IAEA-TECDOC-1143

Modelling of the transfer of radiocaesium from deposition to lake ecosystems

Report of the VAMP Aquatic Working Group

Part of the IAEA/EC Co-ordinated Research Programme on the Validation of Environmental Model Predictions (VAMP)

INTERNATIONAL ATOMIC ENERGY AGENCY

IAEA

March 2000

The originating Section of this publication in the IAEA was:

Waste Safety Section
International Atomic Energy Agency
Wagramer Strasse 5
P.O. Box 100
A-1400 Vienna, Austria

MODELLING OF THE TRANSFER OF
RADIOCAESIUM FROM DEPOSITION TO LAKE ECOSYSTEMS
IAEA, VIENNA, 2000
IAEA-TECDOC-1143
ISSN 1011-4289

Printed by the IAEA in Austria
March 2000

IAEA SAFETY RELATED PUBLICATIONS

IAEA SAFETY STANDARDS

Under the terms of Article III of its Statute, the IAEA is authorized to establish standards of safety for protection against ionizing radiation and to provide for the application of these standards to peaceful nuclear activities.

The regulatory related publications by means of which the IAEA establishes safety standards and measures are issued in the **IAEA Safety Standards Series**. This series covers nuclear safety, radiation safety, transport safety and waste safety, and also general safety (that is, of relevance in two or more of the four areas), and the categories within it are **Safety Fundamentals**, **Safety Requirements** and **Safety Guides.**

- **Safety Fundamentals** (silver lettering) present basic objectives, concepts and principles of safety and protection in the development and application of atomic energy for peaceful purposes.
- **Safety Requirements** (red lettering) establish the requirements that must be met to ensure safety. These requirements, which are expressed as 'shall' statements, are governed by the objectives and principles presented in the Safety Fundamentals.
- **Safety Guides** (green lettering) recommend actions, conditions or procedures for meeting safety requirements. Recommendations in Safety Guides are expressed as 'should' statements, with the implication that it is necessary to take the measures recommended or equivalent alternative measures to comply with the requirements.

The IAEA's safety standards are not legally binding on Member States but may be adopted by them, at their own discretion, for use in national regulations in respect of their own activities. The standards are binding on the IAEA for application in relation to its own operations and to operations assisted by the IAEA.

OTHER SAFETY RELATED PUBLICATIONS

Under the terms of Articles III and VIII.C of its Statute, the IAEA makes available and fosters the exchange of information relating to peaceful nuclear activities and serves as an intermediary among its members for this purpose.

Reports on safety and protection in nuclear activities are issued in other series, in particular the **IAEA Safety Reports Series**, as informational publications. Safety Reports may describe good practices and give practical examples and detailed methods that can be used to meet safety requirements. They do not establish requirements or make recommendations.

Other IAEA series that include safety related sales publications are the **Technical Reports Series,** the **Radiological Assessment Reports Series** and the **INSAG Series**. The IAEA also issues reports on radiological accidents and other special sales publications. Unpriced safety related publications are issued in the **TECDOC Series**, the **Provisional Safety Standards Series**, the **Training Course Series,** the **IAEA Services Series** and the **Computer Manual Series**, and as **Practical Radiation Safety and Protection Manuals**.

The IAEA does not normally maintain stocks of reports in this series. However, electronic copies of these reports can be obtained from:

INIS Clearinghouse
International Atomic Energy Agency
Wagramer Strasse 5
P.O. Box 100
A-1400 Vienna, Austria

Telephone: (43) 1 2600-22880 or 22866
Fax: (43) 1 2600-29882
E-mail: CHOUSE@IAEA.ORG
Web site: http://www.iaea.org/programmes/inis/inis.htm

Orders should be accompanied by prepayment of 100 Austrian Schillings in the form of a cheque or credit card (MasterCard, VISA).

FOREWORD

Following the Chernobyl accident and on the recommendation of the International Nuclear Safety Advisory Group (INSAG) in its Summary Report on the Post-Accident Review Meeting on the Chernobyl Accident (Safety Series No. 75-INSAG-1, IAEA, Vienna, 1986), the IAEA established a Co-ordinated Research Programme on "The Validation of Models for the Transfer of Radionuclides in Terrestrial, Urban and Aquatic Environments and the Acquisition of Data for that Purpose". The programme used the information on the environmental behaviour of radionuclides which became available as a result of the measurement programmes instituted in countries of the former Soviet Union and in many European countries after April 1986 for the purpose of testing the reliability of assessment models. Such models find application in assessing the radiological impact of all parts of the nuclear fuel cycle. They are used in the planning and design stage to predict the radiological impact of nuclear facilities and in assessing the possible consequences of accidents involving releases of radioactive material to the environment and in establishing criteria for the implementation of countermeasures. In the operational phase, they are used together with the results of environmental monitoring to demonstrate compliance with regulatory requirements concerned with radiation dose limitation.

The programme, which had the short title "***Va***lidation of Environmental ***M***odel ***P***redictions (VAMP)", ran from 1988 to 1995. It was sponsored by the IAEA and supported by the European Commission. There were four working groups within the VAMP programme: the Terrestrial Working Group, the Urban Working Group, the Aquatic Working Group and the Multiple Pathways Assessment Working Group.

The **VAMP Aquatic Working Group** studied the turnover of caesium-137 in freshwater systems. It was divided in two subgroups, one on lake modelling and one on modelling rivers and reservoirs. This report summarizes the work of the **Subgroup on Lakes**. The objectives of the subgroup were to assess how various kinds of models can be applied to different lake types, to compare the model predictions with environmental data sets and to analyse the influence of model parameters on the predictions.

The report is the outcome of a joint effort by the participants of the subgroup. It also includes two annexes, the first describing experiences gained in applying certain remedial measures to lakes and river systems contaminated by radionuclides including caesium-137 and the second containing the results of the specific model applied to one of the scenario lakes. A special acknowledgement is due to the Chairman of the Working Group, L. Håkanson (Sweden), for directing the group and to J. Brittain (Norway) for his valuable and devoted efforts in developing and editing the report. The IAEA staff members responsible for the report were D. Calmet and K.-L. Sjoeblom of the Division of Radiation and Waste Safety.

Other reports issued under the VAMP programme are:

Modelling of Resuspension, Seasonality and Losses during Food Processing. First Report of the VAMP Terrestrial Working Group, IAEA-TECDOC-647 (1992).

Assessing the Radiological Impact of Past Nuclear Activities and Events, IAEA-TECDOC-755 (1994).

Modelling the Deposition of Airborne Radionuclides into the Urban Environment. First Report of the VAMP Urban Working Group, IAEA-TECDOC-760 (1994).

Validation of Models Using Chernobyl Fallout Data from the Central Bohemia Region of the Czech Republic, Scenario CB. First Report of the VAMP Multiple Pathways Assessment Working Group, IAEA-TECDOC-795 (1995).

Modelling of Radionuclide Interception and Loss Processes in Vegetation and of Transfer in Semi-natural Ecosystems. Second Report of the VAMP Terrestrial Working Group, IAEA-TECDOC-857 (1996).

Validation of Models Using Chernobyl Fallout Data from Southern Finland: Scenario S. Second Report of the VAMP Multiple Pathways Assessment Working Group, IAEA-TECDOC-904 (1996).

EDITORIAL NOTE

In preparing this publication for press, staff of the IAEA have made up the pages from the original manuscript(s). The views expressed do not necessarily reflect those of the governments of the nominating Member States or of the nominating organizations.

The use of particular designations of the countries or territories does not imply any judgement by the publisher, the IAEA, as to the legal status of such countries or territories, of their authorities and institutions or of the delimitation of their boundaries.

The mention of names of specific companies or products (whether or not indicated as registered) does not imply any intention to infringe proprietary rights, nor should it be construed as an endorsement or recommendation on the part of the IAEA.

CONTENTS

1. INTRODUCTION

The environmental impact of releases of radionuclides from nuclear installations can be predicted using assessment models. For such assessments information on their reliability must be provided. Ideally models should be developed and tested using actual data on the transfer of the nuclides which are site specific for the environment being modelled. In the past, generic data have often been taken from environmental contamination that resulted from the fallout from the nuclear weapons testing in the 1950s and 1960s or from laboratory experiments. However, it has always been recognized that there may be differences in the physico-chemical form of the radionuclides from these sources as compared to those that could be released from nuclear installations. Furthermore, weapons fallout was spread over time; it did not provide a single pulse which is generally used in testing models that predict time dependence. On the other hand, the Chernobyl accident resulted in a single pulse, which was detected and measured in a variety of environments throughout Europe.

The acquisition of these new data sets justified the establishment of an international programme aimed at collating data from different IAEA Member States and at co-ordinating work on new model testing studies. The possibilities for data acquisition and model testing in this "natural laboratory" were recognized at the Post-Accident Review Meeting, held in Vienna from 25 to 29 August 1986. In the Summary Report of that meeting prepared by the International Nuclear Safety Advisory Group, it was recommended that:

> "In order to improve predictions of the consequences of accidental releases of radioactivity, the IAEA should, in collaboration with WMO, review and intercalibrate models of atmospheric transport of radionuclides over short and long distances and of radionuclide deposition on terrestrial surfaces (soils, vegetation, buildings, etc.) and establish a data base for validation studies on such models. In addition, it should carry out similar activities with regard to models of the transfer of radionuclides through the terrestrial environment and in food-chains, their transfer through surface waters (freshwater and seawater) and their transfer in urban environments."

Following these recommendations, the IAEA established a Co-ordinated Research Programme (CRP) on "Validation of Environmental Model Predictions" (acronym VAMP).

VAMP was concerned with models and data relevant to the terrestrial, aquatic and urban environments. It did not deal with models for atmospheric transport, but, however, considered the interactions of aerosols in the surface air with terrestrial and aquatic surfaces.

The principal objectives of the VAMP Co-ordinated Research Programme were:

(a) To facilitate the validation of assessment models for radionuclide transfer in the terrestrial, aquatic and urban environments. It is envisaged that this will be achieved by acquiring suitable sets of environmental data from the results of the national research and monitoring programmes established following the Chernobyl release.
(b) To guide, if necessary, environmental research and monitoring efforts to acquire data for the validation of models used to assess the most significant radiological exposure pathways.
(c) To produce a report or reports reviewing the current status of environmental assessment modelling, including a review of the improvements achieved as a result of post-Chernobyl validation efforts and identifying the principal remaining areas of uncertainty in models used for radiation dose assessments.
(d) To run "test scenarios" for model validations selected for their importance in relation to radiation dose assessments. In selecting scenarios and processes for model validations it is necessary to bear in mind that there should be a clearly demonstrable need to improve the reliability of predictions of radionuclide transfer in the pathways chosen.

VAMP therefore established four working groups on terrestrial, urban, aquatic and multiple pathway analysis. Since there was an obvious relationship between VAMP and the research of other international programmes (IUR: International Union of Radioecologists; BIOMOVS: Biospheric Model Validation Study), effort was made to guarantee the exchange of information and avoid possible overlap.

2. PROJECT SET-UP

For practical reasons the Aquatic Working Group has been divided into two sub-groups, one studying the turnover of caesium-137 in lake systems and the other for river systems. In this document the results of the lake model validation is described. The river model validation is documented in a separate report.

The aim of the sub-group on lakes was to study:

(a) The causal relationships governing radionuclide concentrations, especially caesium-137, in lake waters and the uptake in fish;
(b) The factors regulating the decline of caesium-137 concentration in fish (i.e. the factors regulating the transport of caesium-137 from land to water and the factors in lakes regulating internal loading/resuspension);
(c) The extent, potential and results of remedial actions.

Institutions which had data sets and/or models for lake systems were identified in 1989 through a circulated questionnaire. The Lake Sub-Group reviewed the answers to the questionnaire and selected seven institutes able to provide relevant data sets and six to provide mathematical modelling work. A new questionnaire was sent to these institutes in order to assess how their involvement in the VAMP Aquatic Group might be adapted to the scope of the CRP.

Following the answers to the second questionnaire and a review of the scientific data provided, a formal model validation approach was considered which consisted of formulating scenarios to test models based upon predictions of peak and tail values for water and predator fish. Modellers then performed calculations, which were subsequently analysed and compared with the observed data.

It should be emphasized that the primary aim of the Lakes Subgroup was not to duplicate the work carried out within the framework of BIOMOVS, such as 'blind' tests of various models. Instead, the objective was to try to assess how various models apply to various lake types, to establish criteria for this and to explain the model characteristics (parameters, rate constants, etc.) in a clear and structured way. The extent, potential and results from remedial actions in the aquatic environment were also addressed.

Model considerations

The deposition of radionuclides following a nuclear accident gives rise to at least two principal concerns in respect to the freshwater environment:

(a) Are the concentrations of radionuclides in aquatic foodstuffs and raw waters likely to exceed values at which restrictions should be placed on their use and consumption, i.e. what is the peak concentration?
(b) If such concentrations are exceeded, over what period of time are restrictions on the harvesting of freshwater foodstuffs and the use of raw waters likely to be required, i.e. what is the recovery time of the system?

Models have been developed to describe the behaviour of radionuclides in freshwater systems so that estimates may be made of the potential impact of either authorized, routine discharges from

nuclear facilities or accidental inputs. The Chernobyl accident is an example of the latter and the monitoring and research data subsequently collected provide a basis for testing the validity of the models as descriptions of the real freshwater environment. There are a large number of lakes for which, following the Chernobyl accident, data have been collected concerning the distributions of caesium in the water, sediment and biota. The data have been collected for a variety of purposes and show marked differences in the frequency of sampling both in space and time. Nevertheless, these data sets do provide a basis of comparison for model predictions of the behaviour of caesium in freshwater lakes and, hence, a means of validating the models.

3. LAKE SITES

From the data sets made available to the VAMP Aquatic Group, seven localities have been chosen to provide, as far as possible, the widest range of lake characteristics. However, this selection clearly does not include all possible lake types. The lakes are:

Øvre Heimdalsvatn, Norway
Devoke Water, United Kingdom
Esthwaite Water, United Kingdom
IJsselmeer, The Netherlands
Iso Valkjärvi, Finland
Hillesjön, Sweden
Bracciano, Italy

The locations of the lakes are shown in Figure 3.1. Estimates of the caesium deposition at these sites from the Chernobyl plume are shown in Figure 3.2.

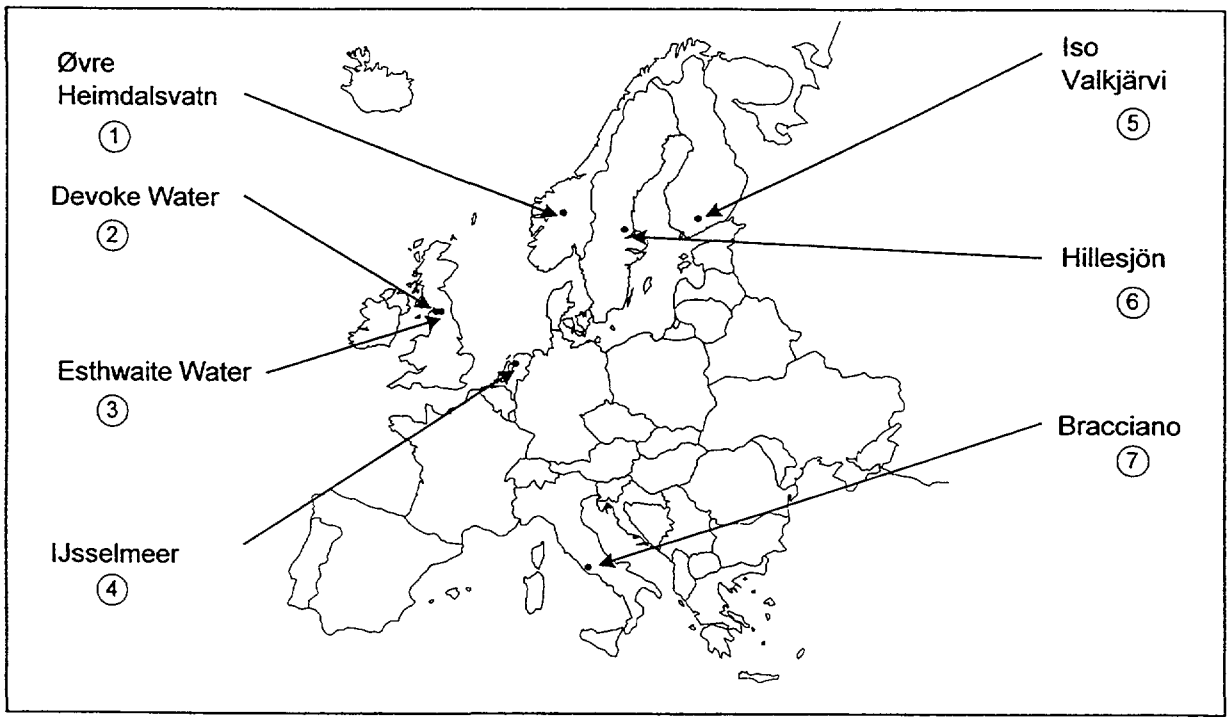

FIG. 3.1. The location of the lakes used in the VAMP study.

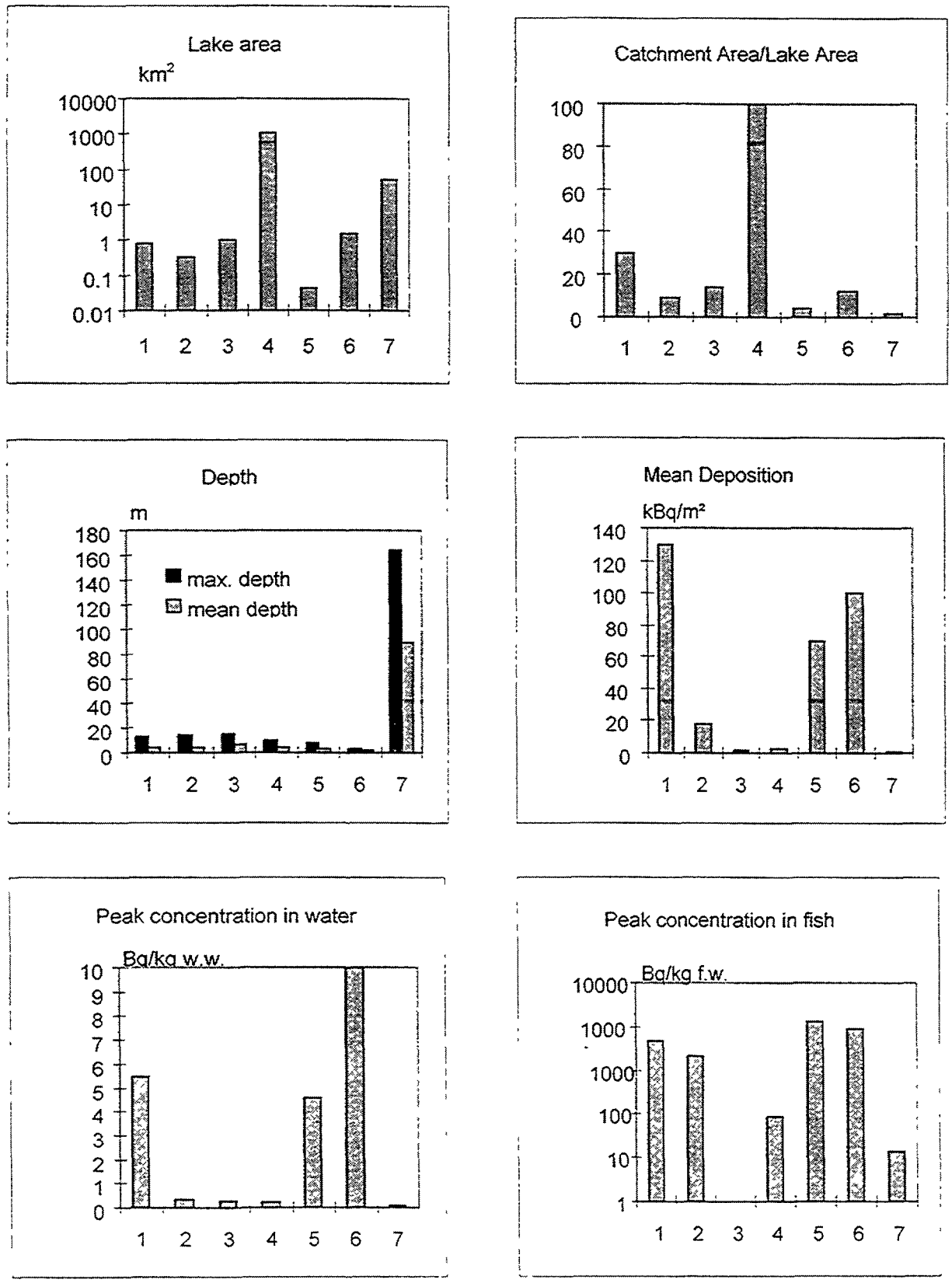

[a] Perch if data available, otherwise trout.

FIG. 3.2. Some characteristics of the VAMP lakes. The brown numbers 1–7 refer to Figure 3.1.

TABLE 3.1. BASIC SITE DATA FOR THE VAMP LAKES

Lake	Alt. m a.s.l.	Lat. °N	Lake area km^2	Max depth m	Mean depth m	Lake volume m^3
Øvre Heimdalsvatn	1090	61	0.78	13	4.7	3.7×10^6
Devoke Water	233	54	0.34	14	4	1.36×10^6
Esthwaite Water	66	54	1.0	15	6.4	6.4×10^6
IJsselmeer	0	52	1147	10[a]	4.3	4.9×10^9
Iso Valkjärvi	126	61	0.042	8	3	1.3×10^5
Hillesjön	10	61	1.6	3	1.7	2.7×10^6
Bracciano	164	42	57	165	89	5.1×10^9

[a] Approximate value.

Lake	Catchment/ lake area	Rainfall mm/a	Water res. time	Ice cover % of year	Ice cover during fallout
Øvre Heimdalsvatn	30	800	63d[b]	60	yes
Devoke Water	9	1840	88d[c]	<2	no
Esthwaite Water	14	1750[c]	70d[c]	<2	no
IJsselmeer	100[c]	750[c]	150d	<2	no
Iso Valkjärvi	4	600	3a	50	yes
Hillesjön	12	650[c]	130d[b]	40	yes
Bracciano	1.6	900	137a	0	no

[b] Major seasonal variation – see site descriptions (Appendix I).
[c] Approximate values.

The lakes have a number of characteristics which have a potential influence on the behaviour of the caesium deposition and its incorporation in the food chain leading to fish. Basic lake data are summarized in Figure 3.2 and Table 3.1. The altitudes of the lakes vary from sea level to 1100 m with the majority at the lower end of the range. With the exceptions of IJsselmeer (1.15×10^3 km^2) and Lago Bracciano (57 km^2), the lakes are small with surface areas in the range 0.04–1.6 km^2, and all except Bracciano (165 m) are shallow with maximum depths less than 15 m. The catchment areas, relative to the lake area, show a relatively wide range, with a maximum of approximately 100 for IJsselmeer. This is a potentially important factor in terms of the possible secondary input of Chernobyl derived caesium to the lakes from the drainage area. Secondary inputs are also likely to be affected by precipitation levels over the catchment area.

TABLE 3.1. (continued)

Lake	T<4°C month	Summer temp.: epilimnion	Stratification	pH	K mg/L	Ca mg/L	Cond. µS/cm
Øvre Heimdalsvatn	8	10–15	winter strat.	6.8	0.4	1.7	7–32
Devoke Water	0–2	12–21	polymictic	6.5	0.55	5.8	–[e]
Esthwaite Water	0–2	12–21	warm, monom.	8[d]	0.9	8.2	100
IJsselmeer	0–2	12	polymictic	8.5	7.0	60	700
Iso Valkjärvi	6	15–20	dimictic	5.1	0.4	1.0	17
Hillesjön	5	18	winter strat.	7.3	3.0	1.0	360–570
Bracciano	0	20–25	warm, monom.	8.5	40	17	465

[d] Varies from 6.8 in winter to >9 in summer.
[e] Value not known.

Lake	Humic status	Trophic status	Prim. prod. g $C \cdot m^{-2} \cdot a^{-1}$	Susp. load mg/L	Sediment. rate $g \cdot m^{-2} \cdot a^{-1}$
Øvre Heimdalsvatn	Oligo.	Oligo.	25–30	0.3	60
Devoke Water	Meso.	Oligo.	–[e]	0.5	300[f]
Esthwaite Water	Oligo.	Eutro.	350[f]	1.0	700
IJsselmeer	Oligo.	Eutro.	10–15	40	500
Iso Valkjärvi	Meso.	Oligo.	25	<1	70[f]
Hillesjön	Oligo.	Meso.	100	5.0	–[e]
Bracciano	Oligo.	Oligo.	290	<1	–[e]

[e] Value not known.
[f] Estimated value.

All of the parameters discussed so far have relevance to the water residence times for the lakes, which on an annual basis vary between 63 days for Øvre Heimdalsvatn and 137 years for Bracciano. Particularly in the case of Øvre Heimdalsvatn the 63 day value is a yearly average which conceals a wide seasonal variation between a low of a few days during peak snow melt in the spring and a theoretical high of some 400 days when the lake is ice-covered in winter. For all the other lakes, apart from Hillesjön which shows a similar but less pronounced pattern, there is relatively little seasonal variation in residence time.

With respect to water chemistry, Iso Valkjärvi is the only acid lake, but most, except Bracciano and IJsselmeer, have low alkalinity. Esthwaite Water, Hillesjön and IJsselmeer have significant inputs

TABLE 3.2. DEPOSITION AND WATER DATA FOR CAESIUM-137 IN THE VAMP LAKES

Lake	Deposition kBq/m^2		Unfiltered water	
	Mean	Range	Max. obs. conc. Bq/L	Date
Øvre Heimdalsvatn	130	26–260	5.5	12.06.86
Devoke Water		15–20	0.35	late July '86
Esthwaite Water	2.0		0.3	13.05.86
IJsselmeer		1.5–3.0[a]	0.2	01.05.86
Iso Valkjärvi	70		4.6	10.06.87
Hillesjön	100		10	15.05.86
Bracciano	0.9	0.3–1.5	0.1	20.05.86

[a] Deposition on lake and near lake areas.

TABLE 3.3. CAESIUM-137 DATA FOR FISH POPULATIONS IN THE VAMP LAKES

Lake	Species	Main food items[b]	Max. obs. conc. Bq/kg w.w.	Date of obser-vation.	Size of fish measured at max. obs. conc.	No. of fish measured at max. obs. conc.
Øvre Heimdalsvatn	Minnow	B, A	5800	28.08.86	3–10 cm	~100
	Trout	B	4700	28.08.86	262–412 g	6
Devoke Water	Perch	F	2100	17.02.87	231–409 g	10
	Trout	B, F	1400	16.02.87	298–492 g	7
IJsselmeer	Smelt	Z	30	08.04.87	2.2 g	226
	Roach	Z, B, A	20	08.04.87	179 g	15
	Perch[1]	Z, B	34	03.07.87	<10 g	242
	Perch	Z, B, F	85	12.04.87	189 g	11
Iso Valkjärvi	Whitefish	Z	9500	03.06.88	35 cm	2
	Perch	B, Z	13 800	16.09.88	15–20 cm	8
	Pike	F	27 000	23.07.87	23–35 cm	2
Hillesjön	Roach	Z, B, A	3600	10.03.87	18–24 cm	10
	Perch	Z, B	5900	10.03.87	10–12 cm	26
	Perch	Z, F	9200	10.03.87	18–20 cm	2
	Pike	F	5000	24.02.88	250–3200 g	50
Bracciano	Whitefish	Z	14	21.08.86	24–29 cm	50

[a] 1986 year class.
[b] A = algae; B = benthos; F = fish; Z = zooplankton.

of nutrients and are mesotrophic or eutrophic, while the remainder are oligotrophic. Devoke Water and Iso Valkjärvi are the only lakes with a significant content of dissolved organic carbon and have been classified as mesohumic.

Three lakes, Øvre Heimdalsvatn, Hillesjön and Iso Valkjärvi are icebound for at least 50% of the year and show winter stratification. The remaining lakes experience little or no ice cover and are well mixed during the winter. All the lakes except Øvre Heimdalsvatn and IJsselmeer develop a thermocline in the summer and are stratified for a substantial period.

In Table 3.2. available information on the deposition to the lakes and the maximum observed caesium-137 concentration in the lake water, together with the dates of observation are presented.

A summary of the maximum radiocaesium content for fish from six of the lakes is given in Table 3.3. A more detailed description of the seven selected sites is given in Appendix I.

4. BASIC CONCEPTS, MODELS AND MODEL COMPARISON

4.1. BASIC CONCEPTS

4.1.1. The distribution coefficient

Background and definitions

In radioecology it is important to distinguish between the total concentration in water and sediments and the bioavailable fraction. However, this is hard to accomplish. The aim of this Section is to give a brief survey of definitions for the distribution coefficient (K_d) and some examples illustrating the important role that this coefficient plays for the modelling of radiocaesium in lake ecosystems. It is important to note the difference between the particulate fraction (= the suspended phase or the particulate phase) of a contaminant and the dissolved fraction (or phase), which is often more available for biouptake by plankton, bacteria, plants and fish. This Section focuses on the distribution of radiocaesium between dissolved and particulate phases in lake waters [4.1]. The VAMP Rivers sub-group has focused on definitions and approaches to determine the distribution coefficient for sediments, i.e., the distribution between caesium in interstitial water and sediment particles [4.2]. This is a function of many factors related to the inorganic materials of the sediments (e.g. illite clays and frayed edge sites), of redox potential and sediment chemistry (e.g. activity of ammonium).

TABLE 4.1. SELECTIVE EXTRACTION SCHEME FOR DIFFERENT METAL FORMS IN SEDIMENT [4.3]

STEP	EXTRACTANTS	EXTRACTION-TIME	TEMP. (°C)	FRACTION
1	1 M $MgCl_2$ at pH 7.0	15 minutes	-	Exchangeable metal
2	1 M Acetate buffer at pH 5.0	0.5 hour	-	Carbonate-bound metals
3	Leached with 0.04 M NH_2OH*HCl in 25 % (v/v) HOAc	6 hours	96	Metals bound to Fe-Mn oxides
4	30 % H_2O_2 (pH 2.0) → and then 3.2 M NH_4OAc in 20 % (v/v) HNO_3 →	5 hours 0.5 hour	85 20	Organically bound metals

VARIANT	DEFINITION
1	K_d = Amount of particle-associated contaminat X per mass unit particulate matter / Amount of dissolved contaminant X per volume unit of water
2	K_d = Amount of particle-associated contaminant X per mass unit particulate matter / Amount of dissolved contaminant X per mass unit of water
3	K_d = Amount of dissolved contaminant X / Amount of dissolved + particle-associated contaminant X

FIG. 4.1. Variants of the partition coefficient for a substance. Note the difference between variant 1 and 2 contra variant 3.

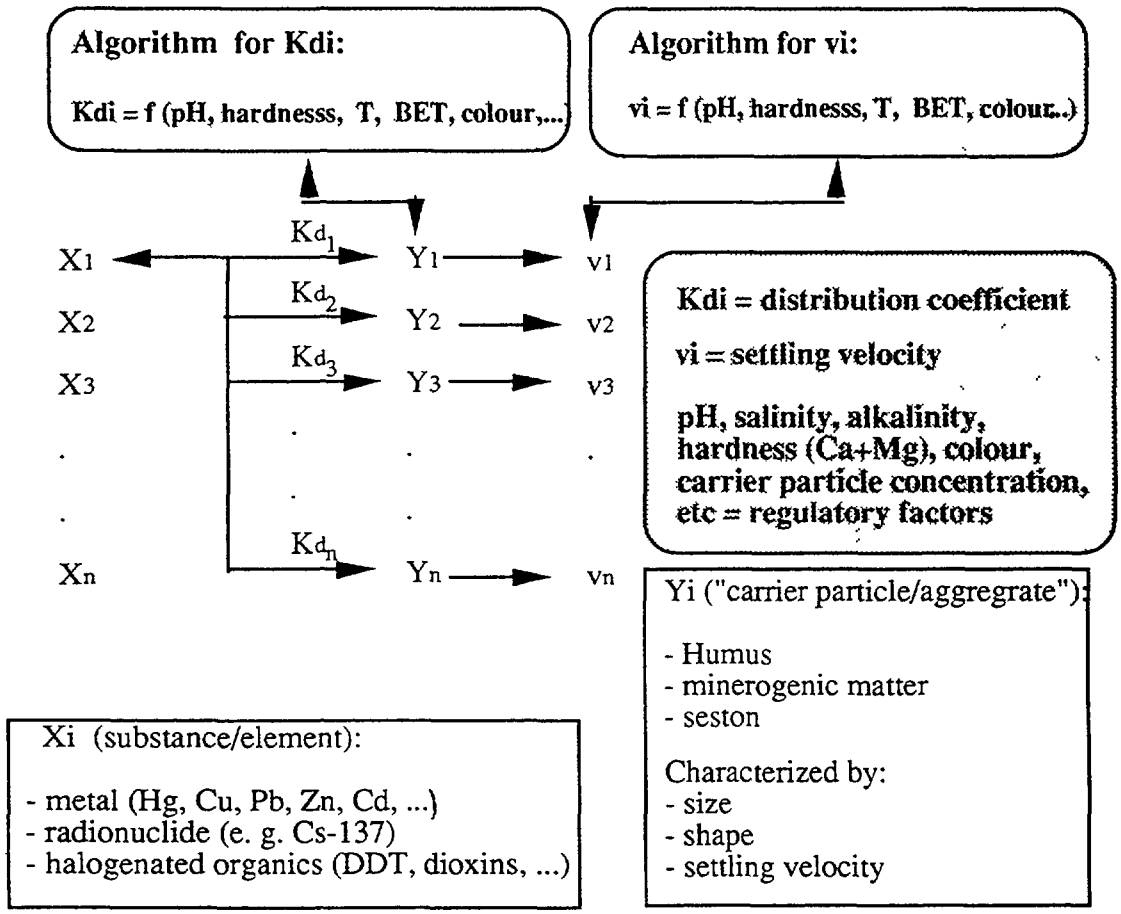

FIG. 4.2. The partition coefficient (K_d) for any given substance X (a metal, a radioisotope or a chlorinated substance like DDT) in relation to different types of "carrier particles", Yi (e.g., humic matter, clays, seston) would be a function (expressed by the algorithm) of several environmental variables [like pH, salinity, water retention time (T), resuspension processes (BET) or lake colour] [4.10].

Among the different separation methods, chemical extractions have been the most frequently used, Table 4.1, [4.3, 4.4]. These extraction methods give information about how strongly the different substances are bound to suspended matter in the water and in the sediment. This will indicate whether these substances could be released from the particles or not. Different authors have often found varying degrees of selectivity for the various extraction methods [4.5].

The exchangeable fraction has normally been regarded as the most "bioavailable" fraction, but it has been shown [4.6] that deposit-feeding clams accumulated much less ^{60}Co, ^{65}Zn and ^{109}Cd in their soft parts than indicated by an acetic-acid fraction. This is because the actual uptake of any metal released by acetic acid, or any other extractants, will depend on the metal, its site, oxidation state, and the type of organism [4.7].

Over the years, a distinction has been made between particulate and dissolved phase, the latter, often operationally defined as the fraction which passes through a 0.4–0.45 μm filter, and the former as the remaining non-filterable fraction [4.8]. It should be noted that the term dissolved in this case does not need to be equivalent to the bioavailable fraction of a substance. To obtain an expression for which form (dissolved or particulate) the substance is present in a system, a ratio commonly expressed as K_d, the partition coefficient (or partitioning or distribution coefficient), is generally used. This ratio can be defined in several ways (Figure 4.1). It could be defined for the dissolved and particulate phase of the lake water, or for the distribution of the metal/radionuclide between the interstitial water and the solid phase of lake sediments. It should be noted that the term partition coefficient also can be used to describe a substance content in a specific extractant step, such as the concentration of a carbonate-bound substance in the sediment relative to the concentration of the substance in its soluble water-phase.

It must be stressed that the partition coefficient is a variable and not a constant in a given ecosystem. Each determined K_d value depends on many chemical and physical parameters, e.g. pH and salinity. For instance, a pH decrease from 7 to 5 has been shown to decrease the K_d value for zinc by a factor of 5.5 [4.9].

No practically useful and empirically validated predictive models for the K_d value of primary interest to model radionuclide transport in lake ecosystems exist. Such a predictive model or sub-model for lake K_d ought to be given as a function of all the major chemical and physical variables governing the K_d value in the water phase of lakes (Figure 4.2). It should also be noted that each K_d value is specifically linked to a certain substance. It has been shown [4.11] for metals that K_d values can differ from 10 000 m^3/kg for Fe or 1000 m^3/kg for Pb to 30 m^3/kg for Cd in a lake. Referring to Figure 4.1, it can be noted that the partition coefficient can be expressed in several ways. K_d is expressed as variant 3 and variant 1, which are, of course, related by the following equation:

$$K_d(variant3) = 1/(K_d(variant1) * Cp + 1) \quad (4.1)$$

Where Cp is the concentration of particulate matter (kg/m^3 = g/L).

K_d is generally defined as variant 1, that is the ratio between the particulate phase (P, caesium-137 in Bq/kg) and the dissolved phase (D, caesium-137 in Bq/m^3). Using this definition, a K_d of 3333 (P/D=3333) means, for example, that 50% is in dissolved phase and 50% in particulate phase in the Øvre Heimdalsvatn lake, where Cp is 0.0003 g/L, and that 25% is in dissolved phase in the IJsselmeer lake, where Cp is 0.04 g/L.

It should be stressed that the size of the carrier particle (i.e., the suspended material) has an influence on the partition coefficient. It has been shown that K_d values decrease with increasing particle size [4.12], which is easy to understand because of an increasing surface area/volume ratio with decreasing particle size. This affects the distribution and sedimentation of the substances in lakes.

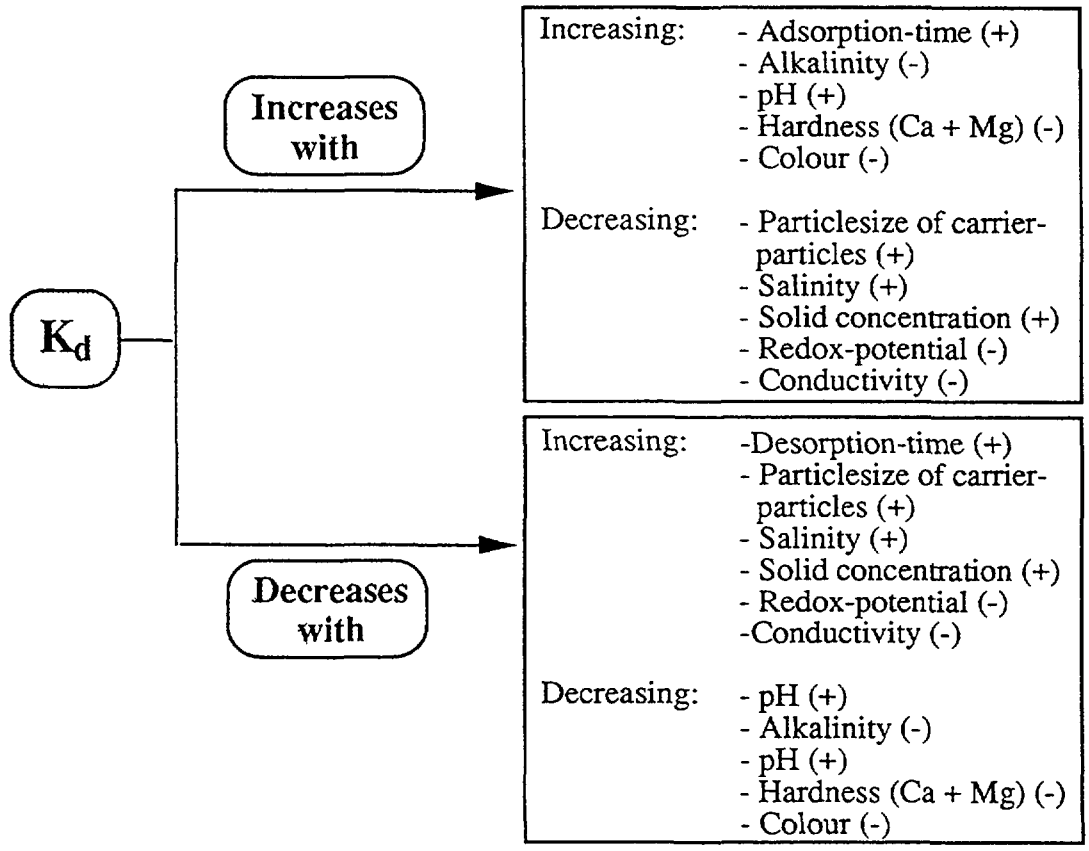

FIG. 4.3. Possible dependencies (-) and already documented dependencies (+) for the partition coefficient (variant 1) of a metal in relation to selected environmental variables [4.13].

Particles of all sizes are introduced to the lake water by primary production, from rivers, through the atmosphere and by resuspension of surface sediments. Particle coagulation, aggregation and break-up continuously renew the particle size spectrum and hence the available surface sites for adsorption of metals. Chemical and physical parameters change with time and this will influence the partition coefficient because these different variables affect coagulation, adsorption, desorption, resolution, precipitation, co-precipitation and complexation (Figure 4.3). These phenomena will also have an impact on the biotic uptake of a substance. Superimposed on these phenomena are kinetic parameters which govern reaction rates, particle sedimentation in question and hydrodynamics.

Studies of the partition coefficient have revealed that the kinetics of the adsorption of easily exchangeable metals is often a two-step reaction [4.13], suggested the "Brownian-pumping" model for metal sorption onto natural particles, and regarded the first step to be of major importance for the K_d value. Most likely, this step has characteristic chemical equilibrium times on the scale of milliseconds to minutes. The second step, which is slower, is believed to take days to months, and it is referred as "slow" particle aggregation of colloidal particles. The second step could also be characterized by ions moving towards more less reachable sites further into the crystal lattice [4.14]. As well as adsorption, desorption has also been shown to be important for the K_d value.

It has been shown [4.15] that the same environmental conditions give higher K_d values for the desorption process relative to the adsorption process for a substance. This is believed to depend on the aggregation of smaller colloidal particles, which may cause the adsorbed substance to be buried inside the aggregated particles, thus making desorption difficult. However, this is this not the case for all substances. Further, it has been shown [4.16] that the adsorption and desorption process for Be gives the same K_d value as soon as equilibrium has been reached.

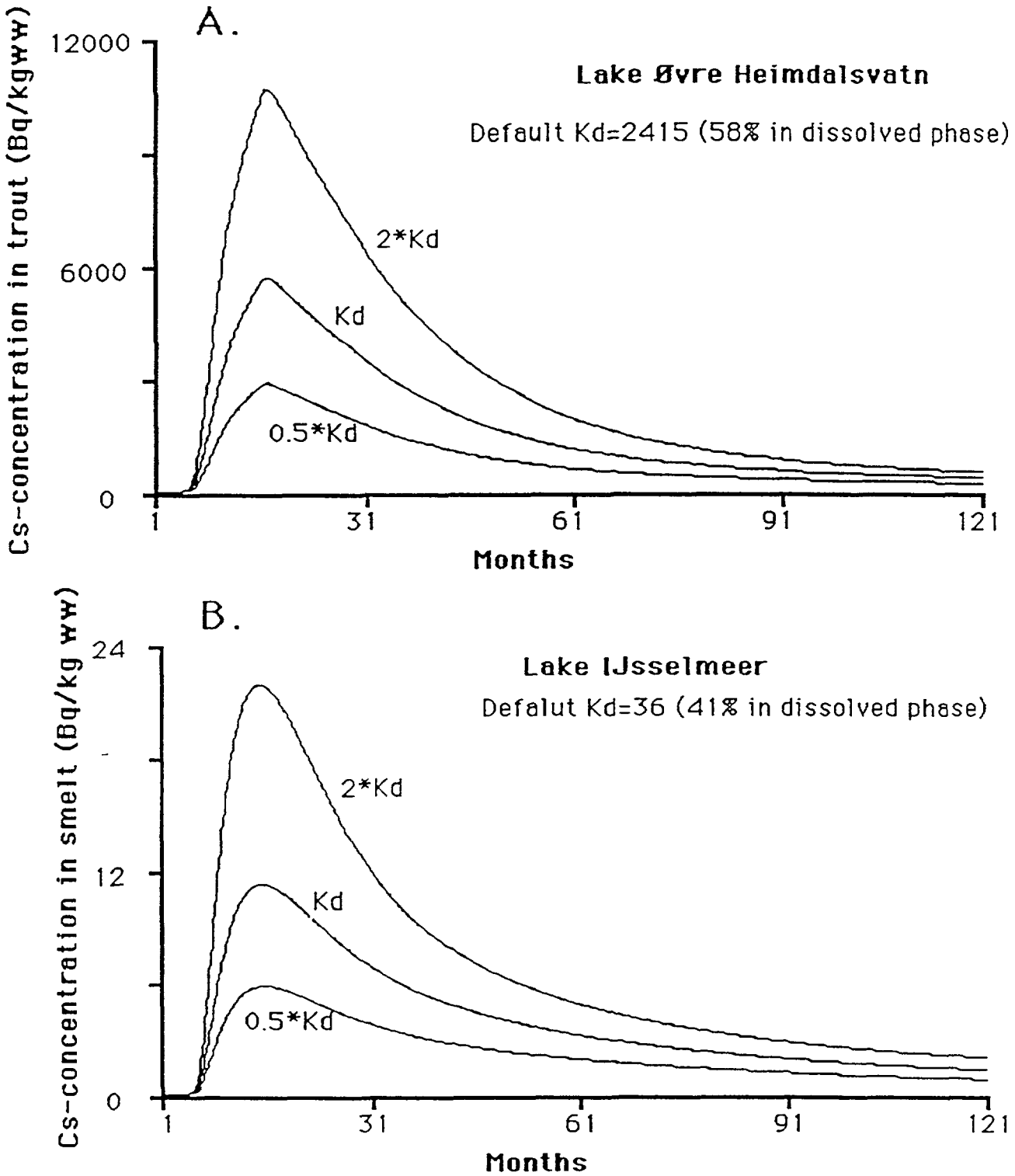

FIG. 4.4. A. Sensitivity test for the concentration of caesium-137 in trout in Øvre Heimdalsvatn, when the partition coefficient (variants 1 and 3) for caesium is varied and the other model variables are kept constant (VAMP LAKE model).
B. The same test for the concentration of caesium-137 in smelt in IJsselmeer.

It should be noted that the partition coefficient generally decreases with increasing concentration of particulate matter. The observed dependency (or slope) between K_d and particulate matter also shows [4.17] that the share of the water soluble phase (K_d, variant 3) decreases with increasing concentration of particulate matter.

The importance of K_d in the modelling of radiocaesium

Caesium-137 seems to have a relatively large particle affinity [4.18, 4.19, 4.20]. If this is true, it will imply that the behaviour of caesium in lakes is largely governed by the chemical and physical properties of the carrier particle, which is especially interesting when studying the effect of the partition coefficient in relation to biological uptake and potential ecosystem effects.

The aim of this Section is to give an example of the importance of K_d values in modelling radiocaesium in lakes, and the VAMP model is used as a tool to simulate the spread and biouptake of caesium-137. The VAMP model is only used in this exercise to demonstrate how the target variable, caesium-137 in fish, is influenced by the partition coefficient. It can be clearly seen that the partition coefficient for caesium is of major importance for caesium-137 in fish (Figure 4.4).

Figure 4.4 shows that it is very important to use a realistic value for the partition coefficient. It would therefore be of great interest to be able to predict the K_d value, its variability in time and with location, as well as its linkage to chemical and physical parameters. In this sensitivity test, the partition coefficient was changed by a factor of 4 (from 0.5 K_d to 2 K_d; where K_d is the default value of the K_d as defined in Annex II-4; pH = 6.8 gives 58% in dissolved phase and a K_d of 2415). Then the levels of caesium in fish (here trout in Øvre Heimdalsvatn) also varies by a factor of 4. Therefore, the result of the model prediction is very much dependent on the choice of the K_d value. This is valid, for this species of fish in this Norwegian lake and is also true for all species of fish in all lakes, but the relative importance of the K_d value is different in different lakes. This is exemplified with data for smelt in IJsselmeer (pH = 7.5 gives 41% in dissolved phase and a K_d of 36).

In conclusion, there are several ways to define the distribution, or partition, coefficient, K_d for substances in lake waters into a dissolved and a particulate phase. Sensitivity tests have shown that lake models for radiocaesium are often very sensitive to the choice of the K_d value. Uncertainties in K_d values lead to uncertainties in model predictions. A sub-model, or an algorithm, which predicts the partition coefficient of a metal or a radionuclide and its relationship to different simple and readily available chemical and physical environmental variables (pH, lake colour, lake water retention rate or retention time, mean depth, etc.) is needed if adequate predictions of transport and biouptake of radiocaesium in aquatic systems are to be made.

4.1.2. Rates and concentration factors

This Section deals with some of the most important concepts used to model the behaviour of toxic substances in the environment. The flux of a contaminant Φ_{ij} from compartment i to the compartment j is related to the amount of the matter in compartment i as follows:

$$\phi_{ij}=k_{ij}Q_i \tag{4.2}$$

where k_{ij} ($i \neq j$) is a rate constant whose dimension is 1/time. The dimensions of Q_i and Φ_{ij} are, mass and mass/time respectively. In the case of a radioactive substance, Q_i is expressed as Bq and Φ_{ij} as Bq/time.

The flux of contaminant from a compartment i to the external environment is modelled according to the following formula:

$$\Phi_i = K_i Q_i \tag{4.3}$$

The constants k_{ij} and K_i are called, respectively, transfer rate from compartment i to compartment j and transfer rate out of compartment i. They are independent of the amounts of matter in each compartment and, in case of stationary processes, are also independent of time, although in general they may depend on many time dependent lake variables, such as temperature, water turnover and water chemistry.

Defining the amount of contaminant introduced from the external environment into compartment i for unit time as Ψ_i (input rate), we obtain, as a consequence of mass conservation:

$$\frac{dQ_i}{dt} = -(\lambda + K_i)Q_i - \sum_{j \neq i} k_{ij} Q_i + \sum_{l \neq i} k_{li} Q_l + \Psi i \tag{4.4}$$

The effect of radioactive decay, or of a first order transformation process, is given by λQ_i , where λ is the "decay rate" ($time^{-1}$).

Equation (4.4) is composed of n (n = number of compartments) first order differential equations in n unknown functions (the amount of substance in each compartment). If the volumes or the masses of the compartments (for instance the volume of the contaminated water body or the mass of a fish species) are constant over time, it is possible to divide both members of equations (4.4) by the products of the volumes and masses to obtain, as result of subsequent simple algebraic calculations, a set of differential equations for the radionuclide concentration C_i in each compartment:

$$\frac{dC_i}{dt} = -(\lambda + K_i)C_i - \sum_{j \neq i} K_{ij} C_i + \sum_{l \neq i} K_{li} C_l + \Psi_i^* \tag{4.5}$$

If

$$\lambda = 0 \tag{4.6}$$

and

$$K_i = 0; \ \Psi_i = 0 \tag{4.7}$$

for any i, summing the members of equations (4.4) over i, we obtain:

$$\frac{dT}{dt} = -\sum_i \sum_{j \neq i} k_{ij} Q_i + \sum_i \sum_{l \neq i} k_{li} Q_l = 0 \tag{4.8}$$

where $T = \sum_i Q_i$ is the total amount of substance present in the system that, according to the equation (4.8), is constant over time. Equation (4.6) states that the considered substance is stable; according to equation (4.7), the system is "closed", i.e. the contaminant does not enter or leave the system. In such

a case, the solutions of equation system (4.4), when $t \rightarrow \infty$, reach constant "equilibrium" values that are solutions of the following system of n+1 linear equations in the n unknown Q_i:

$$0 = -\sum_{j \neq i} k_{ij} Q_i + \sum_{l \neq i} k_{il} Q_l \; ; \; T = \sum_i Q_i \qquad (4.9)$$

In such circumstances the system reaches an equilibrium condition, i.e. the values of the amount of contaminant substances in each compartment are constant over time. The time required for Q_i to be experimentally indistinguishable from the values at equilibrium condition depends on k_{ij}. The ratios between the contaminant concentrations in two compartments when $t \rightarrow \infty$:

$$R_{ij} = \frac{C_i}{C_j} = \frac{Q_i}{Q_j} \frac{V_j}{V_i} \qquad (4.10)$$

(V_i and V_j are the constant volumes or the masses of the compartments i and j) generally depend on the initial distribution of the contaminant substance in the various compartments (initial conditions).

If the contaminant is not stable (open system, $\lambda \neq 0$ and/or $K_i \neq 0$) and the input rates Ψ_i are constant over time, the system reaches a unique equilibrium condition, independent of the initial conditions. The equilibrium can be demonstrated by solution of the following set of linear equations:

$$0 = -(\lambda + K_i) Q_i - \sum_{j \neq i} k_{ij} Q_i + \sum_{l \neq i} k_{l \neq i} Q_l + \Psi_i \qquad (4.11)$$

The mathematical form of the solution of system (4.11) is:

$$Q_i = \sum_j \Gamma_{ij} \Psi_j \qquad (4.12)$$

Formula (4.12) shows that the ratio between the amount of substance, at equilibrium, in two different compartments depends on the substance input rates in the other compartments. If only one input rate, Ψ_k, is different from 0 the amount of substance in the generic compartment i is $Q_i = \Gamma_{ik} \Psi_k$. In such case, the ratios at equilibrium between the amounts of substance in different compartments and consequently the concentration equilibrium ratios (see formula (4.10)) are independent of the input rate.

Supposing, moreover, that the system is composed of a surrounding medium (for instance water, soil or sediment) and of various biotic and abiotic components and that:

(a) the system is closed and, at initial time, only the amount of contaminant in the surrounding medium is different from 0;

or

(b) the contaminant substance is not stable and only the input rate of contaminant in the surrounding medium is different from 0 and constant in time;

then the ratios R_{ij} between the concentration in a biological component and the concentration in the surrounding medium, which depend in general on the contaminant, on the biological species and on the environmental system, are independent of the input rate and the initial concentration of the

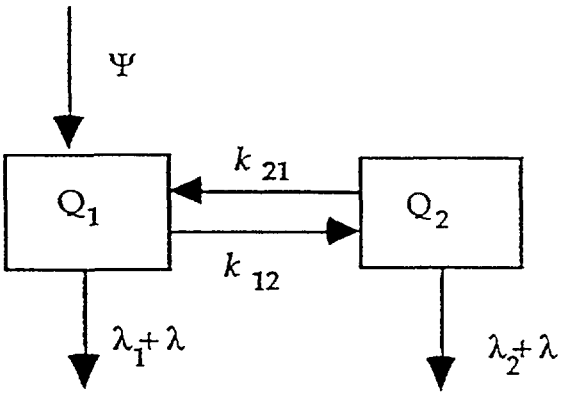

FIG. 4.5. Illustration of the use of the "concentration factor". Q_j is the amount of contaminant in the surrounding medium, Q_2 is the amount of contaminant in a biological species, λ is the radioactive decay rate and λ_1 and λ_2 are the transfer rates out of the surrounding medium and the biotic compartment, respectively.

contaminant in the surrounding medium. These ratios are called "concentration factors" or "bioaccumulation factors".

The above discussion shows that the possibility of defining concentration factors depends on the structure of the system to which the compartments belong. The relationships between the concentration factors and the rates depend on the specific structure of the system.

The following example will illustrate the meaning and the use of the "concentration factor". Consider a system that comprises two compartments (Figure 4.5).

It can be shown that the concentration factor is:

$$R_{21} = \frac{C_2}{C_1} = \frac{Q_2}{Q_1}\frac{V_1}{M_2} = \frac{k_{12}}{\lambda_2 + \lambda + k_{21}}\frac{V_1}{M_2} \qquad (4.13)$$

where V_1 and M_2 are the volume and the mass of the compartments 1 and 2 respectively. The concentration factor (4.13) does not depend on the transfer rate out of compartment 1 (surrounding medium). This is a general result that may be also proved in case of more complex system structure. Indeed, at equilibrium, the input of contaminant to a compartment j from the surrounding medium is $\Phi_{1j} = k_{1j}Q_1$ (see equation (4.2)). Then the values of Q_i, obtained solving the system of the n-1 equations of the mass balance in the other compartments (excepted the surrounding medium), are proportional to Q_1, but do not depend explicitly on λ_1; then the ratios R_{ij} are independent on λ_1. From the experimental point of view it is often easier to evaluate $\lambda + \lambda_2$ and R_{12} than the rates k_{12}, k_{21}.

It is possible to verify that if at time 0 the amount of contaminant in each compartment of an open system is 0 and if:

$$\int_0^\infty \Psi_i dt < \infty \qquad (4.14)$$

(that is the integral in the first member of (4.14) is finite) for every i, by integrating both members of each equation of system (4.4), we derive for the time integrated quantities $\int Q_i dt$ the same algebraic equations that we obtained for the amounts of contaminant in various compartments at equilibrium

(equation (4.11)). Consequently the ratio between the time integrated concentration in a living organism and the time integrated concentration of contaminant in the surrounding medium is equal to the concentration factor for the specific organism if the input rate of contaminant into the surrounding medium accomplishes condition (4.14) and if all other input rates are zero. Condition (4.14) corresponds to very common contamination events; for instance if the input rate shows a finite duration time, condition (4.14) is fulfilled.

4.2. MODEL DESCRIPTIONS

4.2.1. ENEA, Italy

The ENEA model was developed at ENEA by Luigi Monte who is also the user. The model is based on the solution of a set of first order differential equations in which unknown functions are radionuclide concentrations in the various compartments (water, suspended matter, sediment and fish) of the freshwater environment [4.21, 4.22, 4.23]. The migration of a radionuclide from water to sediment is modelled by dividing the sediment into three compartments (interface layer, surface sediment and deep sediment or sink compartment). It is assumed that a radionuclide dissolved in water interacts immediately with the sediment interface layer.

The model may be considered as a generic tool to predict the time behaviour of a radionuclide in a lake system following the deposition of a radionuclide over the surface of the lake and on the lake catchment. The time behaviour of the radionuclide in water, suspended matter, sediment, piscivorous and non-piscivorous fish are predicted.

The model evaluates best estimates of the concentration of caesium-137 in the various compartments of lake systems when a specific set of values for the generic parameters are used (see Annex II-1). The model is mainly focused on the evaluation of radionuclide behaviour in abiotic compartments of the lacustrine environment. The prediction of the behaviour of caesium-137 in fish species are approximate values.

The estimates of the uncertainty of the model results have been carried out by a method described in Section 5.3.2. This method is based on statistical analysis of the results of the comparison between the model output and experimental data collected at various sites.

4.2.2. KEMA, Netherlands

The model, LAKECO, has been developed at KEMA by Rudie Heling [4.24], and is based on several model descriptions in the literature [4.25, 4.26].

The model is a compartment model in which all processes are based on first order differential equations. The tool used to solve the equations is the graphical model tool "I think™ v.2.2.1". The user of this code is Rudie Heling.

The model LAKECO has been developed as one of the aquatic models within the emergency decision support system RODOS, under development in the CEC RODOS project. This model must be very flexible in order to estimate the levels of radionuclides in water, and fishery produce in various lake ecosystems. The model is integrated and coupled to dose and countermeasure models to assess both the short and long term radiological consequences via aquatic exposure pathways in accidental circumstances. LAKECO is linked to a chain of aquatic models handling the transfer of the radionuclide from the drainage area via rivers to the lake, where radionuclides accumulate in both the sediments and fish. The model is documented within the framework of the CEC project RODOS. Some validation results have also been reported [4.24].

The aim of the model is to predict the levels of radionuclides in fishery produce for reasons of health protection. The initial contamination due to direct deposition on the lake surface results in

enhanced levels of radionuclides in fishery produce for many years, especially in top predators like perch and pikeperch, which reach their maximum values when the levels in the lake water are far below the maximum permitted concentration. To estimate the period of restrictions for fishery produce, the lake model must supply at least a relatively good estimation of the peak levels, and the time at which these levels are reached. The required accuracy is within an order of magnitude. Because of this application of the model, underestimates are not desirable, and conservative assumptions in terms of input parameters are accepted.

The model was originally developed to model the behaviour and fate of radionuclides within a lake ecosystem in the Netherlands. After the accident with the reactor in Chernobyl the KEMA carried out many measurements of caesium-137 in the Lake IJsselmeer to obtain more insight into the presence and fate of the Chernobyl fallout in a lake ecosystem. In 1989 the amount of empirical data, especially on biota and raw water, were sufficient to be used as calibration data for a model. The lake model was constructed to predict the long term behaviour of radionuclides both in the abiotic and biotic components. Tests showed adequate agreement between calculations and measurements.

The lake is considered as a box in which complete mixing occurs. The system of linear differential equations obtained by mass balances on all subcompartments is solved numerically. In the sediment layer there are two boxes in which homogeneous concentrations are assumed (Figure 4.6). In the sediment layer both transport of adsorbed and dissolved radionuclides is modelled. The processes which are taken into account are: particle scavenging/sedimentation, molecular diffusion, enhanced migration of radionuclides in solution due to physical and biological mixing processes, particle reworking also due to physical and biological processes and burial, i.e. the downward transfer of radionuclides in the bottom sediment as a result of sedimentation. Transports are the inflow of contaminated river water from the catchment and the outflow at the outlet of the lake.

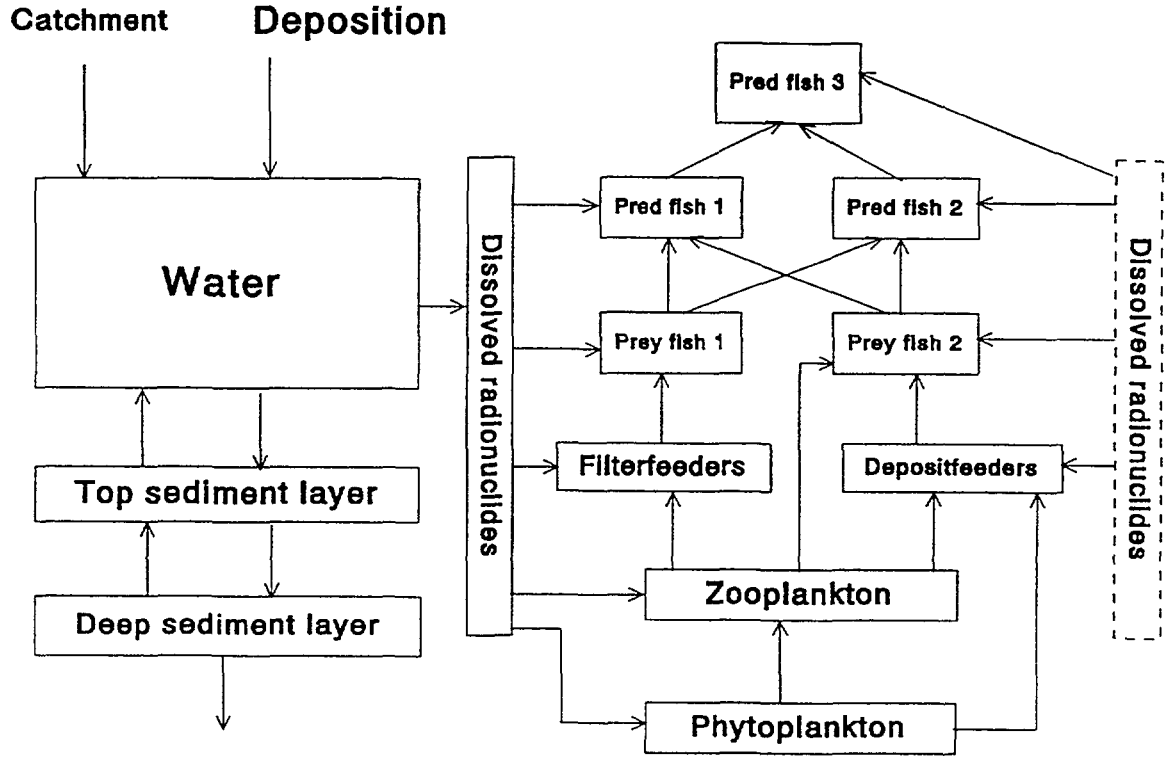

FIG. 4.6. Overview of the compartments of lake model LAKECO.

In case of continuous discharges of radionuclides by nuclear or non-nuclear industries, the uptake of radionuclides by aquatic organisms can be modelled by using the concentration factor approach. In accidental situations, however, a more dynamic approach is necessary, as the concentration factor approach tends to overestimate the concentration in the first period after the initial contamination. To improve predictions, the concentration in an organism can be modelled by means of a combination of the concentration factor approach and the biological half-life of a radionuclide in a specific organism. The delay caused by the time radionuclides need to migrate throughout the several trophic levels is then modelled in a better way. However, this does not model what actually happens, i.e. the transfer of radionuclides from organism to organism due to the prey-predator relationships. Thus, a more complex and accurate approach takes the position in the food chain into account. This requires knowledge about the food chain in a certain water body and specific parameters like consumption rates and food preference, but if these data are available they can be used as direct input data. This approach was adopted in LAKECO because of the presence of an extended set of data, not only to obtain insight in the applicability of this model, but also to get more insight into all processes involved regarding caesium-137 as a tracer. More detailed information on this model can be found in Annex II-2 of this report.

4.2.3. Studsvik, Sweden

The model has been developed at Studsvik Ecosafe AB by Ulla Bergström and Sture Nordlinder, who are also the main users [4.27].

The model is based upon compartment theory with first order differential equations implying that the transfer of elements between the compartments is described by rate constants expressed in turnover per time; in this case per month. Most of the resultant transfers in the model are obtained from expressions based upon biological and physical parameters. This structure makes it possible to:

- apply the same model to different ecosystems using different site-specific values of the parameters,
- perform uncertainty analyses on a rational basis,
- identify important parameters and processes for resultant concentrations in fish or other compartments.

The model is of generic character, whereby site specific conditions are simulated by changing input parameter values. The model can be used for both continuous as well as pulse releases to the system. It predicts concentrations of radionuclides in water, sediment and biota as a function of time. It can be used for both predictions of peak values as well as long term concentrations. The accuracy of the predictions mainly depends on how well the values of the parameters for the system to be studied are known. The model usually provides "best estimates", although somewhat conservatively biased.

The code is used in combination with a statistical error propagation system, PRISM. This programme uses Latin-hyper cube sampling from pre-described distributions to generate in this case 200 sets of values for each parameter. These are used for calculation of 200 model results. Correlation between parameters can be considered independently of the type of distribution of each parameter. Finally, PRISM statistically evaluates and summarizes the joint set of model parameter and predictions. The general statistics include the following:

- the arithmetic mean,
- the standard deviation,
- the coefficient of variation,
- the geometric mean,
- the percentiles,
- the five highest and five lowest values.

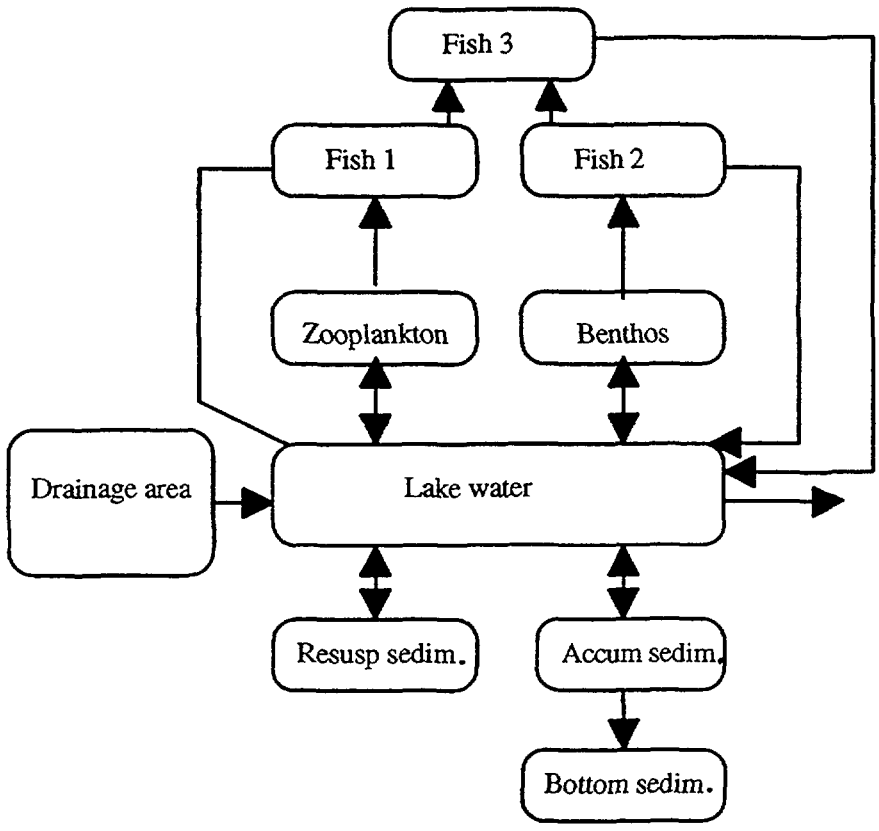

FIG. 4.7. The general structure of the Studsvik model.

These values are analysed statistically by Spearman ranked coefficients and regression procedures. The regression procedures are used for obtaining the relationship between model parameters and model uncertainties.

The basic structure of the model has been used for calculating scenarios within the BIOMOVS study [4.28, 4.29] as well as for modelling caesium-137 turnover in two subarctic lake ecosystems [4.30]. In general, the model simulates concentrations of caesium-137 in fish within a factor of two from observed values. In this particular modelling exercise site specific information was used for each layer. For example, the food habits of the fishes in each layer were considered as well as the consideration of non-homogeneous mixing in the water column of the deep Italian lake, Bracciano.

A generalized structure of the model is given in Figure 4.7. The number of compartments for fish varies according to the ecosystem to be studied. The following compartments are included: drainage area, water, sediments (three compartments for the resuspension accumulation and non-active layers, respectively), plankton, Gammarus (benthos), prey and predatory fish.

Parameters in the model are mostly related either to the nuclide or to the lake ecosystem to be studied. In addition, there are some general parameters, such as consumption values.

The codes for making the calculations are described by the model users in [4.27, 4.29, 4.31].

4.2.4. Uppsala University, Sweden

This Section presents three models for radiocaesium in lakes. They are based on different presuppositions and there are drawbacks and benefits to all of them. They have been developed at Uppsala University (UU) by Lars Håkanson.

4.2.4.1. The empirical model

The general layout of this model is given in Figure 4.8. All equations and presuppositions are given in Annex II-4. This model has been presented in greater detail in [4.33]. It was derived from empirical data for 41 Swedish glacial lakes and their caesium data from 1986 to 1989. This model has not been tested in the VAMP project. It is included in this Section in order to cover as many types of models as possible, and because it highlights and ranks some interesting factors regulating the spread and biouptake of radiocaesium in lakes.

It can be concluded that the radiocaesium concentration in lake water may be predicted by this empirical model if one has access to data on: (i) fallout of radiocaesium, (ii) tributary water discharge, (iii) relief of catchment, (iv) lake volume (i.e., the lake area times lake mean depth), (v) wetland percentage in the catchment (which influences the secondary load, i.e., the transport of caesium-137 from land to water), and (vi) theoretical lake water retention time. The Cs concentration in lake sediments is calculated from a sediment to water concentration factor. The Cs concentration in predatory fish (here 1 kg pike) is determined from the Cs concentration in lake sediments (an indirect

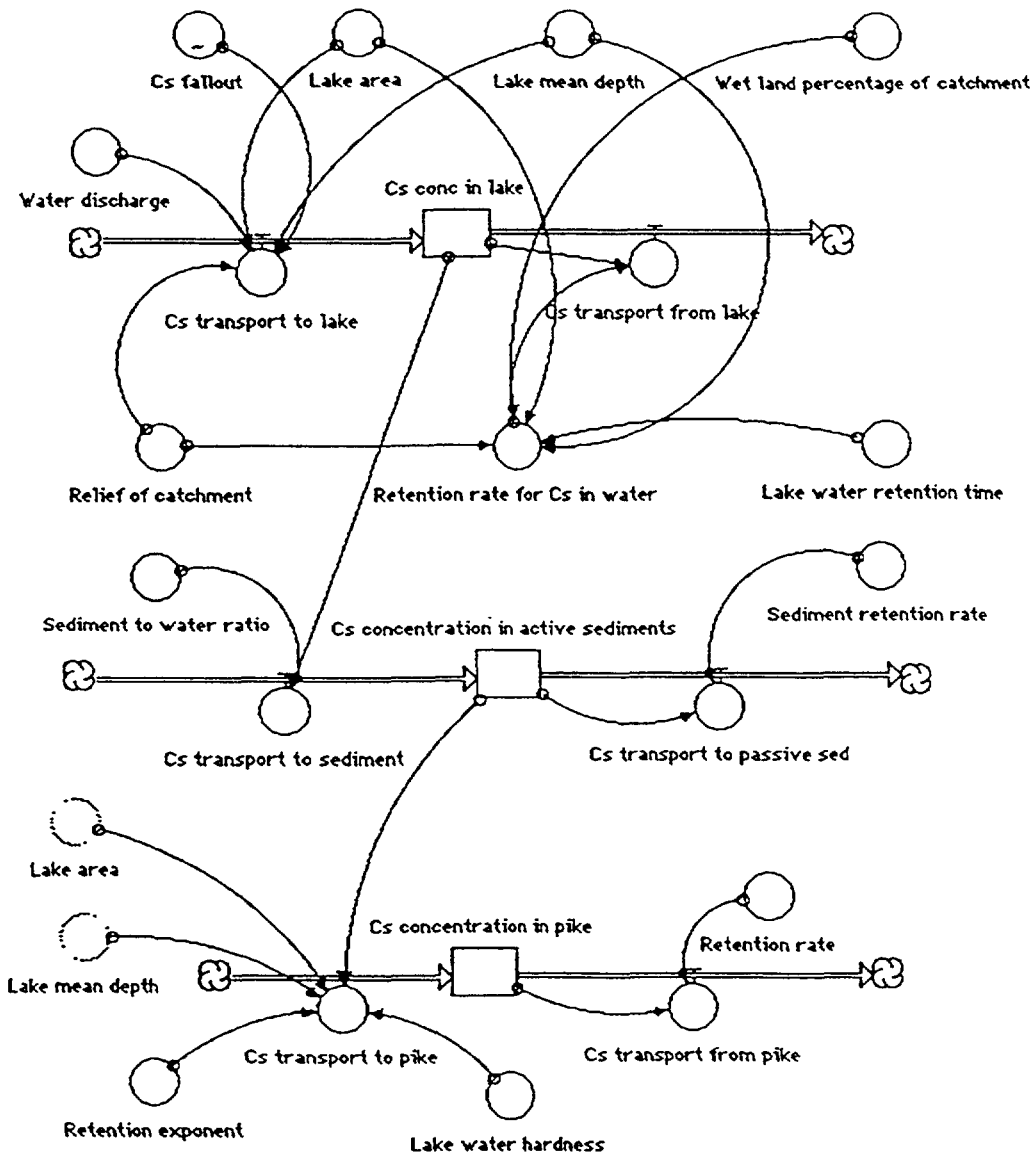

FIG. 4.8. Layout of the UU-Empirical model for radiocaesium in lakes [4.32].

measure of lake load of radiocaesium) and from lake data on water hardness (which influences the bioavailability of radiocaesium). This empirical, statistical model has been obtained by stepwise multiple regression analysis.

The reason why this model has not been tested in the VAMP project is that empirical data on the wetland percentage of the catchments and reliable data on lake water hardness are lacking for several VAMP lakes. Thus, we do not have access to the necessary driving variables. Another reason for not testing this model in the VAMP project is that this is an empirical model derived for small Swedish, glacial forest lakes. It should not be used for other lake types without changing the empirical constants in the model.

4.2.4.2. The mixed model

This is a new version of a model presented earlier by Håkanson [4.32]. For a detailed account, see Annex II-4. This model has been used for all the VAMP lakes. This is a model for the flux of caesium based on calculations using a set of differential equations. The objective with this small mixed model is to predict not all the caesium concentrations in a lake ecosystem, but just the caesium concentrations in lake water, prey fish and predatory fish. To do this, the empirical knowledge gained in deriving the empirical model on the factors regulating the biouptake and retention of caesium in fish was used. This was done by a technique called **dimensionless moderators**. Thus, this model uses **only a minimum** of input data (Figure 4.9). The equations and assumptions are given in Annex II-4, in addition to an account of the development of dimensionless moderators.

Figure 4.9 gives a summary of the model characteristics of the mixed model in terms of compartments, model variables and lake specific variables. It has only three compartments: water, prey and predatory fish, six model variables and five lake specific variables. The total number of driving variables (x) is thus 11. Note that there are no catchment area, sediments, food-web and partition coefficient (K_d) in this very simple model.

4.2.4.3. The generic model

This is a more comprehensive traditional dynamic model. All equations and assumptions are given in Annex II-4. This model has nine compartments, 27 model variables and nine lake-specific variables (see Figure 4.10). It is evident that uncertainty exists in many of these rates and model variables.

In this short model presentation, we will focus on some specific features of this generic model: the outflow rate from the catchment regulating the secondary lake load of radiocaesium and the partition coefficient (K_d).

In most of the affected areas the Chernobyl fallout was shortly before the peak of the spring flood, which also was unusually strong in large parts of the area. Between 0.5 and 10% of the catchment area's total fallout was probably transported to the lakes during May 1986 [4.33, 4.34, 4.35]. During the years 1987–89, the total contribution from the catchment area was probably less than 0.5% of the total deposition owing to a strong decrease in the Cs concentration in the runoff water via streams and rivers. This initial transport to Nordic lakes, and particularly those in northern Sweden, was probably considerably higher than in Central European areas with corresponding fallout levels [4.36]. In this model, we have applied a specific time dependent function to describe the transport (outflow rate of radiocaesium times the amount of radiocaesium in the catchment) from the catchment areas. Thus, the outflow rate and the Cs transport from land are not constant.

Caesium-137 has a marked particle affinity [4.18, 4.19, 4.20] which implies that its behaviour in lakes is partly governed by the chemical and physical properties of the "carrier particle". In addition, the caesium turnover in a lake will be governed by the turnover time of the lake water; the longer the

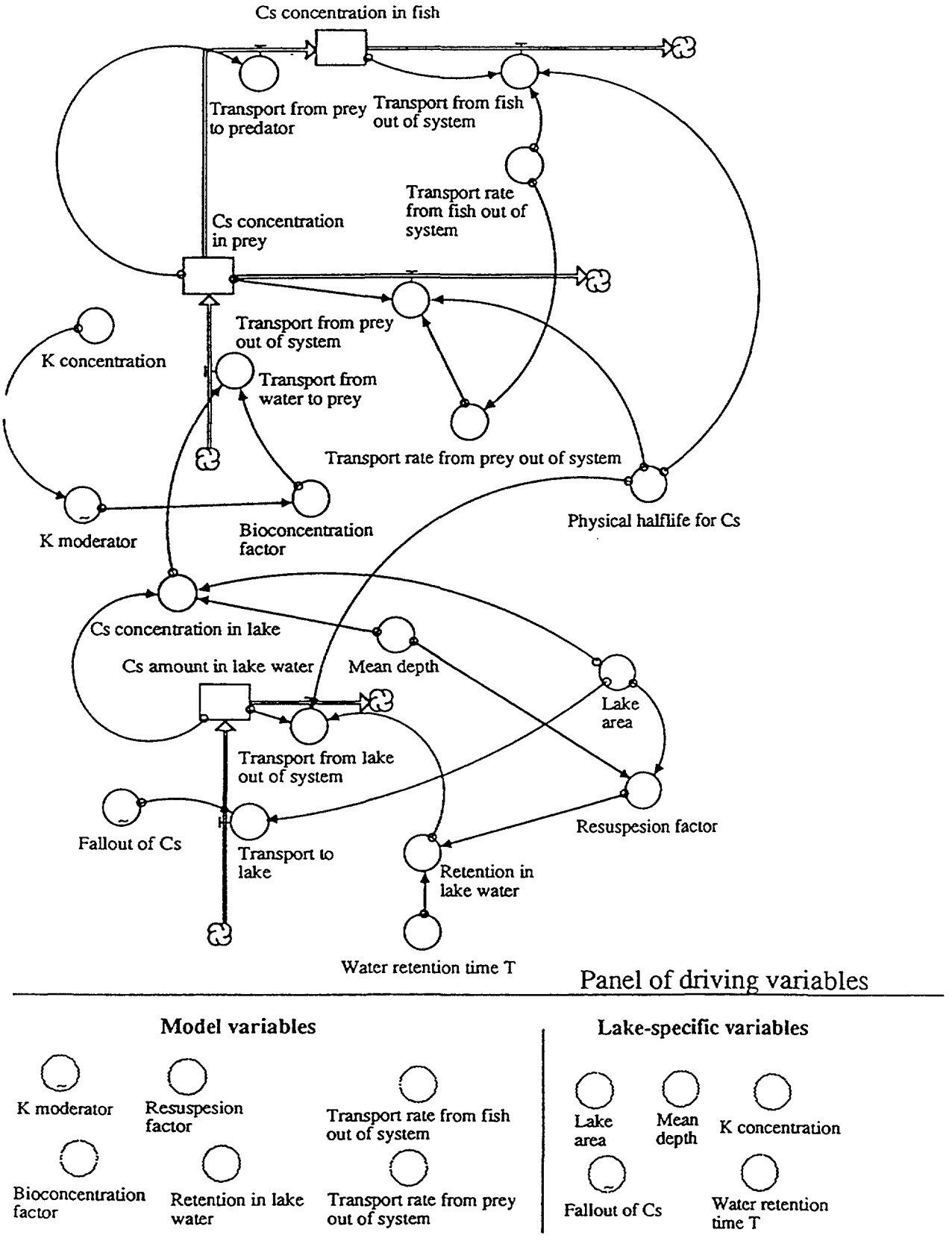

FIG. 4.9. Illustration of the UU-Mixed model and panel of driving variables. The number of model variables, n_1, is six; the number of lake specific variables, n_2, is five.

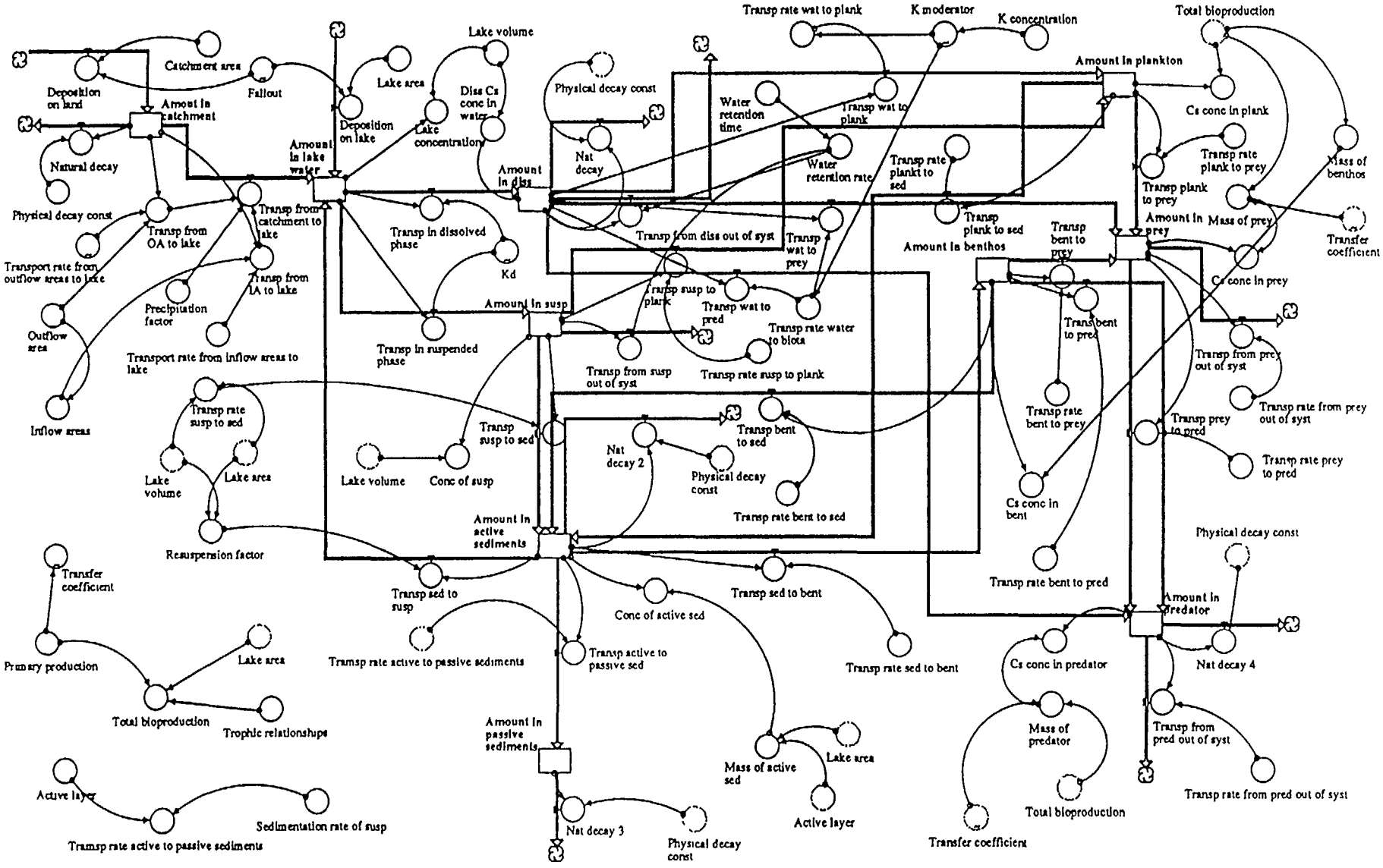

FIG. 4.10. Illustration of the UU-Generic model.

water turnover time the greater the proportion of the initial load that will be retained within the lake. During the spring/early summer of 1986, the radioactive caesium was supplied either bound to aerosols (fine particulate residues from the explosion), in ionic form, or bound to colloids and particles from the catchment areas of the lakes [4.37]. The ability to become bound to particles implies that the retention of caesium-137 in lakes will be relatively large and the turnover time considerably longer than the turnover time of the water; the turnover of caesium-137 in the water masses, however, will be shorter than the turnover of the water itself.

In this model, we assume that also the partition coefficient, K_d, is not a constant, but has a time dependent function.

4.2.5. VTT Energy, Finland

The numerical calculations have been performed employing the computer code DETRA (**D**oses via **E**nvironmental **T**ransfer of **RA**dionuclides) [4.38]. The DETRA code was originally developed by Ilkka Savolainen and Riitta Korhonen from VTT. The present user of the code is Vesa Suolanen, also at VTT.

The DETRA code employs a dynamic compartment approach. The compartment model for the aquatic environment utilized in the present study was created by the user. The theory of the dynamic fish model was, however, developed earlier [4.39].

The computer code DETRA is a generic tool for environmental transfer analysis of radioactive or stable substances. The code has been applied for various purposes, mainly problems related to biospheric transfer of radionuclides both in safety analyses of disposal of nuclear wastes and in consideration of food chain exposure pathways in the analyses of off-site consequences of reactor accidents. For each specific application an individually tailored conceptual model can be developed. The biospheric transfer analyses performed by the code are typically carried out for terrestrial, aquatic and food chains applications.

The accuracy of the model predictions depends on the specific application, but in the type of analyses discussed in this Report, the intended accuracy is roughly within a factor in the of ten, based on the estimation of uncertainty related to the conceptual models and to the input parameters.

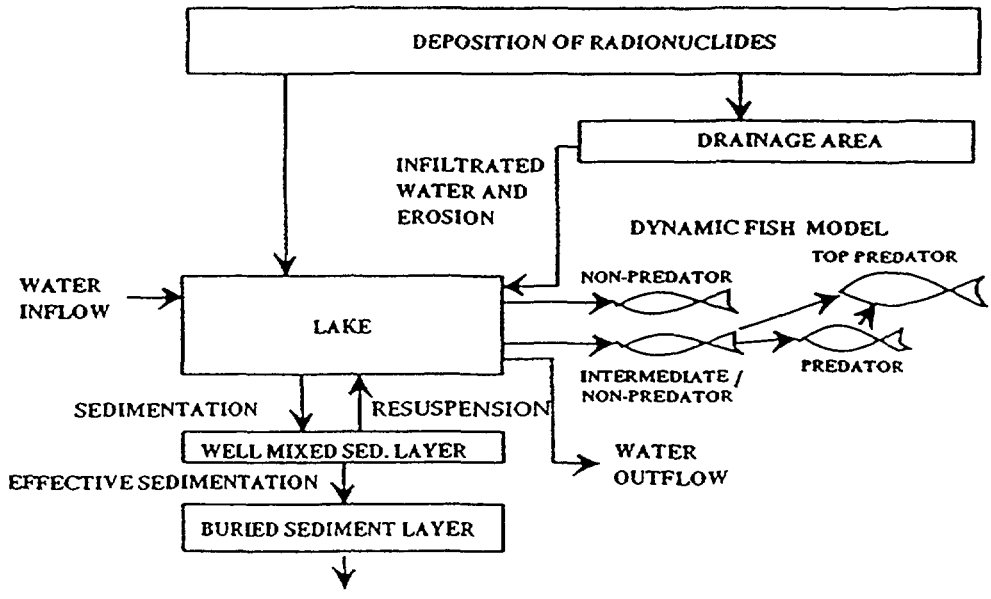

FIG. 4.11. The compartment structure used for the VTT model.

The same type of models as used in this study were employed in the analyses related to the consequences of deposition in aquatic environment caused by the Chernobyl accident. The predictions have been qualitatively consistent with the observations, although some parts of the model may require further development and improvement. Additional detailed data of models of the same type are given in [4.40].

The method of predicting the contamination of freshwater fish is based on utilization of dilution properties of lakes, environmental sorption characteristics and on the dynamic fish model for non-predatory, intermediate and predatory fish types. The compartment structure of the model is presented in Figure 4.11. Methods for calculation of transfer factors between different compartments are presented in Annex AII-5.

The dilution property of a certain lake, that is lake volume multiplied by water exchange rate, is an essential factor when predicting not only the contamination of lake water but also the contamination of various fish types. Additionally, the sorption properties related to the particular aquatic environment under consideration will affect the concentration of radionuclides in fish.

The model accounts for the effects of infiltrated water and erosion from the drainage area. The secondary source term, which is caused by leaching of radionuclides from the drainage area into lake, seems to be more important in long term considerations.

4.3. COMPARISON AND OVERVIEW OF MODEL CHARACTERISTICS

4.3.1. General comparison

The models utilized in the VAMP model comparison excercise vary widely both in nature and size (Table 4.2). Most of them also have their own specific features. In order to compare and evaluate the performance of these different models, it was necessary to take the basic model steps, equations and rates and transform them into a common terminology. Once this had been carried out, it can in fact be seen that the models have many similarities and in many cases there appears to be a common approach to the major problems in modelling the processes of importance in predicting radiocaesium in water and fish.

During the model comparison excercise it became clear that there are many terms for the same process giving rise to considerable confusion. For example, the transfer rate of radiocaesium out of a lake has been expressed by many different terms including elimination rate, outflow flux, outflow rate and retention rate. Another problem term is the transfer rate to the biota. Here there are also many expressions, such as biouptake, bioaccumulation and bioconcentration. All this causes considerable confusion and there is a clear need for a consistent terminology. In the context of this Report the term "transfer rate" is used for all rates and fluxes. Thus, the expressions, transfer rate out of lake, transfer rate catchment to water, transfer rate prey fish to predator and transfer rate water to sediments by scavenging are used in this Report.

4.3.2. Fundamental rates

The ensuing pages provide a breakdown of the definitions of the different transfer equations used in the various models. For any given transfer, some modellers use the equation rate for all lakes modelled, while others may vary this according to lake type, geographical region, fish species, etc.

TABLE 4.2. COMPARATIVE DESCRIPTION OF THE MODELS

MODEL	ENEA	STUDSVIK	KEMA	VTT	UU-emp.	UU-mixed	UU-generic	VAMP LAKE
Institute	ENEA	Studsvik Eco & Safety	KEMA	VTT	.....Uppsala University.....			IAEA
Country	Italy	Sweden	Netherlands	Finland	.....Sweden.....			
Responsible person	L. Monte	U. Bergström	R. Heling	V. Suolanen	.....L. Håkanson.....			L. Håkanson
Size (> 5, 5–15, > 15)	Medium	Medium	Large	Medium	Medium	Small	Large	Medium
Character	Mathematical	Generic probabilistic	Generic deterministic	Generic deterministic	Empirical	Mixed (dynamic & empirical)	Generic (determ-intrinsic & dynamic)	Mixed
Specific features	Sediment interface compartment	Chemical composition of fallout Uncertainty analysis	Food web sediments	Drainage area modelling	Purely empirical	Dim. moderators	K_d = f(time) Transfer rate from catchm. = f(time)	Seasonal moderator
Emphasis of model	Water and predator	Water, fish and sediment	Water, fish sediment	Water, fish sediment	Water and predator	Water and predator	Predator	Water and predator

TRANSFER FROM CATCHMENT TO WATER

MODEL

ENEA:

$$Rate = \frac{\varepsilon \cdot Q}{ADA} f(t)$$

where
ε is the transfer coefficient from the drainage area (m^{-1}),
Q is the tributary discharge (m^3/s),
$f(t) = A_1 e^{-\lambda_1 t} + A_2 e^{-\lambda_2 t}$; λ_1 (5.8×10^{-7} s^{-1}) and λ_2 (2.7×10^{-8} s^{-1}) are the effective decay constants (short and long term components), due to environmental effects, of radionuclide available for migration from catchment to lake; A_1 (0.94) and A_2 (0.06) relative weight of short and long term components, ADA is the area of drainage area (m^2).

KEMA:

If empirical data on Q (discharge in m^3 per time unit) and C (= Cs-conc. in tributary in Bq/m^3) are available then:

$$Transfer\ rate = Q * C\ (Bq/unit\ of\ time)$$

If no empirical data is available, then the transfer of radionuclides from land to the lake water is neglected, under the assumptions that this can be regarded as a secondary load which governs the concentrations of radionuclides in the lake water in the long term.

STUDSVIK:

$$Rate = 0.0001 \cdot D \cdot ADA \cdot f(time) \cdot f(season)$$

$$f(time) = e - \frac{t \cdot ln2}{T_{1/2}}$$

where
D is the fallout (Bq/m^2),
$T_{1/2}$ is the fixation rate, where f(season) = 1 for "lowland" lakes and f(season) = 10 for high altitude Nordic lakes. Default rate (1/month = 0.0001).

UU-mixed:

No rate

UU-generic:

The catchment is first divided into outflow areas (OA; wetland areas with horizontal transport) and inflow areas (IA).
The flux from outflow areas is:
Flux = AOA · 0.01 · Mod · D · ADA

where
AOA is the outflow fraction of drainage area (dim.less),
0.01 is the default rate (1/month),
Mod is the time dependent moderator; dim.less; defined in Appendix II.4,
D is the fallout (Bq/m^2),
ADA is the area of drainage area (m^2).

Flux from inflow areas is given by:

$$Flux = AIA \cdot \frac{0.001}{12} \cdot D \cdot ADA$$

where AIA is the area of inflow areas, fraction of ADA, and rate = 0.001/12 (1/month).

VAMP:

$$Rate = Mod(seas) \cdot \frac{0.04}{12 \cdot \sqrt{time*}}$$

where
Mod(seas) is the seasonal moderator; dim.less defined in Section 5.10,
0.04/12 is the default rate (1/month),
time* is [month of fallout (1 = Jan., 2 = Feb., ... 12 = Dec.) + 1].

DETRA:

$$Rate = \frac{1}{h} \cdot \left(F_s \frac{e}{(1-\epsilon)\cdot\zeta_s} + F_w \cdot \frac{r}{\epsilon}\right)$$

$$F_w = \frac{1}{1 + K_d \cdot SM}$$

$$F_s = 1 - F_w$$

where
F_w is the dissolved fraction of Cs in soil water (dim.less),
F_s is the fraction of Cs in solid material (dim.less),
SM is the concentration of solid material in soil (kg_s/m^3_{tot}),
h is the depth of infiltrated soil layer for precipitation, (m),
r is the rate of average precipitation (m/month),
ϵ is the porosity of soil layer (dim.less),
e is the rate of erosion (erosion from drainage area to lake surface) (kg_s/m^2/month),
ζ_s is the density of solid material in soil (kg_s/m^3_s).

TRANSFER OUT OF LAKE

MODEL

ENEA:

Three compartments: dissolved phase, suspended phase and interface layer:

$$Rate(diss) = \frac{Q(t)}{V}$$

$$Rate(susp) = \frac{Q(t)}{V}$$

$$Rate(interfacelayer) = 0$$

KEMA and STUDSVIK:

If empirical data on Q (i.e. tributary water discharge) are available:

$$Rate = \frac{Q(t)}{V}$$

where V is the lake volume (m^3).

If only site-specific data on theoretical lake water retention time (T=Q/V) are available:

$$Rate = \frac{1}{T}$$

For deep lakes, like Bracciano,

$$Rate = \frac{Q}{V_{epi}}$$

where V_{epi} is the epilimnetic water volume (m^3).

UU-mixed:

$$Rate = \frac{1}{RF \cdot T^{exp}}$$

$$RF \left(\frac{\sqrt{area}}{DM} \right)^2$$

$$\exp = \frac{\frac{30}{T+29} + 0.5}{1.5}$$

where
area is the lake area (m^2),
Dm is the mean depth (m),
RF is the resuspension factor (dim.less),
T is the theoretical lake water retention time (months).

UU-generic:

$$Rate = \frac{0.693}{0.5T}$$

VAMP:

$$Rate = \frac{Mod(seas)}{T^{exp}}$$

$$\exp = \frac{\frac{30}{T+29} + 0.5}{1.5}$$

where Mod(seas) is the seasonal moderator; dim.less, see Section 5.10 for definition.

DETRA:

$$Rate = \frac{Q(t)}{V}$$

where
Q(t) is the water flow rate of lake (m^3/month),
V is the lake volume (m^3).

V means effective (V_{eff}) mixing volume of lake. Therefore, for deep lakes $V_{eff} < V_{real}$, because typically only the upper part of lake volume effectively takes part in water exchange (i.e. dilution).

TRANSFER FROM WATER TO PLANKTON

MODEL

ENEA:

See transfer to predator

KEMA:

$$C_{phyto} = CF_{phyto} \cdot C_W \cdot F_W$$

where
C_w is the ^{137}Cs concentration in water (Bq/m^3),
F_w is the dissolved fraction (dim.less).

$$CF_{phyto} = f(K^+) = [\exp(a \ln(M_k) + b/T)]^{-1}$$

where
T is the lake water temperature in Kelvin, degrees,
a,b are the constants,
M_k is the potassium molarity (mmol/l).

STUDSVIK:

$$Rate = \frac{\ln 2}{T_{1/2}} \cdot CF \cdot \frac{M(plank)}{M(water)}$$

where
$T_{1/2}$ is the fixation rate,
CF is the concentration factor water to plankton,
CF = const × Mod,
const is 3000, empirical constant, (L/kg dw),
Mod = $Mod_{lake\ type} \cdot Mod_k/Mod_{season}$ is moderator (dim.less),

Mod_{season}	$Mod_{lake\ type}$	Mod_k
Summer 1	Oligorophic 3	K ≤ mg/l 2
Winter 5	Mesotrophic 2	K ≥ mg/l 1
	Eutrophic 1	

M(plank) is the biomass of plankton (kg dw),
M(water) is the lake volume (L)

UU-mixed:

Note that this biouptake encompasses water to prey (including phytoplankton and zooplankton and small fish)
Biouptake = CF × Mod_{CaMg}
where
CF is the concentration factor (dim.less); default value = 150,
Mod_{CaMg} is the moderator; dim.less; for the influence of water hardness on this rate defined by a graph.

UU-generic:

$Rate_{diss}$ = 0.002/K moderator
This is the biouptake rate (1/month) of Cs from dissolved phase to plankton (both phyto- and zoo-plankton)
$Rate_{part}$ = 0.001
This is the biouptake rate (1/month) of Cs from particulate phase to plankton (both phyto- and zoo-plankton)

VAMP:

$Rate_{diss} = 0.01 \times Mod_{(K + pH)}$
where
0.01 is the rate (l/month) for Cs biouptake from dissolved phase to phytoplankton,
$Mod_{(K + pH)}$ is the moderator regulating this uptake based on K-conc. and lake pH (dim.less), given by:

$$Mod_{(K+pH)} = \frac{2}{[(K+pH) - 3]^2 + 0.01}$$

DETRA:

$$Rate = P_d \cdot PM \cdot P_w$$

$$P_w = \frac{1}{1 + P_d \cdot PM} \quad ,$$

where
P_d is the distribution coefficient to plankton $(Bq/kg_{PL})/(Bq/m^3_{water})$,
PM is the concentration of plankton in water (kg_{PL}/m^3_{water}),
P_w is the dissolved fraction of Cs in plankton (dim.less).

TRANSFER TO PREDATOR

MODEL

ENEA:

$$Rate = \frac{Kfk}{C_k} \cdot \frac{(\lambda_{cs} + \lambda_b) \cdot M\ (pred)}{v}$$

where
KfK = CF × C_k
where
KfK is the proportionality constant 8×10^{-3} (dim. less),
CF is the concentration factor (conc. in predator conc. in water at equilibrium (Bq/kg × m^3/Bq)),
C_k is the concentration of K in lake (kg/m^3),
λ_{cs} is the radioactive decay rate, 1.9×10^{-3}/month for caesium-137,
λ_b is the elimination rate for predator, 0.054,
M(pred) is the predator biomass (kg),
V is the lake volume (m^3).

KEMA:

$$Rate = (K_{resp} + K_{growth}) \cdot Ex^1 \cdot Mod^1 + K_{wat} \cdot Ex^2 \cdot Mod^2$$

where
K_{resp} is the biouptake rate of respiration, 0.005 (l/day),
K_{growth} is the biouptake rate of growth, 0.0005 (l/day),
K_{wat} is the biouptake rate from water, 0.075 (m^3/kg·l/day),
Ex^1 is the extraction of Cs from food, 0.7 (dim.less),
Ex^2 is the extraction of Cs from water, 0.001 (dim.less),
Mod^1 is the moderator = f(K, species) (dim.less) accordingly:

Large pike	Mod^1	=	1
Large perch	Mod^1	=	1/0.7

Mod^2 is the moderator = f(k); dim.less; accordingly:

Brown trout			
K < 0.5 mg/l	Mod^2	=	300
K > 0.5 mg/l	Mod^2	=	1

STUDSVIK:

$$Rate = UF \cdot MC \cdot \frac{M(pred)}{M(prey)}$$

where
UF is the uptake fraction, 0.7 (dim.less),
MC is the mass consumption (kg/month/kg fish),
M(pred) is the biomass of predator (kg ww),
M(prey) is the biomass of prey (kg ww),
MC = f(temp), accordingly:
f(temp) = 0.1 for winter and 0.6 for summer

UU-mixed:

Rate = 0.01, prey to predator (l/month)

UU-generic:

Rate = 0.02, benthos to predator (l/month)
Rate = 0.01, prey to predator (l/month)

VAMP:

Rate = 0.2/12, prey to predator (l/month)

DETRA:

$$Rate = \frac{m_{pf,pr}}{m_{pf}}$$

where
$m_{pf,pr}$ is the mass of prey fish eaten by the assumed predatory population in the lake considered (kg/month),
m_{pf} is the mass of the assumed prey fish population in the lake considered (kg).

TRANSFER FROM WATER TO SEDIMENTS OR SCAVENGING RATE FOR CAESIUM

MODEL

ENEA:

$$Rate = \frac{v}{Dm \cdot SM}$$

Rate for the particulate phase of Cs, where
v is the mass (net) sedimentation rate ($kg \cdot m^{-2} \cdot day^{-1}$),
Dm is the mean depth,
SM is the concentration of suspended matter (kg/m^3).

Note that the ENEA model also accounts for advective and diffusive transport from sediments to water.

KEMA:

This rate applies to total-Cs in lake water (i.e. dissolved + particulate)

$$Rate = \frac{v \cdot K_d \cdot F_w}{Dm}$$

where
v is the mass sedimentation rate ($kg \cdot m^{-2} \cdot month^{-1}$),
K_d is the distribution coefficient (m^3/kg),
Dm is the mean depth (m),
F_w is the dissolved fraction of Cs in lake water (dim.less).

$$F_w = \frac{1}{1 + K_d \cdot SM}$$

where
SM is the concentration of suspended matter (kg/m^3).

Note that the KEMA model also accounts for advective and diffusive processes in both directions for water and sediment.

STUDSVIK:

Rate = Rate × Mod + Rate (1 – Mod)
Rate is defined as in the KEMA model
Mod is the moderator accounting for distance from Chernobyl (dim.less)

Scandinavia	UK and The Netherlands	Italy
Mod = 0.25	Mod = 0.5	Mod = 1.0

UU-mixed:

No rate used.

UU-generic:

Flux = Rate × Amount in suspended phase × Resuspension factor
Rate = 0.01 (l/month)

$$Resuspension\ factor = \left(\frac{\sqrt{Area}}{Dm}\right)^{0.5}$$

where
Dm is the mean depth (m),
Area is the lake area (m^2).

VAMP:

Rate = 1/Dm
where
Dm is the mean depth (m),
1 is the settling velocity (m/month).

DETRA:

$$Rate = \frac{v \cdot K_d \cdot F_w}{D_m}$$

where
v is the mass sedimentation rate ($kg \cdot m^{-2} \cdot month^{-1}$),
K_d is the distribution coefficient (m^3/kg),
D_m is the mean depth of lake (m),
F_w is the dissolved fraction of Cs in lake water (dim.less).

$$F_w = \frac{1}{1 + K_d \cdot SM}$$

where
SM is the concentration of suspended matter (kg/m^3).

TRANSFER FROM SEDIMENT TO BENTHOS

MODEL

ENEA:

No compartment for benthos.

KEMA:

Benthos is assumed to consume phyto- and zooplankton which are deposited on the sediments, and is therefore modelled as a predator for these species. The transfer from sediment particles to benthos is assumed to be negligible as a result of the strong adsorption of radiocaesium to particles.

STUDSVIK:

$$Rate = \frac{ln2}{T_{1/2}} \cdot CF \cdot \frac{M(benthos)}{M(sed)}$$

where
$T_{1/2}$ is the biological turnover time; months,
CF is the concentration factor, where
CF is the $0.1 \times Mod_K \times Mod_{lake\ type}$,
0.1 is the empirical constant,
Mod_K is the moderator for the influence of K-conc. on this rate; dimensionless,
$Mod_{laketyp}$ is the moderator to illustrate that this rate attains different values in different lake types.
Note that Mod_k and $Mod_{laketype}$ are the same as for the biouptake rate water to plankton.
$M_{(benthos)}$ is the biomass of benthos (kg ww),
$M_{(sed)}$ is the mass of active sediment (kg ww),
Note that the ratio M(benthos)/M(sed) is small, about 0.01.

UU-mixed:

No compartment for benthos.

UU-generic:

Rate = 0.00001 (l/month)
Note that in this model there is also a return flux of Cs from benthos to sediment.

VAMP:

Note that in this model, benthos is included in the compartment called prey.
Rate = $0.0002 \cdot DR^{0.5}$ (l/month)

$$DR\ (dynamic\ ratio) = \frac{\sqrt{Area}}{Dm}$$

DETRA: No compartment for benthos.

5. RESULTS AND DISCUSSION

The results from the Lakes Subgroup are presented in several ways, both as specific model predictions in comparison with empirical data and in terms of overall principles that may be applicable to radionuclide modelling in general. During the course of the VAMP exercise a number of new techniques have been developed as well as a completely new model, the VAMP LAKE model. These are described together with a number of general topics such as model size, dietary shift, lake ice cover and half-lives. Such aspects are of significance either in model optimization or in accurately predicting radiocaesium contamination levels in lake water and fish, and thus of major importance in prediction of dose to man.

5.1. SENSITIVITY ANALYSES

Sensitivity analysis is an important element in any model validation exercise. It not only indicates the sensitivity of individual models to changes in the values of the model parameters, but also provides valuable information on the major processes influencing radionuclide transport, dispersal and biouptake in natural ecosystems. Sensitivity analyses have been carried out for most models used in the VAMP Lakes Subgroup.

In general a local sensitivity analysis identifies the parameters for which the model predictions are the most sensitive through the performance of several model runs in which one of the parameters are changed, while the other parameters retain their default values. When the most sensitive parameters are identified, two main possible actions may then be considered. The first step is to find field measurements data to decrease the uncertainty range of the parameter. The alternative is to replace this parameter by a sub-model, without increasing the uncertainty by the introduction of new variables with their associated uncertainties.

Two types of driving parameters can be distinguished, site-specific or environmental parameters, and model-specific parameters. Site-specific parameters are parameters, like the lake depth and catchment area, which are easily available, while model-specific parameters are parameters which cannot easily be obtained from field or laboratory data, and have to be assessed on the basis of generic literature values, or in the case of incomplete information, on the basis of expert judgement. This generally implies that the predictive power of a model will be greater when the number of site-specific parameters is relatively high in comparison with the number of model-specific parameters.

5.1.1. The ENEA model

Extensive sensitivity analyses of a model output are based on the evaluations of a large number of functions (variation of the time dependent model output with respect to each parameter). To avoid the presentation of an enormous amount of data a compromise was adopted. In Table 5.1, the approximate ranges of the ratio "variation of the output variables/variation of the parameter" are reported. For instance, a value of 10/100 means that if the parameter varies by a factor 100, the output varies within a factor of 10 (around the average value). In the table, the range of the ratio is indicated by a capital letter ($1/100 < L < 5/100$; $5/100 < M < 10/100$; $10/100 < H < 20/100$). The ratios are evaluated at two different points in time: time = 30, corresponding to 30 days after the deposition pulse and time = 1000, corresponding to 1000 days after deposition. Of course, the sensitivity of the model output with respect to a specific parameter may vary with time. The sensitivity analysis was carried out with respect to the following parameters: K_d, K_{alb}, K_{bal}, K_{sd}, D_{al} d_{al} and D_{bs} (see Table II.1 of Appendix II for a complete list of symbols). The evaluation of the sensitivity of the output was not carried out for site-specific parameters (water volume, water surface, lake depth, suspended matter, etc.). The model output is of course linear with respect to D (the deposition on the lake), $D\varepsilon A_1$ and $D\varepsilon A_2$ (the deposition on the catchment multiplied by the transfer factor catchment $\rightarrow$ lake and by the relative weighting of the fast and slow components of transfer function catchment $\rightarrow$ lake).

TABLE 5.1. RANGES IN THE SENSITIVITY OF MODEL PARAMETERS IN THE ENEA MODEL AND THE RATIO BETWEEN THE VARIATION OF THE OUTPUT AND THE VARIATION IN THE MODEL PARAMETER (see text for further explanation)

Parameter	Concentration in water Time = 30 days		Concentration in water Time = 1000 days		Deposition Time = 1000 days	
K_d	H[a]	≈ 20/100	L	≈ 4/100	M	≈ 8/100
K_{alb}	L[b]	≈ 1/100	L	≈ 4/100	L	≈ 2/100
K_{bal}	L	≈ 1/100	H	≈12/100	L	≈ 2/100
K_{sd}	L	≈ 1/100	M[c]	≈10/100	L	≈ 2/100
D_{al} d_{al}	H	≈ 10/100	L	≈ 3/100	L	≈ 2/100
D_{bs}	L	≈ 1/100	L	≈ 1/100	L	≈ 1/100

[a] 10/100 < H < 20/100
[b] 1/100 < L < 5/100
[c] 5/100 < M < 10/100

5.1.2. The KEMA model

On the basis of sensitivity analyses, some new su-models have been incorporated into the lake model LAKECO to estimate important parameters. For the prediction of the caesium concentration in fish, these important parameters were the distribution coefficient of the water column (K_d), the concentration factor phytoplankton-water (CF) and to a lesser extent, the biological half-life of the fish species and the sediment reworking rate (R_w). For the calculation of the concentration of caesium in the sediments, the size of the accumulation area is of great importance. The newly implemented sub-models estimate values for these parameters based on measurable parameters such as the potassium content of the water, lake water temperature and lake morphometry. Through this procedure the number of model-specific parameters has been reduced significantly. The remaining model-specific parameters are of minor importance, and therefore their assessment by means of new sub-models is unnecessary.

The predictions for the various lake ecosystems, presented in this Report (see Section 5.2.2), have been performed with an enhanced version of LAKECO, called LAKECO-B, in which these sub-models have been incorporated.

Three examples of sensitivity analysis are presented in Figure 5.1. Figures 5.1A1–5.1A3 present the sensitivity of the radiocaesium levels in the top predator perch for the biological half-life in the perch, for the concentration factor CF and for the distribution coefficient K_d in Devoke Water, while Figures 5.1B1–5.1B3 present the sensitivity of this species to these parameters in Hillesjön. These two lakes are selected because they have different trophic status — Devoke Water is oligotrophic, while Hillesjön is mesotrophic.

Figure 5.1B3 demonstrates that a variation in the K_d between 2 and 0.01 times the default value (28.8–0.14 m^3/kg), which results in a significant change in the perch peak. This can be explained by the fact that the dissolved fraction of caesium increases if the K_d decreases, which results in a longer retention time in the water column, since the scavenging from the water column has a minor effect when less of the caesium is attached to particles. The dissolved fraction is a crucial parameter, controlling the relative significance of all processes which occur in the dissolved phase such as diffusion compared to the processes which are controlled by the behaviour in the particulate phase, like scavenging, particle reworking and the burial of particles to deeper sediment layers. In the case of a higher dissolved fraction, the uptake by phytoplankton also increases due to enhanced bioavailibility.

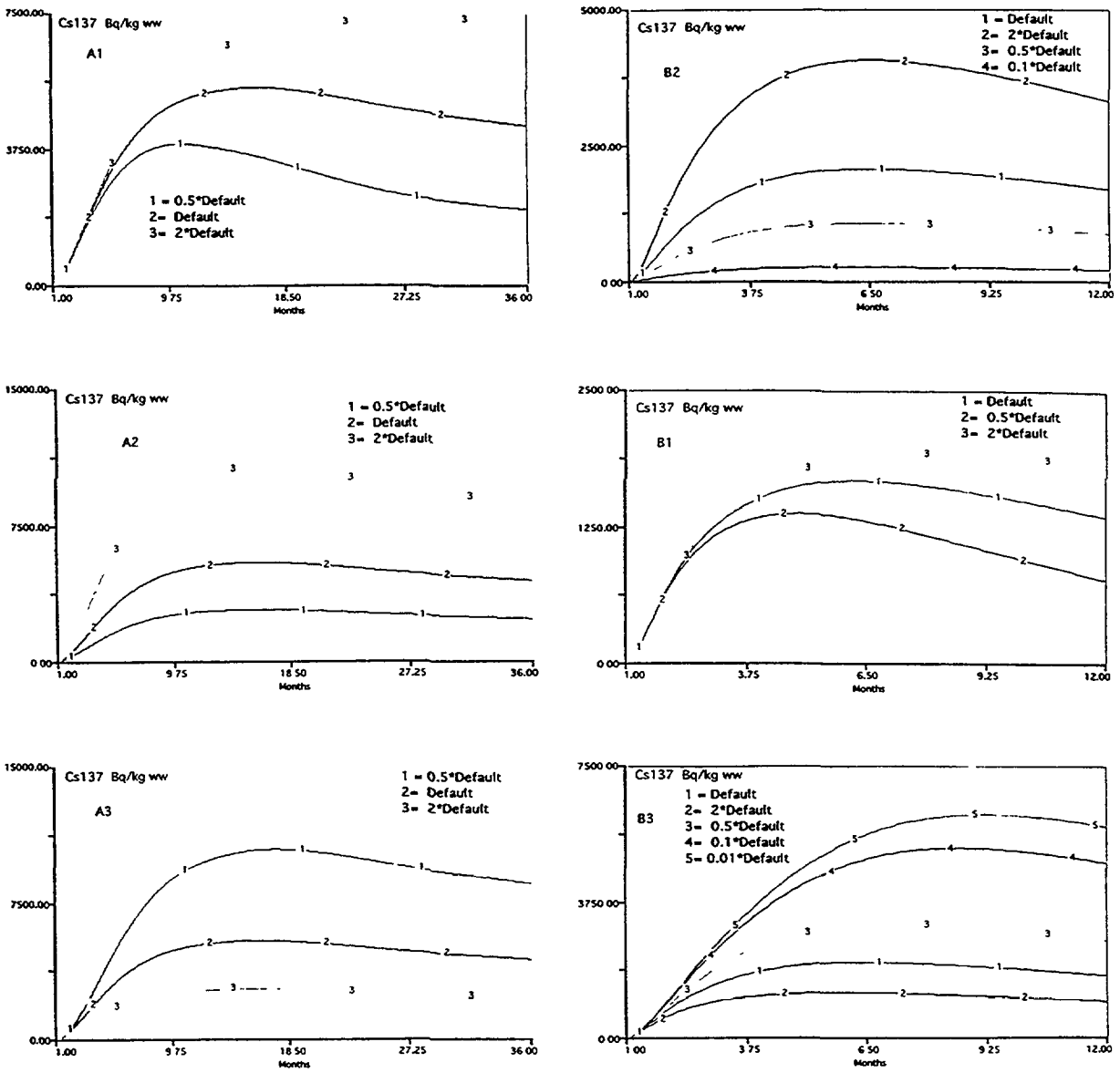

FIG. 5.1. Sensitivity of the modelled ^{137}Cs concentration in large perch in Devoke Water (A) and Hillesjön (B) to the biological half-life (1), the concentration factor phytoplankton-water (2) and the distribution coefficient K_d in the water (3). Default values are: biological half-life 289 days (Devoke) and 356 days (Hillesjön); concentration factor and 1150 (Devoke) and 470 L/kg (Hillesjön) distribution coefficient 53.7 (Devoke) and 14.4 m^3/kg (Hillesjön).

As a consequence the transfer throughout the food chain increases. The CF for phytoplankton-water governs the uptake of radionuclides from the water to phytoplankton, through which radiocaesium is transferred to higher trophic levels. The significance of this CF is demonstrated in Figures 5.1A2 and 5.1B2.

The biological half-life is also important. In the literature it has been shown (see Section 5.5) that the biological half-life is dependent on lake temperature, on the fish species and its body weight. Since the biological half-life controls the elimination rate of caesium in aquatic organisms, changing this value affects both the peak level and the shape of the tail. Figures 5.1A1 and 5.1B1 clearly demonstrate this strong effect on the tail shape.

Another very important parameter is the residence time of the lake water. However, this parameter is site-specific, and can be derived from tributary discharge.

The sediment reworking rate, R_w, is a sensitive model parameter, but less sensitive than the above mentioned parameters. It describes the rate of sediment mixing by bioturbation and wind induced waves, causing the enhanced transfer of particles through the sediment-water interface. In LAKECO-B this parameter is also assessed by a sub-model, in which the lake morphology governs the extent to which particles are transferred through the water sediment interface. Although this parameter is not extremely important, it needs to be predicted from a sub-model in order to obtain a more flexible model which can be applied to lakes with different morphometry.

Furthermore, the fraction of small particles in the mixed sediment layer influences the shape of the recovery curve and the timing of the peak concentration in adult perch. These particles govern the overall K_d of the sediments. At present this parameter is based on an estimated value of some 10% fine particles. This cannot be verified, so a new sub-model has to be constructed to estimate the K_d of the sediments.

The percentage of the lake bottom which acts as an accumulation area for fine materials suspended in the water is of importance for the calculation of the concentration activity in the sediments. On the basis of a newly implemented sub-model the accumulation area has been estimated. However, this sub-model is only important in cases where the activity concentration in the sediments is required. Due to the very large variation in the radionuclide concentration in the sediments, the sediment sub-model of LAKECO could not be properly validated.

Modifications of the LAKECO model on the basis of the sensitivity analysis

The validations and sensitivity tests within the framework of the VAMP project have lead to modifications of some of the processes in the LAKECO model, giving a more appropriate tool which can be applied to other lake ecosystems for which no detailed information is available. Parameters such as K_d and CF can be substituted by sub-models in which these parameters are related to site-specific environmental parameters like the potassium concentration. The uncertainty of the K_d and the CF value is then substituted by the uncertainty in the potassium concentration in the lake water. However, this value is relatively easy to determine compared with the determination of K_d and CF in the field. The model-specific parameter R_w (sediment reworking rate) is fixed at a default value for lake ecosystems, but modified by the so called dynamic ratio (DR). This value relates the surface of the lake to the mean depth of the lake, and expresses the extent of the lake bottom which is influenced by wind-induced waves. The biological half-life (BHL), another important parameter, controls both the peak level in the organism and the shape of the tail of the curve. This value can be expressed by an empirical relationship based on a set of literature values, in which the BHL is a function of the body weight of the fish, in combination with a temperature dependency (see Section 5.5). These sub-models are briefly described below.

The K_d sub-model

A partition coefficient can be based on soil properties, like the grain size distribution, the capability of the soil to exchange cations (CEC), and the concentration of competitive ions like potassium and ammonium, which are in some cases known parameters [5.1]. A first attempt to obtain a lake partition coefficient, K_d, is the empirical derived relationship between the CEC, potassium, and ammonium concentration on the one hand and the K_d on the other:

$$K_d = \frac{1.5}{[K^+]/39.1 + 5[NH_4^+]/18} \qquad (5.1)$$

where
K_d is the lake distribution coefficient for suspended matter (m^3/kg),
$[K^+]$ is the concentration of potassium ions (mg/L) in the lake water,
NH_4^+ is the concentration of ammonium ions (mg/L) in the lake water.

The equation is based on the measurement of a large number of soils and sediments ranging from very poor sandy soils with a low CEC to soils with a high clay content and consequently a high CEC. It does, however, introduce a new uncertainty, the ammonium content, and in the model calculations it has been assumed that the levels in lake waters are low: 0.1 mg/L in eutrophic lakes and 0.05 mg/L in oligotrophic lakes.

These sub-models have been incorporated into the LAKECO model and gave good agreement between observed data and predicted levels of the caesium in lake waters and top predator (see Section 5.2.2).

The CF sub-model

The CF sub-model supplies an estimate of the concentration factor water-phytoplankton based on the temperature of the lake water and potassium concentration of the water. Equation (5.2) is derived from the Nernst electrochemical equation. The coefficients in the equation are based on measurements on the changing electropotential in varying potassium conditions over the cell membranes of a floating macrophyte *Riccia* [5.2]. By means of several equations based on these measurements, an equation relating the potassium level in the aquatic environment and the caesium uptake of the cell can be derived:

$$CF = \frac{1}{EXP\ (0.73\ \ln\ (K^{+}/39.1) \times \frac{1.22 \times 10^{3}}{(\ T + 273\ )})} \qquad (5.2)$$

where
CF is the concentration factor phytoplankton-water (L/kg),
T is the temperature of the lake water (°C,
K^{+} is the potassium concentration of the lake water (mg/L).

This sub-model is also applied to the lakes of the VAMP study. The combination of this sub-model and the K_d sub-model was tested. In Table 5.2 the values for the K_d and CF calculated by means of these sub-models are presented for the lakes in the VAMP project.

TABLE 5.2. THE APPLICATION OF THE K_d AND CF SUB-MODEL TO A NUMBER OF EUROPEAN LAKE ECOSYSTEMS

Lake	Lake temperature (°C)	K^{+} (mg/L)	CF (L/kg)	K_d (m^3/kg)	Trophic status
Iso Valkjärvi	11	0.4	2100	62	Oligotrophic
Bracciano	23	40	61	1.4	Oligotrophic
Øvre Heimdalsvatn	7	0.4	2200	62	Oligotrophic
Hillesjön	12	3	470	14	Eutrophic
Devoke Water	15	0.55	1600	54	Oligotrophic
Esthwaite Water	15	0.9	1100	30	Eutrophic
IJsselmeer	11	7	260	7.3	Eutrophic

In Figure 5.2 (A = Devoke Water, B = Hillesjön) the sensitivity of the radiocaesium levels in adult perch to the potassium level is presented. In natural conditions, potassium levels range between 0.1 in oligotrophic situations up to 20 mg/l in eutrophic situations. This graph shows a relatively

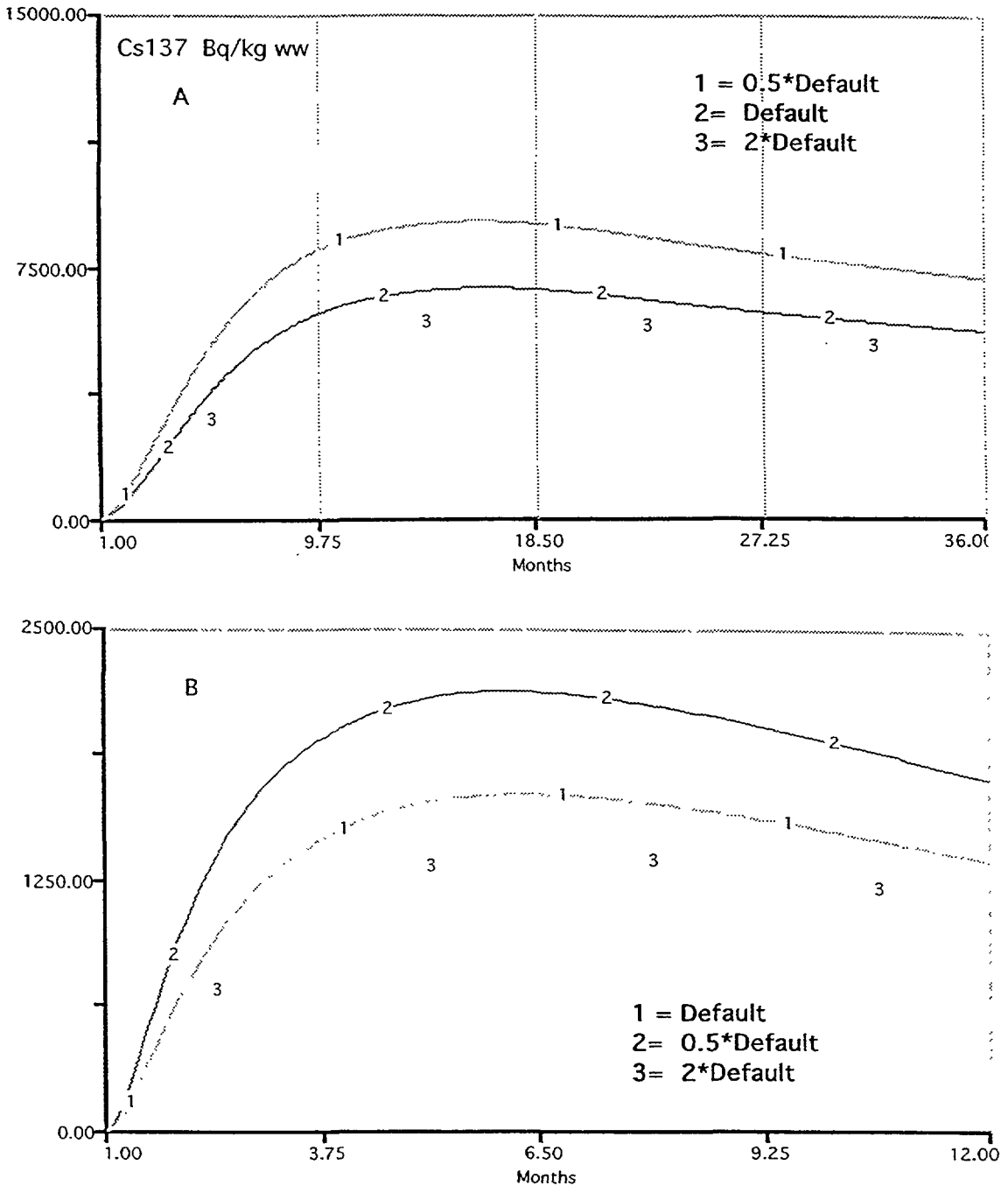

FIG. 5.2. The sensitivity of the ^{137}Cs concentration in large perch for the potassium concentration in lake water, after the implementation of the K_d and the CF sub-models. A, Devoke Water; B, Hillesjön.

narrow uncertainty range for the caesium concentration in large perch in comparison with the ranges as shown in Figure 5.1.

The dynamic ratio as a moderator for the sediment mixing rate

Resuspension and remobilisation by wind-induced waves play an important role in the behaviour of radionuclides in lake ecosystems. Resuspension causes an ongoing release of radionuclides from the bottom sediments to the water column. Such effects will be greater in shallow lakes, where sediment mixing and resuspension is caused by wind-induced waves. Håkanson and Jansson [5.3] proposed a method to link bottom dynamics with the shape of the lake by introducing the so-called

dynamic ratio (DR). This is the square root of the lake area divided by the mean depth, and is a measure of the bottom sediments dynamics, low values indicating a relatively low effect of wind on lake bottom dynamics and vice versa. Based on this principle, it was derived [5.3], by means of empirical data of nine Swedish lakes, the following expression for the determination of the accumulation area (A_a) , and the transportation and erosion area (A_{e+t}):

$$A_{e+t}=100-A_a=25\ DR\ 41^{\frac{0.061}{DR}} \tag{5.3}$$

The accumulation area is dominated by fine particles, while in the erosion area coarse particles are present, and no net accumulation occurs. For radionuclides, the fine particles play a dominant role, since caesium is attached to these fine particles. For the lake ecosystem model LAKECO, the accumulation area plays a major role in the sediment water transfer. This calculated value is used to estimate the size of the accumulation area, which is important in the calculation of the ^{137}Cs concentration in the sediments. This expression is valid for lakes with a surface area between the 1.9 and 3583 km^2. However, in this Study it is also applied to lakes with a smaller surface area under the assumption that such an extrapolation is acceptable.

TABLE 5.3. BATHYMETRIC INFORMATION AND SEDIMENT DYNAMICS FOR VAMP LAKES

Lake	Mean depth (m)	Area (km^2)	DR[a]	A_a[b] (%)	R_w[c]	Class[d]
Iso Valkjärvi	3	0.042	0.07	55	7×10^{-6}	A
Bracciano	89	57	0.08	66	8×10^{-6}	A
Øvre Heimdalsvatn	4.7	0.78	0.19	84	2×10^{-6}	B
Hillesjön	1.7	1.6	0.7	76	7×10^{-5}	B
Devoke Water	4	0.34	0.15	83	2×10^{-6}	B
Esthwaite Water	6.4	1.0	0.16	83	2×10^{-6}	B
IJsselmeer	4.3	1147	7.9	0	8×10^{-4}	E

[a] DR is the dynamic ratio;
[b] A_a is calculated percentage area of accumulation;
[c] R_w is the modified sediment reworking rate;
[d] Classification in accordance with Håkanson and Jansson [5.3].

The DR is useful as a moderator of the sediment reworking rate R_w. Instead of using a literature value for this rate, a generic value can be modified with this moderator. This value ranges between 9×10^{-5} and 9×10^{-4} m/d for freshwater lakes [5.4]. For very shallow lakes this value can be a factor of ten higher. Considering the fact that the DR value ranges between the 0.1 and 7.9 [5.3], combined with the experience gained within the VAMP project, the following expression for the R_w has been chosen:

$$R_w=10^{-4}*DR \tag{5.4}$$

In Table 5.3 the calculated values for the modified sediment reworking rate and the size of accumulation area for the lakes of the VAMP project are presented. According to the empirical equation, IJsselmeer has no accumulation area, but the estimated percentage of the lake bottom, which acts as a sedimentation area, is close to 10%.

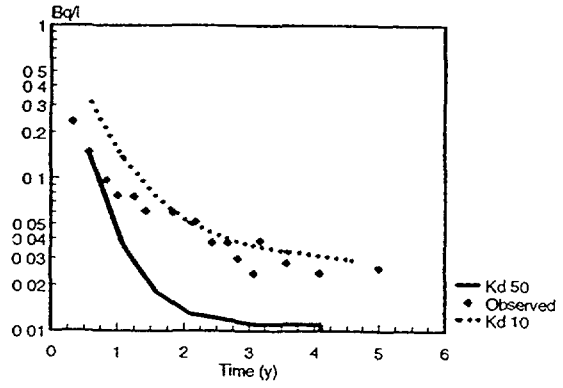

FIG. 5.3. Concentrations of ^{137}Cs in water for Devoke Water with K_d 10 and 50 m^3/kg, respectively.

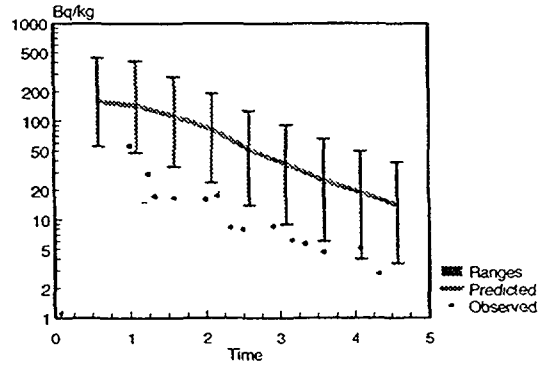

FIG. 5.4. Initial predictions for perch in IJsselmeer.

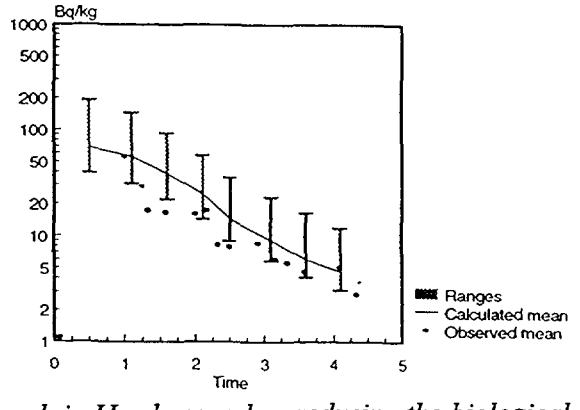

FIG. 5.5. Predictions for perch in IJsselmeer when reducing the biological half-life by a factor of two.

The results of the global (ranked) sensitivity analysis are given in Section 5.3.3 together with the uncertainty analyses of the KEMA model, LAKECO.

5.1.3. The Studsvik model

A sensitivity analysis was carried out using the Studsvik model by changing parameter values systematically by a factor of five up and down. The variation in sensitivity is dependent upon time as various processes act differently on the distribution of ^{137} Cs as a function of time. The water retention time was not varied since it is a site-specific parameter. However, it is clear that it is an important factor in addition to the actual deposition. Both these factors are directly related to the concentrations.

In the expression used for obtaining the sedimentation rate, the K_d value may be important. After the first two months following deposition, the concentration of ^{137}Cs in water is greatly influenced by the K_d values, especially if it is increased by a factor of five. A fivefold increase in leakage rate from the drainage area also influences the concentration in water to an increasing degree, as does the resuspension rate from the sediments. The model is, however, not sensitive to the concentrations of suspended matter in the lake. One example of changing the K_d value by a factor of five is given for Devoke Water (Figure 5.3). As can be seen from the figure, the predictive accuracy increases substantially when a K_d value of 10 m^3/kg is used, as compared to the K_d of 50.

Concerning fish, the results for perch are also sensitive to the K_d values, the leakage rate from the drainage area and resuspension from the sediments. However, these predictions are even more sensitive to the value used for the bioaccumulation factor for plankton as it is a direct multiplier in the model for the rate describing the uptake to fish. This value was also changed by a factor of five up and down. However, the uptake fraction was even more sensitive, as according to the structure of the model it will be multiplied. The extreme case of lowering it by a factor of five reduces the concentrations in perch by a factor of 15. In the model this could also reflect lower consumption values for the fish, which is important for the build up of ^{137}Cs [5.5]. The importance of the biological half-life in fish was studied in the same manner. It had considerable importance. One typical example is shown for perch in IJsselmeer, where the initial overestimation is substantially reduced by lowering the biological half-life (Figures 5.4 and 5.5).

According to these sensitivity analyses the predictions for perch are very sensitive to the intake of ^{137}Cs, bioaccumulation factors and fish metabolism described by the biological half-life. However, it should be pointed out that the values used in these sensitivity analyses were in many cases extreme.

5.1.4. The UU-mixed model

Many sensitivity analyses are presented in this Section and in other parts of this Report (e.g. in Section 5.10.9). The UU-Generic model will not be dealt with here. This model has many features in common with the STUDSVIK model and the VAMP LAKE model. Instead, the results of sensitivity analyses for the UU-Mixed model are given.

The UU-Mixed model is a very small model based on a mixture of dynamic and empirical concepts. It has very high predictive power (see Section 5.8.5). Selected sensitivity analyses using data from Øvre Heimdalsvatn are presented. All these sensitivity analyses have been done in a similar way. Each model variable has been altered by a factor of 1.25 (i.e. a 25% change from the default value), then by 1.5, 2 and a factor of 4. Thus each graph presents five curves, where curve one represents the default values (see Section 4.2.4.2).

Figure 5.6.A shows that the UU-Mixed model is very sensitive to changes in the values of the "ecological half-life" for prediction of radiocaesium in predatory fish: the shorter the ecological half-life, the faster the recovery. This is quite logical, but the characteristics of the "tail" are different for different models: small models generally use high values for the "ecological half-life" in a given fish species (like six years for pike and three years for trout). Larger models that account for many lake processes will apply lower values of this rate, since this value includes many processes regulating the actual value of the rate.

Figure 5.6.B gives five curves for different bioconcentration factors. The default value is given by 150 × K moderator. The lower the bioconcentration factor, the lower the Cs concentration in fish, such as seen in trout in Øvre Heimdalsvatn.

Figure 5.6.C gives similar curves for different values of the transport (or transfer) rate of radiocaesium from prey to predator. The default value of this rate is 1 in the UU-Mixed model. From this graph, we can note that the model is not very sensitive to the choice of this value. From Figure 5.6.D, we can also note that the model is also not sensitive to the value used for the "ecological

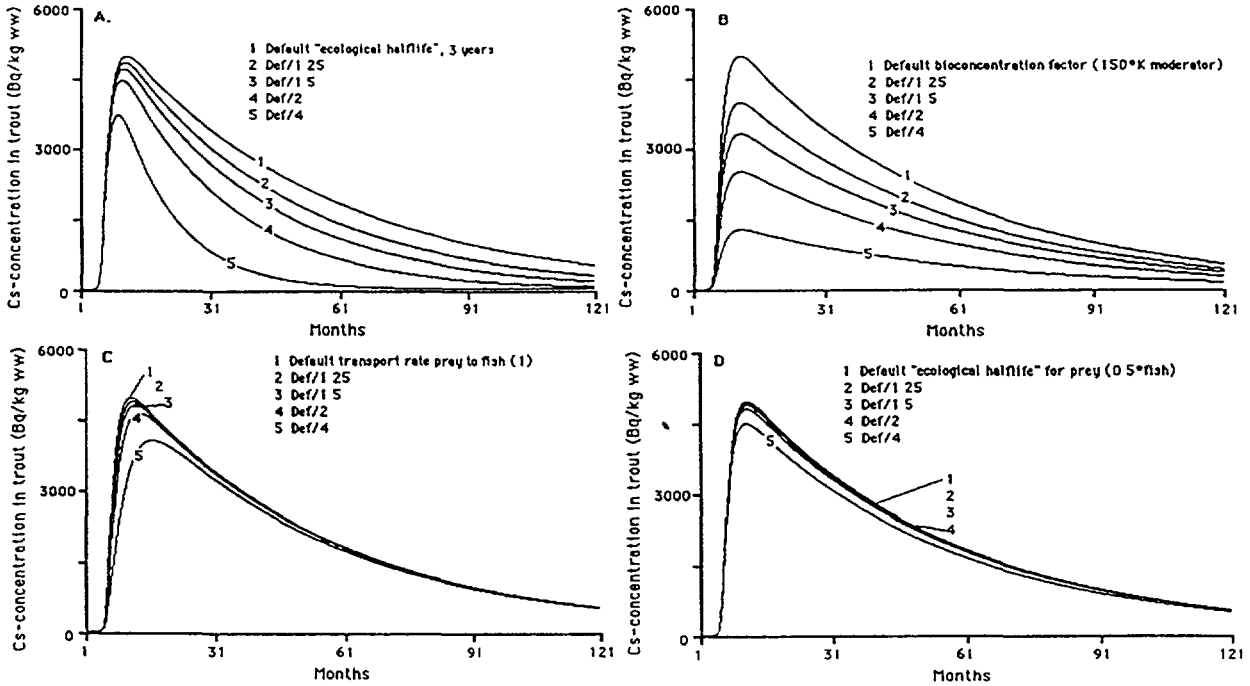

FIG. 5.6. Sensitivity analyses for important model variables in the UU-Mixed model using data for Øvre Heimdalsvatn to predict ^{137}Cs concentration in trout

A. Different "ecological half-life" for fish.
B. Different bioconcentration factors.
C. Different values for the transport rate of radiocaesium from prey to fish.
D. Different "ecological half-life" for prey.

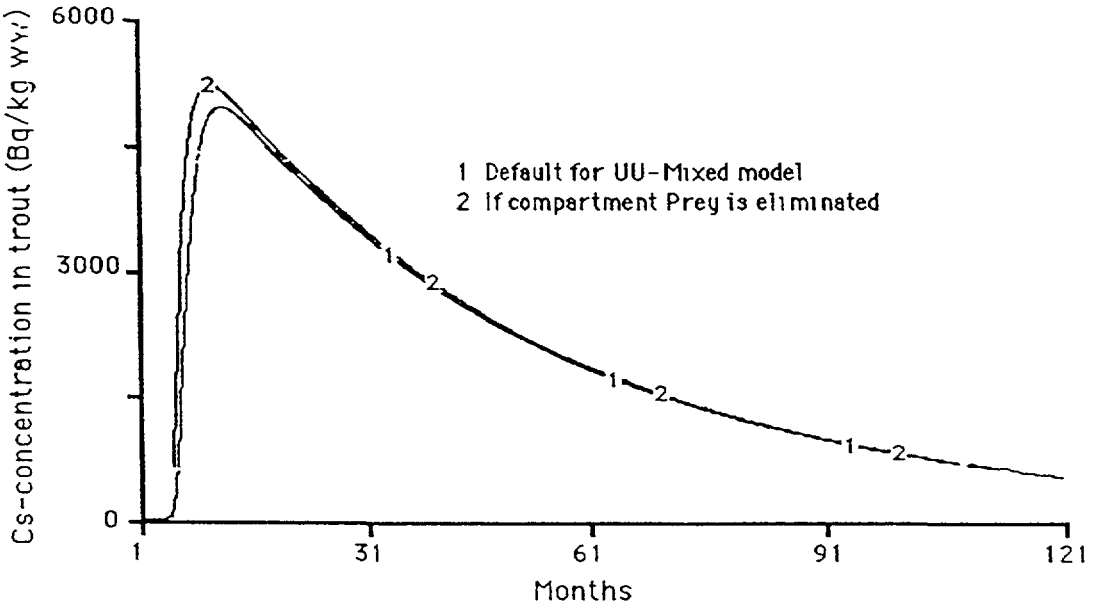

FIG. 5.7. Predictions for Cs concentrations in trout from Øvre Heimdalsvatn using the UU-Mixed model with (curve 1) and without (curve 2) compartment for prey

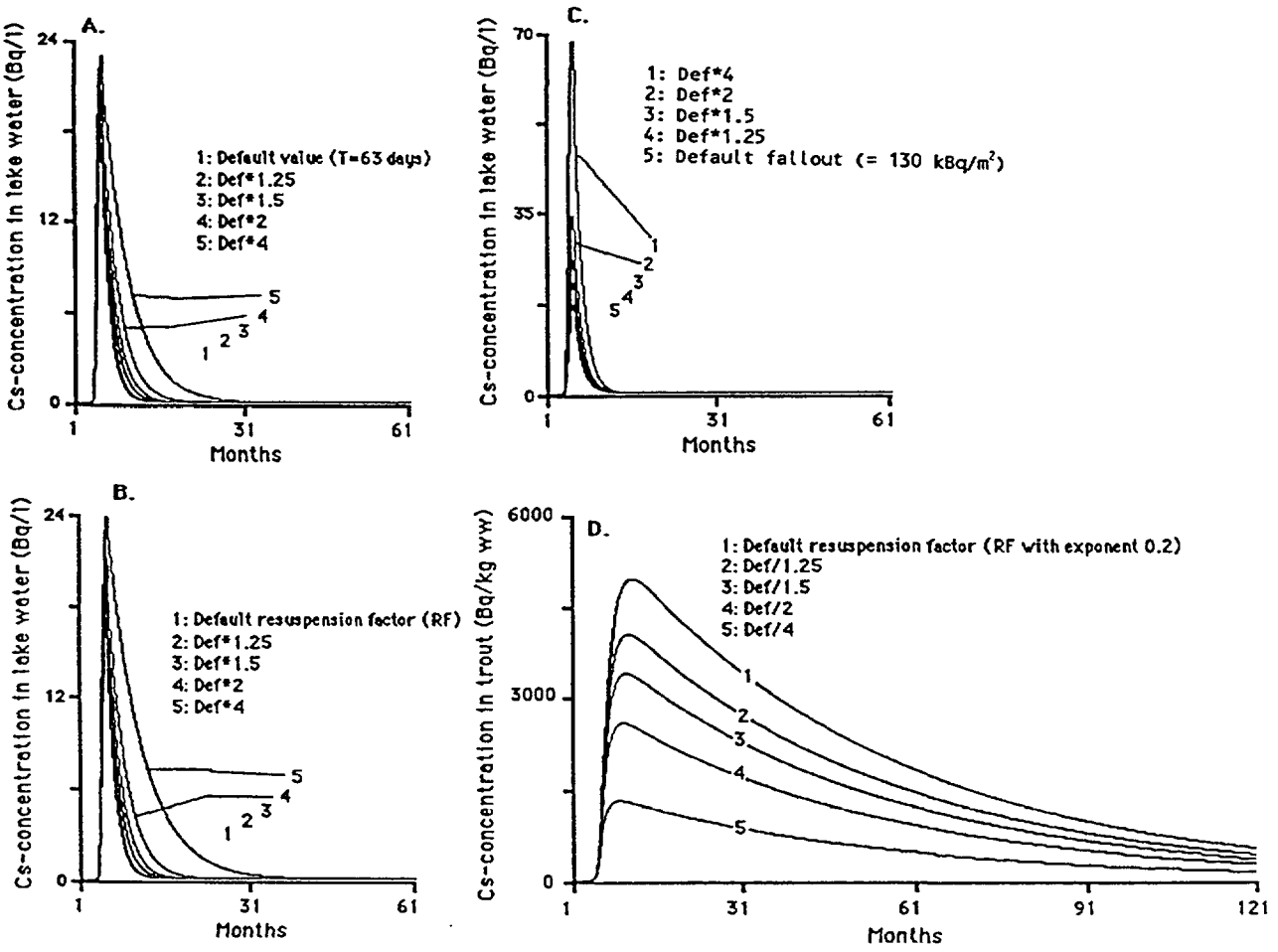

FIG. 5.8. Sensitivity analyses for important model variables in the UU-Mixed model using data for Øvre Heimdalsvatn to predict Cs concentration in lake water and trout.

A. Cs concentrations in lake water for different values of the lake water retention time.
B. Cs concentrations in lake water for different values of the resuspension factor.
C. Cs concentrations in lake water for different values of fallout. Note the change in scale of the y-axis.
D. Cs concentrations in trout for different values of the exponent in the resuspension factor.

half-life" in the prey. As a default value, this half-life was set to 0.5 times the ecological half-life for fish. These results indicate that the prey compartment in this model could be omitted. If this is done (Figure 5.7.), the model produces almost the same results as it does with the prey compartment. Thus, for even simpler, predictive models, one could recommend that this compartment be eliminated.

The basic aim of this model is to predict radiocaesium in lake water and predatory fish from as few and as readily available variables as possible. In Figure 5.8, four sensitivity analyses are presented for Cs concentration in lake water when different model variables are altered. (A) shows the results when the lake water retention time is changed. The default value is 63 days in this lake, and the graph illustrates that the Cs concentration in lake water, reaches a higher level and decreases slower if the retention time is longer (Def*4 means that the lake water retention time is 252 days (63 × 4). An increase in the resuspension factor (B) will mean that the lake is more dominated by internal loading and resuspension, resulting in a higher Cs concentration in water a slower recovery. Figure (C) illustrates the very important, and logical, effect of increasing fallout (note that the scale is different in this figure). Graph (D) illustrates how the choice of the exponent in the resuspension factor

influences the prediction of caesium in fish, in this case trout in Øvre Heimdalsvatn. If we alter the default value of exponent, 0.2, in steps (division by 1.25, 1.5, 2 and 4), we can note a significant change in resuspension factor, internal loading, and, finally, in the Cs concentrations in fish.

In conclusion, these sensitivity analyses indicate that this simple model could be even more simplified by omitting the prey compartment. The model is especially sensitive to the values for the "ecological half-life" for predatory fish, the bioconcentration factor and the definition of the resuspension factor.

5.1.5. The VTT model

The VTT model (DETRA) applied in this exercise uses a compartmental modelling approach. Sensitivity analyses have shown that the predictions using this model are sensitive to the parameter values for the water exchange rate, sedimentation, suspended sediment load, sorption distribution coefficient (K_d), solubility and consumption rates of plankton by fish.

Variation in the lake water exchange rate affect almost linearly the caesium concentration in lake waters. If the exchange rate increases, the water concentration of caesium decreases correspondingly. For elements which have high solubility this relationship can be clearly obtained. Caesium nuclides are relatively soluble and the K_d value $[Bq/kg_{solid\ material}]/[Bq/l_{water}]$ of caesium is quite low. Therefore, caesium concentrations in aquatic ecosystems are sensitive to water exchange rates.

Sedimentation rates and the amount of suspended sediment in lake waters affect the loss rates of nuclides from water to sediment. Radionuclides which are easily sorbed on to particles are very sensitive to changes in sedimentation rate. Because of its relatively high solubility, caesium is not very sensitive to this parameter. However, if the sedimentation rate in the lake is increased by a factor of ten, the caesium concentration in lake water decreases by about 60%. The concentrations in fish will then decrease correspondingly.

The distribution coefficient (K_d) describes the sorption intensity of various elements on solid material. The sedimentation rate of caesium is rather sensitive to K_d values. The total caesium concentration in lake water is, however, not very sensitive to K_d, because over 90 % of the caesium activity is distributed in the soluble phase.

The concentration of caesium in fish is directly proportional to the consumption rate of plankton by fish.

5.2. COMPARISON OF MODEL PREDICTIONS AND OBSERVED VALUES

One of the main tasks in the VAMP Lakes Subgroup has been to compare model predictions with the empirical values. The range of models employed has furnished an opportunity to assess both the accuracy of specific models and of particular model types. This has provided insight into the strengths and weaknesses of particular models when applied to a certain lake type. Comparisons between empirical data and model predictions are also treated in other sections of this Report, including empirically based uncertainty analysis (Section 5.3), detailed model comparisons (Section 5.4) and optimal model size (Section 5.8).

All modellers have compared observed peak values and model predicted peak values. In addition, some modellers have compared tail values, defined as of June 1990 (or 50 months after fallout), for predicted and observed values.

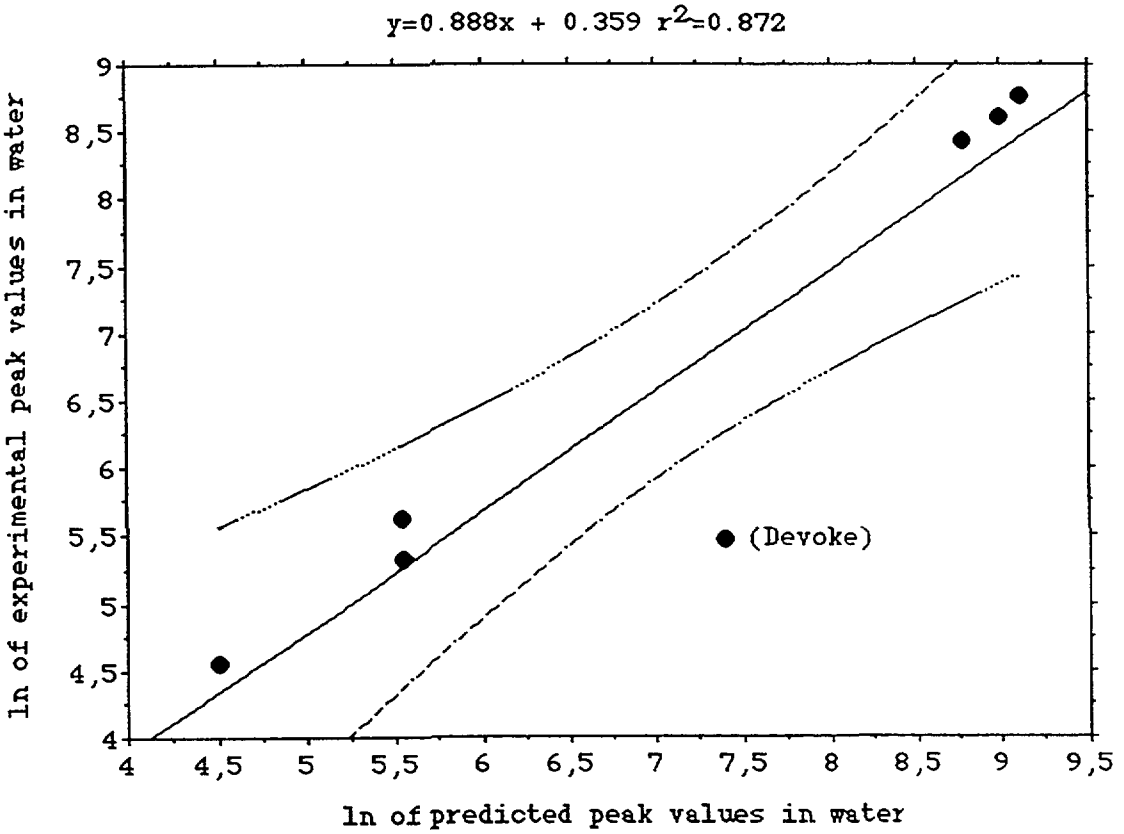

FIG. 5.9. Natural logarithms of the measured peak values versus the predicted peak values of ^{137}Cs in water (data from seven VAMP lakes).

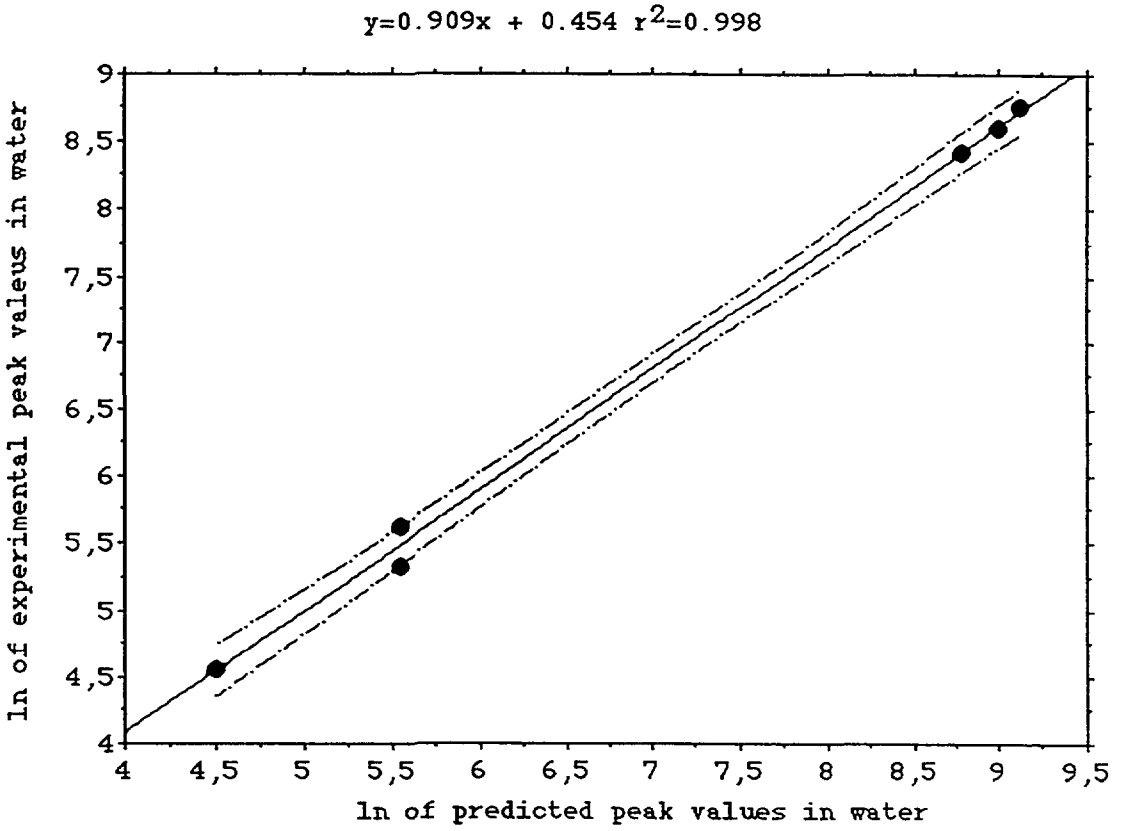

FIG. 5.10. Natural logarithms of the measured peak values versus the predicted peak values of ^{137}Cs in water (data from six lakes, Devoke Water is excluded).

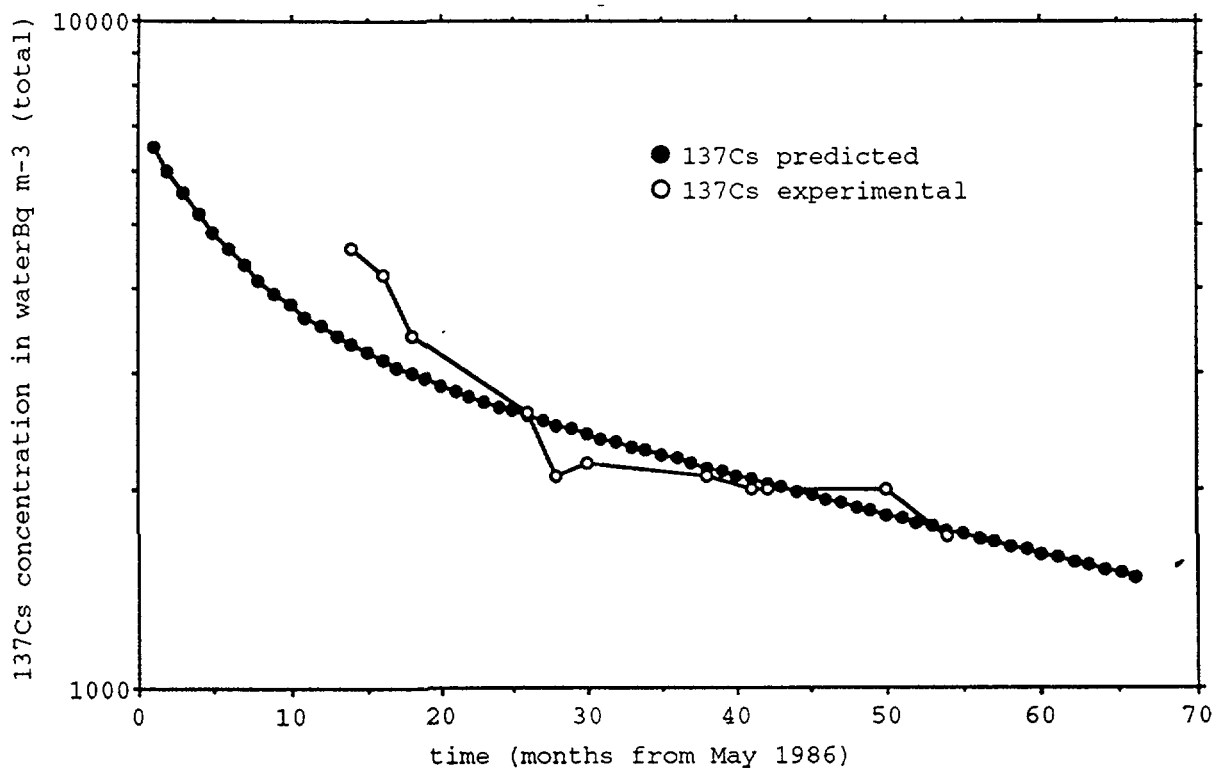

FIG. 5.11. Comparison of the measured and predicted ^{137}Cs concentration in water for Iso Valkjärvi.

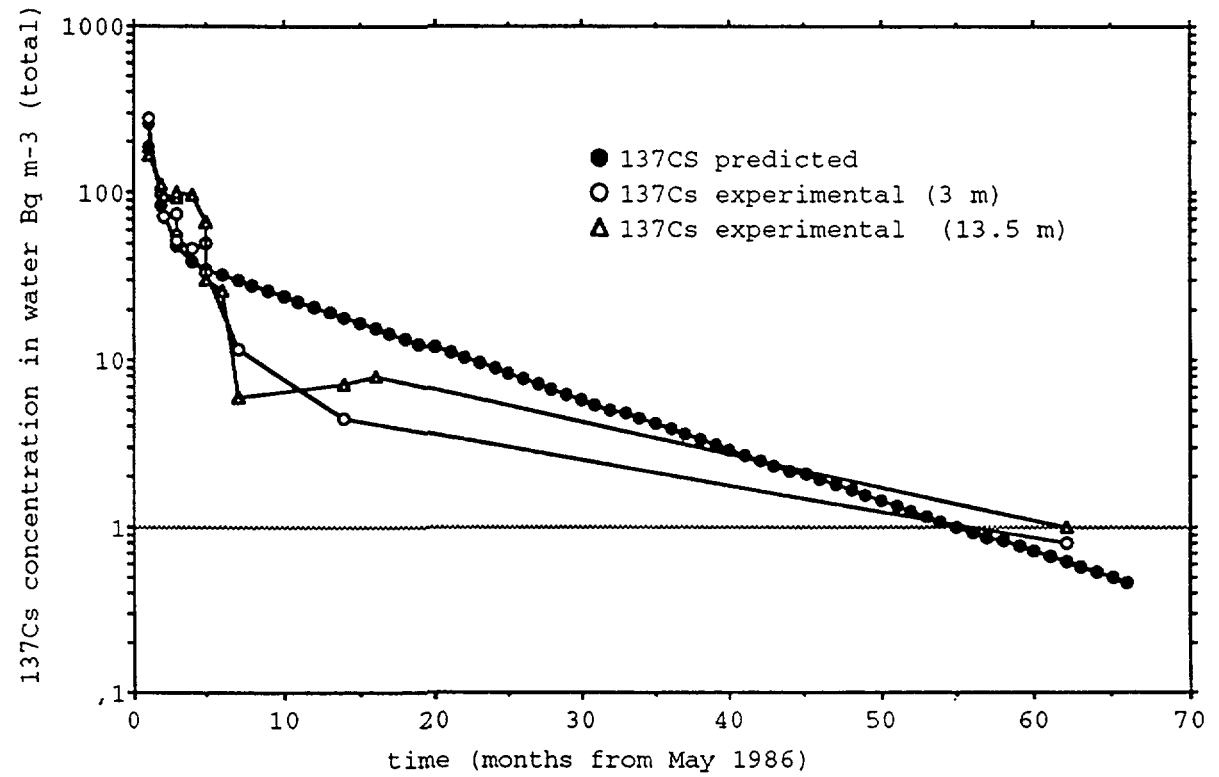

FIG. 5.12. Comparison of the measured and predicted ^{137}Cs concentration in water for Esthwaite Water.

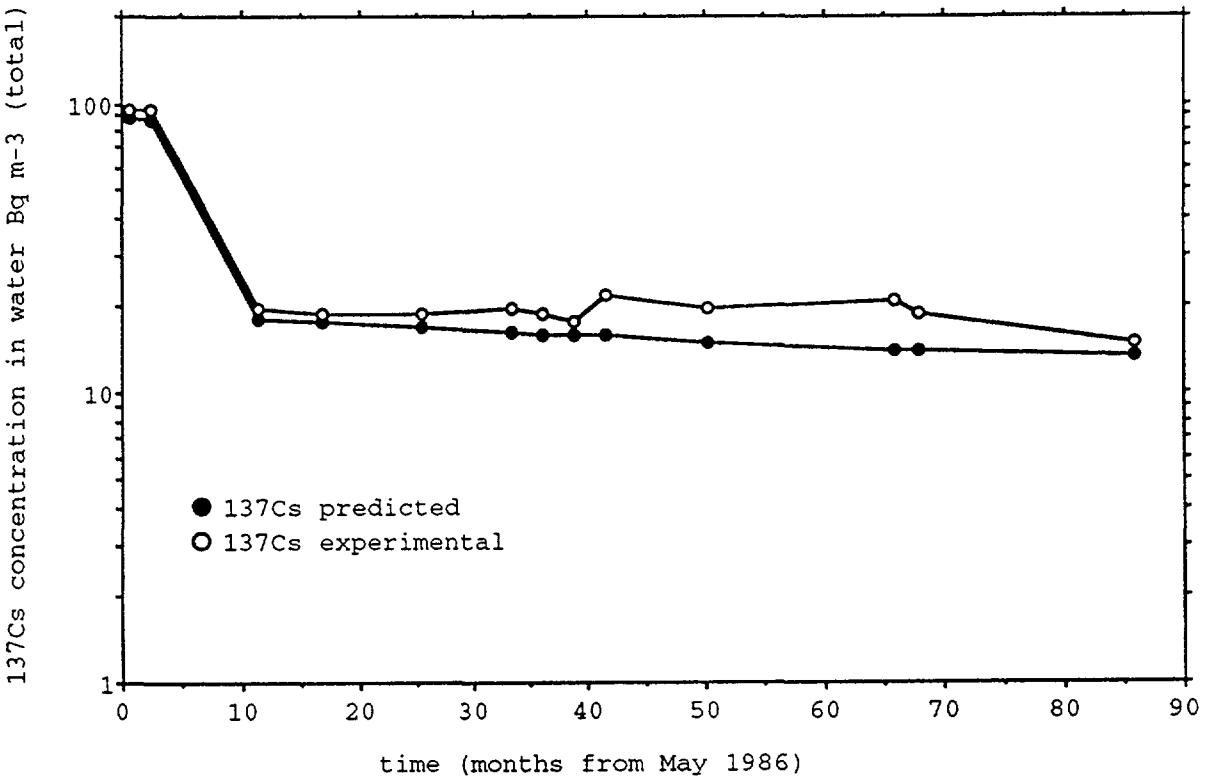

FIG. 5.13. Comparison of the measured and predicted ^{137}Cs concentration in water for Bracciano.

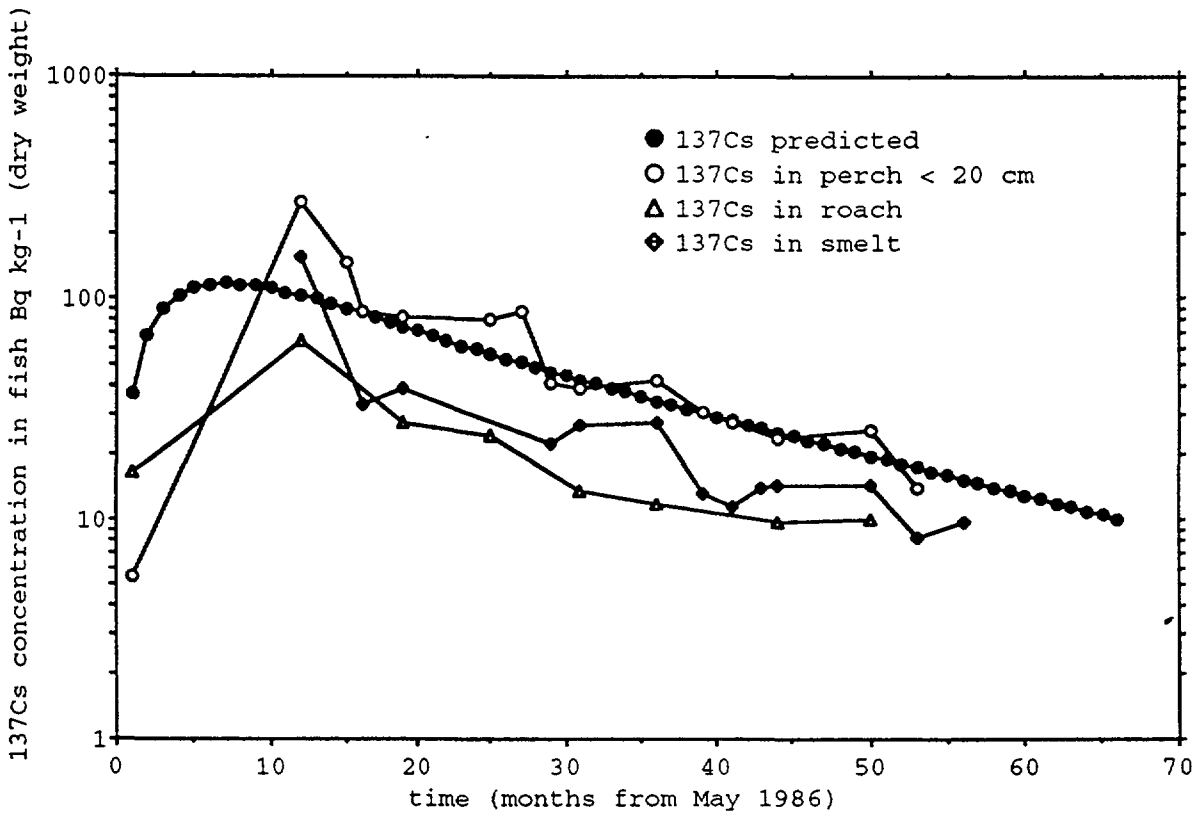

FIG. 5.14. Comparison of the measured and predicted ^{137}Cs concentration in fish for IJsselmeer.

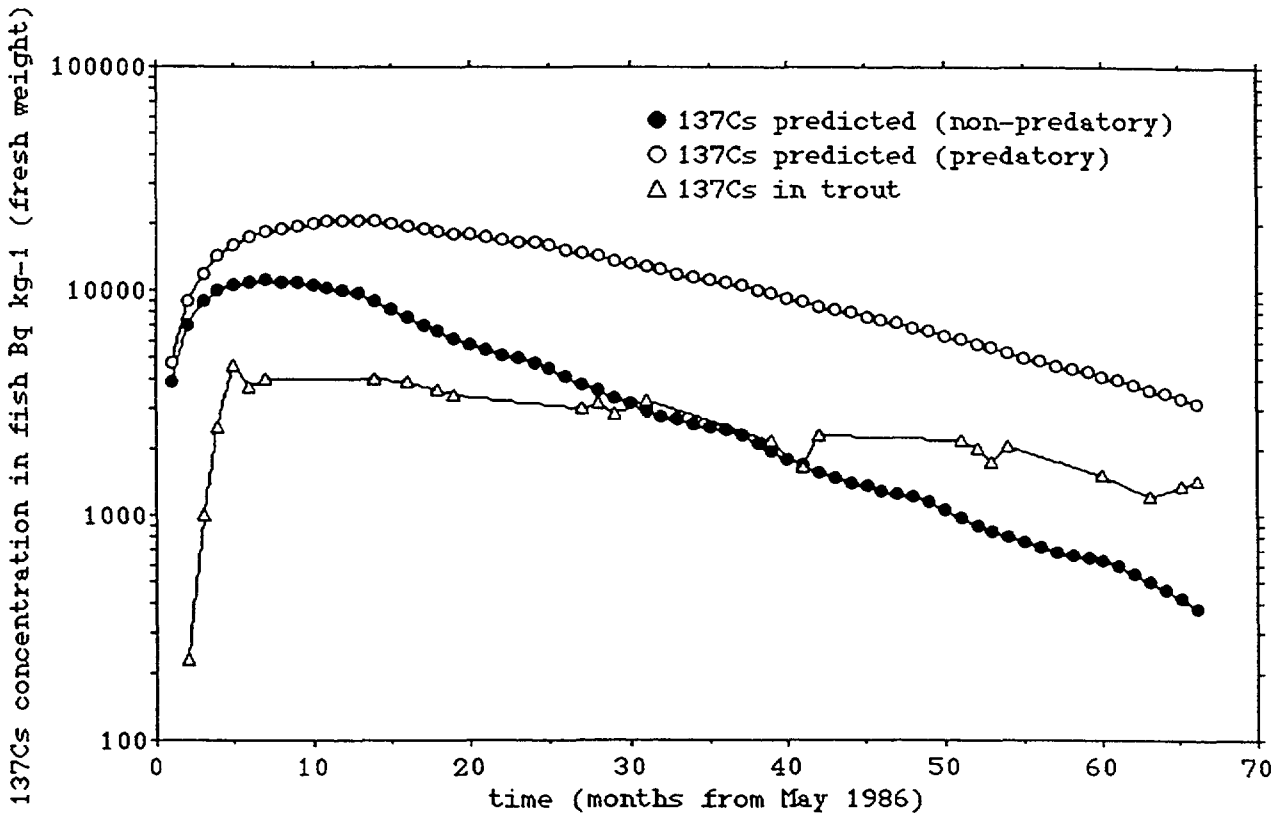

FIG. 5.15. Comparison of the measured and predicted ^{137}Cs concentration in fish for Øvre Heimdalsvatn.

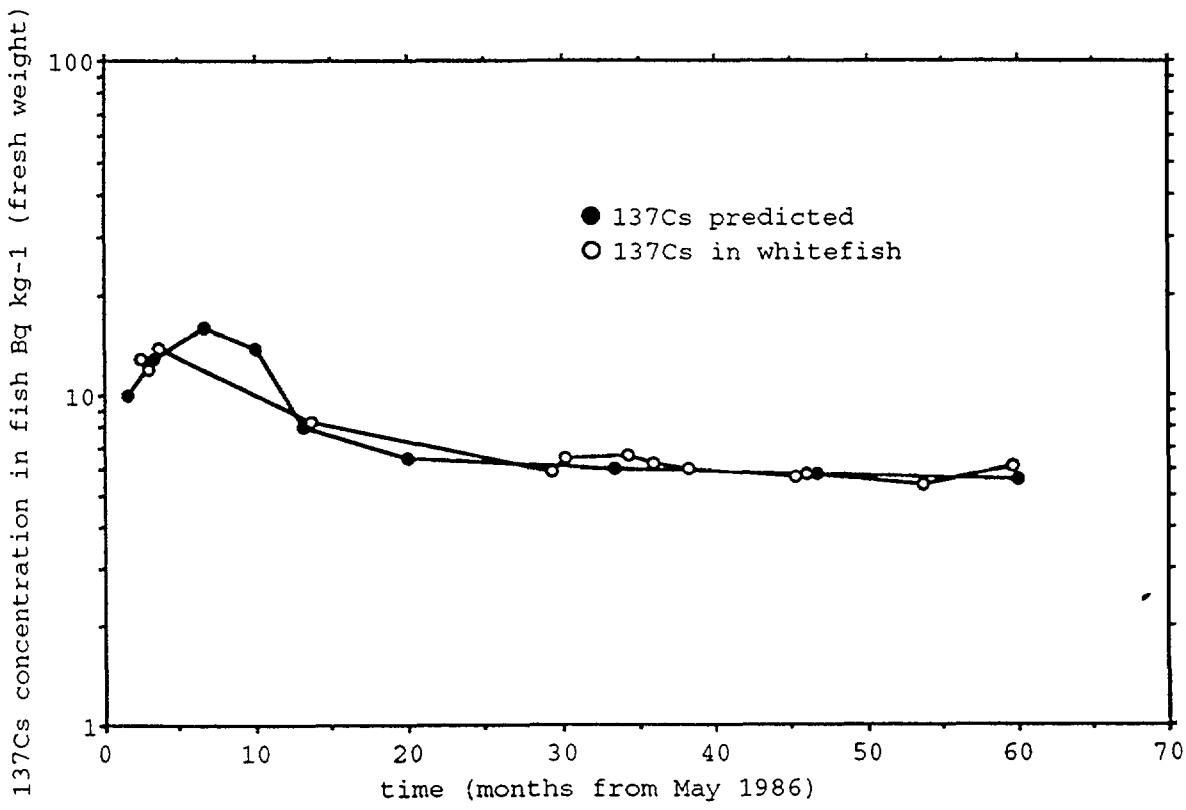

FIG. 5.16. Comparison of the measured and predicted ^{137}Cs concentration in fish for Bracciano.

5.2.1. The ENEA model

Using generic values for the parameters used by the model, the predicted concentrations of ^{137}Cs in water are generally within less than a factor of two from the empirical values, except for Devoke Water. The model predictions for this lake are within a factor of between four to five from the empirical values. Figures 5.9 and 5.10 show the results of the regression analysis between the logarithm of the experimental radionuclide concentration peak values in water and the logarithm of the predicted values. The results from all seven lakes are included in Figure 5.9, while in Figure 5.10 the results from Devoke Water are excluded.

The comparisons between the experimental ^{137}Cs concentration in lake water of Iso Valkjärvi, Esthwaite Water and Bracciano and the model outputs are reported in Figures 5.11, 5.12, and 5.13.

The sub-model used to predict the concentrations of radionuclide in fish species was developed to evaluate estimates of fish flesh contamination. The predicted values were generally within a factor of four from the empirical values. Some results of the comparison of the empirical concentrations and of the model predictions are reported in Figures 5.14 and 5.15. The sub-model predictions would probably be more accurate if site specific data for model parameters were available.

In the case of Bracciano an accurate knowledge of the site-specific bioaccumulation factor is available, resulting in a very reliable prediction of the long-term time behaviour of ^{137}Cs in whitefish flesh (Figure 5.16).

5.2.2. The KEMA model

In this Section the results of the validation test are presented. The bathymetric, hydrological, and radiological data supplied within the project have been used to run the lake ecosystem model LAKECO for several lakes. The equations and assumptions are presented in Appendix II.2.

Basically, LAKECO has been applied to each lake without substantial modifications. However, to deal with special environmental conditions, some extensions are introduced to handle specific phenomena such as ice-cover and the catchment runoff. Sensitivity runs (see Section 5.1.2) demonstrated the necessity of the implementation of new sub-models to improve the flexibility and applicability of the model. Subsequently, the important parameters are estimated by means of new sub-models. The extended version, LAKECO-B, has been used to perform the final calculations. The results of these calculation are presented below. Although LAKECO predicts the activity concentration of radiocaesium in water, sediments, and in many aquatic organisms in the food web, only the predicted values for water and the top predator for each lake is given in this Section.

The modifications were implemented to the extent to which information was given. Thus, for Hillesjön, Øvre Heimdalsvatn and IJsselmeer time dependent discharge rates were used. For Øvre Heimdalsvatn an ice-cover delay was used and for Hillesjön and IJsselmeer secondary load information was used. If information was lacking, general information and averaged values such as residence time were used.

In principle, LAKECO is not constructed to calculate the transfer of radionuclides from the catchment area to the lake. The transfer from the catchment has been assumed to play a minor role in the peak levels of radiocaesium in water and fish when a deposition of radionuclides takes place on the lake surface. Besides, this study is focusing on the lake ecosystem, so that the transfer from the catchment area to the lake has been regarded as a boundary condition. A simple catchment transfer approach could have been applied by assuming that of the total inventory of radionuclides in the catchment, 0.1 per cent is annually leached to the lake. This approach, however, was not adopted, since no detailed data are available to validate this assumption.

For Bracciano, a deep lake, it appeared that neglecting the stratification resulted in underestimation of the caesium concentrations. Mixing appears to govern the retention of radiocaesium in the epilimnion (see Annex II-2). Therefore, for this lake LAKECO has been modified to predict the radiocaesium levels in the epilimnion, the thermocline and in the hypolimnion.

For the model specific parameters, such as biota specific parameters, which could not be derived from the available information, consistent values were selected as input to avoid fitting. Another example of fitting is the duration of the deposition, which directly controls the peak levels of radiocaesium. If the total deposition is transferred to the lake instantaneously in the modelling process, higher peak levels in the water and consequently in the biota can be expected than if it is assumed that the deposition took place over a period of several days. Since no data concerning deposition rates and duration of the deposition were available, the initial concentration was calculated by using the total deposition on the lake area. This might result in deviating predictions, but shows the extent to which the generic model is able to give accurate predictions for the various lake ecosystems.

Tables 5.4 and 5.5 illustrate the observed levels and predicted peak levels for radiocaesium in the water column and in fish. Figure 5.17 shows the predicted radiocaesium levels in the water column

TABLE 5.4. PREDICTED AND OBSERVED PEAK LEVELS (Bq/L) ^{137}Cs IN WATER (BRACCIANO ^{134}Cs). RATIO OF PREDICTED AND OBSERVED PEAK VALUES

Lake	Predicted	Observed	Ratio P/O
Øvre Heimdalsvatn	28	5.5	5.1
Hillesjön	35	10	3.5
Iso Valkjärvi	0.82	4.6	0.2
IJsselmeer	0.42	0.19	2.2
Devoke Water	0.05	0.24	0.2
Esthwaite Water	0.23	0.03	0.8
Bracciano	0.04	0.05	0.8

TABLE 5.5. PREDICTED AND OBSERVED PEAK LEVELS (Bq/kg ww) OF ^{137}Cs IN FISH (BRACCIANO ^{134}Cs). RATIO OF PREDICTED AND OBSERVED PEAK VALUES

Lake	Fish	Predicted	Observed	Ratio P/O
Øvre Heimdalsvatn	Brown Trout	21 700	4660	4.7
Øvre Heimdalsvatn	Minnow	6340	5800	1.1
Hillesjön	Pike	5240	4680	1.1
Hillesjön	Perch 2+	5410	9160	1.2
Hillesjön	Perch 0+	6810	5880	1.2
Hillesjön	Roach	3760	2760	1.4
Iso Valkjärvi	Pike	17 800	27 000	0.7
Iso Valkjärvi	Perch 2+	17 000	13 800	1.2
Iso Valkjärvi	Whitefish	11 000	9500	1.2
IJsselmeer	Perch 2+	73.1	82.7	0.9
IJsselmeer	Perch 0+	85.5	25.6	3.3
IJsselmeer	Roach	52.6	17.2	3.0
IJsselmeer	Smelt	26.6	34.7	0.8
Devoke Water	Perch	2040	2080	1.0
Devoke Water	Brown Trout	2290	1250	1.8
Bracciano	Whitefish	3	4	0.8

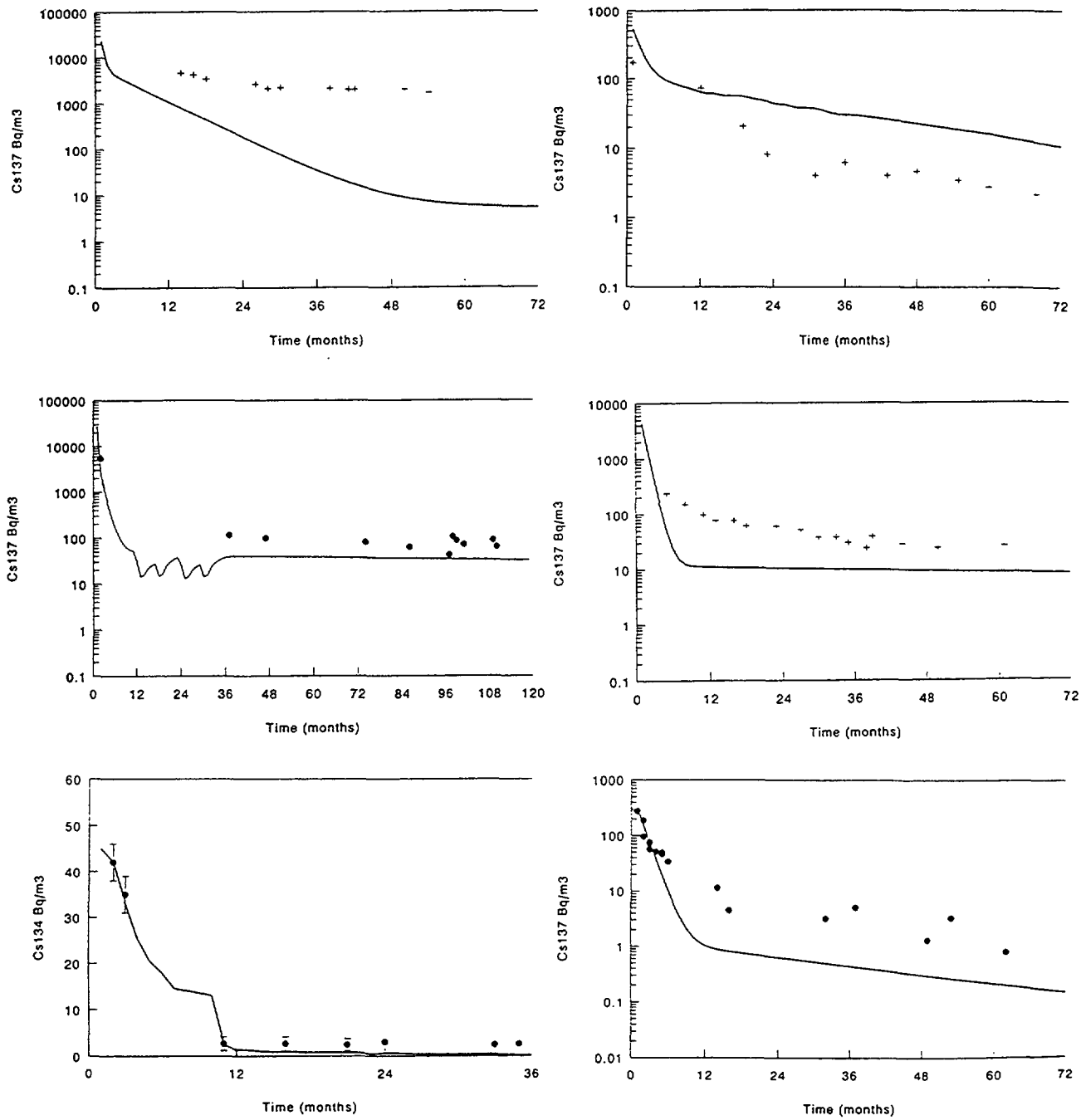

FIG. 5.17. Simulation results of LAKECO. Total ^{137}Cs (Bq/m^3) in the water column. Comparison of predicted radiocaesium concentration with measurements data. Left: Iso Valkjärvi, Øvre Heimdalsvatn, Bracciano (^{134}Cs). Right: IJsselmeer, Devoke Water, Esthwaite Water.

and Figure 5.18 presents the radiocaesium levels in the top predator. In the graphs dots represent the empirical data as contained in the database. In Figure 5.19 the predicted peak values for the concentration in the water and in the fish, prey and predatory fish, have been plotted against the observed values. However, empirical data were not available in all cases to compare the predicted peak levels properly. For example, the radiological data concerning the smelt in lake IJsselmeer were probably from a year after the peak concentration. In these cases the highest available values were compared with the predicted values on the same date. This approach was applied for the concentration in the water, in the prey fish and for the predatory fish showing peak levels one up to two years after the deposition. In all cases the maximum predicted levels were compared with the maximum observed levels of radiocaesium.

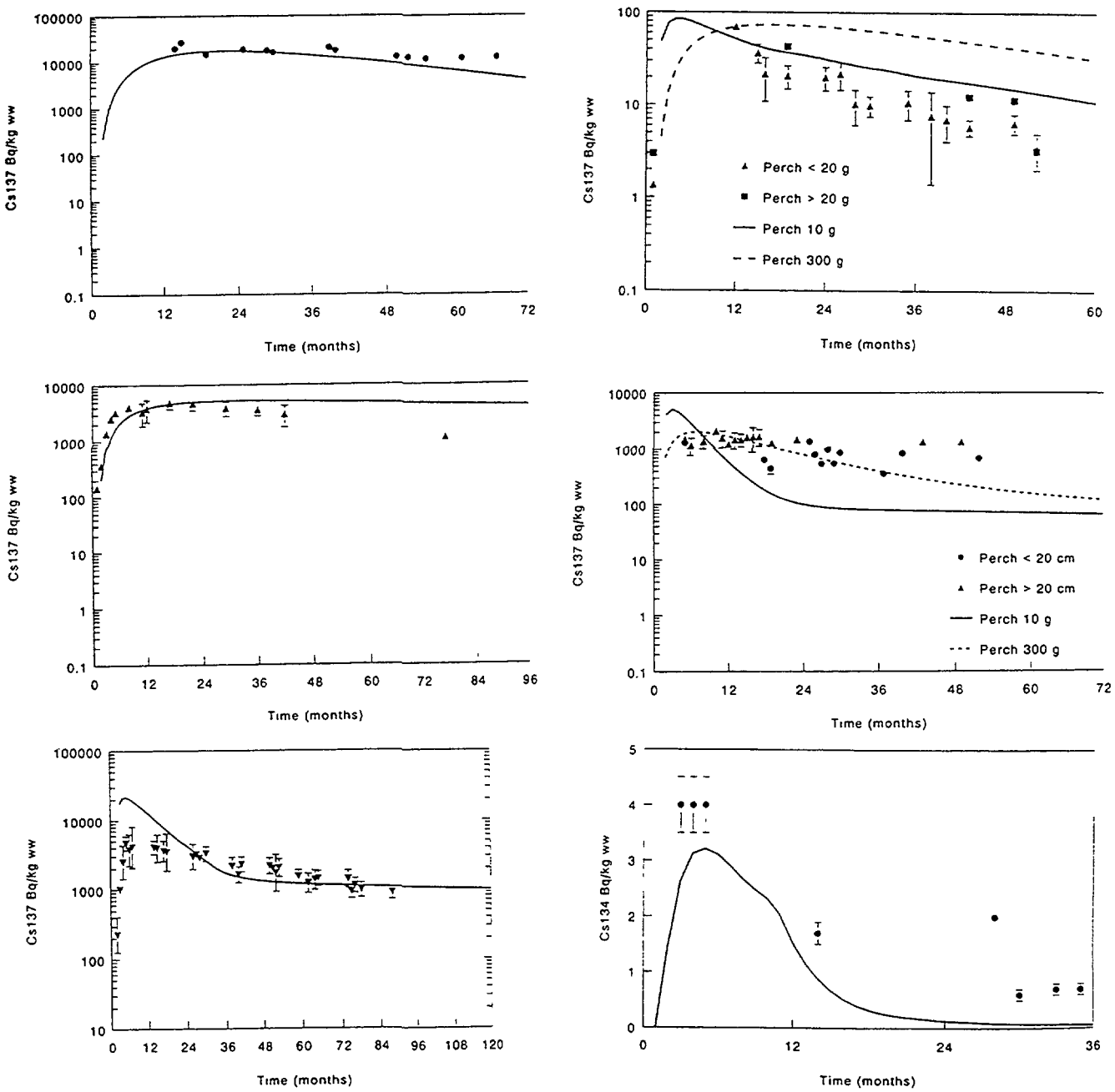

FIG. 5.18. Simulation results of LAKECO. Total ^{137}Cs (Bq/kg^{1} ww) in the top predator. Comparison of predicted radiocaesium concentration with measurements data. Left: Iso Valkjärvi (Pike), Hillesjön (Pike), Øvre Heimdalsvatn (Brown Trout). Right: IJsselmeer (Perch), Devoke Water (Perch), and Bracciano (Whitefish (^{134}Cs)).

The peak in the radiocaesium concentration in the water in the Scandinavian lakes Hillesjön and Øvre Heimdalsvatn appears to be overestimated. About 50% of predicted caesium levels in water consists of non-soluble caesium. It is possible that the removal of non-soluble radiocaesium from the water column is faster than assumed in the model, so that the actual radiocaesium concentration would be lower by at lease a factor of two. For Iso Valkjärvi, the predicted value is lower than the maximum observed value. However, the observed is measured one year after deposition, and is certainly not the maximum value which occurred in the lake. The estimated value based on calculations was about 23 Bq/L. As also demonstrated in the plots of the time series, the tail of the water peak seems to be underestimated by the model. The reason for this disagreement between the predicted and observed values in the long term is probably the absence of a catchment model. Leaching of radionuclides, in

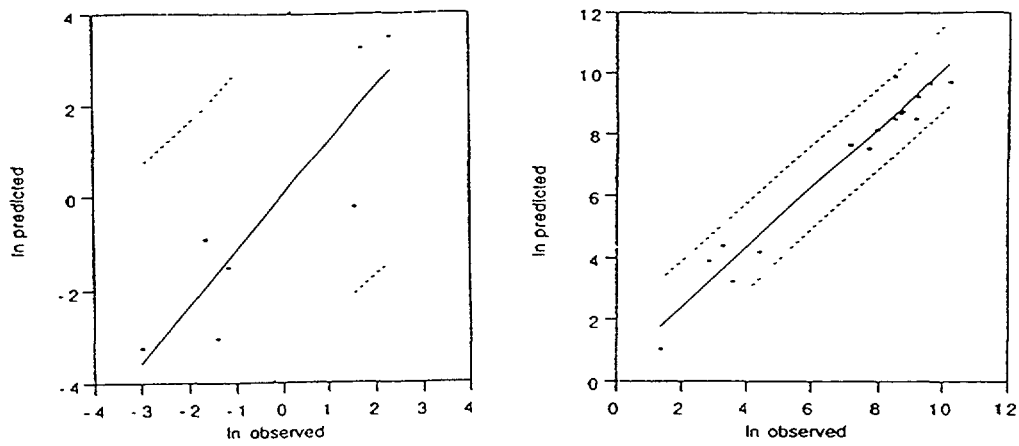

FIG. 5.19. Fitted lines of the predicted against the observed peak values with 95% uncertainty bounds for the individual values. Left: radiocaesium concentration in water. Right: radiocaesium concentration in fish.

combination with remobilization of radionuclides, controls the levels in lake waters. This secondary load plays an important role after one to two years. The underprediction of the peak level in water in Devoke Water could be explained by this effect, due to the presence of peat bogs. The leaching of radionuclides from the catchment could thus be enhanced in comparison with other lake ecosystems. Nevertheless, the predictions are in accordance with the accuracy required for the model predictions, and none of the predictions differ from the observed values by more than one order of magnitude.

The predicted values for fish seems to be more in agreement with the observed values than the predictions for the water concentrations. The predicted versus observed ratio varies between 0.2 and 4.7, which is again lower than the required accuracy of the model of one order of magnitude. However, the predicted peak levels for trout appears to exceed the measured values significantly. The reason for this is probably the high assumed water uptake due to the low potassium concentrations in the lake water. An extraction of caesium passing the gills of 100% was assumed, which might be an overestimation. Models on the basis of processes for the uptake of caesium via the gills in oligotrophic lakes must be developed to account for this gill effect more accurately.

5.2.3. The Studsvik model

The results from the Studsvik model are presented as predicted/observed (P/O) values and also for predators in graphical form (Figure 5.20). Ratios for predicted to observed maximum levels and tail values in water for each lake are shown in Tables 5.6 and 5.7, respectively. The predicted values correspond to the arithmetic mean from the calculated distributions.

The model consists of one compartment for the water, with the exception of Bracciano, which is not considered completely mixed until the autumn. The average values of the two concentrations given for Esthwaite Water were used in the comparison.

There is a tendency for the model to overestimate the levels of ^{137}Cs in water. This is most pronounced for Hillesjön, which is considered in more detail in Section 5.4. Naturally, the model which is run on a monthly basis gives the highest values during the first months after the deposition. However, due to the lack of empirical data such values could not be used in the evaluation. Apart from a single measurement in June 1986, no reliable measurements of the levels in water were available for Heimdalsvatn until May 1989. Outflowing water had then a level of 0.116 Bq/L, while the model predicts 0.152 Bq/L.

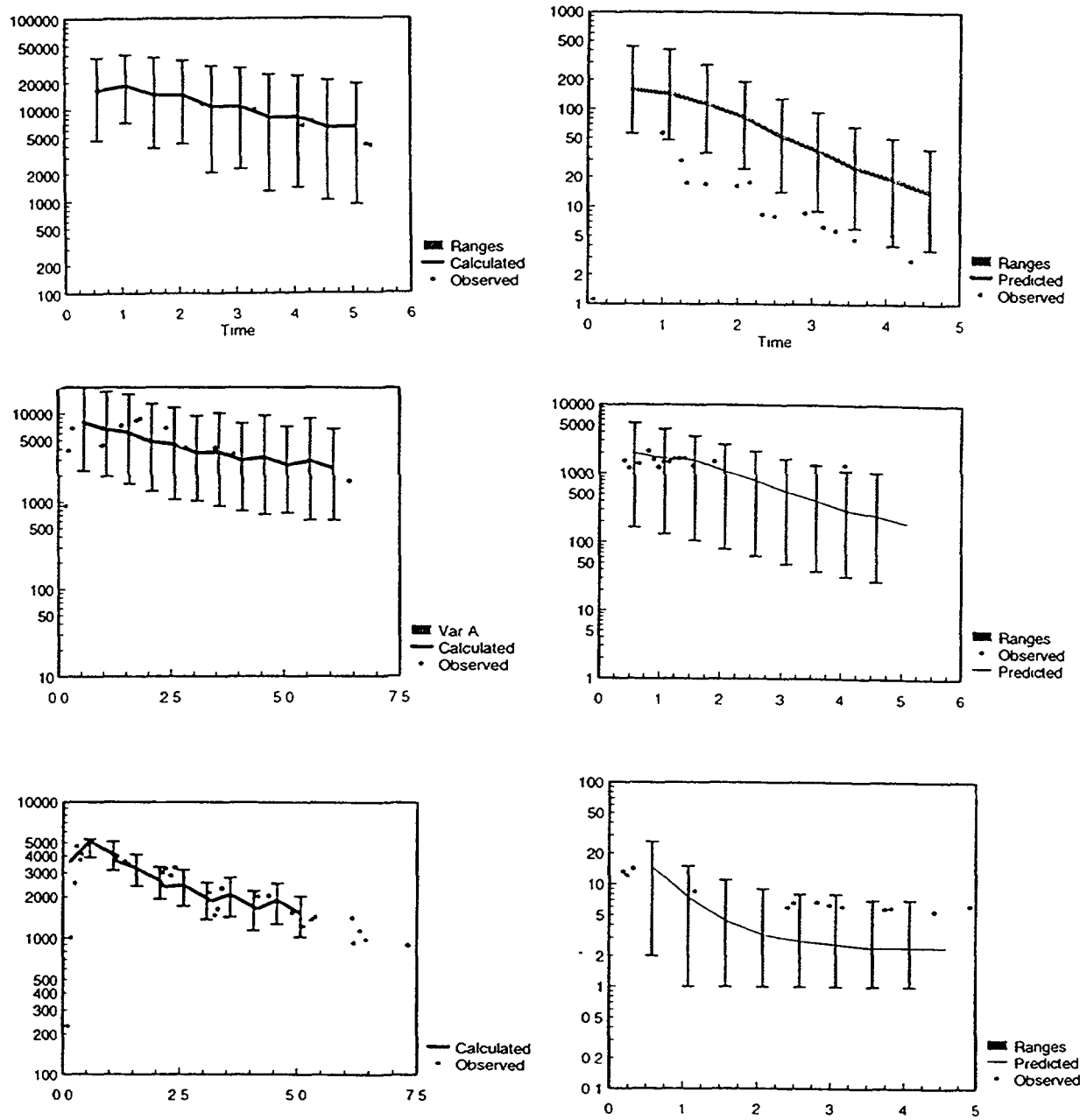

FIG. 5.20. Observed and predicted concentrations (Bq/kg ww) of ^{137}Cs versus time (years) in top predators in different lakes. Left: Iso Valkjärvi (perch), Hillesjön (perch) and Øvre Heimdalsvatn (trout), right: IJsselmeer (perch), Devoke Water (perch) and Bracciano (whitefish).

The model predicts the peak and tail concentrations of ^{137}Cs in lake waters within a factor of two (Tables 5.6 and 5.7).

Peak and tail values have also been compared for the observed maximum predatory fish levels (Table 5.8). Consideration was given to the potassium content in the water when selecting values for the bioaccumulation factors. It should also be pointed out that the basic structure of the model has been used in earlier model evaluations concerning Nordic lakes [5.6–5.9]. When predicting the results for Bracciano, the bioaccumulation factor to plankton was reduced to 500 because of the very high content of potassium in this lake. This can easily be seen as a tuning of the model, but it should be kept in mind that this study was not a pure validation test, but rather addressed the basic principles of ^{137}Cs turnover in lakes. This lake is also deep, such that total mixing in the water column was not used until

TABLE 5.6. PREDICTED TO OBSERVED RATIOS OF THE MAXIMUM MEASURED CONCENTRATIONS OF ^{137}Cs IN WATER

Lake	P/O water
Bracciano	1.4
Devoke Water	1.1
Esthwaite Water	1
Hillesjön	3
IJsselmeer	1.7
Iso Valkjärvi	1.4

TABLE 5.7. PREDICTED TO OBSERVED RATIOS FOR TAIL VALUES OF THE LEVEL OF ^{137}Cs IN WATER

Lake	P/O Water
Devoke Water	1.3
Esthwaite Water	0.61
Hillesjön	1.5
IJsselmeer	1.4
Iso Valkjärvi	0.8

TABLE 5.8. PREDICTED TO OBSERVED RATIOS FOR PEAK LEVELS IN FISH

Lake	P/O	Species
Bracciano	1.4	Whitefish
Devoke Water	1.5	Perch
Heimdalsvatn	1.1	Trout
Hillesjön	0.7	Perch
IJsselmeer	2.6	Perch
Iso Valkjärvi	1.1	Perch

TABLE 5.9. PREDICTED TO OBSERVED RATIOS OF TAIL VALUES FOR THE CONCENTRATION OF ^{137}Cs IN PREDATORY FISH

Lake	P/O	Species
Bracciano	2.4	Whitefish
Devoke Water	0.3	Perch
Heimdalsvatn	1.3	Trout
Hillesjön	1	Perch
IJsselmeer	5.4	Perch
Iso Valkjärvi	1.1	Perch

the autumn. For Devoke Water as seen below in the sensitivity analyses, the results for perch are very sensitive to the choice of K_d value for the suspended matter.

The model has a tendency to overestimate, although mostly within a factor of two.

Results for tail values are shown below in Table 5.9. There is a clear overestimation in the predictions, with the exception of Devoke Water. This is probably due to the following reasons. For Bracciano, no consideration was given to earlier fallout from weapons testing during the 1960s, which according to the observations must be the most probable explanation to the almost constant values in fish after the initial pulse. For IJsselmeer, the loss by fishing was not included in the model and according to subsequent information there is considerable fishing activity in the lake. The good agreement for the Nordic lakes reflects experience in modelling such ecosystems.

5.2.4. The UU-Mixed model

This Section compares empirical data and predicted values using the UU-Mixed model. The focus is on water and predatory fish, as well as situations where the model predictions either agree well or poorly with the empirical data. Possible explanations are given for this.

Bracciano

From Figure 5.41A in Section 5.3.2., we can note that this model gives rather poor predictions for whitefish. The main reason is that this model does not account for "old" nuclear tests caesium, which still remains in this lake due to its very long water retention time (137 years). For the same reason, the model also gives poor predictions for ^{137}Cs in lake water. If it is assumed that only 10% of the entire lake volume participates in the mixing of the radiocaesium after the Chernobyl fallout, then one obtains a rather good correspondence between modelled peak values and empirical peak values (Figure 5.21A). The modelled values would have been one order of magnitude lower had one used the entire lake volume in the calculation of the Cs concentration.

Øvre Heimdalsvatn

The small UU-Mixed model gives very good predictions not only for trout in this lake, but also for the minnow (Figure 5.22).

Iso Valkjärvi

Figure 5.40A in Section 5.3.2 presents the relationship between modelled values and empirical data for caesium in lake water, and Figure 5.41 presents the same comparison for whitefish. There is a good correspondence between observed and predicted values for small perch, and quite good predictions for pike and large perch. The main reason why the model gives rather poor predictions of the tail values for caesium in lake water has to do with the fact that it includes neither secondary load nor seasonal variability.

Hillesjön

The results are discussed in detail in Section 5.4. The modelled values for caesium in lake water are initially much too high; the predicted peak value is about 50 Bq/L in relation to the empirical peak of about 10 Bq/L. The model gives good predictions for small perch (< 10 cm), pike and roach, but too high values compared to the empirical data for large perch.

Esthwaite Water

There is a very good correspondence between modelled values and empirical data for caesium in water in this lake, as illustrated in Figure 5.21B.

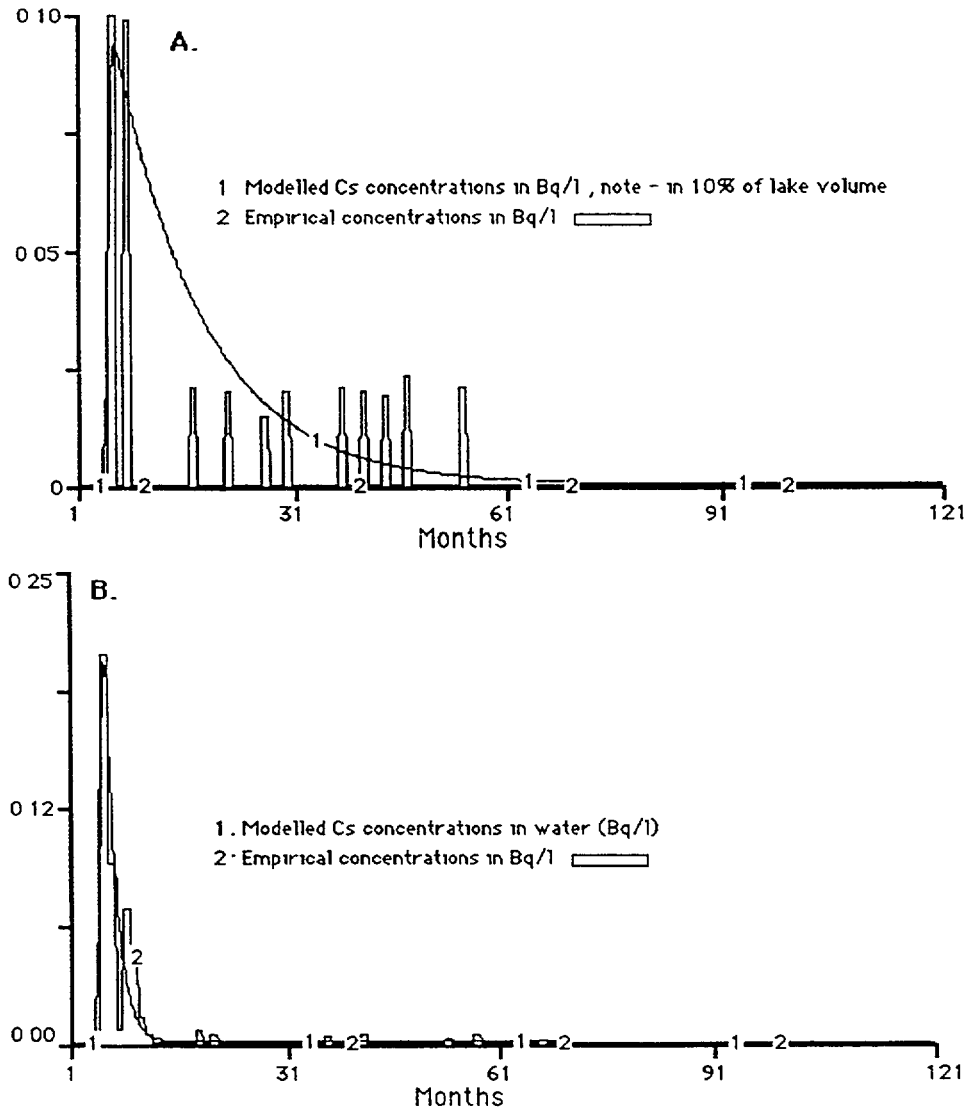

FIG 5.21. Caesium in water in Bracciano (A) and Esthwaite Water (B): the UU-Mixed model versus empirical data

Devoke Water

The results are presented in Figure 5.23. The predicted initial values for caesium in lake water are much higher than the empirical values. The model gives good predictions for trout (Figure 5.23D). There is considerable scatter among the empirical data, but the model seems to predict too low values for both large perch (Figure 5.23B) and small perch (Figure 5.23C).

IJsselmeer

The model gives rather good predictions of caesium in lake water, although the initial values are a little high (Figure 5.24A). The modelled values for large predatory perch are also higher than the empirical values, and this is especially so for the tail values (Figure 5.24B). The predictions are quite good for smelt (Figure 5.24C).

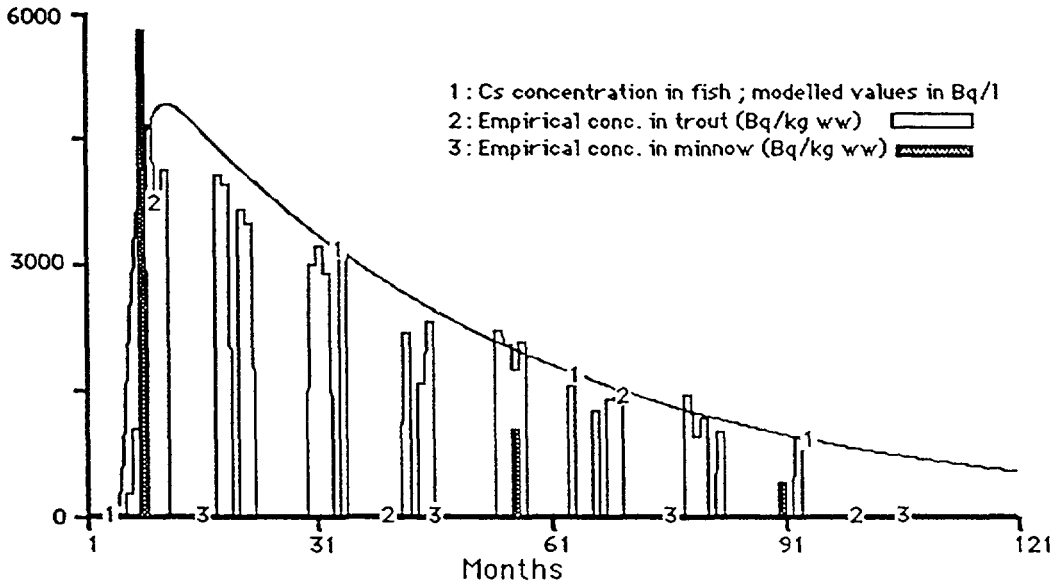

FIG. 5.22. Caesium in trout and minnow in Øvre Heimdalsvatn: the UU-Mixed model versus empirical data.

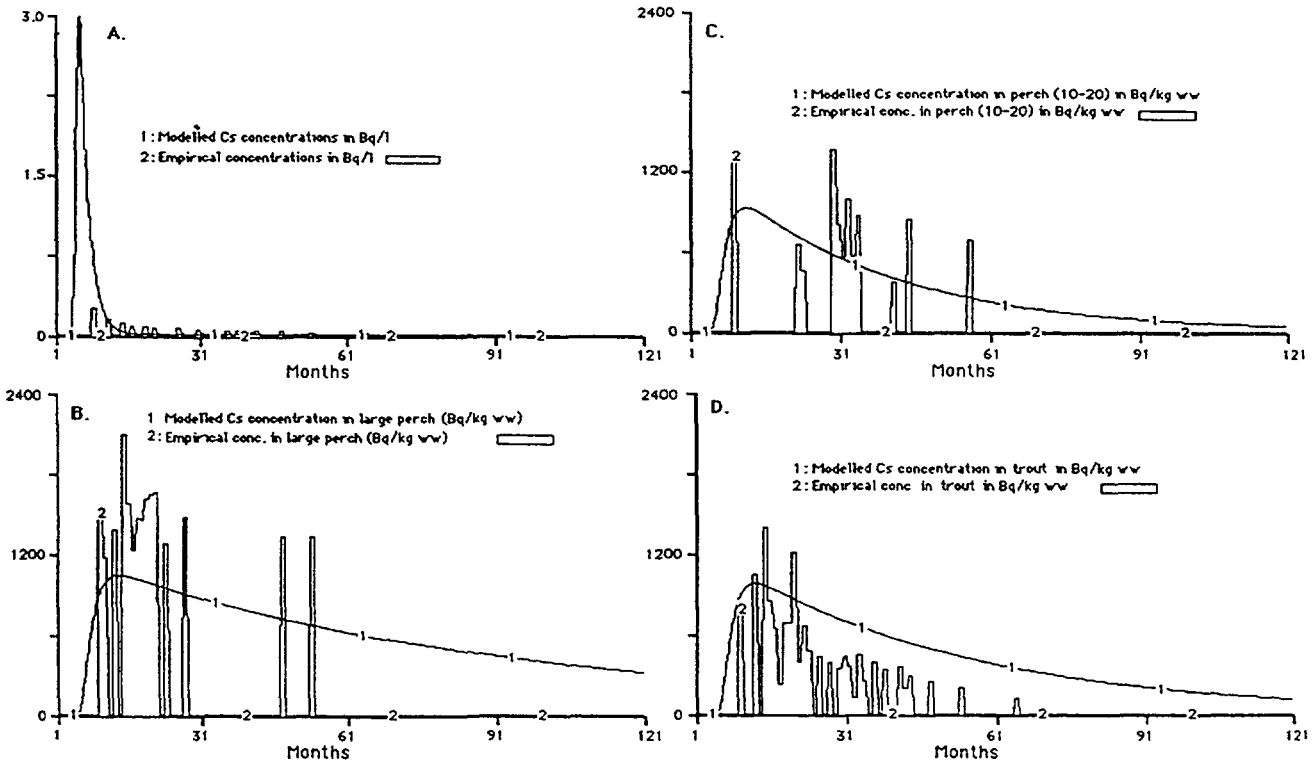

FIG. 5.23. Caesium in lake water (A), large perch (B), small perch (C), and trout (D) in Devoke Water: the UU-Mixed model versus empirical data.

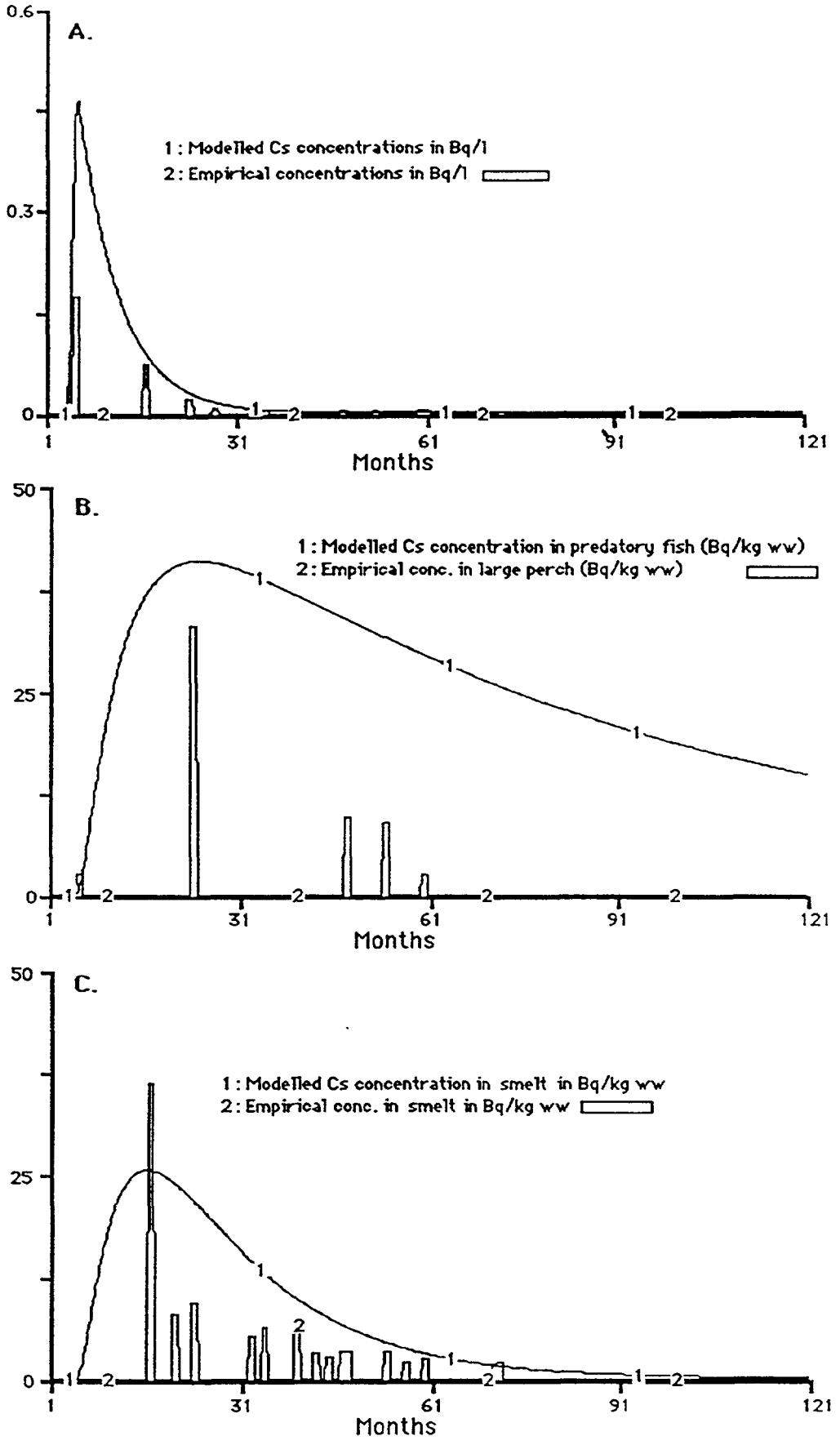

FIG. 5.24. Caesium in lake water (A), large perch (B), and smelt (C) in IJsselmeer: the UU-Mixed model versus empirical data.

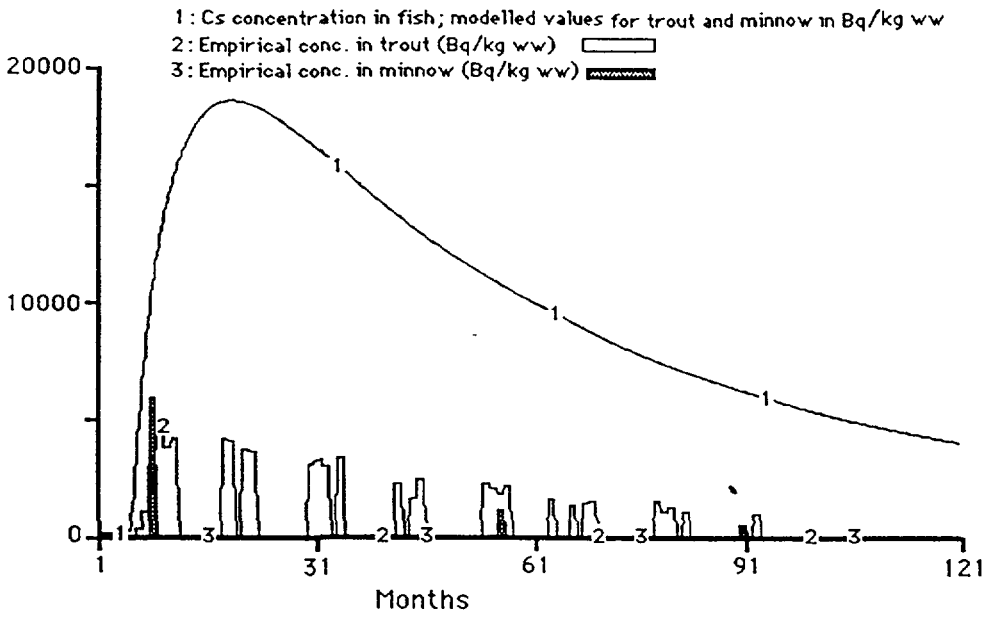

FIG. 5.25. Caesium in trout and minnow in Øvre Heimdalsvatn: the UU-Generic model versus empirical data.

5.2.5. The UU-generic model

Bracciano

Figure 5.41C in Section 5.3.2. shows that this model gives very poor predictions indeed for whitefish. The model does not account for "old" caesium, so these results are not unexpected. For the same reasons, the model also gives poor predictions for ^{137}Cs in lake water.

Øvre Heimdalsvatn

This model overestimates the values for trout and minnow in this lake by a factor of three, as illustrated in Figure 5.25. Since this is a large model where we have keep all model variables the same for all lakes and only varied the lake-specific parameters, there are many possible reasons for the poor fit linked for example to uncertainties in the biouptake rates, the K_d values and the retention rates. The great uncertainties in this model probably lie in the biouptake and bioaccumulation rates, which are likely to be too high.

Iso Valkjärvi

Figure 5.40C in Section 5.3.2 shows the relationship between modelled and empirical data for caesium in lake water, while Figure 5.41F presents the same for whitefish. This model overestimates the values for whitefish, and also for pike, large perch and small perch in this lake by a factor of 2. The biouptake rates are probably too high.

Hillesjön

The results are also discussed in Section 5.4. The modelled values for caesium in lake value are also initially too high for this model (by a factor of three to four). The model gives good predictions for small perch, and large perch, but too low values for pike (by a factor of two) and roach (by factor of three to four).

Esthwaite Water

The modelled values are too high (by a factor of two) for caesium in water in this lake, as illustrated in Figure 5.26.

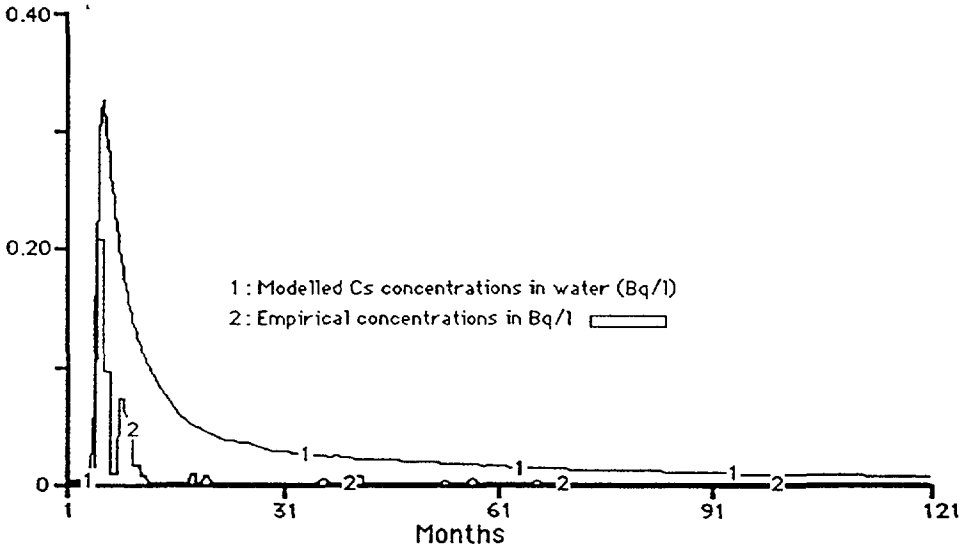

FIG. 5.26. Caesium in lake water in Esthwaite Water: the UU-Generic model versus empirical data.

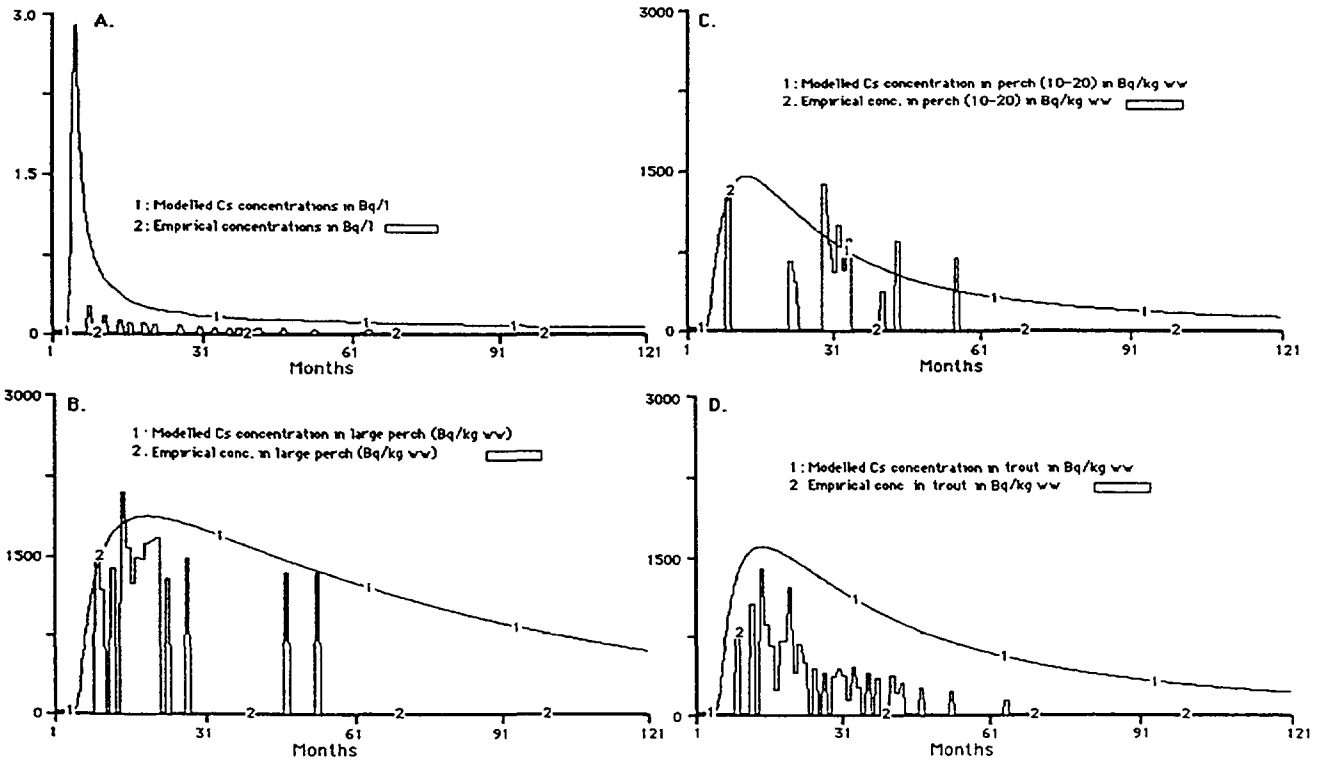

FIG. 5.27. Caesium in lake water (A), large perch (B), small perch (C), and trout (D) in Devoke Water: the UU-Generic model versus empirical data.

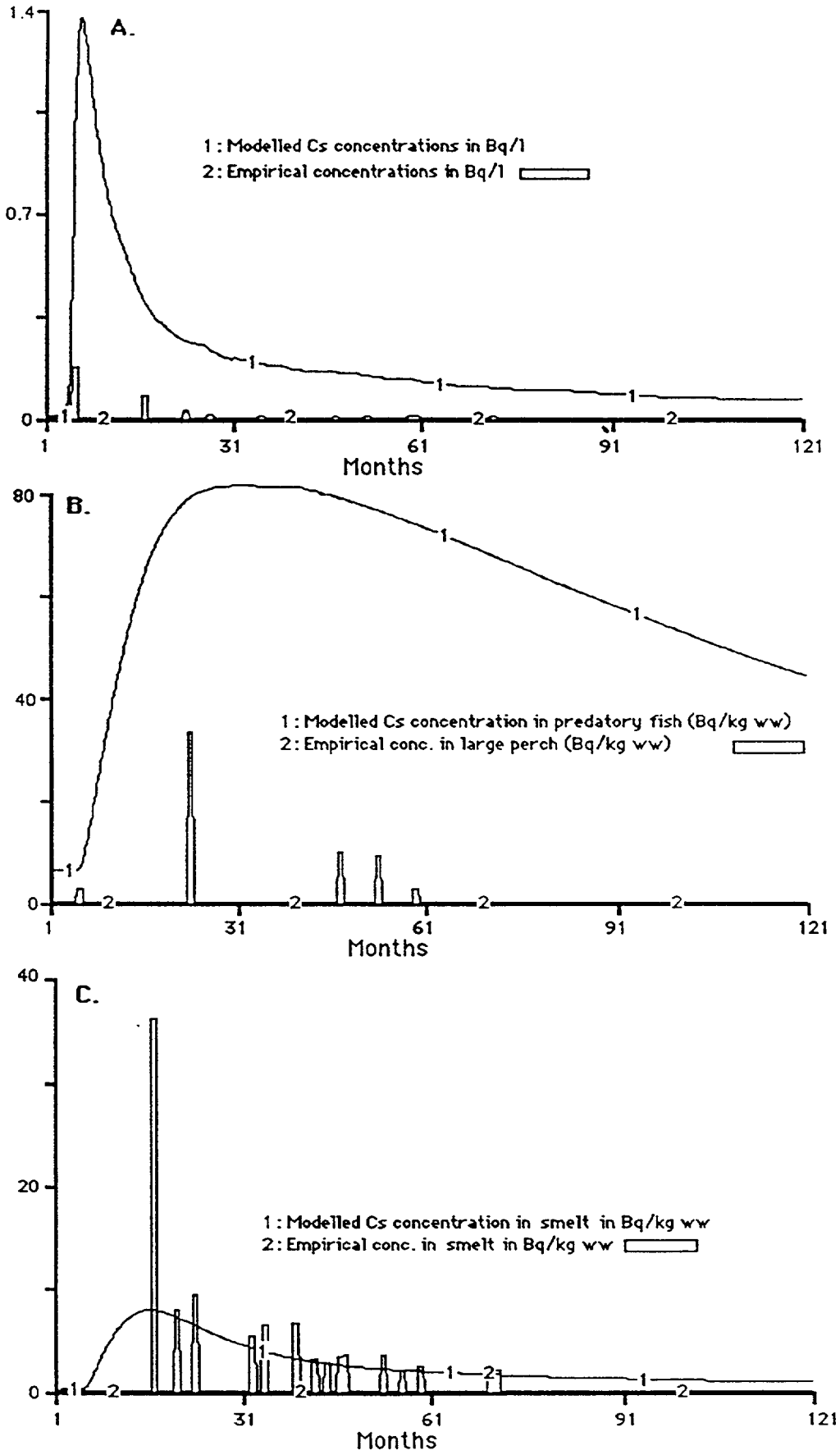

FIG. 5.28. Caesium in lake water (A), large perch (B), and smelt (C) in IJsselmeer: the UU-Generic model versus empirical data.

Devoke Water

The results are presented in Figure 5.27. The predicted values for caesium in lake waters are much higher than the empirical values (by a factor of four in the initial phase and a factor of two after two years (Figure 5.27A). The model gives good predictions for large perch (Figure 5.27B) and small perch (Figure 5.27C), and reasonable although too high values for trout (Figure 5.27D).

IJsselmeer

The model gives much too high values for caesium lake water (Figure 5.28A) and large perch (Figure 5.28B). The fit for smelt is much better, except for one initial very high empirical value, which the model cannot predict (Figure .28C). The predictions for roach and small perch agree quite well with the empirical values (no figure included).

5.2.6. The VTT model

The model seems to underestimate the activity content in water in the longterm. Figure 5.28 presents the predicted ^{137}Cs concentrations in the waters of the considered lakes. There are several parameters in the model which affect the activity content in water. The resuspension component from the sediments is probably underestimated. The suspended sediment load, the sedimentation rate and the K_d values all affect the activity content in water. Additionally, the seasonality effect is important in the shortterm because the water exchange rates of the lakes fluctuate during the year. In the model, averaged values for precipitation on drainage areas and for water exchange rates of lakes were applied in the calculations and the seasonality effect was not considered. It is obvious that seasonality affects the temporal concentrations in water, especially for mountain lakes.

The dynamic fish model predicts peak values relatively well. Generally, the predicted peak values in fish are within a factor of three compared to the observed values. In the longterm, however, the model slightly underestimates the activity content in fish, especially for prey fish. The predicted concentrations in fish are related to the predicted concentrations in lake water. As mentioned earlier, the model underestimates concentrations in water and this is one of the reasons for the underestimation of concentrations in fish.

The temporal behaviour of predicted ^{137}Cs concentrations in top predator of different lakes is presented in Figure 5.29. The predicted normalized (with respect to total deposition) concentrations in top predators are presented in Figure 5.30. Figure 5.30 shows that the concentrations in fish are not very sensitive to the lake type if the water turnover times (i.e. the dilution properties of the lakes) are accounted for.

The VTT model is relatively simple, but it was intended to account for the most important processes which are known to contribute to the concentrations in aquatic ecosystems. Most of the results were qualitatively satisfactory. However, the comparison of predicted concentrations to the observed values indicate that especially the modelling of the drainage area (including the effect of seasonality) and sedimentation need improvement.

Predicted ^{137}Cs concentrations in water and predator and values for predicted/observed concentration ratios for different lakes are presented in Tables 5.10 and 5.11.

5.3. UNCERTAINTY ANALYSES

Traditional uncertainty analysis provides a quantitative estimate of the range of model outputs that results from uncertainties in the structure of the model or the inputs to the model. The analysis can also be extended to identify the sources that dominate the overall uncertainty, so that priorities can

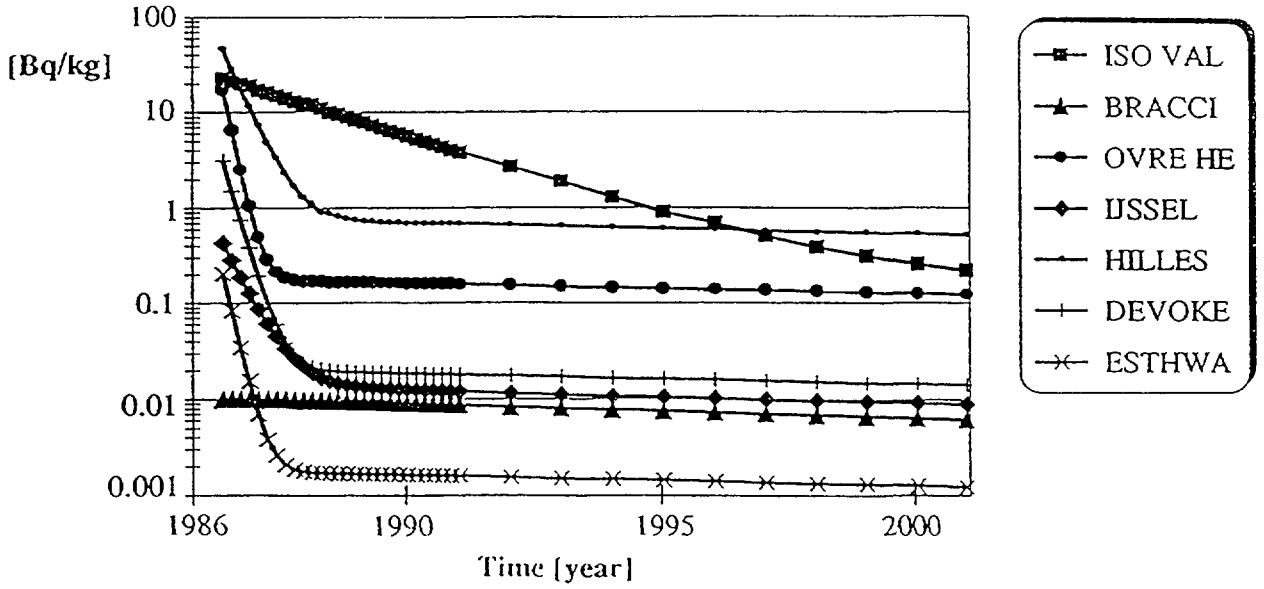

FIG. 5.29A. Predicted ^{137} Cs concentrations in the water of different lakes.

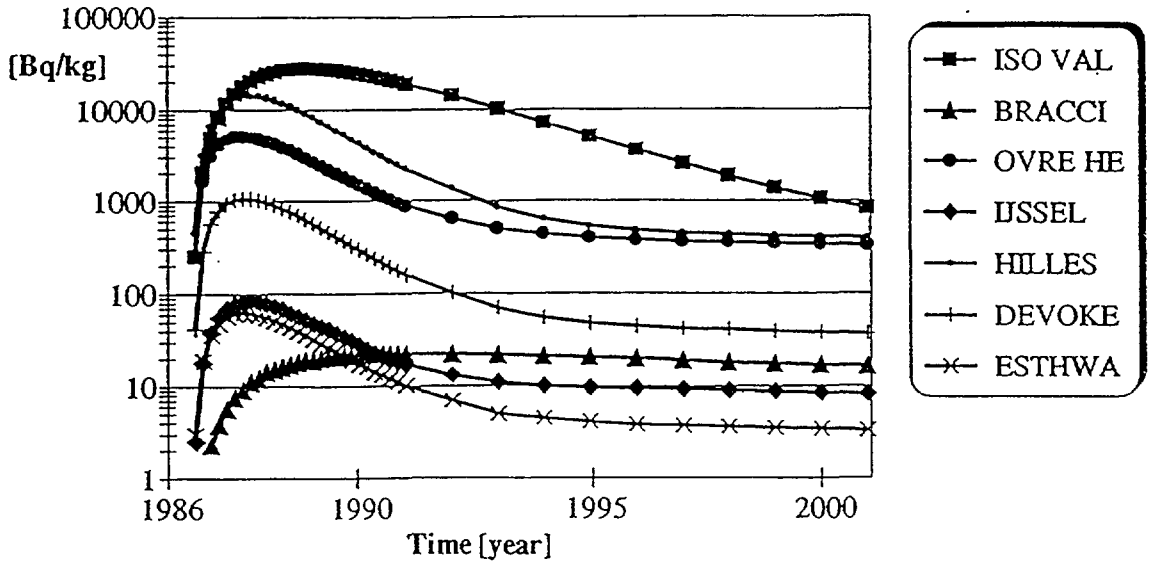

FIG. 5.29B. Predicted ^{137} Cs concentrations in the top predator in different lakes.

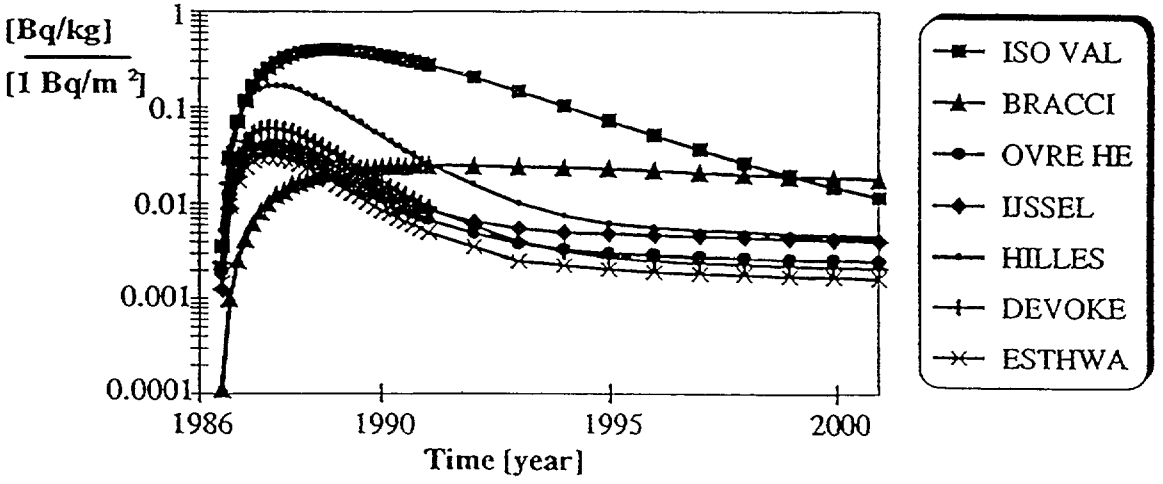

FIG. 5.30. Concentrations (normalized with respect to deposition) in top predator in different lakes.

TABLE 5.10. PREDICTED TOTAL CONCENTRATIONS OF ^{137}Cs (VTT MODEL) AND RATIOS PREDICTED/OBSERVED FOR WATERS OF VARIOUS LAKES AT SELECTED TIME POINTS AFTER THE DEPOSITION

Lake	Date	Predicted concentration in water (Bq/L)	P/O
Iso Valkjärvi	10.06.87– June 1990	14.9 4.5	3.2 2.2
Bracciano	20.05.86 June 1990	0.01 0.009	1.0 0.45
Øvre Heimdalsvatn	12.06.86 June 1990	14.7 0.1	2.7 1.0
IJsselmeer	01.05.86 June 1990	0.5 0.01	2.9 2.1
Hillesjön	15.05.86 June 1990	52 0.7	8.1 0.7
Devoke Water	late July 1986 June 1990	1.6 0.02	6.8 0.83
Esthwaite Water	13.05.86 June 1990	0.3 0.002	1.1 0.06

TABLE 5.11. PREDICTED PEAK AND TAIL CONCENTRATIONS OF ^{137}Cs IN PREDATORY FISH, AND RATIOS PREDICTED/OBSERVED FOR VARIOUS LAKES (VTT MODEL)

Lake	Date	Predicted concentration in predator (Bq/kg)	P/O
Iso Valkjärvi	October 1988 June 1990 June 2040	28 000 (maximum value) 21 700 150	1.0 1.7
Bracciano	June 1990 November 1990 June 2040	22 22.2 (maximum value) 5	4.1 1.6
Øvre Heimdalsvatn	June 1987 June 1990 June 2040	5 020 (maximum value) 1 110 125	1.1 0.57
IJsselmeer	August 1987 June 1990 June 2040	80 (maximum value) 20 3	3.0 3.8
Hillesjön	July 1987 June 1990 June 2040	18 100 (maximum value) 4 870 459	2.1 1.4
Devoke Water	June 1987 June 1990 June 2040	1 060 (maximum value) 210 14	0.76 1.1
Esthwaite Water	June 1987 June 1990 June 2040	60 (maximum value) 10 1	

be set to reduce the uncertainty in model predictions. There are various approaches to uncertainty analysis, but the approach based on Monte Carlo simulations is well matched to the complexity of environmental transfer models. In Section 5.3.1 this approach is used for the KEMA and Studsvik models. However, there may also be considerable uncertainty in empirical data. On the basis of the ENEA, UU models and the VAMP model the concept of empirically based uncertainty analysis is developed and compared with model uncertainty in Section 5.3.2.

5.3.1. Model uncertainty analysis

The KEMA model

In this Section the results of a ranked sensitivity analysis and an uncertainty analysis on the LAKECO lake model are presented. The top predator, perch, in IJsselmeer is selected as an example. For the selected parameters of the lake model, an uncertainty bound by a triangular distribution is estimated based on literature values (Table 5.12). The propagation of these uncertainties is made using the Monte-Carlo method, 1000 runs, with the Latin Hypercube sampling method. Scatter plots show the relationship between the single parameters and one of the output variables (Figure 5.31). The abbreviations in the graphs correspond with the parameter names in Table 5.12. A ranking of sensitivity is also presented on the basis of the use of this Monte-Carlo method. The scatter plots demonstrate that the only significant relationship is the one between the maximum levels in perch and the K_d, especially for K_d in the range 0.1 – 10 m^3/kg. Thus, it is important in the case of eutrophic lakes with high potassium concentrations, where relatively low K_d values can be expected on the basis of the competitive effect of potassium, to have reliable measurements or estimates of the K_d.

TABLE 5.12. UNCERTAINTY ANALYSIS DATA FOR THE KEMA MODEL. PARAMETERS WITH TRIANGULAR DISTRIBUTION WITH UNCERTAINTY BOUNDS (INPUT). RESULTS OF THE PROPAGATION OF ERRORS FOR THE LEVELS OF ^{137}Cs IN PERCH (OUTPUT) ARE ALSO GIVEN

Parameter/variable	Unit	Min	Mode	Max
Input				
Deposition (DEPO)	Bq	2000	2300	2500
K_d (KDW)	m^3/kg	0.1	7.3	250
Susp. matter (SUSP)	kg/m^3	0.03	0.04	0.05
Sediment reworking (RW)	m/d	7.9×10^{-5}	7.9×10^{-4}	16×10^{3}
Porewater turnover (RT)	L/d	7.9×10^{-4}	7.9×10^{-3}	3.9×10^{-2}
Sedimentation (SIGMA)	$kg.m^{-2}\cdot d^{-1}$	1.0×10^{-2}	1.35×10^{-3}	1.5×10^{-3}
BHL zooplankton (THLFZ)	day	4	5	6
BHL smelt (THLFS)	day	50	67	90
BHL perch (THLFP)	day	240	289	350
CF phytoplankton (CF)	L/kg	100	257	2000
Output				
^{137}Cs perch (PERMAX)	Bq/kg ww	1.1	9.5	83

In Table 5.13 the results of the global sensitivity analyses are presented. Instead of constant ranges around the default values, which is usual in local sensitivity analysis, the real uncertainty ranges have been used. The simple correlation coefficient is a measure of the importance of a parameter to the output variable, while the partial correlation coefficient is a measure of the importance of a parameter to the output variable after removing all the linear effects of the other variables. High values correspond to a high level of importance. These parameters are appropriate to evaluate non-linear relationships [5.10].

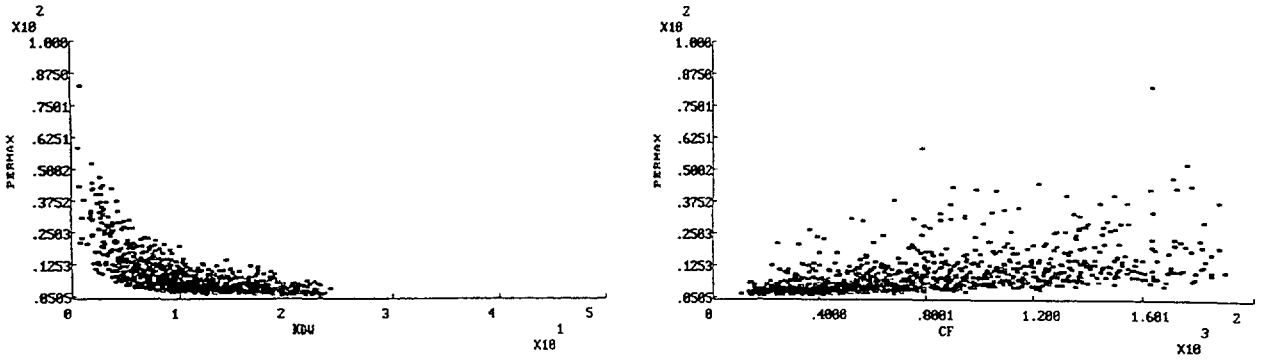

FIG. 5.31. Scatter plots demonstrating the relationship between peak level in perch and the K_d (left), and the CF phytoplankton (right).

The scatter plots and the table demonstrate that there seems to be a linear relationship between the CF and the peak level, and a non-linear relationship between the peak level and the K_d.

TABLE 5.13. RESULTS OF THE GLOBAL SENSITIVITY RUNS: CORRELATIONS OF PEAK LEVEL IN PERCH (PERMAX) WITH INPUT PARAMETERS

Variable coefficient	Simple correlation coefficient	Partial correlation coefficient	Simple ranked correlation coefficient	Partial ranked correlation coefficient
DEPO	-0.01	+0.04	+0.01	+0.30
KDW	-0.63	-0.73	-0.71	-0.96
SUSP	+0.02	-0.06	+0.07	+0.02
RW	+0.06	-0.01	+0.03	-0.22
RT	-0.03	+0.03	-0.04	+0.04
SIGMA	-0.02	-0.01	-0.02	-0.03
THLFZ	+0.06	+0.08	+0.10	+0.38
THLFS	+0.17	+0.23	+0.20	+0.62
THLFP	+0.09	+0.13	+0.12	+0.38
CF	+0.52	+0.65	+0.67	+0.96

The Studsvik model

A statistical parameter analysis has been carried out for two model predictions which describe the turnover of ^{137}Cs within the lakes Hillesjön and Øvre Heimdalsvatn. Results for the concentration of ^{137}Cs in water and trout for Heimdalsvatn and for perch and pike for Hillesjön are given below. The principal aim was to compare and discuss the main parameters contributing to the uncertainty in the model results.

Two different approaches were used for modelling the turnover of ^{137}Cs between the drainage area, the lake water and the sediment. The one applied to Hillesjön uses rate constants based on steady state conditions from the fallout in the 1960s. The other approach used for Heimdalsvatn used K_d values and mass sedimentation rates for obtaining the rate constants from water to sediment. When modelling the transfer of ^{137}Cs from the drainage area to the lake, the available information about type of lake, monthly turnover rate of water and estimations about the variation of deposited amount of ^{137}Cs within the catchment area were taken into consideration. A summary of the main differences in the deposition parameter values used for the two lakes is given in Table 5.14. Personal judgement based on the deposition values was used when estimating the initial source terms to the lakes.

TABLE 5.14. SITE SPECIFIC DEPOSITION PARAMETER VALUES (BEST ESTIMATES AND RANGES)

	Hillesjön	Øvre Heimdalsvatn
Deposition, lake surface (kBq/m^2)	95 (63–125)	180 (28–510)
Deposition, drainage area (kBq/m^2)	63 (53–74)	129 (12–142)
Rate constant, drainage to lake (L/month)	1×10^{-4} ($1 \times 10^{-5} - 1 \times 10^{-3}$)	1×10^{-4} ($1 \times 10^{-5} - 1 \times 10^{-3}$)

The major parameters contributing to the uncertainty in the calculated concentrations of ^{137}Cs in water are shown in Figure 5.32. The parameters are designated as:

Dep drain: the initial deposition of ^{137}Cs in the drainage area,
Drain: the leakage of ^{137}Cs from the drainage area to the lake,
CFZOO: the bioaccumulation factor zooplankton/water,
Dep lake: the initial deposition of ^{137}Cs on the lake surface,
K_d: the distribution coefficient, solid/soluble form,
Sed: the transfer of ^{137}Cs from the water column to the sediments,
Resusp: the resuspension of ^{137}Cs from the sediments back to the water,
CFGAMMA: the bioaccumulation factor *Gammarus* (benthos)/water.

Different parameters contribute in different ways over time to the uncertainty of the calculated concentrations of ^{137}Cs in water, especially for Øvre Heimdalsvatn (Figure 5.32A). The parameters also differ substantially between the lakes. The main parameter contributing to the uncertainty in the predictions of ^{137}Cs in water in Øvre Heimdalsvatn during the first year after deposition is the K_d. Also the amount of ^{137}Cs deposited directly on the lake (Dep lake) contributes significantly to the uncertainties in the predictions. After 18 months, the leakage of ^{137}Cs to the lake water from the drainage area contributes significantly; later on this is the main parameter contributing to the uncertainty. This implies that, according to this model, the leakage from the watershed should be the main process maintaining the ^{137}Cs concentrations in the water. In the model, this leakage is estimated to be about 0.12% of the total deposition. These results agree with the high variability of ^{137}Cs deposition in the drainage area. The initial contribution from the value of the bioaccumulation factor for zooplankton is unexpected and needs further analysis.

In contrast to Øvre Heimdalsvatn, different processes contribute most to the uncertainty in the concentrations of ^{137}Cs in the water of Hillesjön (Figure 5.32B). From November 1986 onwards the resuspension of ^{137}Cs from the sediments seems to be the main contributing process to the uncertainties in the calculated results. Hillesjön is located in an open, flat landscape, and the lake is also shallower than Øvre Heimdalsvatn. These model results are confirmed by measurements carried out in the lake [5.11]. However, with time the parameter describing the leakage from the drainage area will also contribute to the uncertainty. However, the transfer of ^{137}Cs to the sediments from the water column plays a greater role for this lake over a longer period of time than for Øvre Heimdalsvatn.

The parameters contributing to more than about 10% uncertainty in the concentration of ^{137}Cs in the trout in Heimdalsvatn are shown in Figure 5.33A. The abbreviations of the parameters are explained above. In analogy with the results for ^{137}Cs in the water, the value of K_d is initially more important than later on. In this case, however, its contribution lasts for a longer period of time than for ^{137}Cs in the water. This is probably because of the delayed response of ^{137}Cs in fish compared to the water. The analyses showed that the main parameter to the uncertainty after the first two years was

the value of the bioaccumulation factor to *Gammarus*. This is in agreement with the method used for modelling the uptake of ^{137}Cs in fish. In this model the uptake of ^{137}Cs of fish was considered to be caused by their fractional uptake of ^{137}Cs in food *(Gammarus)*. The increase in the ^{137}Cs levels in fish was due to the metabolic turnover time of ^{137}Cs in the food web. The initial deposition onto the lake also plays an important role during the first five years after the fallout. After that, the importance of the secondary load of ^{137}Cs from the drainage area increased.

The major parameters contributing to the uncertainty for the predictions of ^{137}Cs in perch and pike in Hillesjön are shown in Figures 5.33B and 5.33C. The parameters are the same, although with varying percentage contributions. In this model, the uptake of ^{137}Cs to the fish is also based on their

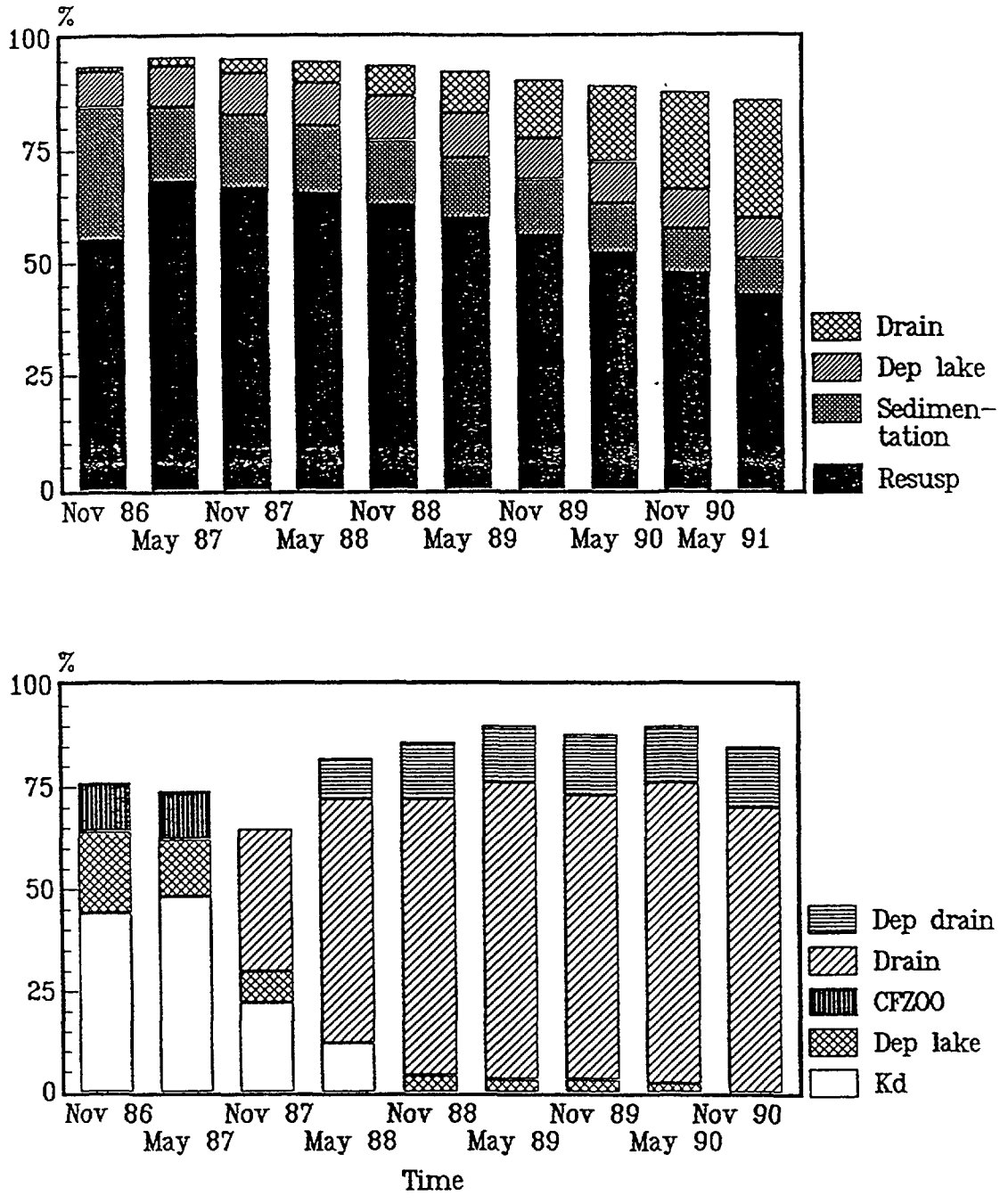

FIG. 5.32. Dominant parameters for the uncertainty in predicted ^{137}Cs concentration in water for Hillesjön (top) and Øvre Heimdalsvatn (bottom).

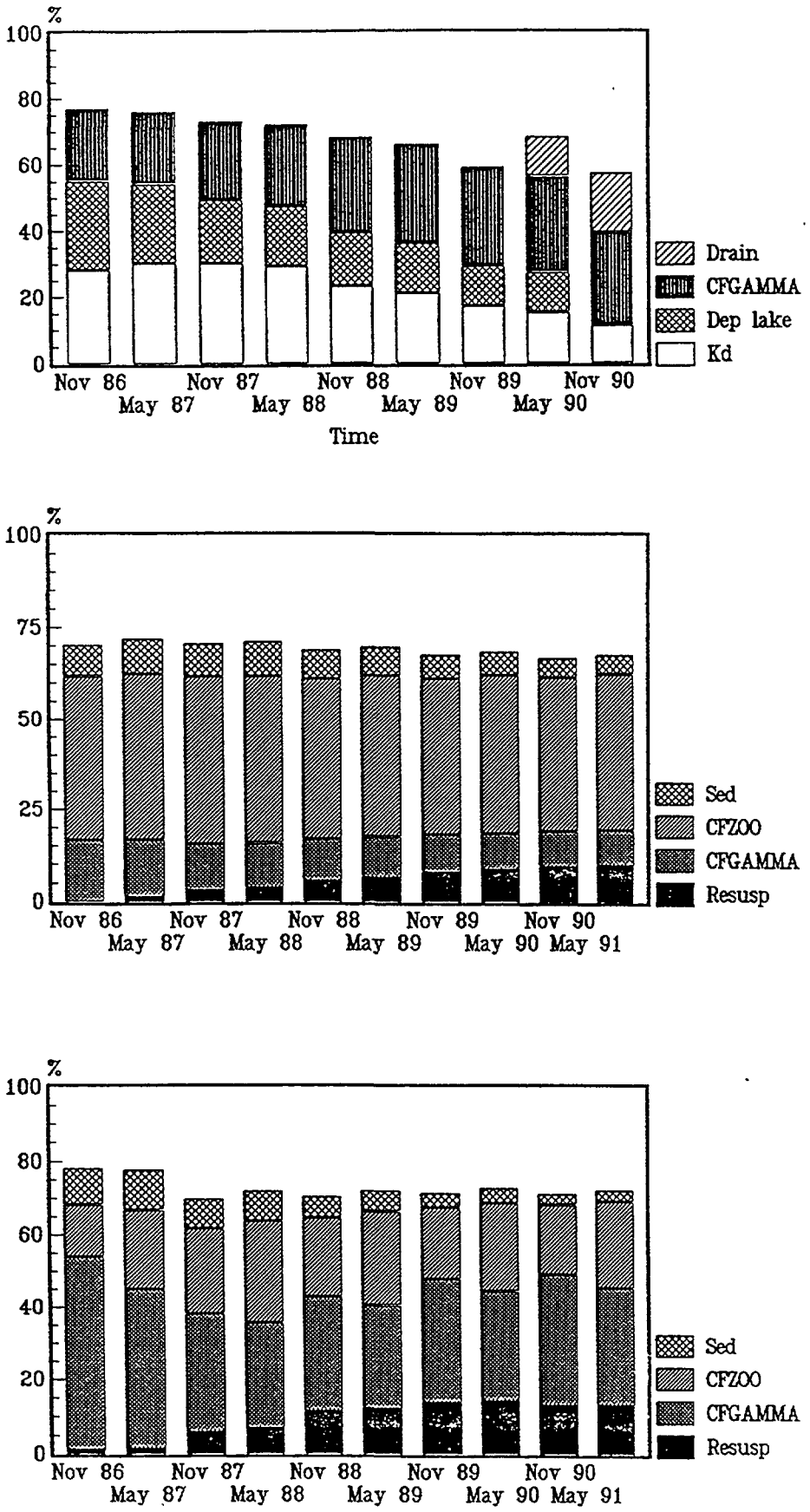

FIG. 5.33. Dominant parameters for the uncertainty in predicted ^{137}Cs concentration in trout from Øvre Heimdalsvatn (top), and in pike (middle) and perch (bottom) from Hillesjön.

position in the food chain. Perch has a mixed diet, while pike is a top predator, consuming only fish. The uptake by the non-piscivorous roach is modelled in the same way as that of trout in Heimdalsvatn, taking into consideration that roach consumes zooplankton instead of benthos. For the first time period, the analysis did not show any contributions to the uncertainty in the concentrations of ^{137}Cs in fish from transport of ^{137}Cs from the drainage to the lake. The importance of the resuspension from the bottom sediments to the lake water increases with time for both fish species. The opposite is valid for the transfer of ^{137}Cs from the water to the sediments.

5.3.2. Comparison of empirical and model uncertainty

The values of the parameters used in environmental mathematical models are often affected by wide uncertainty levels. The experimental values of each model parameter are characterized by a probability distribution (normal, log-normal, triangular etc.) and related "statistics" (mean value, variance, etc.). The uncertainty of the parameters reflects on the model results. The aim of the model uncertainty analysis is to appraise how parameter uncertainties influence the model output, identifying and evaluating the probability distribution and related "statistics" of the model predictions. The above discussion may be easily generalized to also include factors other than parameter uncertainty. The following equation:

$$L(\omega_1,...,\omega_n;t)X(t)=Y(t) \tag{5.5}$$

where t is the time, X(t) is a vector whose components are the quantities to model, Y(t) is a vector whose components are the input functions (for instance the radionuclide deposition rates) and L is a stochastic operator depending on the time and on the stochastic variables $\omega_1,...,\omega_n$, represents the more general formulation of a model. The solutions X(t) of the model is a set of stochastic functions of time. This general equation includes the uncertainty due to stochastic variations in the model "structure", corresponding to the change of the mathematical form of the operator L.

The uncertainty analysis of the model output aims to evaluate the "confidence intervals at confidence level α" with endpoints 0_1, 0_2 around the output values of a modelled quantity (for instance the radionuclide concentration in water, in sediment, in fish, etc.) such that:

$$P(0_1 \le E \le 0_2)=\alpha \tag{5.6}$$

where $P(0_1 \le E \le 0_2)$ is the probability that, at time t, the model output lies within to the interval $[0_1, 0_2]$. Of course 0_1 and 0_2 are generally functions of time. In the {time, model output} plane, the equation 5.6 represents a region: the probability that an output value belongs to this region is α. Such a region may be also given by as a set of curves representing possible outputs of the model, each output being evaluated using a specific set of values of the model parameters.

As the experimental or empirical values of the modelled quantities are affected by random measurement errors, the validation of the model is based on the comparison of two statistical distributions: experimental values versus model results. If the experimental errors of the measured quantities are negligible compared with the uncertainty of the model output and if the model output agrees with the experimental data, the probability that an experimental value belongs to the region defined by equation 5.6 is α.

Unfortunately these hypotheses are generally hard to verify. Indeed, experimental data are often associated with large uncertainty, while model outputs may show significant discrepancies compared to experimental values. Moreover, the comparison of the above mentioned statistical distribution (model versus experimental data), requires large amount of information (knowledge of the distributions of model parameters and of experimental data) and complex calculations. The validation of a model is then carried out by various techniques that, although not complete and rigorous from a mathematical

point of view, nevertheless allow an approximate, objective appraisal of the agreement between the model predictions and the experimental data (see section of "model validation").

The uncertainty analysis of model output entails similar difficulties. In the next Section a simple method for evaluating the uncertainty of the model output is described. This method is based on the comparison of model results with experimental values relevant to different sites. It is applicable when the statistical distributions of model parameters are not known, but a number of experimental evaluations of the modelled quantities carried out in various conditions are available.

Empirically based uncertainty analysis

The model output is function of time and of model parameters:

$$0(t;\mu_1^k,...,\mu_n^k;\nu_1,...,\nu_1) \tag{5.7}$$

μ_i^k represents the "site specific parameters" whose values show negligible uncertainty and are available for each site (identified by k), ν_1 represent "generic" parameters for which site specific values are not available. In the case of lake systems, "site specific" parameters are, for instance, depth, surface area, water volume, amount of suspended matter; "generic" parameters include the radionuclide migration rate from sediments to water, from bottom sediments to deep sediments, etc. Of course, the classification of a parameter as "generic" or "site specific" is, to a large extent, arbitrary, depending on the availability of relevant data and on the state of the art of measurement techniques. Let us suppose that the uncertainties (in terms of distribution functions and of related statistics) of the generic parameter values are not known. For a specific set of values of ν_i it is possible to compare the model output with the experimental values measured at different sites (i.e. in different lakes). For instance, it is possible to evaluate the empirical distribution of the following stochastic variables:

$$D(k)=0(t;\mu_1^k,...,\mu_n^k;\nu_1...\nu_l)/E_k(t) \tag{5.8}$$

or

$$D(k)=0(t;\mu_1^k,...,\mu_k^n;\nu_1,...,\nu_l)-E_k(t) \tag{5.9}$$

where k identifies the site and $E_k(t)$ is the experimental value, measured at time t in site k, of the modelled quantity. A knowledge of the statistical distribution of D(k) allows evaluation of the probability that $O(t;\mu_1^k,...,\mu_n^k;\nu_1,...,\nu_l)$ lies within a specific confidence interval around $E_k(t)$. However, the method has some disadvantages:

(a) it is often difficult or impossible to identify the distribution of D(k);
(b) there are generally not sufficient data to evaluate the distribution of D(k) as function of t.

To avoid the second difficulty, it is possible to identify certain functions that summarize the comparison of the model output with the experimental values in a single real number evaluated over the entire interval of time for which experimental and predicted data are available. The following example explains this approach.

This method is based on the evaluation of the "functional distance" between the experimental data and the model output for a specific site:

$$d^2=\sum_1^n (ln_{E_i}-ln_{0_i})^2/n \tag{5.10}$$

E_i and 0_i are respectively the i^{th} experimental value and the corresponding prediction; n is the number of available experimental data. The functional distance d shows certain characteristics:

(a) d is a positive number that depends solely on the ratio E/O;
(b) overestimates and underestimates of experimental data by the model are not compensated in the equation defining the functional distance.

For example, if the ratios between the experimental data and the model were on average a factor of 2, $d^2 = 0.48$; if these ratios were equal to a factor of 10, $d^2 \approx 5.3$. Parameter d may be intended as a "quality index" of the model predictions, being strictly related to the performances of the model. Values of d very close to 0 indicate a good agreement of model output with experimental data. If d>>0, the model output agrees poorly with experimental values.

The comparison was carried out using the logarithm values of the measured and the predicted quantities. This choice was due to two main characteristics of the distribution of the experimental data:

(a) the ranges of variation of the experimental data, in time and from one site to the other, are very large (orders of magnitude);
(b) in most cases the statistical distribution of the experimental values, showing a marked asymmetrical shape, are approximately log-normal. Figure 5.34 shows the distribution of d for the ENEA model applied to 7 lakes: Vico, Bracciano, Hillesjön, Iso Valkjärvi, Esthwaite Water, East Twin and IJsselmeer [5.12]. The distribution of d is assumed to be approximately log-normal.

The evaluation of the standard deviation of d allows the estimation of the confidence interval of the functional distance d. The experimental data analysed in this case suggest that the geometric mean of d is 0.44, the arithmetic mean of d is 0.56, the arithmetic mean of d^2 is 0.445 and the standard deviation of lnd is 0.758.

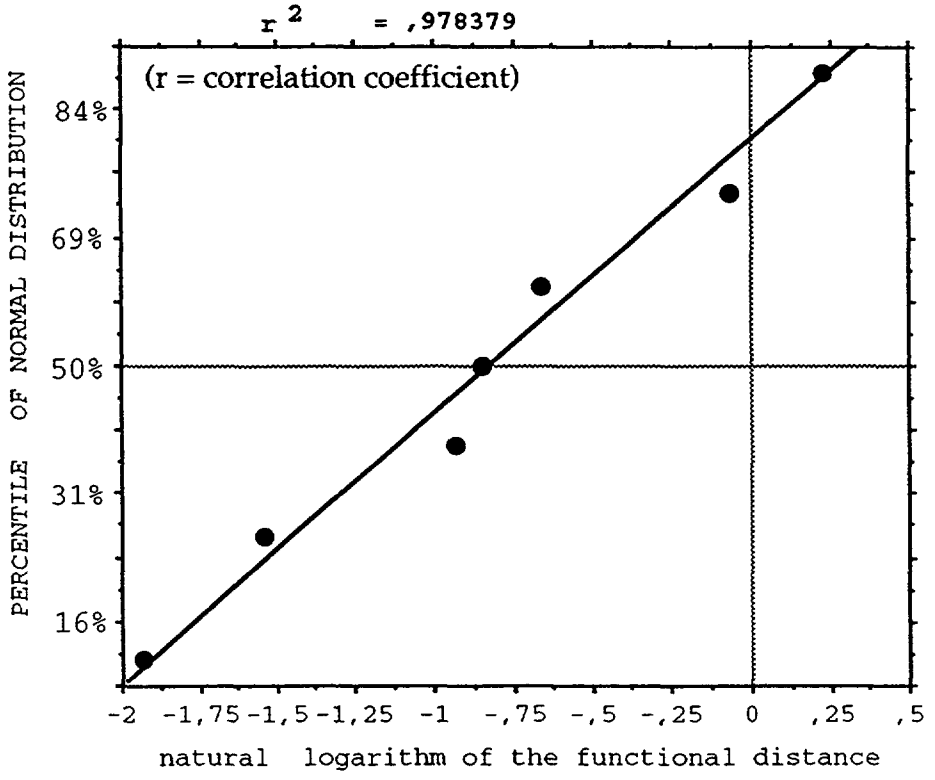

FIG. 5.34. Distribution of the natural logarithm of the "distance d".

The probability that lnd < -0.469 (-0.469=ln0.44 + 0.465 × 0.758; 0.465 is the 68% percentile of the cumulative normal distribution function) is 68%. This means that the average value of $(\ln E - \ln 0)^2$ is less than 0.391. If ln(E/0) shows a normal distribution with mean value μ and variance σ^2, it is possible to show that

$$\langle d^2 \rangle = \sigma^2 + \mu^2 \tag{5.11}$$

where $\langle d^2 \rangle$ is the arithmetic mean of d^2. If $\mu^2 << \sigma^2$ (the model output is not biased) we get

$$\sigma = \sqrt{(\langle d^2 \rangle)} \tag{5.12}$$

for the ENEA model, $\sigma = 0.667$ which corresponds to the following approximate confidence interval for E/0 (68% confidence level): $0.5 < E/0 < 2$.

The functional distance also depends on the uncertainty of experimental data: high values of d may be due both to model inaccuracy in predicting the experimental values and to the uncertainty of experimental values.

Uncertainty in empirical data

Before comparing empirical data to modelled values, it seems appropriate to discuss the uncertainty in the empirical data. Several approaches to this problem exists, and the aim here is to show that the results and interpretations could, in fact, depend very much on the method selected. This will be illustrated by using three different methods.

Table 5.15 illustrates available data for one of the VAMP lakes, Devoke Water. Month 1 is January 1986. Data exists from month 8 till month 64 for ^{137}Cs in lake water, small perch (perch < 20 g, SP), large perch (> 20 g, LP) and trout. Since it is very interesting to predict "the peak and the tail", i.e., the maximum values and the recovery process, we will look at the uncertainties of the empirical data for:

(1) Individual analyses of water samples and fish from the same sampling occasion. This method is, probably, the most common and straightforward to address uncertainty in empirical values;
(2) The maximum values (the "peak"), i.e. the correspondence between empirical maximum values and modelled values for the same month;
(3) The temporal data (the "tail"), i.e. the correspondence between empirical data and modelled values for a given period.

The third method is illustrated in Table 5.15. The empirical uncertainties are given by the SD-values and mean values, in italics, like SD = 398 for MV = 1167 for large perch for month 10. The bold rectangles give the maximum empirical values, like 0.24 Bq/L for month 8 for Cs in water. The modelled value for month 8 will be compared with this value. The same principles apply to the value 2092 Bq/kg ww for lake perch for month 14 and 1383 Bq/kg fresh ww for trout for month 14. This comparison will be called method 2, max. values. The set-up for the "tail" test, method 3, is also given in Table 5.15. The column of empirical data for trout, starting with 779 Bq/kg ww for month 9 and ending with 120 Bq/kg ww for month 64 will be compared to modelled values.

The uncertainty of this series of data can be tested by copying the column containing trout data and pasting it in so that data for April are compared to data from March, etc. By doing so we obtain two empirical sets of data, Emp1 and Emp2. In a steady state they should be identical. Note, (i) that all data from the first half year after the Chernobyl accident (i.e. data up to September 1986) have been excluded in this test since the conditions then were most variable, and significant changes took place, especially in lake water and planktivorous fish, from one month to the next, and (ii) that in order to get enough data from adjacent months, from 1988 of data three months apart were accepted (but not

TABLE 5.15. EMPIRICAL DATA FOR RADIOCAESIUM IN WATER, SMALL PERCH, LARGE PERCH AND TROUT IN DEVOKE WATER

Month 1=Jan-86	Water Bq/l n	Water Bq/l MV	Perch -20 ww Bq/kg n	Perch -20 ww Bq/kg MV	Perch 20- ww Bq/kg n	Perch 20- ww Bq/kg MV	SD	2*CV for n≥4	Brown trout Bq/kg n	Brown trout Bq/kg MV Emp1	Brown trout Bq/kg MV Emp2	SD	2*CV for n≥4
8	4	0,24											
9			1	1312	1	1502			9	779		449	1,15
10					6	*1167*	*398*	0,68					
11	4	0,15											
12					2	*1375*	*359*		5	1032		351	0,68
13													
14	5	0,10			10	2092	*258*	0,25	7	1383	842	555	0,80
15					19	*1573*	*517*	0,66	12	842	633	356	0,85
16	12	0,08			6	*1222*	*239*	0,39	11	633	216	526	1,66
17					16	*1466*	*473*	0,65	10	216	679	230	2,13
18					8	*1457*	*371*	0,51	6	679	678	120	0,35
19	7	*0,08*			*1*	*1610*			*16*	*678*	*1201*	*435*	*1,28*
20					6	*1637*	*761*	0,93	4	1201	374	318	0,53
21	7	0,06			6	*1663*	*560*	0,67	4	374	653	221	1,18
22			1	641					9	653	470	375	1,15
23			2	443	1	*1279*			9	470	420	209	0,89
24													
25									7	420		175	0,83
26	9	0,06											
27					2	*1476*	*134*		24	376		141	0,75
28													
29			3	1361					9	338	422		
30	6	0,05	14	797					5	422	348		
31			9	540					10	348	110		
32			12	981					1	110	431		
33	6	0,04	6	549					7	431	235		
34			3	860					9	235	380		
35													
36	6	0,04							8	380	325		
37													
38	6	0,03							9	325	344		
39													
40													
41	6	0,02	4	356					3	344	179		
42	6	0,04							3	179	278		
43									4	278			
44			4	832									
47	6	0,03				*1330*			9	239	195		
53	1	0,02			9	*1334*			9	195			
56			6	672									
64	6	0,03							1	120			
							MV:	0,59					1,02

more), like 235 Bq/kg ww for month 38 and 344 Bq/kg ww for month 41. This gives data for a very interesting comparison since this is the manner in which modelled values are often compared to empirical data. The measured value M(t) (Emp1) may be considered as the sum of a non-stochastic variable V(t) (the "expected" value at time t) and of a random variable $\xi(t)$ (the error associated to the measurement). It is supposed that $\xi(t)$ is independent on the value of $\xi(\check{t})$ ($t \neq \check{t}$) such that:

$$cov(\xi(t),\xi(t'))=0 \quad for\ every\ t \neq t' \tag{5.13}$$

The "translated" data series is (Emp2):

$$M'(t)=V(t+\Delta t)+\xi(t+\Delta t) \tag{5.14}$$

As $\xi(t)$ and V(t) are independent, we get:

$$|cov(\xi(t),V(t+\Delta t))| \ll |cov(V(t),V(t+\Delta t))| \tag{5.15}$$

$$|cov(V(t),\xi(t+\Delta t))| \ll |cov(V(t),V(t+\Delta t))| \tag{5.16}$$

From (5.13), (5.15) and (5.16) it follows:

$$cov(M(t),M'(t)) = cov(V(t),V(t+\Delta t)) \tag{5.17}$$

From the above equation, we get, if $\Delta t \rightarrow 0$:

$$cov(M(t),M'(t)) = var(V(t)) \tag{5.18}$$

If V(t) is a "regular" function and if Δt is "enough" small, we get:

$$cov(M(t),M'(t)) \approx var(V(t)) \tag{5.19}$$

The correlation coefficient, r, between M(t) and M(t+Δt) is

$$r = \frac{cov(M(t),M(t+\Delta t))}{\sqrt{var(M(t))var(M(t+\Delta t))}} \tag{5.20}$$

From equation (5.18) it follows:

$$r \approx \frac{var(V(t))}{var(M(t))} \tag{5.21}$$

As ξ(t) and O(t) are independent, we get:

$$cov\ (M(t),O(t)) \approx cov\ (V(t),O(t)) \tag{5.22}$$

From equation 5.22 it follows:

$$r_{mp} \approx \frac{cov(V(t),O(t))}{\sqrt{var(M(t))var(O(t))}} \tag{5.23}$$

where r_{mp} is the correlation coefficient between the predicted and the experimental values. When var (ξ(t)) = 0 we get for every t:

$$r_{\lim} \approx \frac{cov(V(t),O(t))}{\sqrt{var(V(t))var(O(t))}} \tag{5.24}$$

where r_{lim} is the correlation coefficient between the "expected" experimental values and the model results. From equation (5.21) it follows:

$$r_{\lim} \approx \frac{r_{mp}}{\sqrt{r}} \tag{5.25}$$

Equation (5.25) allows approximate evaluation of the correlation coefficient between the experimental "expected" data and the predicted values. The correlation coefficient r_{lim} is more reliable than coefficient r_{mp} to assess the model performances in case of comparison of the performances of various models with data relevant to different sites. From the above equations, it is possible to derive some properties of the correlation coefficients.

Of course, due to the approximations, the calculated value of r_{lim} may be, in some cases higher than 1. These parameters must be considered a "quality index" for the model. Equation (5.25) states that the correlation coefficient from the experimental results and the model predictions is strongly affected by the data uncertainty. Low values of r_{mp}, that may be due to high uncertainty of experimental data, do not necessarily mean that the model scarcely predicts the experimental values. r_{mp} and r_{lim} are "quality indexes" of a model. Whereas the values of r_{mp} and "d" (the functional distance) are affected by the uncertainty of experimental data used to validate the model, r_{lim} is strictly related to the model performance.

Figure 5.35 gives the results related to method 1, uncertainty in empirical data. Figure 5.35A first gives the direct results for trout in Devoke Water. This is a graphical display of the information given in Table 5.14, except that 2 SD instead of 1 SD have been used. The reason for this is simply that ± 2 SD corresponds to $\pm 95\%$ confidence limits. The mean values vary very considerably, the peak value, 1383 Bq/kg fresh w.w., being attained during month 14, and after this there is an uneven general decrease with time. The spread around the mean value is initially very large, but decreases with time. This is the result for one species of fish in one lake. Figure 5.35B gives the same results for all fish data for all the VAMP lakes. In this figure, the relative standard deviations (2 CV) are compared to the number of fish analysed (N). The assumption was that a negative correlation may exist such that greater uncertainties might occur if N is small. This does not seem to be the case. The most important factor for the uncertainty is the time after the fallout – the uncertainty decreasing with time (Figure 5.36). The mean CV is 0.55 with a large standard deviation (0.35). The application of this mean, standardized empirical uncertainty to the data on trout from Devoke Water is described in Figure 5.35C. This graph could be compared with that in Figure 5.35A. This is a demonstration of an approximate, standardized method to describe the uncertainty of all empirical fish data.

Figure 5.36 gives a compilation of CV values for the data for the VAMP lakes. Figure 5.36A shows (for water, whitefish, small perch, trout, large perch and pike) that there is a weak negative trend ($r^2 = 0.035$, $p = 0.018$), i.e. CV decreases with time after the Chernobyl accident, but Figures 5.36B–E show that this trend is not apparent at all for many species of fish in several lakes (e.g. for trout in Øvre Heimdalsvatn, in Figure 5.36D, or for small perch in Hillesjön in Figure 5.36C). It can be noted that very high CV values occur; there are many CV values larger than 0.5, and a few even larger than 1. This indicates the great empirical uncertainties in the Cs data for the VAMP lakes. Such uncertainties will be discussed in more detail later on. The results in Figure 5.36 are intended to be used as background information in the discussions on the factors of importance for the optimal size of predictive models for radiocaesium in lakes.

Model validation

The empirical uncertainties will now be compared with modelled uncertainties. Figure 5.37A gives a comparison between peak values from the VAMP LAKE model and empirical peak values (for the same month; according to method 2) for caesium in water (for the 7 VAMP lakes) and in fish (Figure 5.37B, for the 18 available data-pairs). The figure also gives the regression lines and the statistics. It can be noted that the VAMP LAKE model generally predicts the maximum values better in fish than in water ($r^2 = 0.95$ and 0.86, respectively, and the slope is 0.921 and 0.805, respectively). The figure also gives the 95% confidence interval for the predicted y. The confidence intervals are not exactly parallel to the regression line, but almost. 2 SD [from the mean value log (VAMP-mod) = 0 and 2.5, respectively] for the VAMP LAKE model are 0.81 for water and 0.60 for fish. This is a simple method to validate a model and to express the uncertainty of the predicted maximum values. This expression for model uncertainty (2 SD in Figure 5.37) can be compared with the empirical uncertainty (2 CV in Figure 5.35).

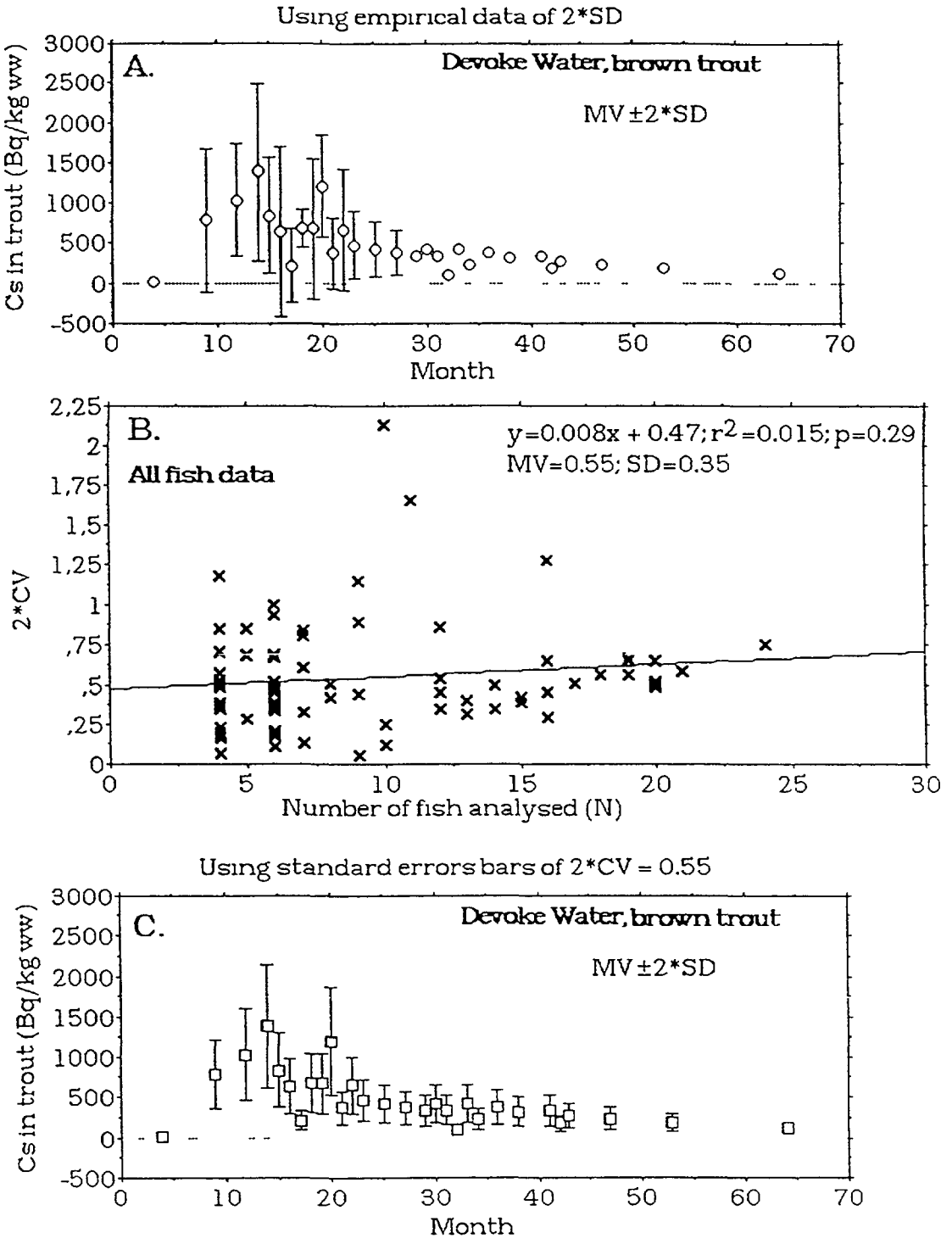

FIG. 5 35. Empirical uncertainties according to method 1.

A. The mean values and standard deviations for trout in Devoke Water. Month 1 is January 1986.

B. Compilation of all available relative standard deviations (or coefficients of variation, CV) for the entire data set for the VAMP lakes. Statistics illustrating the relationship between 2CV (≈ 95% conf. limits) and the number of fish analysed of each species in each lake.

C. Illustration of mean values and standardized empirical uncertainty limits (2CV = 0.55) for trout in Devoke Water.

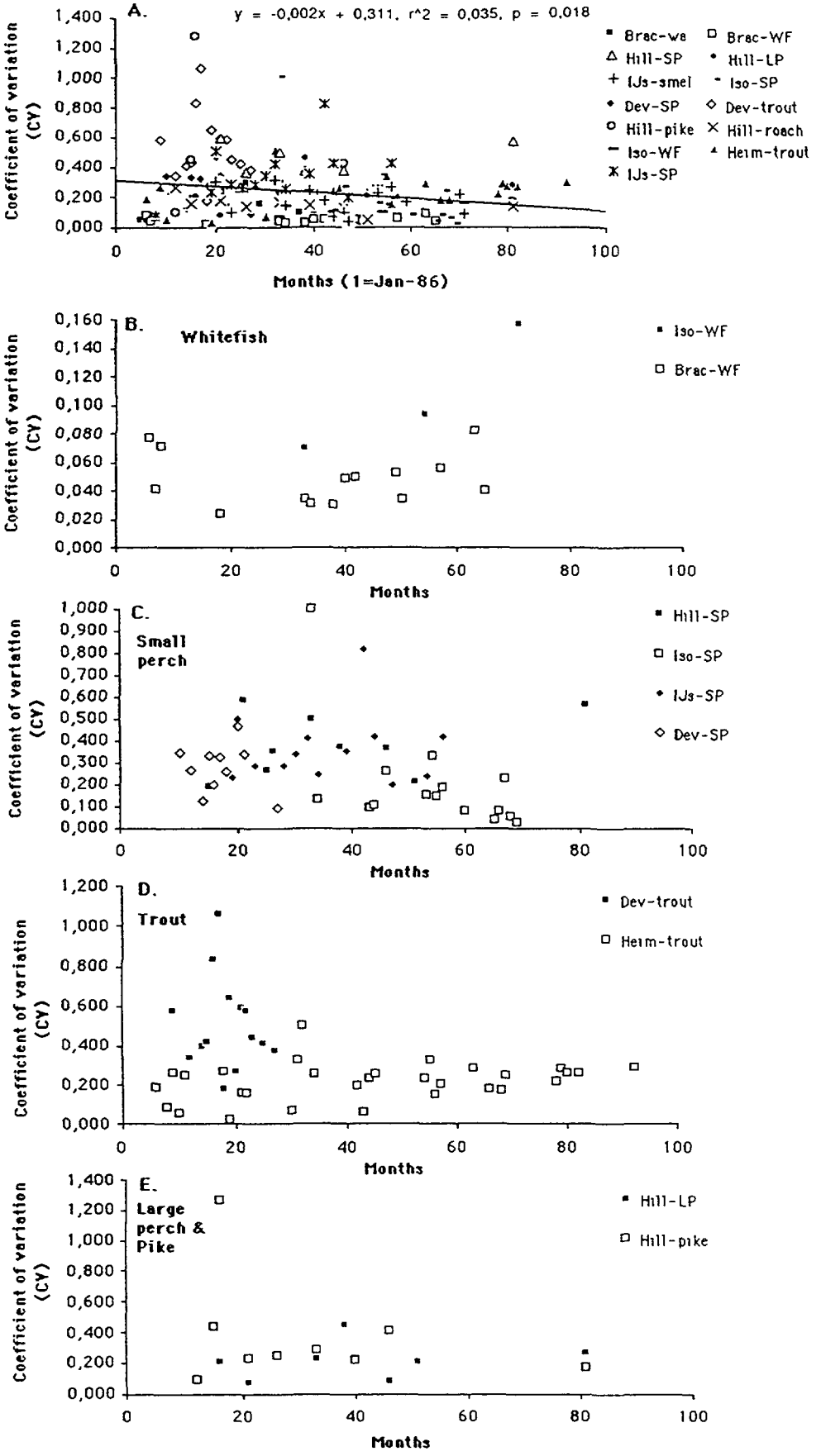

FIG. 5.36. Compilation of CV-values for the VAMP lakes.

Brac = Bracciano, Dev = Devoke, Heim = Øvre Heimdalsvatn, Hill = Hillesjön, IJs = IJsselmeer, Iso = Iso Valkjärvi; SP = small perch, LP = large perch, WF = whitefish.

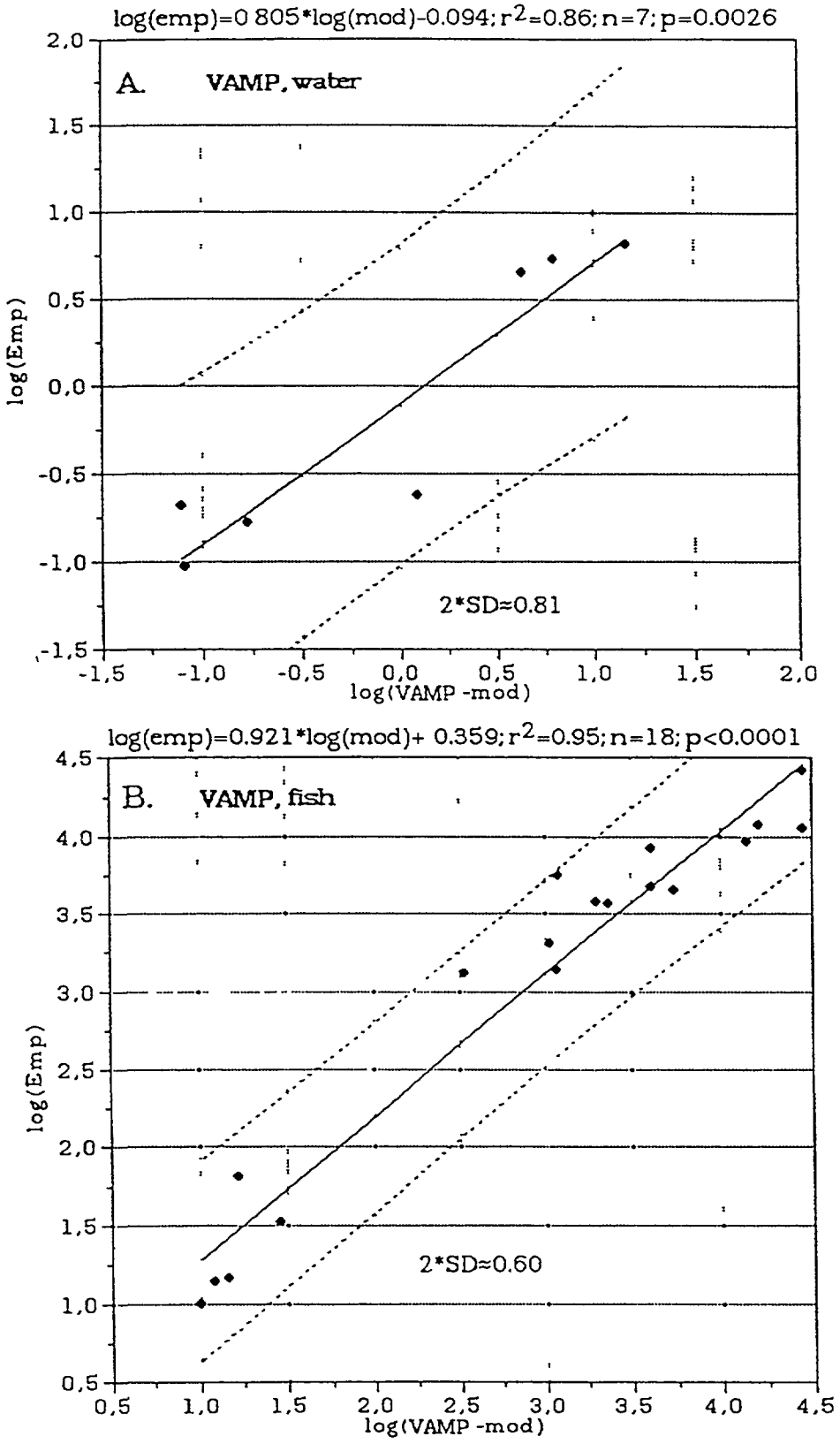

FIG. 5.37. Comparison between maximum empirical data and corresponding values predicted by the VAMP LAKE model for (A) Cs in lake water and (B) Cs in all types of fish. Statistics and 95% confidence limits for the predicted y. The values for 2SD (0.81 for water and 0.60 for fish) describe the smallest distance (in y-direction) between the regression line and the 95% confidence interval as a simple measure of model uncertainty determined by these validations.

Results for trout in Devoke Water are given in Figure 5.38. Here the standardized empirical uncertainty (2 CV = 0.55) gives rather narrow uncertainty limits around the empirical mean values. In Figure 5.38B, a direct comparison to the model uncertainty is made, as expressed by the limits given by 2 SD (= $10^{0.60}$). With this approach, the expected result is obtained: the model predictions give wider uncertainty limits than the empirical data.

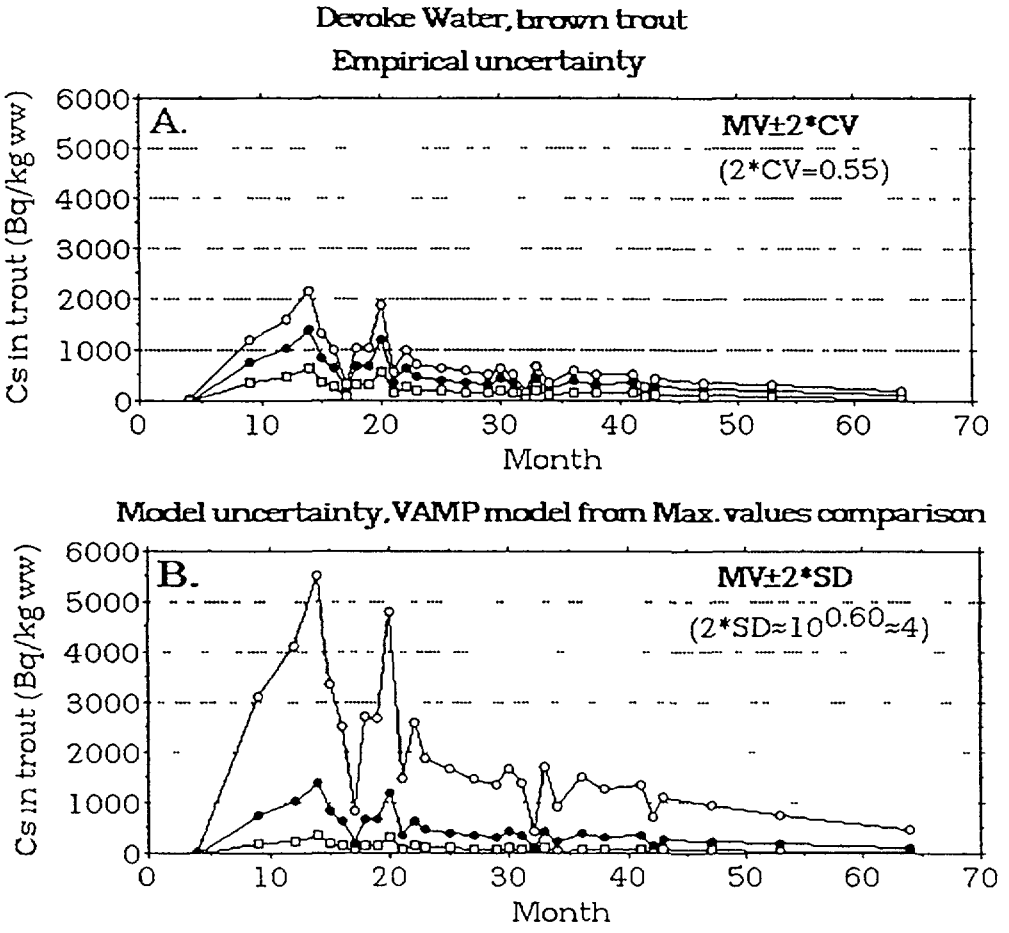

FIG. 5.38. Comparison between uncertainties in (A) empirical data (from the results given in Figure 5.35B), and (B) uncertainties related to the prediction by the VAMP LAKE model (from the results presented in figure 5.37B) for brown trout in Devoke Water.

Figure 5.39 gives a more comprehensive comparison between predicted peak values and empirical peak values (according to method 2) when the data for water and fish have not been separated, as in Figure 5.36. Figure 5.39A shows that the VAMP LAKE model can, in fact, predict maximum values of caesium in water and fish very accurately. The r^2 value is 0.97 for the 25 data-pairs (for logarithmic values). The mixed model (Figure 5.39B) also gives similar predictions; the r^2 value is also 0.97 for this model. This is somewhat surprising since the mixed model is very small. It does not account for many processes perceived to be important. The largest generic model (Figure 5.39C) gives the lowest r^2 value (0.91), but this is mainly due to one outlier, namely large perch in Devoke Water. If this point is omitted, the r^2 value is 0.97. Figure 5.39D gives the results when the two empirical data sets are compared in the same way. An expected very high r^2 value (0.987) is obtained.

It is also interesting to look at how the different models predict in individual lakes and for different species of fish, and especially to study how various processes and model components affect the predictions. It is, however, beyond the objective of this Section to address such issues in detail. A few examples are given, however. The first example (Figure 5.40) concerns the Finnish lake, Iso

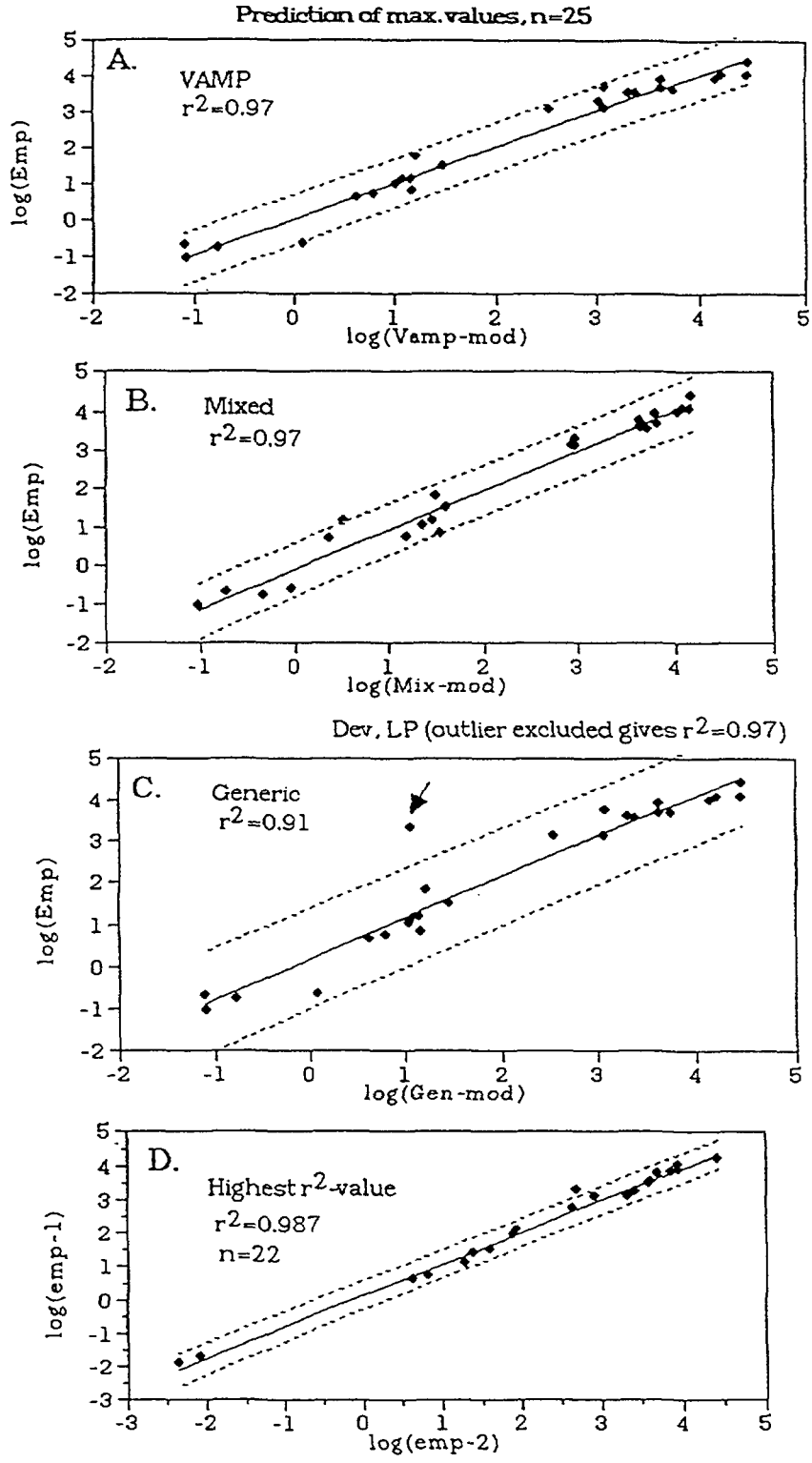

FIG. 5.39. A compilation of validation tests (empirical data versus modelled values) for (A) the VAMP LAKE model, (B) the UU-Mixed model, (C) the UU-Generic model, and (D) the test of the two empirical data sets called Emp1 and Emp2 for caesium in water and fish in Devoke Water. Note that this figure gives a regression (regression line and the 95% confidence interval) for logarithmic data.

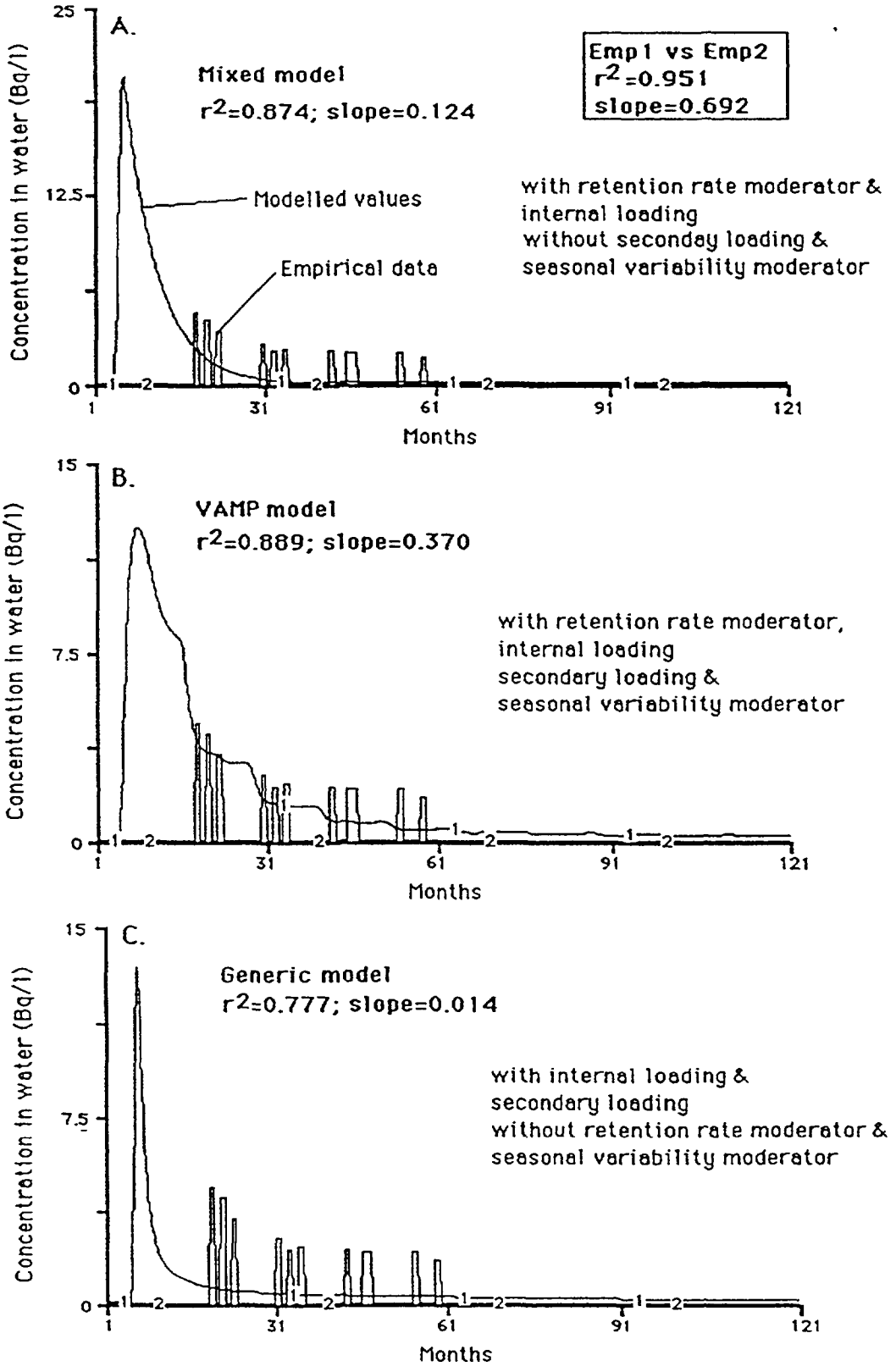

FIG. 5.40. Validation results for caesium in water in Iso Valkjärvi. (A) the UU-Mixed model, (B) the VAMP LAKE model, and (C) the UU-Generic model. The figure also lists the processes influencing the recovery accounted for (and not accounted for) in the three models, and the results from the comparison between the two empirical data sets, Emp1 and Emp2.

Valkjärvi. Figure 5.40A shows that there is a good correspondence between the two data series, Emp1 and Emp2 for caesium in water in this lake, $r^2 = 0.951$. The slope is 0.692, which is expected – the values should be higher for Emp2 since these data are from a month before the data given by Emp1. It can be noted that the small mixed model gives rather poor predictions in this case; r^2 is 0.874, which is reasonable, but the slope is very low, only 0.124. Similarly, the graph (Figure 5.40A), which shows that the mixed model provides very poor predictions for the "tail" values: The empirical data are much higher than the modelled values. This model accounts for the water retention rate and internal loading, but it does not account for secondary loading from the catchment or for seasonal variability in water discharge.

The VAMP LAKE model gives the best predictions in this example. The r^2 value is highest, 0.889, and the slope is closest to 1 (0.370). This model accounts for all the four given processes affecting the recovery process, i.e. the "tail" values, and a much better correspondence between modelled values and empirical data is obtained. However, also in this case, it can be noted that the slope is far from the ideal value of 1.0. The UU-Generic model gives very poor predictions indeed and the slope is 0.014.

It should be stressed that this example of caesium in water in Iso Valkjärvi has been selected to illustrate the importance of the factors included in the definition of predictive power, the r^2 value, the slope and the coefficient of variation. The idea has not been to evaluate the given models, but to discuss predictive power in a general way. Predictive power, especially with respect to dynamic models, is defined and treated in more detail in Section 5.8.5. The next example concerns predictions of caesium in whitefish in the Italian lake, Bracciano, and the Finnish lake, Iso Valkjärvi. Figures 5.41A, B and C give the results for the three models for Bracciano in the same way as Figure 5.40 gave the results for water in Iso Valkjärvi. Correspondence between the two empirical data sets is rather poor in this case, $r^2 = 0.808$ and the slope is 1.208, indicating that, on average, the values from the latest month (Emp1) are higher than the values from Emp2. This indicates something "strange" in Bracciano. This lake has, in fact, high concentrations of "old" caesium [5.13]. These models assume that all caesium emanates from the Chernobyl fallout, and there is no factor accounting for caesium from the weapon tests during the 1950s and 60s. Figures 5.41A, B and C illustrate that all three models provide a low predictive power in Bracciano. The best model is the VAMP LAKE model which gives an r^2 of 0.409, but the slope is very far from 1; it is 0.079. The generic model gives an r^2 of 0.

All this illustrates, in fact, not the weakness of these models, but the strength of modelling. All models provide adequate to very good predictions in most lakes for water and most species of fish, and when this is not the case, then the difference between the model prediction and the empirical value can be discussed in quantitative terms. The model can provide a hypothesis, which could be tested against independent empirical data. In the case of Bracciano, it is evident that models which do not account for "old" fallout should provide poor predictions. If these models were to give good predictions, it would be for the wrong reason.

Figures 5.41D, E and F for whitefish in Iso Valkjärvi provide another interesting example: The r^2 value and the slope for the two empirical data sets are: 0.309 and 0.348, respectively. This indicates great uncertainties in the empirical data for whitefish in this lake. And all three models actually give much higher r^2 values and much better slopes than obtained from the comparison between Emp1 and Emp2: The mixed model gives $r^2 = 0.874$ and slope = 0.956, and from Figure 5.41A we can note the very good correspondence between modelled values and empirical data both for the peak and the tail. The VAMP LAKE model also gives good predictions, although the modelled peak is too high. The generic model gives values that are about 2 times higher (slope = 1.943) than the empirical data.

These are some selected results to highlight how the different models behave. Table 5.16 gives a compilation of many model runs for the three models, for the seven VAMP lakes and for caesium concentrations in water, whitefish, trout, small perch, large perch, roach and pike. The table gives the r^2 values when empirical data are compared to modelled values for the corresponding periods (months). The results are summarized in Figure 5.42. The mean r^2 value from all these validation tests (n = 23)

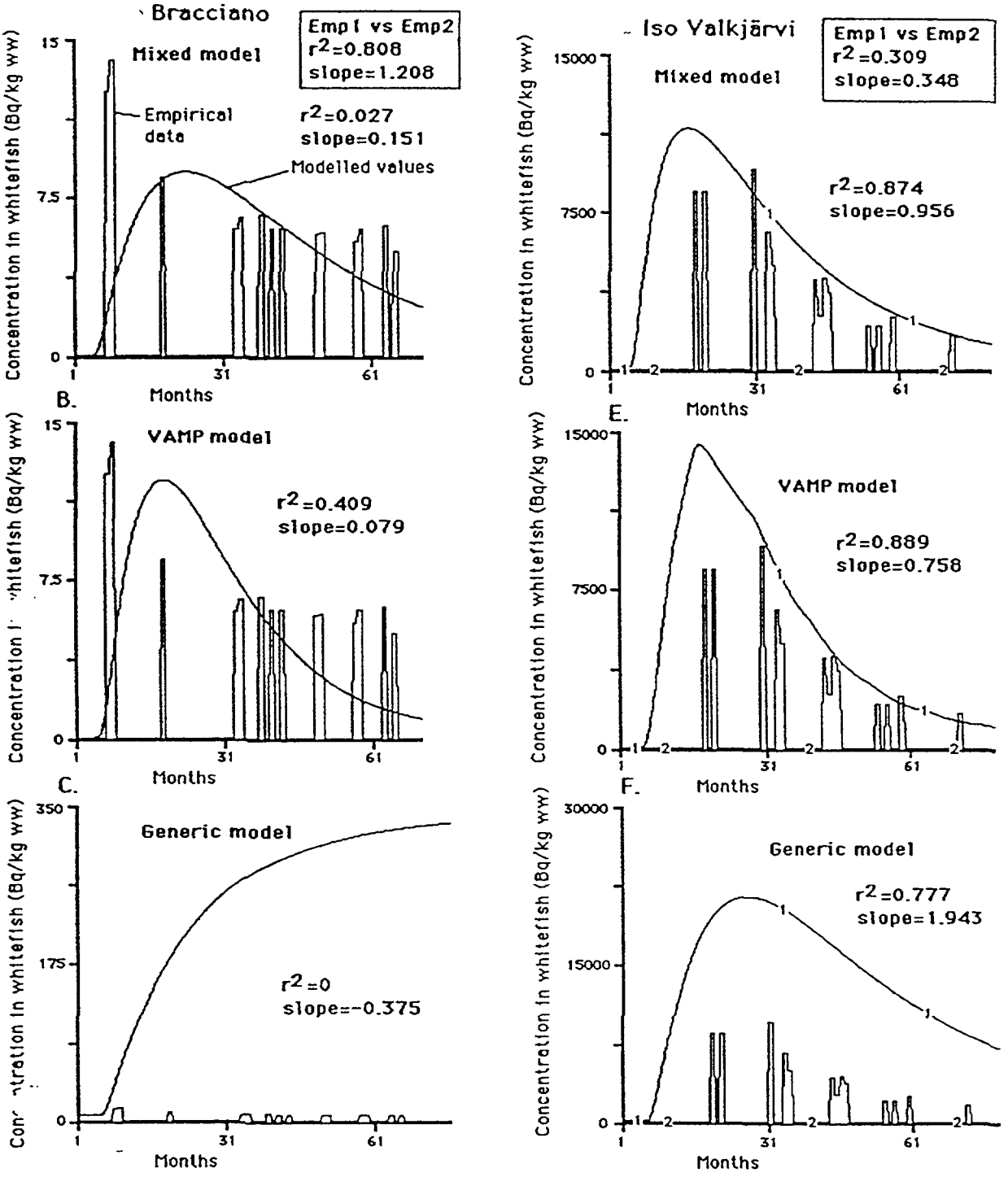

FIG. 5.41. Validations for caesium in whitefish in Bracciano and Iso Valkjärvi for the UU-Mixed model, the VAMP LAKE model, and the UU-Generic model. The figure also gives the results from the comparison between the two empirical data sets, Empl and Emp2.

TABLE 5.16. EMPIRICAL r^2 VALUES OBTAINED IN COMPARISONS BETWEEN EMPIRICAL AND MODELLED RESULTS OBTAINED FROM THE VAMP LAKE MODEL, THE UU-MIXED MODEL, THE UU-GENERIC MODEL AND BY THE TEST SERIES BETWEEN THE TWO EMPIRICAL SAMPLES (EMP1 VS EMP2) FOR DIFFERENT LAKES, ^{137}Cs CONCENTRATIONS IN WATER AND IN DIFFERENT SPECIES OF FISH

	Lake	r^2			
		VAMP LAKE	Mixed	Generic	Emp1 vs Emp2
Water	IJsselmeer	0.89	0.81	0.76	0.88
Water	Iso Valkjärvi	0.84	0.80	0.04	0.95
Water	Devoke Water	0.79	0.81	0.95	0.11
Water	Esthwaite Water	0.66	0.61	0.74	0.40
Water	Hillesjön	0.52	0.39	0.64	0.02
Water	Bracciano	0.31	0.44	0.92	0.99
Whitefish	Iso Valkjärvi	0.89	0.87	0.78	0.31
Whitefish	Bracciano	0.41	0.03	0.00	0.81
Trout	Heimdalsvatn	0.86	0.90	0.83	0.86
Trout	Devoke Water	0.39	0.58	0.50	0.27
Smelt	IJsselmeer	0.81	0.73	0.81	0.92
Small perch	Hillesjön	0.88	0.86	0.87	0.95
Small perch	Iso Valkjärvi	0.84	0.85	0.65	0.72
Small perch	IJsselmeer	0.77	0.85	0.74	0.85
Small perch	Devoke Water	0.01	0.08	0.03	0.02
Roach	IJsselmeer	0.79	0.72	0.79	0.65
Roach	Hillesjön	0.64	0.89	0.62	
Pike	Hillesjön	0.94	0.88	0.94	0.85
Pike	Iso Valkjärvi	0.69	0.60	0.00	0.44
Large perch	Iso Valkjärvi	0.98	0.94	0.18	
Large perch	Hillesjön	0.55	0.68	0.61	0.87
Large perch	IJsselmeer	0.30	0.57	0.32	
Large perch	Devoke Water	0.08	0.06	0.11	0.00

is, in fact, highest for the simplest model, the mixed model, and lowest for the largest model, the generic one. In addition, the mean r^2 value between the two empirical data sets, Emp1 vs Emp2, is about 0.6. This indicates the uncertainty in the empirical data and provides an analogous parallel to the comparison between modelled values and empirical data. Figure 5.43 summarizes the corresponding results for the slope. Figure 5.43A gives the mean values and the standard deviations, and Figure 5.43B the median values, the quartiles, the 90% values and the outliers. Also in this case the comparison between the two empirical data sets gives the largest divergence from 1. The median and the mean value is about 0.6. It is, of course, also logical that this slope should be somewhat less than 1.

The results of many comprehensive validation tests of time dependent data ("tail tests") are summarized in Figure 5.44 (for all variables, for water and different fish). The VAMP LAKE model and the small mixed model generally provide the best predictive accuracy and the large generic model the lowest r^2 values.

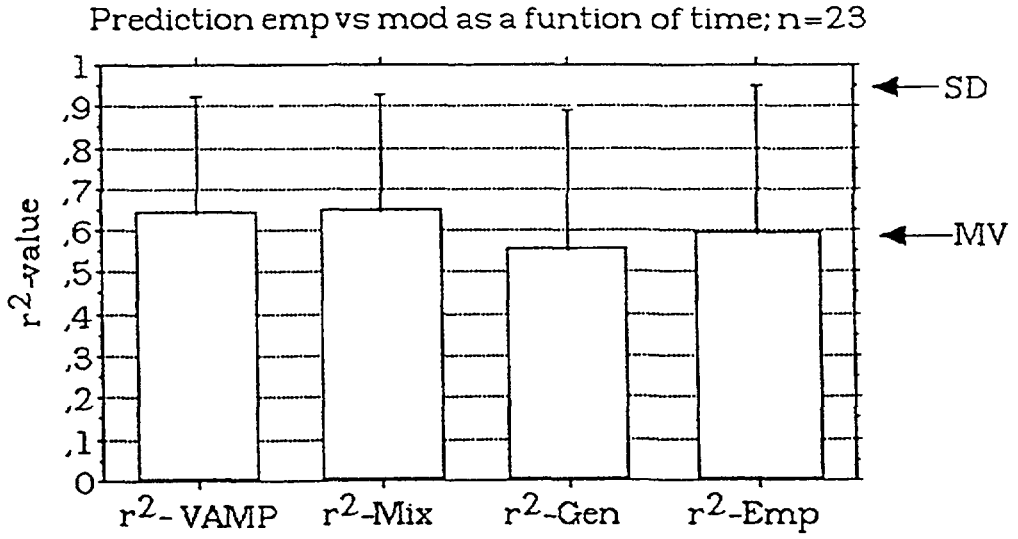

FIG. 5.42. Compilation of validation results for r^2 values obtained for water and all species of fish for the three models (VAMP LAKE, UU-Mixed and UU-Generic) and results from the comparison between the two empirical data sets, Emp1 and Emp2.

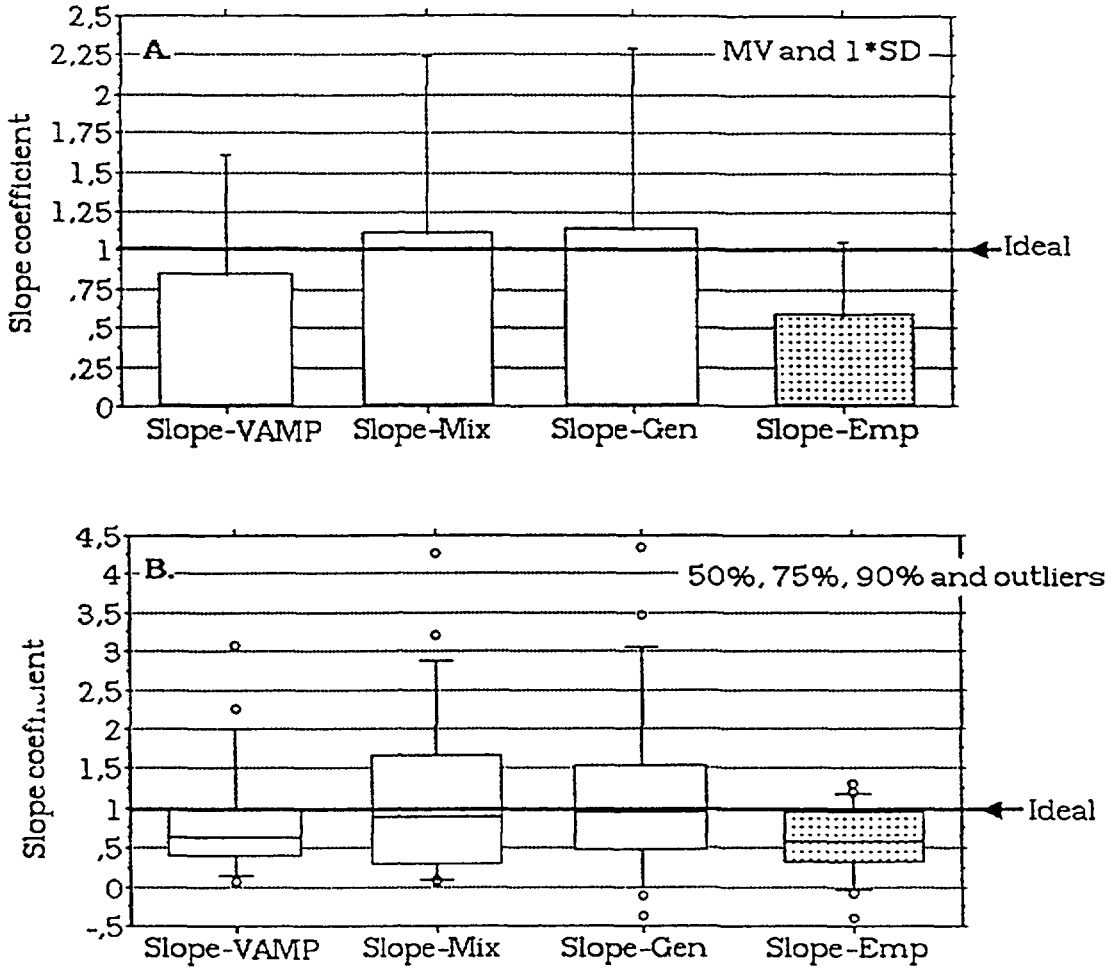

FIG. 5.43. Compilation of validation results for slopes obtained for water and all species of fish (n = 18) for the three models (VAMP LAKE, UU-Mixed and UU-Generic) and results from the comparison between the two empirical data sets, Emp1 and Emp2. (A) gives the mean slopes and the standard deviations (B) gives the median (= 50%), quartiles, percentiles and outliers.

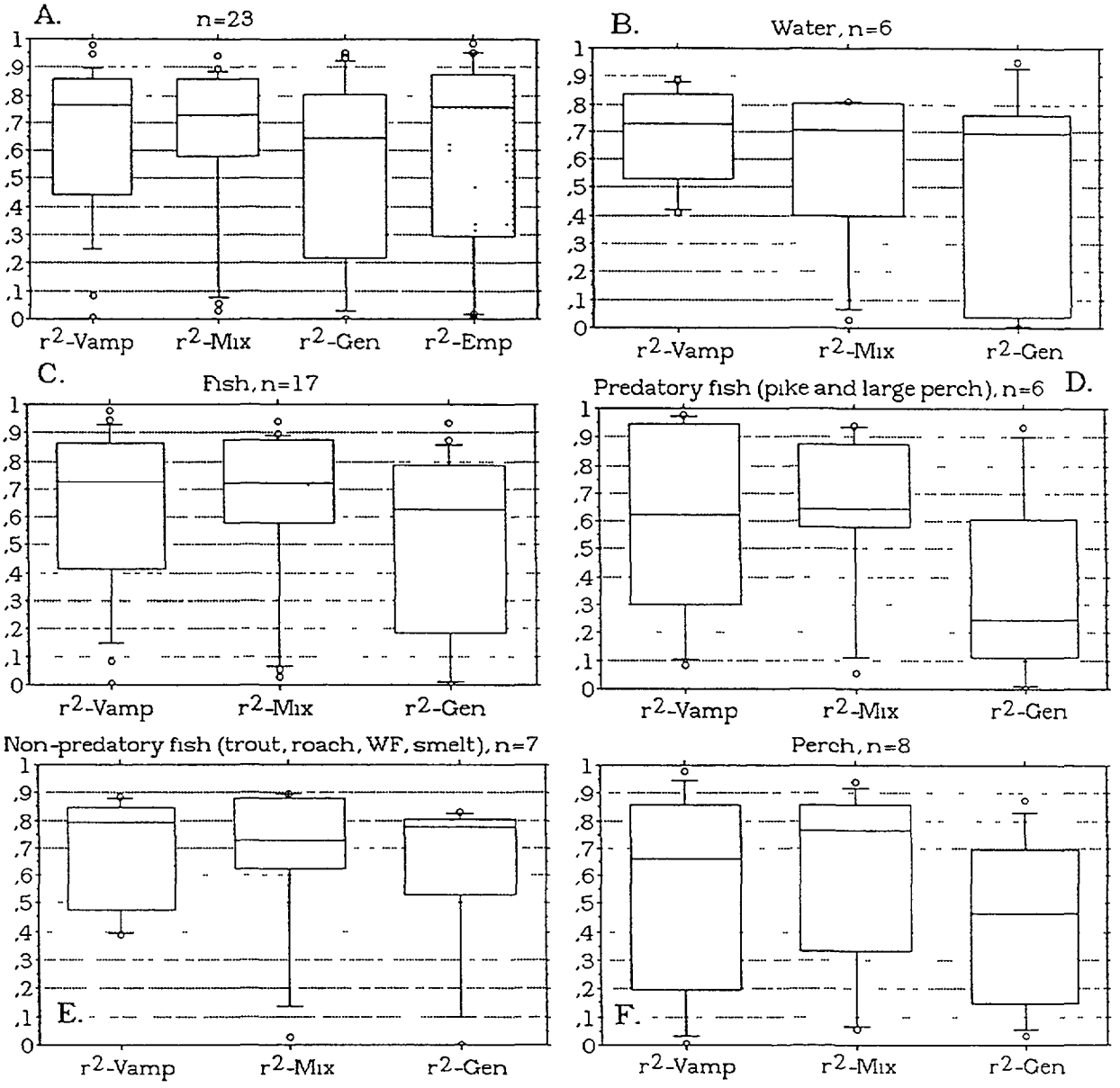

FIG. 5.44. A compilation (box and whisker plot of r^2 values) of validation results ("tail test") for the three models (VAMP LAKE, UU-Mixed and UU-Generic).

(A) Results for all regressions, n = 23, and a comparison between the corresponding two empirical data sets. Emp1 and Emp2.
(B) Results for water (6 lakes).
(C) Results for all types of fish (n = 17).
(D) Results for pike and large perch (n = 6).
(E) Results for trout, roach, whitefish (WF) and smelt (n = 7).
(F) Results for perch (n = 8).

5.4. DETAILED MODEL COMPARISONS FOR HILLESJÖN

When testing model predictions against independent empirical data all the ingoing components should be evaluated as a function of time in order to obtain reliable estimates of the precision in the model results. This is also helpful for identifying the critical components for improving models. However, it is beyond the scope of this study to fulfill such evaluations for all times, lakes

and models. The emphasis has been on analysing peak and tail values of the levels of ^{137}Cs in water and predatory fish in this study. To address these questions and study the time dependence of the models, the Swedish lake, Hillesjön has been selected for a model comparison, in which model predictions for the components water, prey fish and predatory fish have been evaluated against the observations on a continuous basis.

5.4.1. Water

Results for water in Hillesjön are presented in Figure 5.45A and B. All models predict higher peak values than the observed, although no observational data are available until June 1986. The results

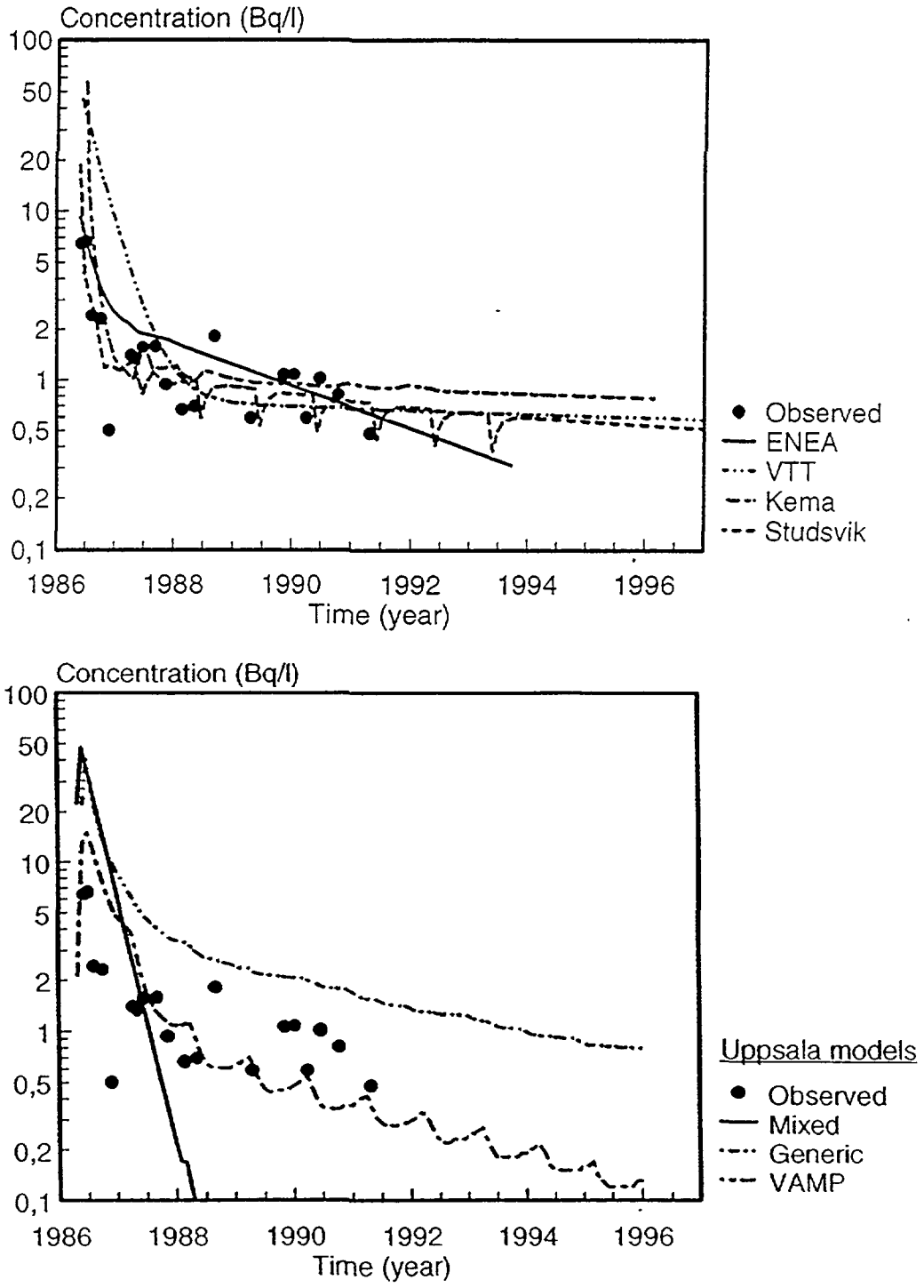

FIG. 5.45. Comparison of observed concentrations of ^{137}Cs in water in Hillesjön with predictions obtained by different models.

from the ENEA and Studsvik models show a better agreement with the initial fast decline in the water than the other models. The decrease in the concentrations of ^{137}Cs in water is due to outflow and sedimentation, while leakage from the catchment area and resuspension from the sediments are processes slowing down the recovery. The only model not considering these latter processes is the UU-mixed model. It is clear from the results (Figure 5.45B) that models which do not account for secondary load give poor long-term predictions for the concentration of ^{137}Cs in water.

Monthly averages of the water retention time were available and showed a pronounced maximum during spring, causing an effective removal of ^{137}Cs from the lake. Models which do not consider this seasonality overestimate the levels of ^{137}Cs. One explanation for the faster decrease in the Studsvik model is due to the assumption that a fraction of the deposition is immediately transferred to the sediments because of its particulate form.

Some models use the same method for obtaining rate constants from the water to the sediments, based on the particulate form and mass sedimentation rates. Several studies have shown the great importance of the K_d values when applying these rates. On the other hand, the UU-mixed model accounts neither for transfer to the sediments nor leakage from the drainage area, although is the model which predicts the most rapid decrease. Only one model, the UU-generic model, consistently overestimates the concentrations of ^{137}Cs in the water.

Models which neglect any significant transfer back from the sediments to water (resuspension/bioturbation) underestimate the levels after the first two years. The important role of resuspension as the main process maintaining increased levels of ^{137}Cs in the waters of Hillesjön is confirmed by observational data [5.11]. The uncertainty analyses for Hillesjön also identify resuspension as the main process responsible for the uncertainty in the predicted levels of ^{137}Cs in the water (see Section 5.3).

The results from the ENEA model, which has a compartment for sediment interface [5.12], show a good agreement to the dynamics of the observations, as does also the Studsvik model. The latter model also considers the seasonal dependency of the initial leakage from the catchment as well as water retention time.

5.4.2. Prey fish

The next component studied is prey fish, represented by the roach. The results are presented in Figure 5.46. All models base their uptake of ^{137}Cs in fish from more a less complicated food webs, all taking their original levels of ^{137}Cs from water concentrations. Most models predict the observed peak values within a factor of two with minor deviations in time compared to the time of occurrence of the observed peak values. The "simplest" food webs are found in the ENEA and the UU-Mixed models which use only bioaccumulation factors and biological or ecological half-lives for obtaining rate constants to predict the transfer from water. However, the predictions agree well to the observations as there was a good agreement for the levels of ^{137}Cs in water. The UU-generic model underestimates the levels in prey in contrast to its overestimation of the levels in water. The underestimation from the VTT model is due to corresponding underestimation of the levels in water. Furthermore, a short biological half-life of ^{137}Cs in roach was used in the VTT model. The results from the UU-Mixed model are slightly higher than the observations due to compensation of the low levels in water by using a long turnover time within the fish. However, this is not a biological half-life and corresponds more to an ecological half-life.

The Studsvik model initially shows a good agreement, but the discrepancies seem to increase with time. However, the results are consistent with the predictions of the levels of ^{137}Cs in water. The KEMA model underestimates the long term concentration of ^{137}Cs in roach due to underestimation of the levels in water. Furthermore, the biological half-life used is shorter than used for instance in the Studsvik model.

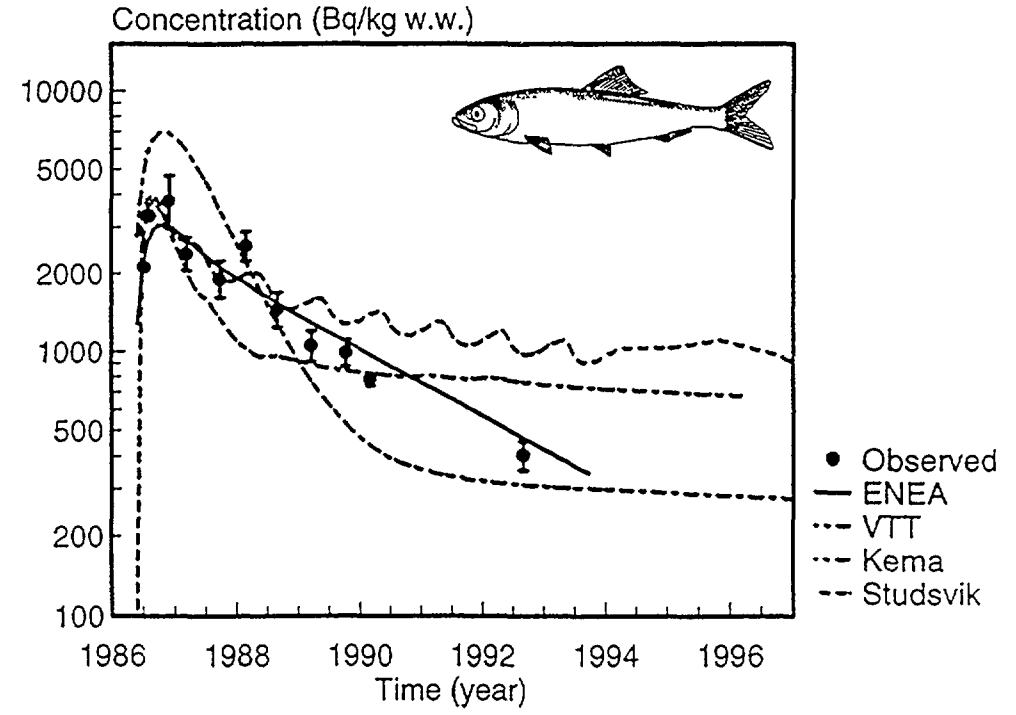

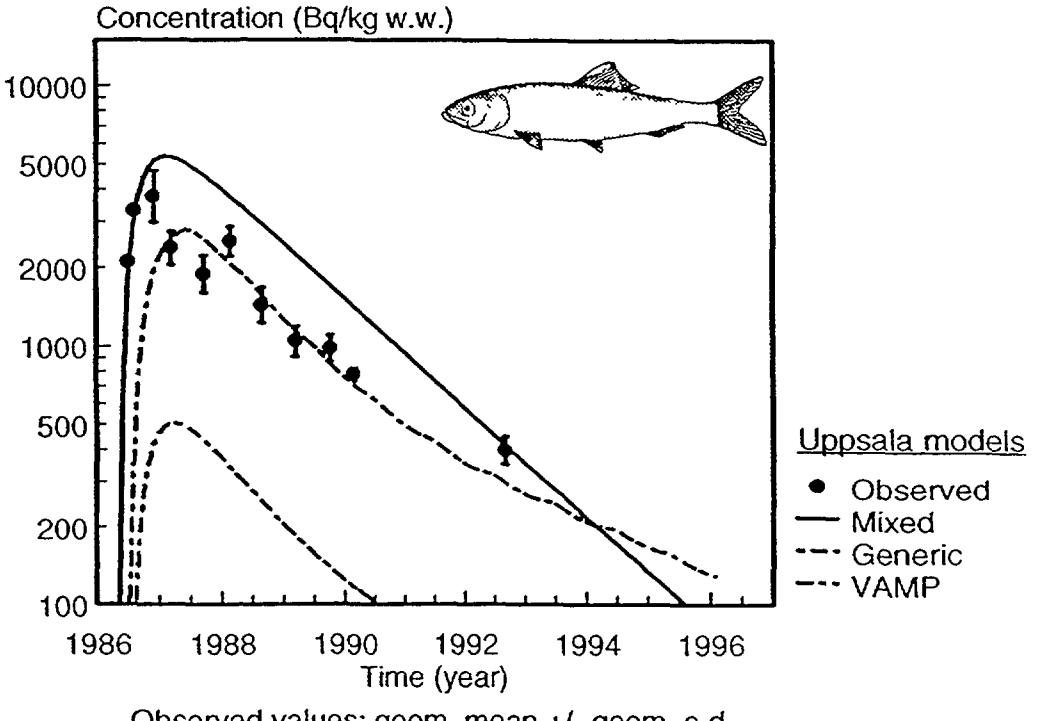

FIG. 5.46. Comparison of observed concentrations of ^{137}Cs in roach in Hillesjön with predictions obtained by different models.

5.4.3. Predatory fish

The results for predatory fish (perch) are presented in Figure 5.47, with geometric means and standard deviation for the observational data.

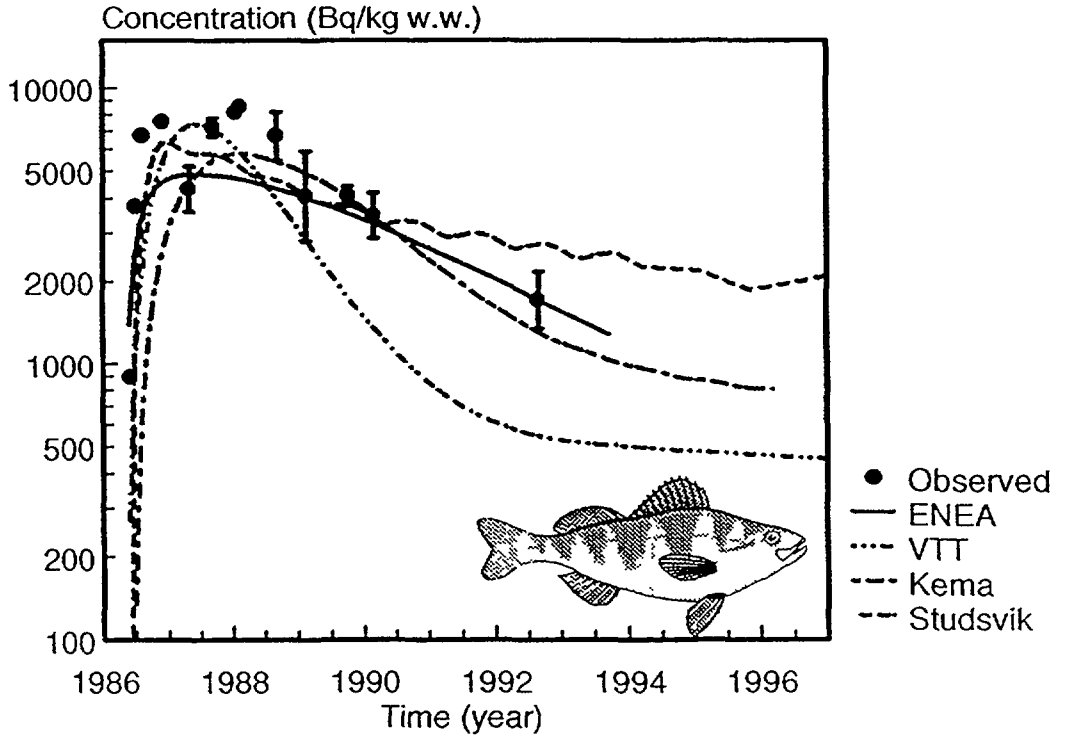

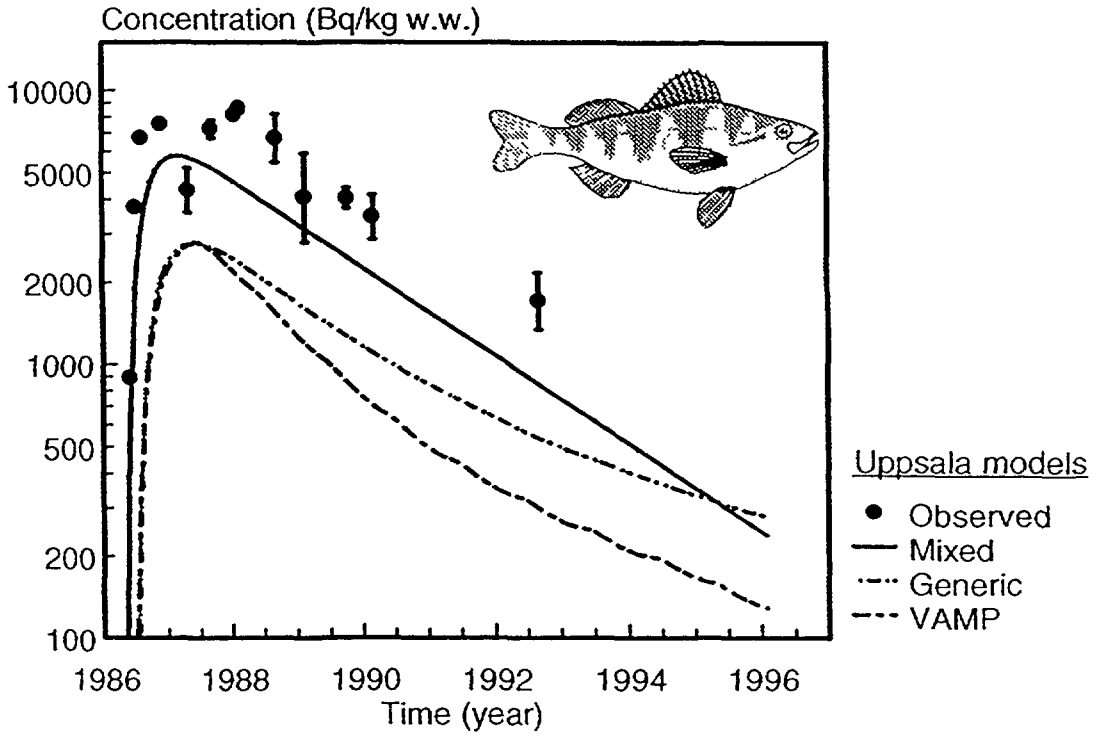

FIG. 5.47. Comparison of observed concentrations of ^{137}Cs in perch in Hillesjön with predictions obtained by different models.

All models underestimate the levels of ^{137}Cs in perch, although, most results for the two first years are within a factor of two. In addition, all models except KEMA predict maximum values somewhat earlier in time than the measured values. This reflects how the uptake to fish is modelled, and is especially obvious for the ENEA model which has a direct relationship water to predators [5.13]. For most models the underestimation in perch is due to the corresponding underestimation of long-term ^{137}Cs concentrations in the water. The lower rate of decrease in the Studsvik model can be explained by an overestimation of the biological half-life, used in combination with a too slow decrease in the content of ^{137}Cs in the prey fish. The results from the KEMA model, which is the model with the most complicated food webs, agrees well with the observations after the initial underestimation. However, if the underestimation of ^{137}Cs in water and prey were compensated for, the predicted values would increase.

Conclusions

Caution must be taken when drawing general conclusions about the precision of models for Hillesjön. The faster recovery for this lake may partly be due to bottom freezing during the cold winter of 1987 and to the possible migration of fish out of the lake which is supported by local interviews. Nevertheless, certain general conclusions may be drawn:

- Most models predict ^{137}Cs concentrations in water within a factor of two for the first two years after deposition.
- The predicted levels are sensitive to the choice of K_d values.
- Secondary load must be considered for precision in the concentrations of ^{137}Cs in water, especially in the long term.
- Simple modelling of uptake to fish using rate constants based on bioaccumulation factors and biological half-lives makes it difficult to simulate the dynamics in a satisfactory manner, although with pertinent values the predicted long term levels of ^{137}Cs in fish are reasonable.

5.5. BIOLOGICAL HALF-LIVES

5.5.1. Theoretical considerations

The biological half-life, $T_{1/2}$, is defined as the time it takes for an organism to loose 50% of its radionuclides after its transfer from a contaminated to an uncontaminated environment. For aquatic invertebrates for ^{137}Cs these values range between 10 and 100 days, while for fishes the values are higher, ranging between 100 and 1000 days [5.14]. Vanderploeg et al. reported a biological half-life of 1–2 days for phytoplankton, 5 days for zooplankton and 7 days for chironomid larvae [5.15], while Kolehmainen et al. found values ranging between 20 and 200 days for fish; 200 days for perch and 85 days for roach [5.16]. Carlsson reported 200 days for large perch, and for the pike values of 400 days (200 g) up to 600 days (1.5 kg) in Lake Ulkesjön with an average annual water temperature of 8-10°C [5.17]. The values were calculated by means of a model fitted to empirical measurements.

Data on molluscs are rather limited, and it is often assumed that the concentration factor of molluscs is usually similar to that of crustaceans. The concentration factor for radiocaesium tends to be some what higher for the freshwater environment than for the marine environment. Biological half-lives for freshwater clams have been reported to vary between 3 and 38 days accounting for 34% and 66%, respectively, of the total content [5.18]. Foulquier found in laboratory experiments that for three freshwater molluscs (*Anodonta cellensis, Anodonta cygnea, Unio margaritana*), close to 58% of the radiocaesium was associated with the soft parts of the molluscs [5.19]. The distribution within the soft part in this experiment was: 42% in the viscera (half-life *Unio* 120 days), 24% in the muscles (half-life 130 days) and 18% in the gills (half-life 100 days). Coughtrey and Thorne [5.20] concluded from this that the half-life of radiocaesium for freshwater molluscs in the edible part is at least 40 days. They advise a ten times lower concentration factor for marine molluscs than for freshwater molluscs (edible part), 20 and 200, respectively, with a retention time of 40 days for both environments based on the above data.

Experiments on the adsorption of radiocaesium in a marine mussel (*Cardium edule*) in water with a constant concentration, gave maximum levels in soft tissues after 17 days, which indicates a relatively short biological half-life for this marine mussel.

Biological half-lives not only vary between the different fish species, but the age or size of the fish and the water temperature also influence the biological half-life [5.21]. However, the age effect differs from species to species. While perch does not show this effect strongly, roach doubles its half-life between the age of 2–3 years and 9–12 years. For rainbow trout the change is even greater; it varies from 20 days at the age of 6 months to 80 days at the age of 2–3 years [5.16]. Another illustration of the differences in the retention times of young fish of the same weight (or age) is the fact that juvenile bluegill with a weight of 60 g have a retention time for potassium, behaving in terms of chemical properties similar to caesium, of 0.11 year, much lower than for pike of the same weight. According to Carlsson this can be explained by the concentration in the food, and more importantly, the higher food uptake per unit weight, which links biological half-life to consumption rates [5.17]. The general conclusion from Carlsson's model study is the strong dependency between the biological half-life and the weight of the fish. Ugedal et al. investigated the dependency of the half-life on body weight and temperature in brown trout (*Salmo trutta*) and found biological half-lives varying from 104 up to 564 days [5.21]. Although there are differences among the different fish species, Reichle et al. derived a generic body-weight biological half-life relationship for cold-blooded vertebrates [5.14]. Based on experimental data from perch, trout, bluegill, and carp, they derived the following power function model:

$$T_{\frac{1}{2}} = 38.02\ W^{0.139} \tag{5.26}$$

where W is the weight of the fish (g). This would mean a biological half-life of 72 for a fish of a weight of 100 grammes, and a biological half-life of 155 days at a weight of 3 kg. This relationship was for a temperature of 20°C. Furthermore, this equation is also suitable for aquatic invertebrates except insects.

The half-life generally doubles when the temperature decreases by 10°C (the so called Q_{10} method) [5.17, 5.14], consequently the values in the example must be doubled to obtain the half-lives at 10°C. This method could be applied to determine the biological half-life at temperatures other than the temperature at the reported biological half-life. The generic equation is expressed in the following way:

$$THB(T) = THB(T_0)e^{\left(-\frac{\ln(2)}{10}(T-T_0)\right)} \tag{5.27}$$

where THB(T) is the biological half-life at temperature T and $THB(T_0)$ the biological half-life at temperature T_0, the temperature of the water in which the biological half-life is determined.

That would imply for the above mentioned empirical equation (5.26), that in lake waters with a temperature of 10°C, the biological half-life is 144 days for fish with a body weight of 100 g, 210 days for 1 kg, and 310 days for a body weight of 3 kg. Figure 5.48 gives the graphical presentation of the equation for temperatures of 20, 10, and 0°C.

Since equation (5.26) is derived from measurements data from fish with a body weight ranging between 5 up to 350 gram, this function cannot simply be extrapolated to larger fish. Therefore piscivorous fish such as pike and large perch are not be properly described by means of this function.

As stated above, Carlsson reported half-lives of 200 days for large perch, and for the pike values of 400 days (200 g) up to 600 days (1.5 kg) in Ulkesjön, with a water temperature of 8–10°C calculated by means of a model fitted to empirical data [5.17]. If equation (5.27) is applied to adjust these half-lives to the higher summer temperature present in the Swedish lake, Hillesjön (18°C), the

biological half-lives for pike of two different weight classes are 230 days (200 g), 350 days (1500 g) respectively, which is significantly higher than in the case of the application of equation (5.26). In the same article Carlsson [5.17] reported a similar equation to Reichle et al. [5.14] for the relationship between biological half-life (BHL) and fish body weight:

$$BHL = a_0 W^{0.2} \tag{5.28}$$

Calculated values for biological half-lives at 8–10°C for pike reported by Carlsson were used to fit the linear power function of the form $Y = a_0 X^{a1}$. Finally, the constant a_0 appeared to be 65.41 for a lake water temperature of 20°C, resulting in the relationship expressed in equation (5.29), valid between 200 and 1500 g. Consequently the biological half-life for pike with a body weight of 1 kg in lake Hillesjön in the summer period at a temperature of 18°C would be 325 days, which is a reasonable value.

$$BHL = 65.41 W^{0.2} \tag{5.29}$$

Summarizing, theoretically two equations can be used to estimate the biological half-lives for aquatic organisms based upon body weight and the water temperature. The first could be applied for a whole range of aquatic organisms including non-piscivorous fish up to a body weight of 300 g, and the second could be applied for piscivorous fish like perch and pike up to a body weight of 1500 g. Both equations could be combined with the temperature correction method, Q_{10}. This results in two sub-models, which can be incorporated into lake models.

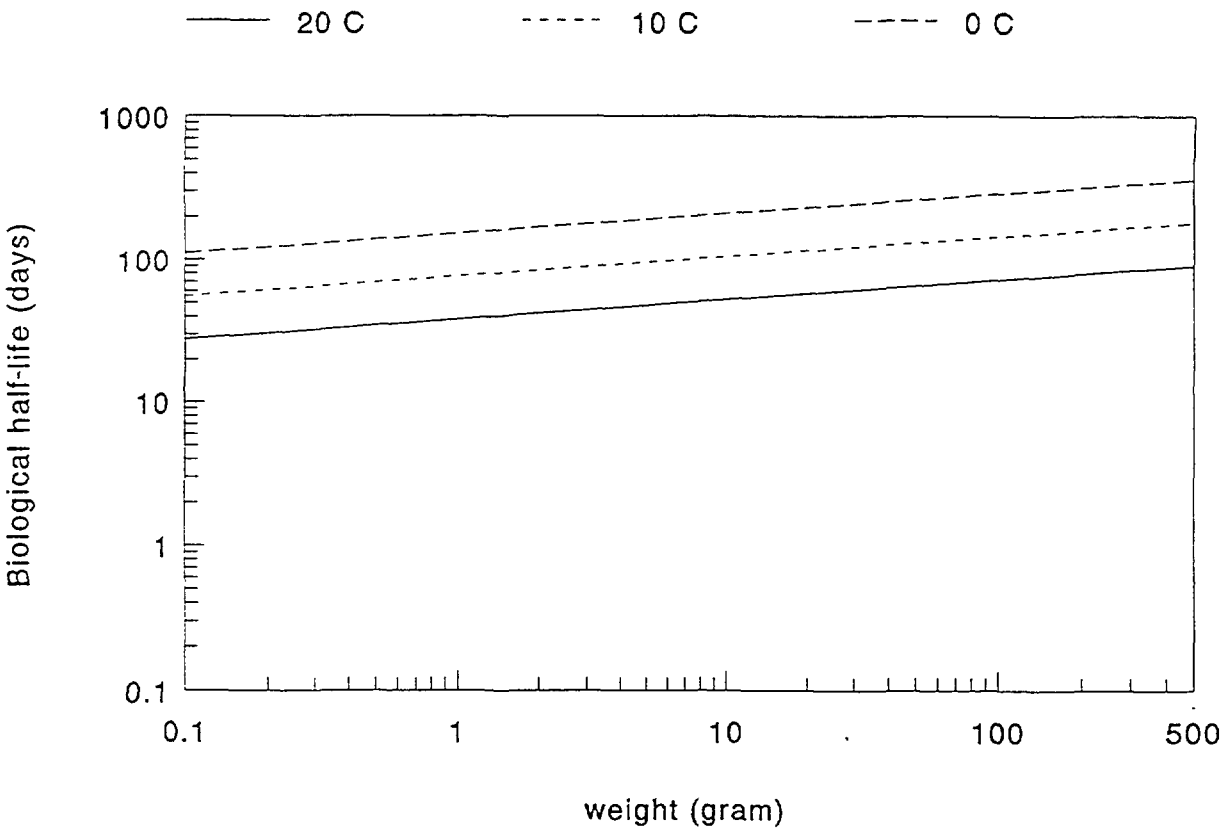

FIG. 5.48. Relationship between body weight of an aquatic organism and its biological half-life for caesium. The graph follows a linear power equation of the form $Y = aX^b$

For prey fish and juvenile predatory fish with a maximum weight of 300 g, equation (5.30) can be used to estimate the biological half-life.

$$BHL = 152.08W^{0.139}e^{-\frac{\ln(2)T}{10}} \tag{5.30}$$

For piscivorous fish with a body weight exceeding the 300 g, equation (5.30) can be applied to estimate the biological half-life. The equation is valid from 100 g up to 1500 g.

$$BHL = 261.64W^{0.2}e^{-\frac{\ln(2)T}{10}} \tag{5.31}$$

Various workers performed laboratory tests to find this relationship for specific fish species. Ugedal et al. [5.21] studied the relationship for brown trout (*Salmo trutta*) measuring the biological half-life at different temperatures (4–15.5°C) and weights (40–500 g), and found a linear power equation with a weight exponent of 0.176, higher than proposed by Reichle [5.14], but lower than in the equation based on Carlsson's [5.17] data. The Q_{10} value appeared to be higher than suggested by Reichle (and in equations (5.30 and 5.31). It was 2.86, i.e. an almost threefold increase of the biological half-life for every 10°C decrease in temperature:

$$BHL = 290\ W^{0.176}\ e^{-\frac{\ln(2.86)\ T}{10}} \tag{5.32}$$

In 1971, Gallegos and Whicker [5.22] studied the elimination rate of ^{137}Cs in the rainbow trout (*Oncorhynchus mykiss*) with weights varying between 30 and 200 g at four water temperatures, from 5.0 to 18.3 °C. The constants found deviated from those found by Ugedal, the weight exponent of the linear power equation turned out to exceed those determined by Ugedal, Reichle and Carlsson. They found a relatively high weight exponent, 0.292, a relatively low Q_{10} value, 1.2, and a low half-life constant A_0 of 20.1 (see equation 5.33).

$$BHL = 20.1\ W^{0.292}\ e^{-\frac{\ln(1.2)\ T}{10}} \tag{5.33}$$

Ugedal explained these deviating values by indicating the low weight range in Gallegos' experiments. However, this could explain the lower value of the half-life, but not the higher weight exponent. One should expect a lower instead of a higher value for the weight exponent over a weight range with an upper limit of 200 g. Hewett and Jeffries found the weight exponent in brown trout at 10°C, with body weight ranging between 1.5 kg and 820 g, to be 0.22 [5.23].

The linear power equation appears to be a reasonable way to express the dependency of the biological half-life on temperature and body weight. However, it is obvious that, probably due to the different experimental methods, even for one fish species such as brown trout, the biological half-life dependency cannot easily be verified under laboratory conditions. Equations (5.30) and (5.31) are selected for model application because of the generic character of the equations, but when they are applied to brown trout or rainbow trout, the resulting half-lives will differ from those found by Ugedal et al. [5.21] and Gallegos and Whicker [5.22]. The proposed equations (5.30) and (5.31) applied on a brown trout of 200 g, at 10°C gives 159, and 377 days for the biological half-life, respectively, whereas Ugedal's equation gives 255 days, and Gallegos' equation, although derived from experiments with rainbow trout, gives 82 days when applied to brown trout.

5.5.2. Application of biological half-life values in food web models

Biological half-lives in food web models

Sensitivity analyses of the various models have demonstrated the importance of biological half-lives. The use of appropriate biological half-lives which are based on empirical models instead of on expert judgement is needed to improve the models. This makes the models more flexible and applicable to a wider range of lake ecosystems. In order to increase predictive power, the sub-model for the assessment of the biological half-life must have as few model specific parameters as possible, otherwise the uncertainty may increase instead of decrease. The first possibility is to apply the empirical relationship between biological half-life and the body weight of the aquatic organism, assuming that some average body weight represents the whole population of a certain fish type. Otherwise the weight of the fish as a function of time must be modelled by means of an empirical curve.

To apply the biological half-life in the models, it must be realized that the reason for decreasing levels of the radionuclides in the body of fish after a initial contamination is not only due to excretion, but also due to the so called "growth dilution". Growth dilution is the decrease of radionuclides per unit of mass, while the total amount on total body weight basis remains constant. Equation (5.34) illustrates the way in which most models handle the loss rate, $K_{½}$. It can be expressed as inversely proportional to the biological half-life:

$$K_{1/2} = \frac{\ln(2)}{T_{1/2}} \tag{5.34}$$

where $T_{½}$ is the biological half-life in days.

If the loss by reproduction is assumed to be negligible, the $K_{½}$ term can be split up into two parts is based on the loss by excretion and growth dilution:

$$K_{1/2} = K_{ex} + K_g \tag{5.35}$$

where K_{ex} is the excretion rate (d^{-1}), and K_g is the growth rate coefficient (d^{-1}).

Generally, "growth dilution" is a very important factor contributing to the loss of radionuclides on a weight basis [5.24], especially for young fish and invertebrates. In zero-growth conditions, i.e. when K_g is equal to zero, the biological half-life is a consequence of loss due to excretion. Thus, when using the "biological half-life" values given in the literature as model input it must be made clear whether this growth dilution is taken into account. If the biological half-life in the literature is defined as the loss rate per unit body weight, in the loss rate $K_{½}$ this growth dilution is automatically taken into account, and therefore does not need to be modelled separately, such that values of $T_{½}$ are suitable as model input. However, if the reported values for $T_{½}$ are results due to excretion, the loss of radionuclides using equation (5.34) is too low; consequently the model will supply underestimations. To counter this, growth dilution must be incorporated as an extra term in the loss rate term as showed in equation (5.35).

Unfortunately, the literature does not in all cases contain detailed information on the exact way the biological half-life has been derived from field measurements or from laboratory experiments. In this case two possible errors can occur as a consequence of using these kinds of biological half-lives. When equation (5.34) is applied, but the biological half-lives is based only on excretion, overpredictions of the caesium levels will be the consequence; if equation (5.33) is applied, while the biological half-life used includes both excretion and growth dilution, underpredictions of the caesium

levels will be the consequence. The latter is not acceptable in emergency support systems and countermeasure support. Therefore, it is recommended that when the exact procedure of obtaining the half-lives is unknown, both the growth dilution and the excretion must assumed to have been taken into account in the reported values. Thus, equation (5.34) instead of (5.35) must be applied, accepting the risk of overestimating the turnover time in the fish species as a consequence.

Recommendations based on the application of a biological half-life sub-model

The sub-models discussed above can be used as guidelines for the use of biological half-lives in predictive models. For use in dose assessment and countermeasure modelling in which these types of predictive model are implemented, the use of biological half-lives related to fish species instead of body weight would make the model more flexible and more easily applicable. Models used in decision support systems must be as generic as possible, but can have special features to govern process like ice-cover, or age class specific radionuclide levels in fish. For instance, fish weights are not known in all cases, especially if the area has not been monitored intensively. Assuming, that the VAMP lakes cover a wide range of lake ecosystems, general recommendations can be made concerning the use of biological half-lives in decision support systems such as RODOS, developed within the framework of the CEC-programme.

The VAMP models were designed to model average fish with a constant body weight, or lakes with a constant biomass for the several fish species (more detailed model approaches, in which the time dependent body weight is also modelled are discussed in Section 5.7). The recommendations concerning biological half-lives are given under the assumption that the fish have a constant body weight during a certain time period, thus representing the average body weight in a specific lake ecosystem.

Three levels of recommendations can be distinguished. The first level is the use of the sub-model for calculating the biological half-life. Level 2 and 3 recommendations are derived from the results of the application of this sub-model on the VAMP lakes, under the assumptions that the range of lake ecosystems of the VAMP project is sufficient to derive these generalisations. However, one has to realize that the produced values are based on a limited set of data, and therefore must be regarded an initial attempt to provide general advice to modellers which is more appropriate than simply guessing this important parameter.

The higher the recommendation level, the lower the accuracy in prediction of the biological half-lives for fish species for an individual lake ecosystem. At level three, the models will overpredict the turnover of radiocaesium levels in central Europe and underpredict the levels in the Nordic region. For dose assessment purposes, the maximum values of the ranges can be selected to avoid underpredictions.

The selection of the level of recommendation must be based on available data, requirements from the modellers and the purpose for which the models are used. In descending order of complexity and dependency on other environmental variables, these are:

Recommendation level 1
Data: Extensive data sets on the aquatic organisms and the lake ecosystem.
Aim: Detailed model studies for scientific purposes.
BHL: Biological half-life as a function of temperature and body weight.
Fish: All species.
Input: Lake water temperature, body weight of the fish species.

Recommendation level 2
Data: Limited data sets on the aquatic organisms and the lake ecosystem.
Aim: Model validation, and screening analysis for dose assessments.
BHL: Biological half-life as a function of average body weight.

Fish: Several fish species.
Input: Mean body weight of the fish species.

Recommendation level 3
Data: No data sets on the aquatic organisms and the lake ecosystem.
Aim *Screening analysis for dose assessments.*
BHL: Generic biological half-life.
Fish: Groups of species: predatory, non-predatory fish.
Input: Not required.

More specifically the levels are elaborated as follows:

1. **Recommendation level 1**

This method which requires the most extensive input data set, uses both linear equations between body weight and biological half-life for any given body weight and temperature. In Table 5.17 the results of the application of these linear power relationships, as presented earlier in this Section, are given for a selection of body weights ranging from 10 up to 3000 g. The dependence of temperature can be expressed by means of equations (5.30) and (5.31). These equations can be applied to determine the biological half-life at temperatures other than the temperature for which the reported biological half-life is valid. The first equation can be applied to non-predatory fish with a body weight from 5 g up to 350 g (FPREY in Table 5.17), while the second equation can be applied to piscivorous fish (FPRED in Table 5.17) with a body weight ranging from 100 up to 1500 g. The biological half-lives for trout or whitefish, for instance, can be estimated by means of the first equation, while in the case of pike the second equation can be applied. Perch can be regarded as an intermediate species, which can be modelled up to 100 g by means of the first equation for non-piscivorous fish, and for higher weights by means of the second equation, for piscivorous fish.

In the table higher values are also presented to show the result of extrapolating to higher values. However, their validity is doubtful. As an example, the 3D-plot (Figure 5.4.9) gives insight into the temperature effect on the body weight versus biological half-life dependency in prey fish.

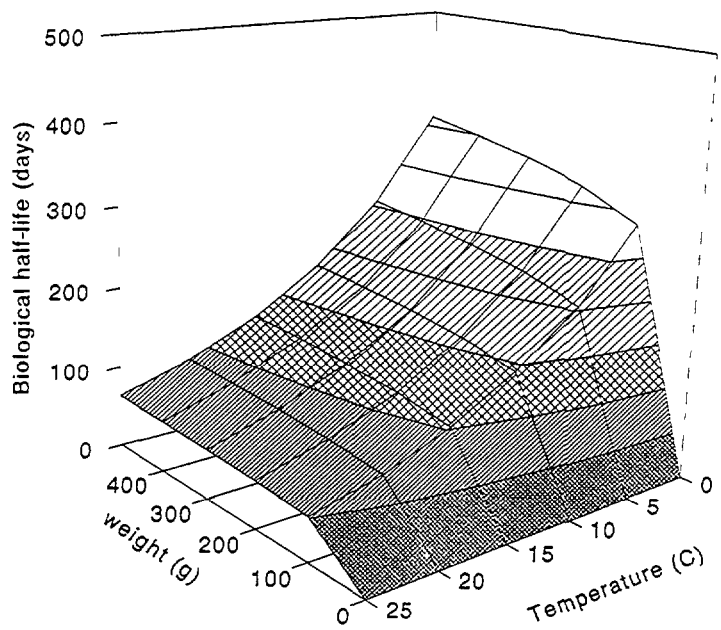

FIG. 5.49. The relationship between biological half-life, body weight and lake temperature for non-piscivorous fish.

TABLE 5.17. CALCULATED VALUES FOR BIOLOGICAL HALF-LIVES OF CAESIUM AS A FUNCTION OF BODY WEIGHT, BASED ON EQUATION (5.26), VALID FOR SMALL AND JUVENILE FISH WITH A BODY WEIGHT 5 TO 350 G (FPREY), AND EQUATION (5.31) FOR PREDATORY FISH WITH A BODY WEIGHT OF 100 TO 1500 G (FPRED) AT FOUR DIFFERENT TEMPERATURES

Weight (g)		Temperature			
		20°C	15°C	10°C	4°C
FPREY	5	48	67	95	144
	10	52	74	105	159
	20	58	82	115	175
	25	59	84	119	180
	50	65	93	131	199
	100	72	102	144	219
	150	76	108	153	231
	250	82	116	164	248
	500	90	128	180	273
	1000	99	140	199	301
	2000	109	155	219	332
	3000	116	164	231	351
FPRED	100	164	232	329	498
	200	189	267	377	572
	300	205	289	409	620
	400	217	307	434	657
	500	227	321	453	687
	1000	260	368	521	789
	1500	282	399	565	856
	3000	324	459	649	983

In accordance to this approach, the fish species in the VAMP database can be subdivided into the following two groups:

1. Perch 0+, roach, smelt, minnow, trout, whitefish, Perch 2+ (<100 gram)
2. Pike and large perch (>100 gram)

The body weights of the fish were not given in all cases; in these cases the weight was estimated on the basis of reported length-weight relationships for similar fish at the same altitude and at similar lake temperatures. These recommendation are presented in Table 5.18.

2. **Recommendation level 2**

Applying the empirical linear power functions for the body weights of the various fish species in the database of the VAMP project and lake temperatures general recommendations on the biological half-lives can be supplied. Obviously, for most of the fish species involved, the body weight ranges from 5 g for juvenile and small fish species like smelt in IJsselmeer and minnow in Øvre Heimdalsvatn, up to 300 g for perch, the upper limit of the data from which the empirical relationship was derived. Large perch and pike have body weights in the range of the second sub-model. Also the range of lake temperatures varied within the expected natural range, from 7°C in the Nordic area up to 23°C in southern Europe. Based on the weight of these species and the average temperature in the lake ecosystems, a summary of biological half-lives, based on Table 5.17, is presented in Table 5.19.

TABLE 5.18. RECOMMENDED VALUES FOR BIOLOGICAL HALF-LIFE (BHL) FOR FISH SPECIES OF DIFFERENT SIZE IN THE LAKES STUDIED IN THE VAMP PROJECT MEAN LAKE TEMPERATURE CALCULATED ON AN ANNUAL BASIS

Lake	Mean temp. (°C)	Species	Average weight (g)	BHL (days)
Iso Valkjärvi	11	Whitefish	250	153
		Perch 0+	10	98
		Perch M	50	157
		Perch L	300	382
		Pike	500	432
Hillesjön	12	Roach	40	111
		Perch 0+	10	91
		Perch M	50	114
		Perch L	300	356
		Pike	1000	453
Øvre Heimdalsvatn	7	Minnow	5	117
		Brown Trout	250	202
IJsselmeer	15	Smelt	5	67
		Roach	177	110
		Perch 0+	10	74
		Perch M	50	93
		Perch L	300	289
Devoke Water	15	Perch 0+	10	74
		Perch M	50	93
		Perch L	300	289
		Brown Trout	250	116
Bracciano	23	Whitefish	250	67
		Pike	150	145

TABLE 5.19. CALCULATED VALUES FOR BIOLOGICAL HALF-LIVES OF CAESIUM AS A FUNCTION OF BODY WEIGHT ACCORDING TO THE EMPIRICAL RELATIONSHIPS (LINEAR POWER RELATIONSHIP) FOR SEVERAL FISH SPECIES CONTAINED IN THE DATABASE OF THE VAMP PROJECT

Fish species	Biological half-life (days)	
	Best estimate	Range
Prey fish		
Smelt	65	–
Minnow	120	–
Roach	100	89–111
Brown trout	160	116–202
Whitefish	110	67–153
Perch juvenile (>0+)	85	74–98
Perch adult (>2+)	125	93–157
Predatory fish		
Pike, large perch (>5+)	300	145–453

To avoid underpredictions for Nordic lakes, the upper range should be selected. However, many fish species are not mentioned in this list, in the case of other lake systems with other fish species, even more general recommendations are required. This is presented as recommendation level 3. In this case the only distinction made is between piscivorous and non-piscivorous fish. The latter group also includes juveniles of large top predatory fish.

3. **Recommendation level 3**

If no clear information is available concerning the aquatic food web, the species involved, and temperature regimes, one single value as a generic biological half-life can be adapted to assess the biological half-life of predatory and non-predatory fish. This is mainly meant for a generic model, as is often used in screening analysis systems, or risk analysis systems, in which the global range is considered relevant. Again, these recommended values are based on the application of the sub-model on the various lakes, and must be considered as a generic approach, not applicable for specific studies on particular lake ecosystems.

The best estimations for the biological half-lives based on Table 5.19 are:

I.	Perch 0+, small roach, smelt, minnow.	90 days
II.	Trout, whitefish, roach, perch 2+ (< 50 gram)	125 days
III.	Pike, large perch (100 gram)	300 days

Recommended values for non-predatory and predatory fish are presented in Table 5.20.

TABLE 5.20. GENERIC VALUES FOR THE BIOLOGICAL HALF-LIFE (DAYS) OF PREDATORY AND NON-PREDATORY FISH

	Non-predatory fish		Predatory fish
	small species, juvenile piscivorous fish (5–100 g)	adult fish (< 300 g)	adult fish (> 100 g)
Biological half-life	90	125	300

Aquatic invertebrates

Aquatic invertebrates including molluscs, benthos (insects) and zooplankton, are not discussed in this Section, as detailed information on body weights were not available in the data base. In principle the biological half life-of these aquatic organisms can be estimated by same sub-model as presented above. Generic values, based on the literature, are presented in Table 5.21.

TABLE 5.21. GENERIC VALUES FOR THE BIOLOGICAL HALF-LIFE (DAYS) FOR AQUATIC INVERTEBRATES

Aquatic organism	Biological half-life
Zooplankton	5
Benthos (deposit feeders)	7
Molluscs (filter feeders)	40

5.6. ECOLOGICAL HALF-LIVES

Radioactive nuclides reduce their radioactivity by physical decay according to their physical half-life. In a similar manner, ecological half-life can be used to describe the resultant decrease in a compartment from all processes acting to reduce the level of radioactivity. When series of observational data are available, an ecological half-life can be determined from an exponential curve fitting the data series. Such half-lives have been calculated from the data for concentration of ^{137}Cs in water and fish species in some of the VAMP lakes. Only a brief account is given here; further details are given elsewhere [5.25].

Information about ecological half-lives is essential from the radiation dose point of view as these can be used to obtain rapid estimates of recovery times in contaminated areas (see papers in Moberg [5.26] and Dahlgaard [5.27]). The examples given below include water and different fish species in selected lakes in the VAMP study, for which sufficient data are available. Some analyses have also been carried out to determine sensitivity to the time period considered. Observational data for ^{137}Cs in water are unfortunately often lacking for the initial period, so caution must be exercised when comparing half-lives.

The best initial data set for water is available from Esthwaite Water (see Appendix III). Concentrations of ^{137}Cs in water are given for the epilimnion and hypolimnion. Mean values of these have been plotted to obtain the exponential regression curves (Figure 5.50). Initially, up to about two months after deposition, there is as expected a very rapid removal rate of ^{137}Cs from the water, corresponding to an ecological half-life of one month. Due to absence of data during corresponding time periods, no comparison can be made with the other lakes. The analysis indicates an effective removal of ^{137}Cs to the sediments, as the water retention time of about 70 days cannot explain such a rapid decline. The subsequent decline is of the same order as the outflow rate of water, which is in fact the shortest for the lakes from which empirical data for water are available.

For other lakes, ecological half-lives have been determined in a similar manner, although with less data (Table 5.22). The time period studied is general about 5 years after deposition. Only average values over two time periods have been calculated, but the analysis show a tendency of increasing ecological half-lives with time. Thus, care must then be taken when using these for predictions.

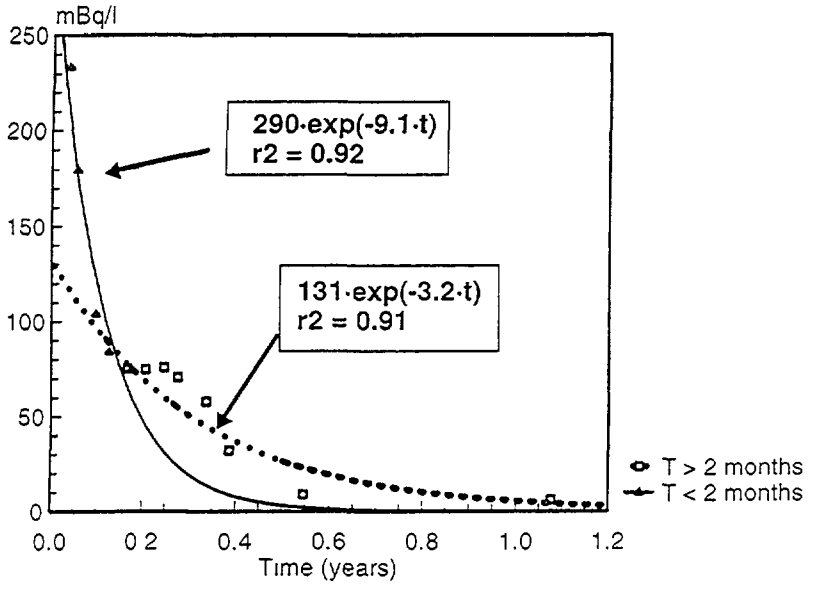

FIG. 5.50. Regression curves fitted to observed mean values of the concentration of ^{137}Cs in epilimnion and hypolimnion waters of Esthwaite Water.

TABLE 5.22. OBSERVED PEAK VALUES, DATES OF OCCURRENCE AND CALCULATED ECOLOGICAL HALF-LIVES FOR LAKE WATERS DURING DIFFERENT TIME PERIODS AFTER DEPOSITION

Lake	Observed peak value (Bq/L)	Date of observed peak value	Ecological half-life (year) up to 1 year	Ecological half-life (year) after 1 year
Devoke Water	0.35	end July 1986	0.4	2
Hillesjön	6.4	12.6.86	0.3	1.5
IJsselmeer	0.2	1.5.86	0.75	1.7–2
Iso Valkjärvi	4.6	10.6.87		2.6

The fit to an exponential decrease for water is good for all lakes, with the exception of Hillesjön, where the correlation coefficient was about 0.6. The probable explanation to this is resuspension from the bottom sediments. The importance of resuspension for maintaining increased levels of ^{137}Cs in water has been confirmed by field measurements [5.11]. Resuspension has also been identified as the main contributor to the uncertainty in the predicted levels of ^{137}Cs in the waters of Hillesjön (see Section 5.3).

In general, the ecological half-life of caesium in lakes is about two years after the first year. The half-lives seem to be correlated to water retention time, as well as reflecting the importance of the secondary load.

Water is one main pathway leading to the fish compartment, which is very important from dose point of view. Ecological half-lives have also been calculated for certain fish species from selected lakes (Table 5.23).

For brown trout in Øvre Heimdalsvatn, there is a suitable complete data set. Different start and end points were tried for the regression, but the results were very consistent, showing an ecological half-life of just below 3 years and correlation coefficients of 0.9 and higher (Figure 5.51). In contrast, brown trout in Devoke Water had an ecological half-life of 1.6 years. However, there is a large scatter in the data, resulting in a correlation coefficient of about 0.7. Shorter half-lives were also found for perch in IJsselmeer compared to perch in the Nordic lakes. However, in IJsselmeer there is intensive commercial fishing which effectively reduces the ecological half-life. The results for small perch in IJsselmeer also indicate an increase in half-life with time. The similar and rapid decline for all fish species in Hillesjön was unexpected. One possible explanation could be migration of fish out of the lake into the Baltic Sea.

The metabolism within the fish is described by the biological half-life, which is one component of the ecological half-life. It is well known that the biological half-life depends, among other things, on water temperature and fish size [5.21, 5.28]. In Section 5.5 it is clearly seen that the more southern VAMP lakes show a much faster recovery than lakes in northern Europe, partly on account of their higher water temperatures.

Simple models are often based on the concept of ecological half-lives to account for all the complicated processes involved. However, further evaluation of the importance of different lakes characteristics and important underlying processes for determining ecological half-lives need to be undertaken.

TABLE 5.23. CALCULATED ECOLOGICAL HALF-LIVES OF CAESIUM FOR FISH

Lake	Species	Ecological half-life (year)
Devoke Water	Brown trout	1.6
Øvre Heimdalsvatn	Brown trout	2.9
Hillesjön	Roach	2
	Perch, mixed	2
	Perch > 20 cm	2
	Pike	2.4
IJsselmeer	Perch, small	1
Iso Valkjärvi	Pike	4.6

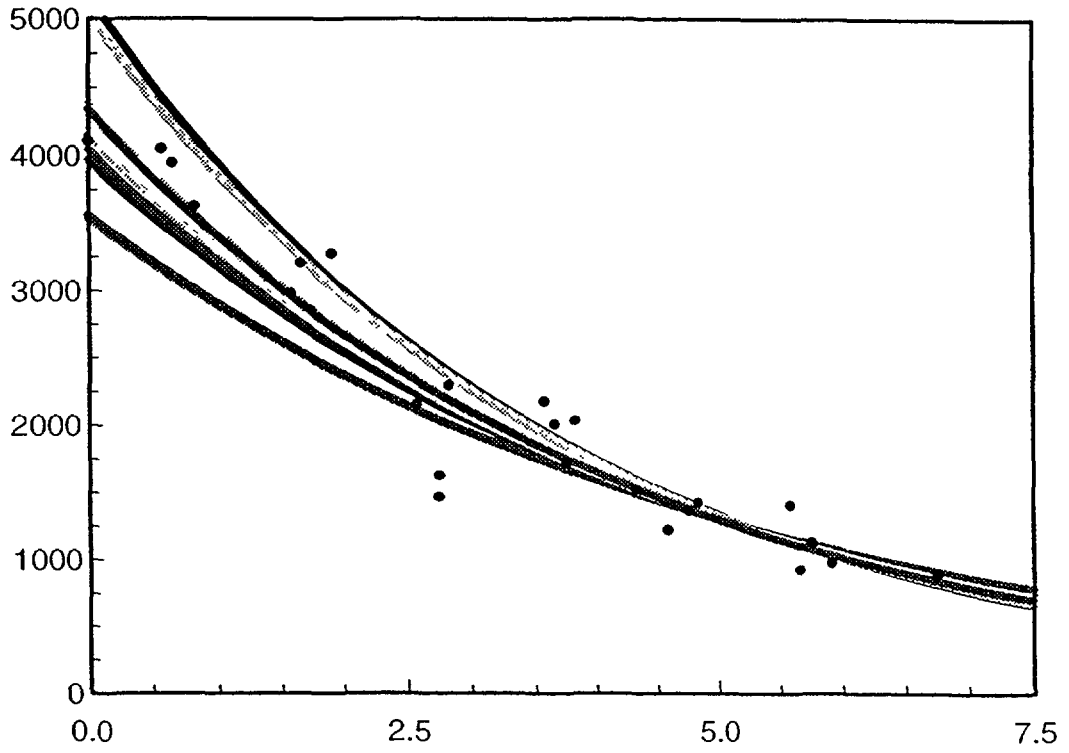

FIG. 5.51. Regression curves for exponential fitting to observed levels of ^{137}Cs in brown trout from Øvre Heimdalsvatn.

5.7. MODELLING DIETARY SHIFT; AN EXPLANATION OF THE "SIZE EFFECT" USING PERCH AS AN EXAMPLE

This Section discusses the so-called weight or size effect in perch contaminated with ^{137}Cs. In several European lakes, there seems to be an almost linear relationship between the ^{137}Cs levels in perch and their body weight at a given time. Some fish like brown trout show a similar effect, while other fish species like bream, rudd and roach do not show it.

This effect may be explained by considering the age of the fish population concerned. In comparison with, for example smelt and roach, large perch has a rather long biological half-life. Due to its position in the food web, the peak in the contamination of the perch normally occurs a relatively long time after the deposition of radionuclides on the water body. The curve for perch shows a slower initial increase of the ^{137}Cs content, and a longer tail in comparison with plankton feeders like smelt (see Annex III and Hadderingh and Van Aerssen [5.29]).

Models can be helpful tools to explain this "size effect" in fish. Many variables, such as uptake rates, seasonal changes, position in the food web and the turnover time of radionuclides in the lake, play a role in the transport of radionuclides up through the food chain. The relative importance of these factors is difficult to quantify without the use of dynamic models.

Modelling the different age classes gives the relationship between the ^{137}Cs levels in perch and their age. For that purpose, a modified version of the dynamic model LAKECO [5.30] has been used to calculate the concentration in smelt and perch as a function of year class. Normally this model predicts the levels of radiocaesium in both young and adult perch present at the time of radionuclide deposition on the lake. This can be considered as "a worst case scenario". However, in the real situation, perch born several years after the fallout will be exposed to less contaminated food than perch present in the lake at the time of deposition. By implementing a shift in the food uptake, perch, born at any time, can be modelled.

Lake IJsselmeer has been selected for a test case of the application of the LAKECO model to better understand the size effect, since extended sets of data are available from this lake [5.29].

In Figure 5.52 the ^{137}Cs concentration in perch has been plotted against its body weight for three different years. It clearly demonstrates the size effect in perch for the IJsselmeer. The figure also shows that the size effect becomes less important in fish caught in later years (see cf. Håkanson et al. [5.31]), although it is still present after 6 years.

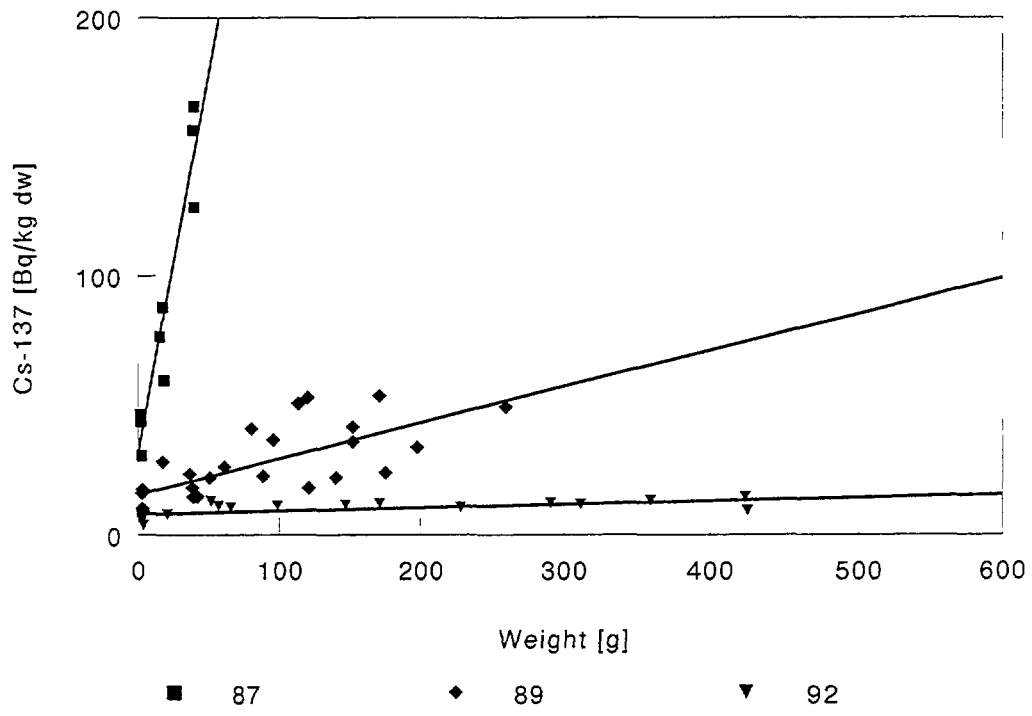

FIG. 5.52. Relationship between body weight (g) and ^{137}Cs concentration (Bq/kg dw) in predatory perch in IJsselmeer in three sampling years: 1987, 1989, and 1992.

Figure 5.53 gives predicted ^{137}Cs levels in perch of distinct ages, born shortly after, and at 12, 24, 36, 48 and 60 months after the deposition on the Lake IJsselmeer. The symbols represent the empirical data. This figure demonstrates that by simply introducing a shift in the fish uptake, the differences in caesium levels among the various year classes can be calculated.

From Figure 5.53 a size effect figure can be reconstructed by drawing vertical intersection lines on specific sampling dates. The ^{137}Cs levels of the various year classes at the intersection points can be plotted against the corresponding body weights in a similar way to Figure 5.52. The upper intersection points with the highest caesium concentrations correspond to higher body weight than the lower intersection points. Figure 5.54 clearly shows that body weight increases exponentially with time. The same figure also shows that in 1988 perch of year class 1986 have a higher body weight (upper intersection point) than perch of year class 1988 (lower intersection point). Consequently perch with higher ^{137}Cs levels correspond to higher body weights. When the "size effect" values for the various sampling dates are reconstructed, plots such as in Figure 5.52 will be obtained.

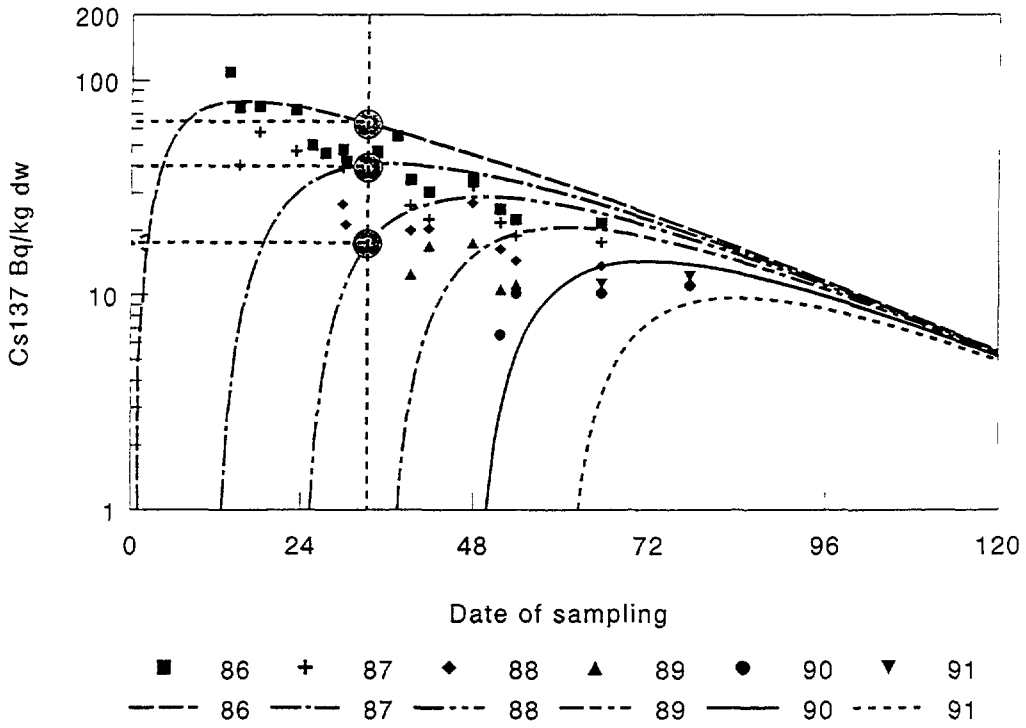

FIG. 5.53. The predicted ^{137}Cs concentration (Bq/kg dw) for the various year classes versus time (months), compared with the empirical data. Calculations performed with the LAKECO model.

Comparison between the observed and the predicted levels (Figure 5.53) shows that the model tends to overpredict the ^{137}Cs levels. The model is based on conservative assumptions to avoid underestimation. Although the predicted values tend to be higher than the empirical data, the predicted maxima occur later than the observed, an effect which occurs in almost each year class. The main reason for this is that the model predicts the caesium levels in adult perch. This causes underestimations, since perch younger than two years have a higher growth rate than adults, and consequently a higher caesium uptake, while in the model the growth rate of the adult perch is selected as a default value. Furthermore, the diet of the juvenile perch consists mainly of zooplankton and benthos, groups which are highly contaminated in the initial period after the deposition. The adult perch in the model are assumed to be a top predator foraging on smelt, which contains lower levels of ^{137}Cs than zooplankton. Incorporating these two factors into the model may result in more accurate predictions. Nevertheless, even using this approximate approach, the shift in food uptake provides a rather good explanation of the size effect in perch.

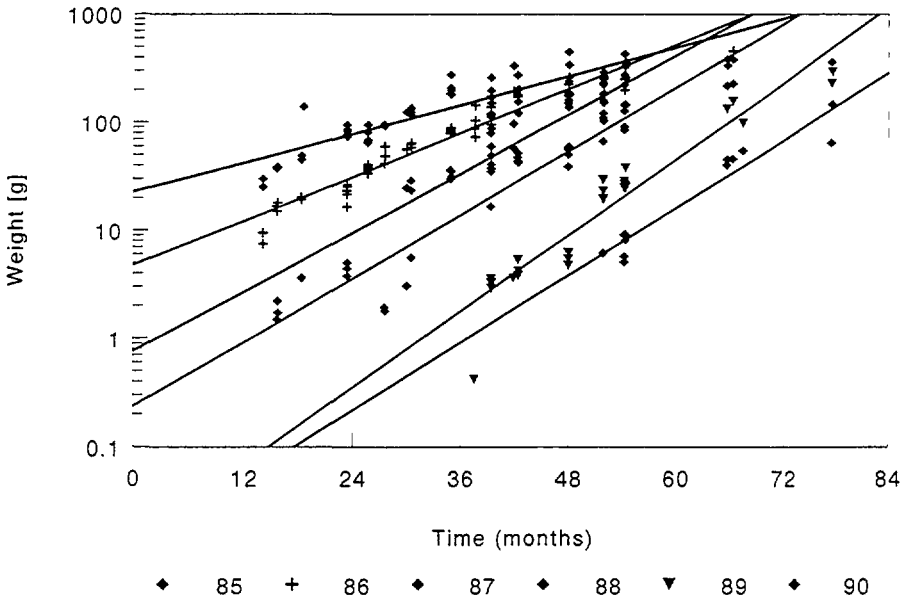

FIG. 5.54. Body weight (g) as a function of time (months) for perch. Each curve represents a year class. Straight lines are fitted lines. The gradient of the curve is the relative growth rate (RGR). Averaged value for the RGR over the year classes 1986 – 1990 is 1.45 × 10^{-3}/d.

According to the observations perch of the year classes 1985 and earlier do not show a size effect [5.29]. This is due to the fact that fish of these year classes were in the adult stage at the moment of the deposition. Their body weight may have differed, but the uptake of ^{137}Cs was the same. The size effect is mainly related to the ^{137}Cs amount in the lake water and therefore decreases in all trophic levels. The next generations of perch are consequently exposed to diminishing levels of radionuclides in their prey.

During the first period after the accident a reversed size effect may also be observed. One reason for this is that high transfer of radionuclides takes place to non-predatory perch (perch 0+ and perch 1+) just after the accident because of the consumption of contaminated zooplankton and benthos, while at that time the prey of adult perch is less contaminated. Because of the relatively lower body weight of the juvenile perch combined with high uptake rates (resulting in high growth rates), an inverse size effect can be assumed: in comparison with perch 2+ the ^{137}Cs content in perch 0+ is higher, while the body weight is lower. Unfortunately there are not enough empirical data available to support this assumption. However, in Figure 5.18, the difference in response between juvenile and adult perch is illustrated.

5.8. OPTIMAL MODEL SIZE AND PREDICTIVE POWER

5.8.1. Introduction and aims

Dynamic models (or mass-balance models) are founded on a causal analysis of the processes governing the fluxes of matter and substances based on relationships expressed by differential equations. If dynamic models are to be used in practice in monitoring and research, the rates that govern the transport between the various compartments need to be known, simulated or estimated. In dynamic modelling, the analysis of dimension (of each parameter) is very important. Dynamic models are mostly used to study complex interactions and time-dependent variations within defined ecosystems, like lakes. Dynamic models are sometimes difficult to calibrate and validate and they tend to grow indefinitely. If dynamic models are not validated against independent, reliable empirical data, they may yield absolutely wrong predictions.

Empirical/statistical models are primarily used to quantify differences between ecosystems/areas from simple, readily accessible data. Empirical models and dynamic models are thus used for different purposes; they do not compete, but complement each other. The presuppositions of models must always be clearly stated.

It is well known for nutrients/eutrophication in lakes that large dynamic models often yield worse predictions than simple empirical/statistical models [5.32, 5.33] and that dynamic models for toxins in lake ecosystems may yield extremely bad predictions with uncertainty limits two orders of magnitude apart as shown in the BIOMOVS study [5.34]. It is simple to give verbal "explanations" of this and very difficult to give clear-cut mathematical explanations where general definitions are used for "predictive power" and "model uncertainty". The aim of this Section is certainly NOT to present the final solution to this problem but rather to present an initial quantitative approach to this important problem. For further discussions of many of the models and results discussed in this Section, see the textbook Håkanson and Peters [5.35].

This Section focuses on models for ecosystems, like lakes and coastal areas, i.e., rather homogenous entities of a certain area (in the order of 10.000 m^2 to 100 km^2). One important definition of such ecosystems is that the areal and temporal variability of defined characteristic mean properties (e.g. zooplankton biomass, Secchi depth and Cs concentration in pike) within the ecosystems should be smaller than the variability between ecosystems.

There are benefits and drawbacks with all types of models. The main disadvantages with empirical models are that they generally only apply under restricted conditions, and that they may give a poor insight into the causal mechanisms [5.36]. The main disadvantages with dynamic mass-balance models [5.37, 5.38, 5.39] are that they may be difficult and very expensive to calibrate and validate, and they tend to be large.

This Section focuses first on a general and principal discussion on the problem of optimization of predictive models, i.e., in contexts where one or a few interesting y-variables are to be predicted from a set of more readily available x-variables. The basic questions is: is it possible to quantitatively address the problem of optimization of model size, i.e., the balance between an increasing generality as dynamic and empirical models account for more processes (more x-variables) and the increase in predictive accuracy and uncertainty associated with this growth? Every process, model variable and/or compartment added to a model entails a certain error. It is evident to many modellers that the risks of predictive failure, as determined from both a decreasing accuracy in the prediction of y and increasing uncertainty limits (e.g., confidence or tolerance limits) around the predicted y-value, will increase if more and more x-parameters (like compartments, boxes, factors, rates, processes, etc.) are accounted for in the model.

First, it should be stressed that it is evident that ecosystem models constructed with the purpose of describing/understanding interactions, food webs, fluxes of contaminants, etc. must generally be extensive. However, it is quite another issue with models for specific predictions, of just one or two y-variables. In predictive modelling there seem to be two avenues to make that ranking of influence: by empirical/statistical methods (correlations, etc.) or by sensitivity analyses.

5.8.2. Problem formulation

Generality and fit

In the balance between generality and accumulated uncertainty, we will here first treat the question of generality. An analogy can be made with lake hydrographic surveys and the construction of bathymetric maps [5.35, 5.40].

Figure 5.55A illustrates a shoreline of a lake. From this simple information, nothing about the topography of the lake is known. The information value I is zero, i.e., for $n = 0$, $I = 0$. The information

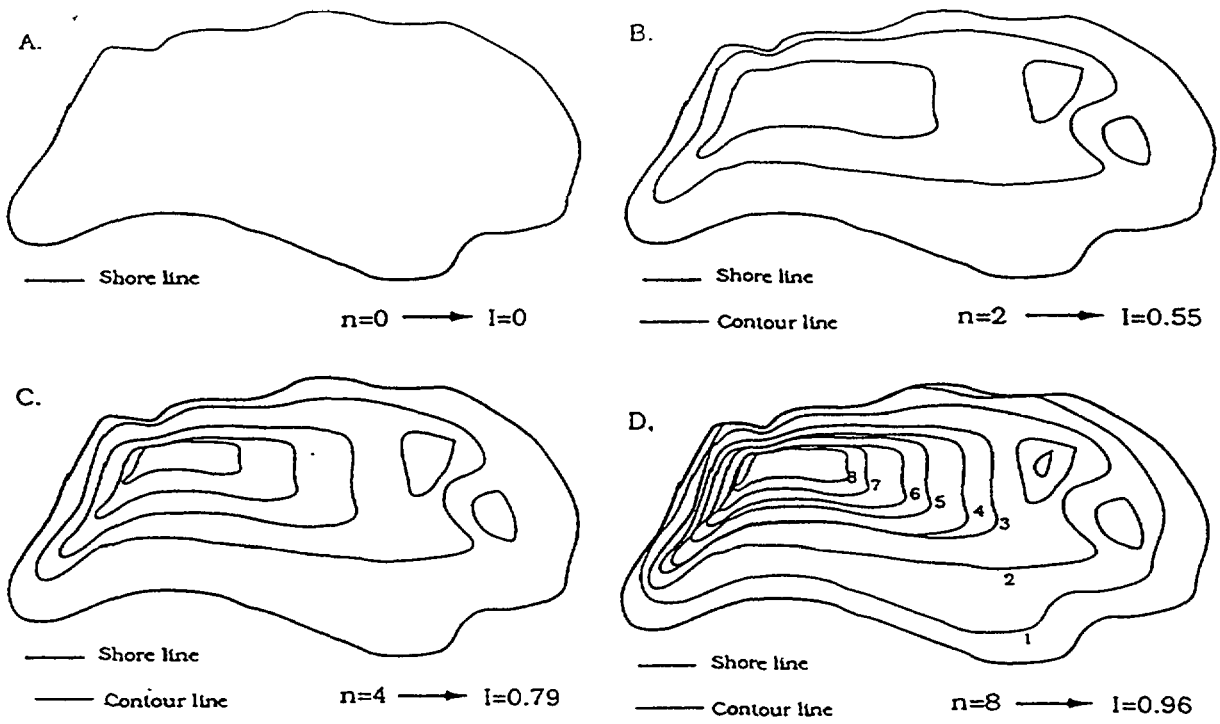

FIG. 5.55. Illustration of how the information value (I) increases with the number of contour lines (n) in a bathymetric map.

value is taken as having a value between 0 and 1; I = 1 means complete and correct information of the entire topography of the lake. By increasing the number of contour lines the information value, I, increases (Figure 5.55A–D) [5.41]. It should be noted that the I-value initially increases very markedly. There is a significant difference in how the I-value increases when n increases from, for instance 2 to 4 as compared to from 8 to 10. The relationship between I and n is given by:

$$I = (e^{0.4n}-1)/(e^{0.4n}+0.22) \tag{5.36}$$

This formula is depicted in Figure 5.56A. The information value, I, asymptotically reaches 1 as n approaches ∞.

The same principles are also valid in context of predictive modelling. It is evident that there would be many specific cases when the relationships between n and I (for modelling) would differ from this particular I-value (for bathymetric maps). In order to challenge this particular definition some tests were made.

Figure 5.56 gives three test series (stepwise multiple regressions) for:

1. A simple biological variable; Hgpe, i.e., the mean lake Hg content in perch fry in mg/kg wet weight based on data from some ten fishes per lake from 25 Swedish lakes [5.42]; predicted from many empirical parameters from the catchment area (like percentage of rocks, lakes and mires), the bathymetric map of the lake (like mean depth, Dm, and dynamic ratio, i.e. $\sqrt{\text{area}}/\text{Dm}$) and from lake chemical variables (like pH and colour).

2. An abiotic (chemical) variable; RHg, i.e., mean lake reactive Hg from water samples; in ng/L predicted from different empirical lake parameters [5.42].

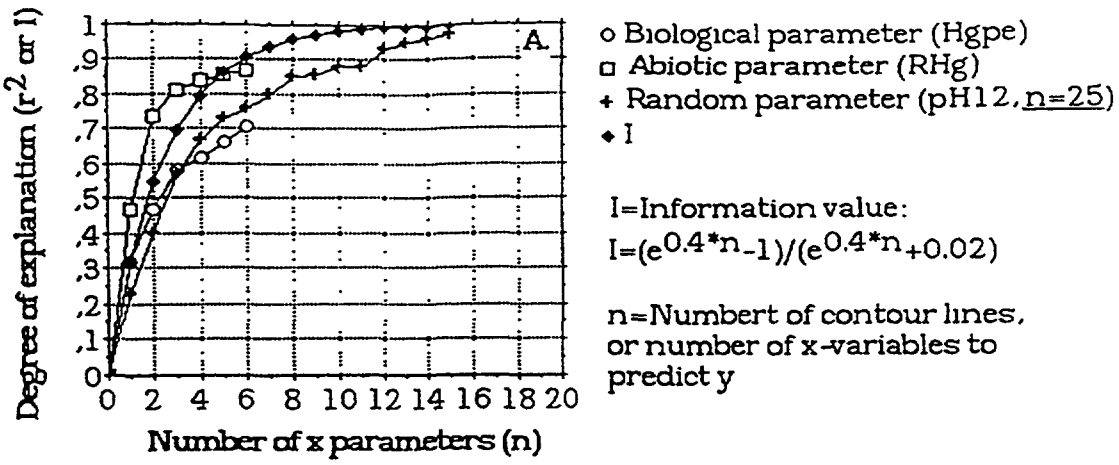

FIG. 5.56. Graphical illustration of the relationship between the degree of explanation (r^2 or I) and the number of contour lines (n) in a predictive model for a biological variable (Hgpe, Hg-content in perch fry in mg Hg/kg ww), an abiotic variable (RHg, Hg-content in lake water in ng/l; see Lindqvist et al., 1991 for definition), a prediction of mean annual lake pH (pH12) based on random parameters for 25 lakes, and the information value (I) as defined by the given formula (valid for bathymetric maps).

3. Mean annual lake pH predicted from random parameters (as given by a random data generator).

The following conclusions may be drawn from Figure 5.56:

- These results indicate that it is more difficult to predict biological variables than abiotic variables. This is evident from this simple example where an elementary biological parameter has been selected, the Hg-concentration in fish: from seven steps a r^2-value of 0.73 was obtained. The abiotic (chemical) variable as given by a specific fraction of mercury in lake water called reactive Hg, is by definition not a biological parameter. It should, however, be noted that the actual value of RHg in a given lake depends on many complex biological processes [5.43, 5.44]. It is often possible when predicting chemical (and also physical) lake variables to obtain higher r^2-values (in this case 0.87) from fewer steps (six instead of seven), as compared to most biological variables.

- It is possible to obtain very high r^2-values in models based entirely on random parameters, given two presuppositions: (i) the number of cases, e.g. lakes (n) must be small (in Figure 5.56 n = 25 was used to obtain comparable data), and (ii) F must be small (1 for pH12; normally F would be set to 4; see Neter et al., 1988 for definition of F), so that many steps would be accepted (there are 15 steps for pH12).

The results for Hgpe, RHg and pH12 are compared to the information value, as defined by Equation (5.36). It can be noted that: (i) the degree of explanation (r^2 or I; where r^2 is the coefficient of determination and r = correlation coefficient) increases as the number of x-variables accounted for in the models increases, (ii) that the curve for the I-value from Equation (5.36) falls between the three other curves, and (iii) that the curves for the biological variable (Hgpe) and the random parameter prediction of pH12 (for n = 25) are very close. However, this is totally dependent on the choice of n. If n is, for example, 35 the curve would be significantly different from the curve for n = 25. The reason for this is simply that it is much more unlikely to obtain high r^2 values for random parameters if n is large.

In conclusion, the predictive accuracy, expressed for example by the r^2 value, when empirical data are compared to modelled values, generally increases with the number of x-variables accounted

for in the predictive model, but differently for biological and chemical variables (and for different modelling presuppositions). This has been exemplified with regression models, but the same principles also apply to dynamical models [5.35].

Accumulated uncertainty

Every state variable and/or rate in a dynamic model and x-variable in an empirical/statistical model has a certain uncertainty (Håkanson, 1992 [5.45]). In dynamic modelling, a mean or a median value for a given ecosystem (e.g. sedimentation rate) can often be applied as a constant in different model calculations/simulations. Uncertainty analysis entails the uncertainties in all the x-variables in the model being accounted for in the determination of the predicted y-value. Sensitivity analysis entails that one model parameter is varied while the rest of the model parameters are kept constant. Uncertainties in x-parameters may, in principle, be added or multiplied in the model.

From statistical textbooks [5.46], it is easy to demonstrate that there exists an exact way of defining the uncertainty of additive models, since the standard deviation, SD, may be written as:

$$SD_y = SD_x\sqrt{n} \tag{5.37}$$

$$y = \sum_{i=1}^{n} x_i \tag{5.38}$$

where SD_y = the standard deviation of the y-variable; SD_x = the standard deviation of all the x-variables. The relationship between the number of x-variables, n, in a simple additive model and the uncertainty, as given by SD_y, is given in Figure 5.57A (the curve linked by crosses). In the following account, Equation (5.37) will be used as a reference and both additive (summation) models and products (multiplicative models) will be tested using x-variables with different standard deviations. Because it is rather difficult to find exact solutions for multiplicative models, Monte Carlo techniques will be used to derive numerical solutions for all types of model uncertainties.

Figure 5.58A gives one example of a frequency distribution for a given standard x-variable used in the following uncertainty exercise. The mean value (MV) is set to 1.0, the standard variation (SD) to 10% of the mean and the distribution is assumed to be normal. This is, in fact, a rather low relative standard deviation (= coefficient of variation, CV = 100SD/MV) in lake ecosystem contexts. Many lake variables, like pH, total-P, and colour, generally appear with significantly higher CV values [5.36]. Section 5.3 gave a compilation of CV-values for the data for the VAMP lakes and showed (for water, whitefish, small perch, trout, large perch and pike) that there is a weak negative trend ($r^2 = 0.035$, $p = 0.018$), i.e. CV decreases with time after the Chernobyl accident, but that this trend is not apparent at all for many species of fish in several lakes (e.g. for trout in lake Øvre Heimdalsvatn, or for small perch in lake Hillesjön). Many CV values are larger than 0.5, and a few even larger than 1. This indicates the great empirical uncertainties in the Cs data for the VAMP lakes.

The frequency distributions in Figure 5.58 have been determined from 10 000 trials using Monte Carlo techniques. In the following, the frequency distribution of Figure 5.58A (SD = 10%), and also distributions where SD is set as 20, 30 and 40% of the mean value will be used. Figure 5.64B shows the uncertainty in a y-variable if one multiplies four x-variables by uncertainty distributions of the type given in Figure 5.58A (SD = 10%). It can be noted that the mean is, naturally, still 1 (1×1×1×1), and that the standard deviation has increased and the confidence interval has widened (from 0.65 to 1.44, as compared with 0.80 to 1.19 — the 95% confidence interval corresponds to about 2SD.

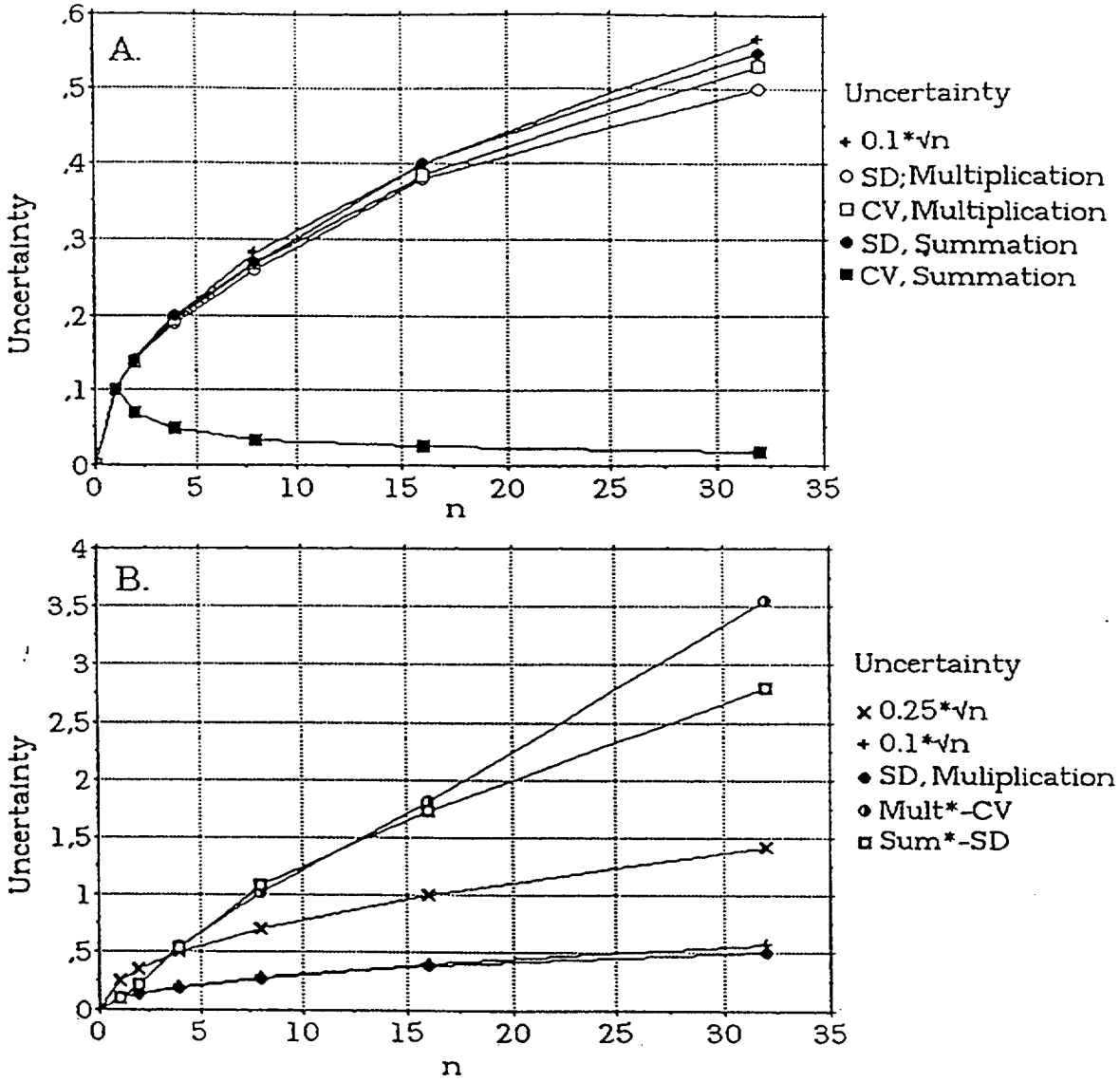

FIG. 5.57.
A. Uncertainty of the y-variable in predictive models with different numbers of x variables (n) determined in two different ways, by summing (SD, Summation and CV, Summation) and multiplying (SD, Multiplication and CV, Multiplication) the x variables in the model. All x variables in this test have a mean value of 1 and a standard deviation (SD) of 0.1. The curve for the exact expression $0.1\sqrt{n}$ is used as a reference line.
B. The same results as A. but for situations when the standard deviation of the x variable is varied (0.1, 0.2, 0.3 and 0.4; Mult-CV and Sum*-SD).*

Figure 5.58C gives analogous results for a summation of four x-variables (of the type in Figure 5.58A), i.e., 1+1+1+1. The mean y-value is 4. The 95% confidence limits vary between 3.61 and 4.39.

Calculations of this type have been made for a whole range of n-values (2, 4, 8, 16, 32) and the results are given in Figure 5.57A and B. In these figures SD, Multiplication means a standard deviation obtained from multiplication where each model variable has a SD of 10%; SD, Summation means the same thing for a summation model; Mult*CV means a coefficient of variation (CV) for a model where each model parameters has a SD-value of 10, 20, 30 and/or 40%. The series is:

n	1	2	4	8	16
SD	x_1	x_1x_2	$x_1x_2x_3x_4$	$(x_1x_2x_3x_4)^2$	$(x_1x_2x_3x_4)^4$

SD_1 = 10%, SD_2 = 20%, SD_3 = 30% and SD_4 = 40% of the mean value (MV).

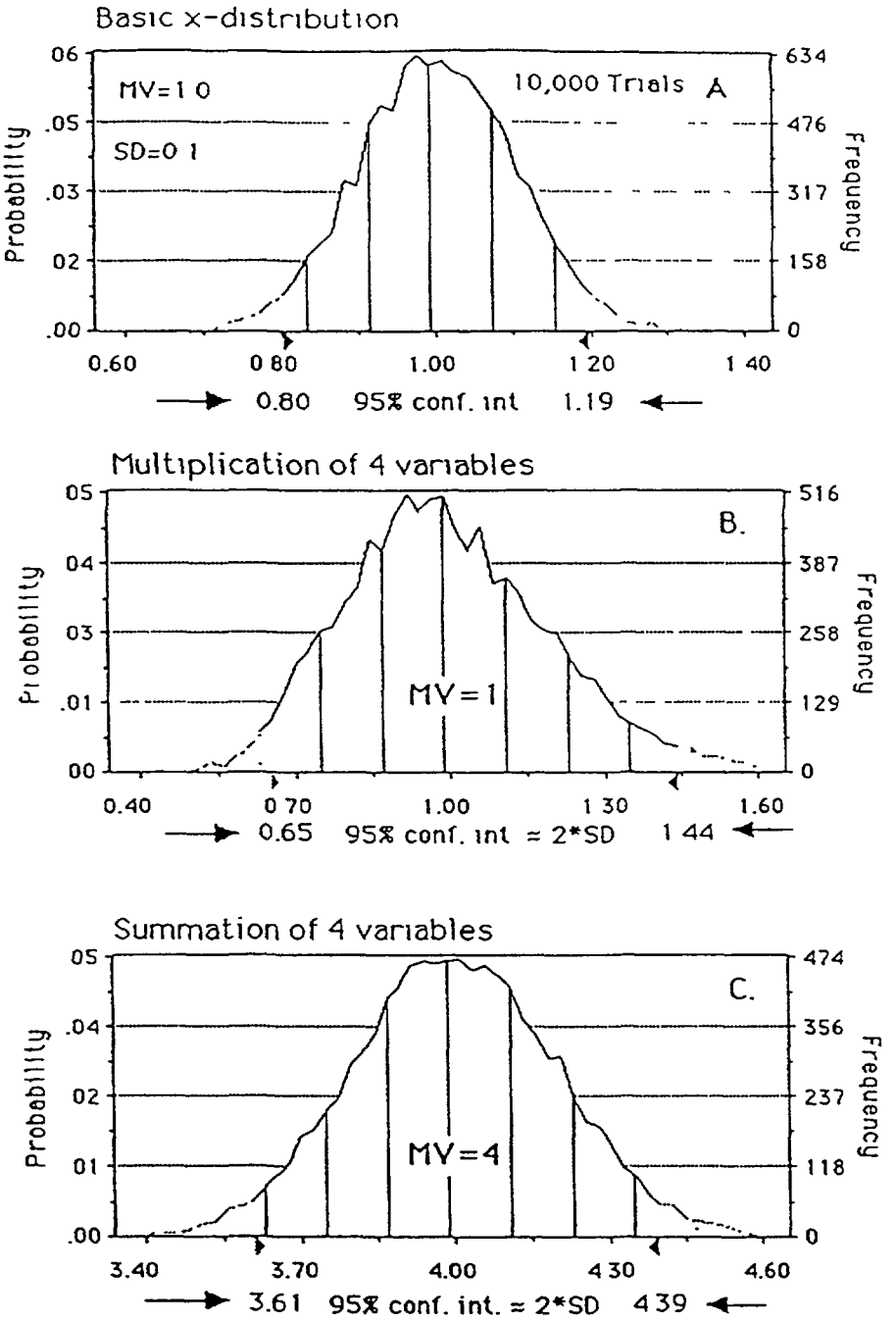

FIG. 5.58. Uncertainty analyses for predictive models.
A. The basic uncertainty distribution for the given standard x variable in this test. MV = 1.0, SD = 0.1, normal distribution, 10,000 trials using Monte Carlo technique.
B. The calculated uncertainty in the y variable after multiplication of 4 x variables.
C. The calculated uncertainty in the y variable after summation of 4 x variables.

The CV-values, would, of course, improve the comparison for x-variables with different mean values.

Using such SD- and CV-values as uncertainty factors for different n, Figure 5.57 shows that, as expected, the three curves for SD = 10% are very close to the exact curve ($0.1\sqrt{n}$). Since these three curves depend on the given presuppositions for the x-variable, they may not be used generally. This is evident from Figure 5.57B, which compares the results for SD = 10% (curve SD, Multiplication and curve $0.1\sqrt{n}$) with two curves with more uncertain x-variables (10, 20, 30 and 40%).

One may also note that the relative standard deviation (CV, Summation) naturally decreases when we add parameters. The reason is that the probability of getting a value which departs 2SD (0.2 units) from the mean of 1 would be about 0.02 for the initial x-distribution, but the probability of getting a value which departs (0.2+0.2 = 0.4 units) from a the new mean of 2 would be much less than 0.02.

From these results, one can note that the uncertainty factor increases significantly as n increases.

5.8.3. Uncertainties in regressions versus model uncertainties

It may seem a paradox that model uncertainty may, in fact, increase as one considers more and more information, i.e., as the number of model variables increase. In the following sections this theme will be discussed. The first focus is on the relationship between the r^2-value and the uncertainty of the slope coefficient of the regression line, the next part deals with the predicted uncertainty in y for individual lakes (which is generally a key issue in lake-specific investigations), and in the last Section of this Report this information will be used to address the important issue of the optimal size of predictive models.

Figure 5.59A illustrates a typical linear regression between an x and a y variable. The regression line is: $y = 0.52x - 6.72$; the r^2 value is 0.61 and n = 30. The figure also gives the upper and the lower 95% confidence limits for the slope of the regression line as a measure of the uncertainty in this regression. It was indicated above that the ratio between the upper and the lower slope coefficients (0.68/0.36 = 0.16) relative to the slope coefficient of the regression line (0.52) is 30.8%. So, 100 × 2SD, as defined in this manner, is 30.8%. This is one measure of the model uncertainty. It is evident that this value depends on the number of data pairs used in the regression (n). The value is also related to the r^2 value obtained in the regression. Results of calculations to create a nomogram linking n, r^2 and 100 × 2SD are given in Figure 5.59B. From this nomogram, the model uncertainty (100 × 2SD) associated with a given r^2 value for a given n can be directly read. The example presented in Figure 5.59B is shown as a dark dot on the line for n = 30. The same type of relationships exist between r^2, n and other confidence limits of the same regression, like the 95% confidence limits for the predicted y, or for the mean y.

From Figure 5.59B, it is evident that the uncertainty of the slope coefficient (100 × 2SD) is very small for high r^2 values; it can be extremely large for low r^2 values, especially if the number of data pairs (n) is low.

Models are generally used for predictions in given lakes of special interest for either research or management. The Figure 5.60 shows that the dynamic ratio (DR) influences the prediction of the Hg content in small perch (Hgpe) more than most other model variables. This means that uncertainties in the DR value may cause relatively large uncertainties in Hgpe predictions. However, for any given lake the DR value can be determined with great precision. The other model variables (RHg, T, pH12 and totP3/3) can generally not be determined with the same precision for any given lake.

In this Section the dependence of the predictive accuracy of a model, in this case a regression model, on the uncertainty of the model variables (x_i) and the model constants, such as the slope coefficient, will be highlighted. The basic problem is depicted in Figure 5.60A. To substantiate the argument, Figure 5.60B gives real data from the Hgpe-model with five model variables. It can be seen that the r^2 value increases as more and more x variables are included in the model, from step 1 (r^2 = 0.18) to step 5 (r^2 = 0.65). The model constants change at each step, for example the model constant for RHg changes from 0.182 at step 1 to 0.006 at step 5. The uncertainty in the slope coefficient decreases steadily with the r^2 value from 1.0 at step 1 to 0.31 at step 5. The decrease in the uncertainty of the slope coefficient could be regarded as a crude measure of how the uncertainty of the model constants change with the r^2 value.

The uncertainty of the model variables for individual lakes (data from Håkanson and Peters [5.35]) are given in Figure 5.60C, which gives the mean values (MV), coefficients of variation (CV) and standard deviations (SD). Thus, with these data, one can determine how uncertainties in model constants and model variables influence the uncertainty in the predicted y-value for a given lake as the number of model variables change in five steps. The results of appropriate Monte Carlo calculations (10,000 trials) are summarized in Figure 5.61. From this figure, it can be seen that the uncertainty for y (defined by the CV-value from the calculated frequency distribution for y) decreases from a very high value (22.1) at step 1 (i.e. with a model with just one model variable, RHg), to a minimum value for n = 4 (when CV = 5.2), and then the model uncertainty increases when the next model variable (total-P) is included. This results can be understood when it is explained that the last model variables were included after the critical F was lowered from 4 to 1, and that total-P is a very variable parameter (CV ≈ 0.35). Without this empirical knowledge, it would seem reasonable to account for total-P and

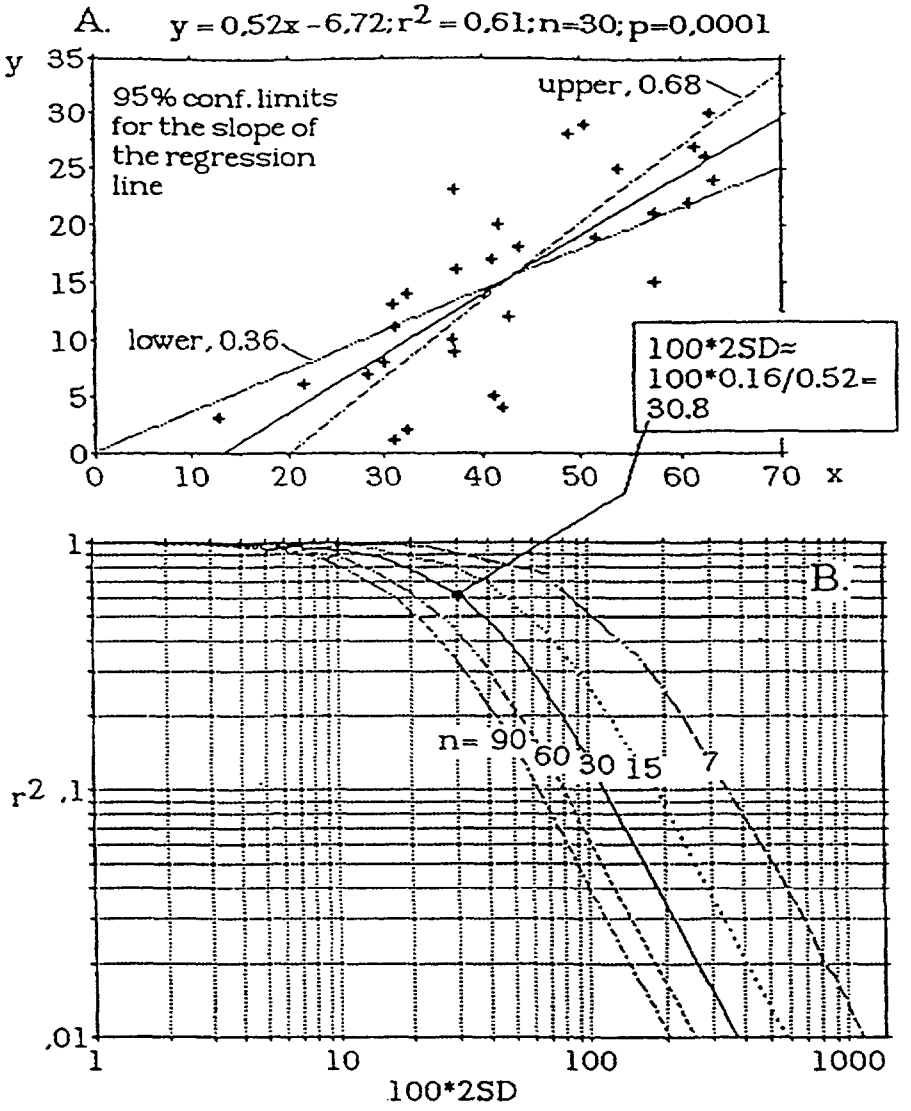

FIG. 5.59

A. A linear regression illustrating the regression line and of the upper and the lower 95% confidence limits of the slope of the regression line. The standard deviation of the slope coefficient is 0.08 [4SD = 0.68–0.36] and the slope coefficient of the regression line is 0.52.

B. A nomogram for the relationship between the uncertainty of the slope coefficient of the regression line (defined in the figure and called 100 × 2SD), the r^2 value and the number of data-pairs used in the regression (n).

Uncertainty in the slope coefficient (a1) decreases as more variables are considered (see B)

A. General set-up

r2-value increase

y1=a1*x1=A1*f(x1) ← Uncertainty in the model variable in individual lake is set constant (see C)
y1=a2*x1+b1*x2=A2*f(x)
y1=a3*x1+b2*x2+c1*x3=A3*f(x)
y1=a4*x1+b3*x2+c2*x3+d1*x4=A4*f(x)
y1=a5*x1+b4*x2+c3*x3+d2*x4+e1*x5=A5*f(x)

Task: Calculate uncertainty in y

B. Example; y=f(x)=Hgpe; n=25; RHg forced into equation

Step	F-value	r2-value	Slope*) uncertainty	Model
1	4	0,18	1,00	log(Hgpe)=0,182*RHg-0,976
2	4	0,42	0,50	log(Hgpe)=0,164*RHg-0,309*log(DR)-1,214
3	4	0,54	0,40	log(Hgpe)=0,096*RHg-0,335*log(DR)-0,151*log(T)-1,198
4	4	0,63	0,35	log(Hgpe)=0,005*RHg-0,307*log(DR)-0,145*log(T)-0,161*pH12-0,071
5	1	0,65	0,31	log(Hgpe)=0,006*RHg-0,278*log(DR)-0,181*log(T)-0,167*pH12-0,181*totP3/3^0.2+0,263

*)=Uncertainty in slope coefficient, A1, related to this r2-value (=2*SD from fig. 3.19)

C. Uncertainty in model variables in individual lakes (CV=SD/MV; see section 4 and Håkanson, 1992)

Variable (x)	MV	SD	CV
RHg	1,17	0,53	0,45
DR	0,14	0,0014	0,01
T	0,48	0,01	0,02
pH12	6,84	0,14	0,02
totP3/3	7,41	2,59	0,35

FIG. 5.60.

A. How would the model uncertainty (i.e., the uncertainty in y) depend on the uncertainties in model constants (a to e) and model variables (x_1 to x_5)?

B. A "ladder" listing the results of stepwise regressions giving F values, r^2 values, uncertainties in slope coefficients for five regression models for the Hg-content in perch (Hgpe).

C. Mean values (for Swedish glacial lakes) of the uncertainties in model variables. The pH12 mean is a mean annual pH, i.e., a mean value for 12 months; the totP3/3 mean is a mean value of lake total-P concentration from 3 months when the last month is month 3 (i.e. from Jan., Feb. and March).

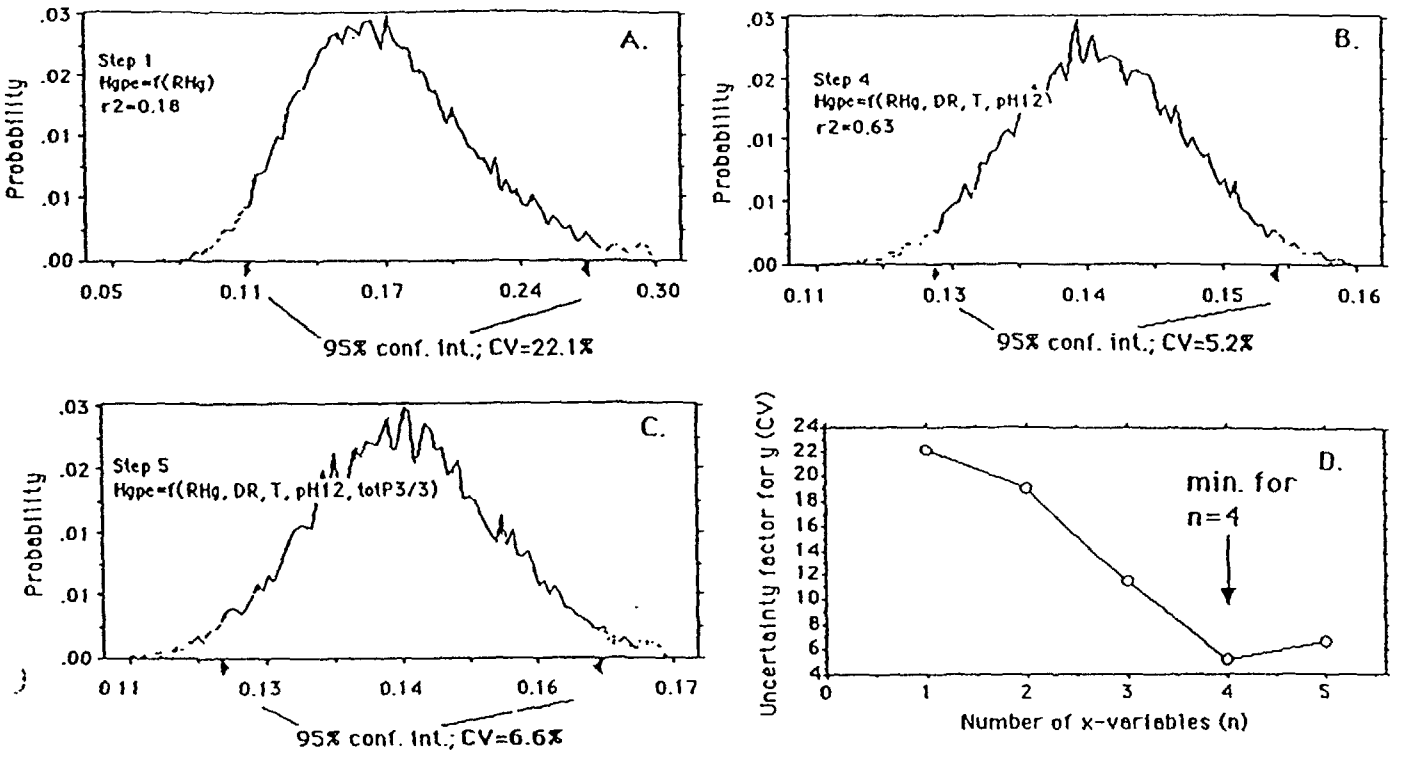

FIG. 5.61. Results illustrating the relationship between the uncertainty in y (as derived from 10 000 Monte Carlo simulations) and the number of model variables (in the Hgpe-models; Hgpe = Mercury content in perch fry in mg/kg ww).

A. The frequency distribution for y (= Hgpe) for the first-step yielding an r^2 of 0.18 shows that the model uncertainty, as given by the coefficient of variation, CV = 22.1%, is very large.

B. The similar distribution for the model based on four model variables gives a much lower CV (5.2%).

C. When the results for the model based on five model variables are used, the CV increases to 6.6%.

D. A comparison of all the results from these tests illustrates that the lowest uncertainty in y in this example is obtained for the model based on four model variables.

lake production in a model of this kind, since an increase in production would biologically dilute a given lake load of mercury, lowering Hgpe-values. However, for these lakes, the data show that the increase in predictive accuracy (from 0.63 to 0.65) is outbalanced by an increase in model uncertainty (for the high CV of 0.35 for total-P). This result motivates the next section, which deals with the problem of the optimal size of predictive models. From Figure 5.61, it is evident that the optimal size of this particular model would be for n = 4. In the next section, this problem will be treated in a more general way, and in the following section, it will be illustrated with data for radiocaesium in lakes.

5.8.4. Optimal size

To determine the optimal size (i.e., number of x-variables) of a predictive model one can combine the information value (r^2 or I) from Figure 5.62 and any of the uncertainty factors (SD or CV) from Figure 5.62 in several ways:

- Maximize I/CV (or r^2/SD), see Figure 5.62A;
- Maximize I(1-CV), Figure 5.62B;
- Maximize I-CV, see Figure 5.62C and D,

since the I-value should be as large as possible and the CV-value as small as possible.

If the uncertainty factor (CV or SD) approaches zero, i.e., if there is no uncertainty linked to the parameters and state variables in the model, then the model would be better as more compartments and processes are added. The expression (1-CV) could, of course, attain negative values if the standard deviation is larger than the mean value and CV larger than 1. So, the expression I(1-CV) is a constructed expression and the optimal model derived from this expression ought to be less interesting than the results from the expressions I/CV and I-CV.

From Figure 5.62, one can note that the optimal size for predictive models (under the given conditions) is generally achieved for a (surprisingly) small n. The reason is that with these definitions, the predictive accuracy (I or r^2) increases rapidly when n is small and the increasing accumulated error or uncertainty (CV or SD) presses down the factor to be optimized for higher n.

5.8.5. Predictive power

The objective in this Section is to use three models, the VAMP LAKE model, the UU-Mixed model, and the UU-Generic model, to illustrate some important principles in all types of modelling, namely predictive power.

Predictive power should be defined scientifically so that its meaning is clear. The aim of this Section is to provide a definition of predictive power and the rationale for that definition.

Figure 5.63A illustrates two hypthetical curves, one based on empirical data, the other on modelled values. There is an almost perfect agreement between the two curves. So, the model provides a very good prediction for this particular y-variable in this particular lake. One way to quantify the fit between empirical and modelled y is to do a regression. The r^2 value, the intercept and the slope of the regression line will reveal the fit. The r^2 value and the slope should be as close to one as possible (Figure 5.63B) and the intercept should ideally cross the origin. Would this model work also for other lakes or ecosystems? If the answer is yes, it seems to be a very useful predictive model. One can, however, safely assume that the r^2 value and the slope will not be equally high in all cases. There will be situations when the model will yield a poor prediction, a low r^2 and a slope much lower or higher than one. Such spread indicates the uncertainty of the model in predictions. This is illustrated in Table 5.24, where the given (hypothetical) model has been tested in 15 situations. For each validation, the r^2 value and the slope between empirical and modelled y can be determined as well as the coefficient of variation (CV = SD/MV) for r^2. If the model generally has a high predictive power, then CV should be small. It is 0.19 in Table 5.24.

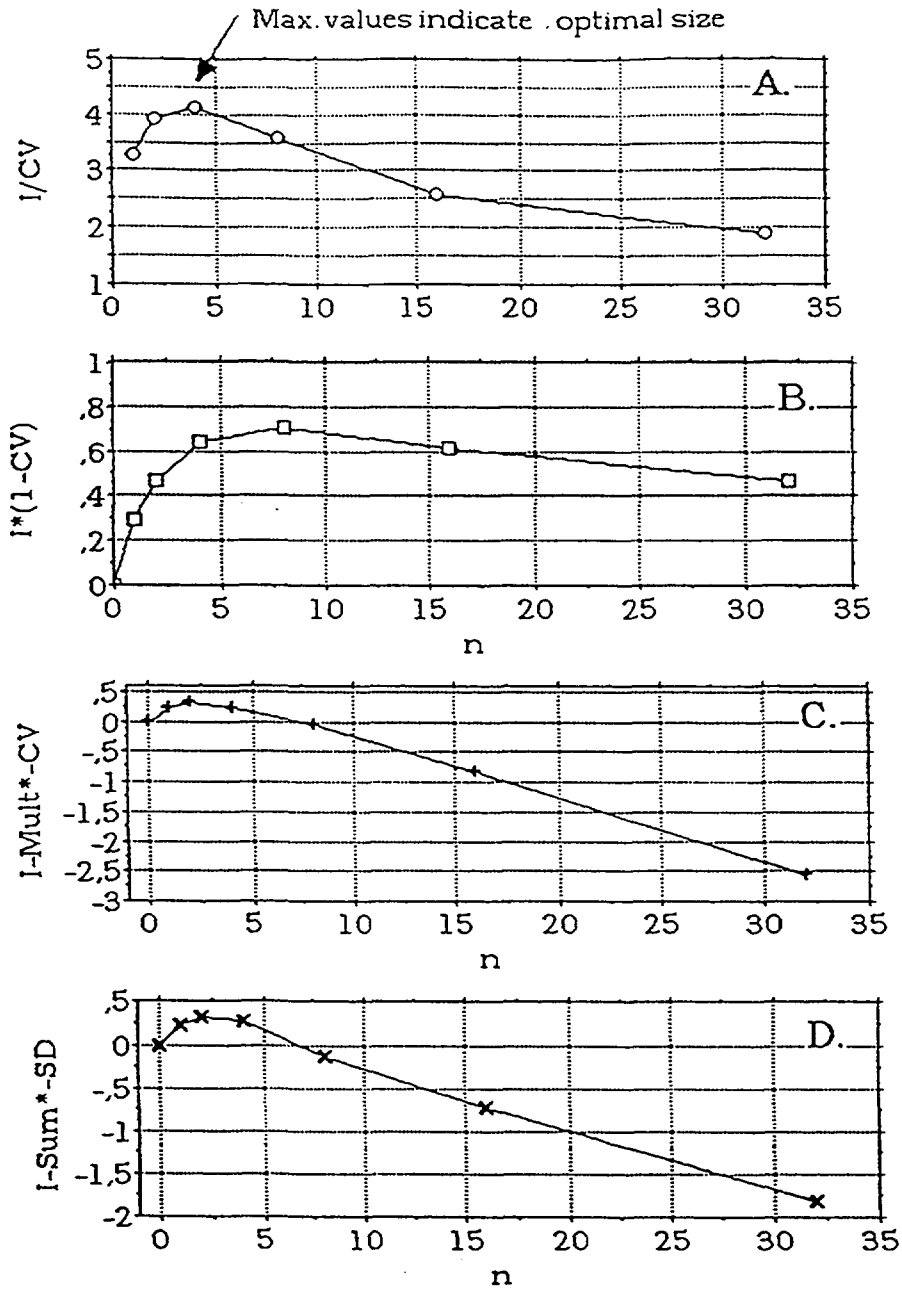

FIG. 5.62. Calculation of the optimal number of x variables in a predictive model (under given conditions). I, the information value (or the r^2 value), which should be as large as possible. The accumulated model uncertainty expressed as the standard deviation (SD) or the coefficient of variation (CV = SD/MV), which should both be as small as possible (n = the number of compartments or x variables in the model).

A. The result for the ratio I/CV, which should be maximized. CV is here equal to CV, Multiplication.

B. The results to maximize the product I(1-CV).

C. The results to maximize I – Mult-CV.*

D. The results to maximize I – Sum-SD.*

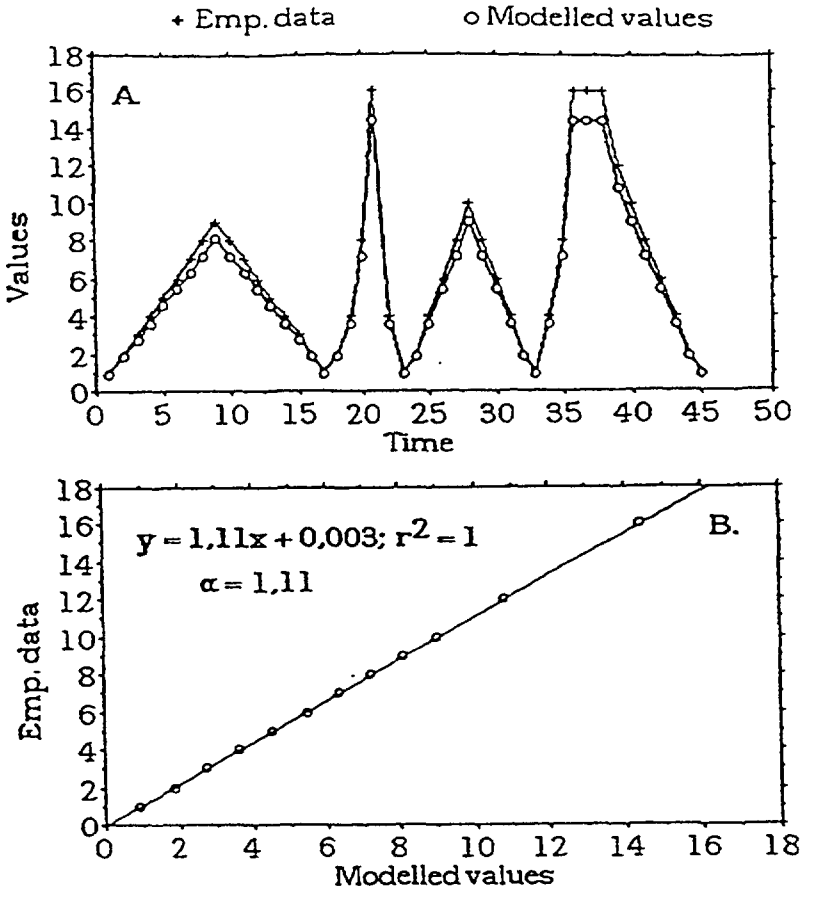

FIG. 5.63. A. Illustration of a very good correspondence between empirical data and modelled values. B. The same data illustrated by a hypothetical regression analysis. The fit is almost perfect, the r^2 value is 1.00, but the slope is 1.11, which is higher than the ideal 1.00.

From these arguments on r^2, slope and CV, we may give a general definition of predictive power (PP):

$$PP = R^2/((1.1 - \alpha)CV) \tag{5.39}$$

where
R^2 is the mean r^2 of all model validations;
α is the slope of the regression line; and
CV is the coefficient of variation for the r^2 values obtained in the empirical tests (Table 5.24).

The higher the R^2, the higher PP. One could also use the median r^2 value. This is a matter of definition, and here we used the mean value. α, the slope, may be smaller and larger than 1. If it is smaller than 1, the influence on PP is quantified by means of the factor $1.1 - \alpha$. Since α may be equal to 1, and since division by zero is not allowed, 1.1 is used instead of just 1. Other constants than 1.1 may be used, but 1.1 will cause PP values to vary between 0 and 100 (see Figure 5.64). This means that the slope factor is always larger than 0.1. If the slope is larger than 1, $1/\alpha$ can be used instead of α and the same factor applied. This means that a slope of 0.5 will give the same factor as a slope of 2, namely $1.1 - 0.5 = 0.6$ or $1.1 - 1/2 = 0.6$. One could also account for the intercept in this approach, but that would add very little since the slope and the r^2 value are already used. The predictive power of the given model is 12. This is a rather high value since the mean r^2 (i.e. R^2) is as high as 0.80, the uncertainty linked to the slope is 0.35 and the CV is 0.19. In this case, the CV value is determined from the spread around the r^2 values. It is a measure of model uncertainty. Similar CV values may be determined in other ways, e.g. by Monte Carlo simulations, which will be illustrated later on.

Figure 5.64 gives two nomograms illustrating how R^2, slope and CV influence PP. One can safely assume that CV in practice will never be zero for models for aquatic ecosystems, neither are models likely to yield r^2 values of 1.00. Very good models may give r^2 values of about 0.95. CV values lower than 0.1 ought to be rare. From Figure 5.64, it can be noted that with this definition, PP will generally be lower than 100. Models yielding PP higher than 10 would be very good. Models giving PP lower than 1 may be useless for all practical purposes for predictions in individual lakes. Such models have a poor fit (a low r^2 and/or a slope much diverging from 1) and great uncertainties (i.e. a high CV).

This expression of predictive power (Equation 5.39) should be regarded like most models for complex systems: A tool which accounts, not for every conceivable situation and factor, but for the most important factors in a simple and useful manner. The fit between modelled values and empirical data is here given by the r^2 value and the slope factor. The fit may, however, be expressed in many alternative ways. Instead of the mean or median r^2 one could use the adjusted r^2. All expressions related to such r^2 values would depend on the number of data pairs (n), the range and the transformation of the x and y variables. Logarithmic x and y variables will give different r^2 values than non-transformed variables. Instead of using this definition of the slope factor, one could use other alternatives and also include the intercept.

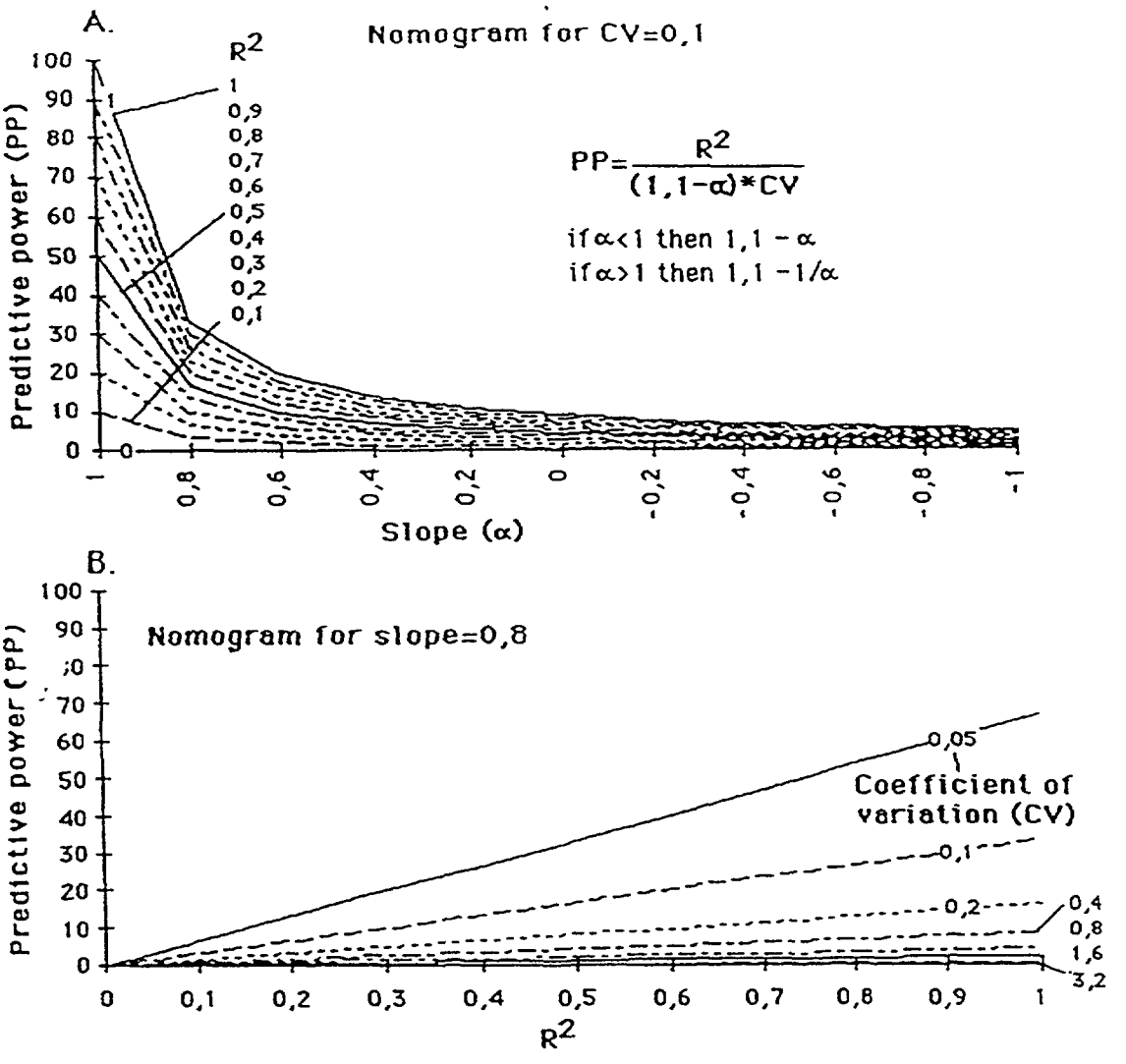

FIG. 5.64. Nomograms illustrating predictive power. A. Gives curves for a constant CV of 0.1. B. Gives curves for a constant slope of 0.8.

It should be stressed that the uncertainty (CV) is determined independently of the fit. One should not use, for example, expressions related to the confidence interval of the regression line for the uncertainty since such measures are directly related to the r^2 value (see Figure 5.59). In this approach, the model uncertainty is expressed in two ways, either by Monte Carlo simulations or from repeated validations which enable the determination of CV from the obtained r^2 values between modelled values and empirical data. There may be other approaches to express model uncertainty.

This definition of predicted power (PP) should not be used in an uncritical manner and PP values determined for different models for different purposes may not be directly comparable. In all modelling situations, it is the responsibility of the modeller to define and explain the presuppositions of the models and its applicability. Since predictive power is such an important concept in ecosystem and environmental modelling and research, it is hoped that the presentation of this approach would stimulate further discussions and tests on this topic.

5.8.6. Predictive power of empirical models for radiocaesium

Limnetic ecosystems are extremely complex and any lake is characterized by many complicated interactions among biological, chemical and physical variables.

One of the important tasks of predictive modelling is to describe such complicated relationships quantitatively and to rank the relative importance of different x variables in predicting a given y variable. To do this, it is important to use a hierarchical mode of thinking. In lake radioecology, one generally wishes to predict concentrations of radionuclides in water and in fish. These are the target y variables to be predicted by the VAMP models. Further, the fluxes to, within and from these compartments (lake water and predatory fish) need to be studied. Everything in the lake could, potentially, influence such fluxes, but everything cannot be of equal importance for these two specific predictions. Good predictive models are based on the most important processes, no more, no less.

So, one needs reliable empirical data on the most important rates and model variables. But all empirical data from natural ecosystems are more or less uncertain. Two main approaches to address the problem of uncertainty analysis exist, analytical methods [5.47] and statistical methods, like Monte Carlo techniques [5.48]. In this Section, only Monte Carlo simulations will be discussed.

Figure 5.65 illustrates schematically why it is important to consider uncertainty. When working with mean values and frequency distributions of empirical data at the ecosystem level, there is always uncertainty about any model variable (x). This uncertainty is illustrated by the frequency distributions in Figure 5.65. It should be noted that many variables are not initially normally distributed and only some of these variables may be transformed to normal distributions.

This uncertainty in x is reflected in almost all descriptions of the observations. The regression parameters and the regression line they describe are uncertain, as are the mean y value and the predicted y value. All ecological descriptions include uncertainties, thus, it is important to describe this uncertainty and to assess its effects with uncertainty tests. For example, all descriptions of a central tendency should be accompanied by a measure of dispersion, the uncertainty may be described in regression with confidence bands, or an uncertainty ellipse may be calculated.

If we have a predictive empirical model, $y = \alpha_1 x_1 + \alpha_2 x_2 + \alpha_3 x_3 + \alpha_4 x_4 + \alpha_5 x_5 + \beta_1$, based on five more or less uncertain empirical x variables, then the r^2 value (the degree of explanation obtained when empirical data are compared to modelled values in regression) would increase for each model variable added to the model, but the model uncertainty might also increase, especially for the last x variables in the model, and especially if these x variables are uncertain. Large empirical models based on many such unreliable x variables carry an accumulated uncertainty. This cumulative uncertainty may be quantified by Monte Carlo simulations.

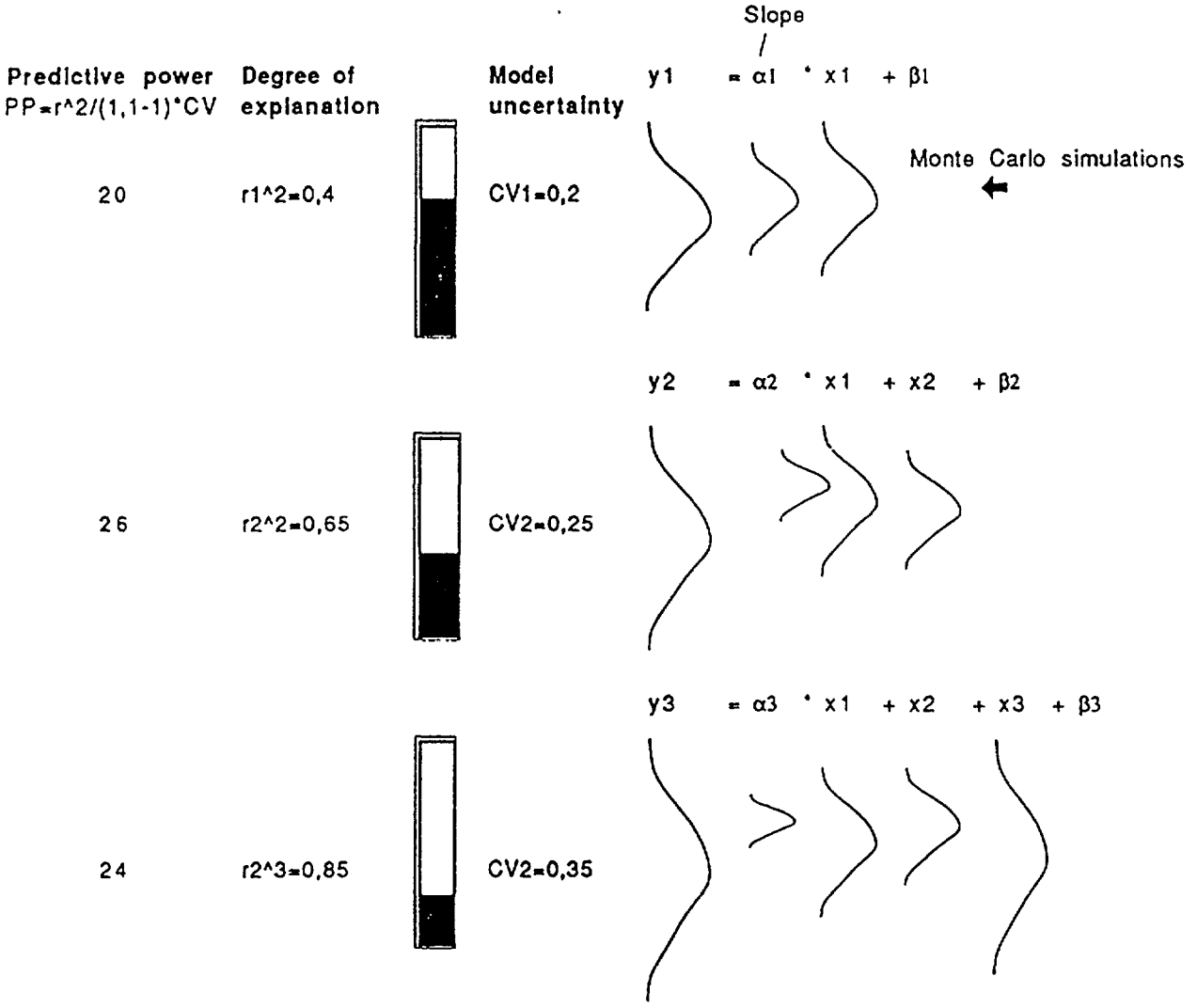

FIG. 5.65. Illustration of predictive power for three regression models. The model uncertainty (CV) is determined from Monte Carlo simulations. CV depends on uncertainties in model variables (x) and slope coefficients (α). The highest predictive power is obtained for two x variables in this hypothetical example.

The uncertainties associated with the simple model $y = \alpha_1 x_1 + \beta_1$ in Figure 5.65 can be evaluated as follows: It is an empirical, statistical model derived for a certain number of lakes. The r^2 value is 0.40. The simulated uncertainty in the x_1 variable and the slope α_1 are given by the two frequency curves (the "gates") showing the probabilities (or the frequencies) of the values. The program generates individual estimates or "shots" through these two "gates", and the result of doing this 10 000 times is the uncertainty curve for the predicted y variable. The graph shows the range of the data for y, or the 95% confidence intervals, or the coefficient of variation (CV), where 1CV corresponds to ±70 % confidence intervals and 2CV to ±95% confidence intervals. The first CV in Figure 5.65 is 0.2. The ± 95% confidence interval for the predicted y could also be determined, but that measure of model uncertainty can be derived directly from r^2 and n, and it does not add any more information. This measure of model uncertainty, on the other hand, is produced by an independent method, Monte Carlo simulations.

The next step uses a model with two x variables. The r^2 value has increased from 0.4 to 0.65. How about the model uncertainty? Adding one model variable does not alter the uncertainty of the first model variable, only the uncertainty of the slope of the first model variable, α_1, which is reduced. This is illustrated by a smaller uncertainty "gate" in Figure 5.65. We must also account for the uncertainty

of the new model variable, x_2. This is shown by the new uncertainty "gate". A new Monte Carlo simulation will give a new coefficient of variation for y, 0.25, as compared to 0.2 for the first model. The predictive power connected to these two steps may now be determined. It is assumed that the slope in regressions is close to 1. The PP value is 20 for step 1 and 26 for step 2. So, PP has increased.

In the next example, one more model variable x_3 is added. In this case, r^2 increases from 0.65 to 0.85, the model uncertainty increases from 0.25 to 0.35, and the predictive power decreases from 26 to 24. This may seem paradoxical, but it has to do with the fact that model uncertainty accumulates as more and more uncertain x-variables are included in the model. Note that this is just a pedagogical example. The argument will be substantiated later by real lake data for radiocaesium.

The first focus is on the relationship between the r^2 value and the uncertainty of the slope coefficient of the regression line. Table 5.25 gives (based on data from Håkanson, 1991) a r-rank table (based on linear correlation coefficients of absolute values) for one of the target y variables, the concentration of radiocaesium in pike in 1988 (Cs-pi88) in relation to:

1. Cs-concentrations in pike (Bq/kg ww) caught in 1986 and 1987 and in fish eaten by pike, namely perch fry (Cs-pe86 and Cs-pe87);
2. fallout, Cs-soil in Bq/m^2;
3. variables indicating the load of caesium to the lake, Cs-wat87 (Cs in lake water in 1987 in Bq/L), caesium in surface sediments (Cs-sed86 and Cs-sed87 in Bq/kg dw) and caesium concentrations in material collected by sediments traps placed 2 m above the bed of the lakes (Cs-bo86 and Cs-bo87 in Bq/kg dw);
4. different lake variables (mean annual values for 1987) for colour (mg Pt/L), Fe (µg/L), conductivity (mS/m), K-concentration (meq/L), alkalinity (meq/L), hardness (CaMg in meq/L), Ca-concentration (meq/L), pH and total-P-concentration (µg/L);
5. various lake morphometrical parameters, Dm = mean depth (m), Q = theoretical water discharge (m^3/sec), lake volume (Vol) (m^3), theoretical water retention time, T (a), lake area (m^2), percentage of the lake bed dominated by accumulation processes and fine sediments, BA (% of lake area), and dynamic ratio, DR (= $\sqrt{}$area/Dm); and
6. different parameters describing the catchment area, Rock% is the percentage of bare rocks in the watershed, ADA is the area of the drainage area (m^2), Bas% is the percentage of basic rocks, RDA is the relief of the catchment area, etc.

It is evident that all the Cs variables may be related to one another and to the fallout (Cs-soil) after the Chernobyl accident, and all the water variables could, potentially, influence the bioavailability and biouptake of radiocaesium as well as the biomasses, and hence the concentration in the biomasses of radiocaesium, the morphometrical parameters could, potentially, influence the retention of radiocaesium in lakes, the resuspension and the internal loading of caesium, and the watershed parameters could, potentially, all influence the runoff of caesium from land to water, i.e., the secondary load of radiocaesium to the lakes. But all these factors could not be of equal importance to predict Cs-pi88. One simple way to quantitatively rank such dependencies is to make a correlation analysis (Table 5.25). It can be noted that some of the factors appear with high r values vs Cs-pi88, like Cs-wat87 (r = 0.88), total-P (r = 0.48), dynamic ratio (r = -0.64) and Rock% (r = 0.40), and some with low r values. Many, if not all, of the variables are related to one another. This is stressed by the small r rank matrix for the water chemical variables related to the K concentration in Table 5.25 (cluster variables). Very high and expected correlations exist between K, conductivity, hardness and alkalinity (r > 0.9). Such interrelated variables can replace one another in predictive models without causing any major loss in predictive power.

There exist great differences in the representativity and reliability of these potential model variables. All water chemical variables vary with time and sampling location in a lake. The CV-values given in Table 5.25 have been determined from frequent within lake samplings during one year. From such analyses a lake-specific mean value (MV), the spread around the mean (the standard deviation, SD) and the relative standard deviation (or coefficient of variation, CV) can be determined. Most data

in this table emanate from references [5.42] and [5.49]. A small uncertainty (CV ≈ 0.01) for the map parameters can be noted, CV is higher or about 10% (or 0.1) for variables like Q and Cs-soil, and much higher for many variables, like 0.38 for total-P (a very variable variable). It can also be noted that the variability decreases with time for caesium in small perch (from 0.59 1986, to 0.28 1987). These uncertainties are very important indeed in predictive modelling.

The next example illustrates a simple regression model with real data for a given y variable, the concentration of radiocaesium in pike in 1988, Cs-pi88 in Bq/kg ww. Many lake variables (like K concentration, pH, total-P and colour) could, as stressed in Table 5.25, influence the biouptake of radiocaesium and the Cs concentration in pike. The result of a stepwise multiple regression is illustrated in the table in Figure 5.66. Note that the concentration of ^{137}Cs in water in 1987 is the most important x variable. It explains statistically about 78% ($r^2 = 0.778$) of the variability in the y variable (Cs-pi88) among these 14 Swedish lakes. The F value is 4. The next factor is the potassium concentration of the lake water (the mean annual K value for 1987 is used). At the second step, the r^2 value has increased to 0.885. The third x variable is the Open Land percent (OL%, a measure of the cultivated land) of the catchment. Accounting for OL% increases r^2 to 0.917. The fourth and last x variable (for F = 1) is lake total-P (mean value for 1987). It increases r^2 to 0.929.

y=Cs-pi88; n=14

Step	F-value	Variable	r^2-value	Model
1	4	Cs-wat87	0,778	y=9479*x1+769
2	4	K	0,885	y=9559*x1-170,6*x2+2524
3	2	OL%	0,917	y=9685*x1-249,5*x2+172*x3+2804
4	1	totP	0,929	y=9259*x1-226,4*x2+191,6*x3-224,6*x4+4939

Step	r^2-value	Variable	Value	CV for variable	Modelled value Cs-pi88, Bq/kg ww	Uncertainty in y CV from MC-sim.	PP
1	0,778	Cs-wat87	0,5 Bq/l	0,26	5509	0,219	36
2	0,885	K	10 µeq/l	0,12	5598	0,223	40
3	0,917	OL%	8%	0,01	6528	0,190	48
4	0,929	totP	11 µg/l	0,38	6368	0,239	39

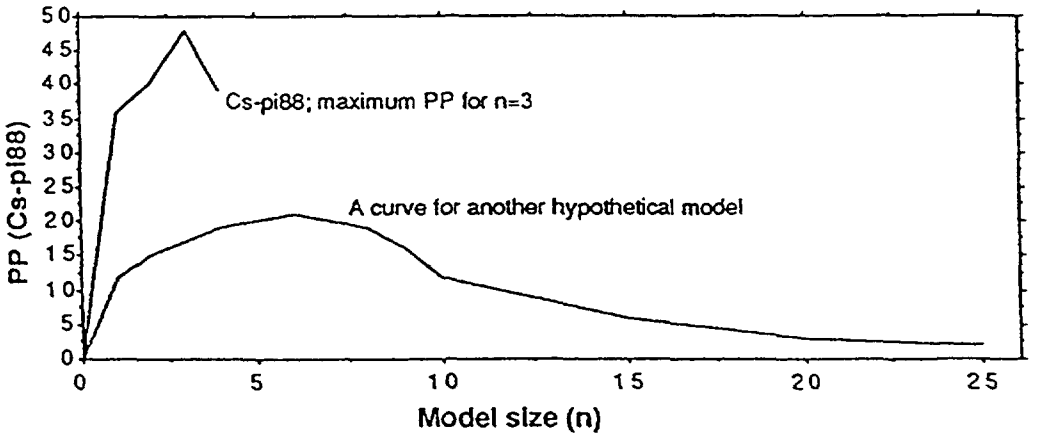

FIG. 5.66. Predictive power for empirical models derived by stepwise multiple regression analysis using caesium in pike in 1988 (Cs-pi88 in Bq/kg ww) as y variable, and caesium in lake water in 1987 (Cs-wat87), lake K concentration, open land percentage (OL%) of the watershed, and lake total-P as x variables. The graph illustrates the relationship between PP and model size (n) for the data given in the table. The other curve illustrates another situation. The main point here is to highlight that different models will yield different curves.

Lake total-P is, as already pointed out, a very variable variable. Its coefficient of variation (CV) is, on average, 38%, or 0.38. The corresponding CV for K is only about 0.12, for caesium in water it is about 0.26 [5.49]. The uncertainty associated with the determination of the Open Land % is much smaller — in the order of 1% (CV = 0.01; Nilsson, 1992 [5.50]). With this information, we can use Monte Carlo simulations to estimate the uncertainty (CV) in our y variable. The results are given in the table in Figure 5.66. We can note that CV is 0.219 at step 1, 0.223 at step 2, 0.190 at step 3 and 0.23 at step 4. Predictive power attains maximum values for n = 3. Thus, by accounting for total-P in this stepwise regression analysis, r^2 is increased, but PP decreased. The reason for this is that an uncertain variable is added which contributes more to the model uncertainty (CV) than to the r^2 value. The net result is a model with a lower PP. Empirical regression analysis automatically yields a slope close to 1. The PP-value of these empirical models are very high, PP > 35 for all four models.

From the graph in Figure 5.66, we can conclude that the maximum PP is not obtained for the largest model size. For other models, the highest PP may very well be obtained for other model sizes. This is illustrated by the other curve in the graph. It should be remembered that empirical models can only be used within given ranges of applicability. These models only apply to small, forest lakes of glacial origin, but these principles apply generally.

5.8.7. Predictive power of dynamic models for radiocaesium

Dynamic models derive from a causal analysis of ecological and biological fluxes. If dynamic models are not validated, they may yield absolutely worthless predictions. As is the case for any model, the presuppositions of the model must always be clearly stated.

Many of the models used in VAMP are typical compartmental model, giving the biotic compartments of a lake ecosystem (top predator, two types of small fish, zooplankton, phytoplankton, algae and benthos), the abiotic compartments (active sediments, passive sediments and water), and the processes and mechanisms regulating fluxes among these compartments for our type substance radiocaesium. The differential equations describe the fluxes to the lake (direct lake load and river input related to catchment load) and from the lake (outflow and sedimentation to the passive sediment layer). Such general model set-ups can apply to any substance, not just radiocaesium.

The Mixed model a simplified version model where the fluxes to the top predator, the y-variable to be predicted, could be estimated from a few compartments (small fish and lake water) and empirical knowledge of the factors regulating the Cs-uptake by small fish. The uptake by small fish can be described as a function of lake K, theoretical water retention (T) and the dynamic ratio of the lake (DR). Basic problems with traditional mass-balance models and methods to derive small predictive mixed models are discussed in [5.35] and [5.36]. For all models, one would need reliable, quantitative data on many rates describing the fluxes (in mass per unit time) among the compartments and the characteristics of each compartment. The following sections give several tables with lists of all the rates and variables linked to the three dynamic models which will be discussed in this Section, and Annex II gives all the equations and assumptions of the models. Moreover, most "rates" are not constants, they vary in time and space. The rates are variables, like most of the variables describing the system and its compartments (e.g., weight and age of the animals).

In this Section, the relationship between predictive power (PP) and model size (n), i.e. the optimal size problem, for dynamic predictive models for radiocaesium in lakes will be discussed. Three models will be tested and these results will be compared with the results in Figure 5.66.

1. A small, mixed model (see Section 4.2.4.2.): it has only three compartments (water, prey and predatory fish), 6 model variables and 5 lake-specific variables. The total number of driving variables (x) is thus 11. Note that there is no catchment area, no sediments, no food-web and no partition coefficient (K_d) in this model.
2. The VAMP LAKE model (presented in Section 5.10): It has 10 compartments, 21 model variables and 11 lake-specific variables. The model size is given by n = 32.

3. The generic model (see Section 4.2.4.3.): It is a traditional model with 9 compartments, 27 model variables and 9 lake-specific variables, which gives n = 36.

These models will be tested using the data for the VAMP lakes (see Figure 3.2 and Tables 3.1–3.3). Since the six VAMP lakes vary in size (from 0.042 to 1147 km^2), mean depth (from 1.7 to 89.5 m), precipitation (from 600 to 1840 mm/year), pH (from 5.1 to 8.5), K concentration (from 0.4 to 40 mg/L), primary productivity (from 0.8 to 350 g $C \cdot m^{-2} \cdot a^{-1}$) and in food-web characteristics, it is a great challenge to try to model the effects of the Chernobyl "spike" on the caesium concentrations in water and biota.

The results of many comprehensive validation tests of time dependent data ("tail tests") were summarized in Section 5.2 (for all variables, for water and different fish). The VAMP LAKE model and the small UU-mixed model generally provide the best predictive accuracy and the large UU-generic model the lowest r^2 values.

The results concerning predictive power of the dynamic models are summarized in Figure 5.67. The table in this figure gives the mean r^2, the CV related to the given r^2 values, the mean slope and the predictive power (PP) for the three models and the corresponding data for the comparison between the two empirical samples (Emp1 vs Emp2). The smallest model, the mixed model, yields the highest PP, the biggest model, the generic model, the lowest PP. So, also in this case, one obtains best predictive power for small models accounting only for the most important processes. Big models with many uncertain rates and model variables give lower PP. The lowest PP value is obtained when comparing the two empirical samples. This indicates the empirical uncertainties associated with the VAMP data. We should also note that the PP values obtained by these dynamic models are much lower than the PP values from the empirical models in Figure 5.66. That is an important indication and a lesson: Within the range of applicability, empirical models often provide better predictive power than dynamic models in ecosystem contexts.

	Model variables n1	Lake-specific variables n2	n= n1+n2	R^2	CV	Slope, MV	1,1-a	PP
Mixed model	6	5	11	0,65	0,427	1,12	0,21	7,42
VAMP model	21	13	34	0,65	0,428	0,85	0,25	6,12
Generic model	27	9	36	0,56	0,602	1,15	0,23	3,99
Emp1 versus Emp2				0,59	0,603	0,59	0,51	1,93

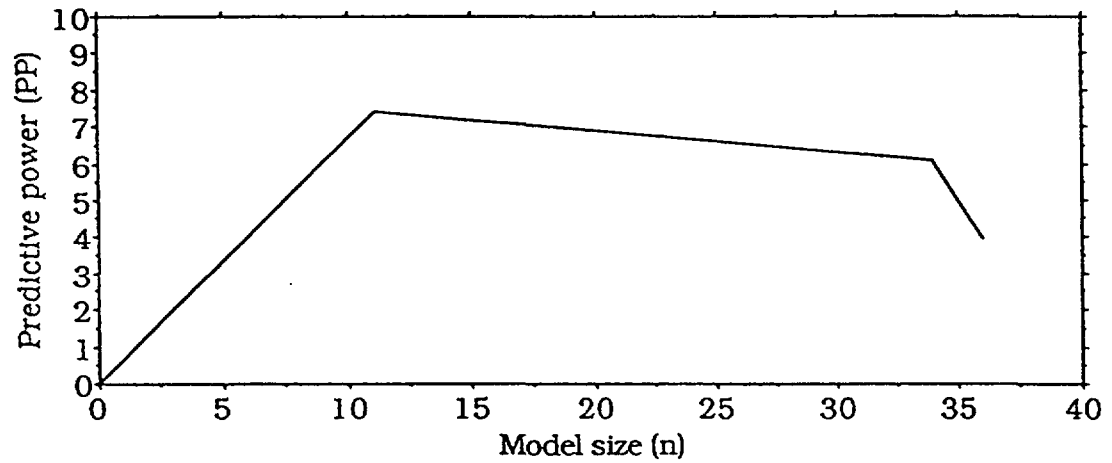

FIG. 5.67. Predictive power for three dynamic models for caesium in lakes. The graph illustrates the relationship between PP and model size (n) for the data given in the table.

5.8.8. Conclusions

These results should be considered as the first step to the very important problem on the optimal size of predictive models. These examples illustrates the need to obtain further insights into the factors that determine "predictive power" and "model uncertainty".

It is evident that there may exist many specific cases when many x-variables would do more good than harm, but it is important to note that the uncertainties are likely to increase the model uncertainty when variables are added to the model. These results support the old statement: The simpler the better.

Many statements and comments about models in general and predictive models in particular have been given. Some of those statements are listed below.

- If the aim is to quantify, rank, predict and simulate, there are few, if any, alternative approaches to quantitative models in complex ecosystems.
- Dynamic models are logical constructions. However, logical reasoning depends on one's personal knowledge and some of that knowledge may be subjective.
- Large models are often "prescriptive" not predictive. Large models may look more objective than small, but this may be self-deception.
- Models are built and validated with empirical data. However, empirical data, and any knowledge based on empirical data, are uncertain. Accumulated uncertainties in the models will cause uncertainties in model predictions.

TABLE 5.24. ILLUSTRATION AND DEFINITION OF PREDICTIVE POWER (PP) FROM MEAN r^2, MEAN SLOPE FACTOR AND CV AFTER 15 MODEL VALIDATIONS

Test number	r^2	slope α	if slope > 1 than 1/slope	1,1−α
1	0,95	0,90		0,20
2	0,82	0,85		0,25
3	0,77	2,10	0,48	0,62
4	0,96	1,50	0,67	0,43
5	0,66	1,20	0,83	0,27
6	0,55	1,00	1,00	0,10
7	0,88	1,30	0,77	0,33
8	0,46	0,60		0,50
9	0,92	0,80		0,30
10	0,91	1,50	0,67	0,43
11	0,68	1,20	0,83	0,27
12	0,86	2,00	0,50	0,60
13	0,88	0,95		0,15
14	0,92	0,67		0,43
15	0,79	0,80		0,30
MV (=R^2)	0,80			0,35
SD	0,15			
CV	0,19			

Predictive power, PP =0,80/(0,35*0,19)=12,0

PP=R^2/((1,1-slope)*CV)

TABLE 5.25. AN r-RANK (LINEAR CORRELATION COEFFICIENT, r) MATRIX BASED ON DATA FROM 14 SWEDISH LAKES ON CAESIUM IN PIKE IN 1988*

r-rank n=14		Cs-pi88	CV		
Other fish	Cs-pi88	1,00	0,22		
	Cs-pi87	0,91	0,33		
	Cs-pe87	0,80	0,28		
	Cs-pe86	0,91	0,59		
Fallout	Cs-soil	0,70	0,10		
Lake load	Cs-wat87	0,88	0,26		
	Cs-sed86	0,85	0,62		
	Cs-bo87	0,76			
	Cs-sed89	0,71	0,62		
	Cs-bo86	0,66			
Water variables	Colour	-0,20	0,19		
	Fe	-0,20	0,28		
	cond	-0,31	0,09		
	K	-0,31	0,12	Cluster variables	
	alk	-0,37	0,39	K	1,00
	CaMg	-0,37	0,14	cond	0,94
	Ca	-0,38	0,12	CaMg	0,92
	pH	-0,42	0,02	alk	0,90
	totP	-0,48	0,38	pH	0,57
Morphometry	Dm	0,53	0,01		
	Q	0,38	0,10		
	Vol	0,27	0,01		
	T	0,23	0,10		
	Area	0,05	0,01		
	BA	-0,47	0,05		
	DR	-0,64	0,02		
Watershed	Rock%	0,40	0,01		
	ADA	0,37	0,01		
	Basic rock%	0,25	0,01		
	RDA	0,12	0,01		
	Mire%	0,09	0,01		
	Fine sed%	0,05	0,01		
	Forest%	-0,02	0,01		
	Lake%	-0,04	0,01		
	Coarse sed%	-0,08	0,01		
	Open land%	-0,11	0,01		
	Till%	-0,18	0,01		

* (Cs-pi88 in Bq/kg ww) versus (1) different caesium variables (Cs-pe87 is Cs in perch fry in 1987 in Bq/kg ww, Cs-soil in fallout in Bq/m^2, Cs-wat87 is caesium in lake water in 1987 in Bq/l, Cs-sed86 is caesium in surface sediments in 1986 in Bq/kg dw, Cs-bo86 is Cs in near-bottom sediment traps in 1986 in Bq/kg dw), (2) different lake variables (mean values for 1987), (3) lake morphometric parameters (Dm = mean depth, Q = theoretical water discharge, Vol = lake volume, BA = areas of fine sediments, DR = dynamic ratio), and (4) different watershed parameters. The table also gives a small r rank matrix illustrating correlations among the water chemical cluster variables linked to K concentration. The column called CV gives mean coefficients of variations for the given variables.

- The predictive power of a model is not governed by the strength of the model's strongest part, but by its weakest part.
- Large models are simple to build, but hard to validate. Small models are hard to build, and simple to validate.
- Small size is necessary, but not sufficient, for utility and predictive power; so useful models must be small. Small models should be based on the most fundamental processes, but this is difficult to accomplish.
- Scientific knowledge does not lie in the model alone, nor in the empirical data alone, but in their overlap as validated, predictive models.
- The key issue is not to verify, but to falsify a model, and thereby to determine its limitations.
- It is important to predict mean values, but it is equally important to predict the confidence interval around the mean.

5.9. THE SIGNIFICANCE OF ICE AND SNOW CONER FOR THE UPTAKE OF RADIONUCLIDES IN AQUATIC ECOSYSTEMS

5.9.1. Introduction

One of the main concerns after the Chernobyl accident has been the concentration of ^{137}Cs in the aquatic food chain and in particular freshwater fish. The environmental impact of radionuclide releases from nuclear installations can be predicted using assessment models. Many of the models have been developed and tested in areas where snow and ice cover are absent or only of a temporary nature. However, much of the fallout from Chernobyl occurred in northern and continental ecosystems at the end of April 1986, a time of the year when many areas were still covered in snow and ice. In cold temperate, arctic and alpine areas the time of the year in which fallout occurs can profoundly affect its significance for both aquatic and terrestrial systems. For example, during winter fallout will be more or less effectively trapped in the snow pack, only being released during snowmelt in the spring.

The amount of primary fallout then reaching various ecosystems will depend on the hydrological characteristics of the system in question. For example, most of the fallout on the ice of a lake with a long water retention period will be retained within that lake, while in the case of a lake with a short retention period, much of the fallout will be flushed out of that particular lake to other lakes further down the watercourse. The physical nature of the fallout and the radionuclides involved will also affect its retention in aquatic systems during the spring spate. For instance, it has been clearly shown that ^{90}Sr in the Chernobyl fallout is much more mobile than ^{137}Cs and is more readily flushed out of lakes and other ecosystems [5.51].

5.9.2. Seasonality and its effect on food chain uptake

Most aquatic systems in cold temperate, arctic and alpine regions have a pronounced seasonal hydrological pattern, characterized by high discharge during the spring snowmelt period which gradually falls during early summer. During the summer and autumn there may be short-term increases in discharge, but their magnitude is rarely as great as the spring spate. During winter discharge is generally very low and water retention periods are long. In addition, groundwater inputs are often of greater importance during the winter period of snow and ice cover, when surface inputs are reduced. The transition from low winter discharge to maximum spring discharge is often fairly rapid and usually takes place during the course of three to five weeks. The magnitude of the spring spate will of course vary from year to year in the same water course, depending on the depth and nature of the snow pack and weather conditions at the time. Cloudy conditions and precipitation in the form of rain during the spring will increase lake flushing rates, while clear weather with frost at night will reduce the magnitude of the spate, although possibly increasing its duration. However, much of the snow pack may dissipate by sublimation under such conditions.

Lakes have received radionuclides from Chernobyl fallout via two sources: direct fallout on the lake surface, the primary load, and by leakage from the catchment, the secondary load. In the first instance the primary load is of major importance, but in the long-term inputs from the catchment can be of importance in determining radiocaesium concentrations in fish. Winter snow and ice cover, coupled with frozen ground, will affect runoff characteristics for radionuclides from arctic/alpine catchments, especially if fallout takes place during winter. Clearly, runoff will be much greater from frozen ground than at times when surface runoff is able to percolate down through the soil. Once in the soil, it may be chemically bound to soil particles, thus arresting its further transport into rivers and lakes. Snow and ice cover will also change the fallout pattern from a single pulse to a more long-term contamination, whose length will vary with the intensity and duration of the spring snowmelt.

Data from Øvre Heimdalsvatn clearly demonstrate the seasonal effects related to fallout on aquatic systems [5.52]. Fallout from Chernobyl reached the area at the end of April 1986, when most of the catchment was covered in snow and the lake itself was ice-covered. The lake remained ice-covered until the beginning of June, although the increase in discharge associated with the spring spate began in mid-May and culminated during the breakup of lake ice at the beginning of June. The water retention period of Øvre Heimdalsvatn varies from a minimum of a few days at the peak of the spring spate to a theoretical value of almost 400 days during winter. The extremely rapid renewal of the water masses during the spring will naturally affect the uptake of radionuclides in the food chain. In 1986, a significant part of the fallout on the lake ice was flushed out of the system and was therefore neither available for the lake food chain nor laid down in the lake sediments. In many lakes lake sediment concentrations are similar to fallout values [5.36]. However, in Øvre Heimdalsvatn, where fallout was in the order of 130 kBq/m^2, mean sediment concentration back calculated to 1986 was only 60 kBq/m^2. Thus less than 50% of the initial radiocaesium fallout has been retained in the lake and most of this loss probably occurred during the spring spate of 1986.

During the course of the validation exercise and in the associated sensitivity analyses the need to take account of such seasonal variation became apparent. The empirical radiological data collected since 1986 from Øvre Heimdalsvatn and the other VAMP lakes, together with basic physical, chemical and biological data from these lakes and their catchments, have been used to develop a seasonal moderator, thus incorporating seasonality into the modelling process.

There is a comprehensive hydrological literature and many hydrological models to describe and predict runoff, tributary water discharge (Q) and lake water retention time (T). The aim is not to introduce an approach for process-oriented hydrologists, but to present a new and simple technique for ecologists to predict seasonal variability in Q when the basic objective is to model ecosystem dynamics rather than hydrological processes. The approach uses smoothing functions to change the seasonal variability of so-called seasonal variability norms. The technique makes it possible to predict these important lake characteristics in a simple and general manner since the only input variables needed are: latitude, longitude, altitude, mean annual precipitation, catchment area and lake volume. The derivation of the model for Q is based on a set of prerequisites concerning the seasonal variability norm. The seasonal variability moderator for Q is a dimensionless expression and it can be used in dynamic models wherever one wishes to account for seasonal variability in rates and coefficients. Details of the development of the seasonal variability moderator, including all equations and presuppositions are given by Håkanson and Peters [5.35] and in connection with the VAMP LAKE model (see Section 5.10 and Annex II).

5.9.3. The timing of the contamination

The Chernobyl accident took place at the end of April. What would be the situation for radiocaesium in brown trout (*Salmo trutta*) in Øvre Heimdalsvatn had this accident happened at another time of the year? It is of utmost importance that the model accounts for such a difference since it is highly unlikely that any possible future accident would happen at the same time of the year. The simulation in Figure 5.82, Section 5.10, is a sensitivity analysis where the month of the fallout has been

changed. The model is run with and without the seasonal moderator for Q/T, while all else was kept constant.

Although these aspects need to be studied in more detail, these results from the sensitivity analyses indicate that late spring and early summer is the most unfavourable time for an accident of this type, just at the very start of the productive season. Lower maximum values would be obtained with fallout in January or March. A significant part of a winter fallout on ice would be quickly transported out of the lake together with the spring spate. This in fact happened in the case of Øvre Heimdalsvatn, where only about 50% of the initial radiocaesium fallout was retained in the lake. Studies in the Italian Alps have shown clear seasonality in radiocaesium concentrations in rivers as a result of accumulation in the snow pack during winter and subsequent release during snowmelt in spring [5.53]. Fallout later in the year, during late summer and autumn, would not affect the plankton in the lake in the same way as a fallout just after the spring spate.

5.9.4. Duration of the contamination

Contamination of aquatic systems by radionuclides and other pollutants may be of quite different duration. A model simulation of the radiocaesium concentration in the waters of Hillesjön as a result of contamination periods of 1 day, 10 days and 1 month (Figure 5.68) clearly shows the importance of the duration of the contamination. A short radionuclide pulse gives a high peak of short duration, while a longer contamination period results in a lower peak, but an extension of high concentrations. Such an extended contamination may result in different concentrations in predatory fish. This was one of the problems comparing and predicting the effect of fallout from the weapons testing in the 1960s with the fallout from the Chernobyl accident. If the fallout radionuclides are present in a particular layer of the lake ice, they may be released over a restricted time period. The release and transfer of radionuclides from snow and lake ice needs to be investigated in more detail and at present a conservative approach should be adopted to avoid underestimates of peak concentrations in aquatic organisms.

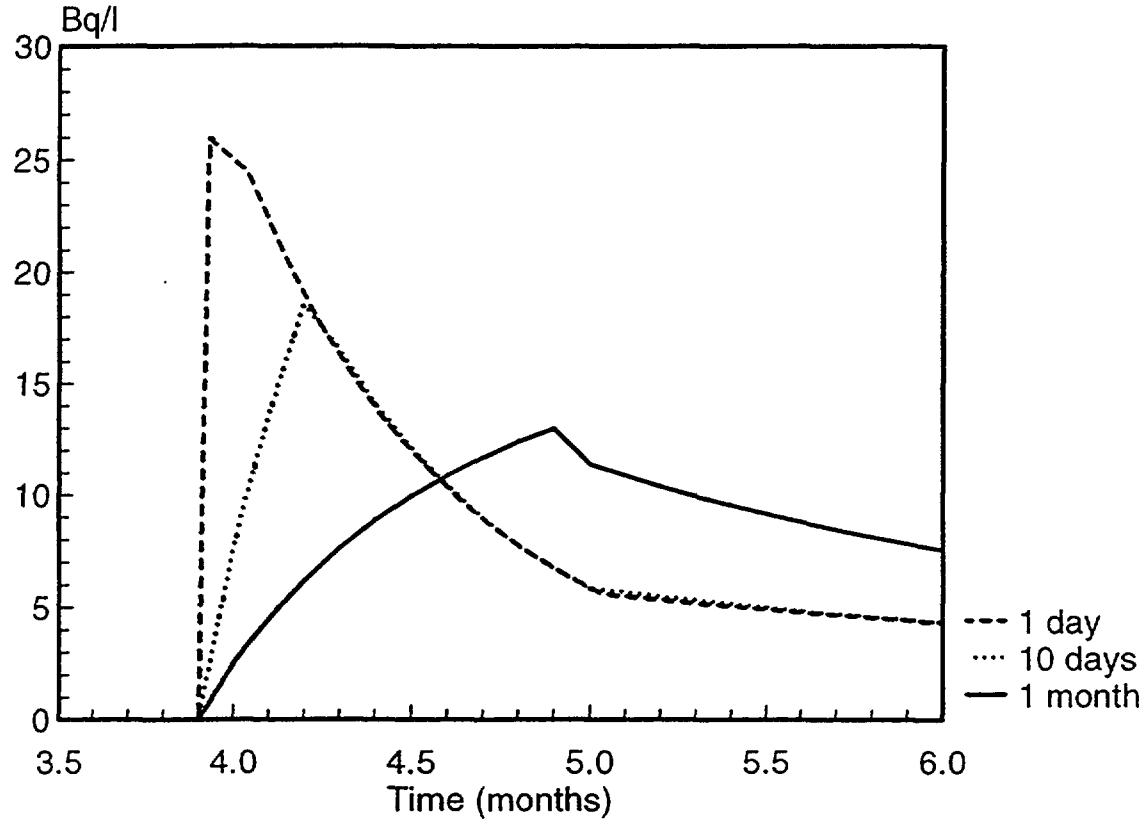

FIG. 5.68. Model simulation (Studsvik model) of radiocaesium concentrations in the waters of the Swedish lake, Hillesjön, as a result of radioactive contamination of different durations.

5.10. THE VAMP LAKE MODEL

During the course of the VAMP project the Lakes Subgroup have developed an entirely new mixed model, the VAMP LAKE model. This new model for radiocaesium in lakes is presented in Figure 5.69. Since this model is meant to be a simple, general, predictive, state-of-the-art model for radiocaesium in lakes, a more thorough presentation of this model than the other models will be given. This model is meant to be based on the most fundamental processes, rates and relationships governing the spread and biouptake of radiocaesium in lakes. The main aim is to predict radiocaesium in predatory fish and in lake water. So, the aim is not to produce a complex lake ecosystem model, but a small, general predictive model driven by readily accessible environmental parameters. All equations and presuppositions are given in Appendix II. The model should also provide reasonable predictions in the event of a future accident. The model variables should, preferably, not be altered for different lakes.

The VAMP LAKE model has six specific components, which should also be applicable in many other modelling contexts. These components, listed below, are intended to increase the predictive power of the model and make it more generally applicable.

1. A seasonal variability moderator for Q and T;
2. A moderator for water retention rate;
3. A transfer coefficient (to calculate relationships between biomasses);
4. An outflow rate function (for the transport of caesium from the catchment to the lake, i.e. the secondary load);
5. A dimensionless moderator for planktonic uptake of radiocaesium, i.e. for the transport of caesium in the dissolved phase in the lake water to phytoplankton; and
6. A dimensionless moderator for the lake partition coefficient (K_d).

5.10.1. Seasonal variability moderator for water discharge and lake water retention time

Climatic variables, like precipitation and river water discharge influence most processes in lake ecosystems. To account for seasonal variability is of paramount importance in most lake models dealing with the distribution, biouptake and ecosystem effects of contaminants, or with processes related to primary and secondary production, or with interactions between abiotic and biotic variables. The basic aim here has been to develop simple sub-models which can be used to account for seasonal variability. More specifically, the objectives are:

1. To develop a "seasonal variability moderator", which is a simple sub-model that may be used to increase the predictive power of larger ecosystem models by accounting for seasonal variability in tributary water discharge (Q) and hence also in lake water retention time (T = V/Q, where V = lake volume);
2. To present a sub-model for the turnover (or retention) rate of lake water, also from readily available map parameters;
3. To illustrate the use of these sub-models within the framework of a larger lake model, in this case the VAMP LAKE model; and
4. To show that the predictive power of dynamic lake models can be increased by accounting for seasonal variability in this simple manner.

Many factors may affect seasonal variability in theory and in practice. The first approach focuses only on the factors regulating the lake water retention time (T), which in turn is governed by tributary water discharge (Q), since the lake volume (V) does not vary appreciably for a given lake.

Tributary water discharge (Q) is governed by many complicated relationships, but a simple approach assumes that the following five factors are vitally important:

1. Latitude (Lat). The higher the latitude, the larger the potential seasonal variability (in Q and T) if everything else is constant. Latitude is usually given in °N, but here is expressed as the distance (m) north of the equator calculated as (Lat/360) × 40.08 × 10^6 m, where 40.08 × 10^6 is the earth's circumference in metres;

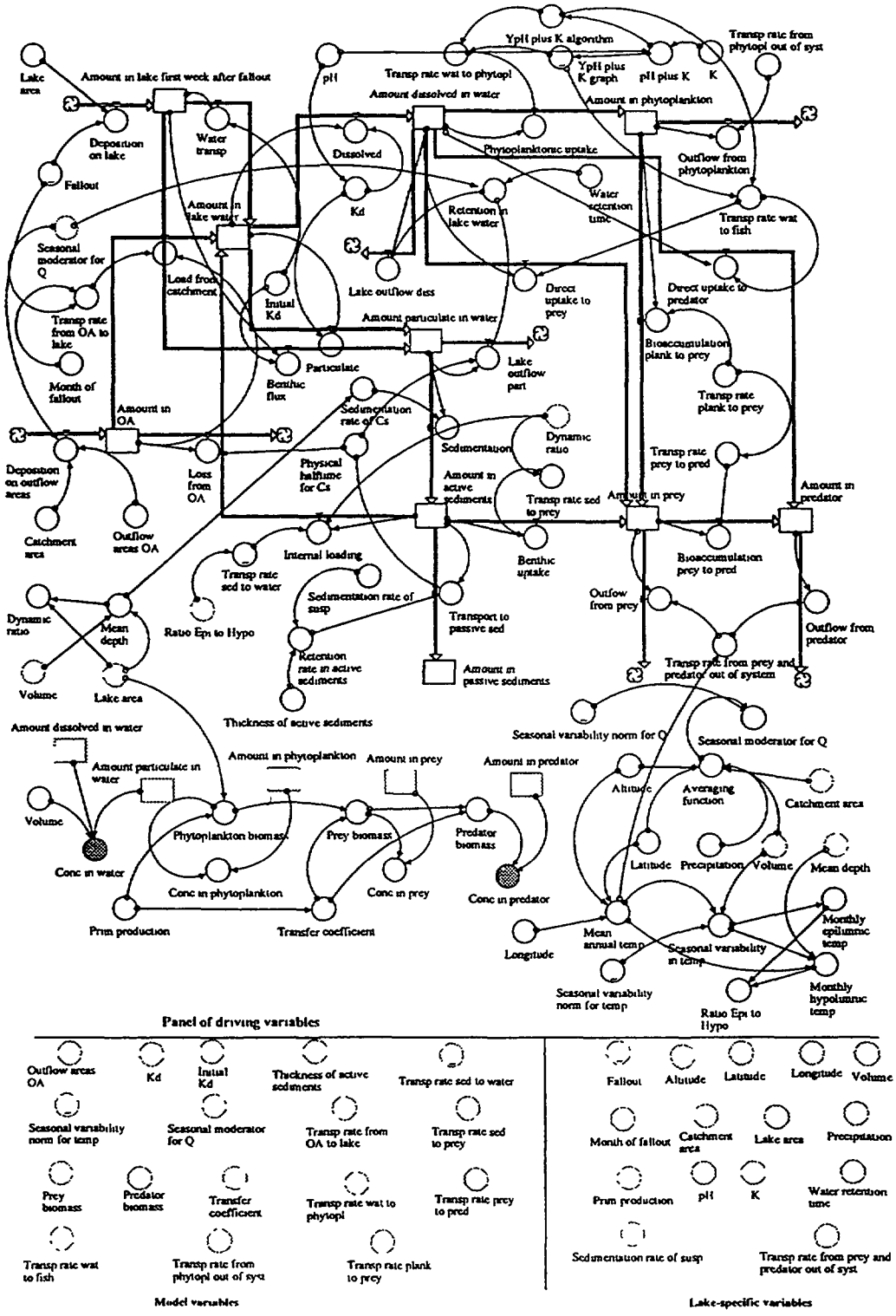

FIG. 5.69. The new VAMP LAKE model for radiocaesium in lakes. The display also gives the biomass sub-model, the seasonal moderator sub-model and the panel of driving variables. This panel is divided into two parts, model variables and environmental, or lake-specific, variables. The environmental variables must be changed for every lake. The model variables, on the other hand, should preferably not be changed, at least not without careful motivations to minimize the elements of "art" and to maximize the elements of science in the model predictions.

2. Altitude (Alt, in m above sea level). The higher the altitude, the larger the potential seasonal variability (in Q and T) if everything else is constant;
3. Precipitation (Precise, usually given in mm/year). The greater the precipitation, the larger the potential seasonal variability (in Q and T) if everything else is constant. In this model, we set the calculation time (dt) to one month, so the model accounts for seasonal variability on a monthly basis. Precipitation is then expressed as m/month (= annual prec $\times$ $10^{-3}/12$);
4. Area of drainage area (ADA, in m^2). The larger the size of the catchment, the larger the potential seasonal variability in Q and T, if everything else is constant; and
5. Lake volume (V in m^3). The larger the volume of the lake, the smaller the potential seasonal variability (in T, but NOT in Q).

There may be several ways to construct a seasonal variability moderator for Q and T but our approach uses two features:

1. A seasonal variability norm. This norm is a curve (Figure 5.70) constructed to illustrate extreme seasonal variability in mean monthly water discharge. The curve has several specific features. The mean annual value (dimensionless) of the selected data should be 1.00. The range between the lowest and the highest value should be high. It is 7000 for this particular seasonal variability norm. The main point is not that this particular curve should give the most realistic description of Q in extreme lakes (with high Alt, Lat, Prec, and large ADA), but rather that the general lake model containing this seasonal variability norm for Q and T and an appropriate smoothing device should give the best possible prediction of the amount of material (like radiocaesium) in lake water, sediments and biota. This Section will describe a general approach to construct a seasonal variability norm for Q and T to use in lake models. The same approach can be used in other contexts, but the details of the seasonal variability norm may have to be changed. The peak may be in any given month and the range between the highest and lowest values may vary (see Figure 5.70).
2. It uses an smoothing function to average out the seasonal variability. By definition, the seasonal variability norm for Q and T is extreme. However, the extremes may be moderated by taking running mean values of the seasonal variability norm over periods of different length – the longer the period, the smoother the curve. The equation that specifies this calculation is a smoothing or averaging function.

The smoothing function is based on the five, easily accessible factors given above. Accessibility is an important criterion in this context.

Several techniques exist to smooth a temporal pattern, like the seasonal variability norm for Q and T. In Figure 5.71A, curve 1 is the seasonal variability norm. Curve 2, which is much smoother, represents the same norm after smoothing by the application of one-sided running mean values (called MV1). This example is designated as MV1 5, which means that the smoothed norm for July is the mean value over the preceding five months (i.e. for July, June, May, April and March). Curve 3 illustrates that the extreme variability of the unsmoothed norm is reduced to almost a straight line when one takes one-sided running mean values for 20 months (MV1 20). The same principles apply if one takes two-sided running mean values. This means that the five-month mean value for July is represented by the average value for May, June, July, August and September (MV2 5).

Another smoothing function called smth, has also been used. This function is presented in the software program, "I think". The smth-function calculates a first-order exponential smooth of the input (here the seasonal variability norm for Q and T, see Figure 5.70), using an exponential averaging time (here the averaging function in time units), and an initial value for the smoothing (also for one- and two-sided running mean values, it is necessary to give initial values for the calculation of the first mean values). The smth-function works in the same way as the one- and two-sided running mean values. It may be written as: smth = smth (input, averaging function, initial value).

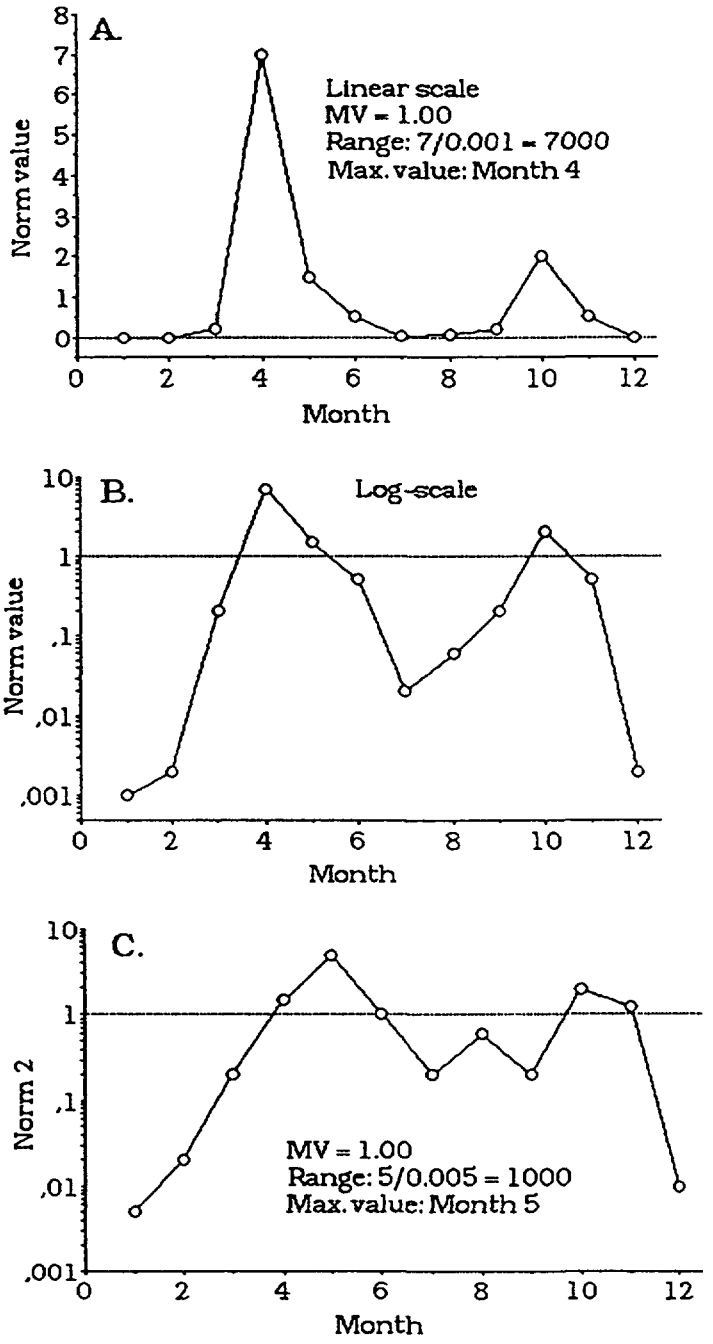

FIG. 5.70. The seasonal variability norm for Q and T on an absolute (A), a logarithmic (B) scale, and an example of another norm for Q and T (C).

In summary, this function smooths the seasonal variability norm for Q and T using a specified averaging function operating over a specified time interval, and an initial value. The development of the averaging function based on Alt, Lat, Prec, ADA and V will be illustrated later in this Section. The initial value is simply the mean value of the seasonal variability norm for Q and T (1). Since the initial results depend on the initial value, this choice is not trivial.

Figure 5.71B compares three curves. Curve 1 represents the one-sided running means calculated over 5 months (MV1 5); curve 2 shows MV2 5; and curve 3 is derived from applying the smoothing function over 3 months (smth 3). These three different smoothing functions yield rather similar seasonal variability curves. Figure 5.71C gives three more examples, where the longer averaging times

are used with each of the smoothing functions (MV1 20, curve 1; MV2 19, curve 2; and smth 12, curve 3). Figure 5.71D provides a sensitivity analysis, comparing the seasonal variability norm to curves generated by the smoothing function applied over 1, 2, 4, 8, and 16 months. The larger the averaging time, the smoother the curve.

To derive an averaging function, a simple dimensional analysis of the expression is carried out. Such dimensional analyses play a fundamental role in dynamic modelling. In statistical modelling, like regression analysis, the model constants carry information about the relationships between the model variables (x) and the predicted y-variable. These constants often have complicated dimensions, but that is rarely recognized in empirical modelling.

An averaging function (AF) based on lake volume, precipitation, lake altitude and latitude and drainage area, may be defined in various ways, and still meet that dimensional criterion. We examine two here:

$$AF_1 = constant_1 \times Vol/(Prec(Alt \times Lat \times ADA)^{1/2}) \tag{5.40}$$

or

$$AF_2 = constant_2 \times Vol^{2/3}/(Prec(Alt \times Lat \times ADA)^{1/4}) \tag{5.41}$$

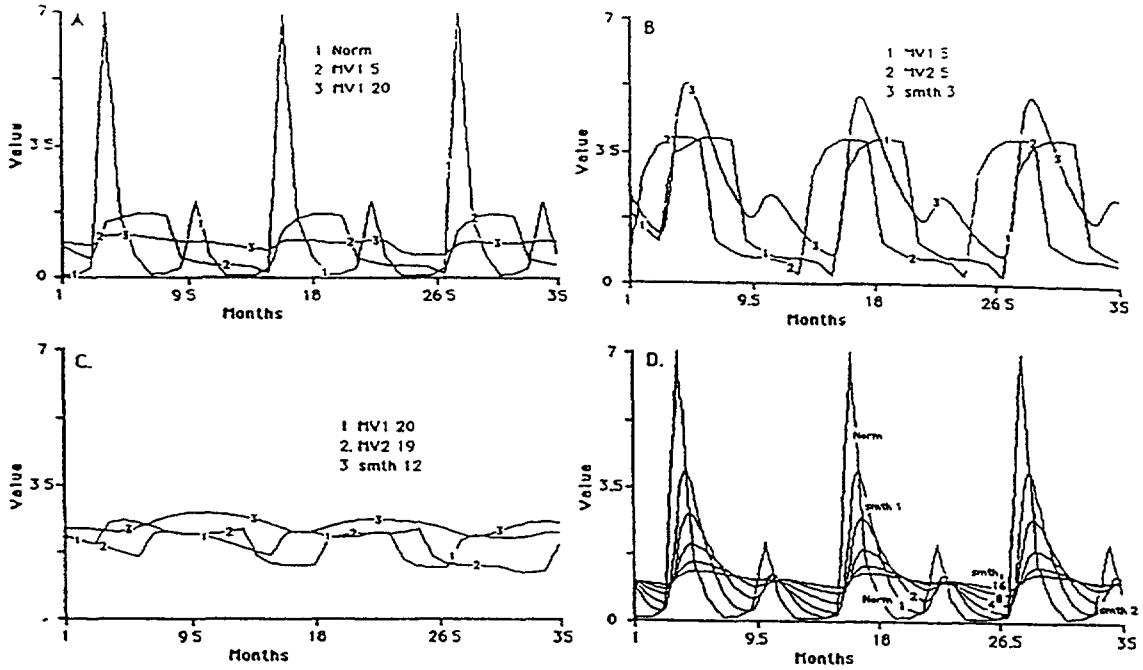

FIG. 5.71. The seasonal variability norm for Q and T and different approaches to modify the seasonal variability of the norm.
A. Curve 1, the seasonal variability norm (norm); curve 2, the norm altered by using one-sided running mean values for five months (MV1 5); curve 3, the norm altered by using one-sided running mean values for 20 months (MV1 20).
B. Curve 1, the norm altered by using one-sided running mean values for five months (MV1 5); curve 2, the norm altered by using two-sided running mean values for 5 months (MV2 5); curve 3, the norm altered by using the smoothing function for 3 months (smth 3).
C. Curve 1, the norm altered by using one-sided running mean values for 20 months (MV1 20); curve 2, the norm altered by using two-sided running mean values for 19 months (MV2 19); curve 3, the norm altered by using the smoothing function for 12 months (smth 12).
D. The norm altered by using the smoothing function for 1, 2, 4, 8 and 16 months.

In Equation (5.40), AF_1 has the dimensions, $L^3/((L/T)(L \times L \times L^2)^{0.5})$, which reduces to time alone. Its units are months. In Equation (5.41), AF_2 has the dimensions, $(L^3)^{2/3}/((L/T)(L \times L \times L^2)^{1/4})$, which also reduces to time (in months). Both these approaches give the required time dimension for AF (i.e., the number of months to be used for the smooth), so the constants in the two equations are dimensionless. If the variables are defined in the following manner, volume in km^3, altitude in m, precipitation in mm/year, latitude in m, and drainage basin area in km^2, then the numerical value of the constant can be calculated by considering the necessary conversions.

$Constant_1$ in Equation (5.40) is $(10^6/((10^{-3})/12)((40.08 \times 10^6) \times 1 \times 10^6))^{0.5} = 1895.7$. The corresponding value for $constant_2$ in Equation (5.41) is 47.6. In the following development, this constant is rounded to 50.

It should be noted that a correct dimensional analysis is generally a necessary component in a model derivation, but it may not be sufficient. In this case, it would be possible to account for other factors that could influence the seasonal variability, and one could also apply different weights to these five factors; instead of using Alt^1, as in this approach, one could use other exponents, like $Alt^{0.65}$.

The smoothing function (smth) for seasonal variation in Q and T plays the same role as other moderators [5.35], influencing (moderating) a rate, or in this case a given seasonal variability norm. It may therefore be termed a seasonal moderator for Q and T and is given by:

$$\textit{Seasonal moderator} = \textit{smth}(\textit{Seasonal variability norm}, AF, 1) \qquad (5.42)$$

This seasonal moderator can be used to provide a simple quantitative description of seasonal variability in Q and T. The model is presented in Figure 5.72, and the compartments and model variables in Table 5.26. Annex II gives all equations and presuppositions.

So far, we have dealt with the technical matter of constructing a seasonal variability moderator for Q and T. We will conduct some sensitivity tests to demonstrate how the derived moderator works.

Figure 5.73A illustrates the seasonal moderator for three of the VAMP lakes. These curves are affected by altitude, latitude, precipitation, catchment area, lake volume, and the defined common seasonal variability norm for Q and T. The Italian lake Bracciano is extremely deep (mean depth 89 m), has an extremely long theoretical water retention time (137 years) and has an extremely low catchment area to lake area ratio (of 1.6); its seasonal variability, as given by the seasonal moderator for Q and T, is also extremely low, as it should be. At the other extreme, the Norwegian lake, Øvre Heimdalsvatn, has very marked seasonal variations. The Swedish lake, Hillesjön, is between these two extremes.

Figure 5.73B gives a sensitivity test with data for Øvre Heimdalsvatn. The altitude has been varied and simulated so as to show how the seasonal moderator for Q and T would be if this lake were located at different altitudes. The figure shows that at lower altitudes the lake is less variable in Q and T. Figure 5.73C gives a sensitivity test where the precipitation is varied and again changes in precipitation produce changes in seasonal variability in Q and T.

What would happen to the averaging function, the seasonal moderator for water discharge, and hence to predicted lake concentrations if the constant in Equation (5.38) would be changed? Negative concentrations may appear if one uses small values of the constant. A small constant gives the averaging function a small value and implies that the seasonal moderator is very close to the seasonal variability norm, which is itself very low during January and February. When the seasonal moderator for Q and T is low and the theoretical water retention time is very short, like 2.1 months for Øvre Heimdalsvatn, the retention rate can exceed 1, so more of the substance is transported out of the lake than into the lake. This causes negative concentrations. To avoid this, the constant and hence the

averaging function must be large enough that retention is less than 1. This is achieved if one uses the theoretical constant of 50.

In the following this seasonal variability moderator for Q and T will be used to predict monthly variations in:

1. Tributary water discharge [Q(t)];
2. Lake water retention time [T(t)]; and
3. Lake water retention rate [$1/T(t)^{exp}$], where the exponent (exp) is a function of the theoretical lake water retention time (T), see next section.

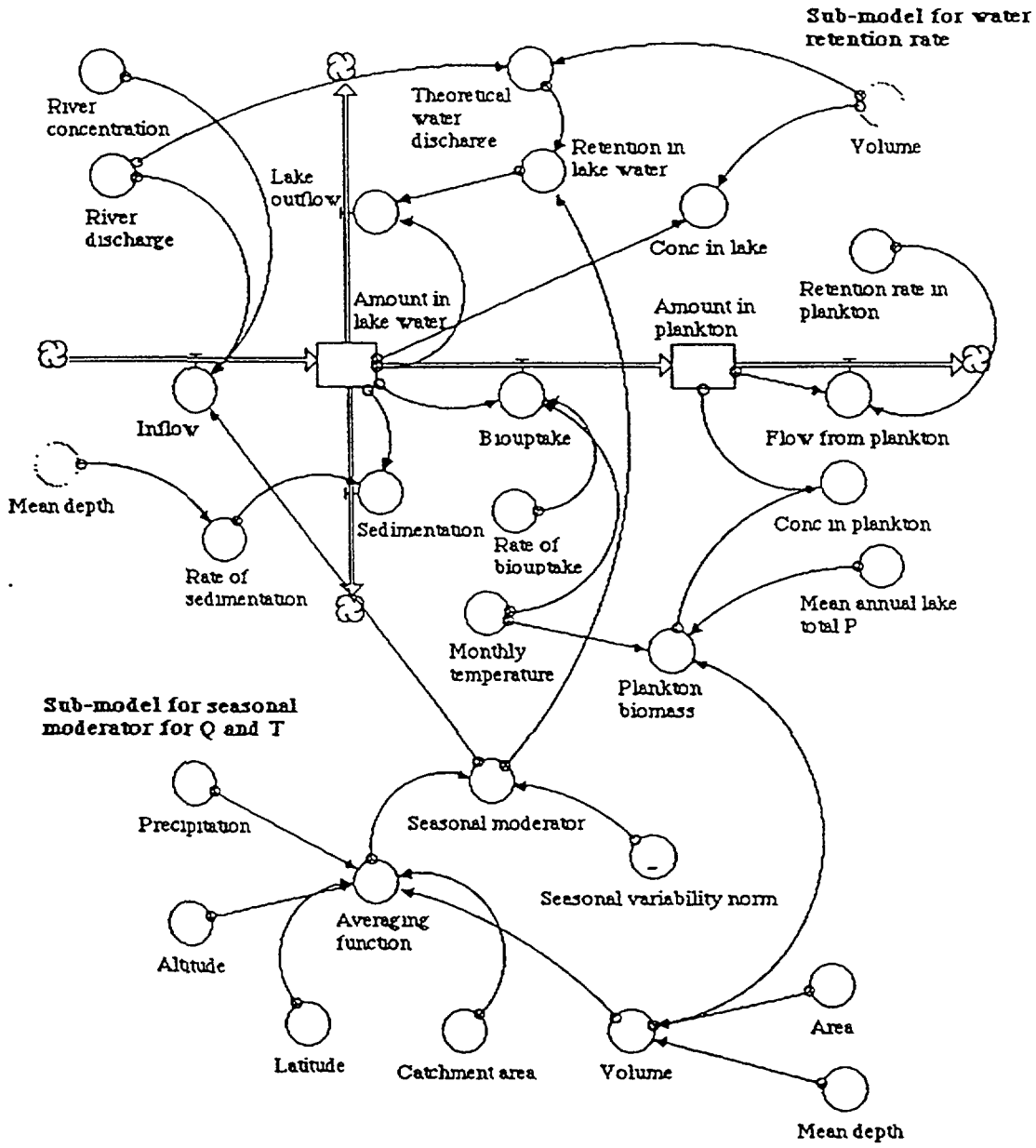

FIG. 5.72. The sub-model for the seasonal variability moderators for lake water retention rate, illustration of the applicability of the moderators to influence inflow, outflow, biouptake of any given toxin, and plankton biomass, the sub-models for the seasonal variability moderators and for tributary discharge.

TABLE 5.26. MODEL CHARACTERISTICS OF THE VAMP LAKE MODEL

A. Compartments:

1. Dissolved phase
2. Active sediment
3. Lake water first week after fallout
4. Lake water
5. Outflow areas of the catchment
6. Passive sediments
7. Phytoplankton
8. Predator
9. Prey
10. Suspended phase

B. Model variables (rates in 1/month, area etc. in m^2):

1. Averaging function 50 × volume$^{2/3}$/Precipitation (Altitude × Latitude × Catchment area)$^{1/4}$
2. Transport rate sediment to benthos = 0.00025
3. Transport rate plankton to prey = 0.25/12
4. Transport rate prey to predator = Bioaccumulation rate plankton to prey = 0.25/12
5. Transport rate dissolved phase to prey and predator (Transp wat to biota) = YpH+0.0004K
6. Initial K_d = 0.5
7. Outflow areas OA = 0.1
8. Transport rate from outflow areas to lake = 0.04 (Seasonal moderator)/12√(Delay(Time, Month of fallout,1))
9. Distribution coefficient K_d = 1/(1.04+(1.75(pH/4-1)^2))
10. Transport rate from phytoplankton out of system = 5/30
11. Transport rate dissolved phase to phytoplankton = YpH + 0.005K
12. Predator biomass = (Prey biomass)/2(Transfer coeff)$^{0.4}$
13. Transport rate (=biological half life) from prey and predator out of system = 0.693/X
    where X is 200 days for large pike and large, predatory perch (> 20 cm)
    125 days for perch (10 – 20 cm), etc.
    100 days for minnow, trout, etc.
    75 days for whitefish, roach, etc.
    75 days for smelt, perch fry (< 10 cm), etc.
    The transport rates for prey out of system = 2(Transport rate for predator)
14. Prey biomass = (Phytoplankton biomass)/(Transfer coeff)
15. Water retention rate = (Seasonal moderator)/T$^{[30/(T+29)+0.5]/1.5}$
16. Retention rate in active sediments = (Sedimentation rate of suspended matter)/(Thickness of active sediments)
17. Sedimentation rate of Cs = 1/(Mean depth)
18. Thickness of active sediments = 2 cm
19. Transfer coefficient = (Prim production+1)$^{0.65}$
20. Seasonal variability norm = GRAPH(TIME)
21. YpH plus K = GRAPH(pH plus K)
22. Internal loading=0.05(Dynamic ratio)

C. Lake-specific variables (examples from Lake Øvre Heimdalsvatn):

1. Altitude = (1090+1) m.a.s.l.
2. Atmospheric load = 130 kBq/m^2
3. Catchment area = 23.4 × 10^6 m^2
4. Lake volume = 3.7 × 10^6 m^3
5. Water retention time = 63/30 months
6. K concentration= 0.4 mg/L
7. Lake area = 0.78 × 10^6 m^2
8. Latitude = 61°N
9. Month of fallout = 5
10. pH = 6.8
11. Precipitation = 800 mm/year
12. Primary production = 27.5 g C·m^{-2}·a^{-1}
13. Sedimentation rate of suspended matter = 60 g·m^{-2}·a^{-1}

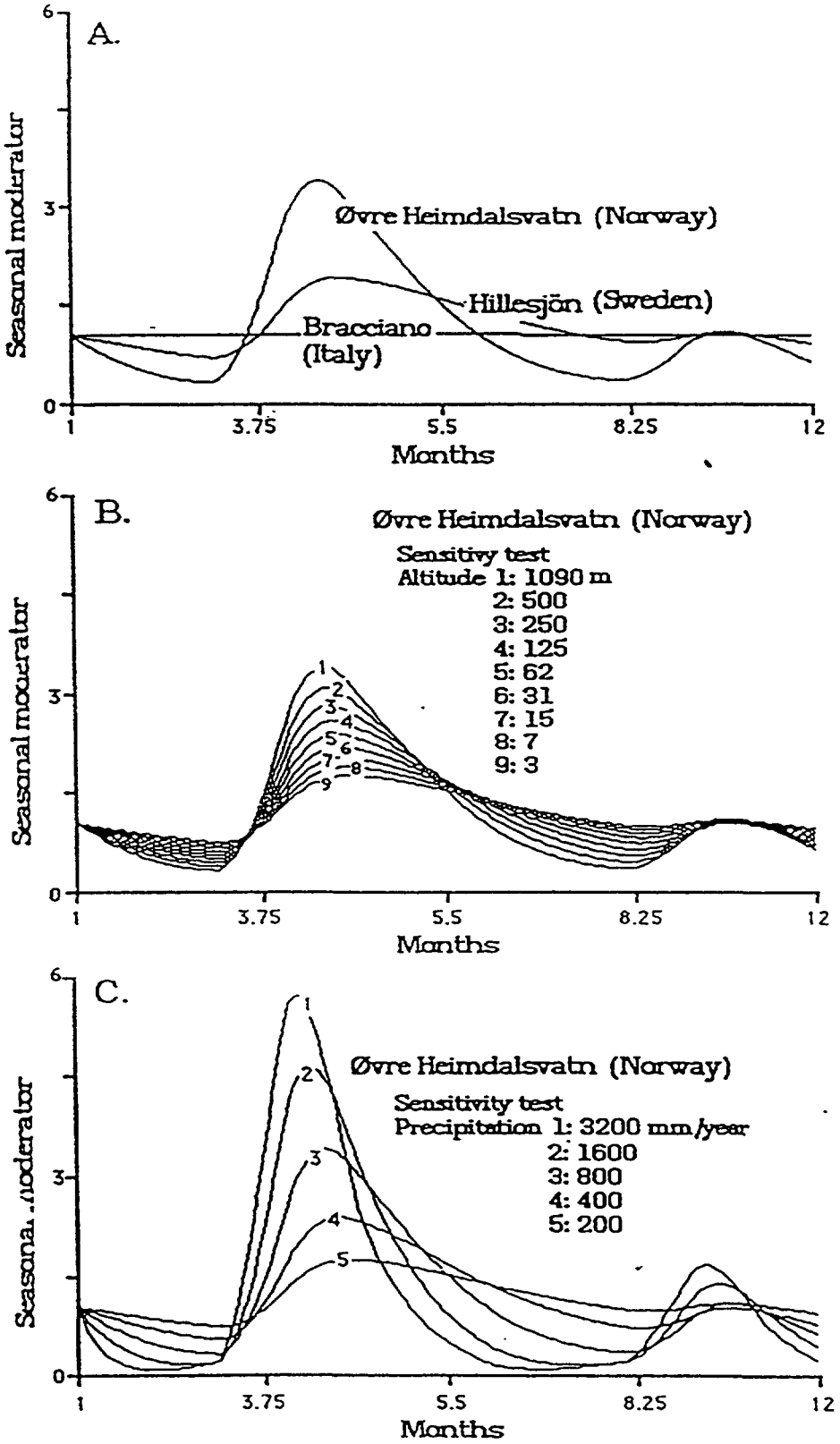

FIG. 5.73. A. Illustration of the seasonal moderator for Q and T for lakes Øvre Heimdalsvatn, Hillesjön and Bracciano. B. Sensitivity analysis of the effects of altitude using data for Øvre Heimdalsvatn. C. Sensitivity analysis of the effects of precipitation using data for Øvre Heimdalsvatn.

To do this, data on mean annual data on Q is needed, where Q is simply predicted from area of drainage area (ADA in m^2), precipitation (or rather precipitation factor which is the rate actual precipitation divided by reference precipitation, dimensionless, here we set it to 600/600, expressed in mm/year) and specific runoff (SR in $m^3 \cdot month^{-1} \cdot m^{-2}$), as:

$$Q(t) = (Seasonal\ moderator) \times ADA \times Prec \times SR \qquad (5.43)$$

The results of the calculations are given in Figure 5.74 (for a typical Swedish forest lake; area, 0.77 km^2; mean depth, 4.2 m; ADA, 10 km^2; [5.35]; SR is set to 11 $L \cdot km^{-2} \cdot a^{-1}$). We can note the spring peak in Q(t) and the retention rate, and the corresponding decrease in lake water retention time, T(t).

Predictions like these are very important in many limnological contexts, and such seasonal variations can in fact be predicted from readily available map parameters, namely:

(a) from the bathymetric map: Area and mean depth; and
(b) from the catchment: Altitude, latitude, mean annual precipitation, catchment area, and specific runoff.

It is evident that these predictions may not be very accurate for every lake every year. But these model predicted values may be considered as normative or normal values. Divergences from the normal can then be discussed in a quantitative manner, and lake-specific calibrations can be used to further increase the lake-specific predictions.

Figure 5.75A illustrates how the model would predict inflow to lake (of a given toxin X in g/month) and Figure 5.75B lake outflow (of X in g/month) with and without the seasonal moderator for Q and T applied both on the inflow and the outflow. Without the seasonal variability moderator, the results are unrealistic.

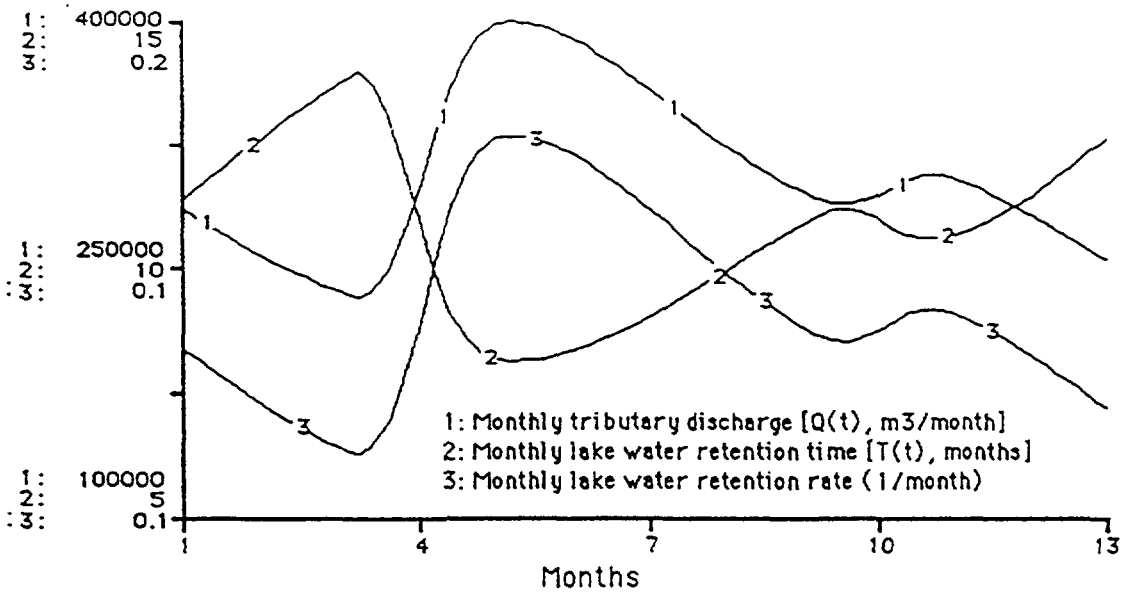

FIG. 5.74. Predictions of seasonal variability in tributary water discharge, Q(t), lake water retention time, T(t), and lake water retention rate, from simple map parameters using seasonal variability moderator technique.

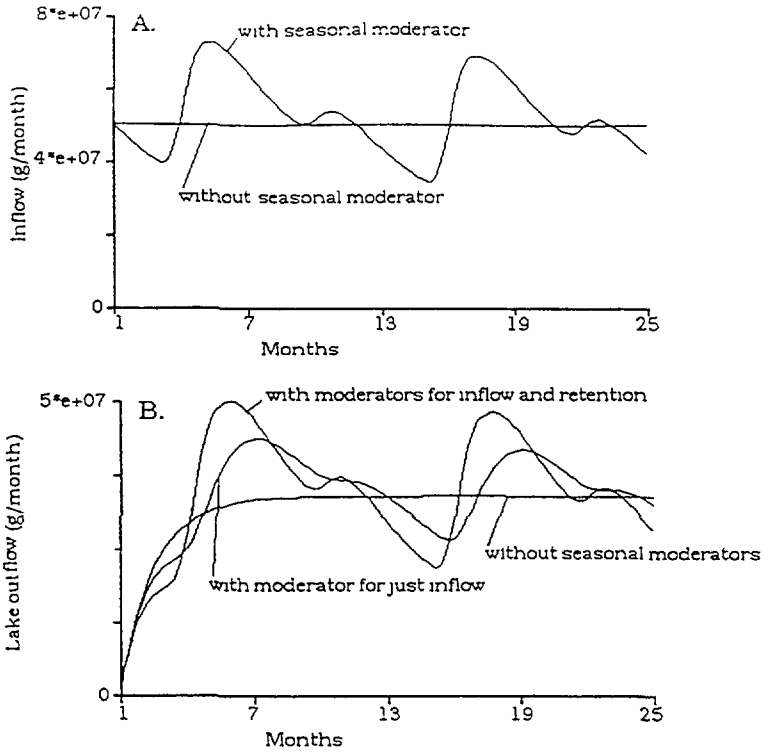

FIG. 5.75. Model predictions of (A) inflow, and (B) lake outflow (of a given toxin X) with and without seasonal variability moderators for Q and T.

5.10.2. Seasonal variability moderator for lake water retention rate

In the basic mass-balance model, the retention in the lake of any given substance X is related to T, the theoretical lake water retention time [5.3, 5.35]. The retention rate would be 1/T or some variant of this such as:

1. 1/T(t), where T(t) is a time dependent function of T, it could be either derived from empirical data or obtained by using the seasonal moderator for Q and T;
2. 0.693/0.5T(t), linked to the half life, where 0.695 = - ln(0.5); or
3. $1/T^{YDm}$, where YDm is a dimensional moderator for the mean depth [5.35].

To describe how the retention rate might vary with time, one can first use the seasonal moderator for Q and T (i.e. a function of time), instead of a mean average water retention (a constant). For example, we could define the retention rate as:

$$\textit{Retention in lake water} = \textit{Seasonal moderator}/\textit{Water retention time} \qquad (5.44)$$

If the seasonal moderator for Q and T has a low value (as during winter), then the theoretical water retention time should be long and the retention rate low, and vice versa. For example, assume that T is 1 year, that the seasonal moderator for Q and T for April is 2.0 and for October 0.2. Then the retention rate for April is 2/1 = 2 and the water is flushed out of the lake and for October the rate is 0.2/1 = 0.2 and much of the water is retained in the lake.

However, for large, well stratified lakes where water turnover is to a large extent regulated by different types of currents [5.54], this approach is evidently a gross simplification. For such lakes, the actual water turnover is quicker, or much quicker, than the value suggested by the simple theoretical

water retention time (i.e. by 1/T), which assumes total mixing. This has been demonstrated in many contexts, including in lake eutrophication modelling [5.55], where it has been shown that the actual turnover time of the water and phosphorus is often quicker than suggested by the theoretical water retention time (1/T). In lake eutrophication contexts, $T^{0.5}$ is often used instead of $KT \cdot T^{1}$ (KT = sedimentation rate) to get better prediction of water and total-P retention in lakes.

The objective in this Section is to provide a simple general sub-model for retention rates for lakes. The rationale for this is further explained in Figure 5.76. The idea is to provide a general expression for the exponent, T^{exp}. The exponent (exp) should be about 1 for small, shallow lakes with large catchments, i.e., for lakes with a short theoretical water retention time (T), and small for lakes with very long theoretical retention times. Based on the empirical data for the VAMP lakes, the following algorithm has been derived (calibrated) for the retention rate (RR):

$$RR = 1/T^{[30/(T+29) + 0.5]/1.5} \tag{5.45}$$

To be modelled with this approach, the lake with the shortest T value must be used as a reference so that T is always equal to or smaller than 1. So, if T is 2 months, which is an extremely short retention time (valid for Øvre Heimdalsvatn, Norway), then the calculation time dt should not be 1 year but rather 1 month.

This gives: For T = 1 (in given units of time, often month), the retention rate is 1, as requested;
For T = 10, the retention rate is 0.14 with this approach, instead of 0.1 with the traditional approach (1/T);
For T = 100, this retention rate is 0.11, and not 0.01.

It is evident that this approach could be improved by calibration against a more extensive set of empirical data than the six VAMP lakes.

5.10.3. The transfer coefficient

It is often assumed that the biomass of the prey (small fish and zooplankton) is about 1/10 of the phytoplankton biomass in a typical Swedish forest lake [5.35]. This is, naturally, a simplification. The ratio between phytoplankton biomass and prey biomass is often about 1/3 in very oligotrophic lakes and as low as 1/50 in hypertrophic lakes. The ratio does not increase linearly with primary production. Here, this ratio is called the transfer coefficient to indicate a transfer (consumption) of biomass (carbon) between different trophic levels in the lake ecosystem. Data on ^{137}Cs may be used to study how this transfer coefficient varies among the VAMP lakes. This is interesting also from a classical limnological perspective, since it means that knowledge may be gained on the relationship between these biomasses at different levels of primary production. The empirical calibrations for the VAMP lakes indicate that the transfer coefficient (phytoplankton biomass/prey biomass) may be given by:

$$Transfer\ coefficient = ((Prim\ production)+1)^{0.6} \tag{5.46}$$

The choice of the transfer coefficient is important for the Cs concentrations of predatory fish because that concentration is calculated as amount/predatory biomass and predatory biomass is calculated as plankton biomass/transfer coefficient.

This means that the transfer coefficient is about 7.5 for a Swedish forest lake with a primary production of 25–30 g $C \cdot m^{-2} \cdot a^{-1}$, and about 34 for a very productive lake (like the Dutch lake, IJsselmeer) with a primary production of 350 g $C \cdot m^{-2} \cdot a^{-1}$, and about 1.5 for an extreme low-productive lake (the Italian lake, Bracciano). This gives a range of about 20 for the VAMP lakes, which cover a very wide range in term of lake primary productivity.

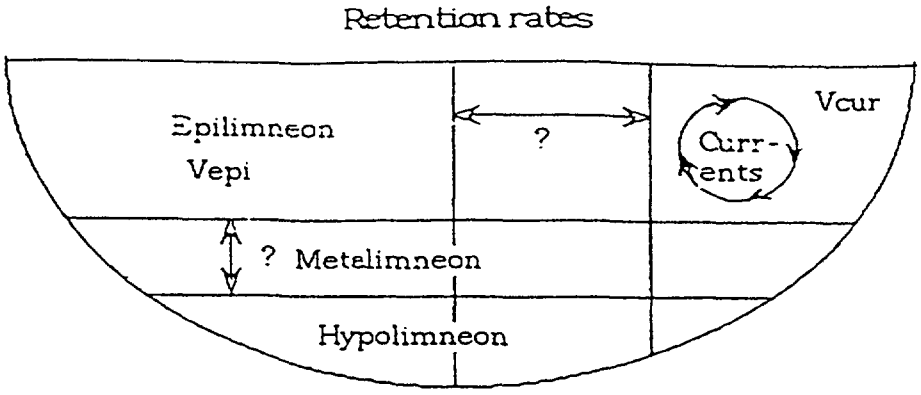

Vtot > Vepi > Vcur
V = Vtot = lake volume (m3); Vepi = volume of epilimneon;
Vcur = volume of lake with active water turnover (current acction, etc.)

T = V/Q; Q = river discharge (m3/month); T = theoretical lake water retention time (months)
1/T = Q/V = lake water retention rate (1/months)

Vtot is a simple morphometric constant
Vepi is a time-dependent, "difficult" lake-specific variable
Vcur is also a time-dependent, "difficult" lake-specific variable

So, it is simple to determine the retention rate if V = Vtot. But for causal reasons, this is NOT a relevant measure in large, deep lakes with long theoretical water retention time (T). For such lakes, a better retention rate would be Q/Vepi or Q/Vcur. Such rates may be estimated in the following manner:

Assume: Vtot = 1; Vepi = 0.7; Vcur = 0.2; and Q = 0.1, then
rate(tot) = 0.1; rate(epi) = 0.14; and rate(cur) = 0.5

rate(tot) = 1/10^1 = 1/T^1
rate(epi) = 1/10^0.85 = 1/T^0.85
rate(cur) = 1/10^0.3 = 1/T^0.3

Task: Which exponent should be used to obtain the best descripition of the retention rate?

This model usew the following algorithm:

exp = ((30/(T+29)) +0.5)/1.5

This gives for T = 1, exp = 1
for T = 50, exp = 0.67 and
for T = 500, exp = 0.40

T must always be > 1 and related to the calculation time dt: If dt is given in months, then T in months must be longer than 1 month.

FIG. 5.76. The rationale for the new approach to define the lake water retention rate.

Analogously, one can also define a transfer coefficient between prey (including zooplankton) and predatory fish. This ratio should be about 1/2 to 1/3 in a typical Swedish forest lake. The range in the ratio between very oligotrophic and very eutrophic lakes should be smaller than the range of 20

for the transfer coefficient between phytoplankton and prey. Using the data for the VAMP lakes for calibrations, we have arrived at the following simple expression for the biomass for predatory fish:

$$Transfer\ coefficient_2 = (Prey\ biomass)/(Transfer\ coefficient)^{0.4} \qquad (5.47)$$

This gives a value of 3.7 for Transfer coefficient$_2$ for a typical Swedish forest lake with a primary production of 25–30 g C·m^{-2}·a^{-1}, and about 4.1 for a very productive lake (IJsselmeer) with a primary production of 350 g C·m^{-2}·a^{-1}, and about 1.15 for an extremely low productive lake (Bracciano). This gives a range of about 3.5 for the VAMP lakes.

Figure 5.77 gives the relationship between primary production and:

A, the transfer coefficient, i.e. the ratio between the prey biomass and the predator fish biomass, and the formula relating the transfer coefficient to the primary production in the different productivity classes;

B, the phytoplankton biomass (linear);

C, the prey biomass (non-linear); and

D, the predator biomass (non-linear).

5.10.4. The outflow rate function

This is the function for the outflow rate of radiocaesium from the catchment, or rather from the outflow areas (the wet land) of the catchment, to the lake. It is given by:

$$Outflow\ rate\ function = 0.1(Seasonal\ moderator)/\sqrt{(time_{FM}+1)} \qquad (5.44)$$

where
FM is the fallout month (5 is May).

This is the general formula for the initial, default rate (0.1 per year), which is modified by the seasonal moderator for Q and T (an increased rate during spring and fall peaks). The rate is time-dependent decreasing with time from the month of the fallout (given by $1/\sqrt{}$time). A delay function initiates the runoff to the month of the fallout plus one month (time$_{FM}$+1). The initial or default value of the runoff is set to 0.1 for the first year after the fallout, i.e. a mean average runoff of 10%. The outflow rate function will cause this initial outflow rate to decrease with time and the seasonal moderator for Q and T influences the seasonal variability in outflow rate. Figure 5.78 illustrates the relationship between outflow rate as a function of fallout month and months after the fallout.

5.10.5. The moderator for planktonic biouptake

This is a dimensionless moderator [5.35], for further information on graphical moderators) expressing the fact that the biouptake of radiocaesium by plankton (here mainly phytoplankton) depends on the pH and the K-concentration of the lake water, the lower pH and K, the higher the uptake, and vice versa [5.36]. This moderator has been derived empirically using the data from the VAMP lakes (Figure 5.79). The moderator operates on the phytoplankton biological-uptake rate, which is set to 0.005 (1/month) as a default value. If this value is higher, biological uptake in phytoplankton is increased so much that unrealistically high values of radiocaesium occur in both prey and predator fish.

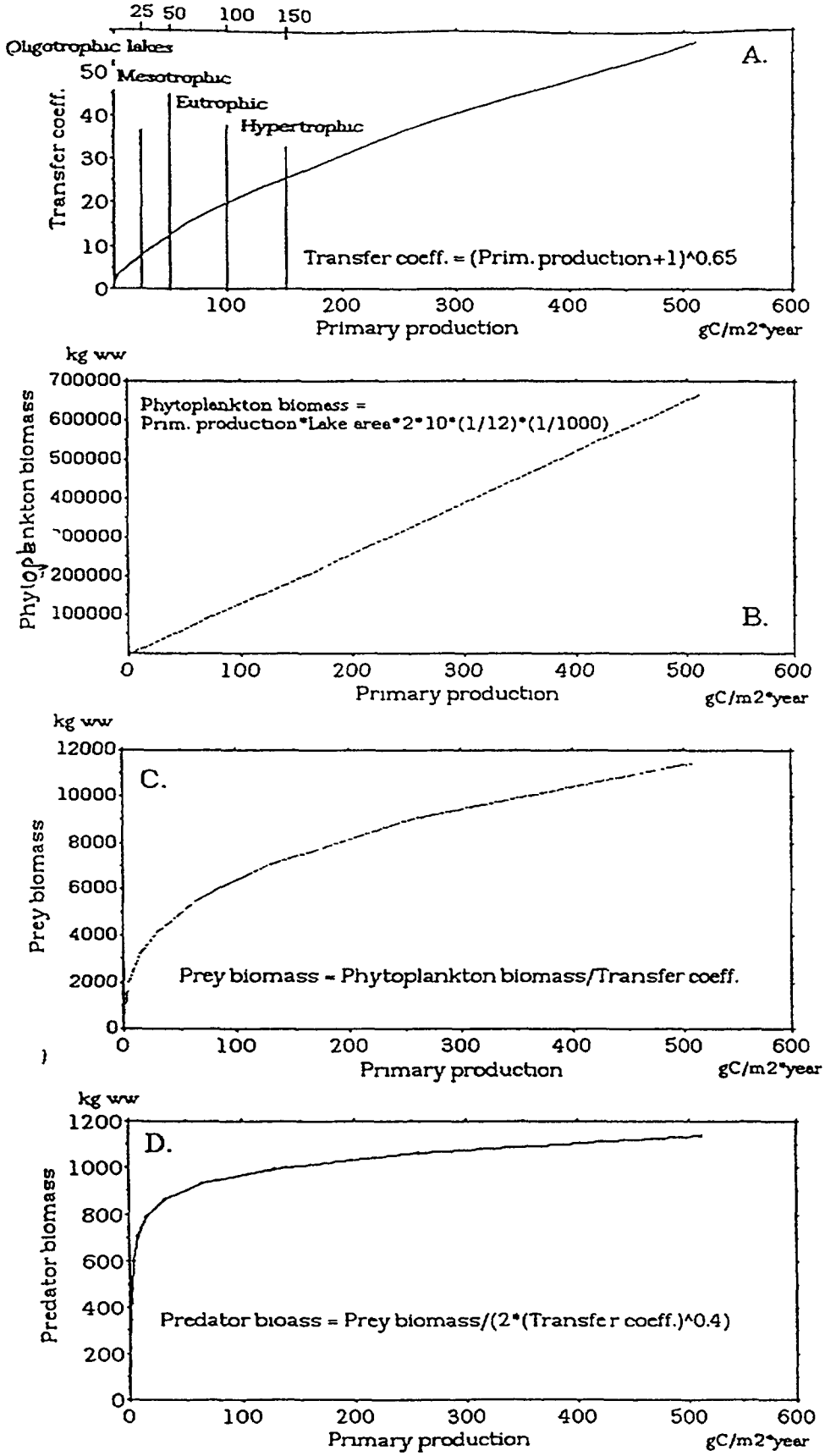

FIG. 5.77. The transfer coefficient. (A) the relationship between the transfer coefficient and the primary production, (B) the relationship between phytoplankton biomass and primary production, (C) the relationship between prey biomass and primary production, and (D) the relationship between predator biomass and primary production.

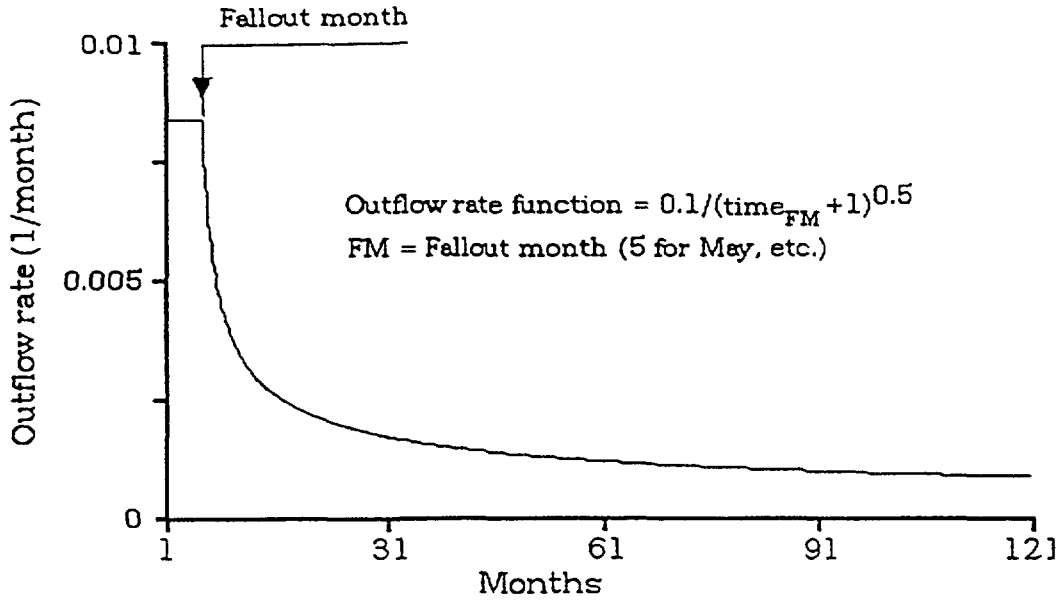

FIG. 5.78. Graphical illustration of the outflow rate function.

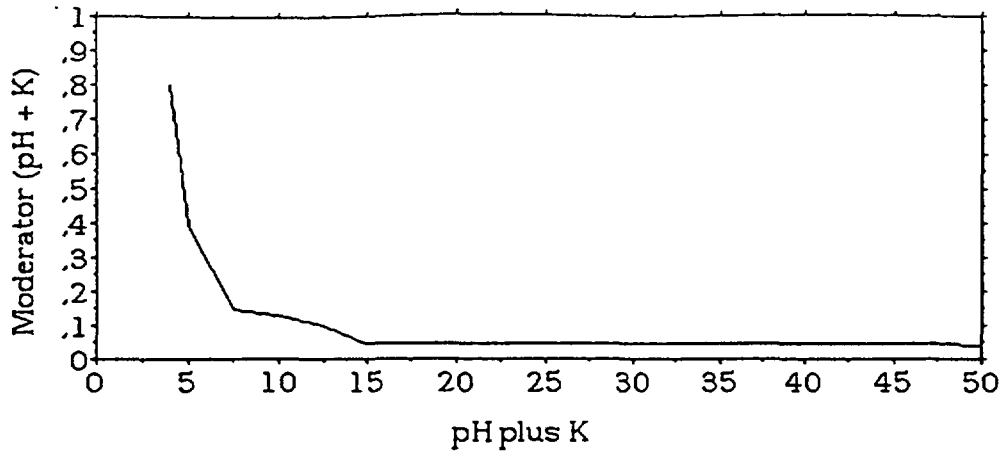

FIG. 5.79. Illustration of the pH plus K moderator.

5.10.6. The moderator for the distribution coefficient (K_d)

The distribution (partition) coefficient (K_d) is used in models to differentiate the caesium in the lake water into a particulate phase and a dissolved phase (see Section 4.1.1). The lake K_d value in this modelling set-up is influenced by lake pH (and/or variables belonging to the same cluster as pH): The lower the pH, the more ^{137}Cs in dissolved phase. pH may influence both the affinity of caesium to the carrier particles (humus, clays, etc.) and the aggregation of the carrier particles and hence the sedimentation rate [5.35].

The following algorithm (a dimensionless moderator) is assumed to be valid for lakes with pH in the range between 4 and 9. For example, it predicts that 96% of the caesium in the lake water is in dissolved phase at pH = 4 and that 26% is in dissolved phase at pH = 9. The formula is the general type:

$$K_d = 1/(x+amp(pH/bord)-1)^z \qquad (5.49)$$

where
x and the exponent z are empirical constants;
bord is a borderline value (set to pH = 4); and
amp is an amplitude value (set to 1.75). This gives:

$$K_d = 1/(1.04+(1.75((pH/4)-1)^2)) \quad (5.50)$$

Figure 5.80 illustrates the relationship between lake pH and K_d. Note that lake K_d is not given in the traditional way, as P/D, where P is caesium in particular phase and D is caesium in dissolved phase. In this case it is given as D/(D+P), i.e. the fraction of the total amount in lake water (D+P) that appears in the dissolved phase.

5.10.7. Using these sub-models

The sub-models to predict seasonal variability in Q and T and lake water retention rate may be used in many different contexts, such as predicting seasonal variability in lake variables from data on mean annual values (or mean values for longer periods than 1 year). Such mean annual values may often be predicted from simple map parameters of the catchment or from the lake itself. This has been demonstrated for many variables, including lake total-P, colour, pH and Secchi depth [5.35], or in models where mean annual total-P is used to predict important lake ecosystem variables [5.56].

Figure 5.69 shows that the seasonal moderator for Q and T is applied twice in the VAMP LAKE model. This seasonal moderator for Q and T influences the outflow rate from the catchment (from outflow- or OA-areas), and modifies water retention time, and thereby changes the lake water retention rate. Our main concern is whether the seasonal moderator for Q and T improves the predictive power of the given model.

Figure 5.81A gives the predicted recovery for Øvre Heimdalsvatn. Given that the lake was contaminated with 130 kBq/m^2 of ^{137}Cs fallout in May 1986, the model predicts how the radionuclide is subsequently distributed among the water, sediments and biota. In doing so, the VAMP LAKE model addresses a series of other questions including what are the most important processes regulating these fluxes and how long does it take to reach the peak value and how high is the peak value in predatory fish used for human consumption.

When the seasonal variability moderator for Q and T is applied, seasonal variation is more pronounced for Cs in water than for Cs in prey, and the curve for Cs in predatory fish is very smooth,

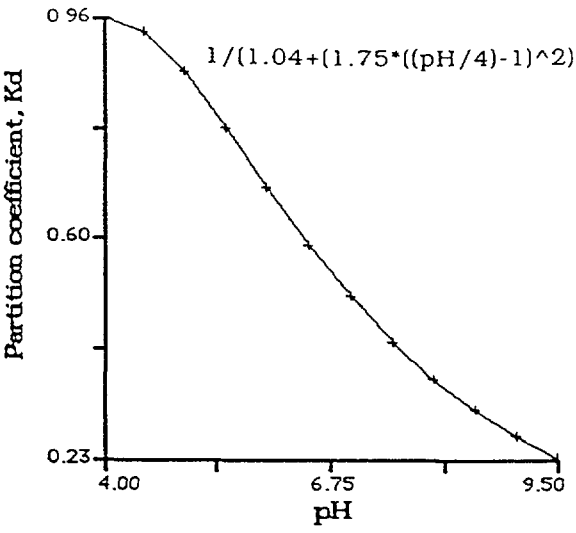

FIG. 5.80. The algorithm for the relationship between lake pH and the distribution coefficient.

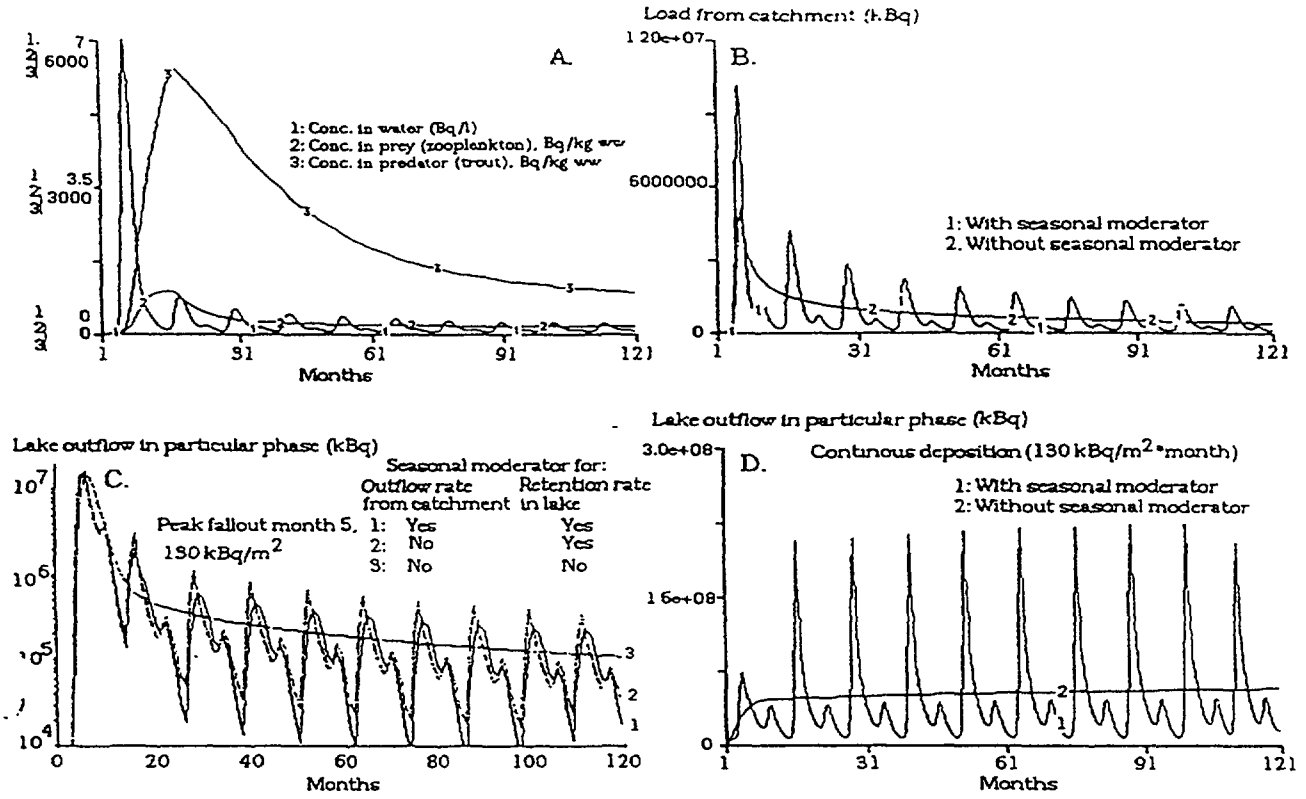

FIG. 5.81. A. Model predictions of Cs concentrations in water (curve 1), prey (zooplankton; curve 2) and predatory fish (trout; curve 3) for Øvre Heimdalsvatn using the VAMP LAKE model with the seasonal variability moderator for Q and T. B. Predictions of the load of radiocaesium from the catchment using the VAMP LAKE model with and without the seasonal variability moderator for Q and T. C. Predictions of the lake outflow of radiocaesium using the VAMP LAKE model with and without the seasonal variability moderator for Q and T to influence the outflow rate from the catchment and/or the retention rate for lake water for a peak fallout of 130 kBq/m² in May 1986. D. The same simulation as in C, but for a continuous deposition of 130 kBq/m².

as expected. Peak values in predatory fish appear some 12 months after the fallout and much earlier in prey. Before we show how these predictions correspond to the empirical data, we will further examine the role of the seasonal variability moderators for Q and T.

Figure 5.81B gives an interesting simulation of the curves for the secondary load of radiocaesium from the catchment with and without the seasonal moderator for Q and T. Without the seasonal moderator, one gets an unrealistically smooth outflow, which disregards the great seasonal variabilities in water discharge.

Figure 5.81C gives the same type of prediction with and without the seasonal moderator for Q and T applied both for the outflow rate from the catchment and the retention rate in the lake in a calculation of the outflow of particulate radiocaesium from the lake. The peak value is about the same but the recovery is quite different without the seasonal moderator for Q and T. This is a simulation for a peak fallout. If we make a simulation for a continuous atmospheric contamination (like for mercury), Figure 5.81D illustrates (otherwise using the same data as in Figure 5.81C), much more marked differences between the results when we use and when we do not use the seasonal moderator for Q and T.

Figure 5.82 gives another simulation to answer the question: What would the curves look like for radiocaesium in predatory fish (trout) in this Norwegian lake had this accident happened at another

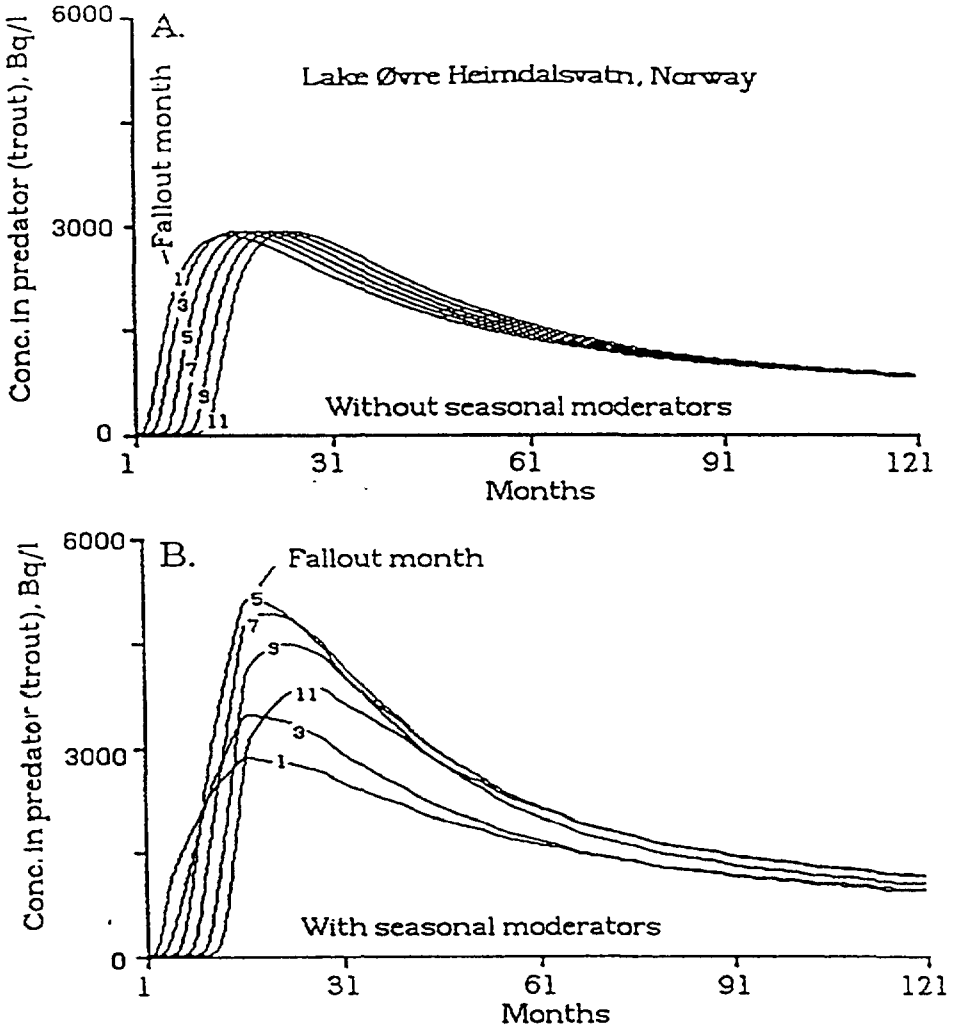

FIG. 5.82. Model predictions of Cs concentrations in predatory fish (trout) for Øvre Heimdalsvatn using the VAMP LAKE model. A. Sensitivity tests without the seasonal variability moderator for Q and T. The curves illustrate the consequences for the Cs concentration in predatory fish when the month of the fallout is varied; curve 1 gives the results in the fallout, 130 kBq/m² happens in January, etc. B. The same type of sensitivity tests with the seasonal variability moderators for Q and T.

season of the year? It is of utmost importance that the model accounts for such a difference since it is highly unlikely that any further accident would happen at the same time of the year and under the same weather conditions. The simulation in Figure 5.82 is a sensitivity analysis where the month of the fallout has been changed with and without the seasonal moderator for Q and T.

This model indicates that May was, it seems, the most unfavourable month for an accident of this type, just at the very start of the bioproductive season. Lower maximum values would have been obtained had this accident happened in January (curves marked 1), March (curves marked 3) and during the autumn. A significant part of a winter fallout on ice would be quickly transported out of the lake together with the spring flood. A fallout later in the year, during late summer and fall, would not be taken up in the plankton in the lake in the same way as a fallout just after the spring flood. The predicted peak value for predatory fish with the seasonal moderator is 5300 Bq/kg w.w.; without the moderator the result is 2900 Bq/kg w.w. The empirical peak value is 4600. The peak values also appear about the same time with and without the moderator for Q and T. However, when the month of the fallout is changed, the model without the seasonal variability moderator for Q and T simply transposes the same curve in simple steps depending on the month of the fallout. This seems very unlikely.

This prediction depends on the use of the seasonal variability moderator for Q and T for this particular lake. These predictions concerning different fallout months have naturally not been validated, but they seem plausible.

5.10.8. Empirical tests

Since the six VAMP lakes vary in size (from 0.042 to 1147 km^2), mean depth (from 1.7 to 89.5 m), precipitation (from 600 to 1840 mm/year), pH (from 5.1 to 8.5), K-concentration (from 0.4 to 40 mg/l), primary productivity (from 0.8 to 350 g $C \cdot m^{-2} \cdot a^{-1}$) and in food web characteristics, it is a great challenge to try to model the effects of the Chernobyl "spike" on the concentrations in water and biota. Traditional dynamic models "succeed" if they produce values within one order of magnitude of the empirical values, and that might serve as a suitable index of success.

Figure 5.83 shows the excellent result of a comparison between empirical data and model data for trout and minnow in Øvre Heimdalsvatn, using model simulations with and without the seasonal moderator for Q and T.

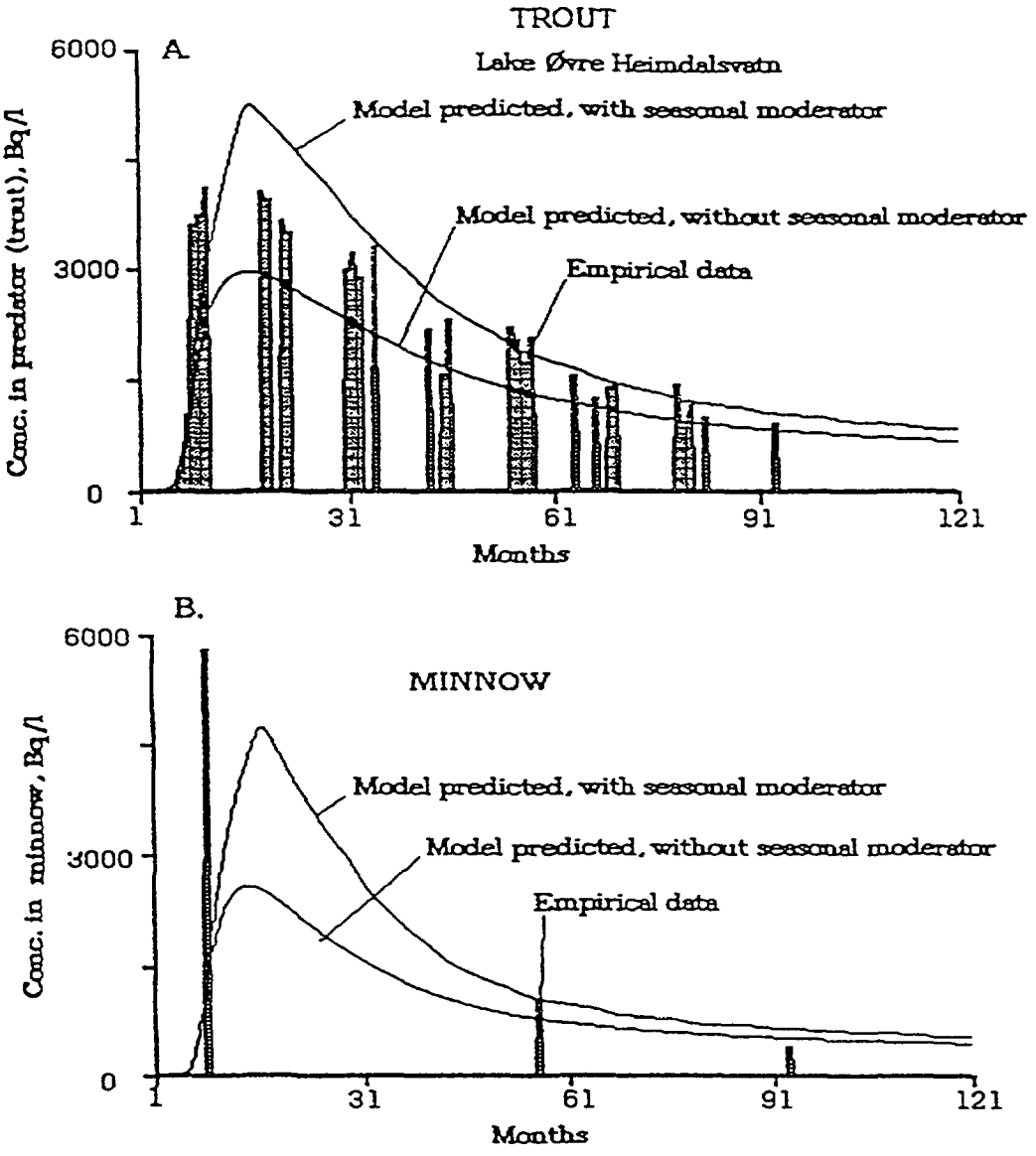

FIG. 5.83. Comparison between empirical data and model predictions of (A) radiocaesium in trout, and (B) in minnow for Øvre Heimdalsvatn using the VAMP LAKE model with and without the seasonal variability moderator for Q and T.

Figure 5.84 shows the remarkable result that the r^2 value between empirical peak values and peak values predicted by the VAMP LAKE model for all the VAMP lakes is 0.998. All lakes more or less lie right on the regression line. The Norwegian lake is in fact the "worst" case. The slope is about 1, i.e. close to the ideal y = x, and the 95% confidence interval for the predicted y is close to the regression line.

It should, however, be stressed that these fine results are not derived after blind tests. There has been considerable "tuning" of the model, but – and this is important – only for the simple environmental variables. The model variables illustrated in Table 5.26 have not been changed, just the lake-specific, environmental variables.

The VAMP LAKE model apparently provides great predictive accuracy for the maximum values, and with the seasonal variability moderator, the results seem plausible for any fallout event. It is very difficult to produce accurate predictions in lakes of this type, for there are great uncertainties in the data for radiocaesium and most lake characteristics (like pH and K concentration). To obtain peaks within a factor of 20% of the observed values for top predator is very good.

These techniques ought to apply in many other modelling contexts, although, one may have to alter the seasonal variability norm for Q and T. The norm for Q and T may require a higher peak in the fall for lakes from certain climatological regions, or to have another averaging function to account for differences in the soils and geology of the catchment. The basic argument is that seasonal variability moderators, like these two, may increase the predictive power of many models. This can be achieved simply, by using only a few readily available driving variables.

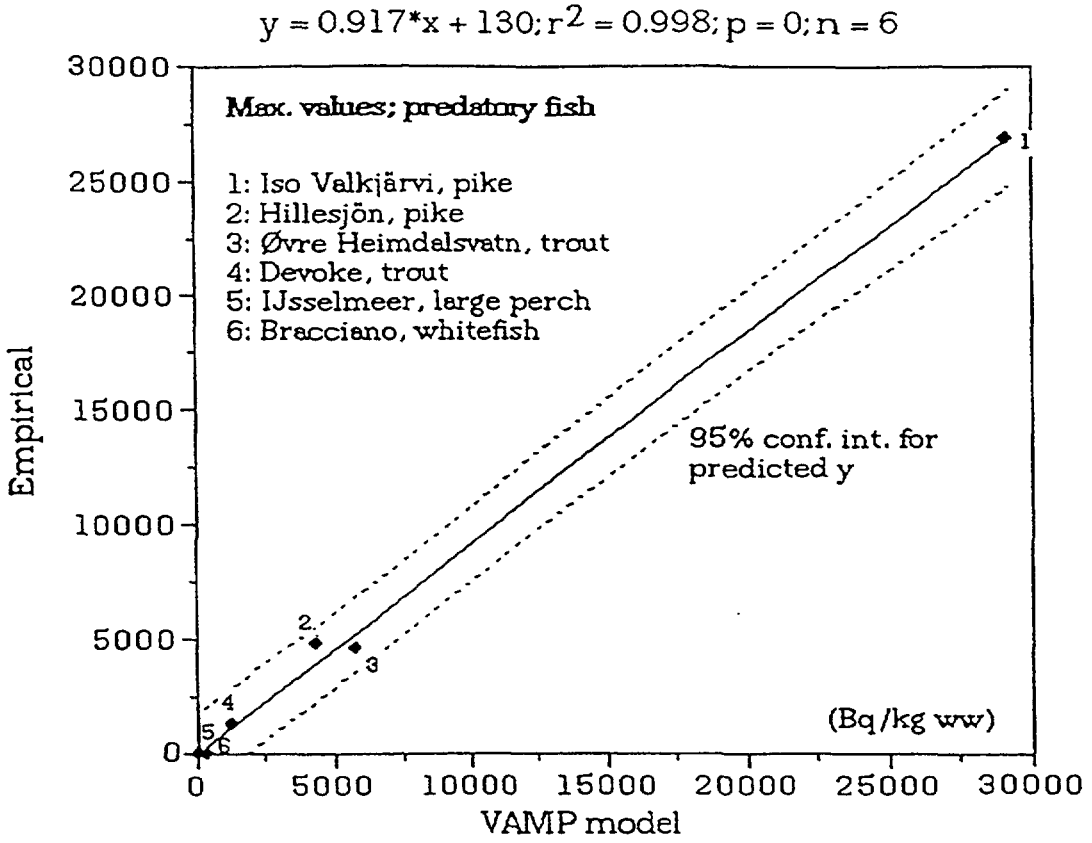

FIG. 5.84. Comparisons between empirical data for peak Cs concentrations in predatory fish after the Chernobyl accident, and values predicted by the VAMP LAKE model.

5.10.9. Sensitivity analyses

Since the VAMP LAKE model is meant to be "the-state-of-the-art" in lake modelling of radiocaesium, some selected sensitivity analyses are presented here to reveal how the model works. All these sensitivity analyses have been done in a similar way, by altering each model variable by a factor of 2 and a factor of 0.5. So, each graph presents three curves, where curve 2 represents the default values.

Figure 5.85 shows that the VAMP LAKE model is very sensitive to changes in variables related to different sedimentological processes, like the lake partition coefficient, K_d (note that in Figure 5.85A the scale on the y-axis goes to 12,000; this is marked by the arrow), but not so sensitive to changes in the sedimentation rate for Cs, the thickness of the active sediment layer (C) and the averaging function for the seasonal moderator (D). Figure 5.86 shows that the model is sensitive to changes in several of the biouptake rates, especially to the direct uptake from dissolved phase in the lake water to predatory fish (trout; Figure 5.86D). The model is less sensitive to the rates for biouptake plankton to prey (C), prey to predator (D) and dissolved phase to top prey (F), and rather insensitive to the values for the rates for dissolved phase to phytoplankton (A) and sediment to benthos (B). Thus, these rates have different influence on the model predictions.

Figure 5.87 gives six sensitivity tests rates regulating different transports from the system. These rates can also be called retention rates, since they also regulate how long radiocaesium will remain in the given compartment. The model is most sensitive to the rates regulating the outflow of dissolved caesium from lake water, and the flow of caesium from predator and out of the system (D). The model predictions are not very sensitive to the choice of the other rates, like transport rate from outflow areas (A), from phytoplankton and out of the system (B), from prey out of the system (C) and from suspended phase in lake water and out of the system (F).

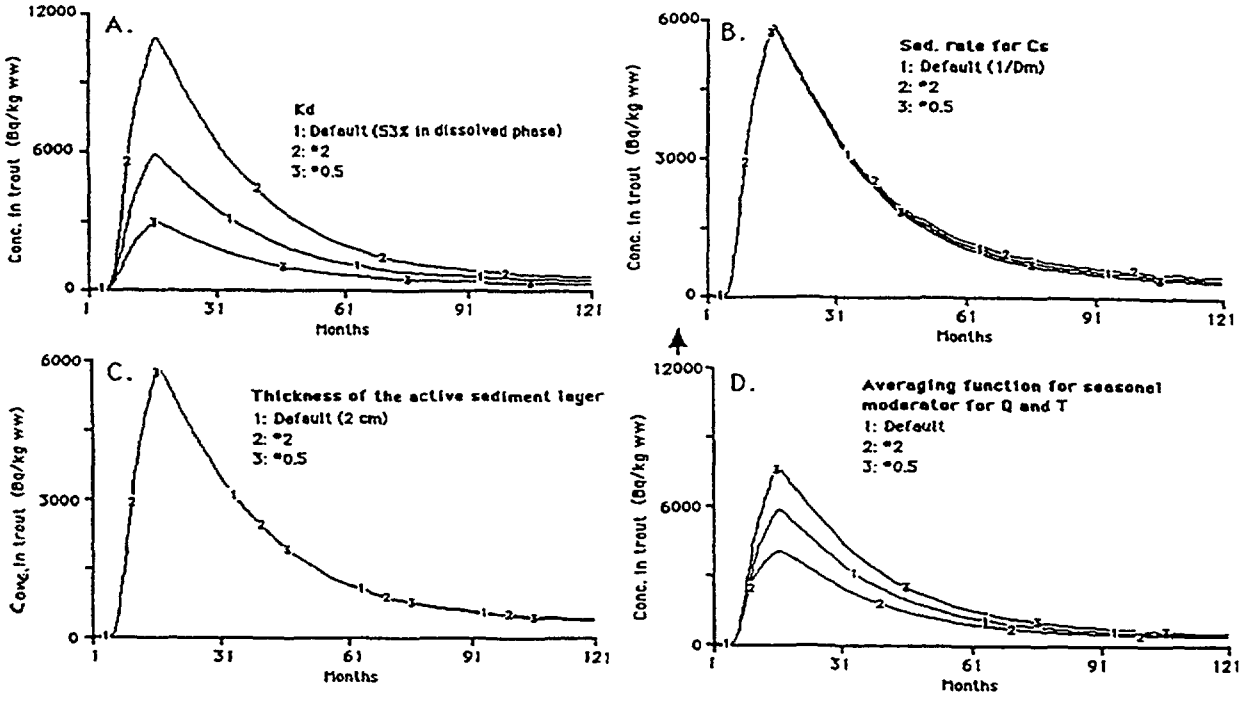

FIG. 5.85. Sensitivity analyses for important model variables related to sedimentological processes in the VAMP LAKE model using data for Øvre Heimdalsvatn to predict Cs concentration in trout (top predator in this lake). A. Lake partition coefficient, K_d. B. Sedimentation rate for Cs. C. Thickness of the active sediment layer. D. Averaging function for the seasonal moderator.

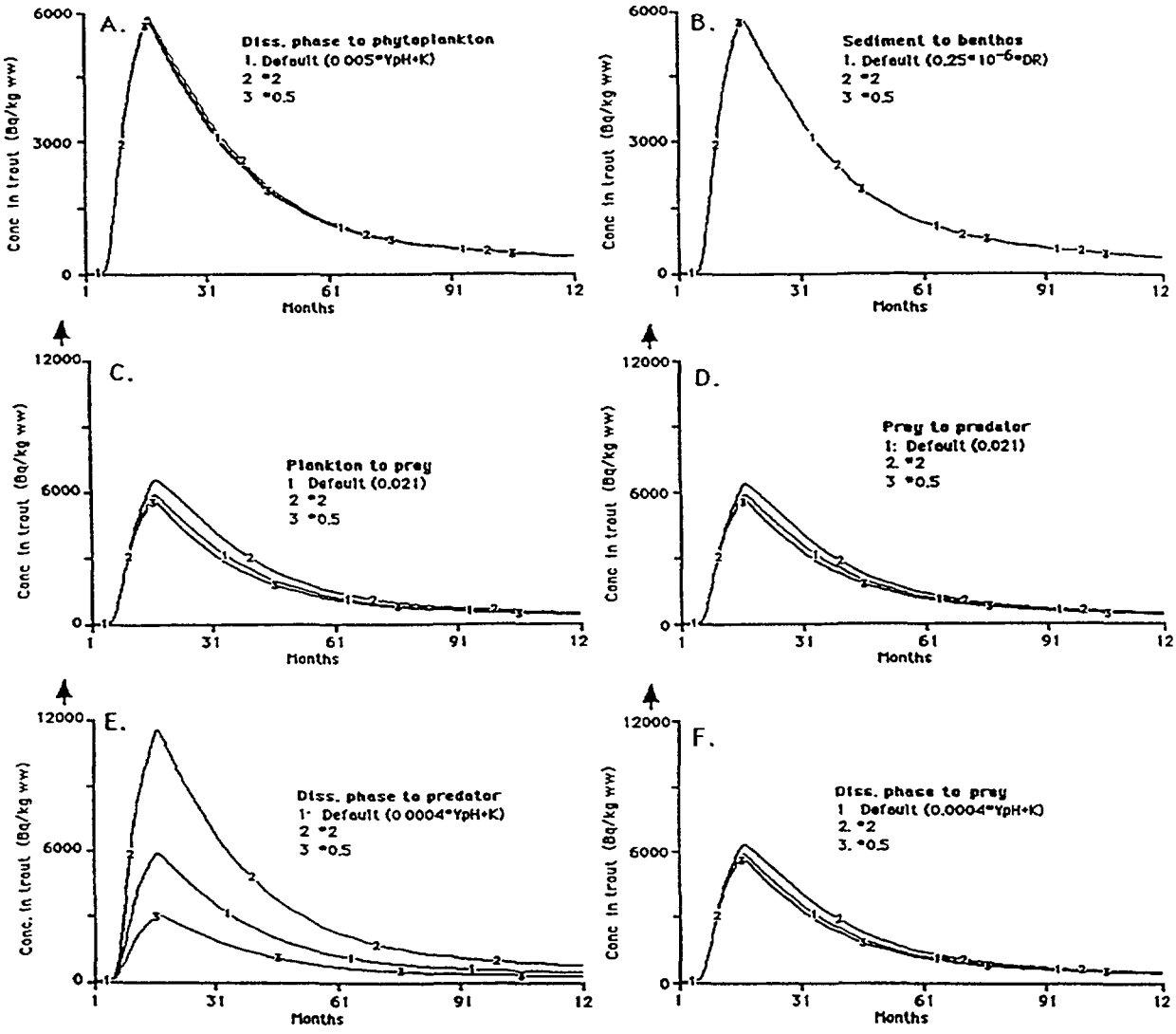

FIG. 5.86. Sensitivity analyses for important model rates regulating biouptake (= bioaccumulation) of radiocaesium in lakes in the VAMP LAKE model using data for Øvre Heimdalsvatn to predict Cs concentration in trout. A. Transport rate dissolved phase in lake water to phytoplankton. B. Transport rate sediment to benthos. C. Transport rate phytoplankton to prey. D. Transport rate prey to predator. E. Transport rate dissolved phase in lake water to predator. F. Transport rate dissolved phase in lake water to prey.

Figure 5.88 gives eight similar graphs for different values of important lake-specific variables. For lakes with a low pH, the predicted values of radiocaesium in trout are very high indeed (A). It should be stressed that pH, by definition, is a logarithmic value, and the differences in lake water acidity from pH = 5 (curve 2) to pH = 8 (curve 5) are most significant: the lower the pH, the higher the values of caesium in fish. It would not be appropriate to make a "standard" sensitivity analysis and change the default pH for Lake Øvre Heimdalsvatn from 6.8 to 2 × 6.8 = 13.4 and to 0.5 × 6.8 = 3.4. The most important lake-specific variables for these model predictions are those for lake water retention time (D) and precipitation (E). All other lake-specific variables are of less importance (like K-concentration, B), the value used for the percentage of outflow areas of the catchment (C), the primary production (F), or the rate of sedimentation of suspended matter (G). Naturally, the fallout is a very important driving variable (H) – uncertainty in fallout leads to uncertainties in all subsequent predictions.

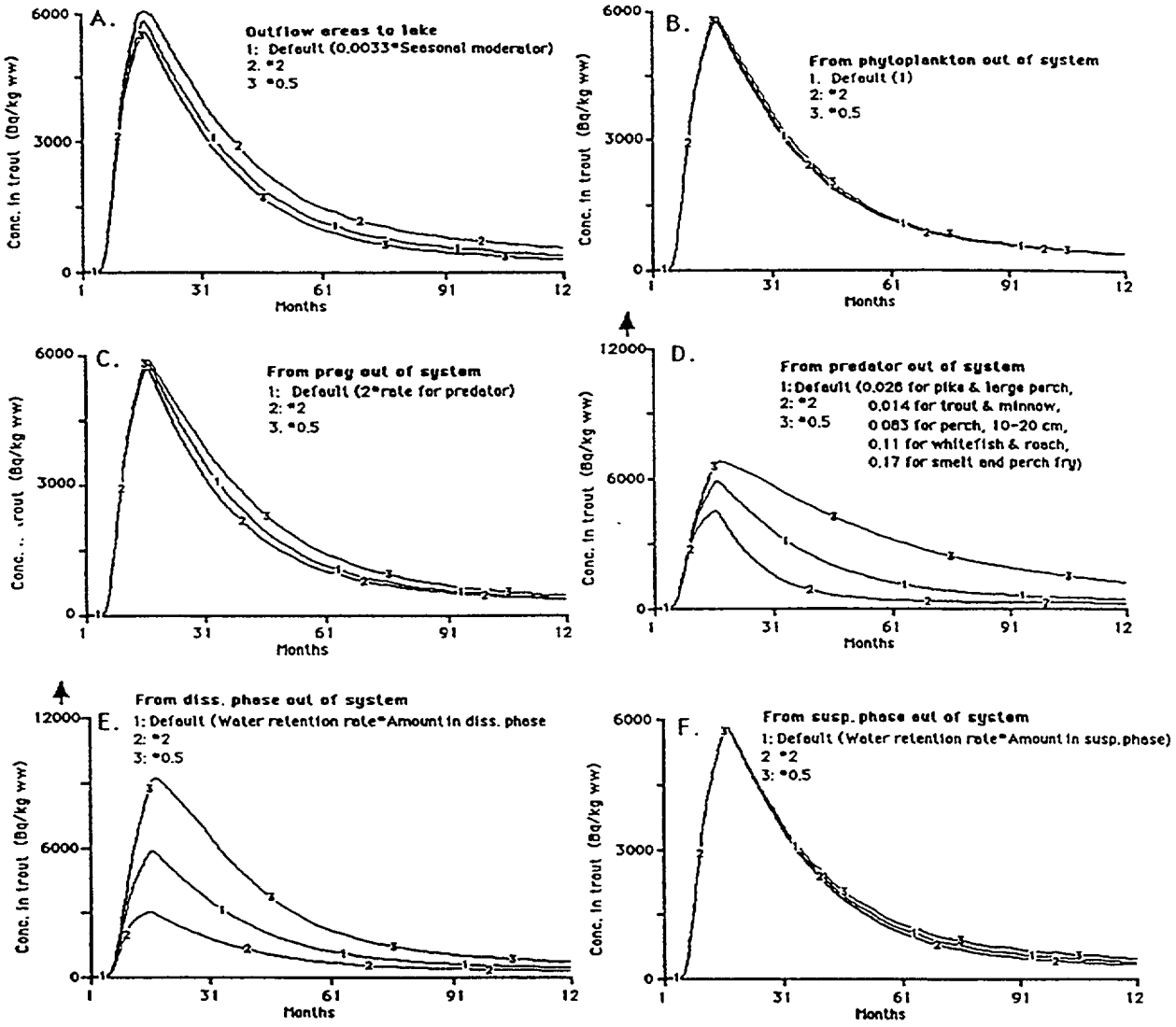

FIG. 5.87. Sensitivity analyses for important model rates regulating different outflow (or retention) processes in the VAMP LAKE model using data for Øvre Heimdalsvatn to predict Cs concentration in trout. A. Transport rate from outflow areas to lake. B. Transport rate from phytoplankton and out of the system. C. Transport rate from prey and out of the system. D. Transport rate from predator and out of the system. E. Transport rate from dissolved phase in lake water and out of the system. F. Transport rate from suspended phase in lake water and out of the system.

5.10.10. Concluding remarks

The main objective here has been to present the basic ideas behind the VAMP LAKE model, the new technical tools (like the seasonal variability moderators and the dimensionless moderators for biouptake) and to give some examples how they may be applied in lake ecosystem models for predicting radionuclide concentrates in water and biota. The construction of these moderators is very important and it depends on the objective of the model. The same comments could be given regarding these models and sub-models as for most models: they are logical constructions. Validations against independent sets of reliable and representative empirical data are essential.

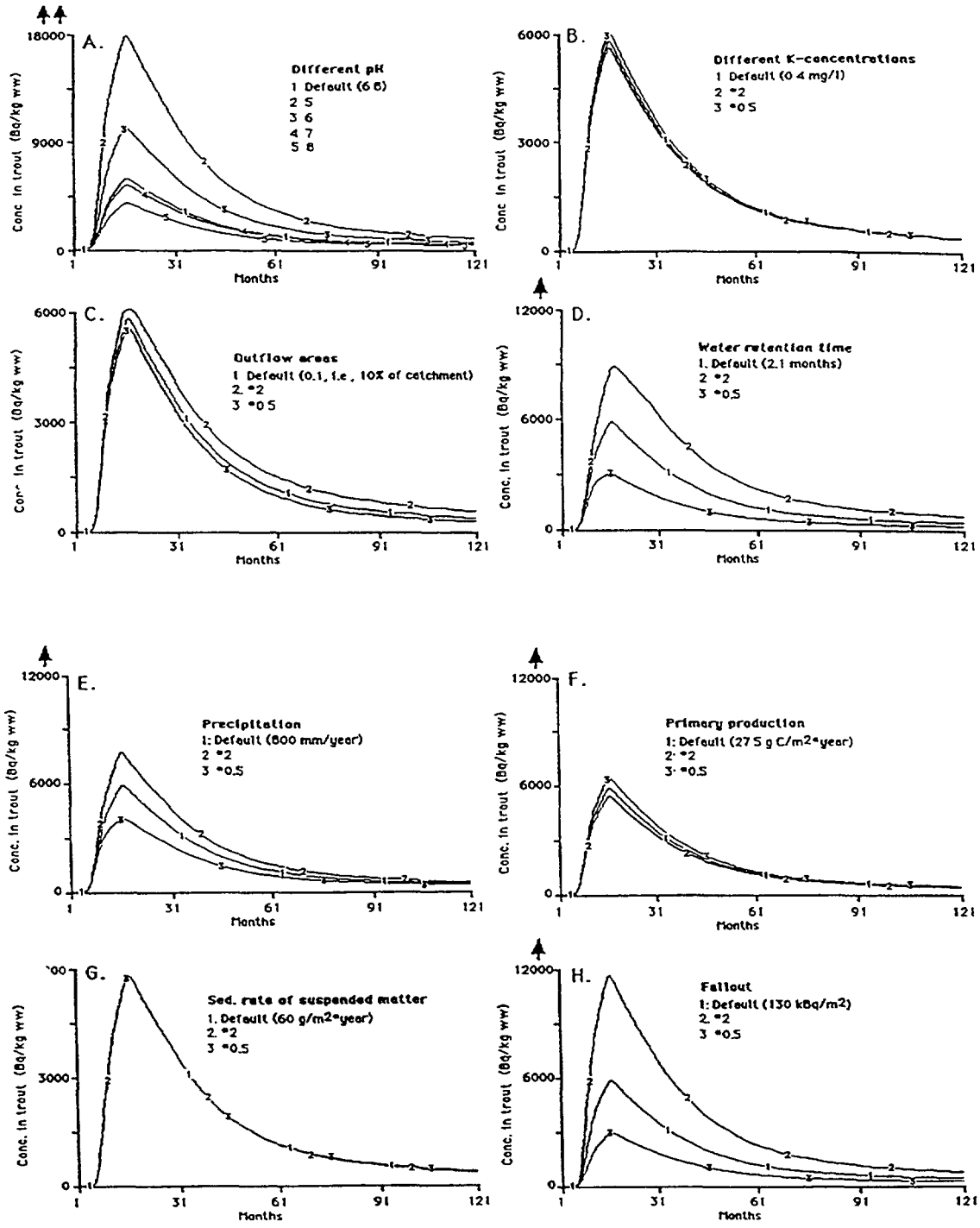

FIG. 5.88. Sensitivity analyses for important lake-specific variables in the VAMP LAKE model using data for Øvre Heimdalsvatn to predict Cs concentration in trout. A. Different lake pH. B. Different K concentrations. C. Different values of the size of the outflow areas. D. Different lake water retention times. E. Different annual precipitation. F. Different primary production. G. Sedimentation rates of suspended materials. H. Different fallout of caesium.

6. CONCLUSIONS

1. The VAMP project has put us in a much better position to predict the spread and biouptake of radiocaesium in lakes. The most important processes have been identified, as well as gaps in our understanding of these processes. A range of sensitivity and uncertainty analyses have revealed that one of the major model variables regulating predictive power is the partition coefficient, K_d, for caesium in lake waters, although biouptake rates, extraction rates and biological half-lives are also important.

2. Various methods to evaluate the reliability of the empirical data for the VAMP lakes have been tested. One interesting approach is to test one time series of empirical data against itself by transforming the data by one month prior to or after the original date. This is analogous to the standard comparison using empirical data tested against model output values. Such comparison revealed great uncertainties amongst some of the empirical data and illustrated that models can only do as well or as poorly as the empirical measurements. Thus accessibility to good empirical data is crucial for model validation and the VAMP database is one of the largest for radiocaesium in lakes.

3. The definition of predictive power (PP) enables to evaluate objectively the fit of model predictive values with empirical data. PP accounts for the fit and the model uncertainty. An important conclusion from the VAMP project is that predictive models should be small and based only on the most fundamental processes/rates and model variables, no more no less.

4. Many new tools in modelling in general have been developed during the VAMP project. These include:

   - a seasonal variability moderator;
   - a general algorithm for dimensionless moderators to account for empirical knowledge within the framework of dynamic ecosystem models;
   - a moderator for lake water retention rate;
   - a transfer coefficient which enables estimates of the relationships between prey and predatory fish biomass;
   - a K-moderator for regulating the phytoplankton biouptake rate.

   These technical tools substantially improve the predictive power of models for radiocaesium in lakes and can also be applied in many other modelling contexts.

5. In order to predict the long-term concentrations of radiocaesium in lakes it is essential to account for the processes regulating the secondary load, i.e. the transport from land to water and the remobilization from sediment to water.

6. Much effort has been devoted to sensitivity and uncertainty analyses of the models. The basic objective of these tests is to reveal the most sensitive parts and processes in the models. Many processes used with the expectation that they would improve predictive accuracy in actuality failed to do so, only adding complexity and uncertainty to the model. This was especially the case for many food web characteristics, the sediment K_d, the thickness of the active sediment layer and the sedimentation rate.

7. A new model, the VAMP LAKE model, was developed during the project. This is a small to medium-sized model, incorporating a seasonal moderator. It is based on the most fundamental processes, rates and relationships governing the spread and biouptake of radiocaesium in lakes. The model displays excellent predictive power for the VAMP lakes, but needs further testing against independent data sets.

8. The modelling of seasonal variation in water discharge, water retention rate, water temperature and stratification is very important in all lakes, but especially so for the high latitude and/or high altitude lakes. The snow and ice conditions during fallout are also of paramount importance for the turnover and retention of radiocaesium during the first year.

9. Interactions with lake sediments is important for all lakes, especially large and shallow lakes dominated by wind and wave induced suspension of bottom sediments. The priorities seem to be in the following order:

- bottom dynamics, i.e. areas of erosion, transport and accumulation;
- wind/wave action and slope induced advection;
- redox potential induced diffusion;
- microbiological degradation of particulate organic matter and sediment K_d.

10. It is of fundamental importance to account for the retention rate of radiocaesium in lake waters. There are different techniques for this: Rate = $1/T(t) = Q(t)/V$, where Q(t)= the seasonal variation in water discharge and V=lake volume. This is, however, a simplistic approach, especially in large stratified lakes. For such lakes one can use the following approach: rate = $1/T(t)^{exp}$, where the exponential is given by the equation, exp = [a(T(t)+(a-1)) +b]/(1+b), where a=30 and b=0.5 in the VAMP model.

11. The most crucial and sensitive part of any model for caesium in lakes as well as for the VAMP LAKE model, is the lake K_d. This is not a constant, and present knowledge suggests that it depends on lake pH (or related water chemistry variables), which influences both the binding of radiocaesium to carrier particles and the aggregation of carrier particles. An algorithm for this relationship is included in the VAMP LAKE model. The lower the pH, the more radiocaesium in the dissolved phase. There are also indications that the distribution of radiocaesium between dissolved and particulate phases depends on water temperature, stratification and water retention time. More research is needed in this area to develop predictive sub-models for lake K_d.

12. Criteria have been developed to assess biological half-lives for radiocaesium in fish. Biological half-lives may be calculated using models based on fish weight and water temperature. Recommendations are given for their use in lake models.

13. The empirical data has enabled the calculation of representative ecological half-lives for lake water and several fish species. These values can be used for rapid dose estimations and can also be incorporated into simple predictive models to account for a wide range of processes.

14. Major uncertainties in the most important driving parameter, the distribution of the fallout, have a direct influence on the accuracy of the model predictions. Thus, efforts should be made to measure fallout more accurately. Alternatively, it is possible to calibrate the models within a few weeks when a certain degree of mixing has occurred.

15. It is very important to apply an ecosystem perspective to modelling of radiocaesium in lakes. Assessment of the representativity of field samples is necessary on account of variation in fundamental lake properties, such as stratification, bottom dynamics and food web characteristics.

16. Lakes differ in their sensitivity to fallout depending on lake and catchment characteristics. Using data from the VAMP lakes and the VAMP LAKE model, the impact of various remedial measures has been tested. Specifically, the effects of liming, potash treatment and fertilization have been simulated. The results demonstrate that potash treatment is likely to be the most effective method to speed up recovery in lakes with low potassium concentrations.

Appendix I

LAKE DESCRIPTIONS

I.1. ØVRE HEIMDALSVATN, NORWAY

The lake Øvre Heimdalsvatn is situated at 1090 m above sea level in the Jotunheimen Mountains of central southern Norway (61°25' N, 8°54' E) (Fig. I.1). The catchment vegetation ranges from subalpine birch forest by the lake to high alpine vegetation above 1600 m. There is no permanent human habitation or activity in the 23.6 km^2 catchment, although during summer the near lake areas are used for grazing of cattle and sheep. The lake has an area of 0.78 km^2 and a mean depth of 4.7 m. The water residence time varies between 2 days at the peak of the spring spate and in excess of 400 days in winter with a mean of 60–70 days (Table I.1). The lake is covered with ice from October until the beginning of June. Lake outflows vary from 0.1 m^3/s in winter to in excess of 10 m^3/s during the spring spate. Rainfall at the lake outflow is about 800 mm/a. The lake only stratifies for short periods during the summer.

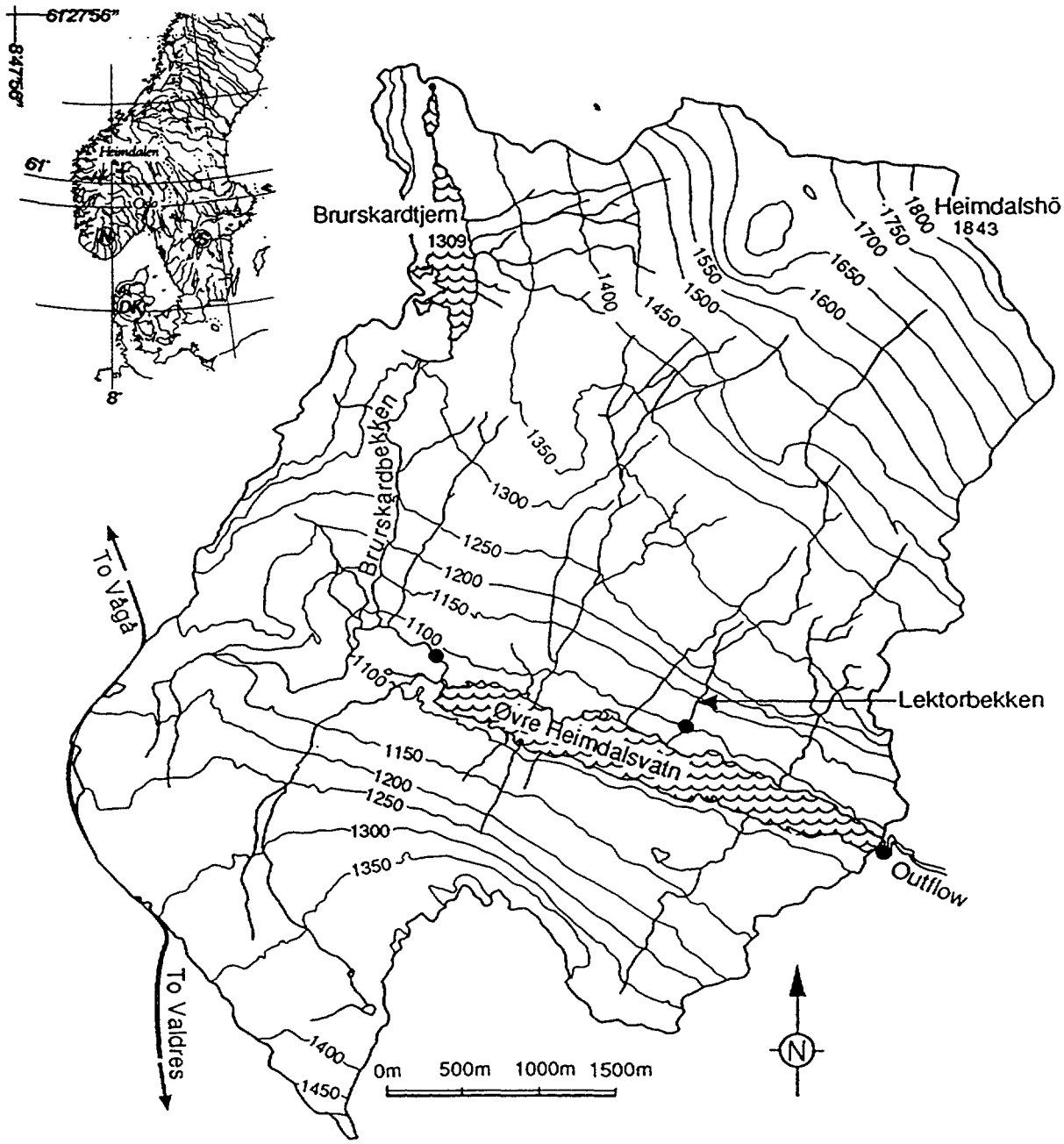

FIG. I.1. Øvre Heimdalsvatn, its location and catchment area.

Øvre Heimdalsvatn is an oligotrophic soft water lake, with a conductivity of 7–32 µS/cm and a pH of 6.2–7.2. The mean potassium concentration is 0.4 mg/L and the mean calcium concentration is 1.7 mg/L. Terrestrial plant material from the catchment is a major source of primary production for the lake ecosystem. Total primary productivity of the lake is 25–30 g $C \cdot m^{-2} \cdot y^{-1}$. Sedimentation is low (60 $g \cdot m^{-2} \cdot y^{-1}$) and the organic content of the sediments is only close to 20%. There are two fish species in the lake, brown trout (*Salmo trutta*) and minnows (*Phoxinus phoxinus*). The latter species colonized the lake in the 1970s.

Deposition on the lake and catchment varied considerably, but with a mean of about 130 kBq/m^2 of ^{137}Cs. The concentration of ^{137}Cs in lake waters was 5.5 Bq/L in June 1986 just after ice break. The concentration fell to about 250 mBq/L by the spring of 1989. ^{137}Cs concentrations in trout rose to a peak of almost 5000 Bq/kg f.w. in August 1986. By 1990 the ^{137}Cs concentration in trout had fallen to about 2000 Bq/kg.

TABLE I.1. ØVRE HEIMDALSVATN – DISCHARGE AND WATER RESIDENCE TIME

Month	Discharge[a] (lake outflow) (m^3/s)	Residence time[b] (days)
January	0.26	163
February	0.17	249
March	0.10	424
April	0.09	471
May	1.73	25
June	2.91	15
July	0.80	53
August	0.55	77
September	0.49	87
October	0.37	115
November	0.33	128
December	0.26	163
Year	0.67	63

[a] Discharge is based on daily measurements of water level in 1970–73.

[b] In the spring spate (May/June) the highest recorded daily mean discharge is 26.2 m^3/s, which gives a water residence time of 1.6 days.

I.2. DEVOKE WATER, UNITED KINGDOM

Devoke Water is typical of the Lake District of north-west England. It is set in rolling hills supporting bracken, heather and coarse pasture; there is no woodland or agricultural cultivation within the lake catchment. The pasture is grazed by sheep.

The lake has a surface area of approximately 0.4 km^2 at an altitude of 230 m. The catchment area is approximately 6 times larger than the lake and rises to an altitude of 494 m to the south. The fells (hills) in the southern area are drained by five small, but permanent, becks (streams) discharging into the lake; there is one additional permanent inlet at the eastern end. The smaller part of the catchment

to the north of the lake rises to a height of 304 m but does not contain any permanent streams; there is, however, likely to be groundwater flow into the lake from this area. The single outlet, Linbeck Gill, is at the western end of the lake and discharges into the River Esk (Fig. I.2). The precipitation is approximately 2000 mm/a and it has been estimated that the water residence time in the lake is of the order of 130 days.

The lake water is very soft (total cations approximately 9 mg/L) and very slightly acidic (average pH=6.5). There is a small amount of dissolved organic carbon and the suspended load is always very low; productivity is also low. During the winter the lake is well mixed over its full depth (12 m) and very occasionally freezes over; thermal stratification develops in May, persists throughout the summer and breaks down in October.

Aquatic macrophytes are present in the lake and it supports populations of brown trout (*Salmo trutta*) and perch (*Perca fluviatilis*) which are subject to sport fishing.

^{137}Cs deposition was estimated to be 15–20 kBq/m^2. The maximum value observed in lake waters was 1.8 Bq/L while a peak value of 2100 Bq/kg f.w. was measured in perch during 1987.

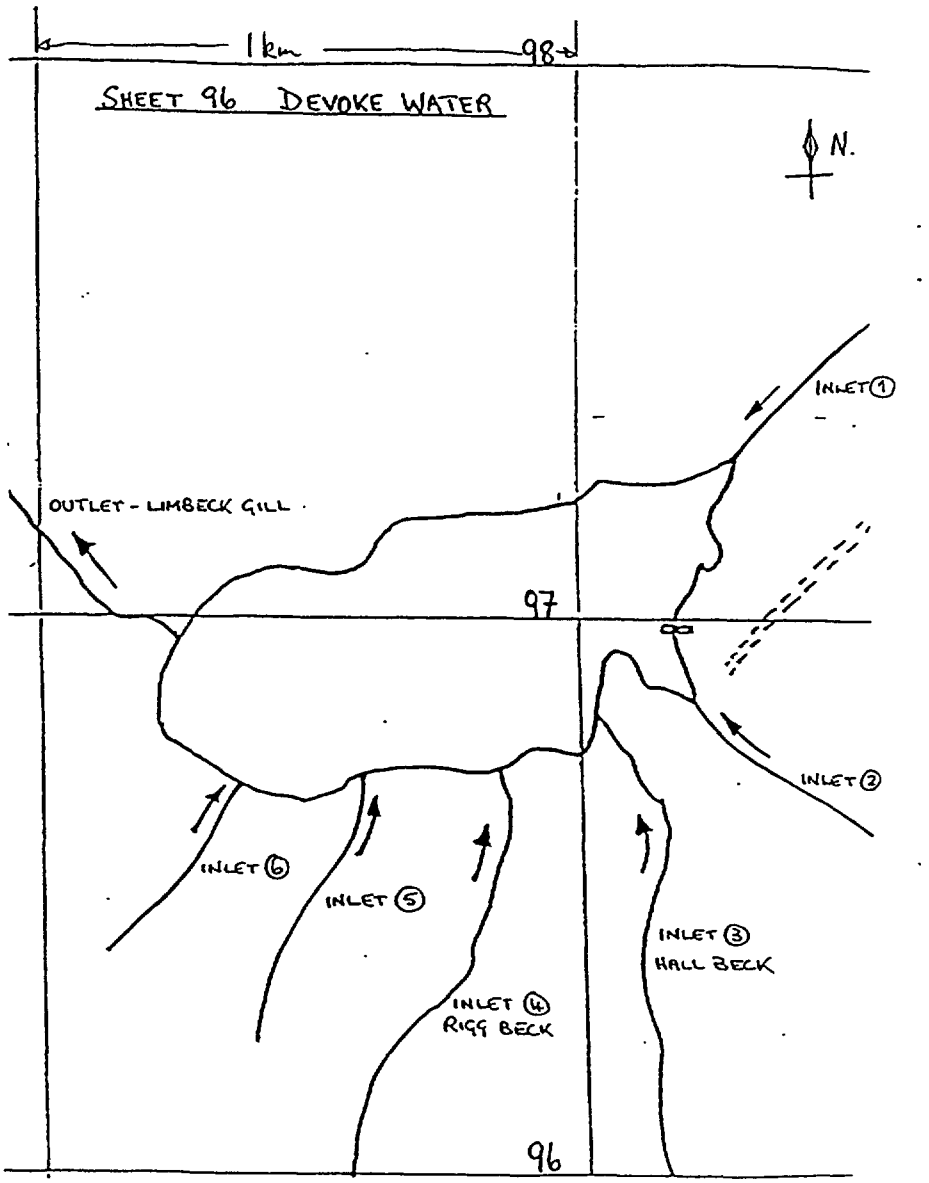

FIG. I.2. Devoke Water.

I.3. ESTHWAITE WATER, UNITED KINGDOM

Esthwaite Water is situated in the English Lake District (54°21' N, 03°00' W) at an altitude of 65 m (Fig. I.3). The lake to catchment area ratio is 1 km^2: 16 km^2 and the maximum and mean depths are 15 m and 6.4 m, respectively. The catchment comprises rolling hills (max. altitude ~300 m) with extensive soil cover (principally brown earths and gleys). It is used mainly as pasture with some forestry. The local population numbers about 100 persons/km^2 but this is greatly enhanced by tourism, especially in summer. The lake is used for sport fishing and supports small-scale fish farming.

Precipitation is close to 1750 mm/a, giving a lake water residence time of about 90 days with no great seasonal variation. The lake is stratified in summer (typically May–October) and generally remains well-mixed through the winter (i.e. warm monomictic). The source waters and, for much of the time, the lake waters have near neutral pH (mean pH = 7.1) and low ionic strength and low hardness (mean = 0.39 meq/L alkalinity). The lake is eutrophic, receiving substantial sewage discharges. These have increased substantially in recent years. The eutrophic character and shallow depth result in a seasonally anoxic hypolimnion (Fig. I.4). Its eutrophic character and lack of buffering result in high surface water pH (maximum > 9.0) in summer. The profundal sedimentation rate is about 1.2 $kg \cdot m^{-2} \cdot a^{-1}$. The sediments are organically rich (some 50%), unconsolidated muds (>90% porosity), generally anoxic but with an 'oxidized' surface layer in winter. The main clay minerals are chlorite and illite.

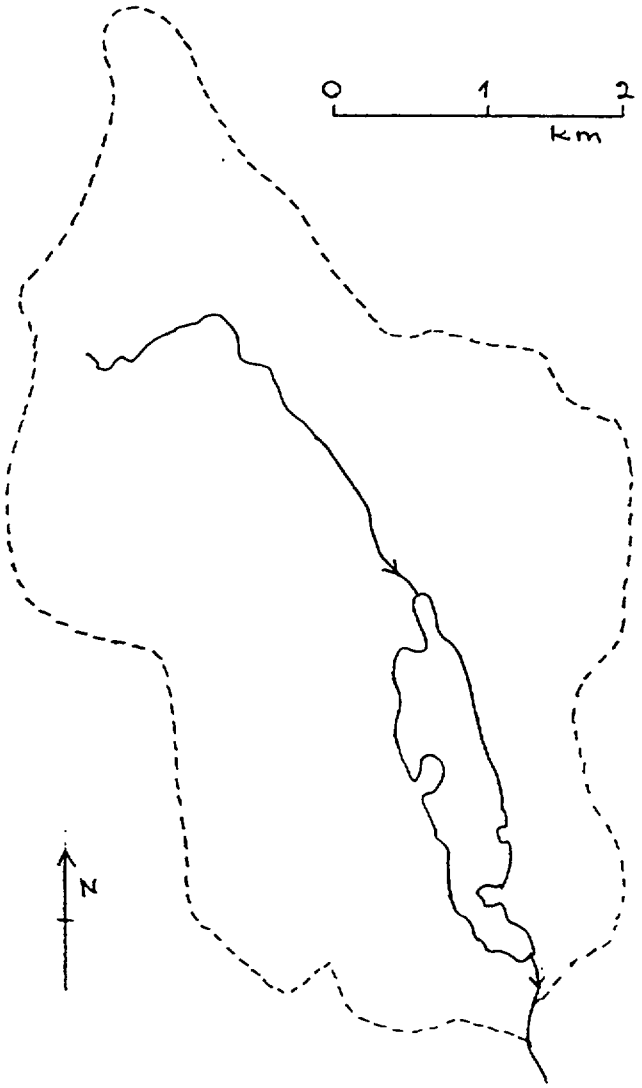

FIG. I.3. Esthwaite Water and its drainage area.

^{137}Cs deposition has been estimated to be 2.0 kBq/m^2. The maximum observed concentration of ^{137}Cs in lake waters was about 0.3 Bq/L. No data on fish populations are available.

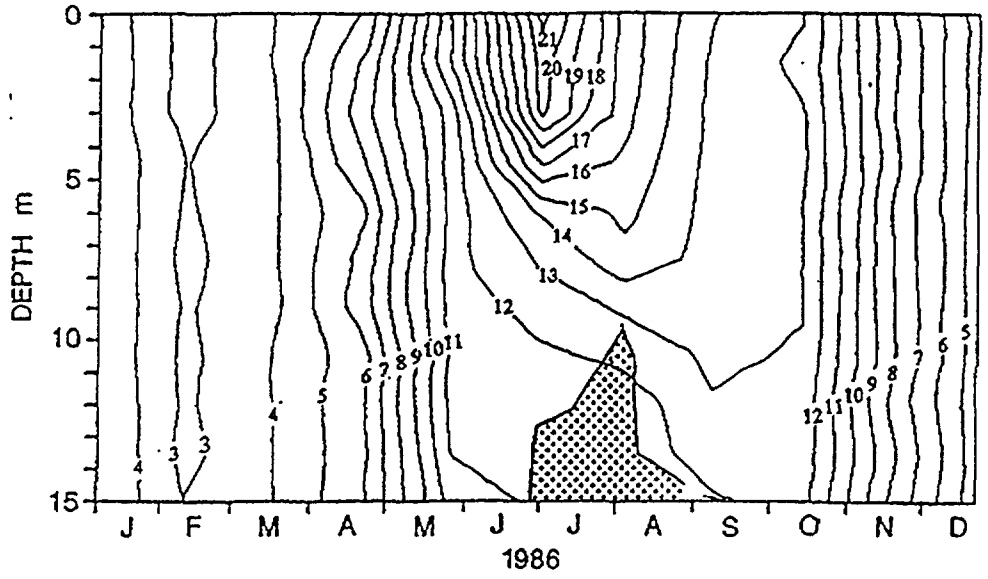

FIG. I.4. Temperature (°C) isopleths for Esthwaite water (stippled area = anoxic waters).

I.4. IJSSELMEER, THE NETHERLANDS

The lake IJsselmeer was developed after closing the former Zuider Sea by a dam in 1931. Due to further land reclamation works it is now divided into three main parts, i.e. the IJsselmeer (1140 km^2) in open connection with the Ketelmeer (60 km^2) and, separated from the IJsselmeer by a dyke, the Markermeer (650 km^2)

The lake is located in the northern part of the Netherlands at sea level and is bordered by agricultural land, pasture and several small towns. In the north it is divided by a dam from the Wadden Sea; to the south-west it is separated by a dam from the Markermeer (Fig I.5). The lake water is used for irrigation and as a source of drinking water.

The lake is very shallow, with a mean depth of some 4 m. Owing to its size, shallowness and location near the coast it is exposed to wind, leading to considerable resuspension of sediments. Its shallowness also means that the lake does not stratify. It is fed via the Ketelmeer, by the river IJssel, a branch of the river Rhine. Its catchment area can be considered to be the drainage area of the whole Rhine, an extremely large and heterogeneous area. This renders assessment of catchment fallout and lake nuclide inflows complicated. The yearly average discharge from the river Rhine is 2200 m^3/s, of which 300 m^3/s is discharged by the river IJssel into the lake. Rainfall in the area is approximately 750 mm/a. Owing to its large surface area direct deposition accounts for about 10% of water inputs to IJsselmeer. Apart from around 10% of the inflow which is sluiced to the Markermeer, the lake waters are sluiced to the Wadden Sea on the opposite side of the lake from the inflow. The water residence time is about 150 days. It is only occasionally covered with ice.

The lake is eutrophic and oligohumic and the waters have a fairly high ionic strength. The average concentration of potassium ions is 0.18 meq/L and that of calcium ions 60 mg/L. Its minimum conductivity is 70 mS/m. The average sedimentation rate is 500 g·m^{-2}·a^{-1}. However, sedimentation is not uniform due to the presence of pre-impoundment channels. Most sedimentation takes place in these channels which cover 10–15% of the lake bottom. These sediments are largely inorganic, composed mainly of clay minerals such as illite. The remaining bottom areas are predominantly covered by sand.

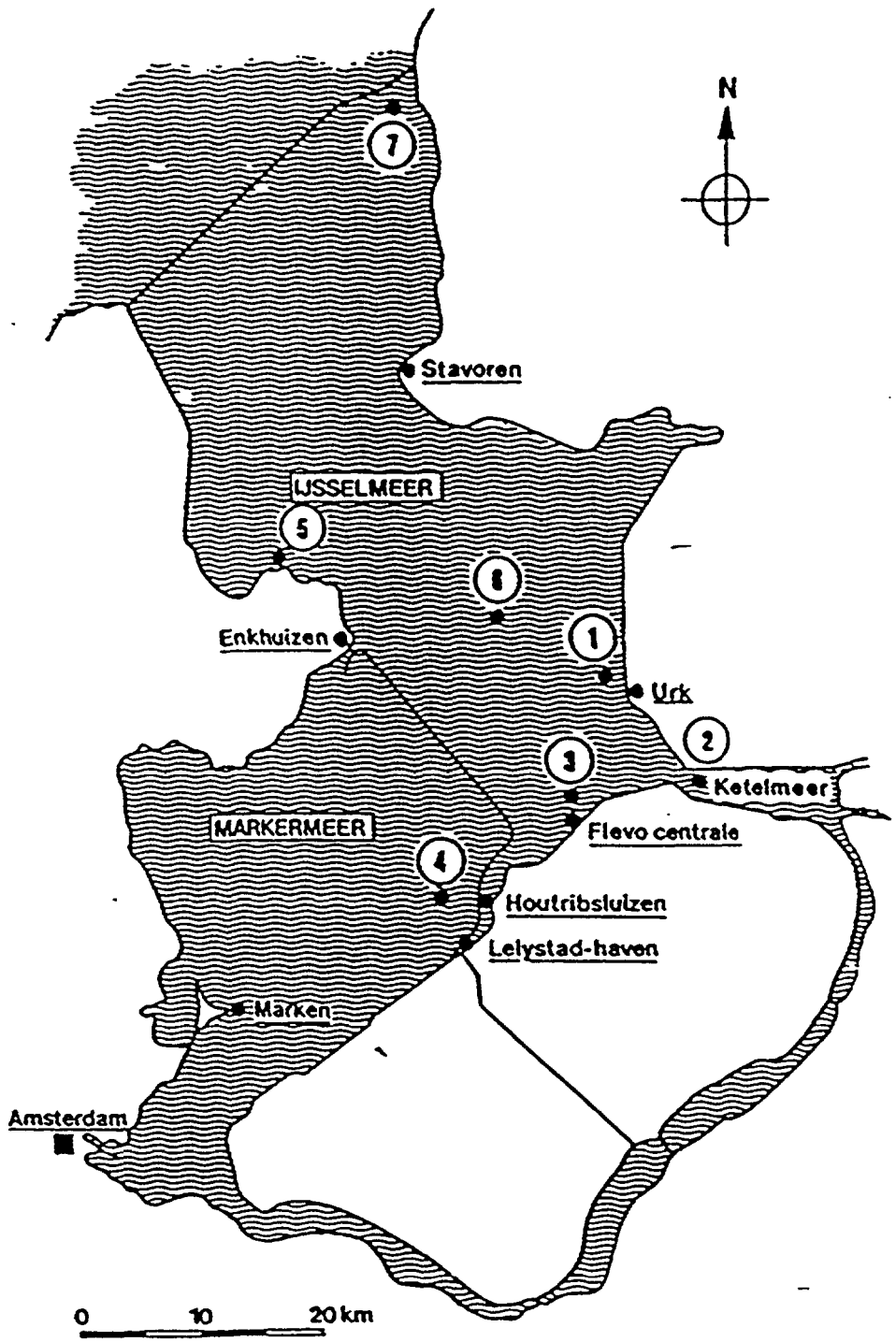

FIG. I.5. IJsselmeer with dam sluices into the Wadden Sea and Markermeer.

The lake has a dense fish population, and the dominant species are smelt (*Osmerus eperlanus*), roach (*Rutilus rutilus*), bream (*Abramis brama*), perch (*Perca fluviatilis*), pike (*Esox lucius*), perch-pike (*Stizostedion lucioperca*), ruffe (*Gymnocephalus cernua*) and eel (*Anguilla anguilla*). *Dreissena*, a freshwater mussel, and *Chironomus* are the major benthic taxa. Both these and zooplankton are the main food items for roach, ruffe and bream. Smelt and young perch feed mainly on zooplankton, while pike-perch and older perch are piscivores. There is an extensive commercial fishing centred on eels, roach and perch.

The direct deposition of ^{137}Cs on the lake, caused by passing of the plume in the early days of May 1986, was estimated to be between 1.5 and 3 kBq/m^2. This gives a total deposition of 1.7–3.4 × 10^{12} Bq ^{137}Cs.

The inflow from the river IJssel varied between 550 Bq/m^3 in May 1986 and 45 Bq/m^3 at the end of that year. At the end of 1987 the inflow decreased to the level of 15 Bq/m^3. Total inflow in 1986 and 1987 was estimated to be 8 × 10^{11} Bq and 2.5 × 10^{11}, respectively. Peak contaminations of ^{137}Cs in perch reached values of 280 Bq/kg dry weight in the summer of 1987, compared to the peak of 65 Bq/kg in roach in spring 1987 (Table I.2).

I.5. ISO VALKJÄRVI, FINLAND

Lake Iso Valkjärvi is a small lake located in the municipality of Lammi in the province of Häme, Finland (61°11' N, 25°07' E, altitude 126.3 m). The catchment area of the lake is 17 × 10^4 m^2. Some 75% of the catchment area is forest and close to 25% bogs. The soil types are morainic (75%) and peat (25%).

The area of the lake is 0.042 km^2. Its maximum depth is 8 m and mean depth 3 m (Fig. I.6). The trophic status of the lake is oligotrophic and the humic status is mesohumic. It is rather acidic, with a pH of 5.1 and an alkalinity of 0.01 meq/L. The average annual concentration of potassium is about 0.4 mg/L and that of calcium 1.0 mg/L. The conductivity is about 1.7 mS/m (25°C). The primary productivity is estimated to be about 10 g $C \cdot m^{-2} \cdot a^{-1}$.

The mean annual precipitation in the catchment area of the lake is about 600 mm/a. The lake has no major inlets. Taking into account evaporation and the ratio of the catchment area to that of the lake, the water residence time of the lake is estimated to be about 3 years. In normal winters Iso Valkjärvi is ice-covered from November to the end of April (50% of the year). It is a dimictic lake and during the summer stratification the temperature of the epilimnion (0–2 m) is 15–20°C, and that of the hypolimnion (3–8 m) 5–6°C. In winter the temperature of the epilimnion is 1–2°C and that of the hypolimnion 4°C. On account of the lack of major inlets the sedimentation rate is low.

The fish species in the lake are perch (*Perca fluviatilis*), pike (*Esox lucius*) and whitefish (*Coregonus lavaretus*). ^{137}Cs deposition has been estimated to be 70 kBq/m^2. The initial lake water concentration of ^{137}Cs has not been measured, but a value of 4.6 Bq/L was measured for concentration of ^{137}Cs in lake waters in June 1987. This subsequently declined slowly to 1.7 Bq/L in October 1990. A similar slow decline in ^{137}Cs between 1987 and 1990 has been observed for perch and pike, while there has been a more rapid fall in ^{137}Cs concentrations in whitefish during the same period. Peak values of 27 000 Bq/kg f.w. ^{137}Cs were detected in summer 1987 in pike.

I.6. HILLESJÖN, SWEDEN

The lake Hillesjön is situated north of the town of Gävle near the eastern coast of central Sweden (60°45' 02" N, 17°14' 07" E). Over 80% of the catchment (19 km^2) is covered by forest (Fig. I.7).

The lake has a surface area of 1.6 km^2. It is shallow with a mean depth of 1.7 m and a maximum depth of 3.1 m. Sediment resuspension is important in Hillesjön because of its shallow depth combined with its coastal location. In summer large areas of the lake become covered in macrophytes, mainly water lilies, bulrushes and horsetails.

Hillesjön is mesotrophic, with a pH of 7–7.5 and a conductivity of 50–150 mS/m. The mean potassium concentration is 3.0 mg/L. Primary production is approximately 100 $g \cdot Cm^{-2} \cdot a^{-1}$. The lake sediments have an organic content of close to 35%.

The mean water residence time is about 140 days, although there is considerable seasonal and annual variation. The lake is ice-covered between December and April/May (Table I.3).

TABLE I.2. AVERAGE WATER DISCHARGE IN THE RIVER RHINE AT LOBITH, AVERAGE SUSPENDED LOAD, AVERAGE ^{137}Cs ACTIVITY IN SUSPENDED LOAD, AVERAGE TOTAL ^{137}Cs ACTIVITY, AVERAGE MONTHLY ^{137}Cs DISCHARGE IN THE RIVER RHINE AND THE RIVER IJSSEL DURING THE PERIOD MAY 1986 – DECEMBER 1987

Month	Water discharge, Lobith (m^3/s)	Suspended load, Lobith (g/m^3)	^{137}Cs activity suspended load (Bq/kg dw)	Total ^{137}Cs activity water[c] (Bq/m^3)	Average ^{137}Cs discharge (Bq/s)	Monthly discharge ^{137}Cs, River Rhine (Bq)	Monthly discharge ^{137}Cs, River IJssel[d] (Bq)
1986							
May (5–19)	3200	45	4836	548.8	1.76×10^6	2.3×10^{12} (15 days)	3.1×10^{11} (15 days)
May (20–31)	3200	45	2110	239.5	7.66×10^5	7.9×10^{11} (12 days)	1.1×10^{11} (12 days)
June (1–15)	3450	50	1360	161.2	5.56×10^5	7.2×10^{11} (15 days)	9.8×10^{10} (15 days)
June (16–30)	3450	50	578	68.5	2.36×10^5	4.8×10^{11} (15 days)	4.2×10^{10} (15 days)
July	2100	45	750	85.1	1.79×10^5	4.8×10^{11}	6.5×10^{10}
August	1600	40	492	53.4	8.54×10^4	2.3×10^{11}	3.1×10^{10}
September	1700	35	636	65.8	1.12×10^5	2.9×10^{11}	4.0×10^{10}
October	1650	45	357	40.5	6.69×10^4	1.8×10^{11}	2.4×10^{10}
November	2000	50	493	58.4	1.17×10^5	3.0×10^{11}	4.1×10^{10}
December	2050	25	470	43.9	9.01×10^4	2.4×10^{11}	3.3×10^{10}
1987							
January	3450	50	341	40.4	1.39×10^5	3.7×10^{11}	5.1×10^{10}
February	1900	35	286	29.6	5.62×10^4	1.4×10^{11}	1.9×10^{10}
March	3750	50	204	24.2	9.06×10^4	2.4×10^{11}	3.3×10^{10}
April	3250	40	188	20.4	6.62×10^4	1.7×10^{11}	2.3×10^{10}
May	2750	30	219	21.6	5.93×10^4	1.6×10^{11}	2.2×10^{10}
June	2600	45	261	29.6	7.70×10^4	2.0×10^{11}	2.7×10^{10}

TABLE I.2. (cont.)

Month	Water discharge, Lobith (m^3/s)	Suspended load, Lobith (g/m^3)	^{137}Cs activity suspended load (Bq/kg dw)	Total ^{137}Cs activity water[c] (Bq/m^3)	Average ^{137}Cs discharge (Bq/s)	Monthly discharge ^{137}Cs, River Rhine (Bq)	Monthly discharge ^{137}Cs, River IJssel[d] (Bq)
July	3600	40	27 [a]	2.9[a]	1.05×10^4 [a]	2.8×10^{10} [a]	3.9×10^9 [a]
August	2800	40	– [b]	– [b]	– [b]	– [b]	– [b]
September	2000	40	233	25.3	5.06×10^4	1.3×10^{11}	1.8×10^{10}
October	2100	35	187	19.4	4.06×10^4	1.1×10^{11}	1.5×10^{10}
November	2150	35	156	16.1	3.47×10^4	9.0×10^{10}	1.2×10^{10}
December	2500	50	136	16.1	4.03×10^4	1.1×10^{11}	1.5×10^{10}
					Total	7.6×10^{12}	1.0×10^{12}

[a] Uncertain.

[b] No data available.

[c] Calculated with distribution coefficient $K_d = 14.6$ m^3/kg [I.1].
Formula used: Total activity – Suspended load – Activity suspended particles + Activity suspended particles/Distribution coefficient

[d] Assuming yearly average discharge in River Rhine to be 2200 m^3/s and that of River IJssel 300 m^3/s, then the discharge ratio River IJssel/River Rhine would be 1/7.33.

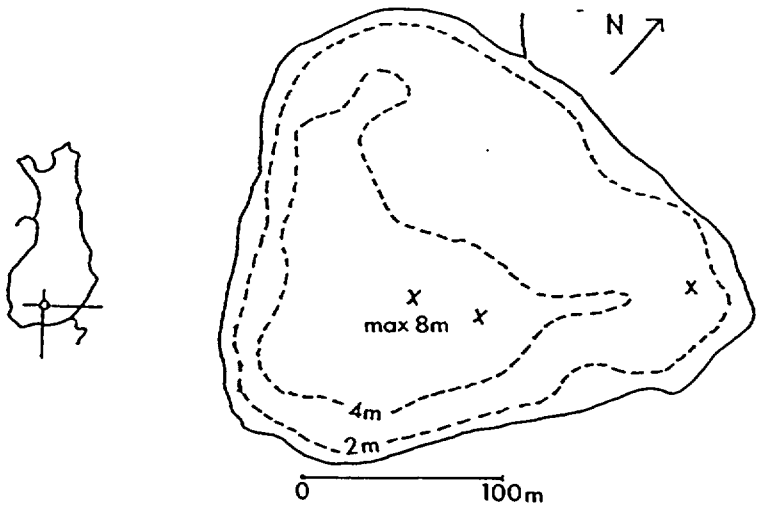

FIG. I.6. Outline map of Iso Valkjärvi and its location in Finland.

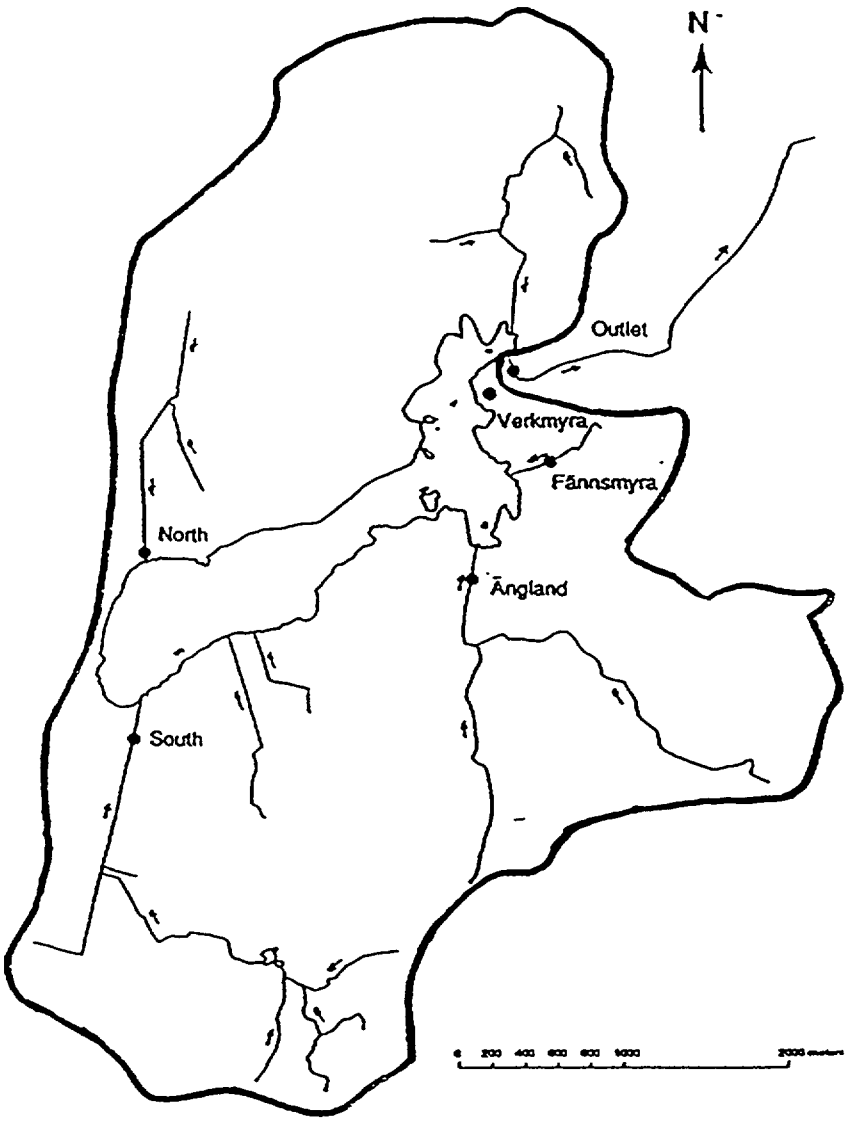

FIG. I.7. Hillesjön and its catchment.

The three fish species in the lake, in order of abundance, are roach (*Rutilus rutilus*), perch (*Perca fluviatilis*) and pike (*Esox lucius*).

Deposition of ^{137}Cs from Chernobyl was estimated to be 100 kBq/m. The initial peak concentration of ^{137}Cs in lake waters was approximately 6.5 Bq/L. This declined to about 1 Bq/L by 1990 although winter values were generally lower. All three fish species showed a rapid rise in ^{137}Cs concentrations during 1986. However, while concentrations in roach and small perch declined slowly in 1987 and 1988, concentrations in pike and large perch remained high and peaked in 1988. Pike had the highest ^{137}Cs concentration, peaking at about 8000 Bq/kg f.w.

TABLE I.3. MONTHLY DISCHARGE FROM HILLESJÖN

Month	Discharge (m^3)	
	1986	1987
January	2.50×10^5	4.70×10^5
February	1.80×10^5	2.50×10^5
March	1.90×10^5	2.00×10^5
April	4.95×10^5	1.15×10^6
May	3.00×10^6	1.47×10^6
June	3.55×10^5	3.90×10^5
July	8.80×10^4	3.10×10^5
August	7.80×10^5	2.40×10^5
September	1.25×10^6	3.60×10^5
October	4.20×10^5	3.20×10^5
November	5.40×10^5	2.50×10^5
December	6.10×10^5	2.70×10^5
Ice break-up	10 May 1986	29 April 1987
Ice freeze-up	1 December 1986	15 December 1987

I.7. BRACCIANO, ITALY

The volcanic lake, Bracciano, is located in north Latium (central Italy), a few kilometres from the Tyrrhenian Sea in an area with a typical Mediterranean climate (mean annual temperature in the range of 15°C and mean annual precipitation 900 mm).

The lake is located at 164 m above sea level. The 'volume development' of the lake is 1.61; it has a circular form and steep sides, with a mean lake depth of 89 m (Fig. I.8).

The inflow of surface water to the lake from the catchment area, which is mainly covered by woods and grasslands, is negligible. The ratio of catchment areas to surface of lake water is 1.6. The discharge from the lake, due to the presence of a small outflow, is approximately 1.17 m^3/s, giving a water residence time of 137 years.

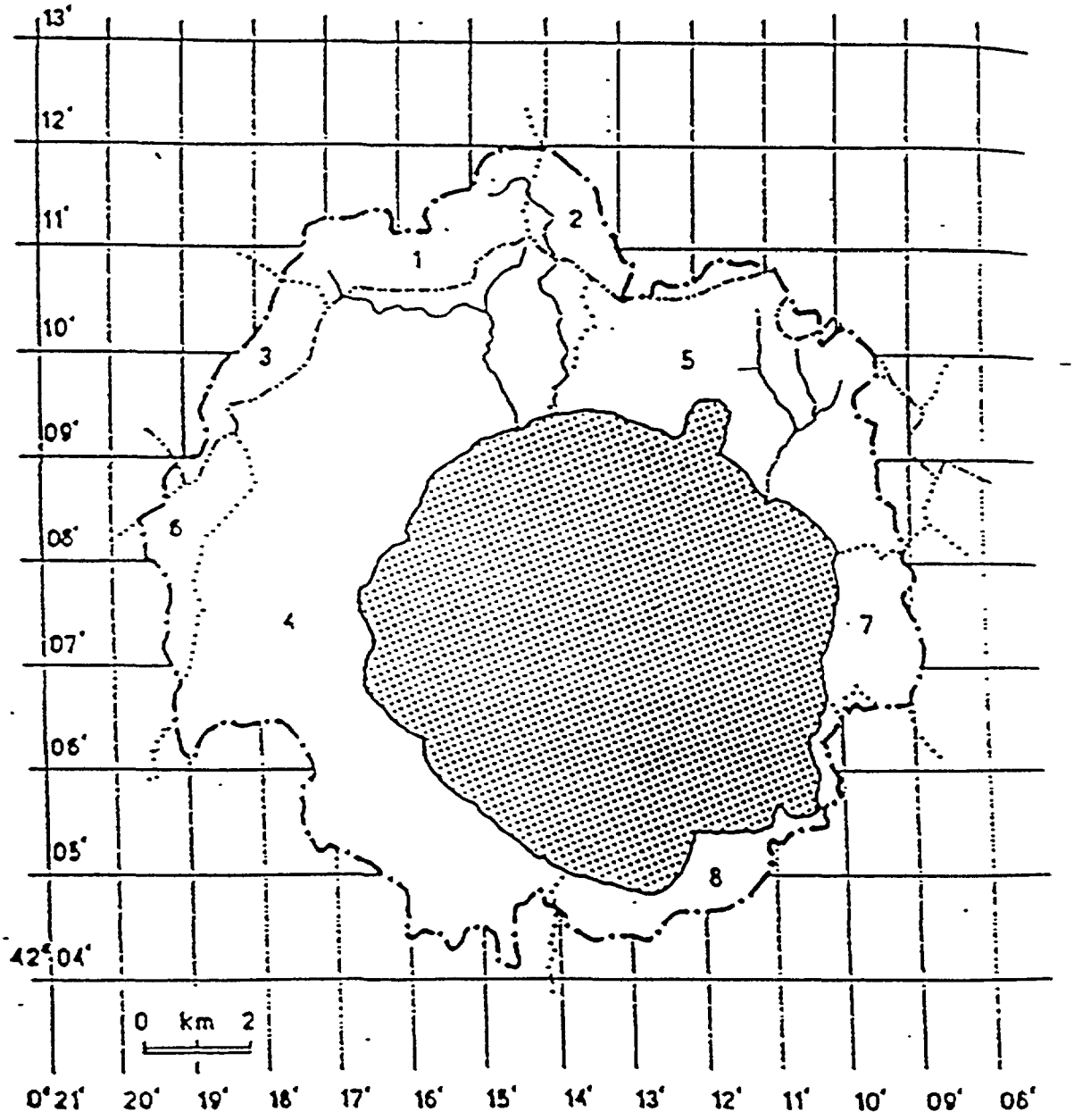

FIG. I.8. Lake Bracciano with its drainage area.

Suspended matter in the lake waters is negligible. Potassium and calcium concentrations are high, 40 g/m^3 and 17 g/m^3, respectively. The lake sediments in the epilimnion are predominantly composed of sand.

The lake waters show a stratified thermal structure during the period May–November. The lake is periodically stocked with whitefish (*Coregonus* hybrids). These fish are usually caught commercially when they reach an average length of 25–30 cm. The whitefish are strictly planktonic and during stratification they prefer the cooler waters of the hypolimnion.

It is important to note that the amount of ^{137}Cs arising from nuclear weapons testing is not negligible in lake waters and the catchment. The deposition of Chernobyl ^{137}Cs (900 Bq/m^2) took place during the first two weeks of May. Deposition values were obtained by measuring ^{134}Cs contents in

undisturbed catchment soils (0–30 cm horizon) and using a figure of 0.5 for the ratio of Chernobyl $^{134}Cs/^{137}Cs$. The initial concentration of ^{137}Cs in epilimnetic water was approximately 90 Bq/m^3. After the winter mixing a steady state value of about 20 Bq/m^3 was reached.

Concentrations in whitefish reached maximum values of 14 Bq/kg fresh weight during the summer of 1986. Afterwards fish contamination decreased to a more or less constant concentration of some 6 Bq/kg.

Appendix II

MODEL DESCRIPTIONS

II.1. DESCRIPTION OF THE ENEA MODEL

II.1.1. Model description

The MARTE model (Model for Assessing the migration of Radionuclide Transport in the aquatic Environment) was developed to assess the levels of radionuclide contamination in non biotic components of lacustrine systems and the migration of radioactive substances in catchment basins. In the present exercise the model was used as a generic tool to evaluate the contamination of waters and sediments of some European lakes (Hillesjön, Øvre Heimdalsvatn, Devoke Water, IJsselmeer, Iso Valkjärvi, Bracciano, Esthwaite Water).

The model consists of the following compartments: water, suspended matter, "interface" layer of bottom sediments, "bottom sediments" and "deep sediments".

The following processes were included in the model:

(a) direct deposition of the radionuclide onto water surface;
(b) radioactive decay;
(c) outflow of the radionuclide in dissolved form;
(d) outflow of the radionuclide attached to suspended matter;
(e) sedimentation;
(f) migration of radionuclide from sediment "active layer" to bottom sediment;
(g) migration of radionuclide from bottom sediment to "active layer";
(h) migration of radionuclide from bottom sediment to deep sediment;
(i) migration of the radionuclide from the catchment basin to the lake.

The uncertainty of the model output was evaluated by an "*a posteriori*" analysis of the comparison between the model outputs and the experimental values. The method was based on the evaluation of the so called "functional distance" defined as follows:

$$d^2 = \sum_{1}^{n}{}_i (ln\ E_i - ln\ M_i)^2 / n \qquad \text{(II.1)}$$

In formula (II.1) E_i and M_i are respectively the i^{th} experimental value and the corresponding i^{th} model prediction; n is the total number of experimental values. The evaluation of the parameters of the statistical distribution of d, obtained comparing the model outputs with experimental data collected for a number of lakes, allows estimation of the confidence limit of the uncertainty of the model. The above analysis shows that the model uncertainty is approximately a factor of 1.9 at 68% confidence level.

Two groups of parameters were used in the model:

group (a) "site specific" parameters: parameters for which site specific data are available: lake volume, lake mean depth, discharge water flux, water outflow, ^{137}Cs deposition, amount of suspended matter, sedimentation rate;
group (b) "generic value" parameters: parameters for which a generic value was used due to the lack of site specific data.

Among the second category of data, the transfer rate of radionuclide from the sediment "interface layer" to the bottom sediment (K_{alb}), the transfer rate of radionuclide from the bottom sediment to the "interface layer" (K_{bal}), the transfer rate from bottom to deep sediment (K_{sd}) and the parameters used to calculate the contribution from the drainage area, are the most important. These parameters affect the time behaviour of radionuclides in lacustrine systems.

In the present work the model was tested to appraise its validity as a generic tool for predicting the migration of ^{137}Cs in lacustrine systems when site specific values of the parameters are not available. As the MARTE model was not developed to predict the radionuclide concentrations in fishes, the present version was updated by including a simple generic submodel for the assessment of fish contamination. The intended purpose of the submodel is the approximate evaluation of ^{137}Cs concentration in fish flesh. The accuracy of the model may be very high if site specific values of the water/fish accumulation factors are available (for instance in the case of lake Bracciano the model results predict experimental values within 10% over a period of several years). Unfortunately in the case of non-site specific evaluations of the accumulation factors, the submodel, connected with MARTE model, shows a lower accuracy. However, the present exercise showed that the ratios between the experimental and the predicted values were never larger then a factor of 4. The detailed description of the MARTE model was published by Monte in 1993) [II.1]. The description of the fish submodel [II.2] and the evaluations of the accumulation factors for some species of fishes living in lake Bracciano were given in references [II.2] and [II.3].

II.1.2. Description of procedures, equations and parameters used in the model

The model structure is illustrated in Figure II.1. A list of symbols used in the present description is given in Table II.1. The process of radionuclide absorption by suspended matter was modelled according to the "k_d concept" (k_d = partition coefficient, "suspended matter/water") based on the hypothesis of a reversible and rapid equilibrium between the dissolved and the adsorbed phases of the radionuclide:

$$C_s/C_w = k_d \tag{II.2}$$

The contribution from the drainage area (I_{tot}) due to a single impulsive deposition pulse D_{imp} was calculated by means of the following formula:

$$I_{tot} = \epsilon\, D_{imp}\Phi(t)(A_1 e^{-\lambda_1 t} + A_2 e^{-\lambda_2 t}) \tag{II.3}$$

where ε is an empirical coefficient describing the ratio of initial water concentration to the deposition (D_{imp}), $\phi(t)$ is the water inflow, and the two terms in parentheses of equation (II.3) represent a fast and a slow component of radionuclide transport due to the vegetation washout and to the runoff. The radionuclide concentration in water (C_w) was calculated as follows:

$$\begin{aligned} dC_w/dt = {} & I_{tot}/(V\,R) + D(t)/(R\,\underline{h}) - C_w\phi_o(t)/(V\,R) \\ & -k_d C_w W_{ssd}\phi_o(t)/(V\,R) - K_{alb}k_d C_w D_{al}\delta_{al}/(\underline{h}\,R) - \lambda_r C_w \\ & -k_d C_w R_s/(\underline{h}\,R) + K_{bal}D_{bs}\delta_b C_b/(\underline{h}\,R) \end{aligned} \tag{II.4}$$

The retardation coefficient, R, is defined as:

$$R = 1 + k_d(P_{ss} + P_{sa})/V \tag{II.5}$$

The terms of equation (II.4) represent:

- the rate of change of the radionuclide concentration in water (left term);
- the input to the lake of the radionuclide from the catchment basin;
- the direct deposition of the radionuclide onto the water surface (D(t)= rate of deposition of radionuclide on lake water);
- the outflow of the radionuclide in dissolved form;
- the outflow of the radionuclide attached to the suspended particles;
- the migration of the radionuclide from the sediment "interface layer" to the bottom sediment;

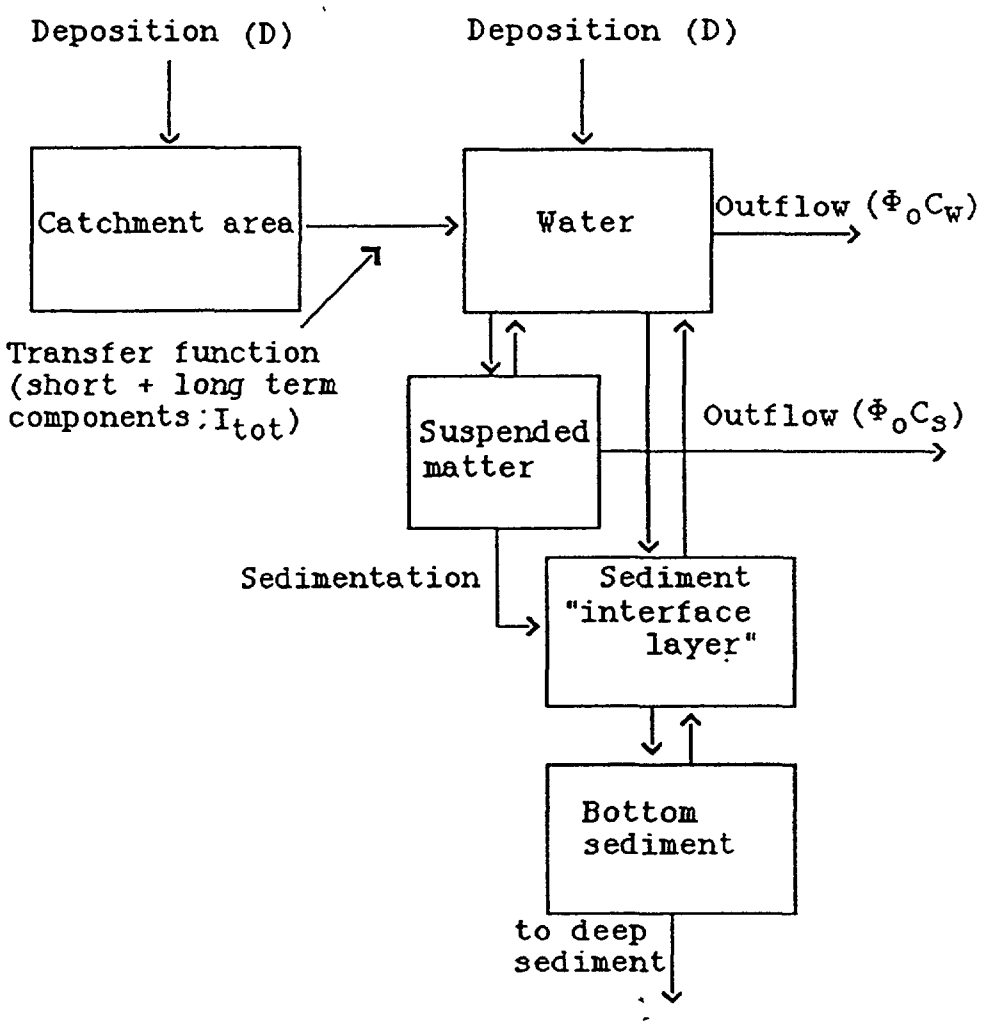

FIG. II.1. Model structure – flow chart of the transfer processes.

- the radioactive decay;
- the removal of the radionuclide by sedimentation;
- the migration of the radionuclide from the bottom sediment to the "interface layer".

The total concentration of radionuclide in water (C_t) was calculated as follows:

$$C_t = C_w + W_{ssd}C_s = C_w(1+W_{ssd}k_d) \tag{II.6}$$

The time variation of the concentration of radionuclide in bottom sediment (C_b) was calculated by means of the following differential equation:

$$\begin{aligned} dCb/dt = &-[\lambda_r + K_{sd} + K_{bal} + R_s/(\delta_b D_{bs})]C_b \\ &+ [R_s k_d/(D_{bs}\delta_b) + k_d K_{alb} D_{al}\delta_{al}/(D_{bs}\delta_b)]C_w \end{aligned} \tag{II.7}$$

The terms on the right hand side of equation (II.7) represent respectively:

- the radioactive decay;
- the migration of the radionuclide to deep sediment;
- the migration of the radionuclide from the "bottom sediment" to the "interface layer";
- the sedimentation;

- the radionuclide migration to the deep sediment as result of the upward movement, due to the sedimentation, of the interface and bottom sediment layers;
- the migration of radionuclide from the "interface layer" to the "bottom sediment".

The lost deposit of radionuclide per unit surface (L) was evaluated as follows:

$$d\Lambda/dt = [K_{sd} + R_s/(D_{bs}\delta_b)]C_b D_{bs}\delta_b - \lambda_r \Lambda \qquad \text{(II.8)}$$

TABLE II.1. LIST OF SYMBOLS

A_1 = relative weight of the short term component of the transfer function "drainage area->lake" (dimensionless);
A_2 = relative weight of the long term component of the transfer function "drainage area->lake" (dimensionless);
B = bioaccumulation factor water->fish (m^3/kg);
C_b = radionuclide concentration in bottom sediment (Bq/kg);
C_f = concentration of the radionuclide in fish (Bq/kg fresh weight.);
C_k = concentration of potassium in water (kg/m^3);
C_s = radionuclide concentration in suspended matter (Bq/kg);
C_t = total concentration of the radionuclide in water (Bq/m^3);
C_w = dissolved concentration in water of the radionuclide (Bq/m^3);
D(t) = deposition rate of the radionuclide ($Bq \cdot m^{-2} \cdot s^{-1}$);
D_{al} = thickness of the sediment "interface layer" (m);
D_{bs} = *thickness of the bottom sediment (m);*
D_{imp} = total deposition due to a single contamination event (Bq/m);
$\underline{h}$ = mean depth of the lake (m);
I_{tot} = total rate of input of the radionuclide from the catchment (Bq/s);
K_{alb} = transfer rate of the radionuclide from the sediment "interface layer" to the bottom sediment (s^{-1});
K_{bal} = transfer rate of the radionuclide from the bottom sediment to the "interface layer" (s^{-1});
k_d = suspended matter/water partition coefficient (m^3/kg);
K_{fk} = constant relating the transfer factor B with the inverse of potassium concentration in water (dimensionless);
K_{sd} = transfer rate of the radionuclide from bottom to deep sediments (s^{-1});
P_{sa} = total mass of the "interface layer" of sediment (kg);
P_{ss} = total mass of suspended matter (kg);
R = retardation factor (dimensionless);
R_s = sedimentation rate ($kg \cdot m^{-2} \cdot s^{-1}$);
S_{dep} = radionuclide deposit in the sediment (Bq/m);
t = time (s);
V = volume of lake water (m^3);
W_{ssd} = weight of suspended matter per unit volume of water (kg/m^3);
$\Phi(t)$ = water discharge into the lake (m^3/s);
$\Phi_o(t)$ = water outflow (m^3/s);
ε = transfer coefficient "deposition -> water" in catchment basin (m^{-1});
Λ = lost deposit of radionuclide per unit surface (Bq/m^2);
λ_b = transfer rate out of fish (s^{-1});
λ_r = radioactivity decay constant (s^{-1});
λ_1 = effective decay constant of the short term component in the transfer function "drainage area -> lake" (s^{-1});
λ_2 = effective decay constant of the long term component in the transfer function "drainage area -> lake" (s^{-1});
δ_{al} = density of the "interface layer" (kg/m);
δ_b = density of the bottom sediment (kg/m).

The total sediment deposit, per square meter at time t, was calculated using the following formula:

$$S_{dep} = D_{al}\delta_{al}C_s + D_{bs}\delta_b C_b + \Lambda \quad \text{(II.9)}$$

The model was solved using STELLA™ [II.4] Software running on a Macintosh IIci computer.

Modelling fish contamination

The evaluation of fish contamination was carried out according to the following single-compartment model:

$$dC_f/dt = -(\lambda_r + \lambda_b)C_f + B(\lambda_r + \lambda_b)C_w \quad \text{(II.10)}$$

The value of the bioaccumulation factor (B) was related to the inverse of potassium concentration in water (C_k):

$$B = K_{fk}/C_k \quad \text{(II.11)}$$

where K_{fk} is a constant depending on the fish species. In the present model two generic values were used according to the fish species is piscivorous or non-piscivorous.

TABLE II.2. GENERIC VALUES OF NON-"SITE SPECIFIC" MODEL PARAMETERS

Parameter	Units	Value
A_2	dimensionless	0.06
A_1	dimensionless	0.94
λ_1	s^{-1}	5.8×10^{-7}
λ_2	s^{-1}	2.7×10^{-8}
ε	m^{-1}	0.4
D_{bs}	m	0.1
D_{al} d_{al}	kg/m^2	0.5
K_{alb}	s^{-1}	4.6×10^{-8}
K_{bal}	s^{-1}	2.9×10^{-8}
k_d	m^3/kg	15
K_{fk} (piscivorous)	dimensionless	8.1×10^{-3}
Kfk (non-piscivorous)	dimensionless	3.0×10^{-3}
K_{sd}	s^{-1}	5.8×10^{-9}
δ_b	kg/m^3	1000
λ_b (piscivorous)	s^{-1}	2.1×10^{-8}
λ_b (non-piscivorous)	s^{-1}	5.7×10^{-8}

II.2. DESCRIPTION OF THE LAKE ECOSYSTEM MODEL LAKECO

II.2.1. Introduction

The model LAKECO has been developed to model the behaviour of radionuclides in lake ecosystems in accidental situations. This model is a box model, which predicts the concentration of ^{137}Cs in the water column, in the sediment and in biota due to an accidental release of radionuclides, by means of a dynamic model applicable on a wide range of lake ecosystems. In the food chain part of the model, the uptake of ^{137}Cs in biota through food and water is taken into account. The set of input parameters consists of physical parameters, which can be obtained with or derived from field data. The dynamic uptake is based on studies on mercury in fish carried out by Delft Hydraulics [II.5]. The model LAKECO can be converted to any possible food pattern in a lake ecosystem. The physical expressions for the transfer of radionuclides from the water column to the sediments are based upon the enhanced COLDOS-SEABED model [II.6].

II.2.2. The hydrological part

Figure II.2 gives a schematic overview of the compartments into which the lake including sediments are subdivided. Arrows give the direction of the transport of radionuclides. For each compartment a differential equation expresses the gradient of the radionuclide present in that particular layer.

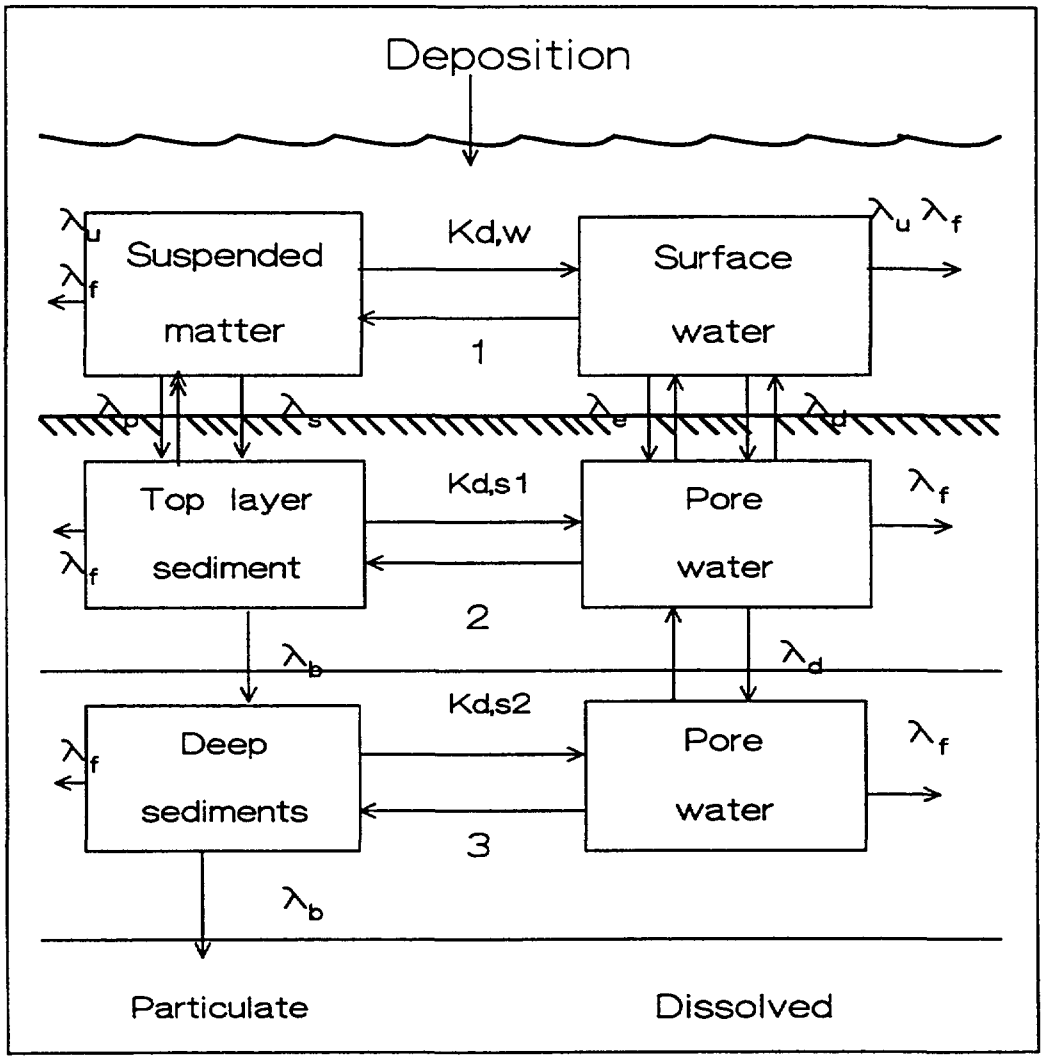

FIG. II.2. Schematic overview of the compartments.

The concentration in the water column can be described by expression (II.12):

$$\frac{dN_i}{dt}=\sum_{j=1}^{n}(K_{ji}N_j-K_{ij}N_i)-{}^{w}\lambda_i^{s1}N_i+{}^{s1}\lambda_i^{w}M_1-\lambda_f N_i \qquad \text{(II.12)}$$

where
N_i is the number of atoms of the radionuclide in compartment i at time,
k_{ji} is the transfer rate of the nuclide from compartment j to i (s^{-1}),
k_{ij} is the transfer rate of the nuclide from compartment i to j (s^{-1}),
M_i is the number of atoms of radionuclide in the top layer of the sediment in compartment i,
${}^{w}\lambda_i^{s1}$ is the transfer rate from the water column to the top layer (s^{-1}),
${}^{s1}\lambda_i^{w}$ is the transfer rate from the top layer of the sediment to the water column (s^{-1}).

Where:

$$\begin{aligned}{}^{w}\lambda_i^{s1}&=\lambda_s+{}^{w}\lambda_d^{s1}+{}^{w}\lambda_e^{s1}+{}^{w}\lambda_p^{s1}\\ {}^{s1}\lambda_i^{w}&={}^{s1}\lambda_d^{w}+{}^{s1}\lambda_e^{w}+{}^{s1}\lambda_p^{w}\end{aligned} \qquad \text{(II.13)}$$

where
λ_s is the rate constant for removal of the radionuclide due to particle scavenging (s^{-1}),
${}^{w}\lambda_d^{s1}$ is the rate constant for the transfer by molecular diffusion of the radionuclide from the water column to the top layer of the sediment bed,
${}^{w}\lambda_e^{s1}$ is the analogous rate constant for the transfer by pore-water mixing,
${}^{w}\lambda_p^{s1}$ is the analogous rate constant for the transfer by particle mixing,
${}^{s1}\lambda_d^{w}$, ${}^{s1}\lambda_e^{w}$, ${}^{s1}\lambda_p^{w}$are the rate constants for these three mechanisms for the transfer from the to sediment layer to the water column (s^{-1}).

The activity concentration in the top layer can be described by expression (II.14).

$$\frac{dM_i}{dt}={}^{w}\lambda_i^{s1}N_i-{}^{s1}\lambda_i^{s2}M_1-{}^{s1}\lambda^{w}M_1+{}^{s2}\lambda_d^{s1}M_2-\lambda_f M_i \qquad \text{(II.14)}$$

where
$M_{1,i}$ is the number of atoms of the radionuclide in the top layer of the sediment in compartment i,
$M_{2,i}$ is the number of atoms in the second sediment layer,
${}^{s1}\lambda^{s2}$ is the transfer rate from the top sediment to the second sediment layer (s^{-1}),
${}^{s2}\lambda_d^{s1}$ is the rate constant for transfer by molecular diffusion of the radionuclide from the second sediment layer to the top sediment layer (s^{-1}).

Where:

$${}^{s1}\lambda_i^{s2}={}^{s1}\lambda_d^{s2}+{}^{s1}\lambda_b^{s2} \qquad \text{(II.15)}$$

where
${}^{s1}\lambda_d^{s2}$ is the rate constant for the transfer by molecular diffusion from the top sediment layer to the second sediment layer,
${}^{s1}\lambda_b^{s2}$ is the rate constant for the transfer of the radionuclide by burial from the top to the second sediment layer (s^{-1}).

The activity concentration in the second layer can be described by expression (II.16).

$$\frac{dM_{2,i}}{dt} = {}^{s1}\lambda_i^{s2} M_{1,i} - {}^{s2}\lambda_b^{s3} M_{2,i} - {}^{s2}\lambda_d^{s1} M_{2,i} - \lambda_f M_{2,i} \qquad \text{(II.16)}$$

where
${}^{s2}\lambda_b^{s3}$ is the transfer rate from the second sediment layer to deeper sediments (s^{-1}).

Rate constants

The rate constants can be expressed by means of equations which contains physical parameters, which can be derived from field data [II.7].

Molecular diffusion

Using Fick's First Law, an expression for the transfer by molecular diffusion between the several compartments can be derived. The rate constant for diffusion from water to the sediments is expressed in equation II.17.

$${}^{w}\lambda_d^{s1} = \frac{D_m F_w}{d_{s1} d_w} \qquad \text{(II.17)}$$

where
D_m is the diffusion coefficient in the pore water (m^2/d),
d_{s1} the thickness of the top sediment layer in m, d_w the depth of the water column (m),
F_w the fraction of N which is in solution (see equation II.18).

$$F_w = \frac{1}{(1 + K_{dw} L)} \qquad \text{(II.18)}$$

where
L is the suspended sediment concentration (kg/m^3),
K_{dw} is the distribution coefficient (m^3/kg).

The rate constant for diffusion in the opposite direction, from the top sediment layer to the water column, is:

$${}^{s1}\lambda_d^{w} = \frac{D_m F_{s1}}{d_{s1}^2 \phi_1} \qquad \text{(II.19)}$$

where
D_m is the diffusion coefficient in the pore water (m^2/d),
d_{s1} is the thickness of the top sediment layer (m),
ϕ_1 is the porosity of the top sediment layer,
F_{s1} is the fraction of the radionuclide which is in solution in the interstitial water of the top sediment layer (see equation II.20).

$$F_{s1} = \frac{\phi_1}{\phi_1 + K_{d1} \rho_{d1} (1 - \phi_1)} \qquad \text{(II.20)}$$

where
ρ_1 is the density of the top sediment layer (kg/m^3),
K_{ds1} is the distribution coefficient of the radionuclide in the top sediment layer.

The rate constant for diffusion from the top sediment layer to the second sediment layer is given by equation II.21.

$$ {}^{s1}\lambda_d^{s2} = \frac{D_m F_{s1}}{d_{s1} d_{s2} \phi_1} \qquad \text{(II.21)} $$

where
d_{s2} is he thickness of the second sediment layer (m).

The rate constant for diffusion in the opposite direction, from the second sediment layer to the top sediment layer, is:

$$ {}^{s2}\lambda_d^{s1} = \frac{D_m F_{s2}}{d_{s2}^2 \phi_2} \qquad \text{(II.22)} $$

where
ϕ_2 is the porosity of the second sediment layer,
F_{s2} the fraction of the radionuclide which is in solution in the interstitial water of the second sediment layer (see equation II.22).

$$ F_{s2} = \frac{\phi_2}{\phi_2 + K_{d2} \rho_{d2} (1 - \phi_2)} \qquad \text{(II.23)} $$

where
ρ_2 is the density of the top sediment layer (kg/m^3),
K_{ds2} is the distribution coefficient of the radionuclide in the second sediment layer.

Sediment mixing

Physical mixing and bioturbation in the top sediment layer will result in the turnover of particles which are in intimate contact with the overlying water. Through their borrowing activities organisms will also promote the exchange of porewater with the water column.

The rate constant for radionuclide transfer from the sediment porewater to the overlying water column by porewater exchange will be:

$$ {}^{s1}\lambda_e^{w} = R_T F_{s1} \qquad \text{(II.24)} $$

where R_T is the porewater turnover rate (d^{-1}).

The rate constant for the transfer from the surface water to porewater is given by:

$$ {}^{w}\lambda_e^{s1} = \frac{R_T \phi_1 F_w d_{s1}}{d_w} \qquad \text{(II.25)} $$

where R_w is the sediment reworking rate (m^3·m^{-2}·d^{-1}).

The rate constant for the transfer from the top sediment layer to surface water due to particle mixing is:

$$ {}^{s1}\lambda_p^{w} = \frac{R_w (1 - F_{s1})}{d_{s1}} \qquad \text{(II.26)} $$

The rate constant for the transfer from the water column to the top sediment layer due to particle mixing:

$$\frac{R_w\ \rho_{d1}\ K_{ds1}\ (1-\phi_1)\ F_w}{d_w} \tag{II.27}$$

The relation between the sediment reworking rate R_w and the porewater turnover R_t rate is:

$$R_T = \varepsilon\ \frac{R_w}{d_{s1}} \tag{II.28}$$

Sedimentation (particle scavenging)

Radioactivity is transferred from the water column to the sediment bed by the scavenging action of particulate material settling from suspension. The rate constant for this process is:

$$\lambda_s = \frac{\sigma\ K_{dw}\ F_w}{d_w} \tag{II.29}$$

where σ is the sedimentation rate ($kg \cdot m^{-2} \cdot d^{-1}$).

Burial

The burial mechanism moves with both sediments and porewater downward relative to the sediment/water interface. However an upward movement of the porewater will take place because of the compaction of the sediment in deeper layers. So it is assumed that only particles are transported to the deeper layers. So the rate constant for transfer of radioactivity from the top layer to the second layer is:

$${}^{s1}\lambda_b^{s2} = \frac{\sigma(1-F_{s1})}{\rho_{d1}\ (1-\phi_1)\ d_{s1}} \tag{II.30}$$

and similarly for the transfer from the second layer to deeper sediments:

$${}^{s2}\lambda_b^{s3} = \frac{\sigma(1-F_{s2})}{\rho_{d2}\ (1-\phi_2)\ d_{s2}} \tag{II.31}$$

II.2.3. The food chain model

In case of continuous discharges of radionuclides by nuclear or non-nuclear industries the uptake of radionuclides by aquatic organisms can be modelled by using a concentration factor. In the case of accidents, however, a more dynamic approach is necessary. The concentration in an organism can be modelled by means of a concentration factor in combination with the biological half life of a radionuclide. A more complex approach is takes the position in the food chain into account, which requires knowledge about the food chain in a certain water body and specific parameters like consumption rates.

For regular discharges of radionuclides the concentration in the organisms can be described by means of equation (II.32).

$$C_{organism} = CF * C_{water} \tag{II.32}$$

For accidental discharges and for regular discharges before equilibrium, equation II.32 can be enhanced with the biological loss coefficient λ_b. In this equation II.33 the concentration in the organism in the long run is determined only by the concentration factor, while the time to the equilibrium concentration is determined by the loss coefficient.

$$C_{organism}=CF*C(t)_{water}\ (1-e^{\lambda_b t}) \tag{II.33}$$

where λ_b is the biological loss rate (d^{-1}), which can be expressed by:

$$\lambda_b=\frac{\ln(2)}{T_{0.5}} \tag{II.34}$$

where $T_{0.5}$ is the biological half-life in days.

Taking the position in the food chain into account requires extensive input data which are not always available. The basic equation on which this approach is based is:

$$\frac{dC_{(pred)}}{dt}=a\ k_1C_f+b\ K_wC_w(t)-K_{0.5}C_{(pred)} \tag{II.35}$$

where
$C_{(pred)}$ is the concentration of the radionuclide in the organism (Bq/kg fw),
C_f is the concentration in the food (Bq/kg ww),
C_w is the concentration of the radionuclide in water (Bq/m^3),
K_1 is the food consumption rate (kg prey)/(kg predator/day) where $K_1 = K_{resp}+K_{growth}$,
K_{resp} is the respiration rate and K_{growth} the growth rate coefficient, *a* the food extraction efficiency,
b the water extractability,
K_w the water uptake rate (m^3/d),
$K_{1/2}$ the biological half-life.

The radionuclide concentration in the food of a predator can be expressed by equation II.36.

$$C_f=\sum_{i=1}^{n} C_{prey,i}\ P_{prey,i}\ \frac{dw_{pred}}{dw_{prey,i}} \tag{II.36}$$

where
$C_{prey,i}$ is the concentration in prey i (Bq/kg ww),
$P_{prey,i}$ the preference for prey (range 0–1),
dw_{pred} is the dry weight fraction of the predator,
$dw_{prey,i}$ is the dry weight fraction of prey i.

The basic philosophy behind the LAKECO model is to use as many parameters as possible based on physical parameters, avoiding the use of fitting parameters in the biological uptake model. The growth rate coefficient K_{growth} can be coupled with the Relative Growth Rate (RGR) of a specimen if measurement data on body weight versus time are available. If no measurement data on fish weight versus time in a particular system are present, literature values must be used as input data.

The RGR can be expressed by the following equation:

$$RGR\equiv\frac{1}{W}\cdot\frac{dW}{dt} \tag{II.37}$$

where W is the weight of the organism.

II.2.4. Input and assumptions in the application of LAKECO on the lakes in this study

In the application of the aquatic model LAKECO the model is enhanced to the extent to which information is available in the databank. For instance, if time dependent discharge rates were available, a time dependent turnover rate was introduced, otherwise a mean value on annually basis has been used. To cope with all the different specific properties of the lakes it was also necessary to construct some modifications and extensions of the model. In general however, as many assumptions as possible were made, to have a flexible model system, applicable to a wide range of lake ecosystems. The assumptions, modifications, and generic and specific parameter values are presented in this Section in more detail.

First of all, stratification seemed to occur in all lakes in this study, except in the shallow lake IJsselmeer. In the application of LAKECO it was assumed that the stratification was negligible. One of the main reasons for neglecting this phenomena was the additional set of parameters which are needed to run such a submodel. Only in the case of the very deep lake Bracciano, would this lead to extreme underestimation in the water column if stratification were omitted. Regarding the whole lake as one single completely mixed box would result in an underprediction of the caesium levels in the water column in the initial period after radionuclide deposition. The mixing period from November till March causes rapid removal of radionuclides to the hypolimnion. Instead of a loss rate mainly due to outflow, like in the other lakes in this study, the loss of radionuclide is governed by this mixing; the caesium inventory in the first 6 metres of the lake (epilimnion) is mixed with the total volume in the autumn. Therefore, in the case of lake Bracciano a submodel on stratification, reported in the recent literature [II.3], was implemented in the model LAKECO to handle this effect.

For each lake, the mean residence times are given. However in the case of the strong seasonal variations in the Swedish and Norwegian lakes, the residence time was substituted by a function based on the monthly averaged discharge. In the case of extreme seasonal variations, it is of great importance when the deposition takes place. When the radionuclides are deposited in the winter when the lakes are covered with ice, the radionuclides will be flushed away during a ice breakup when the flushing rate reaches its maximum value. If the radionuclides enter the lake ecosystem in the summer, when relatively long residence times exist, the extent to which radionuclides affect the system will be greater. Therefore, for Hillesjön and Øvre Heimdalsvatn, time dependent outflow rates have been used to calculate the residence time.

Aquatic systems are very sensitive to the initial deposition and consequently these wide ranges cause large uncertainties in the model results. As well as the amount of deposited radionuclides the time at which the deposition takes place determine the peak values in water, sediments and in biota. Aquatic systems with high seasonal effects are especially sensitive. In the case of Øvre Heimdalsvatn a delay in the model has been build in, in order to predict the actual exposure of radionuclides to the lake water after the ice break-up at the beginning of June, a month after the deposition of radionuclides from the Chernobyl cloud. For Hillesjön and Iso Valkjärvi the deposition took place during the ice-breakup, and no special modification has been implemented for these lakes.

The transfer of radionuclides can be modelled in two different ways: (i) assuming an immediate transfer of radionuclides during the ice-smelt; (ii) assuming a slow transfer of radionuclides when the ice melts. If in the model the latter assumption is accepted, lower levels of ^{137}Cs are the result, since the immediate release from ice to water causes higher peak levels in the water. This is illustrated in Section 5.9.

Non-soluble particles or fuel particles, diminish both the bioavailability of caesium in the water column and reduce the retention time of radiocaesium in the lake water. For the Scandinavian lakes Hillesjön and Øvre Heimdalsvatn a fraction of 50% undissolvable particles has been assumed in accordance with the approach presented by Korhonen [II.8]. For Iso Valkjärvi, a fraction of 75% was

selected. One of the reason in Korhonen's study to introduce this non-soluble fraction, was the discrepancy between measurements and predicted values. This notion was based on the work of Salbu [II.9], who suggested that in Norway about 75% of the deposited caesium was bound to colloids or particles in insoluble form. The phenomena of hot particles and their behaviour near the reactor site is described by several authors [II.10, II.11]. This approach was not applied to the other lakes in the study.

In the model a modification has been implemented to cope with the problem of the non-soluble fraction. The soluble fraction has been treated as radiocaesium with a traditional K_d value, while fate and behaviour of the non-soluble fraction has been modelled by means of the same model with an extremely high K_d value, under the assumption that little caesium is released from the non-soluble particles.

The model is extremely sensitive to the K_d value. Originally the K_d was based on generic literature value, modified by widespread ideas about the relationship between the distribution coefficient and competitive ions like potassium. Values between 10^{-3} and 50 m^3/kg were found in the literature [II.12]. Generally, it can be expected that higher concentrations of potassium in lake water decrease the adsorption to the suspended sediments, since the frayed edge sites on the clay minerals will be occupied by this competitive ion. In the absence of illite or other clay minerals, this relationship might not be found. To estimate the K_d on the basis of the K^+ concentrations is therefore possible. This can be achieved by some expert opinion, but it is better is to implement a submodel to estimate the K_d based on environmental parameters like the potassium concentration in lake water. This results in a narrower uncertainty range for the K_d, and in a more flexible and reliable approach, which can also be applied in emergency decision support systems for nuclear accidents. This submodel is described in Section 5.1.2, in which the outcome of a sensitivity analysis with the subsequent modifications of the model are presented.

The K_d of the bottom sediment can be calculated by means of the same relationship, in the sediments, where the NH_4 concentration will play an important role. A decrease of the K_d in the bottom sediments with increasing depth has been reported [II.13]. In the deeper layers of the sediment of Lake Ketelmeer the K_d was about 0.5 m^3/kg, while at the sediment/water interface the K_d was about 1 m^3/kg. This effect is probably caused by the presence of NH_4 in the deeper anoxic layers, a competitive ion of ^{137}Cs [II.13].

However, in this stage of the model development another approach based on the presence of small particles was selected. Since the particles in the bottom sediments with a fine grain size are mixed with coarse particles, to which radionuclide hardly adsorb, the K_d of the bottom sediments is estimated to be about 0.2 times the value of the K_d of suspended particles. The notion behind this can be expressed in the following equation:

$$K_d(bottom\ sediment) = \alpha K_d(small\ particles) + (1-\alpha)K_d(sand) \qquad \text{(II.38)}$$

where α is the fraction of small particles in the bottom sediment. With the conservative assumption that K_d(sand) is 10 % of K_d(small particles), the equation becomes:

$$K_d(bottom\ sediment) = (0.9\ \alpha + 0.1)\ K_d(small\ particles) \qquad \text{(II.39)}$$

Assuming a fraction of ± 10 % small particles, equation II.39 becomes:

$$K_d(bottom\ sediment) = 0.19 K_d(small\ particles) \approx \alpha_{dw} \qquad \text{(II.40)}$$

If the K_d of sand is negligible in comparison with that of small particles, K_d(sand) becomes a infinitesimal fraction of the K_d(small particles). In that case the equation becomes:

$$K_d\ (bottom\ sediment) = \alpha K_d\ (small\ particles) = K_{dw} \qquad \text{(II.41)}$$

In the model application α is estimated as 0.1, i.e. 10% of the bottom sediment is considered as small particles, and K_d for coarse particles as 0.1 of the K_d of the fine particles, except for IJsselmeer, where sand contributes significantly to the bottom sediments, since the lake was a former sea (Zuiderzee). For this lake the K_d for sand particles was considered negligible.

Originally in the LAKECO the sediment reworking rate, a model specific parameter value, was based on literature values. This process is caused by wind induced waves and biological activity of benthos and fish (bioturbation). Generic values reported [II.6] vary between 10^{-4} and 10^{-3} m d^{-1} for freshwater systems. For shallow waters also values of 10^{-2} were reported. Shallow lakes show higher reworking rates due to the fact, that wind has more effect on the mixing of the sediment layers than in deep lakes. In deep lakes the downward transport in the sediments will be governed by burial, since in these cases benthos in the bottom sediments are present in very low densities. In shallower lakes bioturbation will be the dominant process in burial [II.14]. Although the sediment reworking rate is not the most sensitive parameter, in LAKECO the reworking rate has been modified by a dimensionless moderator, the so called dynamic ratio, which is dependant of the morphology of the lake. This is described in more detail in Section 5.1.2. Due to the introduction of this moderator, the reworking is estimated from the lake morphology, instead of generic literature values or expert judgement.

For η, which governs the relationship between the sediment reworking rate R_w, and the porewater turnover rate R_t was 10 selected, in accordance with Nicholson and MacKenzie [II.6] or Nicholson [II.7], except for the IJsselmeer, for which the value 1 was selected.

Morphological information like volume, depth and surface area are given in the data description of the lakes. Mass sedimentation rates were also given, except for Hillesjön, where the mass sedimentation rate had to be estimated, and for Bracciano, where due to the negligible amount of suspended matter, sedimentation plays a minor role in the removal of radionuclides from the water column.

In LAKECO, most of the species in the food web are modelled with the assumption that the food preference of the predator does not change with time. In reality, the preference of a predator is determined by both the food supply and by the age of the fish. Piscivores like perch and pikeperch change the composition of their diet during their life. In the case of a shortage of the preferred prey predators switch to another item. The food supply also shows seasonal variation, related to the water temperature. In the model, seasonal variation of the food supply is assumed not to result in a change of diet, but in a change of the food consumption rate.

Extreme seasonal changes in food supply, especially with respect to blooms of phytoplankton followed by a zooplankton bloom, are not included in the model. Sufficient food is assumed to be present in the system throughout the whole year. The variation in the mass of zooplankton and phytoplankton is taken into account by using consumption rates averaged annually. For eutrophic lake ecosystems, optimal food conditions for all trophic levels occur, which implies optimal feeding conditions during the year. For oligotrophic lakes, however, this assumption is not quite so realistic.

The model is very sensitive to the parameter for the concentration factor water-phytoplankton. According to the literature it varies between 500 and 2500 L/kg [II.15] (see Section 5.1.2). Therefore, a submodel has been incorporated into LAKECO to supply more realistic estimations of the CF based on the potassium levels in the lake. Higher potassium levels result in relatively lower uptake, and subsequently in lower CF values.

The food preference of each species is important in the transfer of radionuclides in the food chain. Detailed information on the food preferences for a wide range of species can be found in the literature. For each lake ecosystem, however, the structure of the food web differs. Generic information can be used as a first approach in the model, but more site specific information is necessary for the description of the food web in a particular aquatic system. For instance, perch is the top predator in IJsselmeer, while in the Swedish lake Hillesjön perch is eaten by pike, which is hardly present in IJsselmeer. The main food of the perch in IJsselmeer is smelt, while in Hillesjön this is substituted by roach. Investigations of the contents of the fish stomach can give more information on the food preferences of certain fish species, like that on pikeperch and perch in IJsselmeer [II.16]. If there was no information available on a certain fish species, generic information on food has been used. Another possibility is to identify typical predator and prey fish relationships.

Generic information has been used to construct the food webs. Additional information on trout and perch was found in the literature [II.17].

In the model the coefficients are assumed to be constant for a certain type of organism. The food uptake for maintenance, K_{resp}. can be considered independent of the age of an organism. The food uptake for growth, however, will be higher in the first stage of the life, while the relative growth rate is higher than in a later stage. Although in the case of an extended amount of data these parameters can be regarded as variable parameter values, it is more convenient to select average values for the growth rate coefficient and the respiration rate for use in emergency systems.

The biological loss rate, $K_{1/2}$, is a result of excretion, the metabolism of the organism, reproduction, and the growth dilution. Generally growth dilution is the most important factor for the loss of radionuclides on a weight basis. As in the literature the biological loss is generally defined as a loss rate per kilogram body weight, the $K_{1/2}$, this growth dilution is automatically taken into account. Then the $K_{1/2}$ can be expressed inversely proportional to the biological half-life.

$$K_{½}=\frac{\ln(2)}{T_{½}} \qquad \text{(II.42)}$$

where $T_{½}$ is the biological half-life in days.

However, in the literature detailed information on the exact way the biological half-life is derived is not always supplied. When the reported values of the biological half-life are based on total body inventory, these values of $T_{1/2}$ are higher since the $T_{1/2}$ is a only a result of the excretion rate, which is a slower process than the loss due to growth dilution. Then the growth dilution must be introduced as an extra term in equation (II.37). Omitting this term will result in an overprediction of the concentration especially in the fast growing organisms like zooplankton and juvenile fish at the low trophic levels. In the opposite case – the reported values of the biological half life are the result of all loss processes, and due to lack of detailed information on the procedure this reported value is assumed to be the loss rate due to excretion rate only – the levels will be underpredicted if the growth rate loss term is added to the equation. Therefore, if the exact procedure is not given, the growth dilution is assumed to be taken into account, accepting the risk of overestimation in the prediction of the model.

An accurate estimation of the biological half-life is of great importance, governing the retention of caesium in several aquatic organisms. Many studies have been carried out on the subject (see Section 5.5). Rowan [II.18] cited many publications on biological half-lives, and concluded that biological half-lives determined in laboratory experiments gave underestimations, since equilibrium is not reached. There is also a difference in biological half-lives in steady state and accidental situations, the retention time in steady state situations tends to be higher than in the case of an acute exposure. It is therefore important to check the way the biological half-lives have been determined. Based on the relationship between temperature and body weight, suggestions for the biological half-lives for the organisms in the different lakes of this study are presented (see Section 5.5).

In the model the extractability, *a*, of caesium from the food in the fish stomach is fixed at 70%, a rather conservative value. This fraction could be compared with values of the fraction which is eliminated by the slow component of the biological half-life. In the overview of biological half-lives by Rowan [II.18], between 50–80% of the initial burden is eliminated by the slow component. Hewett and Jefferies reported 67% for brown trout [II.19]. However, in the steady state situation, the figure appeared to be 96%. At present there is no appropriate method to estimate this fraction. In the application of LAKECO the fraction is therefore set to 70% for predatory and non-predatory fish, and where this resulted in highly deviating model results, another value has been selected (see Table 3). Lacking good data, the food extraction for the other aquatic organisms was set to 30% for benthos, 10% for zooplankton, and 100% for perch, which is assumed to have a comparatively high extraction factor.

The extraction from the water passing the gills, the water extractability, is fixed at 10^{-3} for all organisms, except for one particular fish in lakes with low potassium levels (see Table 3), the brown trout. The uptake of ions such as caesium via the gills is often discussed in the literature, and regarded as negligible [II.19] and [II.20] in comparison with the food uptake via the gut. For brown trout 5–10% of the caesium uptake is due to the uptake via the gills. That the potassium concentration controls the uptake via the gills, is demonstrated by Fernandez et al. [II.21] by means of laboratory experiments with cyprinids. The concentration factor for caesium found at 0.35 mg/L potassium was close to four times higher than in the case of 35 mg/L potassium, which is evidence both for caesium uptake via the gills and for the influence of potassium on this process.

For Øvre Heimdalsvatn and Devoke Water, however, the high levels and the rapid increase of radiocaesium in brown trout could not be explained by food uptake only. The uptake via the gills could be an explanation of this unusually high uptake in these oligotrophic lakes. This behaviour has also been recently reported for the rainbow trout [II.22]. It was explained by proposing that the major source of ^{137}Cs for a population of trout living in a high mountain lake was not through food items but by ingestion of bottom sediments. The evidence were (i) The major food items of the trout did not contain enough ^{137}Cs to account for the observed levels in fish, (ii) surface sediments and detritus were sufficiently high in ^{137}Cs that less than the 0.1 g would need to be ingested daily to account for the observed levels in trout, and (iii) sediments and detritus were observed in the intestinal tract of the fish. They suggested that the drop in the levels in trout in 1970 was caused by the change in the food pattern from benthos to zooplankton.

However, Kolehmainen [II.23] considered that such uptake was rather unlikely. In laboratory experiments with the bluegill, in which the absorption of ^{137}Cs was tested by feeding the fish with *Chironomus* larvae, contaminated with labelled detritus, and with *Chironomus* larvae fed with labelled algae. It appeared, that the absorption percentage for *Chironomus* larvae that had fed on algae containing ^{137}Cs was much higher, than for *Chironomus* that had fed on labelled detritus. This shows, that the bluegill can adsorb most of the ^{137}Cs associated with tissues, but is able to absorb very little of ^{137}Cs in the detritus and on the clay in the alimentary canal of the chironomid larvae. The adsorption of ^{137}Cs for algae was 68.7%, and for detritus 3.0%. In experiments to test the transfer of radiocaesium from sediments to carp (*Cyprinus carpi,L.*), it was demonstrated, that less than 1% of the caesium was transferred to the fish [II.24]. Uptake experiments with an aquatic food chain carried out with potassium concentrations of 0.6 mg/l showed that 30–50% of the caesium was transferred to the fish via the water [II.25]. However, this was due to the total uptake from all trophic levels of the food chain. In [II.26] the reported fraction via the water for carp fed with Chiromidae was 1–4%, depending on the age of the carp. In an experiment with carp fed with *Daphnia*, however, the contribution of the uptake of radiocaesium via water was about 50%.

For the extractability *b* for brown trout in Devoke Water, and Øvre Heimdalsvatn a value of 0.3 was selected. A more detailed study has to be carried out to find more evidence for the water uptake contribution.

Generic values for model specific parameters are presented in Table II.3 (sediment parameters) and II.4 (biological uptake parameters).

TABLE II.3. GENERIC PARAMETERS FOR THE HYDROLOGICAL PART OF LAKECO

Parameter	Symbol	Unit	Value
Sediment			
Thickness active layer	d_{s1}	m	0.1
Thickness second layer	d_{s2}	m	0.1
Porosity active layer	ϕ_1	–	0.9
Porosity second layer	ϕ_2	–	0.8
Density dry sediment 1	ρ_1	kg dw/m^3	2500
Density dry sediment 2	ρ_2	kg dw/m^3	2500
Diffusion coefficient Cs	D_m	m^2/d	2.7×10^{-5}

TABLE II.4. GENERIC PARAMETERS (RESPIRATION RATE, GROWTH RATE, WATER UPTAKE RATE VIA THE GILLS) FOR THE BIOLOGICAL UPTAKE MODEL OF LAKECO

Organism	Respiration rate K_{resp}[a] d^{-1}	Growth rate K_{growth}[a] d^{-1}	Water uptake rate K_w $m^3 \cdot kg^{-1} \cdot d^{-1}$
Zooplankton	5×10^{-1}	5×10^{-1}	1.5
Chironomidae	1×10^{-2}	5×10^{-2}	1×10^{-1}
Mollusca	5×10^{-2}	1×10^{-2}	1×10^{-1}
Juvenile fish	5×10^{-2}	5×10^{-2}	1×10^{-1}
Non-predatory adult fish	5×10^{-2}	5×10^{-3}	1×10^{-1}
Predatory adult fish	5×10^{-2}	5×10^{-3}	7.5×10^{-2}

[a] The K_{resp}, K_{growth} for fish are default values, in some of the lake deviations occur of about 10%.

II.3. DESCRIPTION OF THE STUDSVIK MODEL

II.3.1. Model structure

The model (see Fig. 4.7) is based upon compartment theory with first order kinetics. It can be adopted for continuous as well as pulse releases and for different elements. The model is of generic type which by changes of site specific parameters could be used for several types of Nordic lakes. The parameters used are those related to environmental conditions, those related to element to be studied, and model parameters.

The latter, such as fish consumption rates, are not changed between varying types of lakes. In practice they vary but there is a lack of data. Uncertainties in parameter values are handled in the model by using distributions of each parameter. By Latin hypercube sampling, 200 sets of input parameters are generated and run through the model. The model responses are given as distributions, and by correlation and regression methods, parameter and processes which have the greatest influence on model outputs are identified. This is done by the PRISM-system [II.27] in combination with the BIOPATH-code for solving the sets of differential equations [II.28]. Uncertainty analysis is a suitable tool for improving models since it points out weak points in an effective way. Another advantage is that correlations between parameters can be considered. One of the conclusions from the BIOMOVS 1 project stressed the importance of modellers making estimates of the uncertainties attaching to their predictions [II.29].

Descriptions of compartments, turnover processes and equations are given below. Earlier versions of the model have been used in a BIOMOVS scenario [II.29] and some preliminary results have also been presented [II.30]. The model and results from this study are also given in [II.31].

The model includes major components in lake ecosystems such as drainage area, lake water, sediments and biota. The actual number of compartments may vary due to the scenario to be studied. The main emphasis is to make predictions of radionuclide concentrations in water and fish.

The drainage area is represented in the model by one generic compartments which is contaminated in accordance to the site descriptions. In general, the water masses are simulated by a single compartment. This simplification seems appropriate in most circumstances as most Nordic lakes are quite shallow and dimictic. In this exercise, the wide scatter of lakes also included one very deep lake, Bracciano, in Italy, with a strong thermocline. This was taken into account in the model by using a smaller dispersion volume until the autumn mixing.

The sediments are simulated by three compartments. Two are used for the transport and accumulations bottoms, respectively, while the third is the deeper sediments acting partly as a sink for the elements. Concerning the food chain, three to five compartments are used. The number depends upon the number of fish species to be considered. A common compartment for plankton and *Gammarus* is used as well as compartments for the respective fish species (e.g. roach, perch, pike).

The turnover of elements in the model is expressed mathematically as turnover rates per month. Major paths for the elements redistributions in the systems are: leakage from the drainage area, transfer out by water outflow and transfer to and from the sediments.

The food chain is by necessity generalized. From the lumped compartments plankton and *Gammarus* the uptake in non-piscivorous fish occurs by the consumption. Predators in turn consume these prey fishes leading to an uptake of ^{137}Cs by gut uptake. Loss from fish occurs by excretion based upon the biological half-life in the fish species, which is dependent on body weight and water temperature. For continuous releases the concentration in fish can be modelled simply by bioaccumulation factors implicitly taking account of all processes.

II.3.2. Description of rate constants

It is worth pointing out again that all rate constants are obtained by the above mentioned error propagation method, that is a best estimate and a statistical distribution for each parameter are used. In general logtriangular distributions are used. The rates are not all constant during the year, for example seasonally dependent parameters such as water retention time, consumption values and biological half-lives.

Transfer rate from catchment to water

When empirical data are missing, the rate constants are obtained from the expression below taking account of seasonality by using a factor 10 higher during the spring season. This is in accordance with observations [II.32]. The change in leakage with time is considered by applying an exponential reduction with a half-life of 3 years.

$$K_{c,w} = Perc \cdot e^{(-t\frac{ln2}{T_{1/2}})} \tag{II.43}$$

where
$K_{c,w}$ is the transfer rate,
Perc is the percentual leakage of deposit amount in the catchment,
t is the time after the deposition,
$T_{1/2}$ is the half-life for fixation of ^{137}Cs in catchment.

Transfer rate out of lake

If empirical data are available:

$$K_{w,o} = \frac{Q(t)}{V} \tag{II.44}$$

where:
Q(t) is the outflow of water as a function of time,
V is the lake volume, with the exception of lake Bracciano where V is epilimnetic volume.

When empirical data are missing:

$$K_{w,o} = \frac{1}{T} \tag{II.45}$$

where T is the theoretical retention time.

Transfer rate from water to sediment

There are several processes interacting for transfer of elements from water to sediments. Interaction with mineral and organic particles may due to the chemical form of the element and environmental conditions cause an effective transfer from water to sediments. In addition, diffusion may also transfer caesium from water to sediments. However, in these scenarios diffusion was neglected because several studies have pointed out the scavenging by particles as a major path. The following expression was used [II.33] for transfer both to transport and accumulation bottoms:

$$K_{ws} = \frac{K_d\, S}{h(1+K_d\, SS)} \tag{II.46}$$

where
K_d is the distribution factor (concentration on solid/concentration in solution) m^3/kg,
SS is the suspended matter (kg/m^3),
S is the mass sedimentation rate ($kg \cdot m^{-2} \cdot month^{-1}$),
h is the average water depth (m).

Transfer rate from sediments to water

The main processes, bioturbation, diffusion and mechanical forces, are lumped into one main flow designated resuspension. The following expression is used for obtaining the rate:

$$K_{s,w} = RESP \cdot \frac{S}{\rho_{sed}} \qquad \text{(II.47)}$$

where
$K_{s,w}$ is the transfer rate from sediments to water ($month^{-1}$),
S is the mass sedimentation rate ($kg \cdot m^{-2} \cdot month^{-1}$),
ρ_{sed} is the density of the sediments per unit area (kg/m^2),
RESP is the resuspension factor.

Transfer rate transport bottoms to accumulation bottoms

It is assumed that there is an effective transfer from the nearshore bottoms to the accumulation bottoms located deeper. The transfer rate is obtained from the following expression:

$$K_{s,s} = (1 - RESP) \frac{S}{\rho_{sed}} \qquad \text{(II.48)}$$

where $K_{s,s}$ is the transfer rate from transport bottoms to accumulation bottoms ($month^{-1}$).

Transfer rate from upper to deeper sediments

A fraction of the sediment surface radioactivity will be transferred to deeper situated parts of the sediments. This describes the role of the sediments as a sink for a part of the radiocaesium. It can be described ananlogically with the equation (II.48):

$$K_{s,s} = (1 - RES) \cdot \frac{S}{\rho_{sed}} \qquad \text{(II.49)}$$

where $K_{s,s}$ is now the transfer rate from accumulation bottom to deep sediment ($month^{-1}$).

Transfer rate water to plankton and Gammarus

The uptake into plankton and *Gammarus* acting in the model as lumped parameters to describe the food-web is based on a bioaccumulation factor in combination with a biological half-life for obtaining the rates. The uptake is considered to be seasonally dependent and described by much longer biological half-lives during the winter. The transfer rate is obtained by:

$$K_{w,f} = \frac{ln2 \cdot M_f}{BHT_i \cdot M_w} \cdot B_f \qquad \text{(II.50)}$$

where
$K_{w,f}$ is the transfer rate to plankton and *Gammarus*, respectively ($month^{-1}$),
M_f is the mass of plankton and *Gammarus*, respectively (kg dw),
BHT_i is the biological half-life, seasonally dependent (month),
M_w is the mass of water (kg),
B_f is the bioaccumulation factor, numerical value is dependent upon type of lake and concentration of potassium in water.

Transfer rate plankton and Gammarus to water

The elimination back to water $K_{w,f}$ is simply described by the biological half-life:

$$K_{f,w} = \frac{ln2}{BHT_i} \tag{II.51}$$

Transfer rate plankton and Gammarus to prey fish

This uptake is modelled by a seasonally dependent consumption rate according to expression below:

$$K_{f,p} = U_f \cdot M_i \cdot \frac{M_p}{M_f} \tag{II.52}$$

where
$K_{f,p}$ is the transfer rate from plankton and *Gammarus*, respectively to prey fish (month^{-1}),
U_f is the proportion of ingested to incorporated caesium,
M_i is the consumption (kg per month and per kg fish),
M_p is the mass of preyfish (kg),
M_f is the mass of plankton and *Gammarus*, respectively (kg).

Transfer rate prey fish to water

This is described by the biological half-life, varying due to season and reflecting the water temperature:

$$K_{p,w} = \frac{ln2}{BHT_i} \tag{II.53}$$

where
$K_{p,w}$ is the transfer rate prey fish to water (month^{-1}),
BHT_i is the biological half-life (month).

Transfer rate prey fish to predator

Predatory fish takes up caesium by their consumption of contaminated food. For perch it is assumed that it consumes a mixture of plankton, *Gammarus* and prey fish while for pike it assumed that it only consumes fish:

$$K_{pi,pp} = FP \cdot U_f \cdot M_p \cdot \frac{M_{pp}}{M_{pi}} \tag{II.54}$$

where
$K_{pi,pp}$ is the transfer rate prey i to predator (month^{-1}),
FP is the fraction of predators consumption of prey i,
U_f is the proportion of ingested to incorporated caesium,
M_p is the consumption rate for predator (kg per month and kg fish),
M_{pp} is the mass of predatory fish (kg),
M_{pi} is the mass of prey fish i (kg).

Transfer rate plankton/Gammarus to predator fish (perch)

$$K_{fi,pp}=(1-FP)\cdot U_f \cdot M_p \cdot \frac{M_{pp}}{M_{fi}} \qquad \text{(II.55)}$$

Transfer rate predator to water

This is due to the metabolism of caesium in the fish, described by the biological half-life, see below:

$$K_{pp,w}=\frac{ln2}{BHT_i} \qquad \text{(II.56)}$$

where
$K_{pp,w}$ is the transfer rate predator to water,
BHT_i is the biological half-life varying with season (months) and species.

II.4. DESCRIPTION OF THE UPPSALA UNIVERSITY MODELS

II.4.1. The Empirical model

The outline of the empirical model is presented in Figure 4.8. Figure II.3 gives data for Cs-concentration in lake water (1986) and pike (1986 to 1989) and predicted recovery curves using this empirical model. We can note that the model predicts too low values for ^{137}Cs in pike and a faster recovery than indicated by the empirical data. These results could be "tuned" to get a better fit with the empirical data by simple calibrations of the retention coefficients in the model. The results presented in Figure II.3 are the first results without any "tuning". An interesting result in Figure II.3 concerns the very slow recovery for the Cs-concentration in pike.

BOX: Cs_conc_in_lake(t) = Cs_conc_in_lake(t - dt) + (Cs_transport_to_lake - Cs_transport_from_lake) * dt
INIT: Cs_conc_in_lake = 0
Every constant in this model must be recalculated when the model is applied to lakes that do not belong to the same lake type as the Swedish forest lakes of glacial origin for which to model was originally developed. The equations, constants, etc. given here are meant as examples. Values in Bq/L.

INFLOWS:
Cs_transport_to_lake = 0.01*(2.53*Water_discharge*Water_discharge+0.005*Lake_mean _depth^2+0.19* LOG10(Relief_ of_catchment)+0.025*Cs_fallout/(Lake_area*Lake_mean_depth) - 0.3)
OUTFLOWS:
Cs_transport_from_lake = Cs_conc_in_lake*Retention_rate_for_Cs_in_water

BOX: Cs_concentration_in_active_sediments(t) = Cs_concentration_in_active_sediments(t - dt) + (Cs_transport_to_sediment + Cs_transport_to_passive_sed) * dt
INIT: Cs_concentration_in_active_sediments = 0
Values in Bq/kg ww.

INFLOWS:
Cs_transport_to_sediment = Cs_conc_in_lake*Sediment_to_water_ratio
Cs_transport_to_passive_sed = Cs_concentration_in_active_sediments* Sediment_retention_rate

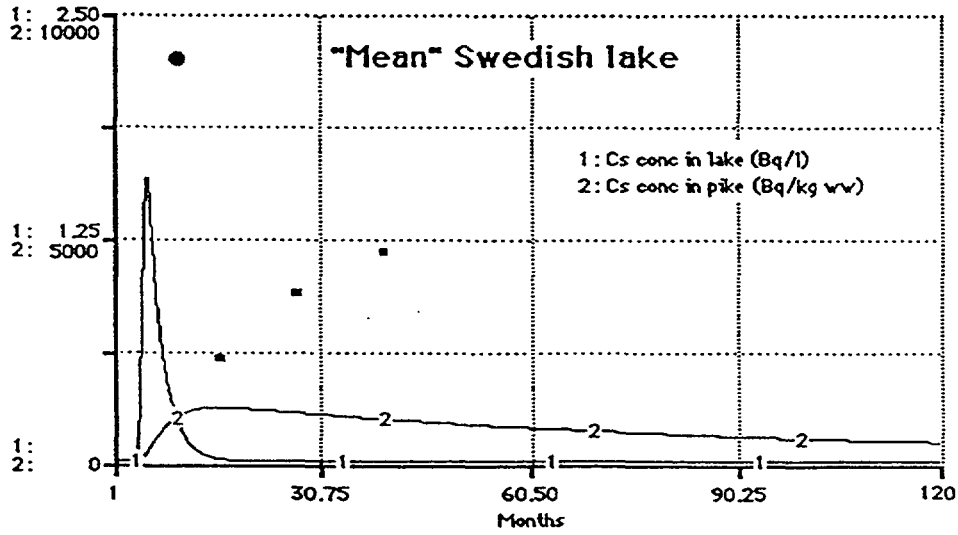

FIG. II.3. A simulation with the empirical model using data for the "average" Swedish lake and corresponding empirical data (see Table II.5) for Cs-concentration in lake water (large black circle) and pike (small black squares). Note that this model has not been calibrated for the VAMP lakes. This figure is included here primarily to illustrate the time dependent predictions may also be obtained with this empirical model.

BOX: Cs_concentration_in_pike(t) = Cs_concentration_in_pike(t - dt) + (Cs_transport_to_pike - Cs_transport_from_pike) * dt
INIT: Cs_concentration_in_pike = 0
Values in Bq/kg ww apply to 1-kg pike.

INFLOWS:
Cs_transport_to_pike = 0.01*(Cs_concentration_in_active_sediments^(Retention_exponent))
*(365-280*Lake_water_hardness*Lake_water_hardness+524*
(Lake_area*Lake_mean_depth)-1.25*SQRT(Lake_area)/Lake_mean_depth)
OUTFLOWS:
Cs_transport_from_pike = Cs_concentration_in_pike*Retention_rate

Lake_area = 0.68
Lake area in km^2.

Lake_mean_depth = 4.1
Lake mean depth in m.

Lake_water_hardness = 0.24
This is the mean annual lake water hardness in meq/L.

Lake_water_retention_time = 0.72
This is the theoretical lake water retention time defined as the ratio between lake volume in km^3 and the mean annual water discharge in km^3/a. Dimension in years.

Relief_of_catchment = 41
The relief of the catchment area is defined from the relationship $dH/\sqrt{ADA}$, where dH is the largest height difference in m the catchment and ADA is the catchment area in km^2.

Retention_exponent = 0.4
This dimensionless constant k is defined from the relationship $Cspi=Cswa^k$, where Cspi=Cs conc in pike in Bq/kg ww and Cswa= Cs conc in lake water in Bq/L. Default value is 0.4.

Retention_rate = 0.693/12*7
It is assumed (see Håkanson, 1991 [II.54]) that the ecological half-life of Cs in 1 kg pike is 7 years.

Retention_rate_for_Cs_in_water = 0.26*SQRT(Lake_water_retention_time)-0.001*Wet_land_percentage_of_catchment+0.069*LOG10(Relief_of_catchment)-0.2*LOG10(SQRT(Lake_area)/Lake_mean_depth)

Sediment_retention_rate = 0.693/(0.2*10*12)
We assume a constant sedimentation rate of 0.2 cm per year and thickness of active layer of 2 cm.

TABLE II.5. A COMPILATION OF DATA FROM 41 SWEDISH LAKES (FROM HÅKANSON, 1991 [II.35]).

	Cssoil (kBq/m^2)	Cswa86-mod (Bq/L)	area (km^2)	Dm (m)	T (year)	ADA (km^2)
n	41	15	41	41	41	41
Min.	2.5	0.04	0.07	1.1	0.02	1.0
Max	70.0	12.9	2.70	10.1	2.90	80.0
Median	15.0	0.9	0.40	4.0	0.47	17.0
MV	25.2	2.2	0.68	4.1	0.72	18.5
SD	21.1	3.3	0.64	2.2	0.68	16.5
V	83.8	148	94.5	53.3	95.12	89.1

	pH	cond (mS/m)	colour (mg Pt/L)	totP (µg/L)	K (µeq/L)
n	41	41	41	41	23
Min.	5.1	1.6	35	4.3	5.9
Max	6.6	8.2	201	26.4	36.7
Median	6.1	2.6	109	10.0	8.7
MV	6.0	3.0	101	10.5	11.1
SD	0.4	1.2	41	4.2	7.3
V	6.4	39.6	40	40.5	65.4

	Cspi87	Cspi88	Cspi89	Cspe86	Cspe87	Cspe88	Cspe89
n	41	41	41	41	41	41	41
Min.	195	304	241	346	103	72	47
Max	7310	13756	20455	104809	19580	7641	3753
Median	1355	2497	2463	3380	2120	682	494
MV	2392	3977	4768	8230	4066	1599	883
SD	2260	3846	5185	16538	4877	1979	960
V	94	97	109	201	120	124	109

Cssoil = fallout, Cswa86-mod = model predicted values of Cs-concentration in lake water (from a model presented in Håkanson, 1991 [II.34]), area = lake area, Dm = mean depth, T = theoretical lake water retention time, ADA = area of drainage area, pH = mean annual lake pH, cond = mean annual conductivity, colour = mean annual colour, totP = mean annual concentration of total-P, K = mean annual concentration of K, Cspi87 = concentration of ^{137}Cs in pike in 1987 (Bq/kg ww), Cspe86 = concentration of ^{137}Cs in perch fry in 1986 (Bq/kg ww).

Sediment_to_water_ratio = 1000
This is the ratio between the Cs-concentration in lake water (median value for 15 Swedish lakes in 1986 was 0.13 Bq/L) and concentration in surface sediments (median value from 22 Swedish lakes was 920 Bq/kg dw, or about 90 Bq/kg ww). This gives a ratio of about 1000 (Bq/kg ww to Bq/L). Data from Håkanson et al. [II.35].

Water_discharge = 0.164
This is the mean annual tributary discharge in m^3/s.

Wet_land_percentage_of_catchment = 16.5
The percentage of lakes, mires, rivers and other types of wetland in the lake catchment area.

Cs_fallout = GRAPH(TIME)
Fallout after Chernobyl on lake and catchment in Bq/m^2.

II.4.2. The Mixed model

Traditional dynamic models (see e.g. [II.36] and Figure II.4A) are based on information on the caesium flow at several levels in a given lake.

This model is first based on the assumption that the Cs-concentration in fish (Csfish) eaten by man (pike, large perch, trout, whitefish, etc.) can be predicted from the Cs-concentration in the fish prey, Csprey, (small perch, smelt, roach, etc.), which in turn depends on the fallout (Cssoil) and on environmental variables describing the lake (theoretical lake water retention time, T, dynamic ratio, DR = $\sqrt{}$area/Dm, Dm = mean depth). Csfish at a certain time (t) can be obtained from the following box model:

$$Csfish(t) = Csfish(t - dt) + (Csprey - Csfish*(k_{1/2}+k_{ret1})) * dt$$

where
Csfish is the Cs-concentration in fish (Bq/kg ww),
Csprey is the Cs-concentration in fish prey (Bq/kg ww),
$k_{1/2}$ is the physical decay (1/month),
k_{ret1} is the caesium retention rate (or transport rate from fish out of the system, or release rate from fish, 1/month).

This means that we only use two of the boxes in Figure II.4A in this model, namely fish and fish prey.

The Cs-concentration in prey at a certain time (t) can be written:

$$Csprey(t) = Csprey(t - dt) + (Cslake*BF - (k_{1/2}+k_{ret2})*Csprey - Csprey) * dt$$

where
Cslake is the Cs-concentration in the lake water (Bq/L), determined from the ratio between the Cs-amount in the lake (Bq) and the lake volume (l),
BF is the bioconcentration factor (dimensionless), which is the ratio between the default bioconcentration factor (150) and the K-moderator (see Figure II.5),
k_{ret2} is the caesium retention rate for prey (or the transport rate from prey out of the system; 1/month).

The Cs-amount (Csamount, Bq) in lake water is given by:

$$Csamount(t) = Csamount(t - dt) + (Inflow - Outflow) * dt$$

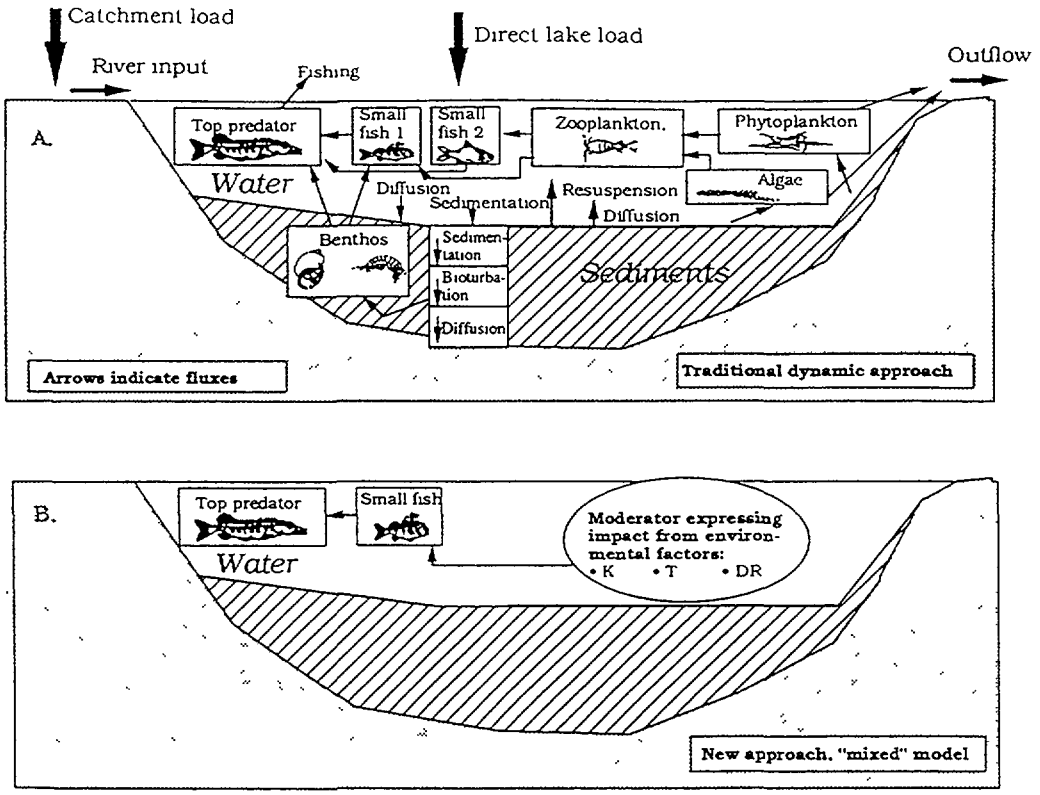

FIG. II.4A. Compartment model illustrating the fluxes (arrows; mass per unit time) in a traditional dynamic model for the type substance radiocaesium in a lake ecosystem with compartments (mass units) for top predator, two types of small fish, zooplankton, phytoplankton, algae, benthos, water and sediments.

FIG. II.4B. Illustration of a small "mixed" model, i.e., a model based on a mass balance model and empirical dimensionless moderators expressing the impact of environmental factors (like K-concentration, theoretical water retention time, T, and dynamic ration DR) on the uptake of radiocaesium from water to small fish.

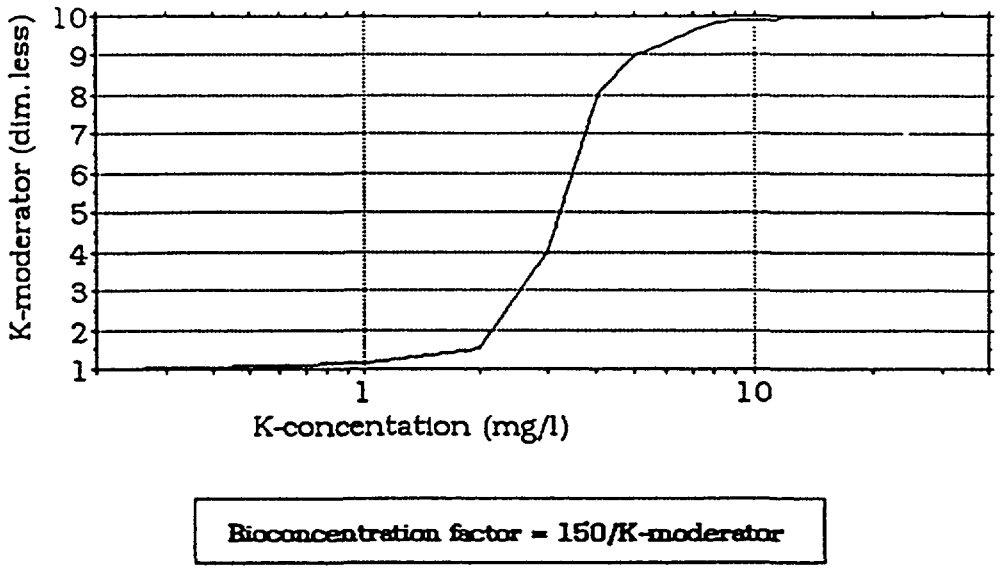

FIG. II.5. Graphical illustration of the dimensionless K-moderator.

The transport of caesium to the lake is simply given by: Fallout (Bq/m^2)*ADA (area of catchment area in m^2), and the transport from the lake by: (k1/2+RR)*Csamount.

The following argument can be given for the definition of the **resuspension factor**. In lakes, resuspension depends on:

(1) An **energy factor** related to the effective fetch (the maximum open water distance) and the wave base (the maximum depth to which surface waves reach to mix the bottom);

(2) A **lake form factor** related to the percentage of the lake bed above the wave base; and

(3) A **lake slope factor** that allows for slope-induced transport (turbidity currents) where the lake bottom slopes more than 4–5 % [II.37].

These determinants may all be expressed quite simply by the lake **dynamic ratio**, DR, which is defined as the ratio $\sqrt{}$area/Dm. The DR will thus increase with lake area, which is a measure of the effective fetch and with decreasing mean depth (Dm), which is an index of the proportion of the bottom area which lies above the wave base. The DR-value may be used to estimate areas of the lake bottom where **erosion** (E), **transport** (T) or **accumulation** (A) prevail [II.38]. E-bottoms are areas where, following Stokes' law, the cohesive materials are not deposited. Such bottoms are dominated by coarse deposits like medium-sized silt, sand and gravel. T-bottoms are, by definition, areas where fine materials are deposited discontinuously. In such areas, one usually finds mixed deposits. A-bottoms appear beneath the wave base, where the fine suspended materials can be continuously deposited. Håkanson and Jansson [II.37] used DR to estimate the percentages of the whole lake bottom which are subject to erosion and transportation (BET) or to accumulation (BA = 100 - BET).

BOX: Cs_amount_in_lake_water(t) = Cs_amount_in_lake_water(t - dt) + (Transport_to_lake - Transport_from_lake_out_of_system) * dt
INIT: Cs_amount_in_lake_water = 0

INFLOWS:
Transport_to_lake = Fallout_of_Cs*Lake_area
This is the transport to the lake (Bq/m^2)
OUTFLOWS:
Transport_from_lake_out_of_system =
(Physical_half-life_for_Cs+Retention_in_lake_water)*Cs_amount_in_lake_water

BOX: Cs_concentration_in_fish(t) = Cs_concentration_in_fish(t - dt) + (Transport_from_prey_to_predator - Transport_from_fish_out_of_system) * dt
INIT: Cs_concentration_in_fish = 0
This is the concentration in Bq/kg ww.

INFLOWS:
Transport_from_prey_to_predator = Cs_concentration_in_prey
OUTFLOWS:
Transport_from_fish_out_of_system = Cs_concentration_in_fish*
(Physical_half-life_for_Cs+Transport_rate_from_fish_out_of_system)

BOX: Cs_concentration_in_prey(t) = Cs_concentration_in_prey(t - dt) + (Transport_from_water_to_prey - Transport_from_prey_out_of_system - Transport_from_prey_to_predator) * dt
INIT: Cs_concentration_in_prey = 0
This is the concentration in Bq/kg ww.

INFLOWS:
Transport_from_water_to_prey = Cs_concentration_in_lake*Bioconcentration_factor
OUTFLOWS:
Transport_from_prey_out_of_system = (Physical_half-life_for_Cs+
Transport_rate_from_prey_out_of_ system)*Cs_concentration_in_prey
Transport_from_prey_to_predator = Cs_concentration_in_prey

Bioconcentration_factor = 150/K_moderator
This is the bioconcentration factor, i.e. the concentration in prey fish (here = perch fry) in Bq/kg ww relative to the concentration of Cs in water in Bq/L. Default value is set to 150.

Cs_concentration_in_lake = 0.001*Cs_amount_in_lake_water/(Mean_depth*Lake_area)
Value in Bq/L.

K_concentration = 0.4

Lake_area = 0.78*10^6
This is the lake area in m^2.

Mean_depth = 4.7
This is the lake mean depth in m.

Physical_half-life_for_Cs = 0.693/(30.2*12)
The physical half-life of ^{137}Cs is 30.2 years = 30.2*12 = 362.4 months. The retention coefficient is ln(0.5)/362.4 = 0.00191
$A(t) = A(0)*e^{-kt}$; $A(t)/A(0) = 0.5$; $\ln(0.5) = -kt$; $k = -\ln(0.5)/t$.

Resuspension_factor = ((SQRT(Lake_area*10^(-6))/Mean_depth))^0.2
This dimensionless factor is given by the dynamic ratio, i.e. the relationship DR=√area/Dm, where the area is given in km^2 (note that area is given in km^2 and NOT in m^2) and the mean depth in m.

Retention_in_lake_water = 1/(Resuspension_factor*(Water_retention_time_T)^((30/((Water_ retention_time_T)+29)+0.5)/(1.5))). See Fig. II.6A.

Transport_rate_from_fish_out_of_system = 0.693/(2*1.5*12)
It is assumed that the retention time (= ecological half-life) of the element in predator fish is x years, and that the retention rate is given by 1/x; x is set to:
6 years for ^{137}Cs for large pike and large, predatory perch (> 20 g);
3 years for minnow, trout, etc.;
2 years for perch (10 - 20 g), etc.;
1.5 years in whitefish, roach, etc.;
1 year for smelt, perch fry (< 10 g), etc.

The retention time (= ecological half-life) for ^{137}Cs in the prey in this model is set to half of that for predatory, or:
3 years for perch, roach, minnow, etc., eaten by large pike and perch;
1 year for perch fry, smelt and other small fishes eaten by perch, trout and minnow;
0.5 years for zooplankton, etc. eaten by whitefish, smelt, roach, perch fry, etc.

Transport_rate_from_prey_out_of_system = Transport_rate_from_fish_out_of_system*2
Water_retention_time_T = (63/30)
This is the theoretical lake water retention time (T = V/Q; V = lake volume in m^3; Q = tributary water discharge in m^3/month). The dimension is months.

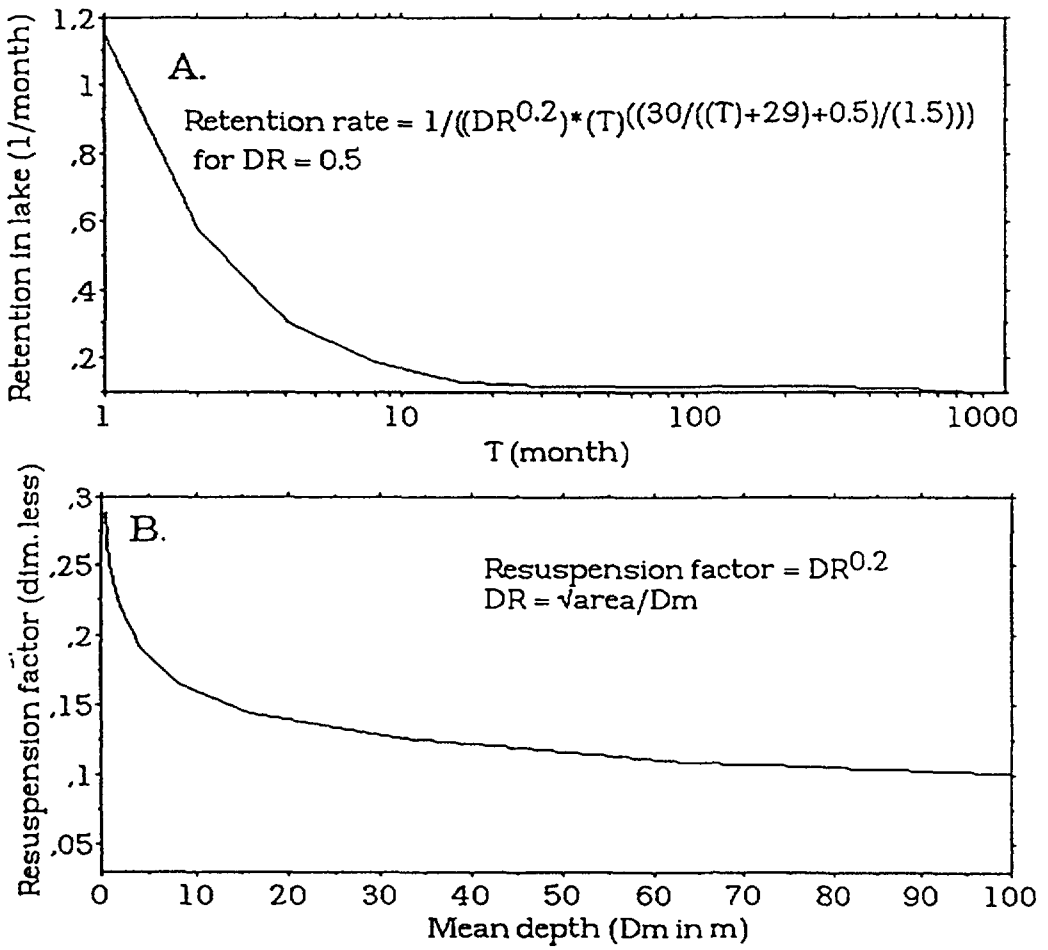

FIG. II.6. Graphical presentations of (A) the retention rate moderator, and (B) the resuspension factor.

Fallout_of_Cs = GRAPH(TIME)
This is the mean fallout of ^{137}Cs on the catchment and the lake after the Chernobyl accident in Bq/m^2.

K_moderator = GRAPH(K_concentration)
(0.00, 1.00), (1.00, 1.13), (2.00, 1.50), (3.00, 4.00), (4.00, 8.00), (5.00, 9.01), (6.00, 9.33), (7.00, 9.64), (8.00, 9.87), (9.00, 9.91), (10.0, 9.87), (11.0, 9.91), (12.0, 9.96), (13.0, 9.96), (14.0, 9.96), (15.0, 9.96), (16.0, 9.96), (17.0, 9.96), (18.0, 9.96), (19.0, 9.97), (20.0, 9.97), (21.0, 9.97), (22.0, 9.97), (23.0, 9.97), (24.0, 9.97), (25.0, 9.97), (26.0, 9.97), (27.0, 9.97), (28.0, 9.98), (29.0, 9.98), (30.0, 9.98), (31.0, 9.98), (32.0, 9.99), (33.0, 9.99), (34.0, 9.99), (35.0, 9.99), (36.0, 9.99), (37.0, 10.0), (38.0, 10.0), (39.0, 10.0), (40.0, 10.0)
This graph is derived from empirical calibrations using the data for the VAMP lakes. The K moderator expresses (in a dimensionless way) how the K-concentration in the lake water influences the bioconcentration factor, i.e., the biouptake of caesium to prey (Fig. II.5).

II.4.3. The Generic model

Figure 4.9 shows the fluxes and compartments of this model.

BOX: Amount_in_active_sediments(t) = Amount_in_active_sediments(t - dt) + (Transp_susp_to_sed + Transp_bent_to_sed + Transp_plank_to_sed - Transp_active_to_passive_sed - Nat_decay_2 - Transp_sed_to_bent - Transp_sed_to_susp) * dt
INIT: Amount_in_active_sediments = 0

INFLOWS:
Transp_susp_to_sed = Amount_in_susp_*Transp_rate_susp_to_sed
Transp_bent_to_sed = Amount_in_benthos*Transp_rate_bent_to_sed
Transp_plank_to_sed = Amount_in_plankton*Transp_rate_plankt_to_sed
OUTFLOWS:
Transp_active_to_passive_sed =
Amount_in_active_sediments*Transp_rate_active_to_passive_sediments
Nat_decay_2 = Physical_decay_const*Amount_in_active_sediments
Transp_sed_to_bent = Transp_rate_sed_to_bent*Amount_in_active_sediments
Transp_sed_to_susp = Amount_in_active_sediments*Resuspension_factor

BOX: Amount_in_benthos(t) = Amount_in_benthos(t - dt) + (Transp_sed_to_bent - Transp_bent_to_sed - Transp_bent_to_prey - Trans_bent_to_pred) * dt
INIT: Amount_in_benthos = 0

INFLOWS:
Transp_sed_to_bent = Transp_rate_sed_to_bent*Amount_in_active_sediments
OUTFLOWS:
Transp_bent_to_sed = Amount_in_benthos*Transp_rate_bent_to_sed
Transp_bent_to_prey = Amount_in_benthos*Transp_rate_bent_to_prey
Trans_bent_to_pred = Amount_in_benthos*Transp_rate_bent_to_pred

BOX: Amount_in_diss(t) = Amount_in_diss(t - dt) + (Transp_in_dissolved_phase - Transp_wat_to_plank - Transp_from_diss_out_of_syst - Nat_decay - Transp_wat_to_prey - Transp_wat_to_pred) * dt
INIT: Amount_in_diss = 0

INFLOWS:
Transp_in_dissolved_phase = (Kd)*Amount_in_lake_water
OUTFLOWS:
Transp_wat_to_plank = Amount_in_diss*Transp_rate_wat_to_plank
Transp_from_diss_out_of_syst = Amount_in_diss*Water_retention_rate
Nat_decay = Physical_decay_const*Amount_in_diss
Transp_wat_to_prey = Amount_in_diss*Transp_rate_water_to_biota
Transp_wat_to_pred = Amount_in_diss*Transp_rate_water_to_biota

BOX: Amount_in_lake_water(t) = Amount_in_lake_water(t - dt) + (Transp_from_catchment_to_lake + Deposition_on_lake + Transp_sed_to_susp - Transp_in_dissolved_phase - Transp_in_suspended_phase) * dt
INIT: Amount_in_lake_water = 0

INFLOWS:
Transp_from_catchment_to_lake =
Transp_from_IA_to_lake+Transp_from_OA_to_lake*Precipitation_factor
Deposition_on_lake = Lake_area*Fallout
Transp_sed_to_susp = Amount_in_active_sediments*Resuspension_factor
OUTFLOWS:
Transp_in_dissolved_phase = (Kd)*Amount_in_lake_water
Transp_in_suspended_phase = (1-Kd)*Amount_in_lake_water

BOX: Amount_in_passive_sediments(t) = Amount_in_passive_sediments(t - dt) + (Transp_active_to_passive_sed - Nat_decay_3) * dt
INIT: Amount_in_passive_sediments = 0

INFLOWS:
Transp_active_to_passive_sed =
Amount_in_active_sediments*Tramsp_rate_active_to_passive_ sediments
OUTFLOWS:
Nat_decay_3 = Amount_in_passive_sediments*Physical_decay_const

BOX: Amount_in_plankton(t) = Amount_in_plankton(t - dt) + (Transp_wat_to_plank + Tranbsp_susp_to_plank - Transp_plank_to_prey - Transp_plank_to_sed) * dt
INIT: Amount_in_plankton = 0

INFLOWS:
Transp_wat_to_plank = Amount_in_diss*Transp_rate_wat_to_plank
Transp_susp_to_plank = Amount_in_susp_*Transp_rate_susp_to_plank
OUTFLOWS:
Transp_plank_to_prey = Amount_in_plankton*Transp_rate_plank_to_prey
Transp_plank_to_sed = Amount_in_plankton*Transp_rate_plankt_to_sed

BOX: Amount_in_predator(t) = Amount_in_predator(t - dt) + (Transp_bent_to_pred + Transp_prey_to_pred + Transp_wat_to_pred - Nat_decay_4 - Transp_from_pred_out_of_syst) * dt
INIT: Amount_in_predator = 0

INFLOWS:
Transp_bent_to_pred = Amount_in_benthos*Transp_rate_bent_to_pred
Transp_prey_to_pred = Amount_in_prey*Transp_rate_prey_to_pred
Transp_wat_to_pred = Amount_in_diss*Transp_rate_water_to_biota
OUTFLOWS:
Nat_decay_4 = Amount_in_predator*Physical_decay_const
Transp_from_pred_out_of_syst = Amount_in_predator*Transp_rate_from_pred_out_of_syst

BOX: Amount_in_prey(t) = Amount_in_prey(t - dt) + (Transp_plank_to_prey + Transp_bent_to_prey + Transp_wat_to_prey - Transp_prey_to_pred - Transp_from_prey_out_of_syst) * dt
INIT: Amount_in_prey = 0

INFLOWS:
Transp_plank_to_prey = Amount_in_plankton*Transp_rate_plank_to_prey
Transp_bent_to_prey = Amount_in_benthos*Transp_rate_bent_to_prey
Transp_wat_to_prey = Amount_in_diss*Transp_rate_water_to_biota
OUTFLOWS:
Transp_prey_to_pred = Amount_in_prey*Transp_rate_prey_to_pred
Transp_from_prey_out_of_syst = Amount_in_prey*Transp_rate_from_prey_out_of_syst

BOX: Amount_in_susp_(t) = Amount_in_susp_(t - dt) + (Transp_in_suspended_phase - Transp_susp_to_sed - Tranbsp_susp_to_plank - Transp_from_susp_out_of_syst) * dt
INIT: Amount_in_susp_ = 0

INFLOWS:
Transp_in_suspended_phase = (1-Kd)*Amount_in_lake_water
OUTFLOWS:
Transp_susp_to_sed = Amount_in_susp_*Transp_rate_susp_to_sed
Transp_susp_to_plank = Amount_in_susp_*Transp_rate_susp_to_plank
Transp_from_susp_out_of_syst = Amount_in_susp_*Water_retention_rate

BOX: Amout_in_catchment(t) = Amout_in_catchment(t - dt) + (Deposition_on_land - Transp_from_catchment_to_lake - Natural_decay) * dt
INIT: Amout_in_catchment = 100000

INFLOWS:
Deposition_on_land = Fallout*Catchment_area
OUTFLOWS:
Transp_from_catchment_to_lake =
Transp_from_IA_to_lake+Transp_from_OA_to_lake*Precipitation_factor
Natural_decay = Amout_in_catchment*Physical_decay_const

Site specific parameters for Øvre Heimdalsvatn

Active_layer = 0.02
Catchment_area = 23.4*10^6
Conc_of_active_sed = Amount_in_active_sediments/Mass_of_active_sed
Conc_of_susp = Amount_in_susp_/Lake_volume
Cs_conc_in_bent = Amount_in_benthos/Mass_of_benthos
Cs_conc_in_plank = Amount_in_plankton/Total_bioproduction
Cs_conc_in_predator = mean(Amount_in_predator/Mass_of_predator,12)
Cs_conc_in_prey = Amount_in_prey/Mass_of_prey
Diss_Cs_conc_in_water = Amount_in_diss/(Lake_volume*1000)
Inflow_areas = 1-Outflow_area
K_concentration = 0.4
Lake_area = 0.78*10^6
Lake_concentration = Amount_in_lake_water/(Lake_volume*1000)
Lake_volume = 3.7*10^6
Mass_of_active_sed = Active_layer*Lake_area
Mass_of_benthos = Total_bioproduction*0.1
Mass_of_predator = Total_bioproduction/(10*Transfer_coefficient)
Mass_of_prey = Total_bioproduction/Transfer_coefficient
Outflow_area = 0.1
Physical_decay_const = 0.00191
Precipitation_factor = 800/600
Primary_production = 27.5
Resuspension_factor = 0.01*((SQRT(Lake_area/10^6))/(Lake_volume/Lake_area))^0.5
Sedimentation_rate_of_susp = 60*(1/13200)
Total_bioproduction = Primary_production*Trophic_relationships*Lake_area*2*(1/12) *(1/1000)
Transfer_rate_active_to_passive_sediments = Sedimentation_rate_of_susp/Active_layer
Transfer_rate_from_inflow_areas_to_lake = 0.001/12
Transp_from_IA_to_lake = Inflow_areas*Transfer_rate_from_inflow_areas_to_lake*Amout_in_catchment
Transp_from_OA_to_lake = Outflow_area*0.01*Transfer_rate_from_outflow_âreas_to_lake *Amout_in_catchment
Transfer_rate_bent_to_pred = 0.02
Transfer_rate_bent_to_prey = 0.001
Transfer_rate_bent_to_sed = 0.5
Transfer_rate_from_pred_out_of_syst = 0.693/(1.5*12)
Transfer_rate_from_prey_out_of_syst = 0.693/(0.25*12)
Transfer_rate_plank_to_prey = 0.001
Transfer_rate_plankt_to_sed = 1
Transfer_rate_prey_to_pred = 0.01
Transfer_rate_sed_to_bent = 0.00001
Transfer_rate_susp_to_plank = 0.00001
Transfer_rate_susp_to_sed = 1/(Lake_volume/Lake_area)

Transfer_rate_wat_to_plank = 0.002/K_moderator
Transfer_rate_water_to_biota = 0.00001/K_moderator
Trophic_relationships = 1
Water_retention_rate = 0.693/(0.5*Water_retention_time)
Water_retention_time = (63/30)
Fallout = GRAPH(TIME)

K_moderator = GRAPH(K_concentration)
(0.00, 1.00), (1.00, 1.13), (2.00, 1.50), (3.00, 4.00), (4.00, 8.00), (5.00, 9.01), (6.00, 9.33), (7.00, 9.64), (8.00, 9.87), (9.00, 9.91), (10.0, 9.87), (11.0, 9.91), (12.0, 9.96), (13.0, 9.96), (14.0, 9.96), (15.0, 9.96), (16.0, 9.96), (17.0, 9.96), (18.0, 9.96), (19.0, 9.97), (20.0, 9.97), (21.0, 9.97), (22.0, 9.97), (23.0, 9.97), (24.0, 9.97), (25.0, 9.97), (26.0, 9.97), (27.0, 9.97), (28.0, 9.98), (29.0, 9.98), (30.0, 9.98), (31.0, 9.98), (32.0, 9.99), (33.0, 9.99), (34.0, 9.99), (35.0, 9.99), (36.0, 9.99), (37.0, 10.0), (38.0, 10.0), (39.0, 10.0), (40.0, 10.0)

Kd = GRAPH(TIME)
(1.00, 0.00), (2.00, 0.00), (3.00, 0.00), (4.00, 0.00), (5.00, 0.5), (6.00, 0.21), (7.00, 0.14), (8.00, 0.1), (9.00, 0.1), (10.0, 0.1), (11.0, 0.1), (12.0, 0.1), (13.0, 0.1), (14.0, 0.1), (15.0, 0.1), (16.0, 0.1), (17.0, 0.1), (18.0, 0.1), (19.0, 0.1), (20.0, 0.1), (21.0, 0.1), (22.0, 0.1), (23.0, 0.1), (24.0, 0.1), (25.0, 0.1), (26.0, 0.1), (27.0, 0.1), (28.0, 0.1), (29.0, 0.1), (30.0, 0.1), (31.0, 0.1), (32.0, 0.1), (33.0, 0.1), (34.0, 0.1), (35.0, 0.1), (36.0, 0.1), (37.0, 0.1), (38.0, 0.1), (39.0, 0.1), (40.0, 0.1), (41.0, 0.1), (42.0, 0.1), (43.0, 0.1), (44.0, 0.1), (45.0, 0.1), (46.0, 0.1), (47.0, 0.1), (48.0, 0.1), (49.0, 0.1), (50.0, 0.1), (51.0, 0.1), (52.0, 0.1), (53.0, 0.1) ...
Transfer_coefficient = GRAPH(Primary_production)
(1.00, 2.00), (18.2, 8.10), (35.4, 15.5), (52.6, 21.0), (69.8, 26.0), (87.0, 29.9), (104, 32.1), (121, 34.1), (139, 35.3), (156, 36.5), (173, 37.5), (190, 38.2), (207, 39.0), (225, 39.2), (242, 39.7), (259, 40.3), (276, 40.8), (294, 41.5), (311, 42.0), (328, 43.0), (345, 43.9), (362, 44.4), (380, 45.3), (397, 46.3), (414, 47.1), (431, 48.0), (448, 48.5), (466, 49.0), (483, 49.5), (500, 50.0)
Transfer_rate_from_outflow_areas_to_lake = GRAPH(TIME)
(1.00, 0.00), (2.00, 0.00), (3.00, 0.00), (4.00, 0.00), (5.00, 30.0), (6.00, 23.6), (7.00, 18.2), (8.00, 15.2), (9.00, 13.1), (10.0, 11.4), (11.0, 10.1), (12.0, 9.45), (13.0, 8.70), (14.0, 7.80), (15.0, 6.90), (16.0, 6.45), (17.0, 6.00), (18.0, 5.55), (19.0, 5.55), (20.0, 5.10), (21.0, 4.95), (22.0, 4.65), (23.0, 4.65), (24.0, 4.65), (25.0, 4.50), (26.0, 4.65), (27.0, 4.05), (28.0, 4.05), (29.0, 3.75), (30.0, 3.75), (31.0, 3.90), (32.0, 3.75), (33.0, 3.60), (34.0, 3.75), (35.0, 3.60), (36.0, 3.45), (37.0, 3.45), (38.0, 3.75), (39.0, 3.30), (40.0, 3.30), (41.0, 3.30), (42.0, 3.30), (43.0, 3.30), (44.0, 3.30), (45.0, 3.30), (46.0, 3.30), (47.0, 3.30), (48.0, 3.30), (49.0, 3.30), (50.0, 3.30), (51.0, 3.15), (52.0, 3.15), (53.0, 3.00) ...

II.4.4. The VAMP LAKE model

A general introduction and description of the VAMP LAKE model is given in Section 5.10. Further details are to be found in Håkanson et al. [II.39]. Site specific parameters are given for Øvre Heimdalsvatn.

BOX: Amount_dissolved_in_water(t) = Amount_dissolved_in_water(t - dt) + (Dissolved - Phytoplanktonic_uptake - Lake_outflow_diss - Direct_uptake_to_prey - Direct_uptake_to_predator) * dt
INIT Amount_dissolved_in_water = 0
Values in kBq.

INFLOWS:
Dissolved_ = Amount_in_lake_water*Part_coeff_Kd
This is the flux (kBq/month) of radiocaesium in dissolved phase.

OUTFLOWS:
Phytoplanktonic_uptake = Amount_dissolved_in_water*Phytoplanktonic_uptake_rate
This is the total uptake of radiocaesium by phytoplankton from the dissolved caesium in lake water in Bq/month.

Lake_outflow_diss = Retention_in_lake_water*Amount_dissolved_in_water
Direct_uptake_to_prey = Amount_dissolved_in_water*Direct_uptake_rate
Direct_uptake_to_predator = Direct_uptake_rate*Amount_dissolved_in_water

BOX: Amount_in_active_sediments(t) = Amount_in_active_sediments(t - dt) + (Sedimentation - Transport_to_passive_sed - Benthic_uptake - Internal_loading) * dt
INIT: Amount_in_active_sediments = 0
This is the total amount of radiocaesium (in kBq) in the bioactive sediment layer in any given month. The initial value is set to 0.

INFLOWS:
Sedimentation = Sedimentation_rate_of_Cs*Amount_particulate_in_water
This is the sedimentation of particulate ^{137}Cs in kBq/month. For simplicity, there is no differentiation on the basis of bottom dynamics, so sedimentation is assumed to take place over the entire lake bottom.

OUTFLOWS:
Transport_to_passive_sed = Amount_in_active_sediments
*(Retention_rate_in_active_sediments+Physical_half-life_for_Cs)
This is the transport from bioactive to biopassive sediments in Bq/month.

Benthic_uptake = Benthic_uptake_rate*Amount_in_active_sediments
This is biological uptake of ^{137}Cs by benthos in kBq/month. For simplicity, we use only one flux from bottom fauna to prey (= zooplankton and small fish) and no flux from bottom fauna to predatory fish in this model.

Internal_loading = Amount_in_active_sediments*0.05*(Dynamic_ratio)
The internal loading of ^{137}Cs (in kBq/month) is assumed to be modified by the dynamic ratio (DR). Lakes with high DR should (by definition) have more resuspension and internal loading than lake with low DR. A default value of the rate is set to 0.05.

BOX: Amount_in_lake_first_week_after_fallout(t) = Amount_in_lake_first_week_after_fallout(t - dt) + (Direct_load_to_lake - Pelagic_flux - Benthic_flux) * dt
INIT: Amount_in_lake_first_week_after_fallout = 0
In kBq.

INFLOWS:
Direct_load_to_lake = Atmospheric_load*Lake_area
This is the total fallout of ^{137}Cs directly to the lake during the fallout event (in kBq/m^2).

OUTFLOWS:
Pelagic_flux = Amount_in_lake_first_week_after_fallout*Initial_Kd
Benthic_flux = Amount_in_lake_first_week_after_fallout*(1-Initial_Kd)

BOX: Amount_in_lake_water(t) = Amount_in_lake_water(t - dt) + (Pelagic_flux + Load_from_catchment + Internal_loading - Particulate - Dissolved) * dt
INIT: Amount_in_lake_water = 0
This is the total amount in lake water at any given month (kBq).

INFLOWS:
Pelagic_flux = Amount_in_lake_first_week_after_fallout*Initial_Kd
Load_from_catchment = Amount_in_OA*Outflow_rate_from_catchment
This is the runoff from land (i.e. from outflow areas = OA) to the lake in kBq/month.
Internal_loading = Amount_in_active_sediments*0.05*(Dynamic_ratio)

The internal loading of ^{137}Cs (in kBq/month) is assumed to be modified by the dynamic ratio (DR). Lakes with high DR should (by definition) have more resuspension and internal loading than lake with low DR. A default value of the rate is set to 0.05.

OUTFLOWS:
Particulate = Amount_in_lake_water*(1-Part_coeff_Kd)
This is the flux (Bq/month) of ^{137}Cs in the particulate phase.

Dissolved_ = Amount_in_lake_water*Part_coeff_Kd
This is the flux (kBq/month) of ^{137}Cs in dissolved phase.

BOX: Amount_in_OA(t) = Amount_in_OA(t - dt) + (Atmospheric_input_to_OA - Loss_from_OA - Load_from_catchment) * dt
INIT: Amount_in_OA = 0
This is the amount in the outflow areas (= OA) at any given month in kBq. The initial value is 0.

INFLOWS:
Atmospheric_input_to_OA = Atmospheric_load*Catchment_area*Outflow_areas_OA
This is the total fallout on the outflow areas (= OA) in kBq.

OUTFLOWS:
Loss_from_OA = Amount_in_OA*(Physical_half-life_for_Cs)
This is the loss from the outflow areas of the catchment due to physical decay.
Load_from_catchment = Amount_in_OA*Outflow_rate_from_catchment
This is the runoff from land (i.e., from outflow areas = OA) to the lake in kBq/month.

BOX: Amount_in_passive_sediments(t) = Amount_in_passive_sediments(t - dt) + (Transport_to_passive_sed) * dt
INIT: Amount_in_passive_sediments = 0
This is the total amount of ^{137}Cs in the biopassive (geological) sediment layer in kBq. The initial value is set to 0. There is no flux from this compartment, not even physical decay, because in this model the passive sediments are just a "sink". The initial value is set to 0 kBq.

INFLOWS:
Transport_to_passive_sed = Amount_in_active_sediments
*(Retention_rate_in_active_sediments+Physical_half-life_for_Cs)
This is the transport from bioactive to biopassive sediments in Bq/month.

BOX: Amount_in_phytoplankton(t) = Amount_in_phytoplankton(t - dt) + (Phytoplanktonic_uptake - Outflow_from_phytoplankton - Bioaccumulation_plank_to_prey) * dt
INIT: Amount_in_phytoplankton = 0
This is the total amount of ^{137}Cs in phytoplankton in the lake any given month in kBq.

INFLOWS:
Phytoplanktonic_uptake = Amount_dissolved_in_water*Phytoplanktonic_uptake_rate
This is the total uptake of ^{137}Cs by phytoplankton from the dissolved ^{137}Cs in lake water in Bq/month.

OUTFLOWS:
Outflow_from_phytoplankton = Amount_in_phytoplankton*Phytoplankton_outflow_rate
This is the outflow of radiocaesium from phytoplankton. There is no feedback in this model. Tests with feedbacks to "amount of particulate in water" and to "amount in active sediments" gave no increase in predictive power of the model. Such feedback loops would complicate the model and might decrease predictive power since their inclusion would require guesses about the feedback rates.

Bioaccumulation_plank_to_prey = Amount_in_phytoplankton*Bioacc_rate_plank_to_prey

BOX: Amount_in_predator(t) = Amount_in_predator(t - dt) + (Bioaccumulation_prey_to_pred + Direct_uptake_to_predator - Outflow_from_predator)
* dt
INIT: Amount_in_predator = 0
This is the total amount of ^{137}Cs (in kBq) in predatory fish any given month. The type of fish is specified under "Predator and predator outflow rates". The initial value is set to 0.

INFLOWS:
Bioaccumulation_prey_to_pred = Amount_in_prey*Bioacc_rate_prey_to_pred
Direct_uptake_to_predator = Direct_uptake_rate*Amount_dissolved_in_water

OUTFLOWS:
Outflow_from_predator = Prey_and_predator_outflow_rate*Amount_in_predator
This is the total monthly outflow from predatory fish in Bq/month.

BOX: Amount_in_prey(t) = Amount_in_prey(t - dt) + (Bioaccumulation_plank_to_prey + Benthic_uptake + Direct_uptake_to_prey - Bioaccumulation_prey_to_pred - Outflow_from_prey) * dt
INIT: Amount_in_prey = 0
This is the total amount of ^{137}Cs (in kBq) in prey any given month. This type of prey fish is specified under "Prey and predator outflow rates". The initial value is set to 0.

INFLOWS:
Bioaccumulation_plank_to_prey = Amount_in_phytoplankton*Bioacc_rate_plank_to_prey
Benthic_uptake = Benthic_uptake_rate*Amount_in_active_sediments
This is biological uptake of ^{137}Cs by benthos in kBq/month. For simplicity, we use only one flux from bottom fauna to prey (= zooplankton and small fish) and no flux from bottom fauna to predatory fish in this model.

Direct_uptake_to_prey = Amount_dissolved_in_water*Direct_uptake_rate

OUTFLOWS:
Bioaccumulation_prey_to_pred = Amount_in_prey*Bioacc_rate_prey_to_pred
Outflow_from_prey = (Prey_and_predator_outflow_rate*2)*Amount_in_prey
This is the total monthly outflow of ^{137}Cs from prey in Bq/month.

BOX: Amount_particulate_in_water(t) = Amount_particulate_in_water(t - dt) + (Particulate + Benthic_flux - Lake_outflow_part - Sedimentation) * dt
INIT: Amount_particulate_in_water = 0
This is the total amount of particulate ^{137}Cs in the lake at any given month in kBq.

INFLOWS:
Particulate = Amount_in_lake_water*(1-Part_coeff_Kd)
This is the flux (Bq/month) of ^{137}Cs in the particulate phase.
Benthic_flux = Amount_in_lake_first_week_after_fallout*(1-Initial_Kd)

OUTFLOWS:
Lake_outflow_part = Amount_particulate_in_water*(Retention_in_lake_water+Physical_half-life_for_Cs)
Sedimentation = Sedimentation_rate_of_Cs*Amount_particulate_in_water
This is the sedimentation of particulate ^{137}Cs in kBq/month. For simplicity, there is no differentiation on the basis of bottom dynamics, so sedimentation is assumed to take place over the entire lake bottom.

Altitude = (1090+1)
Altitude, in m above sea level. To allow for cases where altitude = 0, we will set this value to (alt+1). The higher the altitude, the greater the potential seasonal variability in Q and T, everything else kept constant.

Averaging_function = (50*Volume^(2/3))/(Precipitation*(Altitude*Latitude*Catchment _area)^(1/4))
This is the expression for the averaging function for the seasonal variability norm for Q and T (in months).

Benthic_uptake_rate = 0.00025
A default value for the rate of uptake by benthos in other lakes is set to 0.00025 per month.

Bioacc_rate_plank_to_prey = 0.25/12
It is assumed that, on average, 25% (rate 0.25) of the ^{137}Cs amount in plankton is transported to prey per year. We tested the effect of several different types of seasonal on this rate of biological uptake, but could not increase the predictive power significantly. Initially, we thought that a somewhat smoothed seasonal variability norm for Q and T would reflect the seasonal variability in biouptake better than a mean value. This is so, but predictive power increases very little. Moreover use of a modified seasonal moderator for Q and T here invokes a further assumption about the number of months to be used in the averaging function.

Bioacc_rate_prey_to_pred = Bioacc_rate_plank_to_prey
The bioaccumulation rate prey to predator is set equal to the bioaccumulation rate plankton to prey. We have tested different types of averaging functions for the seasonal moderator for Q and T, and different relationships between these two bioaccumulation rates (for prey and predator), but this, the simplest, approach seems to yield the best predictions of ^{137}Cs in prey and predatory fish.

Catchment_area = 23.4*10^6
The catchment area in m^2.

Conc_in_phytoplankton = 1000*Amount_in_phytoplankton/Phytoplankton_biomass
Values in Bq/kg ww.

Conc_in_predator = 1000*Amount_in_predator/Predator_biomass
Values in Bq/kg ww.

Conc_in_prey = 1000*Amount_in_prey/Prey_biomass
Values in Bq/kg ww.

Conc_in_water = (Amount_dissolved_in_water+Amount_particulate_in_water)/Volume
This is the mean monthly concentration of ^{137}Cs in the lake in Bq/L.

Direct_uptake_rate = YpH_plus_K*0.0004
The direct uptake of ^{137}Cs by prey (mainly small fish and zooplankton) and predatory fish is, for simplicity and to avoid yet another empirical rate that needs to be calibrated, assumed to be governed by the same moderator, YpH_plus_K, that moderates the uptake of ^{137}Cs by

phytoplankton. The default value for the rate is set to 0.0004, i.e., about 13 times lower than for the uptake rate for phytoplankton (0.005).

Dynamic_ratio = (SQRT(Lake_area*10^(-6))/Mean_depth)^0.5
This is the dynamic ratio, DR = $\sqrt{}$area/Dm. Note that lake area is given in km^2, not in m^2, in the definition of DR. Dm is the mean depth in m.

Initial_Kd = 0.5
The empirical data for the Chernobyl fallout for the VAMP-lakes indicate that a significant part of the fallout of ^{137}Cs to the lake surface was strongly bound to particles. This part is quickly transported to the lake bed. The model assumes that this transport of particles to the active sediments occurs during the first week after the fallout. Supported by the empirical data, we will assume that 50% of the initial fallout goes directly to the particulate phase and then to the sediments. This part will subsequently follow benthic pathways to fish. The rest, i.e. ^{137}Cs in solution and ^{137}Cs associated with very small particles (colloids, etc.) and will follow pelagic pathways to fish.

K = 0.4
The characteristic K-concentration of the lake water in mg/L.

Lake_area = 0.78*10^6
The lake area in m^2.

Latitude = 61
Latitude in ° N. The higher the latitude, the greater the potential seasonal variability, when everything else is kept constant.

Longitude = 100
This is NOT longitude *per se* but rather distance from ocean. The idea is to have a relevant measure describing how "continental" the climate of the lake is: The farther the lake lies from the ocean, the more continental is the climate and the colder the lake water. The distance is measured in km.

Mean_annual_temp = 44-((750/(90-Latitude))^1.05)-(0.1*(Altitude)^0.5)-(0.25*
(Longitude+500)^0.5)
This formula gives the mean annual surface water temperature of the given lake. This value is used as an averaging function in the smoothing function: The higher the predicted mean annual lake temperature, the smaller the seasonal variability in lake temperature.

Mean_depth = Volume/Lake_area
The mean depth of the lake in m.

Month_of_fallout = 5
This is the month of the fallout. 1 for January, etc.

Monthly_epilimnic_temp = if Seasonal_variability_in_temp <0 then 0.1 else
Seasonal_variability_in_temp
These are the predicted mean monthly values of epilimnetic temperatures (°C).

Monthly_hypolimnic_temp = if Mean_annual_temp >17 or Mean_annual_temp < 4 or
Seasonal_variability_in_temp <4 then 0.1
else (SMTH1(Seasonal_variability_in_temp, Mean_annual_temp^0.5, Seasonal_variability_in_temp))
/((4*(17-Mean_annual_temp)^0.5+10)/(30*((1.1/(Mean_depth+0.1)+0.2)/1.2)))
These are the predicted mean monthly values of hypolimnetic temperatures (°C). This is only valid

for dimictic lakes, which lie between latitudes 30 and 60° N and at altitudes from 0 to 4000 m [II.40]. The relationship between surface water and bottom water temperatures is also assumed to depend on the mean depth of the lake: The smaller the mean depth, the smaller the difference between surface and water temperatures.

Outflow_areas_OA = 0.1
This is the default value for the percentage of outflow areas in the catchment. The value 0.1 (= 10%) is used as a default value of wet lands (mires, lakes, rivers, bogs, etc.) in catchment areas for the VAMP lakes.

Outflow_rate_from_catchment =
Seasonal_moderator*0.04/(12*(sqrt(DELAY(TIME, Month_of_fallout, 1))))
This is the outflow rate (1/month) from the catchment, or rather from the outflow areas (the wet land) of the catchment. This is the general formula for the rate, which is modified by the seasonal moderator (an increased rate during spring and fall peaks). The rate is time dependent: It decreases with time from the month of the fallout (given by $1/\sqrt{time}$). A delay function initiates the runoff to the month of the fallout. The initial value of the runoff is set to 0.1 for the first year after the fallout, i.e., a mean average runoff of 10%. The outflow rate function will cause this initial outflow rate to decrease with time. The seasonal moderator for Q and T influences the seasonal variability in outflow rate. The equation modifies the mean outflow rate with the seasonal moderator (so rate increases during spring and fall). It also specifies that the rate depends on time after the fallout event: given by $1/\sqrt{(time+1)}$, where time, in months, is measured from the month of the fallout (time = 0).

Part_coeff_Kd = 1/(1.04+(1.75*((pH/4)-1)^2))
This is the distribution (partition) coefficient (K_d) often defined as the ratio between the particulate phase (P) and the dissolved phase (D). The K_d value in this modelling set-up is influenced by lake pH: The lower the pH, the more ^{137}Cs in dissolved phase. This is described by a calibrated algorithm. D+P=T (=total); P/D=1; D/T=0.33; P/T=0.67. This algorithm (a dimensionless moderator) is assumed to be valid for lakes with pH in the range between 4 and 9, and it sets the K_d value to 0.96 for a lake with pH=4 and to 0.26 for a lake with pH=9. The formula is the general type: $1/(x+amp*(pH/board)-1)^z$, where x and the exponent z are empirical constants, board is a borderline value (here set to pH=4), and amp is an amplitude value (here set to 1.75).

pH = 6.8
The characteristic lake pH.

pH_plus_K = (pH+K)
Physical_half-life_for_Cs = 0.693/(30.2*12)
The physical half-life of ^{137}Cs is 30.2 years=30.2*12=362.4 months. The retention rate is ln(0.5)/362.4=0.00191. $A(t)=A(0)*e^{-kt}$; A(t)/A(0)=0.5; ln(0.5)=-kt; k=-ln(0.5)/t.

Phytoplankton_biomass = (Prim_production*Lake_area*2*10*(1/12)*(1/1000))
The phytoplankton biomass is given by the primary production, which is an important driving environmental variable in this model. Primary production in (g $C \cdot m^{-2} \cdot a^{-1}$) times (area) times (1/12 for month) times (2, to get g dw phytoplankton from g carbon) times 10 (to get g ww) divided by 1000 (to get kg ww). The default value for Swedish forest lakes is about 25-30.

Phytoplankton_outflow_rate = 5/30
The retention time for ^{137}Cs in phytoplankton is set to 1 month, i.e. the retention rate is 1/1.

Phytoplanktonic_uptake_rate = YpH_plus_K*0.005
It is assumed that 0.5% of the dissolved ^{137}Cs in the lake water may be taken up by phytoplankton per month, i.e. the phytoplankton biouptake rate is 0.005. This rate is modified by the dimensionless moderator for pH plus K.

Precipitation = 800
The mean annual precipitation in mm/year. The higher the precipitation, the greater the potential seasonal variability, when everything else is kept constant.

Predator_biomass = Prey_biomass/(2*(Transfer_coeff)^0.4)
The biomass of the predatory fish could often be assumed to be about 5% of the biomass of the prey (including zooplankton). But that is a simplification, and in this model we have defined a transfer coefficient which should give a more realistic relationship between the plankton biomass and the prey biomass. So, here the biomass of predatory fish is given not by 0.05*prey biomass but by a function related to the transfer coefficient (Plankton biomass/prey biomass). This function uses the same input (lake primary production), but the ratio between plankton biomass/prey biomass should give a significantly larger range than the ratio between prey biomass/predator biomass; the transfer coefficient gives a range from 2.5 to 22.8, i.e. with a factor of 9 to 10; the ratio prey biomass to predator biomass gives, with this definition, a range of 4.5 to 10.3, i.e. with a factor of about 2.3.

Prey_and_predator_outflow_rate = 0.693/(100/30)
It is assumed that the biological retention time (=half-life) of the element in predator fish is x days, and that the retention coefficient is given by 0.693/x. x is set to:
200 days for ^{137}Cs for large pike (1000 g; main diet = fish) and large, predatory perch (250 g; diet =fish);
150 days for median perch (50 to 250 g; mixed diet = benthos, zooplankton and fish);
125 days for small perch (15 to 50 g; diet =zooplankton)
100 days for minnow (15 g; mixed diet of plant and benthos), trout (200 g; diet = benthos), etc.;
75 days for whitefish (200 g; diet = zooplankton), smelt (15 g; diet = zooplankton), roach (100 g; mixed diet of benthos and zooplankton), perch fry (< 10 g; diet = zooplankton), bream (200 g; diet = benthos), etc.;
7 days for zooplankton; and
5 days for phytoplankton.
The retention time for other predatory species may then be estimated from these guidelines values. The retention time for ^{137}Cs in the prey is generally half of that for predatory.

Prey_biomass = (Phytoplankton_biomass/Transfer_coeff)
The biomass of the prey fish could often by assumed to be about 10% of the biomass of the plankton. But that is a simplification, and in this model we have defined a transfer coefficient which should give a more realistic relationship between the plankton biomass and the prey biomass. So, here the prey biomass is given not by 0.1*phytoplankton biomass but by the ratio between phytoplankton biomass and the transfer coefficient, which is small for low productive lakes and high for eutrophic lakes.

Prim_production = 27.5
This is the mean primary production of the lake in g $C \cdot m^{-2} \cdot a^{-1}$.

Ratio_Epi_to_Hypo = (Monthly_epilimnic_temp+1)/(Monthly_hypolimnic_temp+1)
Retention_in_lake_water = Seasonal_moderator
/Water_retention_time^((30/(Water_retention_time+29)+0.5)/(1.5))
The retention rate (in 1/months) of the lake water. It is generally set to $1/T^1$ in mass-balance calculations; here this expression is first modified by the seasonal moderator for lake water retention time. For large, deep lakes with small drainage areas, i.e. lakes with a long theoretical water retention time (T), it is evident that thermal and chemical stratifications, hydrological flow patterns and currents would influence the retention time of the water and contaminants: Then, should one use the entire lake volume, the volume of the epilimnetic water, or the volume of a defined fraction of the epilimnetic water in the calculation of the retention time? From lake eutrophication studies [II.41], it is well known that better predictions of lake concentrations of total-P are obtained if one uses $\sqrt{T}$ rather than T in mass-balance calculations. In this model, we will

define a function for the exponent in the expression $1/T^{exp}$. This exponent (exp) should be about 1 in lakes with a quick water retention (T<6 months) and it should approach 0.5 for lakes with a long theoretical water retention time (T>48 months). There are several ways to define such a formula, e.g.:

A. 1/T^(1.25-((T)^0.3)/4)
B. 1/T^((x/T)+1)/(z+1)^z; e.g. for x=z=1 or x=z=0.5 of other combinations.
C. 1/T^((x/(T+x-1)+z)/(z+1)); e.g. for x=50 and z=0.25 of other combinations.

In the following model, we have used alternative C. This formula is based on empirical studies in the VAMP lakes. It yields a faster and more adequate retention in lakes with long water retention. It is valid for lake with T larger than 1 month. This approach is meant to give better descriptions of the water retention processes and improve the predictive power of the model.

Figure III.6A illustrates the relationship between T and different retention rates.

Retention_rate_in_active_sediments =
Sedimentation_rate_of_susp_matter/Thickness_of_active_sediments
This is the mean age (in months) of the active sediments. If the thickness of the active sediment layer is 10 cm, the rate of sedimentation is 0.1 cm/year, then the mean age of the active sediment layer is 10/0.1=50 years. The corresponding retention rate is 1/100.

Seasonal_moderator = SMTH1(Seasonal_variability_norm, Averaging_function, 1)
Here we will use a smoothing factor (called smth1), which works similar to a running mean value for a certain number of months before and after a given month). If we take a mean value for many months, the averaging effect will be high and the seasonal variability low. The number of months used for this calculation is given by the averaging function. The initial value is set to one, since this corresponds to the mean value of the averaging function over one year. The seasonal moderator will be used here to influence the outflow rate from the catchment (from outflow areas). A high value of the seasonal moderator (during spring and fall peaks) will increase the runoff from land to water, and *vice versa.*

Seasonal_variability_in_temp = if Mean_annual_temp<(-10) then 0 else
Mean_annual_temp+SMTH1(Seasonal_var_mod_temp, (Mean_annual_ temp/5)*((Volume*10^(-6))^0.1),0)
This is the predicted mean monthly temperature of lake surface water. Monthly temperatures are set to 0 in permanently frozen lakes.

Sedimentation_rate_of_Cs = 1/Mean_depth
It is assumed that the annual settling velocity for the carrier particles for ^{137}Cs is 10 m/month (see Håkanson and Jansson, 1983[II.37]), i.e. for a lake with a mean depth of 10 m, 1/1 of the particulate ^{137}Cs may be deposited during one month, i.e., the sedimentation rate is 10/Dm.

Sedimentation_rate_of_susp_matter = 60/13200
The sedimentation rate, v, in $g \cdot m^{-2} \cdot a^{-1}$ (dw); v*(100/(100-W))*(1/d)*(1/(1000*12))=v/13200 cm/month; W=water content. This relationship, to transform values of sedimentation rates from $g \cdot m^{-2} \cdot a^{-1}$ (dw) to cm/month, may be used if W is set to be 90% and if d=bulk density is set to be 1.1 g/cm^3 (ww). A common value for Swedish lakes is 0.4 cm/year or 430 $g \cdot m^{-2} \cdot a^{-1}$ (dw) [II.38].

Thickness_of_active_sediments = 10
The default value is set to 10 cm. Note that the dimension here is cm not m. Note also that this is a model variable in this model, not an environmental variable. This means that the same value of 10 cm should preferably be used for all lakes. The reason for this simplification is that it is generally very difficult to give any solid scientific estimate concerning this limit, the bioturbation limit, in most lakes. It is not a constant, but a variable [II.38].

Transfer_coeff = (Prim_production+1)^0.65
It is often assumed that the biomass of the prey (small fish and zooplankton) is about 1/10 of the phytoplankton biomass in a typical Swedish forest lake. This is, naturally, a simplification. The ratio between phytoplankton biomass and prey biomass is often about 1/3 in very oligotrophic lakes and as low as 1/50 in hypertrophic lakes. The ratio does not increase linearly with primary production. Here, this ratio is called the transfer coefficient to indicate a transfer (consumption) of biomass (carbon) between different trophic levels in the lake ecosystem. Data on ^{137}Cs may be used to study how this transfer coefficient varies among the VAMP lakes. This is also interesting from a classical limnological perspective, since it means that knowledge may be gained on the relationship between these biomasses at different levels of primary production. The empirical calibrations for the VAMP lakes indicate that the transfer coefficient (=Phytoplankton biomass/Prey biomass) may be given by the function: $(Prim\_production+1)^{0.6}$.

Thus, the transfer coefficient is defined to give a general, simple, realistic relation between the biomass of the plankton and the prey. This transfer coefficient has been derived by empirical calibrations using the data for the VAMP lakes. The choice of the transfer coefficient is important for the ^{137}Cs concentrations of predatory fish because that concentration is calculated as amount/predatory biomass and predatory biomass is calculated as plankton biomass/transfer coefficient.

This means that the value is about 7.5 for a Swedish forest lake with a primary production of 25-30 g $C \cdot m^{-2} \cdot a^{-1}$, and about 34 for a very productive lake (like the Dutch lake IJsselmeer) with a primary production of 350 g $C \cdot m^{-2} \cdot a^{-1}$, and about 1.5 for an extreme low productive lake (the Italian lake Bracciano). This gives a range of about 20 for the VAMP-lakes, which cover a very wide range in terms of lake primary productivity.

In analogy, one could also define a transfer coefficient between prey (including zooplankton) and predatory fish. This ratio should be about 1/2 to 1/3 in a typical Swedish forest lake. The range in the ratio between very oligotrophic and very eutrophic lakes should be smaller than the range of 20 for the transfer coefficient between phytoplankton and prey. Using the data for the VAMP-lakes for calibrations, we have arrived at the following simple expression for the biomass for predatory fish:

Prey_biomass/(Transfer_coeff^0.4)

This gives a value of 3.7 for $Transfer\_coeff^{0.4}$ for a typical Swedish forest lake with a primary production of 25-30 g $C \cdot m^{-2} \cdot a^{-1}$, and about 4.1 for a very productive lake (Lake IJsselmeer) with a primary production of 350 g $C \cdot m^{-2} \cdot a^{-1}$, and about 1.15 for an extreme low-productive lake (Lake Bracciano). This gives a range of about 3.5 for the VAMP lakes.

Figure 5.77 gives the primary production on the x-axis and:
(A) the transfer coefficient, i.e., the ratio between the prey biomass and the predator fish biomass, and the formula relating the transfer coefficient to the primary production; it also illustrates the different classes of lakes: Oligotrophic to hypertrophic;
(B) the linear relationship between primary production and phytoplankton biomass;
(C) the non-linear relationship between the prey biomass and the primary production, and
(D) the non-linear relationship between the predator biomass and the primary production.

Volume = 3.7*10^6
Lake volume in m^3.

Water_retention_time = 63/30
This is the theoretical water retention time for the lake in months.

Atmospheric_load = GRAPH(TIME)
(1.00, 0.00), (2.00, 0.00), (3.00, 0.00), (4.00, 0.00), (5.00, 130), (6.00, 0.00), (7.00, 0.00), (8.00, 0.00), (9.00, 0.00), (10.0, 0.00), (11.0, 0.00), (12.0, 0.00), (13.0, 0.00), (14.0, 0.00), (15.0, 0.00), (16.0, 0.00), (17.0, 0.00), (18.0, 0.00), (19.0, 0.00), (20.0, 0.00), (21.0, 0.00), (22.0, 0.00), (23.0, 0.00), (24.0, 0.00), (25.0, 0.00), (26.0, 0.00), (27.0, 0.00), (28.0, 0.00), (29.0, 0.00), (30.0, 0.00), (31.0, 0.00), (32.0, 0.00), (33.0, 0.00), (34.0, 0.00), (35.0, 0.00), (36.0, 0.00), (37.0, 0.00), (38.0, 0.00), (39.0, 0.00), (40.0, 0.00), (41.0, 0.00), (42.0, 0.00), (43.0, 0.00), (44.0, 0.00), (45.0, 0.00), (46.0, 0.00), (47.0, 0.00), (48.0, 0.00), (49.0, 0.00), (50.0, 0.00), (51.0, 0.00), (52.0, 0.00), (53.0, 0.00) ...
This is the mean fallout on the lake and its catchment area in kBq/m2.

Internal_loading_rate = GRAPH(Ratio_Epi_to_Hypo)
(-5.00, 0.00025), (-2.50, 0.0017), (0.00, 0.0099), (2.50, 0.00575), (5.00, 0.00295), (7.50, 0.0011), (10.0, 0.0009), (12.5, 0.0009), (15.0, 0.00075), (17.5, 0.00065), (20.0, 0.00055), (22.5, 0.00035), (25.0, 0.0003)

Seasonal_var_mod_temp = GRAPH(TIME)
(1.00, -20.0), (2.00, -8.00), (3.00, -2.00), (4.00, 0.00), (5.00, 2.00), (6.00, 8.00), (7.00, 20.0), (8.00, 8.00), (9.00, 2.00), (10.0, 0.00), (11.0, -2.00), (12.0, -8.00), (13.0, -20.0), (14.0, -8.00), (15.0, -2.00), (16.0, 0.00), (17.0, 2.00), (18.0, 8.00), (19.0, 20.0), (20.0, 8.00), (21.0, 2.00), (22.0, 0.00), (23.0, -2.00), (24.0, -8.00), (25.0, -20.0), (26.0, -8.00), (27.0, -2.00), (28.0, 0.00), (29.0, 2.00), (30.0, 8.00), (31.0, 20.0), (32.0, 8.00), (33.0, 2.00), (34.0, 0.00), (35.0, -2.00), (36.0, -8.00), (37.0, -20.0), (38.0, -8.00), (39.0, -2.00), (40.0, 0.00), (41.0, 2.00), (42.0, 8.00), (43.0, 20.0), (44.0, 8.00), (45.0, 2.00), (46.0, 0.00), (47.0, -2.00), (48.0, -8.00), (49.0, -20.0), (50.0, -8.00), (51.0, -2.00), (52.0, 0.00), (53.0, 2.00) ...
This is the seasonal variability norm for surface water temperature. A smoothing function changes this norm, so temperatures in lakes with high predicted mean annual water temperatures vary much less than in colder lakes. Values in °C.

Seasonal_variability_norm = GRAPH(TIME)
(1.00, 0.001), (2.00, 0.002), (3.00, 0.2), (4.00, 6.00), (5.00, 1.50), (6.00, 0.5), (7.00, 0.02), (8.00, 0.06), (9.00, 0.2), (10.0, 1.00), (11.0, 0.1), (12.0, 0.002), (13.0, 0.001), (14.0, 0.002), (15.0, 0.2), (16.0, 6.00), (17.0, 1.50), (18.0, 0.5), (19.0, 0.02), (20.0, 0.06), (21.0, 0.2), (22.0, 1.00), (23.0, 0.1), (24.0, 0.002), (25.0, 0.001), (26.0, 0.002), (27.0, 0.2), (28.0, 6.00), (29.0, 1.50), (30.0, 0.5), (31.0, 0.02), (32.0, 0.06), (33.0, 0.2), (34.0, 1.00), (35.0, 0.1), (36.0, 0.002), (37.0, 0.001), (38.0, 0.002), (39.0, 0.2), (40.0, 6.00), (41.0, 1.50), (42.0, 0.5), (43.0, 0.02), (44.0, 0.06), (45.0, 0.2), (46.0, 1.00), (47.0, 0.1), (48.0, 0.002), (49.0, 0.001), (50.0, 0.002), (51.0, 0.2), (52.0, 6.00), (53.0, 1.50) ...
This graph defines the seasonal variability norm for Q and T. It represents extreme variations in monthly tributary discharge and theoretical lake water retention time. The values are generally without dimension.

YpH_plus_K = GRAPH(pH_plus_K)
(4.00, 1.00), (4.47, 0.805), (4.95, 0.645), (5.42, 0.45), (5.90, 0.31), (6.37, 0.25), (6.85, 0.19), (7.32, 0.17), (7.79, 0.15), (8.27, 0.11), (8.74, 0.09), (9.22, 0.07), (9.69, 0.05), (10.2, 0.037), (10.6, 0.036), (11.1, 0.036), (11.6, 0.036), (12.1, 0.036), (12.5, 0.036), (13.0, 0.036), (13.5, 0.035), (14.0, 0.035), (14.4, 0.035), (14.9, 0.035), (15.4, 0.035), (15.9, 0.035), (16.3, 0.035), (16.8, 0.034), (17.3, 0.034), (17.8, 0.034), (18.2, 0.034), (18.7, 0.034), (19.2, 0.034), (19.6, 0.034), (20.1, 0.034), (20.6, 0.034), (21.1, 0.034), (21.5, 0.034), (22.0, 0.033), (22.5, 0.033), (23.0, 0.033), (23.4, 0.033), (23.9, 0.033), (24.4, 0.033), (24.9, 0.033), (25.3, 0.033), (25.8, 0.033), (26.3, 0.033), (26.8, 0.033), (27.2, 0.033), (27.7, 0.033), (28.2, 0.033), (28.7, 0.033) ...
This is a graph for a dimensionless moderator expressing the fact that the biouptake of ^{137}Cs by plankton (here mainly phytoplankton) depends on the pH and the K-concentration of the lake water: The lower pH and K, the higher the uptake, and *vice versa*.

II.5. DESCRIPTION OF THE VTT MODEL

II.5.1. Model structure

The conceptual model DETRA [II.42] applied for aquatic ecosystems is presented in Figure 4.11. The drainage area, the sediments and the dynamic fish model are connected with the lake recipient which radiologically forms an essential part of the model.

The primary radioactive source term is the direct deposition on the lake surface. With some delay time, part of the fallout which have deposited on the drainage area will also reach the lake water. The activity source from the drainage area is called the secondary source term.

The model used is a general model which can be applied for analyses of various lakes. In each specific application relevant input data have to be used. The flow rates of solid material and water between compartments have to be specified. Additionally the local sorption circumstances have to be considered by selecting reasonable distribution coefficients K_d for the elements. The essential lake specific data which are used in modelling are presented in Table II.6.

The dynamic fish model represents a general modelling approach for non-predator – intermediate – predator fish chain. Assumptions of different fish populations can be flexibly varied and one can select the corresponding input data for the fish model.

In the VAMP exercise for lakes, the same conceptual model presented above in Figure 4.11 is used for each lake. The parameter values, as given in the description of lakes, are however selected separately for each lake in the model.

TABLE II.6. DATA USED FOR THE VAMP LAKES

Lake	Water turnover time, (a)	Suspended sediment load, (mg/L)	Sediment-ation rate, ($g \cdot m^{-2} \cdot a^{-1}$)	Distribution coefficient, K_d, (L/kg)	Area, (km^2)	Mean depth, (m)
Iso Valkjärvi	3	9×10^{-1}	1×10^{2}	1×10^{3}	4.2×10^{-2}	3
Bracciano	137	9×10^{-1}	1×10^{2}	1×10^{3}	5.7×10^{1}	8.9×10^{1}
Øvre Heimdalsvatn	1.7×10^{-1}	3×10^{-1}	9×10^{1}	1×10^{3}	7.8×10^{-1}	4.7
IJsselmeer	4.1×10^{-1}	4×10^{1}	5×10^{2}	1×10^{3}	1.1×10^{3}	4.3
Hillesjön	3.6×10^{-1}	5	4×10^{1}	9×10^{2}	1.6	1.7
Devoke Water	2.4×10^{-1}	5×10^{-1}	3×10^{2}	1×10^{3}	3.4×10^{-1}	4
Esthwaite Water	1.9×10^{-1}	1	7×10^{2}	1×10^{3}	1	6.4

II.5.2. Methods for prediction of transfer

In terrestrial and aquatic environments radionuclides are carried by water and by solid matter. The element specific distribution coefficient, K_d, is used for describing sorption between liquid and solid phases. The fractions of activity present in liquid and solid phases in steady state conditions can be calculated as follows:

$$F_w = \frac{1}{1 + K_d \cdot SM} \tag{II.57}$$

$$F_s = 1 - F_w \tag{II.58}$$

where
F_w is the fraction in water (dimensionless),
F_s is the fraction in solids (dimensionless),
K_d is the distribution coefficient (m^3/kg),
SM is the concentration of solid material in soil (kg_s/m^3_{tot}).

The total transfer rate of a radionuclide can generally be obtained as follows:

$$\lambda_{tot}=F_s\cdot\frac{dm_s}{dt}\cdot\frac{1}{m_s}+F_w\cdot\frac{dm_w}{dt}\cdot\frac{1}{m_w}+\lambda_i \qquad \text{(II.59)}$$

where
λ_{tot} is the total transfer rate (a^{-1}),
λ_i is the radioactive decay rate of radionuclide i (a^{-1}),
m_s is the mass of solid material in a specific compartment (kg_s),
m_w is the mass of water in a specific compartment (kg_w).

In aquatic ecosystems there are several mechanisms which transfer substances from one place to another. Looking at the lake recipient, the radionuclides are transferred to bottom sediments by sedimentation of the suspended material in the lake water. The resuspension of sedimented material causes some return of radionuclides to the lake water. The turnover of lake water affects transfer of radionuclides from and to the lake.

The transfer related to the drainage areas of lakes forms a special case because the radionuclides are transferred, not only by transport of water infiltrated into the surface soil, but also by erosion from the drainage area. These mechanisms gather the activity from the drainage area and the activity will, at least partly, end up into the lake. The activity which ends up into the lake will experience the same transfer mechanisms in the lake as the primary source which originates from the direct deposition on the lake. Additionally, the secondary source term is diluted by precipitation on the drainage area. Therefore, although the drainage area brings about additional activity flow into the lake, it is at the same time compensated to some extent by the additional dilution which is caused by precipitation. Based on a mass balance equation, the total transfer rate from the drainage area into the lake can be estimated as follows:

$$\lambda_{tot,e}=\frac{1}{h}\cdot\left(F_s\cdot\frac{e}{(1-\varepsilon)\cdot\zeta_s}+F_w\cdot\frac{r}{\varepsilon}\right) \qquad \text{(II.60)}$$

where
$\lambda_{tot,e}$ is the total transfer rate from the drainage area into the lake (1/a),
h is the effective depth of soil layer for water infiltration (m),
r is the mean net precipitation rate (m/a),
e is the erosion rate (erosion from drainage area to lake surface) ($kg_s\cdot m^{-2}\cdot a^{-1}$),
ε is the porosity of the soil layer (-),
ζ_s is the density of solid material (kg_s/m^3_s).

Methods for calculation of transfer rates which are applied in the DETRA code are presented in Section 4.3.

II.5.3. The fish model

The dynamic fish model is based on realistic follow-up of activity balance in the lake ecosystem. The K_d values and the mass flow rate approach is applied to describe the transfer of radionuclides from plankton to fish, prey fish to intermediate and predatory fish, etc. The interdependence between

plankton and fish populations determines the consumption rates of plankton by fish. Table II.7 presents the consumption rates used in the model.

The biological half-lives, presented also in Table II.7, are mean values over a year. In reality the metabolism of fishes is faster during the summer compared to the winter. This is because of the rise of the temperature of lake water which stimulates the metabolism of fishes and other organisms in the aquatic environment.

The biological half-lives depict the time constants of activity removal related to different fish types. For prey fish the accumulation rate and removal rate of caesium are faster than in the case of predators. Different time constants reflect the differences between various fish types.

The compartment model employed for fish food chain is presented in Figure II.11. The food chain leading to fish is described by non-predator/intermediate – predator – top predator path. The non-predator/intermediate fish includes fishes such as roach, vendace and small perch. The predator represents fish such as large perch. The top predator includes fish such as pike and trout.

According to the model and experimental data, the maximum concentrations in different types of fish species are obtained after certain time delays. The maximum concentration in non-predatory fish is reached first and the maximum for top predatory fish last. Typically, the maximum in non-predatory fish can be reached after few months and the maximum in top predator after one to two years.

TABLE II.7. FISH MODEL PARAMETERS

Plankton eaten by fish, ($kg_{d\,w\ plankton}/d \cdot kg_{f\,w\ fish}$)	4×10^{-3}
Non-predatory fish eaten by predatory fish, (kg/d·kg)	3×10^{-3}
Intermediate fish eaten by predatory fish, (kg/d·kg)	7×10^{-3}

Fish type:	Biological half-lives of Cs in different fish types, $T_{½,b}$ (day)
Non-predatory fish	100
Intermediate fish	200
Predatory fish	300

Appendix III

CAESIUM-137 DATABASE

This appendix contains data on ^{137}Cs (for Bracciano, ^{134}Cs) concentrations in water, sediments, fish and other biological species in the seven lakes selected by the VAMP Aquatic Working Group/Lake Subgroup for the model validation exercise. It should be noted that the radioactivity measurements in most of the lakes and the samples taken for them were not planned for the needs of model validation but for purposes of radiation protection and radioecological studies. However, in some cases the sampling programme was later modified to meet the needs of the VAMP project.

The fish results given are mainly from pooled samples. In some cases, when the original samples were analysed in many age or size groups the results are given as geometrical means of original pooled samples.

This Appendix contains data collected during the first four to five years after the Chernobyl accident. However, data collection has continued in several of the lakes and this more recent data may be obtained by contacting the data suppliers listed at the end of this Report.

TABLE III.1. CAESIUM-137 IN ØVRE HEIMDALSVATN

Sample	Date			^{137}Cs	Remarks	Remarks
	day	month	year	(Bq/m^3)		
Water		6	86	5500	lake	unfiltered
Water	23	5	89	48	inflow	$M<10^4$ Dalton
Water	23	5	89	203	inflow	$M<10^4$ Dalton
Water	23	5	89	251	inflow	total
Water	22	3	90	160	inflow	total
Water	25	5	89	51	outflow	$M<10^4$ Dalton
Water	25	5	89	65	outflow	$M<10^4$ Dalton
Water	25	5	89	116	outflow	total
Water	22	3	90	100	outflow	total
Sample	**Date**			**^{137}Cs**	**Remarks**	**Remarks**
	day	**month**	**year**	**(Bq/kg dw)**		
CPOM	23	5	89	3089	inflow 1	> 0.9 mm
CPOM	25	5	89	3108	inflow 1	> 0.9 mm
CPOM	30	9	89	530	inflow 1	> 0.9 mm
CPOM	23	5	89	5216	inflow 2	> 0.9 mm
CPOM	25	5	89	10782	inflow 2	> 0.9 mm
CPOM	30	9	89	300	inflow 2	> 0.9 mm
CPOM	23	5	89	22201	lake outflow	> 0.9 mm
CPOM	30	9	89	675	lake outflow	> 0.9 mm
Sample	**Date**			**^{137}Cs**	**Remarks**	**Remarks**
	day	**month**	**year**			
Sediment	28	8	86	690	Bq/kg ww	mean upper 10 cm
Sediment	2	10	89	50.6	kBq/m^2	mean S.D. 31.4
				45	kBq/m^2	median
Sample	**Date**			**^{137}Cs**	**Remarks**	
	day	**month**	**year**	**(Bq/kg ww)**		
Macrophytes	28	8	86	420	Isoetes lacustris	
Zooplankton	28	8	86	3500	Bosmina longispina	
Stonefly	25	7	86	860	Diura nanseni	
Stonefly	25	7	86	2720	Arcynopteryx compacta	
Mayfly	28	8	86	1850	Siphlonurus lacustris	
Gammarus	28	8	86	1850	Gammarus lacustris	

TABLE III.1. CAESIUM-137 IN ØVRE HEIMDALSVATN (cont.)

Sample	Date			^{137}Cs (Bq/kg fw)				No. of fish
	day	month	year	Geom. mean C.L. 95%		Aritm. mean C.L. 95%	Range	
Brown trout	11	6	86	227	125–410	259 ± 140	91–414	6
Brown trout	8	7	86	1000				5
Brown trout	4	8	86	2495	1431–4349	2802 ± 1525	1441–4778	6
Brown trout	28	8	86	4653	3668–5889	4753 ± 1134	3444–6405	6
Brown trout	24	9	86	3716	2193–6300	4159 ± 2439	2209–8395	6
Brown trout	4	10	86	4101	2059–8171	4810 ± 2777	1494–7909	6
Brown trout	23	6	87	4048	3221–5087	4294 ± 987	2260–7360	12
Brown trout	11	7	87	3942	2493–6233	4484 ± 1525	1670–7030	9
Brown trout	6	9	87	3619	2852–5072	4117 ± 1220	1320–8400	13
Brown trout	3	10	87	3473	1872–6443	4091 ± 2078	1070–7330	7
Brown trout	28	6	88	2976	1953–4531	3264 ± 1485	1650–6390	7
Brown trout	20	7	88	3196	2682–3809	3392 ± 552	1770–4860	19
Brown trout	30	8	88	2853		3340	1300–5430	6
Brown trout	4	10	88	3268	2556–4179	3524 ± 753	1650–7680	14
Brown trout	20	6	89	2149	1593–2898	2429 ± 642	660–4590	15
Brown trout	5	8	89	1461	954–2237	1709 ± 707	720–3410	10
Brown trout	27	8	89	1621	1237–2123	1755 ± 453	750–3020	12
Brown trout	30	9	89	2291	1794–2933	2578.± 550	720–4481	20
Brown trout	12	6	90	2174	1658–2847	2334 ± 436	831–4080	16
Brown trout	8	7	90	2002	1685–2378	2119 ± 313	729–3282	20
Brown trout	25	8	90	1712	931–3147	2018 ± 616	825–4420	16
Brown trout	28	9	90	2030	1509–2731	2235 ± 549	680–3514	13
Brown trout		3	91	1517	1220–1888	1672 ± 370	708–3380	19
Brown trout		6	91	1216	885–1671	1370 ± 461	666–2806	12
Brown trout		8	91	1358	985–1872	1552 ± 471	564–3625	14
Brown trout		9	91	1419	1103–1826	1599 ± 339	353–2998	20
Brown trout		6	92	1399	1053–1860	1584 ± 458	610–3190	15
Brown trout biomass c. 1000 kg								
Brown trout density c. 15 kg/ha								

TABLE III.1. CAESIUM-137 IN ØVRE HEIMDALSVATN (cont.)

Sample	Date			^{137}Cs
	day	month	year	(Bq/kg fw)
Minnow	25	8	86	5800
Minnow	25	8	90	1010
Brown trout, milt	28	8	86	860
Brown trout, milt	8	9	90	1720
Brown trout, eggs	28	8	86	2400
Brown trout, eggs	6	9	87	1300
Brown trout, eggs	3	10	87	1880
Brown trout, eggs	29	9	89	840
Brown trout, eggs	29	9	89	813
Brown trout, eggs	29	9	89	1012
Brown trout, eggs	25	8	90	605
Brown trout, eggs	27	9	90	665
Deposition to lake and catchment				
Mean 130 kBq/m^2				
Range 26–260 kBq/m^2				

TABLE III.2. CAESIUM-137 IN DEVOKE WATER

Sample	Nominal date			^{137}Cs	No. of samples	Sampling period	
	day	month	year	(Bq/m^3)			
Water	30	8	86	236	4	7.8–22.9	
Water	17	11	86	149	4	29.10–7.12	
Water	8	2	87	97	5	15.1–4.3	
Water	26	4	87	77	12	20.4–1.6	
Water	20	7	87	76	7	6.7–3.8	
Water	26	9	87	61	7	3.9–15.10	
Water	28	2	88	60	9	28.1–28.3	
Sample	**Nominal or actual date**			**^{137}Cs**	**No. of samples**	**Sampling period**	**Weight range**
	day	**month**	**year**	**(Bq/kg fw)**			**(g)**
Perch	5	9	86	834	1		295
Perch	11	9	86	1312	2		30–150
Perch	22	9	86	1502	12		30–250
Perch	31	10	86	1168	6	29.10–1.11	148–369
Perch	8	12	86	1375	2	7–8.12	148–225
Perch	17	2	87	2092	10	13–20.2	231–409
Perch	12	3	87	1636	2		292–294
Perch	21	3	87	1591	13	20–23.3	147–450
Perch	1	4	87	1483	6	31.3–1.4	157–387
Perch	14	4	87	1222	10		150–274
Perch	1	5	87	1466	8		128–304
Perch	14	5	87	1287	8		131–277
Perch	1	6	87	1052	6		
Perch	1	6	87	911	6		
Perch	2	6	87	1616	6		166–185
Perch	7	7	87	1610	6		
Perch	5	8	87	2055	6		207–628
Perch	4	9	87	1663	6		194–287
Perch	15	10	87	641	1		92
Perch	23	11	87	722	3		63–153
Perch	30	3	88	1473	2		96–104

TABLE III.2. CAESIUM-137 IN DEVOKE WATER (cont.)

Sample	Nominal date			^{137}Cs	No. of samples	Sampling period	Weight range
	day	month	year	(Bq/kg fw)			(g)
Brown trout	15	4	86	14	2		210–218
Brown trout	5	9	86	542	3		100–289
Brown trout	19	9	86	687	2		59–285
Brown trout	21	9	86	605	1		326
Brown trout	22	9	86	744	3		312–475
Brown trout	29	10	86	1951	1		519
Brown trout	8	12	86	1032	5	7–8.12	55–378
Brown trout	16	2	87	1383	7	12–20.2	298–492
Brown trout	6	3	87	1371	2		262–390
Brown trout	21	3	87	934	3	20–21.3	265–308
Brown trout	24	3	87	520	1		282
Brown trout	31	3	87		1		133
Brown trout	31	3	87	722	10	29.3–1.4	81–491
Brown trout	15	4	87	539	7		65–295
Brown trout	1	5	87	528	6		69–257
Brown trout	14	5	87	305	4		171–230
Brown trout	2	6	87	679	6	1–2.6	123–359
Brown trout	7	7	87	761	8	6–8.7	60–344
Brown trout	20	7	87	595	8	16–24.7	78–296
Brown trout	4	8	87	1201	4		150–417
Brown trout	2	9	87	307	3		159–211
Brown trout	5	9	87	577			
Brown trout	16	10	87	653	9	15.10–16.10	124–362
Brown trout	20	11	87	384	6		83–185
Brown trout	23	11	87	644	3		133–166
Brown trout	30	1	88	420	7	29–31.1	86–165
Brown trout	2	3	88	364	7	1–2.3	61–202
Brown trout	29	3	88	339	6	27–31.3	30–189
Brown trout	30	3	88	405	11		131–199

TABLE III.3. CAESIUM-137 IN ESTHWAITE WATER

Sample	Date			^{137}Cs (Bq/m^3)		
	day	month	year	Particulate	Soluble	Total
Depth 3.0 m						
Water	13	5	86	73.96	203.40	277.30
Water	21	5	86	37.34	151.50	188.84
Water	4	6	86	14.47	81.51	95.97
Water	16	6	86	7.61	64.34	71.95
Water	2	7	86	14.47	61.41	75.88
Water	14	7	86	6.00	50.43	56.43
Water	30	7	86	17.16	34.30	51.46
Water	11	8	86	11.66	34.35	46.01
Water	1	9	86	7.13	42.26	49.39
Water	22	9	86	8.82	24.84	33.66
Water	20	10	86	< 2.15	< 2.81	
Water	19	11	86	2.72	8.73	11.45
Water	15	12	86	< 2.39	< 3.51	
Water	2	4	87		< 2.60	
Water	1	6	87		4.48	4.48
Water	24	8	87	< 1.87	< 2.88	
Water	30	11	87		< 3.23	
Water	25	4	88	< 6.10		
Water	8	12	88	< 7.90		< 3.2
Water	15	5	89	< 7.80		< 5.1
Water	2	5	90	< 1.60		< 1.3
Water	6	9	90			< 3.3
Water	24	6	91	< 0.40		0.8 ± 0.4

TABLE III.3. CAESIUM-137 IN ESTHWAITE WATER (cont.)

Sample	Date			^{137}Cs (Bq/m^3)		
	day	month	year	Particulate	Soluble	Total
Depth 13.5 m						
Water	13	5	86		189.20	189.2
Water	21	5	86	37.66	132.10	169.76
Water	4	6	86	11.26	99.98	111.24
Water	16	6	86	10.63	85.20	95.83
Water	2	7	86			
Water	14	7	86			92.38
Water	30	7	86			99.51
Water	11	8	86			94.67
Water	1	9	86			66
Water	22	9	86			30.42
Water	20	10	86	< 1.58	28.85	25.85
Water	19	11	86	< 2.24	6.06	6.06
Water	15	12	86	< 2.51		
Water	2	4	87		< 2.67	
Water	1	6	87		7.21	7.21
Water	24	8	87		8.08	8.08
Water	30	11	87		3.15	
Water	25	4	88	< 5.3		
Water	8	12	88	< 8.7		2.3 ± 1.4
Water	15	5	89	9.1 ± 4.0		< 2.5
Water	2	5	90	< 1.5		< 1.3
Water	6	9	90	< 5.0		< 3.7
Water	24	6	91	< 1.0		1.0 ± 0.6

TABLE III.3. CAESIUM-137 IN ESTHWAITE WATER (cont.)

Sample	Date			Bq/kg dw								
	day	month	year	0–1 cm	1–2 cm	2–3 cm	3–4 cm	4–5 cm	5–6 cm	6–7 cm	7–8 cm	8–9 cm	9–10 cm
Sediment	8	5	86	159	118	122	107	100					
Sediment	13	5	86	407	137	130	111	115					
Sediment	21	5	86	2479	189	122	144	137					
Sediment	4	6	86	1225	174	130	141	174					
Sediment	16	6	86	685	159	144	130	159					
Sediment	2	7	86	2357	263	211	207	215					
Sediment	14	7	86	3730	2810	455	202	232					
Sediment	30	7	86	2480	3080	487	182	193					
Sediment	11	8	86	2360	490	192	152	161					
Sediment	?	9	86	151	922	431	209	179					
Sediment	22	9	86	520	193	138	139	140					
Sediment	20	10	86	1550	394	161	140	163					
Sediment	3	11	86	1060	1460	358	157	159					
Sediment	19	11	86	751	312	174	157	142					
Sediment	15	12	86	751	477	184	140	< 11.1					
Sediment	2	4	87	433	555	202	155	145					
Sediment	1	6	87	399	331	224	179	206					
Sediment	24	8	87	619	595	392	256	185					
Sediment	30	11	87	351	505	668	426	183					
Sediment	25	4	88	410 ± 22	988 ± 43	798 ± 30	205 ± 15	157 ± 9					
Sediment	8	12	88	239	295	315	206	159					
Sediment	15	5	89	214 ± 14	169 ± 9	146 ± 9	157 ± 8	187 ± 9					
Sediment	2	5	90	226 ± 13	296 ±14	784 ± 32	463 ± 20	257 ± 12	195 ± 10	156 ± 8	143 ± 8	162 ± 8	225 ± 11
Sediment	6	9	90	260 ± 18	310 ± 16	265 ± 14	339 ± 18	472 ± 21	811 ± 33	593 ± 25	289 ± 14	237 ± 16	215 ± 11

TABLE III.4. CAESIUM-137 IN IJSSELMEER

Sample	Date			^{137}Cs
	day	month	year	(Bq/m^3)
Raw water	8	5	86	172.1
Raw water	15	5	86	207.5
Raw water	2	4	87	73.7
Raw water	11	11	87	20.8
Raw water	28	3	88	8.2
Raw water	7	11	88	4.1
Raw water	10	4	89	6.3
Raw water	13	11	89	4.1
Raw water	19	4	90	4.7
Raw water	7	11	90	3.5
Sample	**Date**			^{137}Cs
	day	month	year	(Bq/kg dw)
Plankton	24	8	87	9.16
Plankton	11	11	87	64.2
Plankton	28	3	88	27.5
Plankton	25	5	88	19.6
Plankton	20	6	88	53.1
Plankton	22	8	88	13.7
Plankton	7	11	88	8.4
Plankton	10	4	89	27.4
Plankton	26	6	89	21.1
Plankton	13	11	89	6.7
Plankton	19	4	90	20.2
Plankton	5	6	90	8.1

TABLE III.4. CAESIUM-137 IN IJSSELMEER (cont.)

Sample	Date			^{137}Cs(Bq/kg dw)	
	day	month	year	muscle	bones
Perch	8	5	86	6.9	5.3
Perch	13	5	86	9.6	8.3
Perch	8	4	87	391	211.8
Perch	16	11	87	190.5	116.4
Perch	11	4	88	155.5	90.4
Perch	31	10	88	64.3	40
Roach	3	10	84	a	a
Roach	8	5	86	12.1	6.7
Roach	13	5	86	23.4	22.3
Roach	8	4	87	82.7	57.2
Roach	16	11	87	35.4	23.7
Roach	11	4	88	32.5	21.1
Roach	31	10	88	17.5	10.6

Sample	Date			^{137}Cs	Year–class	No. of fish	Length	Weight
	day	month	year	(Bq/kg dw)			(cm)	(g)
Perch	3	10	84	2	1981	11	22.9	167.7
Perch	8	5	86	5.4	> 1984	6	22	170.8
Perch	13	5	86	9.9	> 1984	9	26.3	246.2
Perch	8	4	87	279.1	> 1984	11	23.5	189
Perch	3	7	87	112.3	1986	242	8.8	8.5
Perch	3	7	87	179.5	1985	75	13.1	27.7
Perch	18	8	87	40.4	1987	550	5.5	1.8
Perch	17	8	87	74.8	1986	90	11.1	16.6
Perch	17	8	87	143.5	1985	75	14.8	40.7
Perch	10	11	87	57.6	1987	368	7.2	3.6
Perch	9	11	87	75.9	1986	86	12.3	19.8
Perch	9	11	87	113.6	1985	30	15.8	47.3
Perch	16	11	87	142.3	> 1984	12	26.5	331.9
Perch	13	4	88	47	1987	194	11.1	4.4
Perch	11	4	88	74.6	1986	646	12.9	24.1

[a] Under the detection limit.

TABLE III.4. CAESIUM-137 IN IJSSELMEER (cont.)

Sample	Date			^{137}Cs	Year–class	No. of fish	Length	Weight
	day	month	year	(Bq/kg dw)			(cm)	(g)
Perch	11	4	88	86.7	1985	317	16.3	58.9
Perch	11	4	88	109.4	> 1984	110	21	142.2
Perch	20	6	88	54.9	1986	276	14.2	36.5
Perch	20	6	88	80.2	1985	177	17.4	68.2
Perch	20	6	88	125	1984	45	22.1	145.3
Perch	16	8	88	18.4	1988	343	5.5	1.9
Perch	16	8	88	45.9	1986	63	15.7	48.6
Perch	16	8	88	59.3	1985	35	19.2	97.6
Perch	31	10	88	23.9	1988	363	7.4	4.4
Perch	31	10	88	40.7	1987	41	13	25.8
Perch	31	10	88	43.5	1986	142	16.4	60.7
Perch	31	10	88	50.5	1985	81	20.7	130.1
Perch	30	3	89	18.3	1988	31	7.5	4.2
Perch	30	3	89	44.1	1987	24	13.9	33.9
Perch	30	3	89	48.9	1986	173	17.7	83.8
Perch	30	3	89	58.5	1985	125	22.4	194.4
Perch	21	6	89	5.6	1989	563	3.5	0.4
Perch	21	6	89	55.4	1986	61	19.7	101.7
Perch	15	8	89	12.5	1989	1104	6.7	3.2
Perch	15	8	89	20	1988	70	14.1	33.7
Perch	15	8	89	26.2	1987	13	18.2	79.7
Perch	15	8	89	34.5	1986	44	21.2	136.3
Perch	15	8	89	46.1	1985	21	23.5	178.8
Perch	15	11	89	18.5	1989	1242	7.7	4.2
Perch	15	11	89	20.4	1988	96	15.7	48.9
Perch	15	11	89	23.2	1987	11	22	159.2
Perch	15	11	89	30.4	1986	43	22.7	180.8
Perch	15	11	89	40.9	1985	20	24.6	243.3
Perch	3	5	90	17.5	1989	1969	8	5.6
Perch	3	5	90	27	1988	112	16.3	53.1
Perch	3	5	90	32.3	1987	37	23	158.6
Perch	3	5	90	34.6	1986	50	24.6	207.1
Perch	3	5	90	41.3	1985	15	26.4	290
Perch	28	8	90	6.5	1990	139	8.3	6.2

TABLE III.4. CAESIUM-137 IN IJSSELMEER (cont.)

Sample	Date			^{137}Cs	Year–class/	No. of fish	Length	Weight
	day	month	year	(Bq/kg dw)	age		(cm)	(g)
Perch	28	8	90	10.6	1989	227	13.2	24.3
Perch	28	8	90	16.3	1988	50	20.3	112
Perch	28	8	90	21.8	1987	17	23.9	180.3
Perch	28	8	90	25.2	1986	20	25.5	233.1
Perch	11	11	90	10.8	1990	367	8.7	7.1
Roach	3	10	84	0.5	> 5 years	19	23.2	173.1
Roach	8	5	86	9.2	> 5 years	6	24	171.1
Roach	13	5	86	23.4	> 5 years	17	22.8	171.7
Roach	8	4	87	64.2	> 5 years	15	23.2	179.1
Roach	16	11	87	27.7	> 5 years	14	23.3	174.5
Roach	11	4	88	23.8	> 5 years	141	21.9	164.1
Roach	31	10	88	13.7	> 5 years	98	23.1	184.9
Roach	30	3	89	11.8	> 5 years	66	22.3	164.6
Roach	21	11	89	10.2	1 year	515	8	4.5
Roach	16	11	89	9.8	> 5 years	49	24.4	205.5
Roach	3	5	90	10.1	> 5 years	47	23.1	168.7
Roach	11	11	90	5.6	> 5 years	17	25.1	223.2
Smelt	16	8	88	29.2	1986	219	11.9	11.5
Smelt	16	8	88	15.3	1988	2517	5.5	0.9
Smelt	31	10	88	25.3	1987	166	9.9	4.7
Smelt	31	10	88	20.3	1988	5936	6.2	1.3
Smelt	31	10	88	29.5	1987	386	9.6	4.5
Smelt	31	10	88	30.2	1986	52	13.1	14.8
Smelt	31	10	88	30	1985	23	15.9	30.9

TABLE III.5. CAESIUM-137 IN ISO VALKJÄRVI

Sample	Date			^{137}Cs
	day	month	year	(Bq/m^3)
Water	10	6	87	4600
Water	3	8	87	4200
Water	8	10	87	3400
Water	21	6	88	2600
Water	25	8	88	2100
Water	19	10	88	2200
Water	21	6	89	2100
Water	11	9	89	2000
Water	24	10	89	2000
Water	28	6	90	2000
Water	24	10	90	1700

Sample	Date			^{137}Cs
	day	month	year	(Bq/kg dw)
Zooplankton	9	6	87	11100
Zooplankton	28	7	87	19500
Zooplankton	30	10	87	22000
Zooplankton	10	11	89	2500
Asellus aquat.	9	6	87	17400
Asellus aquat.	30	10	87	17900

Deposition (1986): 70 kBq/m^2

Sample	Length (cm)		Date			^{137}Cs
	min.	max.	day	month	year	(Bq/kg fw)
Perch	13	19	30	6	87	12000
Perch	8	15	22	7	87	8500
Perch	11	14	28	10	87	8300
Perch	14	15	25	5	88	8000
Perch	14	14	16	9	88	9000
Perch	15	20	16	9	88	13800
Perch	23	23	16	9	88	11500
Perch	11	14	26	10	88	9100
Perch	15	18	26	10	88	7000
Perch	10	14	6	7	89	6900
Perch	15	19	6	7	89	8300
Perch	15	20	11	8	89	5500
Perch	24	24	11	8	89	7000
Perch	10	12	22	8	89	5100
Perch	12	14	22	8	89	5500
Perch	14	16	22	8	89	5900
Perch	16	18	22	8	89	7000
Perch	18	20	22	8	89	6300
Perch	21	21	22	8	89	13000
Perch	12	14	11	10	89	5200
Perch	14	16	11	10	89	4700
Perch	16	18	11	10	89	5200
Perch	18	20	11	10	89	8500
Perch	10	11	17	5	90	5200
Perch	12	13	17	5	90	6100
Perch	14	15	17	5	90	7500

TABLE III.5. CAESIUM-137 IN ISO VALKJÄRVI (cont.)

Sample	Length (cm)		Date			^{137}Cs
	min.	max.	day	month	year	(Bq/kg fw)
Perch	16	18	20	6	90	3600
Perch	18	20	20	6	90	7200
Perch	21	25	20	6	90	6600
Perch	10	11	19	7	90	5300
Perch	12	13	19	7	90	5700
Perch	14	15	19	7	90	4000
Perch	10	11	24	8	90	5800
Perch	12	13	24	8	90	5500
Perch	14	15	24	8	90	4500
Perch	16	17	24	8	90	7500
Perch	21	21	24	8	90	8300
Perch	27	27	24	8	90	6600
Perch	12	14	3	12	90	3500
Perch	15	17	3	12	90	4100
Perch	10	11	19	5	91	4200
Perch	12	13	19	5	91	4500
Perch	10	12	18	6	91	4400
Perch	12	14	18	6	91	4800
Perch	14	16	18	6	91	5300
Perch	16	18	18	6	91	4400
Perch	10	11	23	7	91	4400
Perch	12	13	23	7	91	4200
Perch	14	15	23	7	91	4100
Perch	16	17	23	7	91	4700
Perch	18	19	23	7	91	2200
Perch	20	21	23	7	91	4100
Perch	11	12	20	8	91	5200
Perch	13	14	20	8	91	4900
Perch	15	16	20	8	91	4300
Perch	17	18	20	8	91	4600
Perch	21	22	20	8	91	4000
Perch	11	12	30	9	91	4600
Perch	13	14	30	9	91	4800
Pike	27	43	30	6	87	20000
Pike	23	35	23	7	87	27000
Pike	50	50	2	11	87	15000
Pike	43	43	25	5	88	21700
Pike	55	55	26	5	88	16300
Pike	30	30	16	9	88	18100
Pike	53	53	26	10	88	18400
Pike	50	50	27	10	88	14800
Pike	35	40	6	7	89	21000
Pike	47	47	11	8	89	18000
Pike	39	39	28	6	90	11200
Pike	57	57	28	6	90	14500
Pike	47	47	8	8	90	12500
Pike	–[a]	–	28	11	90	11500
Pike	40	40	10	5	91	11200
Pike	76	76	24	5	91	12800
Pike	–	–	3	11	91	12400

[a] No information available.

TABLE III.5. CAESIUM-137 IN ISO VALKJÄRVI (continued)

Sample	Lenght (cm)		Date			^{137}Cs
	min.	max.	day	month	year	(Bq/kg fw)
Pike	–	–	3	11	91	11100
Pike	–	–	3	11	91	14800
Pike	–	–	3	11	91	11600
Whitefish	57	57	30	6	87	8400
Whitefish	30	30	27	8	87	8400
Whitefish	35	35	3	6	88	9500
Whitefish	36	36	16	9	88	6900
Whitefish	38	38	23	9	88	6000
Whitefish	41	45	27	10	88	4900
Whitefish	43	43	12	7	89	4200
Whitefish	45	45	17	8	89	2500
Whitefish	21	41	22	8	89	4300
Whitefish	45	45	11	10	89	3600
Whitefish	25	25	20	6	90	1700
Whitefish	27	27	20	6	90	2100
Whitefish	28	28	21	6	90	2000
Whitefish	28	28	28	6	90	2200
Whitefish	– [a]	–	8	8	90	2000
Whitefish	30	33	2	11	90	2400
Whitefish	–	–	11	11	91	1400
Whitefish	–	–	11	11	91	1400
Whitefish	–	–	11	11	91	1900
Whitefish	–	–	11	11	91	1500
Whitefish	–	–	11	11	91	2000

[a] No information available.

TABLE III.6. CAESIUM-137 IN HILLESJÖN

Sample	Date			^{137}Cs	Site
	day	month	year	(Bq/m^3)	
Water	12	6	86	6400	Outlet
Water	8	7	86	6600	Outlet
Water	13	8	86	2400 ± 900	Outlet
Water	8	10	86	2300 ± 340	Outlet
Water	2	12	86	500	Outlet
Water	8	4	87	1660 ± 500	Outlet
Water	8	4	87	1630 ± 50	Outlet
Water	18	4	87	1130 ± 50	Outlet
Water	18	4	87	1110 ± 50	Outlet
Water	6	5	87	1330 ± 50	Outlet
Water	24	6	87	1550 ± 90	Outlet
Water	7	9	87	1570 ± 70	Outlet
Water	19	11	87	930 ± 30	Outlet
Water	24	2	88	660 ± 30	Outlet
Water	10	5	88	690 ± 30	Outlet
Water	8	9	88	1800 ± 200	Outlet
Water	19	4	89	590 ± 20	Outlet
Water	10	10	89	1060 ± 50	Outlet
Water	11	1	90	1070 ± 50	Outlet
Water	29	3	90	590 ± 30	Outlet
Water	23	6	90	1010 ± 50	Outlet
Water	16	10	90	810 ± 20	Outlet
Water	9	2	91	10 ± 80	Outlet
Water	26	4	91	480 ± 120	Outlet
Water	11	8	86	620 ± 110	South
Water	30	9	86	460 ± 140	South
Water	2	12	86	200 ± 30	South
Water	8	4	87	780 ± 30	South
Water	18	4	87	650 ± 30	South
Water	7	9	87	190 ± 20	South
Water	10	5	88	180 ± 230	South
Water	19	4	89	110 ± 10	South
Water	10	10	89	50 ± 10	South
Water	11	1	90	60 ± 60	South
Water	29	3	90	50 ± 20	South
Water	23	6	90	40 ± 10	South
Water	16	10	90	100 ± 20	South
Water	29	10	90	100 ± 20	South
Water	9	2	91	40 ± 20	South
Water	16	4	91	50 ± 20	South
Water	11	8	86	1280 ± 490	Ångland
Water	2	12	86	790 ± 330	Ångland
Water	8	4	87	570 ± 20	Ångland
Water	18	4	87	400 ± 20	Ångland
Water	7	9	87	180 ± 20	Ångland
Water	19	11	87	200 ± 10	Ångland
Water	24	2	88	150 ± 20	Ångland
Water	10	5	88	690 ± 30	Ångland
Water	19	4	89	100 ± 10	Ångland
Water	10	10	89	190 ± 10	Ångland

TABLE III.6. CAESIUM-137 IN HILLESJÖN (cont.)

Sample	Date			^{137}Cs	Remarks
	day	month	year	(Bq/m^3)	
Water	29	3	90	50 ± 20	Ångland
Water	23	6	90	30 ± 10	Ångland
Water	16	10	90	80 ± 20	Ångland
Water	29	10	90	80 ± 20	Ångland
Water	23	6	90	30 ± 10	Ångland
Water	16	10	90	80 ± 20	Ångland
Water	29	10	90	80 ± 20	Ångland
Water	9	2	91	60 ± 20	Ångland
Water	26	4	91	50 ± 20	Ångland
Water	30	9	86	860 ± 250	Fännsmyra
Water	2	12	86	480 ± 100	Fännsmyra
Water	8	4	87	960 ± 340	Fännsmyra
Water	7	9	87	220 ± 30	Fännsmyra

Sample	Date			^{137}Cs	
	day	month	year	(Bq/kg dw)	
Plankton	12	6	86	8300	
Plankton	16	7	86	59700	
Plankton	13	8	86	1040	
Plankton	7	10	86	6780	
Plankton	2	12	86	2270	

Sample	Size	Date			^{137}Cs (Bq/kg fw)	
		day	month	year	geom. mean	SD
Perch	< 10 cm	13	9	87	3235	–
Perch	< 10 cm	15	2	88	3842	–
Perch	< 10 cm	20	2	89	2039	–
Perch	< 10 cm	10	10	89	1478	–
Perch	< 10 cm	1	3	90	1672	–
Perch	10–20 cm	4	12	86	10064	–
Perch	10–20 cm	10	3	87	7405	1307
Perch	10–20 cm	29	4	87	6970	–
Perch	10–20 cm	13	9	87	5272	2513
Perch	10–20 cm	20	1	88	6489	1527
Perch	10–20 cm	15	2	88	5947	1822
Perch	10–20 cm	15	9	88	3183	1316
Perch	10–20 cm	20	2	89	2543	810
Perch	10–20 cm	10	10	89	2493	785
Perch	10–20 cm	1	3	90	1944	372
Perch	10–20 cm	5	9	92	703	325
Perch	> 20 cm	5	6	86	888	–
Perch	> 20 cm	8	7	86	3732	–
Perch	> 20 cm	13	8	86	6705	–
Perch	> 20 cm	4	12	86	7523	–
Perch	> 20 cm	20	4	87	4318	812
Perch	> 20 cm	13	9	87	7197	544
Perch	> 20 cm	20	1	88	8110	–
Perch	> 20 cm	15	2	88	8554	–
Perch	> 20 cm	15	9	88	6693	1367
Perch	> 20 cm	20	2	89	4068	1554
Perch	> 20 cm	10	10	89	4055	339
Perch	> 20 cm	1	3	90	3461	654

TABLE III.6. CAESIUM-137 IN HILLESJÖN (cont.)

Sample	Date			^{137}Cs (Bq/kg fw)	
	day	month	year	geom. mean	SD
Roach	8	7	86	2101	–
Roach	13	8	86	3301	–
Roach	4	12	86	3753	865
Roach	10	3	87	2372	348
Roach	23	9	87	1890	305
Roach	24	2	88	2524	329
Roach	19	9	88	1441	222
Roach	15	3	89	1043	141
Roach	10	10	89	983	115
Roach	1	3	90	777	40
Roach	5	9	92	400	50
Pike	15	2	86	8	–
Pike	5	5	86	147	–
Pike	5	6	86	376	–
Pike	8	7	86	1400	–
Pike	13	8	86	2590	–
Pike	24	9	86	3310	–
Pike	4	12	86	4091	366
Pike	10	3	87	3315	1234
Pike	29	4	87	3802	3475
Pike	10	9	87	4828	1005
Pike	24	2	88	4681	1054
Pike	15	9	88	3841	973
Pike	12	4	89	3642	729
Pike	1	10	89	3012	1075
Pike	5	9	92	1161	179

TABLE III.7. CAESIUM-134 AND -137 IN BRACCIANO

Sample	Date			^{134}Cs	^{137}Cs
	day	month	year	(Bq/m^3)	(Bq/m^3)
Water	20	5	86	42 ± 4	96 ± 5
Water	15	7	86	35 ± 4	95 ± 5
Water	14	4	87	2.7 ± 1.5	20 ± 3
Water	22	9	87	2.7 ± 1.5	19 ± 4
Water	1	2	88	2.5 ± 1.3	14 ± 4
Water	31	5	88	3.1 ± 1	19 ± 3
Water	31	1	89	2.5 ± 0.4	20 ± 2
Water	17	4	89	2.7 ± 0.8	19 ± 2
Water	14	7	89	1.5 ± 0.7	18 ± 3
Water	2	10	89	< 3.8	22 ± 2[a]
Water	2	10	89	< 2.4	22 ± 1[a]
Water	20	6	90	< 3	20 ± 4
Water				< 3	21 ± 3
Water				< 3	19 ± 3

[a] Samples collected in two different sites in the lake.

Sample	Date			^{134}Cs	^{137}Cs	Size (cm)	
	day	month	year	(Bq/kg fw)[b]	(Bq/kg fw)[b]	min.	max.
Fish	15	7	86	4 ± 0.5	13 ± 1	–	–
Fish	31	7	86	4 ± 0.5	12 ± 0.5	–	–
Fish	21	8	86	4 ± 1	14 ± 1	–	–
Fish	16	6	87	1.7 ± 0.2	8.4 ± 0.2	–	–
Fish	29	9	88	< 2.0	5.9 ± 0.2	–	–
Fish	26	10	88	0.6 ± 0.1	6.5 ± 0.2	–	–
Fish	22	2	89	0.7 ± 0.1	6.6 ± 0.2	–	–
Fish	14	4	89	< 0.5	6.2 ± 0.3	24	26
Fish	20	6	89	0.5 ±0.1	6.0 ± 0.3	–	–
Fish	16	1	90	< 0.5	5.7 ± 0.3	26	29
Fish	8	2	90	0.4 ± 0.07	5.8 ± 0.2	–	–
Fish	28	9	90	< 0.3	5.4 ± 0.3	–	–
Fish	21	3	91	< 0.3	6.1 ± 0.5	–	–
Fish	9	5	91	< 0.3	4.9 ± 0.2	–	–

[b] Dry weight represents 28% of the fresh weight.

Sample	Date			^{134}Cs	^{137}Cs	Depth
	day	month	year	(Bq/kg dw)	(Bq/kg dw)	(m)
Sediment	29	4	87	2.3 ± 0.4	13.5 ± 1.0	1
Sediment	19	3	90	2.9 ± 1.9	66.3 ± 3.5	1
Sediment	19	3	90	1.8 ± 0.6	42.0 ± 0.6	1
Sediment	19	3	90	4.3 ± 0.8	88.0 ± 2.7	4
Sediment	20	6	90	0.6 ± 0.1	12.7 ± 0.3	16
Sediment	20	6	90	< 1.0	17.5 ± 0.5	27
Sediment	20	6	90	< 1.0	22.6 ± 0.7	30
Sediment	20	6	90	< 1.5	17.5 ± 1.0	65

REFERENCES

[4.1] JOHANSSON, H., HÅKANSON, L., "Partitioning coefficients in aquatic systems; metals partitioning between water and particulate matter; impact on ecosystems – modelling", Proc. 21st Nordic Sediment Symposium 1993, Erken Lab., Uppsala Univ., LIU, B:7 (1993) 23–36.

[4.2] INTERNATIONAL ATOMIC ENERGY AGENCY, Modelling of Radionuclide Transfer into Rivers and Reservoirs, IAEA-TECDOC (in preparation).

[4.3] TESSIER, A., CAMPBELL, P.G.C., BISSON, M., Sequential extraction procedure for the speciation of particulate trace metals, Analyt. Chem. **51** (1979) 844–851.

[4.4] REUTHER, R., "The Metal Conference in Athens, 1985: A growing interest in metal speciation", Speciation of Metals in Water, Sediment and Soil Systems (LANDNER, L., Ed.), Springer Verlag, Heidelberg (1987) 3–9.

[4.5] SALOMONS, W., FÖRSTNER, U., Metals in the Hydrocycle, Springer Verlag, Berlin, Heidelberg (1984) 349 p.

[4.6] LUOMA, S.N., JENNE, E.A., Estimating bioavailability of sediment-bound trace metals with chemical extractants, Trace Substances in Environmental Health, X, (Hemphill, D., Ed.) University of Missouri, Columbia, MO (1976) 343–351.

[4.7] LORRING, D.H., Potential bioavailability of metals in eastern Canadian estuarine and coastal sediments, Rapp. P.-v. Réun. Cons. Int. Explor. Mer, **181** (1981) 93–101.

[4.8] HAAPALA, K., Glass fibre and polycarbonate filters for the determination of suspended solids, Vatten **47** (1991) 226–231.

[4.9] TESSIER, A., CARIGNAN, R., DUBREUIL, B., RAPIN, F., Partitioning of zinc between the water column and the oxic sediments in lakes, Geochim. Cosmochim. Acta **53** (1989) 1511–1522.

[4.10] HÅKANSON, L., PETERS, R.H., Predictive Limnology – Methods for Predictive Modelling. SPB Academic Publishing, Amsterdam (1995) 464 p.

[4.11] SIGG, L., "Metal transfer mechanisms in lakes; the role of settling particles", Chemical Processes in Lakes, (STUMM, W., Ed.) John Wiley & Sons, New York (1985) 283–310.

[4.12] RANCON, D., "Influence of concentration distributions in solid medium on the assessment of radioelement distribution between the liquid and solid phases", Application of Distribution Coefficients to Radiological Assessment Models, (SIBLEY, T.H., MYTTENAERE, C., Eds) Elsevier Applied Science Publishers, London (1986) 64–71.

[4.13] SANTSCHI, P.H., HONEYMAN, B.D., "Radioisotopes as tracers for the interactions between trace metals, colloids and particles in natural waters", Heavy metals in the environment (Proc. Int. Conf., Geneva, 1989), (VERNET, J-P. Ed.) CEP Consultants Ltd, Edinburgh (1989) 243–252.

[4.14] NYFFELER, U.P., LI, Y-H., SANTSCHI, P.H., A kinetic approach to describe trace-element distribution between particles and solution in natural aquatic systems, Geochim. Cosmochim. Acta **48** (1984) 1513–1522.

[4.15] LI, Y.-H., BURKHARDT L., BUCHHOLTZ, M., O'HARA, P., SANTSCHI, P. H., Partition of radiotracers between suspended particles and seawater, Geochim. Cosmochim. Acta, **48** (1984) 2011–2019.

[4.16] YOU, C-F., LEE, T., LI, Y-H., The partition of Be between soil and water, Chem. Geol. **77** (1989) 105–118.

[4.17] YAN, L., STALLARD R.F., KEY, R.M., CRERAR, D.S., Trace metals and dissolved organic carbon in estuaries and offshore waters of New Jersey, USA, Geochim. Cosmochim. Acta **55** (1991) 3647–3656.

[4.18] BROBERG, A., ANDERSSON, E., Circulation of Caesium in Limnic Ecosystems, Inst. of Limnology, Uppsala Univ. (1989) 30 (in Swedish).

[4.19] RIISE, G., BJÖRNSTAD, H.E., OUGHTON, D.H., SALBU, B., A study on radionuclide associations with soil components using sequential extraction procedure, J. Radioanal. Nucl. Chem. **142** (1990) 531–538.

[4.20] SALBU, B., BJÖRNSTAD, H.E., BRITTAIN, J.E., Fractionation of Cs-isotopes and ^{90}Sr in snow melt, runoff and lake water from contaminated area in Norway, J. Radioanal. Nucl. Chem. **156:7** (1992).

[4.21] MONTE, L., FRATARCANGELI, S., POMPEI, F., QUAGGIA, S., BATTELLA, C., Bioaccumulation of caesium-137 in the main species of fishes in lake of Central Italy, Radiochimica Acta **60** (1993) 219–222.
[4.22] MONTE, L., A predictive model for the behaviour of radionuclides in lake systems, Health Physics **65** (1993) 288–294.
[4.23] MONTE, L., FRATARCANGELI, F., POMPEI, S., QUAGGIA, S., ANDRASI, G., A predictive model for the behaviour of dissolved radioactive substances in stratified lakes, J. Environ. Radioactivity **13** (1991) 297–308.
[4.24] HELING, R., LAKECO, the Ecological Consequences of an Accidental Release of Radionuclides on a Lake Ecosystem and its Integration into the Real-time-On-line Decision Support System for the Off-site Emergency Management Following a Nuclear Accident (RODOS), KEMA, Arnhem (1994).
[4.25] MACKENZIE, J., NICHOLSON, S., COLDOS, A Computer Code for the Estimation of Collective Doses from Radioactive Wastes to the Sea, Implications for the Collective Dose Assessments, Safety and Relativity Directorate, UK Atomic Energy Authority, Warrington (1987).
[4.26] DE VIES, M.B., PIETERS, H., Accumulation of Heavy Metals in Organisms, Bioaccumulation of Mercury in Pike Perch, Data Analysis on IJsselmeer, Ketelmeer and Marchermeer, RIVO, DIFT, Hydraulics Report T-250, Delft Hydraulics, Delft (1989) (in Dutch).
[4.27] BERGSTRÖM, U., EDLUND, O., EVANS, S., RÖJDER, B., BIOPATH – A Computer Code for Calculation of the Turnover of Nuclides in the Biosphere and the Resulting Doses to Man, STUDSVIK/NW-82/261, Studsvik Energiteknik AB, Nyköping (Sweden) (1982).
[4.28] SUNDBLAD, B. (Ed.), "Dynamics within lake ecosystems". BIOMOVS Technical Report 12, Swedish Radiation Protection Institute, Stockholm (1992).
[4.29] BERGSTRÖM, U., NORDLINDER, S., "Comparison of predicted and measured Cs-137 concentrations in lake ecosystem" (Proc. XVth Reg. Cong. of IRPA) Visby (1989).
[4.30] NORDLINDER, S., BERGSTRÖM, U., HAMMAR, J., NOTTER, M., Modelling turnover of Cs-137 in two subarctic salmonid ecosystems, Nordic J. Freshwater Res. **68** (1993).
[4.31] GARDNER, R.H., RÖJDER, B., BERGSTRÖM, U., PRISM – A Systematic Method for Determining the Effect of Parameter Uncertainties on Model Predictions STUDSVIK/NW-83/555, Studsvik Energiteknik AB, Nyköping (Sweden) (1983).
[4.32] HÅKANSON, L., Ecometric and Dynamic Modelling: Exemplified by Caesium in Lakes after Chernobyl, Springer-Verlag, Berlin (1991) 158 p.
[4.33] BERGMAN, R., et. al., Uptake, Re-distribution and Transport of Radionuclides in a Forest Ecosystem, FOA-rapport E 40040, SLU, Umeå (1988) (in Swedish).
[4.34] HÅKANSON, L., ANDERSSON, T., NEUMANN, G., NILSSON, Å., NOTTER, M., Caesium-137 in perch in lakes from northern Sweden after Chernobyl – present situation, relationships, trends, Swed. Env. Prot. Agency, Report 34 97 (1988).
[4.35] SUNDBLAD, B., EVANS, S., BERGSTRÖM, U., The Turnover of Chernobyl Fallout Within Two Catchment Areas – Hillesjön and Slägsjön – in the Gävle Area, Sweden, Studsvik/NP-89/51, Studsvik Energiteknik AB, Nyköping (Sweden) (1989).
[4.36] SANTCHI, P.H., BOLLHALDER, S., ZINGG, S., LUCK, A., FARRENKOTHEN, K., The self-cleaning capacity of surface waters after radioactive fallout. Evidence from European waters after Chernobyl, 1986–1988, Environ. Sci. Technol. **24** (1990) 519–527.
[4.37] KANSANEN, P.H., JAAKKOLA, T., KULMALA, S., SUUTARINEN, R., Sedimentation and distribution of gamma-emitting radionuclides in bottom sediments of southern Lake Päijänne, Finland after the Chernobyl accident, Hydrobiologia **189** (1990) 221–234.
[4.38] KORHONEN, R., SAVOLAINEN, I., Biospheric Transfer Model DETRA for Assessment of Radiation Impacts, Technical Research Centre of Finland, Nuclear Engineering Laboratory, Research Reports 323, Espoo (1984) (in Finnish).
[4.39] KORHONEN, R., Modeling transfer of caesium-137 fallout in a large Finnish watercourse. Health Physics **59** (1990) 443–454.
[4.40] KORHONEN, R., Model Studies of the Transfer of Radionuclides in the Finnish Environment, PhD Thesis, Technical Research Centre of Finland, Nuclear Engineering Laboratory, Publication 81, Espoo (1991).

[5.1] COMANS, R.H.J., personal communication (1994).
[5.2] FERNANDEZ, J.A., personal communication (1994).
[5.3] HÅKANSON, L., JANSSON, M., Principles of Lake Sedimentolgy, Springer-Verlag, Berlin (1983) 316.
[5.4] MACKENZIE, J., NICHOLSON, S., COLDOS, A Computer Code for the Estimation of Collective Doses from Radioactive Wastes to the Sea. Implications for the collective dose assessments. Safety and Reliability Directorate. U.K. Atomic Energy Authority, Warrington (1987).
[5.5] MEILI, M., "The importance of feeding rate for the accumulation of radioactive caesium in fish after the Chernobyl accident", The Chernobyl Fallout in Sweden, Results from a Research Programme on Environmental Radiology, (MOBERG, L., Ed.), Swedish Radiation Protection Institute, Stockholm (1991) 177–182.
[5.6] SUNDBLAD, B. (Ed.), Dynamics within lake ecosystems, BIOMOVS Technical Report 12, Swedish Radiation Protection Institute, Stockholm (1992).
[5.7] BERGSTRÖM, U., NORDLINDER, S., "Comparison of predicted and measured Cs-137 concentration in a lake ecosystem", The Radioecology of Natural and Artificial Radionuclides, (Proc. of the XVth Regional Congress of IRPA, Visby, (1989)) Swedish Radiation Protection Institute, Stockholm (1989).
[5.8] NORDLINDER, S., BERGSTRÖM, U., HAMMAR, J., NOTTER, M., Modelling turnover of Cs-137 in two subarctic salmonid ecosystems, Nordic J. Freshw. Res. **68** (1993) 21–33.
[5.9] BERGSTRÖM, U., SUNDBLAD, B., NORDLINDER, S., "Models for predicting radiocesium levels on lake water and fish", Nordic Radioecology, The Transfer of Radionuclides Through Nordic Ecosystems to Man, (DAHLGRAARD, H., Ed.) Elsevier, Amsterdam (1994) 93–104.
[5.10] KIRCHNER, T.B., Time-zero, The Integrated Modeling Environment, Reference Manual, Quaternary Software, Inc., Fort Collins, CO (1990).
[5.11] SUNDBLAD, B., BERGSTRÖM, U., EVANS, S., "Long term transfer of fallout nuclides from the terrestrial to the aquatic environment. Evaluation of radioecological models", The Chernobyl Fallout in Sweden, Results from a Research Programme on Environmental Radiology (MOBERG, L., Ed.) Swedish Radiation Protection Institute, Stockholm (1991) 207–238.
[5.12] MONTE, L., A predictive model for the behaviour of radionuclides in lake systems. Health Physics, **69**, No. 3 (1993) 289–294.
[5.13] MONTE, L., FRATARCANGELI, S., POMPEI, F., QUAGGIA, S., BATTELLA, C., Bioaccumulation of ^{137}Cs in the main species of fishes in lakes of Central Italy, Radiochimica Acta, 60 (1993) 219–222.
[5.14] REICHLE, D.E, DUNAWAY, P.B., NELSON, D.J., Turnover and concentration of radionuclides in food chains, Nuclear Safety, **11** 1 (1970).
[5.15] VANDERPLOEG, H., PARCZYK, D.C., WILCOX, W.H., KERCHER, J.R., KAYE, S.V., Bio-accumulation for Radionuclide in Freshwater Biota, Rep. ORNL-5002, Oak Ridge National Laboratory, Oak Ridge, TN (1975).
[5.16] KOLEHMAINEN, S., HÄSÄNEN, E., MIETTINEN, J.K., Biological half-times of ^{137}Cs and ^{22}Na in different fish species and their temperature dependence, in Radiation Protection, Part 1 (SNYDER, W.S. et al., Eds.), Pergamon Press, New York (1968).
[5.17] CARLSSON, S., A model for the turnover of ^{137}Cs and potassium in pike (*Esox Lucius*), Health Physics, **35** (1978) 549–554.
[5.18] HARVEY, R.S., Uptake and loss of radionuclides by the freshwater clam *Lampsilis radiata*, Health Pysics, **17** (1969) 149–154.
[5.19] FOULQUIER, L., Donnees Synthetiques sur les Publications de Radiohydrobiologie de la Section de Radioecologie, CEA Centre d'Etudes Nuclaires de Cadarache, Bibliographie CEA-BIB – 229, Cadarache (1978).
[5.20] COUGHTREY, P.J., THORNE, M.C., Radionuclide Distribution and Transport in Terrestrial and Aquatic ecosystems, A Critical Review of Data, Vol. 1, Balkema, Rotterdam (1983).
[5.21] UGEDAL, O., JONSSON, B., NJÅSTAD, O., NÆUMANN, R., Effects of temperature and body size on radiocaesium retention in brown trout *(Salmo trutta L.)*. Freshwater Biology, 28 (1992) 165–171.

[5.22] GALLEGOS, A.F., WHICKER, F.W., "Radiocaesium Retention by Rainbow Trout as Affected by Temperature and Weight", Radionuclides in Ecosystems (NELSON, D.J., Ed.), USAEC Report CONF-710501-P1, Washington, DC (1971) 361–371.
[5.23] HEWETT, C.J., JEFFRIES, D.F., The accumulation of radioactive caesium from water by the brown trout (Salmo trutta), and its comparison with plaice and rays, J. Fish Biology, **9** (1976) 479–489.
[5.24] THOMANN, R.V., Bioaccumulation model of organic chemical distribution in aquatic food chains, Environ. Sci. Technol. **23** (1989) 699–707.
[5.25] BRITTAIN, J.E. et al., "Estimation of ecological half-lives of Cs-137 in lakes contaminated by Chernobyl fallout", Proc. Int. Symp. on Environmental Impact of Radioactive Releases, 1995, IAEA, Vienna (1995) 291–298.
[5.26] MOBERG, L., (Ed.), The Chernobyl Fallout in Sweden, Swedish Radiation Protection Institute, Stockholm (1991).
[5.27] DAHLGAARD, H., (Ed.), Nordic Radioecology, The Transfer of Radionuclides through Nordic Ecosystems to Man, Elsevier, Amsterdam (1994).
[5.28] EVANS, S., Biological Half-time of Cs-137 in Roach Exposed to the Chernobyl Fallout. Clearance of Cs-137 in Roach Exposed to Various Potassium Concentrations in the Water, An Experimental Study, Rep. STUDSVIK/NP-89/74, Studsvik Energieteknic, Nyköping (1989).
[5.29] HADDERINGH, R., VAN AERSSEN, G.H.F.M., Distribution of ^{137}Cs in the lake IJsselmeer as a Consequence of Chernobyl, Period 1986–1992, Rep. 40356-KES/WDR/93-3132, KEMA, Arnhem (1994) (in Dutch).
[5.30] HELING, R., LAKECO, the Ecological Consequences of an Accidental Release of Radionuclides on a Lake Ecosystem and its Integration into the Real-time On-line Decision Support System for the Off-site Emergency Management Following a Nuclear Accident (RODOS), KEMA, Arnhem (1994).
[5.31] HÅKANSON, L., ANDERSSON, T., NILSSON, Å., Radioactive caesium in fish in Swedish lakes 1986-1988 – general pattern related to fallout and lake characteristics, J. Environ. Radioactivity **15** (1992).
[5.32] AHLGREN, I., FRISK, T., KAMP-NIELSEN, L., Empirical and theoretical models of phosphorus loading, retention and concentration vs. lake trophic state, Hydrobiologia **170** (1988) 285–303.
[5.33] PETERS, R.H., A Critique for Ecology, Cambridge Univ. Press, Cambridge (1991).
[5.34] BIOMOVS, Scenario A1, Mercury in Aquatic Ecosystems, Tech. Report 7, Swedish Radiation Protection Institute, Stockholm (1990).
[5.35] HÅKANSON, L., PETERS, R.H., Predictive Limnology – a Methodological Textbook for Predictive Modelling, SPB Academic Publishers, Amersterdam (1995).
[5.36] HÅKANSON, L., Ecometric and Dynamic Modelling: Exemplified by Caesium in Lakes after Chernobyl, Springer-Verlag, Berlin (1991) 158 p.
[5.37] VEMURI, V., Modeling of complex systems, Academic Press, New York (1978) 448 p.
[5.38] STRAŠKRABA, M., GNAUCK, A., Freshwater Ecosystems, Modelling and Simulation, Developments in Environmental Modelling, 8, Elsevier, Amsterdam (1985).
[5.39] JÖRGENSEN, S.E., JOHNSEN, J., Principles of Environmental Science and Technology (2nd edition), Studies in Environmental Science, 33, Elsevier, Amsterdam (1989).
[5.40] HÅKANSON, L., A Manual of Lake Morphometry, Springer-Verlag, Berlin and New York (1981).
[5.41] HÅKANSON, L., Optimization of lake hydrographic surveys, Water Resources Research **14** (1978) 545–560.
[5.42] HÅKANSON, et al., Measures to Reduce Mercury in Lake Fish, Final Report from the Liming-mercury-cesium project, Rep. SNV PM 3818, National Environment Protection Agency, Solna, Sweden (1990).
[5.43] LINDQVIST, O., et al., Mercury in the Swedish environment, Water, Air and Soil Pollution, **55** (1991).
[5.44] MEILI, M., Mercury in Boreal Forest Lake Ecosystems. Acta Univ. Upsaliensis 336, PhD Thesis, Uppsala University (1991).

[5.45] HÅKANSON, L., Considerations on representative water quality data, Int. Rev. Ges. Hydrobiol., 77 (1992) 497–505.
[5.46] NETER, J., WASSERMAN, W., WHITMORE, G.A., Applied statistics, 3rd Edition, Allyn and Bacon, Boston, MA (1988).
[5.47] COX, D.C., BAYBUTT, P., Methods for uncertainty analysis: a comparative survey, Risk Analysis 1(4), (1981) 251–258.
[5.48] INTERNATIONAL ATOMIC ENERGY AGENCY, Evaluating the Reliability of Predictions Made Using Environmental Transfer Models. Safety Series No. 100, IAEA, Vienna (1989).
[5.49] ANDERSSON, T., HÅKANSON, L., KVARNÄS, H., NILSSON, Å., Remedial Measures Against High Levels of Radioactive Cesium in Swedish Lake Fish, SSI Rapport 91–07, Swedish Radiation Protection Institute (1991) (in Swedish).
[5.50] NILSSON, Å., Statistical Modelling of Regional Variations in Lake Water Chemistry and Mercury Distribution, PhD Thesis, Umeå University (1992).
[5.51] BRITTAIN, J.E., BJØRNSTAD, H.E., SALBU, B., OUGHTON, D.H., Winter transport of Chernobyl radionuclides from a montane catchment to an ice-covered lake, Analyst **117** (1992) 515–519.
[5.52] BRITTAIN, J.E., HÅKANSON, L., BERGSTRÖM, U. & BJØRNSTAD, H.E., The significance of hydrological and catchment processes for the transport and biological uptake of radionuclides in northern aquatic ecosystems (SAND, K., KILLINGTVEIT, Å., Eds.), (Proc. 10th Int. Northern Research Basins Symposium and Workshop, Spitzbergen, 1994) SINTEF Report STF-22-A96415, Trondheim, Norway (1996) 201–217.
[5.53] SPEZZANO, P., BORTOLUZZI, S., GIACOMELLI, R., MASSIRONI, L., Seasonal variation of ^{137}Cs activities in the Dora Baltea River (Northwest Italy) after the Chernobyl accident. J. Environ. Radioact. **22**, (1994) 77–88.
[5.54] SIMONS, T.J., Circulation models of lakes and inland seas, Can. Bull. Fish. Aquat. Sci., **203** (1980) 1–146.
[5.55] VOLLENWEIDER, R.A., The Scientific Basis of Lake Eutrophication, with Particular Reference to Phosphorus and Nitrogen as Eutrophication Factors, Tech. Rep. DAS/DSI/68.27, OECD, Paris (1968) 159 pp.
[5.56] PETERS, R.H., The role of prediction in limnology, Limnol. Oceanogr. **31** (1986) 1143–1159.

[II.1] MONTE, L., A predictive model for the behavior of radionuclides in lake systems, Health Physics **65** 3 (1993) 288–294.
[II.2] MONTE, L., "A Model Assessing the Levels of Radioactivity Contamination of the Main Species of Fishes Living in Some Lakes of Central Italy", (Proc. 2nd Italian-Austrian Radiation Protection Symposium, AIRP, Bologna, 1991) (1991) 227–234.
[II.3] MONTE, L., FRATARCANGELI, S., POMPEI, F., QUAGGIA, S., BATTELLA, C., Bioaccumulation of ^{137}Cs in the main species of fishes in lakes of Central Italy, Radiochimica Acta **60** (1993) 219–222.
[II.4] RICHMOND, B., VESCUSO, P., PETERSON, S., User's Guide to STELLA™, software from High Performance Systems, Dartmouth, NH (1987).
[II.5] DE VRIES, M.B., PIETERS, H., Accumulation of Heavy Metals in Organisms, Bioaccumulation in Pikeperch, Data Analysis of the IJsselmeer, Ketelmeer and Markermeer, Delft Hydraulics and National Institute for Fishery Research (1989) (in Dutch).
[II.6] MACKENZIE, J., NICHOLSON, S., COLDOS – A Computer Code for the Estimation of Collective Doses from Radioactive Wastes to the Sea; Implications for the Collective Dose Assessments, Safety and Reliability Directorate, U.K. Atomic Energy Authority, Warrington (1987).
[II.7] NICHOLSON, S., MACKENZIE, J., The Remobilisation of Radionuclides form Marine Sediments; Implication for the Collective Dose Assessment, SRD Report R 453, Safety and Reliability Directorate, U.K. Atomic Energy Authority, Warrington (1988).
[II.8] KORHONEN, R., Modeling the transfer of ^{137}Cs fallout in a large Finnish watercourse, Health Physics **59** (1990) 443–454.

[II.9] SALBU, B., "Radionuclides Associated with Colloids and Particles in the Chernobyl fallout", Recent Advances in Reactor Accident Consequence Assessment, Proc. of an OECD(NEA)/CEC Workshop, Rome, 1988, OECD Nuclear Energy Agency, Paris (1988) 53–57.
[II.10] AL RAYYES, A.H., et. al., Radiocaesium in hot particles; solubility vs chemical speciation, J. Environ. Radioactivity **21** (1993) 143–151.
[II.11] TCHERKEZIAN, V., SHKINEV, L., KHITROV, L., KOLESOV, G., Experimental approach to Chernobyl hot particles, J. Environ. Radioactivity **22** (1994) 127–139.
[II.12] ONISHI, Y., SERNE, N.J., ARNOLD, E.M., COWAN, C.E., THOMPSON, F.L., Critical Review of Radionuclide Transport, Sediment Transport and Water Quality Modeling, and Radionuclide Adsorption/Desorption Mechanisms, Rep. NUREG/CR-1322 PNL-2901, Battelle, Richland, WA (1981).
[II.13] COMANS, R.H.J., HALLER, M., VAN DER WEIJDEN, C.H., Reversibility of Caesium Interaction with Clay Minerals, Suspended Matter, and Sediments of Dutch Watercourses, Department of Geochemistry, Institute of Earth Sciences, University of Utrecht (1989) (in Dutch).
[II.14] FISHER, J.B., LICK, W.J., McCALL, P.L., ROBBINS, J.A., Vertical mixing of lake sediments in tubificid oligochaets, J. of Geoph. Res. **85** (7) (1980) 3997–4006.
[II.15] COUGHTREY, P.J. THORNE, M.C., Radionuclide Distribution and Transport in Terrestrial and Aquatic Ecosystems, A Critical Review of Data, Vol 1., A.A Balkema, Amsterdam (1983).
[II.16] WILLEMSEN, J., Population dynamics of percids in Lake IJssel and some smaller lakes in the Netherlands, J. of Fish. Res. Board of Can. **34** (1977) 1710–1719.
[II.17] ELLIOTT, J.M., et. al., Sources of variation in post-Chernobyl radiocaesium in fish from two Cumbrian lakes (north-west England), Journal of Applied Biology **29** (1992) 108–119.
[II.18] ROWAN, D.J., RASMUSSEN, J.B., CHANT, L., "A bioenegetic approach to modeling seasonal patterns in the bioaccumulation of radiocesium", Freshwater and Estuarine Radioecology (DESMET, G., et al. Eds) Elsevier, Amsterdam (1997) 387–393.
[II.19] HEWETT, C.J., JEFFERIES, D.F., The accumulation of radioactive caesium from water by the brown trout (*Salmo trutta*), and its comparison with plaice and rays, J. Fish. Biology **9** (1976) 479–489.
[II.20] HEWETT, C.J., JEFFERIES, D.F., The accumulation of radioactive caesium from food by the plaice (*Pleronectes platessa*) and brown trout (*Salmo trutta*), J. Fish. Biology **13** (1978) 143–153.
[II.21] FERNÁNDEZ, J.A., et. al., "Mechanisms of radiocesium uptake and accumulation in Riccia fluitans", Freshwater and Estuarine Radioecology (DESMET, G., et al. Eds) Elsevier, Amsterdam (1997) 329–337.
[II.22] HINTON, T.G., SCOTT, D.E., "Radiological techniques for herpetology, with an emphasis on freshwater turtles", Life History and Ecology of the Slider Turtle (WHITFIELD GIBBONS, J., Ed.) Smithsonian Institution Press, Washington, DC (1990).
[II.23] KOLEHMAINEN, S., The balances of ^{137}Cs, stable Caesium and Potassium in Bluegill *(Lipmis Macrochirus Raf.)* and other fish in White Oak Lake, Health Physics **23** (1972) 301–315.
[II.24] LAMBRECHTS, A., FOULQUIER, L., Etude expérimentale des possibilités de transfert direct du césium 137 du sédiment vers la carpe (*Cyprinus carpio, L*), Rapport CEA-R-5227, Centre d'Etudes Nucléaires de Cadarache (1983).
[II.25] FOULQUIER, L., LAMBRECHTS, A., Essai d'évolution des taux de transferts directs et indirects du césium 137 dans une chaîne alimentaire d'eau douce simplifiée, Rapport CEA-R-5183, Centre d'Etudes Nucléaires de Cadarache (1982).
[II.26] LAMBRECHTS, A., Essai de modélisation du transfert du césium 137 dans les compartiments d'un écosystème d'eau douce simplifié, Rapport CEA-R-5268, Centre d'Etudes Nucléaires de Cadarache (1984).
[II.27] GARDNER, R.H., RÖJDER, B., BERGSTRÖM, U., PRISM – A Systematic Method for Determining the Effect of Parameter Uncertainties on Model Predictions, Rep. STUDSVIK/NW-83/555, Studsvik AB, Sweden (1983).
[II.28] BERGSTRÖM, U., EDLUND, O., EVANS, S., RÖJDER, B., BIOPATH – A Computer Code for Calculation of the Turnover of Nuclides in the Biosphere and the Resulting Doses to Man. Rep. STUDSVIK /NW-82/261 Studsvik Energiteknik AB, Nyköping (Sweden) (1992).

[II.29] SUNDBLAD, B. (Ed), BIOMOVS – Scenario A5, Dynamics Within Lake Ecosystems, BIOMOVS Technical Report 12, Swedish Radiation Protection Institute, Stockholm (1991).
[II.30] NORDLINDER, S., BERGSTRÖM, U., HAMAR, J., NOTTER, M., Modelling turnover of Cs-137 in two subarctic salmonid ecosystems, Nordic J. Freshwat. Res. **68** (1993) 21–33.
[II.31] BERGSTRÖM, U., SUNDBLAD, B., NORDLINDER, S., Models for Predicting Radiocaesium Levels in Lake Water and Fish, In: Nordic Radioecology (Dahlgaard, H., Ed.), Elsevier Science Publishers, Amsterdam (1994) 93–104.
[II.32] SPEZZANO, P., BORTOLUZZI, S., GIACOMMELI, R., MASSIRONI, L., Seasonal variation of ^{137}Cs activities in the Dora Baltea River (Northwest Italy) after the Chernobyl accident, J. Environ. Radioact. **22** (1994) 77–88.
[II.33] HILL, M.D., LAWSON, G., An Assessment of the Radiological Consequences of Disposal of High-level Waste in Coastal Geological Formations, Rep. NRPB-R108 National Radiological Protection Board, Oxfordshire (1980).
[II.34] HÅKANSON, L., Ecometric and Dynamic Modelling – Exemplified by Cesium in Lakes after Chernobyl, Springer-Verlag, Berlin, (1991) 158 p.
[II.35] HÅKANSON, L., ANDERSSON, T., Remedial measures against radioactive caesium in Swedish lake fish after Chernobyl, Aquatic Sci. **54** (1992) 141–164.
[II.36] CARLSSON, S., A model for the turnover of ^{137}Cs and potassium in pike (*Esox Lucius*). Health Phys. **35** (1978) 549–554.
[II.37] HÅKANSON, L., JANSSON, M., Principles of Lake Sedimentology, Springer-Verlag, Berlin, (1983) 316 pp.
[II.38] HÅKANSON, L., The influence of wind, fetch and water depth on the distribution of sediments in Lake Vänern, Sweden, Can. J. Earth Sci. **14** (1977) 397–412.
[II.39] HÅKANSON, L., et al., Modelling of radiocesium in lakes – the VAMP model, J. Environ. Radioactivity (1996) 255–308.
[II.40] WETZEL, R.G., Limnology, Saunders College Publ. (1983) 767 p.
[II.41] VOLLERNWEIDER, R.A., The Scientific Basis of Lake Eutrophication, with Particular Reference to Phosphorus and Nitrogen as Eutrophication Factos, Tech. Rep. DAS/SDI/68.27, OECD, Paris (1968) 159 p.
[II.42] KORHONEN, R., SAVOLAINEN, I., Biospheric transfer model DETRA for assessment of radiation impacts, Technical Research Centre of Finland, Nuclear Engineering Laboratory, Research Reports 323, Espoo (1984) (in Finnish).

Annex I

REMEDIAL MEASURES AGAINST HIGH LEVELS OF RADIOISOTOPES IN AQUATIC ECOSYSTEMS

O. Voitsekhovitch, Hydrometeorological Institute of Ukraine
L. Håkanson, Uppsala University, Sweden

I-1. INTRODUCTION AND AIMS

This Annex has been prepared within the framework of the Aquatic Working Group of the Co-ordinated Research Programme on Validation of the Environmental Model Predictions (VAMP). The main objectives of this Annex are:

(1) To provide an outline of a broad set of remedial measures and strategies tested and suggested for aquatic systems to speed up the recovery after the nuclear accident at Chernobyl in April 1986. This Report covers case studies from rivers and lakes and includes results from field and laboratory experiments, as well as measures directed at reducing radioisotopes in food by different food preparation procedures in the home.
(2) To provide results from selected case studies, focusing on general, strategic results rather than site-specific details.
(3) To provide conclusions which specifically address practical matters concerning how to select remedial measures in different situations, how to avoid inefficient measures, and to suggest important areas for future research.
(4) To provide an analysis of the concept of lake sensitivity using both empirical and modelled data. One and the same fallout may give rise to very different radionuclide concentrations in water and biota depending on the characteristics of the lake and its catchment [I-1] .

Section I-3 is mainly a summary of experiences gained on remedial measures in the Chernobyl area [I-2][1] and from field experiments in Swedish lakes to try to speed up the natural recovery by means of adding lime, potash and nutrients [I-3, I-4] .

It should be noted that this Report is very brief on all matters concerning sampling methods, analyses and data processing, as well as on descriptive matters concerning the rivers and lakes and their drainage areas. The aim is not to provide an overview of the international literature in this fast growing field (see for example reference [I-5]), but to focus on results and practical matters concerning remedial measures.

I-2. REMEDIAL STRATEGIES

There are a range of possible practical remedial actions, either in the drainage area or the watercourse itself. These are listed below.

I-2.1. Measures in the drainage area

(a) Removal of contaminated soil (e.g. by bulldozers);
(b) Alterations in the catchment area to minimize the runoff of radioisotopes from land to water (the secondary load) by planting of trees, digging of channels/ditches, or adding of chemicals to bind the radioisotopes (e.g. lime, potash or dolomite);
(c) Prevention of flooding in the most contaminated areas (e.g. floodplain dams);
(d) Constructions to minimize radionuclide transport to surface water bodies by groundwater flow (e.g. contra-seepage walls in soils).

I-2.2. Measures in the aquatic ecosystem

(a) Constructions to increase the sedimentation of contaminated suspended materials in rivers, (e.g. the building of dams, ditches and spurs);

---

[1]This Study was initiated and funded by the Ministry of Chernobyl of Ukraine. The authors wish to thank Dr. S. Kazakov and E. Panacevitc from SPA "Pripyat" and also Dr. O. Zvekov from the Institute "Ukrwaterproject" for permanent attention and assistance in this study. We are also grateful to the Ukrainian Hydrometeorological Institute for providing monitoring data.

(b) Constructions to separate the most contaminated parts of the water bodies from the main flow (e.g. dikes and dams dividing water bodies);
(c) Dredging of contaminated deposits (e.g. mechanical dredging, suction or removal of material with bulldozers after lowering the water level);
(d) Changes of reservoir operation to optimize the results from the viewpoint of radioecology;
(e) Change of drinking water intake, e.g. choosing intake points with less contaminated surface waters and/or groundwaters;
(f) Adding of chemicals (like potash, lime or fertilizers) to change the partition coefficient of the radionuclides to suspended particles (like humus, clays, fulvic acids, algae), thereby lowering the biological uptake of the radionuclides;
(g) Changing the structure of the food web, e.g. by intensive fishing of predators, which could alter the predation pressure and increase the primary productivity of the water system. This may cause a "biological dilution" of the radionuclides.

I-3. EXPERIENCE FROM CASE STUDIES

I-3.1. The Chernobyl area

I-3.1.1. Introduction

More than 12 years have passed since the wide ranging application of emergency water protection measures to clean up and rehabilitate the environment were first implemented around the Chernobyl Nuclear Power Plant (NPP). The main objective of these remedial activities was to prevent significant secondary contamination of the surface water bodies that are hydraulically linked to the original contaminated area and to mitigate the expansion of expected groundwater contamination. Although some countermeasures and cleanup activities applied to radionuclides sources in catchments proved to have positive effects, many actions were evaluated as ineffective and even useless. The priority and available technologies for water remediation have also changed over time. However, social and political pressures to complete a 1993–1998 remedial action plan for water continues to have significant influence on the outcome of the cleanup. Most of the water protective countermeasure carried out were applied to Chernobyl exclusion zone. Many other mitigation actions were applied to the water intakes and irrigation channels. The water remedial actions in Belarus and Russia were mainly focused on restriction of water usage, recreation and fishery for the water bodies affected by the Chernobyl release. The main thrust was to prevent subsequent radionuclide contamination from entering the Pripyat River and the Kiev Reservoir, as well as other reservoirs along the Dnieper River from downstream of Kiev to the Black Sea. These countermeasures required large financial and human resources for their implementation and it is useful to learn from post-Chernobyl radiation protection practice. This Report briefly describes more than 12 years of scientific and technological activities, carried out mainly in the Ukraine and focused on implementation of countermeasures for contaminated water bodies surrounding the Chernobyl exclusion zone. This Report reviews the measures to prevent significant expansion of the radioactive contamination beyond the Chernobyl exclusion zone, the specific methods applied and new options, based on risk assessment and cost-benefit approaches.

Radioactive contamination of water, water protection, and remediation efforts at the Chernobyl Nuclear Power Plant site are worth assessing for possible lessons in controlling the redistribution of radionuclides via aquatic pathways [I-2, I-6, I-7]. An analysis of the remedial actions taken to mitigate the effects of secondary water contamination after the Chernobyl accident can provide decision-makers with a unique opportunity to optimize their approaches to surface and groundwater protection. As surface water and groundwater may act as secondary contamination sources, most engineering measures taken inside the Chernobyl 30 km exclusion zone were focused on prevention of radionuclide dispersal and migration.

Numerous studies have described the extensive radioactive contamination of large regions of the Ukraine, Belarus, Russia and parts of western Europe that resulted from the 1986 accident in Reactor 4 at Chernobyl. Most radioactive atmospheric fallout was deposited within the Dnieper River drainage

basin that lies adjacent to the Chernobyl Nuclear Power Plant site (Figure I-1(a)). This and adjacent drainage basins form an extensive area from which contaminated runoff flows downstream through the Pripyat and Dnieper River systems across the Ukraine to the Black Sea (see Figure I-1(b) [I-8, I-9].

After the Chernobyl accident, overland flow across the contaminated landscapes has continued to be a major factor in radionuclide transport. This flow contributes to the diverse migration pathways by which radionuclides are transported from the Chernobyl area to the greater Dnieper region with its

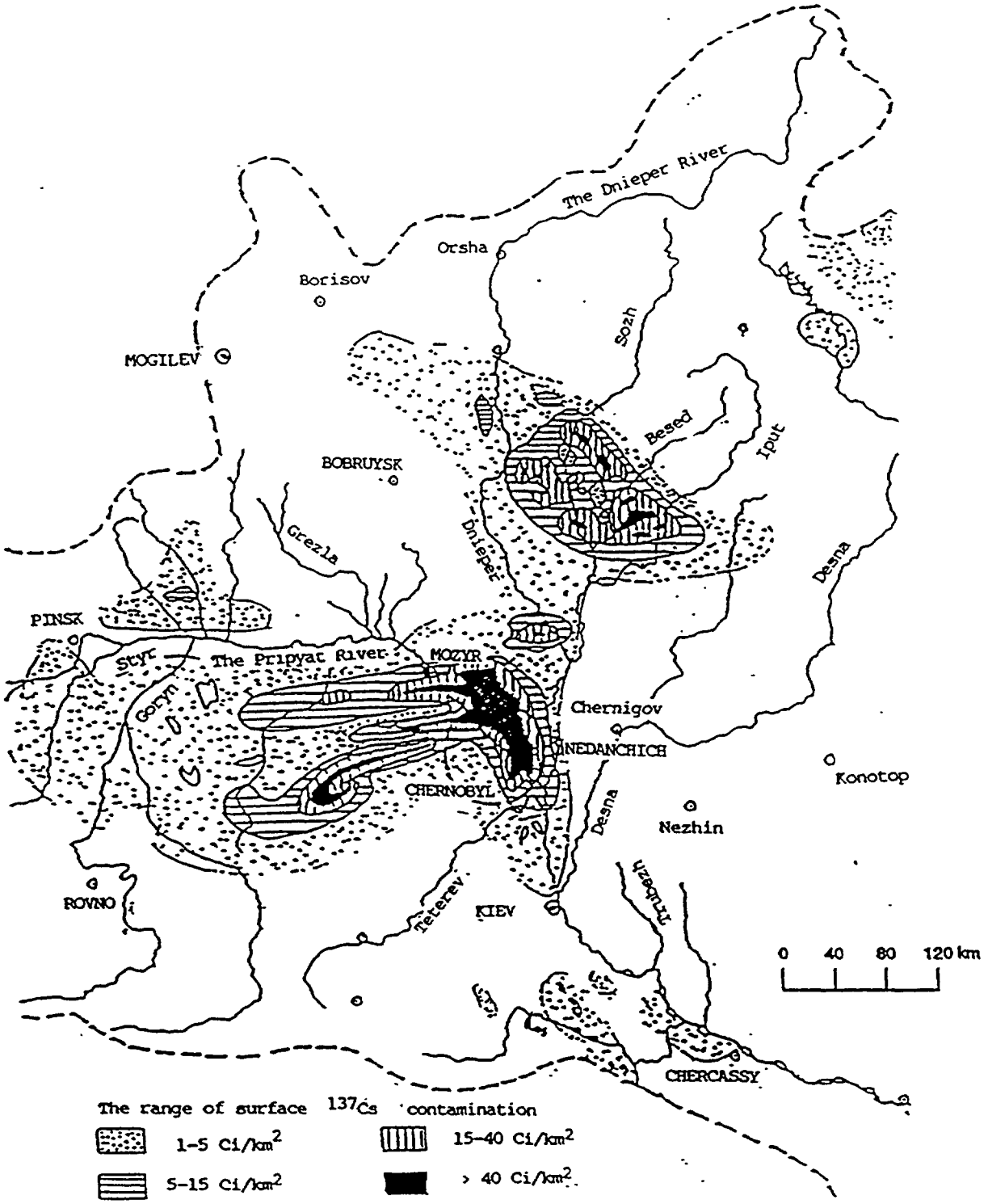

FIG. I-1(a) ^{137}Cs contamination of the catchment areas of the Pripyat and the Upper Dnieper River Basins.

more than 20 million inhabitants. In order to better understand how contaminants are spread across the landscape into relatively uncontaminated areas and to better protect water resources, regional surface and groundwater pathways have been studied. These investigations form a basis for a risk assessment for people living along the Dnieper River and/or consuming water and foodstuffs arising from aquatic systems in the Dnieper catchment.

I-3.1.2. Review of radioactive contamination within the Dnieper River system

A regular sampling programme was organized for the water bodies in the vicinity of Chernobyl NPP, for all the reservoirs of the Dnieper cascade and also in the Belarussian part of the Pripyat River basin as well as in the lakes and rivers flowing from the catchments of the so-called Bryansk (Russian-Belorussian) "hot spot". Many different institutions in the Ukraine, Belarus and Russia were also involved in monitoring groundwater contamination both on- and off-site. These studies showed that groundwater could be significantly polluted in the neighbouring areas of Chernobyl NPP and at short distances from the waste disposal sites. In general, the groundwater pollution contributes no more than 2 to 3% of the total transfer (washout) from terrestrial environment. However, groundwater contamination in the Chernobyl exclusion zone continues to be under the long-term control.

During the initial period immediately after the 1986 Chernobyl nuclear accident, the surface water bodies were directly contaminated by atmospheric fallout. The highest levels of water contamination were observed during the first fortnight. The largest radionuclide contributors to drinking water contamination was ^{131}I and some others short lived radionuclides that could not be controlled due to their food chain transfer through drinking water. Strict restrictions were imposed on the use of open water sources in contaminated areas and evacuation of citizens from the Chernobyl exclusion zone was carried out.

Between 1986 and 1998, surface runoff and other water exchange processes dispersed contaminants from the Chernobyl accident within the Dnieper River drainage system (Figure I-2). Data collection from the Pripyat River illustrates the changes in ^{90}Sr and ^{137}Cs with time near Chernobyl. These data suggest a close relationship between ^{90}Sr concentrations in the river and river discharge. Riverine concentrations of ^{137}Cs are, however, less dependent on surface hydrology. This difference in the nature of radionuclide transport depends on soil/bottom sediment properties and solid-liquid contaminant interactions. Peaks in fluvial ^{90}Sr contamination levels correspond with the inundation of floodplains within a 5–10 km areas around the Chernobyl NPP. This higher radioactivity in soils of this floodplain remain a major source of secondary contamination in the Dnieper aquatic system (Figure I-3, see also Figure I-2).

Moving downstream to the series of reservoirs along the Dnieper cascade, most ^{137}Cs from the Chernobyl accident has accumulated in the bottom sediments of Kiev and other reservoirs. Differences in the concentrations of ^{137}Cs in the inlet and outlet of the different reservoirs is demonstrated in the radionuclide's budget in the reservoirs and their accumulation in the sediments. As a result of the settling of suspended particles, bioaccumulation and adsorption, only 2–5% of the ^{137}Cs that enters the Dnieper through surface runoff reaches the Black Sea. In contrast, most dissolved ^{90}Sr remains in solution and passes through the Dnieper's reservoirs without significant fall in concentration.

Since 1992, more than 4000 small ponds and lakes in six regions of the Ukraine have been studied to assess the consequences of the Chernobyl accident. A special register for their water use and ecosystem contamination as well recommended restrictions was also recently created. Such monitoring actions, together with the results of mathematical modelling, make it possible to obtain reliable data on contamination of the water supply sources for Kiev and other principle water intakes from the rivers and reservoirs affected by the Chernobyl accident and justify particular restrictions and recommendations to eliminate radionuclides migration within aquatic pathways. Development and sustainable support of monitoring programmes for the affected water bodies during the whole post-accident period was one of the most important tasks for governmental bodies, as these activities provided data to support water quality management in the contaminated areas.

I-3.1.3. Scenario simulation (principle events)

Beginning in the spring and summer of 1986, the most serious radioactive contamination (focusing on ^{137}Cs and ^{90}Sr) was in water bodies along the Dnieper River cascade downstream of Chernobyl and the Kiev Reservoir. After the spring and summer of 1986 (when direct radioactive fallout on to the surface of water bodies took place), the most significant sources of surface water contamination of the Dnieper River were surface runoff from the initially contaminated floodplains and catchment areas as well as infiltration of heavily contaminated water from the cooling pond and other water bodies to the river. The first flood period in 1987 showed that the main sources of radioactive contamination of the Dnieper cascade are the whole catchment of the upper part of the Pripyat river basin and a significant part of the upper Dnieper river catchment (mainly the Sozh River). Ten years after the accident, more than 70% of annual radionuclide input has arisen from sources situated in the Chernobyl exclusion zone. The results of radionuclides spatial budget studies derived from the regular monitoring observations provided an important basis for the current strategy on water remedial actions. The time series of the varying concentrations of different radionuclides during the entire post-Chernobyl period have been presented by Voitsekhovitch et al. [I-10].

Since the accident at Chernobyl, no long periods of high river water level or flooding have occurred in the contaminated areas. The spring water flow of the Pripyat River, with discharges of 800–2200 m^3/s, did not exceed the normal flood levels compared to the maximum possible discharge in excess of 5000 m^3/s, as happened in 1979. After river floodplain flooding in 1988, 1991 and in 1994 it became clear that unless mitigating actions were conducted in the contaminated area, the floodplain would remain a hazard in the future. As a matter of fact, the discharges in 1991 and 1994 were not very high, but due to specific conditions during the winter–spring period (ice jams) the floodplain was inundated.

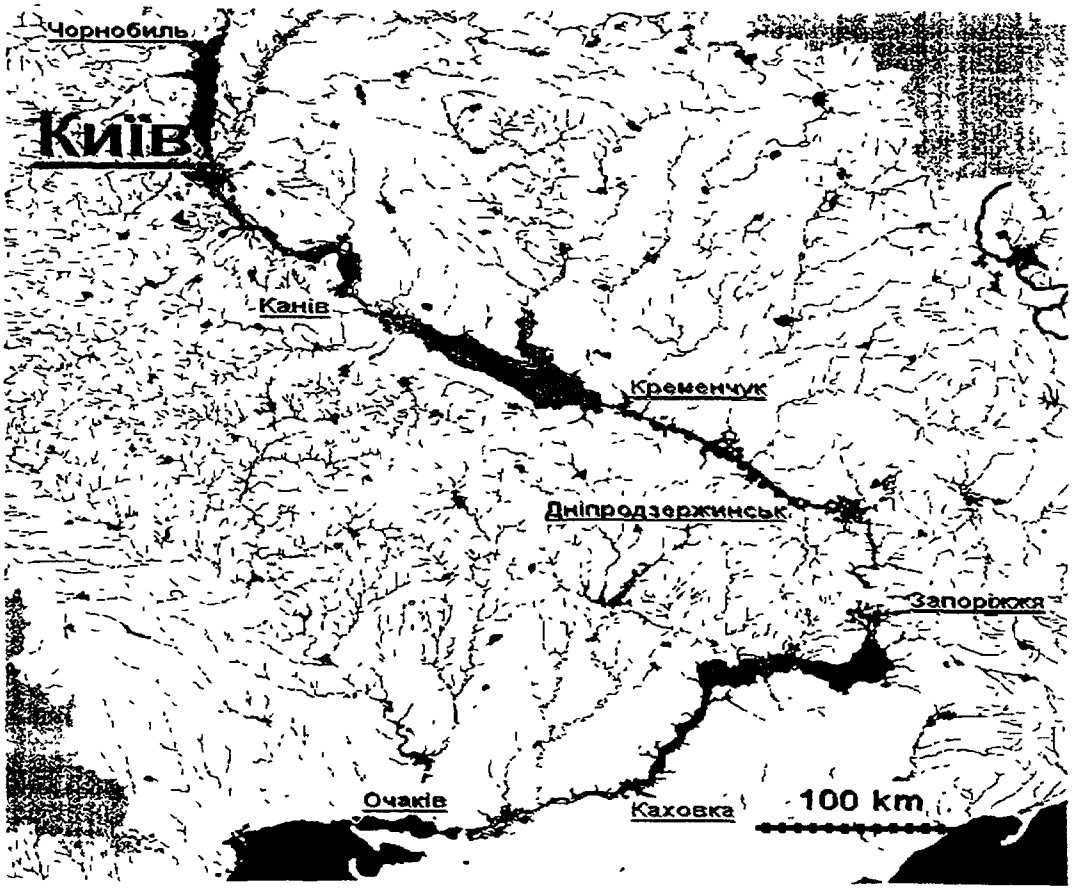

FIG. I-1(b) The Dnieper River Reservoir cascade.

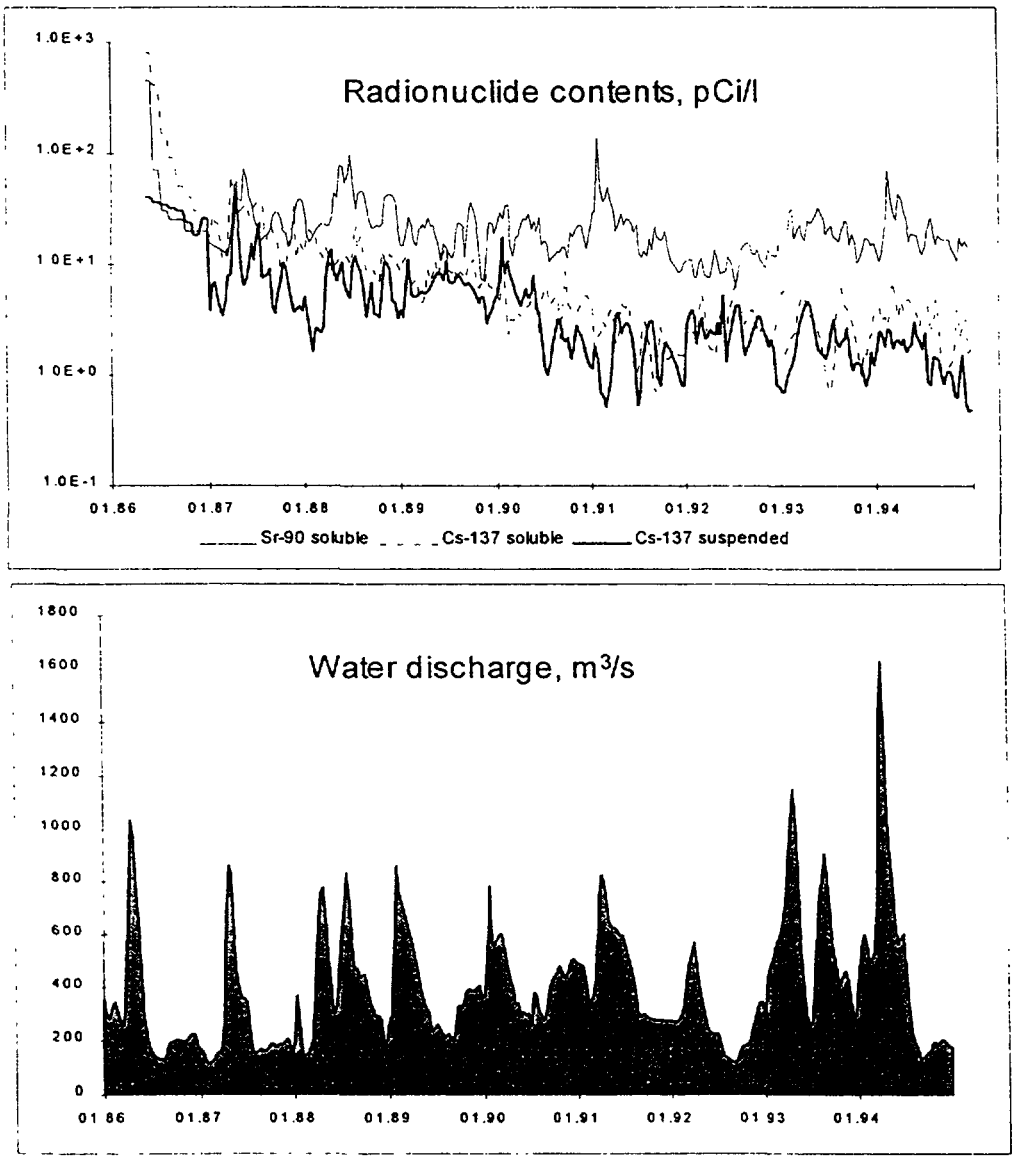

FIG. I-2. ^{137}Cs and ^{90}Sr concentrations in the Pripyat River near Chernobyl averaged over 10 day periods in pCi/L. River discharge (m^3/s) is shown in the lower figure.

For this reason, actions focusing on the prevention of further significant removal of radionuclides from the areas of the Pripyat River floodplain close to the Chernobyl NPP were accepted as a first priority in the water remedial strategy for the period after 1992. The current radionuclides concentrations in the Dnieper River are not considered to pose a significant health risk. However, considering potential runoff and the risk of existing chemical pollution, some measures for preventing and mitigating the risk have been approved.

In order to estimate the potential consequences of the flooding of the Chernobyl area, future contamination levels within the Dnieper Cascade have been simulated, based on a probabilistic hydrological and physico-chemical scenario incorporating migration processes in the contaminated areas. Some results of the simulation are illustrated in Figure I-4(a) and I-4(b), describing results of radionuclides contamination forming downstream of the river's contaminated floodplain in the zone close to Chernobyl and in the Dnieper cascade. The description of models are presented in reference [I-11]. The results of mathematical simulations for different hydrological scenarios and studies of the fate of radionuclide migration in the potentially inundated soils were used to support the water remediation optimization procedure during the post-Chernobyl decade.

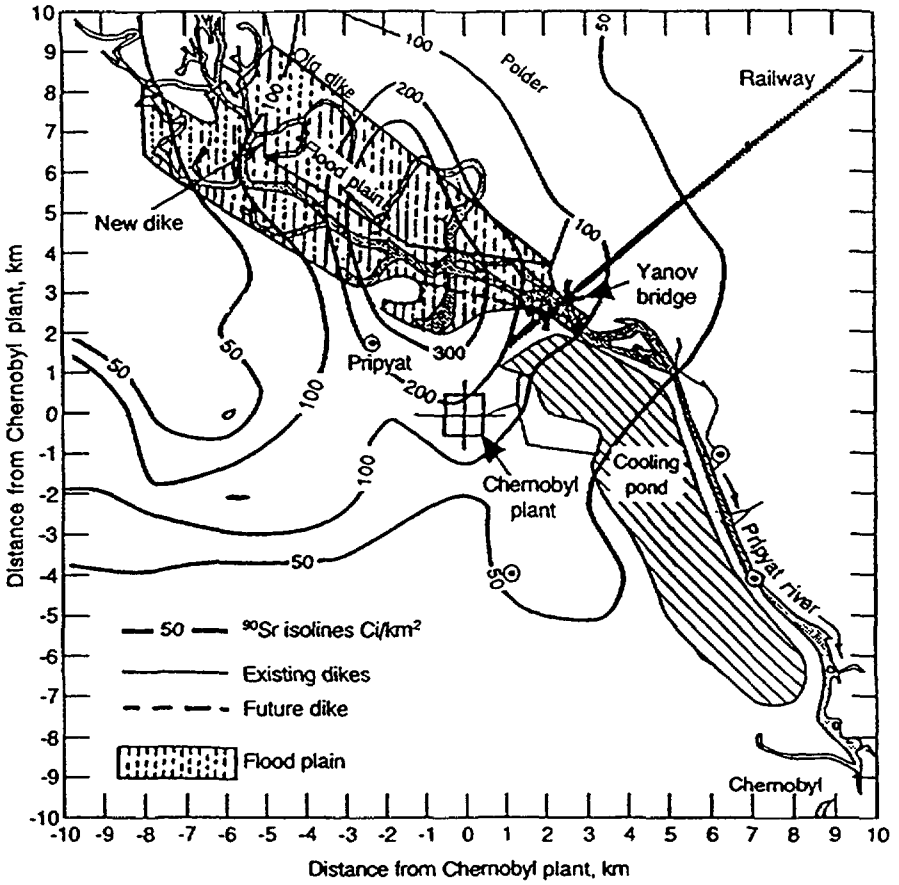

FIG. I-3. ^{90}Sr soil contamination on the Pripyat River floodplain due to atmospheric fallout in April–May 1986 near Chernobyl NPP. This area is a major source of secondary contamination for the Pripyat/Dnieper aquatic system.

I-3.1.4. Assessment of water protection countermeasures

Brief analysis of different stages of water remedial actions

The chronology of governmental decisions focusing on water protection activities carried out after the accident for the period from early May 1986 and up to 1989 are reported in [I-12].

Since the accident, engineering and administrative countermeasures have been taken to mitigate the risk for the population that resides along the Dnieper Reservoir system downstream of Chernobyl. In this respect, three phases of water protection activitieshave been carried out:

Emergency phase: (two to three months after the accident)

During the first two to three months after the accident, short-lived radionuclides, such as ^{131}I, ^{137}Cs, ^{90}Sr, ^{140}Ba, ^{144}Ce, ^{103}Ru, ^{106}Ru, ^{95}Nb and ^{95}Zr formed a significant component of the radiation dose to local residents from aquatic sources. This contrasts with the present time when ^{90}Sr and ^{137}Cs dominate the radiological impact to the human health via aquatic pathways.

Countermeasures during this period were based mainly on administrative decisions and were aimed at controlling the situation. These countermeasures included:

- restriction of water use and fishery, avoiding contaminated surface water resources where possible;
- supplementary purification of drinking water in municipal water treatment plants, development of new technologies, sorbent materials and methods for drinking water treatment;

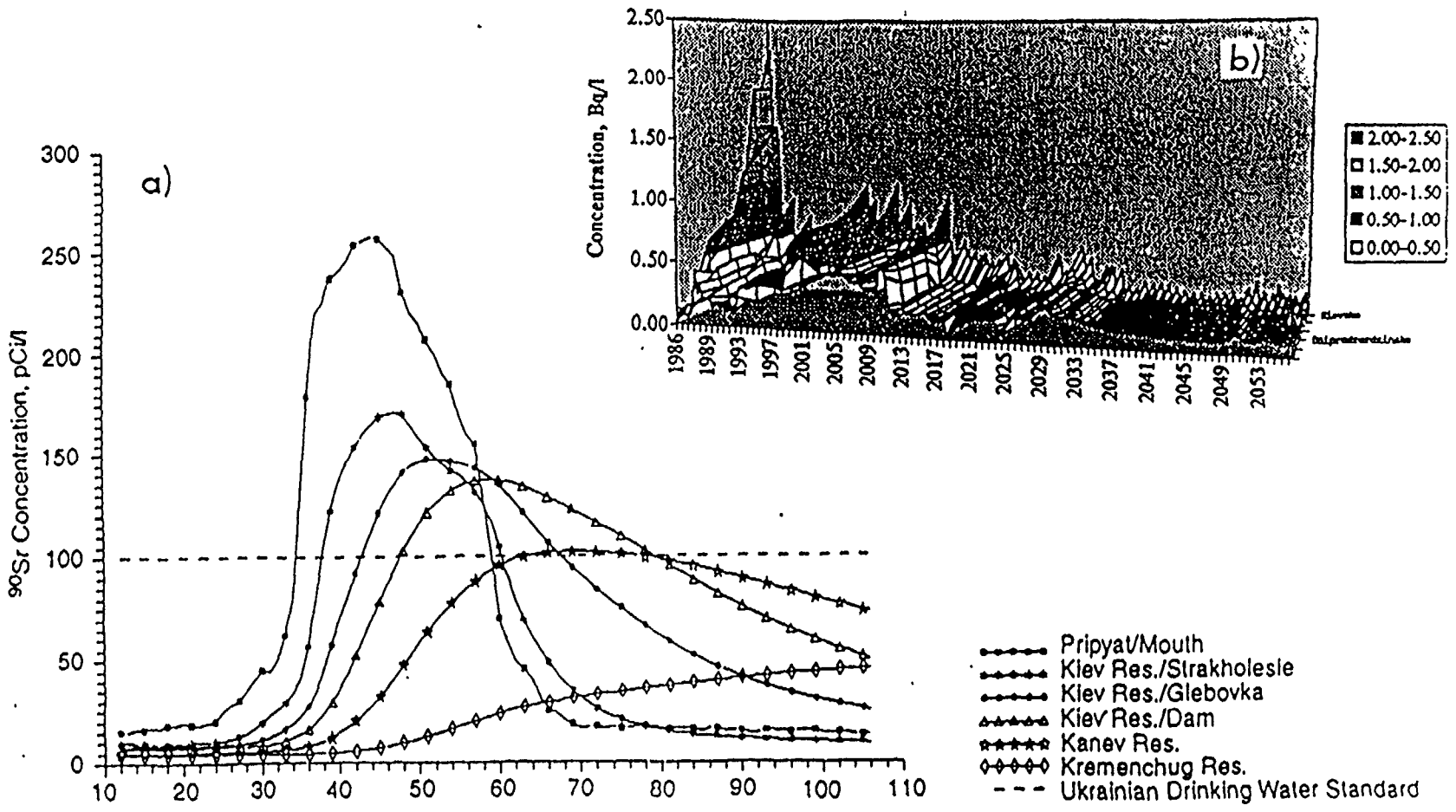

FIG. I-4. Simulations of ^{90}Sr concentrations in the Dnieper Reservoirs: (a) flooding of the floodplain for a scenario discharge of 2000 m^3/s without water protection measures; (b) long-term simulation of the contamination of the Dnieper Reservoirs.

- attempts to regulate the flow of contaminated water through the Kiev Reservoir by dam operation;
- increased use of groundwater sources by municipalities and construction of supplementary groundwater supply wells.

Most of these measures have been implemented without cost-benefit analyses. However, consideration was given to the stress on society and the availability of the resources of the former USSR that were directed to the elimination of the consequences of the accident. The main reasons for implementing only a limited number of the cost-effective actions during the early period after the accident were the lack of experience, time and required expertise. Therefore, most measures to reduce the radiation risk to the public from water usage were very expensive and limited in success [I-13].

Decision-makers also made many errors because of the lack of adequate information concerning spatial and temporal variations in contamination of water bodies and the catchment area. For example, due to the lack of experimental data and disagreement between scientists and decision-makers, the first assessment of the adsorption/desorption parameters for radionuclide liquid-solid interactions was incorrect and the amount of radionuclide runoff from catchments to rivers was greatly overestimated. As a result, many ineffective water protection actions were taken in the first months after the accident. For example, zeolite was washed away into the river from soil-clay barriers constructed along the Pripyat River banks.

As another example, in early May 1986, surface gates were opened and bottom gates closed in the dams of the Kiev Reservoir. It was thought that clean water was being let out of the reservoir so that the highly contaminated near bottom water associated with adsorbed radionuclides could be retained in the reservoir. In reality, during the first week after radioactive release the vertical mixing of water was slow and therefore the lower water layers of the reservoir were much less contaminated than the upper layers, which had been directly contaminated by atmospheric fallout. A better approach would have been to open the bottom dam gates and to close the surface gates, at least for a period of several weeks in May 1986. This action would have reduced the levels of radioactivity in downstream drinking water during the first weeks after the nuclear accident, when the main exposure from drinking water intake occurred.

Early intermediate phase (summer 1986 to 1988)

In the summer of 1986, several kilometres of protective dikes were constructed along the right bank of the Pripyat River to retain the contaminated urban runoff from the cities of Chernobyl and Pripyat. This action was not effective because runoff from such a wide area could not be readily controlled. However, this action did regulate the direction of the contaminated runoff over time. A protective dam 11.2 km long was also built on the left bank of the Pripyat river by the institutions of the USSR.

An enormous range of protection structures were constructed beyond the exclusion zone. Among these were the embankment dams along the Uzh and Teteriv rivers.

In the early years after the accident, attempts to isolate the Chernobyl Plant cooling-pond from the Pripyat River was a major issue. A special drainage and well system was built around the cooling pond to retain infiltrating radioactive water. At present, the drainage system is not in operation because of uncertainty as to the consequences of its operation. Indeed, pumping water from the wells back into the cooling pond may cause problems with the water balance and dissolved salts in the pond. The cost of construction and maintenance of this system was, and still is, very high.

Drainage systems of wells bored at a depth of 20–30 m, with deep well pumps and pressure lines joined by a main collector were built in the exclusion zone of the Chernobyl NPP. The drainage water has to be discharged into the cooling pond. This reserve system is now kept in a state of complete

readiness, although there has been no need to use it up to now. To protect the groundwaters from the river and diversion drainage, the design of the drainage screen for the cooling pond was modified.

Another action during this period was the construction of a slurry wall and a series of drainage wells to prevent subsoil underground migration. A vertical anti-filtration screening wall of ball clay, 2.8 km long and 33 m deep, was built from July to September 1986 on the border between the main NPP building and cooling pond by the method "a wall in the ground".

A special drainage section of Pripyat city's sewage system has been diverted to the cooling pond to reinforce the foundation plate under the reactor N-4 of the NPP. Drilling of wells for the industrial site drainage, construction of the burial points for the radioactive waste as well as a vertical anti-filtration screening wall using the method, "a wall in the ground", were carried out.

Five, and then later on sixteen wells were bored at the industrial Chernobyl NPP site with the purpose of regulating the groundwater level. Liquid wastes of high radioactivity were washed out into the reservoir that was modified in the canal stretch at the third stage of the NPP construction. Additional studies have shown that migration of radionuclides within underground flows is much too slow to allow the drainage wells to be effective. Moreover, the slurry wall and wells could not prevent the contamination of surrounding groundwater. Therefore, the project was stopped.

During 1986 and the early months of 1987, over 130 special filtration dams with sorbing screens containing zeolite (klinoptololite) were built. Filtration dams, with a total length of 4.9 km, were used for retaining radionuclides while letting the water through, were built on a large number of tributaries of the rivers and diversion canals. The zeolite filtration dams captured the short lived radionuclides more or less effectively during the summer 1986, but very soon after their adsorption capacity decreased dramatically because the pores of zeolites bodies became blocked by suspended matter and because of other non-foreseen reasons. Subsequent studies of their effectiveness indicated that only 5% to 10% of ^{90}Sr and ^{137}Cs was adsorbed by the zeolite barriers within the dams. Special technologies of zeolites and other natural sorbent materials used for aquatic radionuclides control were required for sorbent fraction preparation. The river flow through the dam filtration bodies also needed to be controlled. Such requirements vastly increased the cost of such countermeasure and limited their effectiveness. Moreover, the streams that were dammed contributed only a few percentage points to the total flow of the Pripyat and Dnieper River drainage basins. After the spring flood of 1987, the construction of new dams was terminated and a decision was made to destroy most of the existing dams. At present some ten dams are still in use.

During 1986 and 1987, an early mitigating measure was the construction of several Sites of Temporary Radioactive Waste Localisation (STRWL) near the Chernobyl Plant. These sites were used to bury contaminated soils, vegetation, debris, and even small buildings. Wood from the highly contaminated "Red Forest" pines, killed by high radiation levels, was also buried there. These measures were thought necessary to protect the emergency response groups and power plant workers from high doses of radiation. The highly contaminated wood was buried in shallow trenches without any protective measures to prevent future contamination of groundwater, resulting in significant long term contamination problems.

During the first summer after the accident, several sedimentation traps were dredged in the Pripyat River to increase the width of the river and thus reduce the water velocity in attempt to increase sedimentation of suspended radioactive particles. However, subsequent studies [I-2, I-12] showed these traps to be ineffective. The suspended radioactive particles were much too small to settle in such a large natural river with high water discharges and turbulent flow conditions.

To operate all the water protection facilities in the Chernobyl exclusion zone a special Water Management Division was created in July 1987. In 1993 the Administration of the Chernobyl exclusion zone renamed this Division the State Specialised Production Water-protective Enterprise " Chernobyl-water management".

According to its Statute, the activities of the enterprise are aimed at:

- operation of the water protection installations and systems intended for reducing transfers of radionuclides from the contaminated areas by surface water flows to the Pripyat River;
- designing and conducting measures involved in preparation of the water protection installations for floods to pass through;
- hydrological aspects of the water protection measures;
- maintenance of wells for the decrease of water levels and control and observation of wells;
- boring experimental, control and observational wells;
- sealing of the wells that are out of order;
- maintenance of the wells located where people have resettled (so called "self-settlers").

Later intermediate phase (1988 to 1993)

A new phase of hydrological remediation began after the 1988 summer flood. This flood was the first time after the nuclear accident that high river water levels covered much of the contaminated floodplain, thus producing the secondary ^{90}Sr contamination of the river. After this flood event, a special study was made of runoff processes from the contaminated floodplain near the Chernobyl NPP [I-2].

Surface hydrological modelling shows that a realistic, worst-case scenario, one that would cause the highest radionuclides concentration in rivers, would be a spring flood with a maximum discharge of 2000 m^3/s. Such a flood has a probability of occurrence close to 25% per year. It is assumed that the maximum possible increase of ^{90}Sr in waters downstream of the considered areas could be up to 10 Bq/L, clearly exceeding the permissible sanitary level for ^{90}Sr in waters declared in the Ukraine (4 Bq/L). Computer simulation results on the flooding indicated that if radionuclides in the floodplain were isolated from the river, the ^{90}Sr concentration in the river would be decreased by two to four times [I-13]. Thus, several approaches have been proposed to reduce the radionuclide concentration in the river and the potential effectiveness of each approach has been simulated. The construction of a dike around the contaminated area on the left (east) bank of the river has been chosen as the best protective option. Construction of the dike was finished before the spring of 1993. As a result of this action, during the summer flood of 1993 more than 3.7×10^{12} Bq (100 Ci) of ^{90}Sr were prevented from being washed from the floodplain of the Pripyat river into the Dnieper River Cascade. Simulation of the same events for scenario of winter flood on the Chernobyl site in January 1991 and subsequently on the basis of observation of similar events in the summer of 1993 and during the winter flood of 1994 confirmed the accuracy of the simulations [I-13, I-14].

It became gradually clear that other countermeasures at the Chernobyl site could not be planned without the designation of a general strategy for water remediation. However, taking into account that among the CIS countries all contaminated water fluxes reached Ukrainian territory, the Governmental Water Remedial Programme was created and exclusively funded in the Ukraine.

I-3.1.5. Present understanding of the problem

Recent stage of problem evaluation and its solution (1993–1997)

The finding of the first water protection stage at the Chernobyl site was that a realistic understanding that technological possibilities to control the existing sources of radioactive contamination on such a large catchment scale are very limited. It became clear that optimization of any water protection actions can only be done by comparing actual human doses that could be averted as a result of engineering activities at the Chernobyl site [I-15, I-16]. Based on the principles of the Ukrainian Water Remedial Action Plan (1993) and on computer simulation results of the potential effectiveness of different water protection action plans under various Pripyat River hydrological

regimes, a comprehensive Water Remedial Action Plan for the Dnieper River was established in 1994. This plan contained the following priorities:

- To construct a dike in the floodplain area along the Pripyat River containing extremely high soil contamination, also on right bank bordering the Chernobyl NPP; thus isolating the highly contaminated floodplain from the river during flooding (to be finished in 1998).
- To design a project to clean up contaminated bottom sediments in the Chernobyl cooling pond after the Chernobyl nuclear reactors have been shut down (this project is still not terminated because of lack of funds and uncertainty with regard to the future of the Chernobyl NPP).
- To provide water regulation of the Chernobyl wetlands sites (at present the project design is completed and it is ready for implementation).
- To provide expanded groundwater monitoring of STRWL; to provide reliable monitoring and controls of transuranic materials due to surface water and groundwater transport beyond the currently contaminated area (the programme is underway).
- To prevent expansion of radionuclide transport beyond present locations in the waste disposal site, as a result of groundwater mobility, by constructing engineering and geochemical barriers around STRWL (a number of actions are included in the future Chernobyl site Remediation Action Plan).

However, since 1994 new efforts regarding aquatic remedial activities at the Chernobyl NPP site have been practically suspended due to the lack of funds needed to complete the projects. Achieving cost-effectiveness in the remediation measures is uncertain because the criteria for a cleanup strategy have not yet been fully developed. However, at present, large amounts of radioactive materials are still concentrated in the Chernobyl area. For instance, the Pripyat River floodplain areas alone (see Figure I-6) has a 40 to 50% probability of being inundated by the river water each spring. Even after construction of an earthen dike along the left bank of the river in 1992, several thousand curies (1 Ci = 37 GBq) of ^{90}Sr and ^{137}Cs still remained in the lowland soils. A large amount of radioactive waste is also present in the STRWL and in contact with the groundwater flow moving in the direction of the Pripyat River.

During the next 60 years (up to 2056), implementation of this Action Plan should reduce annual runoff influx of radionuclides from the wetlands and floodplain and other radioactive leakage from water bodies. If no action were to be taken, the Pripyat River would introduce 1500–2000 Ci of ^{90}Sr and up to 500–700 Ci of ^{137}Cs into the Dnieper River Cascade. With the remediation plan implemented, the safety level (when no additional action is required) of 1 Bq/L of ^{90}Sr for the Dnieper River water near the Kiev City water intake would be met. These actions would also satisfy the safety level (0.25 Bq/L) of ^{90}Sr contamination in the lower Dnieper River reservoirs that are used extensively for irrigation. In order to predict the beneficial effects in floods with maximum water discharge of 2500 m^3/s, computer simulations were also performed with and without water protection dikes installed along the floodplain on both riverbanks [I-14].

I-3.1.6. Recent justification of the measure based on the radiological risk assessment

Recent approaches for aquatic remedial actions in the Ukraine are based on dose and radiation risk assessment methodology applied to water protection practice. In order to estimate the collective effective doses integrated over 70 years from ingestion of ^{90}Sr and ^{137}Cs to the population of the Dnieper regions, the results of predicted radionuclide concentrations in the Dnieper water up to the year 2056 were used. The average collective effective dose from water usage to the population living along the Dnieper River consists of the dose received from drinking water (35%), fish consumption (40%) and consumption of irrigated products (25%) [I-7].

The dose estimations were based on the results and predicted scenarios (most probable simulated) of radionuclides contents in the Dnieper River reservoirs up to the year 2056. The structure of irrigated land and tap water consumption is taken into account. In accordance with these results, in 1986 the

collective doses from water use in the Kiev region exceeded the current dose level by six to seven times. An opposite effect was observed in the Crimean region, where the initial contamination level of the lower Dnieper River was caused mainly by primary fallout. Studies have shown that for different regions of the Ukraine the structure of the dose pattern is different [I-17]. These studies also show those annual averaged individual effective internal doses for different regions of the Ukraine vary strongly (see Figure I-5). A recent study also showed that the ^{90}Sr contribution to the radiation exposure due to drinking water consumption of the population is much higher than was assumed before. For instance in the same year, for the population of Kiev, the contribution of the aquatic pathway to the total internal dose from ^{137}Cs was only 2%, compared with close to 46% for ^{90}Sr (Figure I-6).

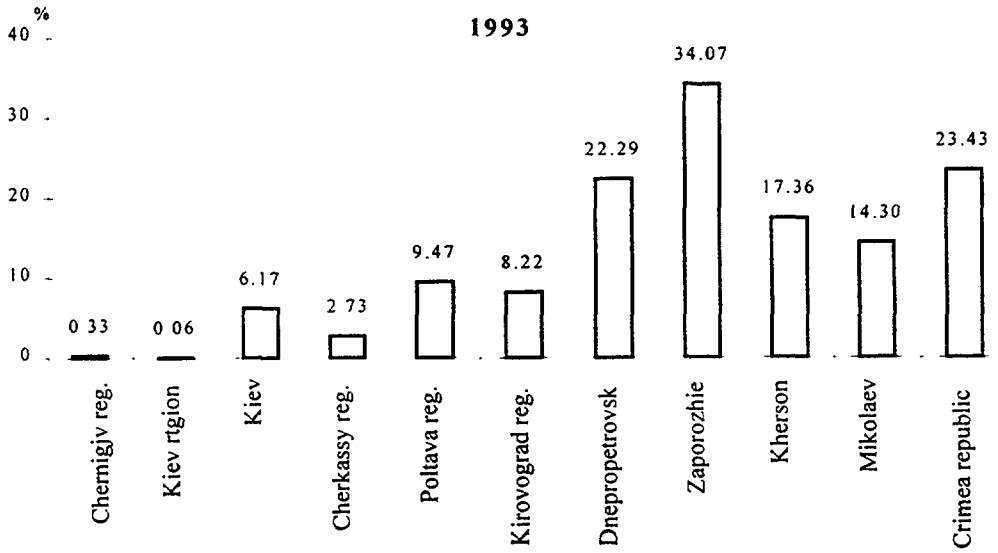

FIG. I-5. Aquatic components contributing an annual averaged individual effective dose for people living in different regions of Ukraine through water usage from the Dnieper Reservoirs during 1993.

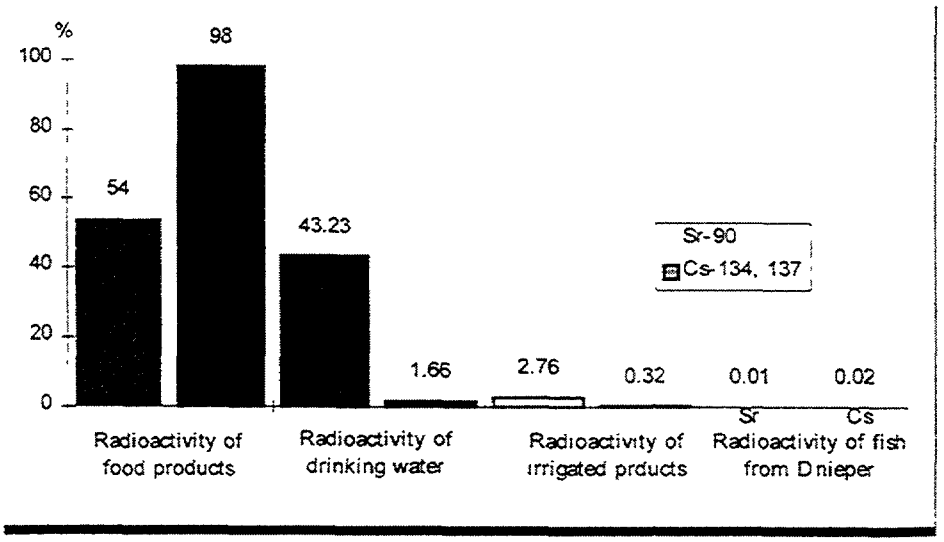

FIG. I-6. Partial contribution of ^{90}Sr and ^{137}Cs components by different elements of food chain pathways to averaged individual effective dose for Kiev citizens during 1993.

The risk assessment procedure includes analysis of radionuclide sources, radionuclide transfer in the environment and assessment of their impact on man. A selection of values for dosimetric coefficients and analysis of radiation risk to man were made in accordance with ICRP recommendations [I-18]. The total collective internal equivalent dose expected due to aquatic pathways for the period 1986–2056 was estimated to be some 3000 man·Sv. Using the ICRP nominal probability coefficient of 7.3×10^{-2} cancer deaths per Sv, the stochastic cancer effects due to water usage of the Dnieper River were estimated. During a 70 year exposure, the projected cancer deaths were estimated at about 200 cancer deaths in 21 million people. During the 1986 to 1993 exposure period, about 60 cancer deaths were predicted [I-13]. A calculation of the dose to the total population shows the individual human radiation risk from Dnieper River water is no higher than 1×10^{-5}.

Moreover, it appears that for more than 30% of the interviewed people with different levels of education, but without special knowledge about radiation protection, the actual health risk is higher from water consumption that from other exposure pathways. Water pathways affect some critical groups of water users more than average persons. In fact, the expected individual risk may be a factor four to five times higher, or in particular cases the risk may be even higher. The most significant radiation risk from annual consumption of fish from the Dnieper River for 1986 was estimated to be in the range of 1×10^{-4} to 1×10^{-5} through uptake of ^{131}I, ^{134}Cs, and ^{137}Cs. After 1987, the radiation risk from fish consumption was assessed to be one order of magnitude less than that for 1986. Implementation of the most effective water protective action could reduce the estimated risk from water usage by up to three to four times. In fact, the radiation risks from water consumption are low compared to other factors in the total radiation risk. At the same time, the risk stress component, caused by the psychological reaction in the population, was greater than the purely physical component of the radiation risk.

In spite of the low exposure level of the Ukrainian population from aquatic pathways, the radionuclide transfer by the river flow (caused mainly by contaminated runoff from sources situated at the Chernobyl Site) will remain a sensitive factor. When all the sources of radioactive contamination of the water are known, it is preferable to derive an optimal set of water protective countermeasures, rather than taking ad hoc actions. However, any countermeasures should be cost effective and chosen according to well-known ALARA principles.

Other environmental contaminants

Unfortunately, at the present time there is no clear basis for estimation of total and partial risks of environmental contamination, particularly from water usage with respect to the multicompartment contamination of water bodies. For instance, all Dnieper River reservoirs are situated in industrial and agricultural areas with high non-radioactive pollution. Toxicological investigations have shown the presence in reservoir waters of a number of other toxic substances with strong cancerogenic and mutagenic properties. In many cases, compared to radionuclide input their origin is uncertain, or they are not controlled. Naturally occurring radionuclides in the water also have their negative effects on the water consumers. For instance, the average individual effective dose from natural radionuclides such as ^{226}Rn, ^{222}Rn, and ^{238}U in drinking water in considered regions can be 0.17 mSv/a and even reach several mSv/a in some regions. This is can be more than the post-Chernobyl risk component. However, these sources of contamination are not controlled and managed. Therefore, it is very difficult to clarify immediate water protective countermeasures. However, in the case of Chernobyl when the sources of water contamination are known, it was decided to realize a reasonable set of actions on the basis of doses and cost optimization. Also taking into account social reasons for decreasing the stress component of the population living along the Dnieper, it was preferable to realize the Water Remedial Action Plan for Chernobyl site rather than be passive.

Strategy of the modern phase of the water protection at the Chernobyl site

The New Radiation Safety Regulations (NRB-98) were implemented in the Ukraine in January 1998, and may provide a basis for using a cost-benefit procedure to optimize water remediation

measures. The expected effectiveness of remediation measures depends on the hydrological regime of the river, for example the timing and duration of low, high, and average river discharges. The effectiveness of designed hydro-engineering constructions, such as dikes, will be significantly greater in preventing additional radioactive washoff from the Chernobyl Plant zone to the river during years when river water floods the contaminated areas.

The first priority action includes the construction of a dike on the right bank of the Pripyat River and mitigation action against filtration of contaminated water from the cooling pond. The cost for such actions was estimated at 5 to 6 M US dollars. Therefore, it was necessary to estimate and compare the cost of the intended countermeasure and radiation risk reduction, as a result of the implementation of a water remedial plan (i.e. the cost to reduce the risk in equivalents of 1 man·Sv).

Computer simulation indicates the effectiveness of the countermeasures will be much greater under high flood conditions, but these remedial actions can be useless under low water levels without river flooding [I-17]. Furthermore, their effectiveness will also be low when contamination levels of the reservoirs are already low due to natural factors. Thus, the use of available funding to implement measures in the Chernobyl exclusion zone is appropriate in spite of their relatively lower contribution to reduce the global health risk to the population from the Chernobyl accident.

For the period of water usage up to 2056 and with 20 million persons affected in the Ukrainian population, construction of the right-bank dike would reduce population doses by an estimated 300 to 400 man·Sv under the most probable hydrological conditions, as opposed to doing nothing. This reduction would be in addition to the 600 to 700 man·Sv dose reduction from the left-bank dike already constructed in 1993.

Cost–benefit analysis application

The cost to reduce the dose through the installation of a right-bank dike and the other actions set forth above were estimated to be approximately US $15 000 to 20 000 per 1 man·Sv reduction. If the running and maintenance costs are taken into account during the lifetime of the dike, the cost will double and can be estimated as 30,000 to 40,000 US per 1 man·Sv. Such a remediation cost for risk reduction could be considered in developed countries and is comparable to similar criteria in the United States and some other countries [I-19].

However, due to the severe economic situation, it is financially difficult for the Ukraine to implement this remediation plan and it is looking for additional funding sources. At present, because of the economical situation in the Ukraine, the dose effective criteria for implementation of countermeasure is estimated to be about 2000 US per 1 man·Sv. However, if the water remedial plan is implemented, its beneficial social effect is very high, an added argument to complete the current water protective action plan. In accordance with new Radiation Safety Regulations in some cases, when the social effect of countermeasure is very high, the dose effective cost can be only 5–10% of the total socially reasonable cost. This means that the actual cost of risk reduction due to suggested water remedial actions on the floodplain near the Chernobyl NPP can be socially acceptable.

Currently, justification for the water protective plan may include reducing the cost of the technology, or optimizing the remedial and cleanup activity, or obtaining additional outside funding. Even though the remediation cost-benefit criterion may not be met for this plan implementation, the cost can still be justified by controlling radioactivity outflow from the Chernobyl Plant zone and by considering the social factors or human stress for those persons living in the Dnieper River water use regions.

The analysis results demonstrate that the effectiveness of mitigating measures depends on proper applications of technologies and on the selection of specific clean-up locations offering a significant reduction of human health risk. Further action in the Chernobyl exclusive zone should thus be focused on the decontamination or rehabilitation of the bottom sediment of the cooling pond after the shutdown

the Chernobyl NPP (after 2000). The application of appropriate remediation technologies to prevent secondary re-suspension of the dry solids, when the water is drained from the cooling pond, will be necessary.

After completing the diking of the "hot spots" on the river floodplains of the zone close to Chernobyl to prevent erosion, air re-suspension and washout of radionuclides by inundated groundwater, the most effective measure is a short rotation forest technology using a special species of willow. At present several national and international groups of experts are developing this methodology and evaluating potential effectiveness of willow growing on the contaminated floodplain areas to control the fluvial radionuclide transport and modify the water budget of the contaminated wetlands.

An aquatic remedial decision support modelling system, based on modern modelling approaches, adequate criteria for intervention levels for decision making and expert systems for appropriate choice of the water remedial technology has to be developed and applied for international radiation protection practice.

Evaluations of the prior data and analyses have demonstrated the correctness of the Chernobyl remediation decisions implemented to prevent subsequent contamination of the natural water bodies. Their success depend on openness and availability of accurate monitoring information, appropriate regulations, development of required remedial technology, the social and political readiness of society, but most of all, on the decision-makers themselves, who are facing the enormous problems created by the Chernobyl nuclear accident.

I-3.2. Swedish lakes

I-3.2.1. Lakes: methods and remedial measures

The results presented here emanate from extensive field experiments to reduce the concentration of ^{137}Cs in fish following the Chernobyl accident, conducted in 41 Swedish lakes during the years 1986-1989 [I-3, I-4, I-20]. The basic question has been: What is the best way of reducing the Cs-concentration in lake fish for human consumption, by means of liming or other chemical measures that would be ecologically acceptable? Alternative remedial strategies are illustrated in Figure I-7.

Many of the processes controlling the flow and biological uptake of ^{137}Cs in aquatic systems are linked to hydrological and morphological parameters of the lake and its drainage area, and thus may not be influenced by measures changing the water chemistry, such as liming and potash treatment. However, other processes are clearly linked to the water chemistry of lakes, such as pH and conductivity, which would influence the affinity of ^{137}Cs to suspended particles [I-22, I-23]. The addition of nutrients would also alter the trophic characteristics and the distribution of ^{137}Cs in various organisms (see for example [I-24]). The remedial measures tested in this Swedish project were therefore aimed at either reducing the uptake of ^{137}Cs in biota by blocking the transfer of ^{137}Cs from water or from sediments, or by reducing the secondary load by blocking run-off of ^{137}Cs by means of wetland liming or full-scale drainage area liming using not only limestone but also potash and dolomite. Potassium can replace caesium in different chemical and biological processes [I-25]. Other ions may also, potentially, participate in different blocking processes (e.g. Ca, Na and Mg), which implies that different liming measures, which produce a general increase in the ionic strength of the water may also have a positive effect. The adding of nutrients (especially phosphorus) would increase the primary productivity and this may cause a "biological dilution", i.e. a decrease in concentration of ^{137}Cs in fish; this method is based on theories involving biological buffering [I-26].

Figure I-8 gives the experimental plan for the Swedish tests. The lakes included in the study are rather small (0.07 to 2.7 km^2). Forest land (mainly pine and spruce) dominates the catchment areas on a till overlying acidic and intermediary bedrocks. Mires are also common in the drainage areas. The

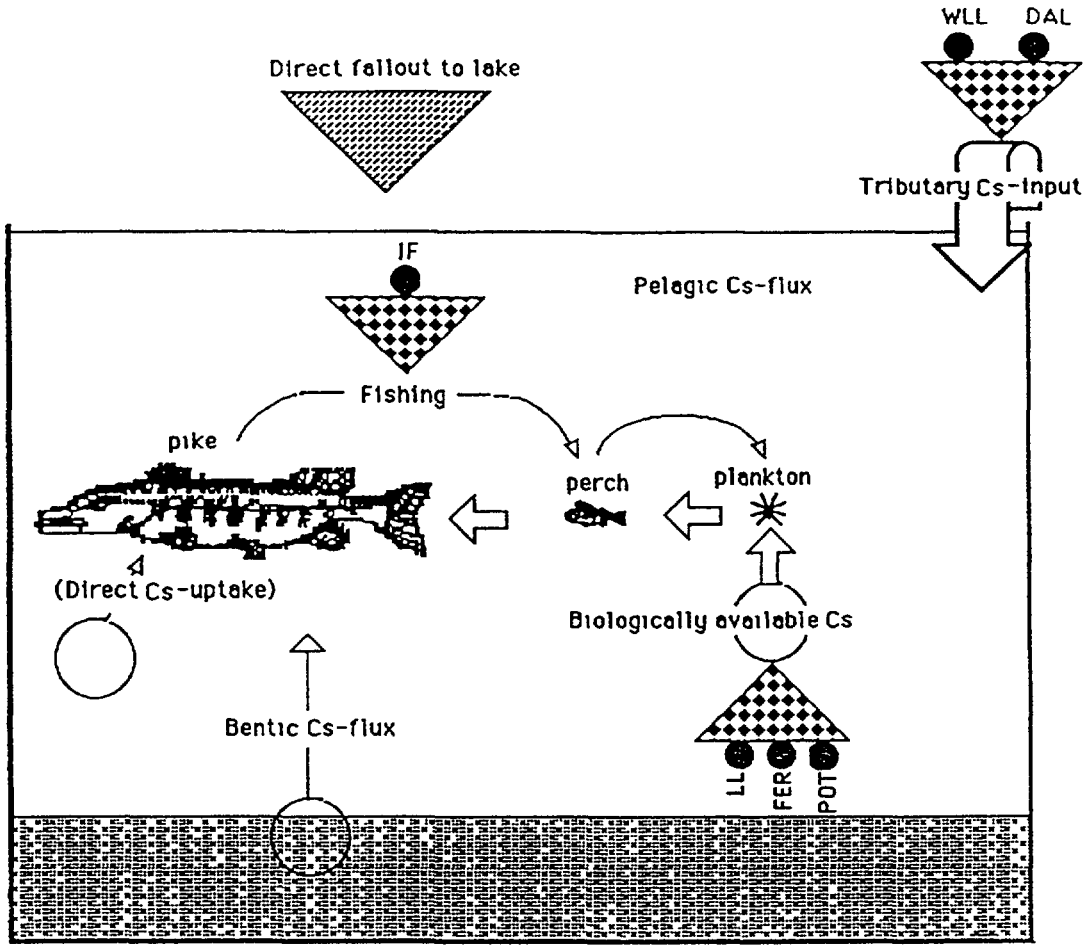

Remedial strategies: IF = Intensive fishing
WLL = Wet land liming
DAL = Drainage area liming
LL = Lake liming
FER = Fertilization
POT = Potash treatment

Cs-137 in fish = f(L-tri, L-water, L-part, L-sed, L-int., Sensitivity)
Kd = Partition coefficient = L-water/L-part = f(pH, totP, K, T, Dm,)

Liming
Fertilization
Potash treatment
Not changeable

L-tri = Tributary input
L-water = Load in water phase
L-part = Load in particulate phase
L-sed = Load in active sediments
L-int = Internal load from sediments to lake water
Sensitivity = Sensitivity factors

FIG I-7 An illustration of some remedial strategies for Cs-contamination

Wetland liming (WLL) and drainage area liming (DAL) are designed to reduce the transport of ^{137}Cs from land to water Remedies involving lake liming (LL), fertilization (FER) and potash treatment (POT) aim at reducing the amount of bioavailable ^{137}Cs in the lake water Intensive fishing (IF) aims at reducing the pool of ^{137}Cs in the lake and modifying the predation pressure The equation under the diagram illustrates the relation between the partition coefficient, Kd, and a number of variables that can be changed by remediation (e g , pH, total-P and K-concentration) and factors that cannot be manipulated (e g the water turnover time of the lake, T, and the bottom dynamic conditions, BA) [21]

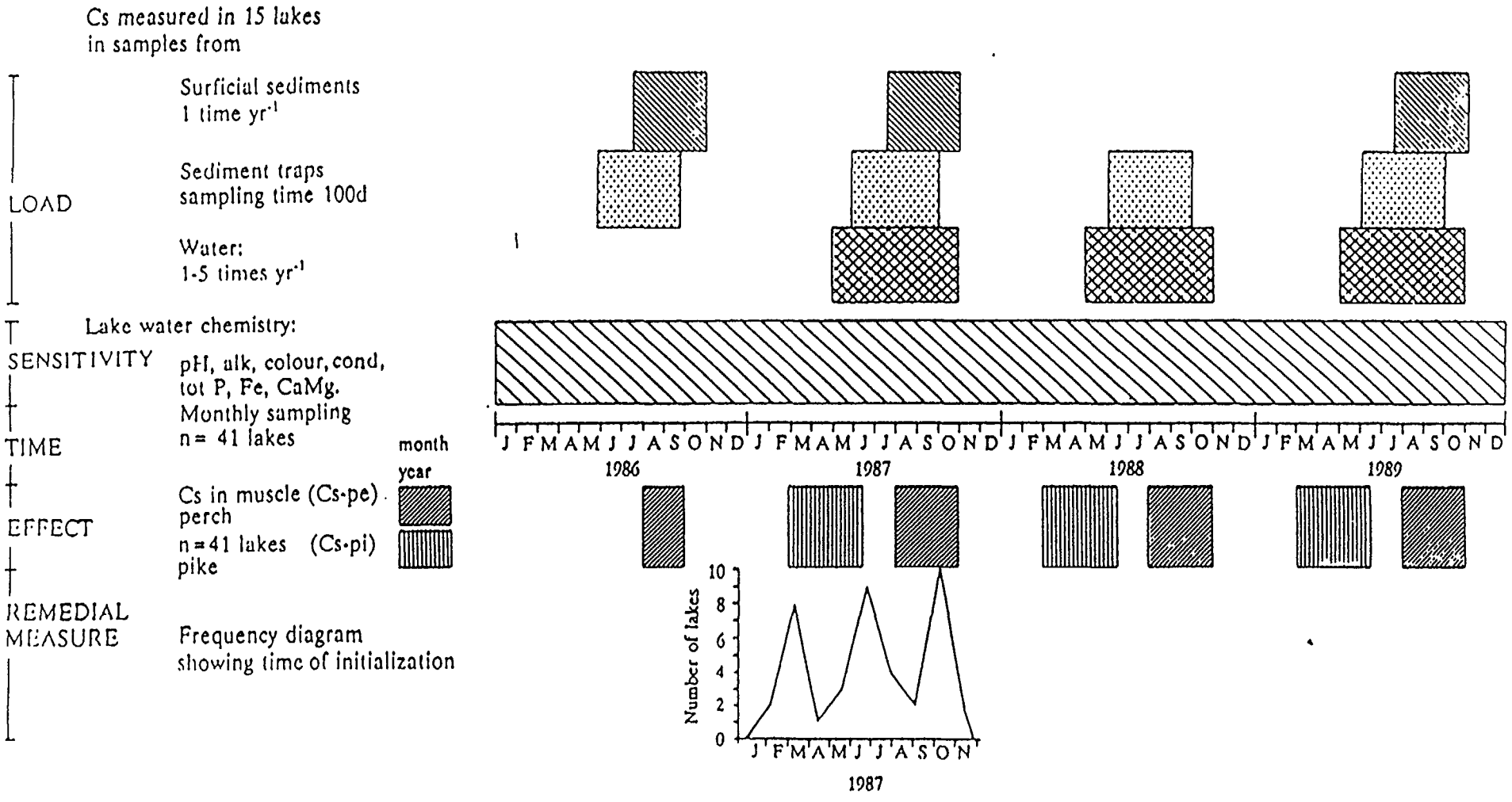

FIGURE I-8. Time schedule illustrating the intensity and duration of the sampling activities in the 41 lakes and a frequency diagram showing when the remedial measures were carried out.

low percentage of lakes and open (= cultivated) land in the catchment areas complement the picture of the "average" lake as being an oligotrophic forest lake situated in the upper reaches of the drainage area.

The following remedial methods were tested:

- Lake liming (LL; tested in 18 lakes. Different types of lime were used: primary rock lime (PR) was used in ten lakes, sedimentary rock lime (SR) in 6 lakes, so-called mixed lime (M; a lime also containing various trace elements and nutrients). The amount of lime added to the lakes has been calculated using data on the initial pH-value (or alkalinity) and the theoretical water retention time of each lake. In most of the lakes, it was assumed that the resulting pH should be about 6.5. However, in 4 of the lakes more lime was added to increase the pH to about 7. The lime was spread over the lakes by different methods, like helicopters, pontoon boats and dosers in the inflowing tributaries. The lime was applied in one or several applications, either on ice or directly onto the water.

- Wetland liming (WLL) was carried out in the catchment areas of 17 lakes, eight of which were limed with primary rock lime, seven with sedimentary rock lime and two with mixed lime. About 0.3 tonnes per hectare were used where the wetlands make up about 2% of the area, and three tonnes per hectare on wetlands making up 10% of the area. The application was carried out with helicopters in single operations. Wetland liming has several advantages compared to lake liming, including prolonged durability, a reduced "lime shock" to the lake ecosystem, improved conditions for animals and plants in streams and rivers and a reduced transport of several metals (e.g. Fe and Al) into the lakes from the catchment area.

- Drainage area liming (DAL) was carried out in two entire drainage areas using dolomite. Since dolomite is less soluble than ordinary limestone, this method will have considerable duration.

- Intensive fishing (IF) was carried out as a major remedial measure in four lakes and as a supplementary measure in three lakes. This resulted in a reduction of the fish population by about 5-10 kg per hectare. The species reduced were mainly pike, perch and roach.

- Potassium treatment (POT) was carried out in 13 lakes. Potassium was added to the lakes either as potash or as an additive in the mixed lime. The fertilizer "Osmocoat", added to two of the lakes, also contains 11% K.

- Fertilization (FER) was carried out in two lakes using "Osmocoat" (5% P and 15% N). In one lake a fish farm, emitting faeces and nutrients, was in operation.

Table I-1 lists the costs (in Sweden) of the different measures in individual lakes, both the total costs and as cost per unit of lake volume. The most expensive measure (calculated per unit of volume) was full-scale drainage area liming, followed by intensive fishing. The least expensive remedial measures were "normal" lake liming and potash treatment. It should be noted that wetland liming and drainage area liming are expected to have several biological and chemical advantages in these acidified lakes and a longer duration. It should also be mentioned that the Swedish liming programme against acidification costs about 100 million SEK (about 20 million US dollars) annually and that most of the measures in the lakes listed in Table I-1 would have been done within the normal provincial liming programmes.

I-3.2.2. Results

Being able to achieve a reduction in the concentration of radioactive caesium in fish was a clear effect of a certain remedial actions on water quality. The mean pH of the lakes increased from 6.0 to 6.7. Other parameters which are directly linked to the liming remedies, e.g. hardness and alkalinity,

TABLE I-1. REMEDIAL MEASURES IN THE 41 SWEDISH LAKES

Lake	MEA	TYPE	AM	Period	Cost	C/Vol	CM
2101	LL	SR	103	Jun87	51	14.2	
2102	LLI	SR	447	Feb87–Dec89	585	1329.5	POT
2103	LLI	SR	99	June87–Mar89	38	24.7	POT
2104	LL	SR	311	Jun87–Mar89	175	33.5	
2105	LL	PR	12	Sep87	10.5	26.9	Se
2106	LL	PR	29	Mar87–Mar89	28	56.0	Se
2107	LL	M	159	Sep87	111.5	20.1	
2108	WLL	M	334	Jul87	323	119.6	
2109	WLLI	SR	415	Jul87–Mar89	241	349.3	POT
2110	WLL	PR	352	Jul87–Mar89	201	97.6	POT
2111	WLL	M	468	Jul87–Mar88	433	481.1	
2112	WLL	PR	104	Jun87	64	168.4	Se
2113	WLL	SR	358	Mar87	275	423.1	
2114	WLL	SR	557	Mar87	341	831.7	
2115	WLL	PR	67	Mar87	42	161.5	Se
2116	WLL	PR	783	Jun87	493	146.7	
2117	LL	PR	181	Jun87–Mar89	62	25.4	POT
2118	WLLI	SR	300	Jul87–Mar89	177	442.5	POT
2119	DAL	DO	419	Sep87	293	714.6	
2120	LL	PR	14	Jun87	12	36.4	FER
2121	IF			May87–Jun89	185	637.9	
2122	L	PR	38	Jun87–Mar89	36	80	IF
2201	LL	PR	239	Mar87–Jul89	201.7	96.0	PO
2202	LL	M	84	Sep87–Jul88	122.5	49.0	
2203	LLI	SR	1159	Aug87–Jun88	629.3	36.6	POT
2204	LLI	SR	768	Aug87–Jun88	434.4	40.6	POT
2205	LL	PR	150	Mar87	95.8	13.3	
2206	WLL	PR	1257	Sep87–Oct87	1114.1	293.2	POT
2207	WLLI	SR	1800	Oct87–Oct88	1485.0	150.0	POT
2208	WLLI	SR	1749	Oct87–Apr88	1522.7	192.7	POT
2209	WLLI	SR	1950	Sep87–Oct87	1569.4	307.7	POT
2210	WLL	PR	2639	Sep87–Dec87	2242.4	228.8	Se
2211	WLL	PR	1561	Sep87–Apr88	1314.6	79.7	
2212	LL	PR	79	Mar87–Mar89	65.1	47.8	FER
2213	DAL	DO	1667	Sep87–Oct87	2075.2	864.7	
2214	LL	PR	64	Mar87–Mar89	56.5	282.6	IF
2215	LL	PR	33	Mar87–Apr88	29.9	28.0	IF
2216	IF			May87–Jun88	320.8	501.2	
2217	IF			May87–Jun88	416.3	612.3	
2218	IF			May87–Jun88	490.6	943.4	
2219	WLL	PR	1750	Sep87–Nov87	1627.6	176.9	Se

KEY:
Lake number, type of measure (MEA), type of line (TYPE), amount of lime used (AM, tons), period when measures were carried out, costs (Cost, SEKx10^3), costs per unit lake volume, (C/Vol, SEK/m^3x10^3) and complementary measures (CM) are given. LL=lake liming, LLI=lake liming to higher pH, WLL=wet land liming, WLLI=wet land liming to higher pH, DAL=full-scale liming with dolomite, Se=selenium treatment, IF=intensive fishing, POT=potash treatment, FER=fertilization, SR=Sedimentary rock lime, PR=primary rock lime, M="mixed lime", DO=dolomite.

showed strongly increasing long-term mean values. A certain decrease in the colour of the lakes was also noted. It was not possible to demonstrate any clear change in the character of the sedimenting material expressed, for instance as the C/N ratio during the period, which could be linked to the measures. The lakes treated with potash had a relatively greater increase in pH (Figure I-9(a)) and alkalinity than the other lakes subjected to lake-liming and wetland-liming. This mainly depends on many of the potash-treated lakes also being given an overdose of lime. The concentrations of total-P generally showed no change in the long term mean value, and consequently fertilization was not effective. Despite the fact that the concentration in lakes increased, it cannot be excluded that the bioproduction in the lakes had increased. The potash treatment generally led to a strong increase in the potassium concentrations in the water. Most of the treated lakes had average potassium concentrations in excess of 20 meq/l after the treatment, from previous mean values of less than 10 meg/l. The results of the potash treatment varied depending on the turnover time of the lakes; in lakes with short turnover times, the potash dose was insufficient to produce a long term effect.

The concentrations of ^{137}Cs in both water and sedimenting material decreased strongly during the project period (Figure I-10). The decrease was particularly strong between 1986 and 1987, i.e. before the treatments. The half-life for the activity in the sedimenting material was, on average, slightly more than 100 days. The continued decrease in concentration was considerably slower; during recent years the half-life period has been in the magnitude of 2-5 years. During 1988 and 1989, the sampling

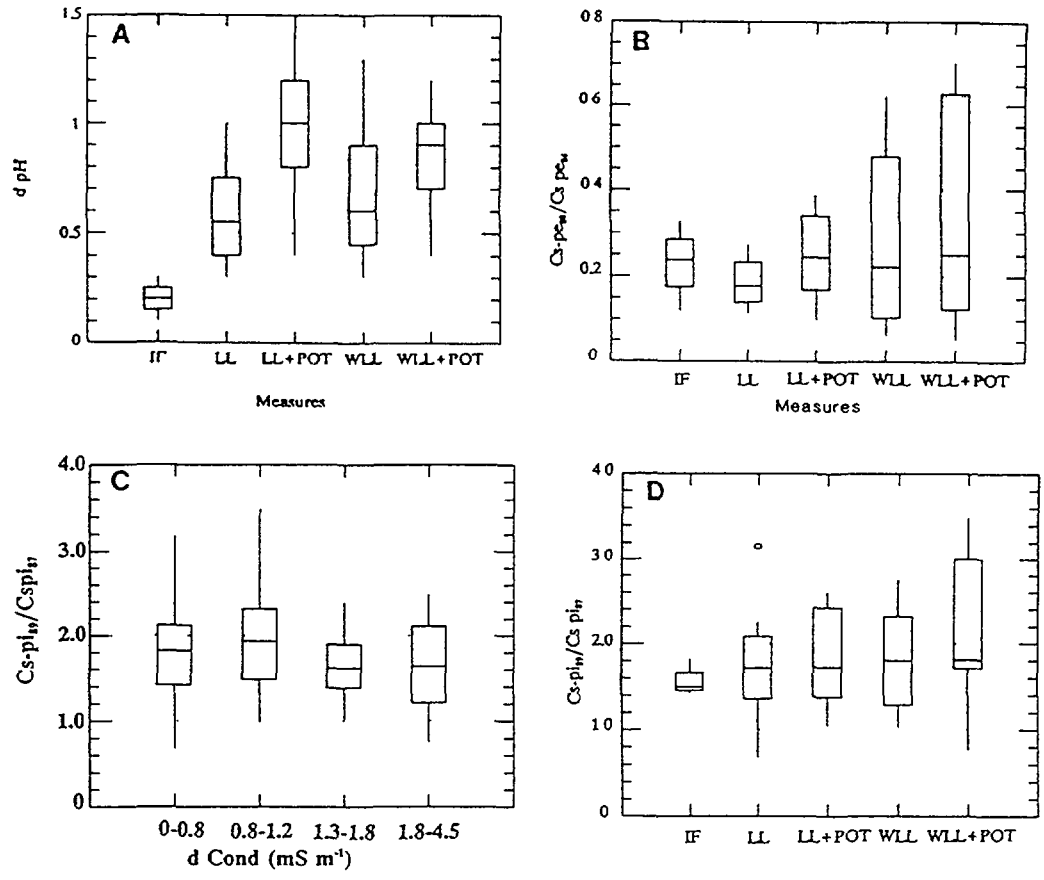

FIG. I-9. (a) Illustration of how the different remedial measures have influenced mean lake pH – IF=intensive fishing, LL= lake liming, POT=potash treatment, WLL=wetland liming [I-20]; (b) Change in ^{137}Cs in pike before (Cs-pi87) and after Cs-pi89) treatment in relation to the change in lake mean conductivity (dCond) linked to the remedial measures; (c) Change in ^{137}Cs in small perch before (Cs-pe86) and after Cs-pe88) treatment in relation to the different remedial measures; (d) Change in ^{137}Cs in pike before (Cs-pi87) and after (Cs-pi89) treatment in relation to the different remedial measures [I-20].

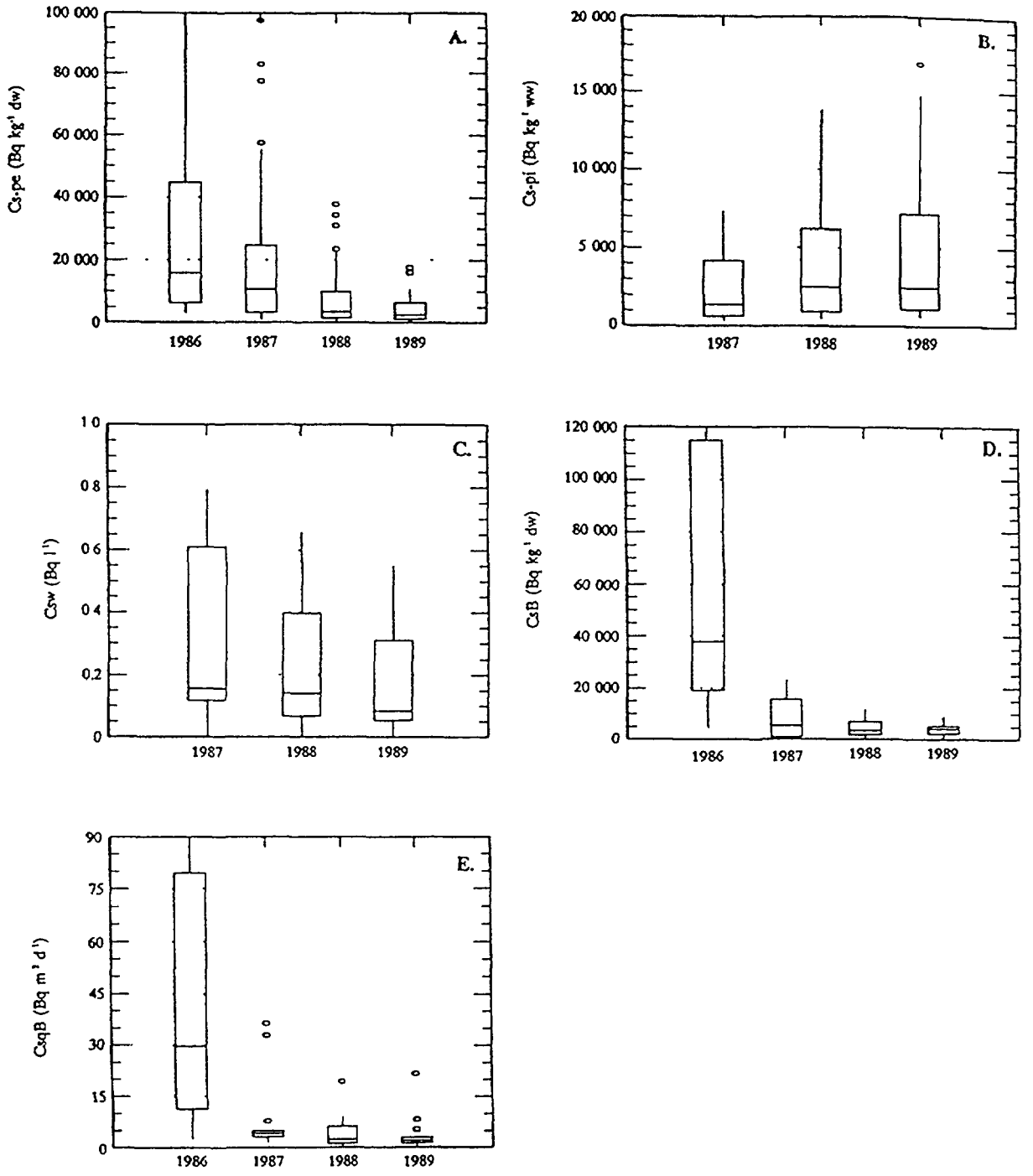

FIG. I-10. Empirical data from concerning the 41 lakes the recovery process for: (a) ^{137}Cs in pike (data from 1987, 1988 and 1989); (b) ^{137}Cs in small perch; (c) ^{137}Cs in material from bottom sediment traps; (d) sedimentation of ^{137}Cs in bottom sediment traps; (e) ^{137}Cs in lake water samples (data from 1987, 1988 and 1989).

programme was extended with regard to sediment traps to cover all 41 lakes. The trend was the same in this larger series of lakes, i.e. the changes between 1988 and 1989 were small, and in some lakes the concentrations had even increased. Thus, the concentrations of ^{137}Cs in water and sedimenting material will probably remain high for many years.

The shallower lakes had a slower decrease in Cs-concentration in fish than the deeper lakes, which may be explained by greater resuspension in shallow lakes. In turn, this implies that a larger proportion of the highly contaminated material in 1986 occurred in the water masses of shallow lakes and is therefore also available for biological uptake.

In relation to the fallout, shallow lakes and lakes with naturally high hardness values had lower concentrations of ^{137}Cs during 1986 in sedimenting material. The most important explanation for this may be that the composition of the sedimenting material differs between lakes. In lakes with low hardness, which here are also less productive and humic, ^{137}Cs appears to be bound to humus colloids or other organic material with low densities. The retention time for Cs in lake water is also shorter in lakes with high natural hardness.

Perch

The mean Cs-value in small perch during the autumn of 1989 was only 15% of the mean value in the autumn of 1986. The decrease in perch can be described fairly well by an exponential decline. In comparison with the concentrations in sediment traps, the decline was considerably more uniform, and the same function can be used for the entire period.

Between-year variations which may be linked to factors controlling perch growth and food choice will also occur in the future, but in comparison to the large-scale decrease, which is controlled by the secondary, mainly internal load, this variation is of minor importance. A comparison between 1988 and 1989 gave an average half-life of 1.5 years, which is also considerably shorter than the half-life of ^{137}Cs in settling material. This implies that the biologically easily absorbable Cs-fraction in the sedimenting material decreases.

The difference in the rate of decrease between different lakes is, however, considerable and extremely important in this context. Significant correlations with the decrease in concentration ($p<0.05$) were obtained for the lake dynamic ratio, ($r=-0.57$; DR=area/Dm; Dm = mean depth) and max. depth, Dmax ($r=0.45$); and among the water chemical parameters, colour ($r=-0.35$). Other correlation coefficients, such as for pH 8-9 ($r=0.23$) and the water turnover time, Tw ($r=0.17$) were not significant. Lakes with the slowest decrease during the period of investigation were relatively shallow brownwater lakes. A logical link to the results shown for the load parameters can be made: the magnitude of the continued decline will be primarily influenced by factors affecting the continued internal load of the lakes and the internal turnover of caesium.

There was no clear difference in the size of the decrease in concentration between lakes where different types of measures were implemented (Figure I-9(c)). The difference in the change in concentration between groups of lakes with different water chemical changes was not significant in any case; both mean values and median values were very similar between groups. The magnitude of the decrease in concentration in perch and the increase in concentration in pike must thus primarily be linked to factors other than the different measures undertaken.

Lakes where average potassium concentrations were increased by more than 5 meq/L had a relatively greater (but not significant, $p=0.07$) decline in the Cs-concentrations in perch fry. This group of lakes was, however, also made up of deep lakes, which, as mentioned earlier, have a faster rate of decline in perch fry. A decrease in the Cs-concentrations in perch fry by 5-10% per year, which is the maximum feasible reduction which could be linked to increased potassium concentrations on the basis of these results, suggests that potash may have a certain effect in the long term, but that K-addition is insufficient as "acute medicine" to counteract high Cs-concentrations in perch.

Pike

In contrast to ^{137}Cs in water, sedimenting material and perch fry, the concentrations in pike increased during the period investigated. The highest concentrations in pike were reached either in 1988

or in 1989. This implies that pike generally reach almost as high levels as the highest levels measured in perch fry, although with a delay of 2–3 years.

Figure I-9(d) shows how the changes of caesium concentration in pike between 1987 (i.e. before the measures), and 1989 were distributed among the lake groups where different remedial measures were tested. The concentrations of ^{137}Cs in pike increased on average, by more than 80% during the two years, and, as can be seen from the figure, there were no major differences between the median values of the groups.

Tests have been made to see how the results were influenced when consideration was given to changes in water chemistry. This is shown in Figure I-9(b), where the division of the lakes into four classes has been made on the change in conductivity. The increase in concentration in pike up to 1989 was, on average, slightly lower (but not significantly) in lakes where the total ionic strength in water had been increased by more than about 1.5 mS/m. However, there are, as mentioned, other factors which have a higher correlation to the relative change in the concentration in pike than changes in conductivity. In the longer term, though, a reduced Cs-uptake in pike of about 5% per year, which is the reduction which may possibly be linked to an increased conductivity as a result of the remedial measures undertaken, may be of value. The possible reduction in uptake at lower levels in the food web may be added to this effect. For example, in perch fry, a maximum of 5-10% which has not yet become apparent in "one-kilo-pike".

The slower increase, reflecting the fact that pike is at a higher level in the food chain, also implies that contamination will have a more extended development in comparison to the plankton-eating perch fry. The good correlation between Cs-concentrations in perch fry and pike shows that the factors that have been found important for the development over time of the load in the lakes and the Cs-concentrations in perch fry are also important for the development of concentrations in pike. Since the main prey of "kilo-pike" is not perch of the size class investigated (<10 g), factors linked to the structure of the food web should also influence the concentration in pike.

I-3.2.3. Modelling

Figure I-11 shows the model predicted effects of a shorter ecological half-life corresponding to the maximum feasible decrease as a result of liming and/or potash remedies (7% per year for perch fry and 5% per year for pike). In a relatively short time perspective (months to years), the gain in recovery time produced by the remedial measures will be relatively moderate. However, in the long term and for fish high up in the food chain ("one-kilo-pike"), the liming and potash remedial measures may have greater importance.

I-3.2.4. Conclusions concerning lake remedial measures

In general, the remedial measures produced the intended response in water chemistry. This also applies to the potash treatment, where the long-term mean value of the potassium concentration in many lakes was above 20 meq/L after the treatment, i.e. the addition of potassium frequently gave more than a twofold increase in natural concentrations. In lakes with very short water turnover times, it was, as expected, difficult to obtain an increased long-term mean K-value.

No rapid and clear reduction in the concentrations of radioactive caesium in fish was obtained compared to lakes where water chemistry or biological conditions were not changed.

The large, initial uptake of radioactive caesium in perch fry that occurred during 1986, before the remedial measures were introduced, can be linked to differences in water chemistry and the morphometric characteristics of the lakes. In lakes with a long water turnover time and with low values of especially conductivity, hardness and potassium, the fish had relatively higher concentrations given the same fallout levels. There was a clear difference between sedimentation of ^{137}Cs in lakes, linked

to particle composition and sedimentation properties which is better indicated by the natural hardness and conductivity of the lake water than by for instance the carbon content of the precipitating material. The Cs-sedimentation was not, however, controlled to any particular degree by the CaMg-concentration in water within the hardness range of these lakes.

The differences between the lakes as regards the continued magnitude of the change in concentration in perch fry can primarily be linked to factors controlling the secondary load (i.e. the internal load and the input from the catchment). In this connection, the depth of the lakes seems to be the most important factor. Shallow lakes generally have a slower reduction in Cs-concentrations in fish, probably as a result of greater resuspension and thus a larger internal load. The transport of caesium into the lake from the catchment area is generally of less importance for the recovery process, except in cases where lakes situated upstream have large internal loads, or when other temporary sinks (certain types of wetlands) supply radioactive caesium.

The lakes treated with potash, where the long-term mean value of the potassium concentrations increased by more than 5 meq/L had had a larger decrease in perch fry concentration up to 1989 (but not statistically significant) than other lakes. The increase in the potassium concentrations, hardness and conductivity resulting from the measures has hitherto been of subordinate importance for the changes in concentration in comparison with other factors, such as differences in the maximum depth of the lakes. An increased reduction of 5-10% per/year in perch fry, which is the maximum conceivable reduction, from a well conducted potash treatment with massively increased potassium concentrations, may be important in a long-term perspective, not for perch fry but for fish high up in the food chain, such as pike.

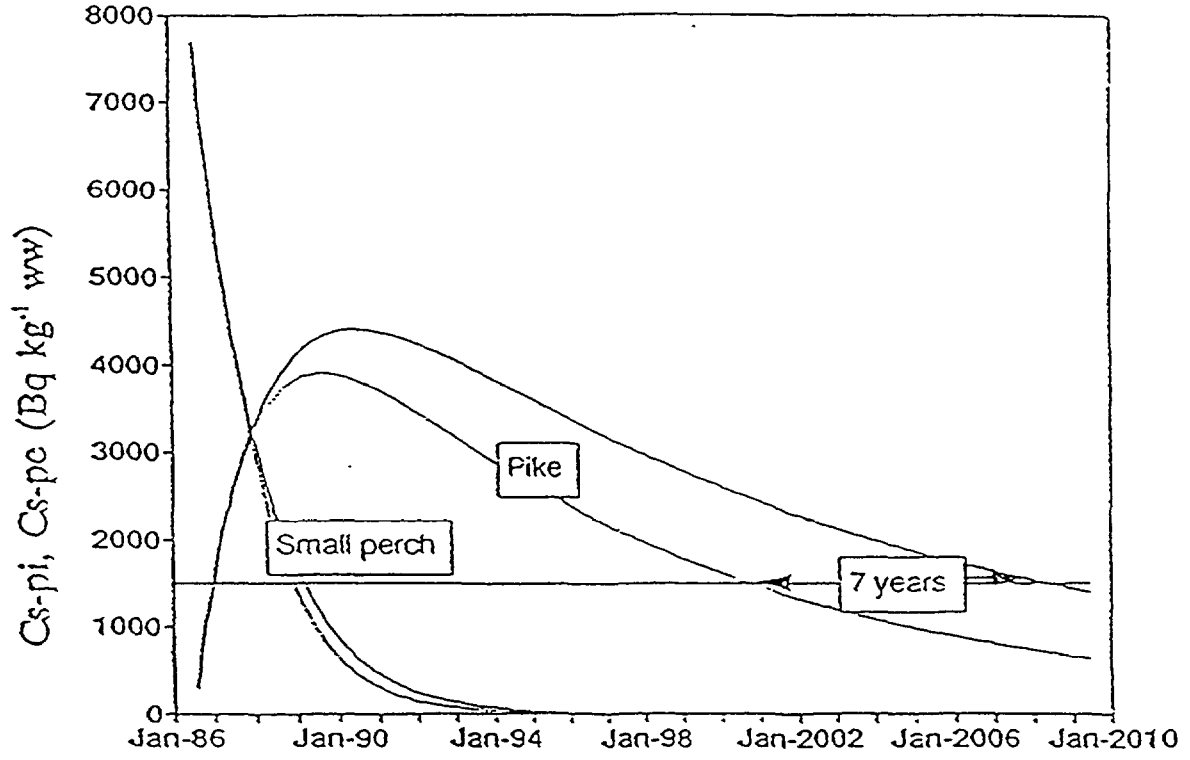

FIG. I-11. Dynamic modelling of ^{137}Cs in pike and perch and simulation of how an effective potash treatment may speed up the natural recovery (7% per year in perch, 5% per year in pike) [I-20].

Up to 1989, there was a weak trend (but not statistically significant) for the increase in concentration in pike to be slightly less, corresponding to a decreased uptake of about 5% per year, in lakes where the conductivity had been increased considerably (> 1.5 mS/m). This may lead to a reduction in the ecological half-life for ^{137}Cs in pike which is important in a longer time perspective.

The time interval between the remedial measures undertaken and the latest fish analyses (about 2 years on average) is not sufficient to statistically establish the small effects of the measures. A longer time series of data would be required.

I-3.3. Laboratory tests

Evans [I-27] made a series of laboratory tests to find out if an adding of potassium (as KCl) could increase the recovery (= decrease) of ^{137}Cs in roach. During these tests, roach from lake Öjaren, Sweden, which received a fallout of 50-100kBq/m^2, were exposed to K-concentrations of 4, 6 and 16 ppm for 3 months. The initial K-concentration of the water of this lake was 0.7 ppm. The fish were fed on dry food. No significant reduction of Chernobyl ^{137}Cs could be detected in these experiments. This is in good agreement with the results from the field experiments in the 41 Swedish lakes.

I-3.4. Household methods

The results presented here emanate from Wallström and Håkanson [I-28]. Extensive tests were made to try to find out if it was possible to reduce the concentration of ^{137}Cs in meat (from moose, deer and fish), by means of simple household techniques.

It has been known for a long time that salting may eliminate ^{137}Cs in meat. It would "normally" take about two to four days to remove 60-70% of ^{137}Cs in a 500 g. piece of meat placed in a concentrated salt solution. The result would depend on many things, such as the size and form of the meat, the type of salt (pure NaCl, mineral salt, salt with I, salt with K, etc.) and the time of exposure. There are at least three severe drawbacks to this salting method:

(1) The amount of vitamins (e.g. B_6, B_{12}) decreases significantly with the time of exposure; after two to four days most of these vitamins are lost;
(2) The levels of Na (and K) would increase and this would influence the taste of the meat; a large intake of Na and K may also give rise to negative health effects in man;
(3) The colour and texture of the meat would change, and most people would probably agree that the grayer and harder meat obtained after 2-4 days in a salt solution would be less "appetizing" than normal, fresh meat.

The idea with these tests was to try to speed up the salting procedure from two to four days to two to four hours. Different types of salt were tested, as well as different types of meat, and different form and size of the meat. Two different approaches to speed up the salting procedure have also been tested; to rotate the meat in the salt solution (called centrifugation) or to rotate the salt solution around the meat (called rotation). The results may be summarized as follows:

(1) The best results in terms of ^{137}Cs reduction were obtained in meat that has been frozen. The difference to unfrozen meat was about 20 - 40% in ^{137}Cs reduction;
(2) Both rotation and centrifugation can reduce 60 - 70% of ^{137}Cs in meat (moose, deer and fish) in two to three hours;
(3) The first round (of centrifugation or rotation) is most efficient in reducing ^{137}Cs; about 30–50% of the ^{137}Cs may be reduced in the first round (depending on the salt and meat used), about 10–15% in subsequent rounds;
(4) There is no significant change in vitamin B_6 if the treatment lasts for two to three hours;
(5) There is no significant change in the texture of the meat, but an increase in the Na concentration;

(6) The main drawback with this method concerns the practical handling. This procedure takes two to three hours and it requires access to a household machine that could either centrifuge the meat (about 1000 rotation/min.) or rotate the salt solution.

The conclusion is that this may be a practical method in areas with heavily contaminated meat, especially for larger kitchens (schools, military, restaurants, etc.), but it may also be used in homes, because there may be people who, from a primarily psychological point of view, would like to feel that they have a possibility to do something themselves to reduce their intake of radioactive caesium.

I-4. LAKE SENSITIVITY AND REMEDIAL STRATEGIES

I-4.1. Introduction

The aim of this Section is to discuss radiocaesium in lakes from a practical, engineering perspective. The focus is on remedial measures, but the initial parts of the work concern an analysis of lake sensitivity to radiocaesium contamination in more general terms. One and the same load (fallout) of any substance to a given lake may cause very different concentrations in water and biota, and ecological effects, depending on the characteristics of the lake and its catchment [I-3].

The results presented here are based on simulations using the VAMP LAKE model (Section 5.10). The basic components of the model are outlined in Figure 5.74. This model is meant to be a simple, general, predictive, state-of-the-art model for radiocaesium in lakes. It has been validated against an extensive set of data for seven European lakes which cover a wide range of lake and catchment characteristics (Table 3.2, Section 3).

The VAMP LAKE model gives accurate predictions for all lakes for all species of fish. The main objective of the model is to predict radiocaesium in predatory fish (used for human consumption) and in lake water (used for irrigation, drinking water, etc.). The VAMP LAKE model is not a very complex lake ecosystem model, but a comparatively small, general predictive model driven by readily accessible environmental parameters. Available environmental parameters can be related to different ecologically relevant and practically useful remedial strategies. By changing different environmental parameters related to different remedial strategies, like pH related to lake liming, K-concentration for potash treatment, lake total-P for lake fertilization (see [I-29] and Section I-3.2 for results and discussions of different remedial measures tested to minimize concentrations of ^{137}Cs in lake water and fish), it is possible to simulate realistic, expected effects for the target variables, ^{137}Cs in lake water and in predatory fish. Since it is also possible to put a price tag on these remedial measures, it is also possible to relate the costs of the remedial measures to the environmental benefit, as expressed by changes in the target variables. This means that relevant cost/benefit analysis can be made. The rationale of this approach is illustrated in Figure I-12. The model variables illustrated in the panel in Figure 5.74 should, preferably, not be altered for different lakes.

I-4.2. Differences in lake sensitivity to radiocaesium

The aim of this Section is to analyse the concept of lake sensitivity using both empirical and modelled data. Figure I-13 gives empirical data on Cs-concentrations in waters of six lakes at different intervals after the Chernobyl accident (month 1 = January 1986). There is a very wide spread in concentrations of about four orders of magnitude. This is understandable, since the fallout also varies by about four orders of magnitude (from 0.9 kBq/m^2 to about 100 for these six lakes, Iso Valkjärvi, Hillesjön, Devoke Water, Bracciano, IJsselmeer and Esthwaite Water, see Table 3.2, Section 3). If one normalizes for fallout (Figure I-14), it can be noted that the range is significantly reduced, but still, the variation covers more than two orders of magnitude. This simply means that there are many other factors regulating the concentrations of ^{137}Cs in lake water besides fallout. One fundamental objective of the VAMP project is to address this question and develop and test models accounting for the most important processes regulating such variations.

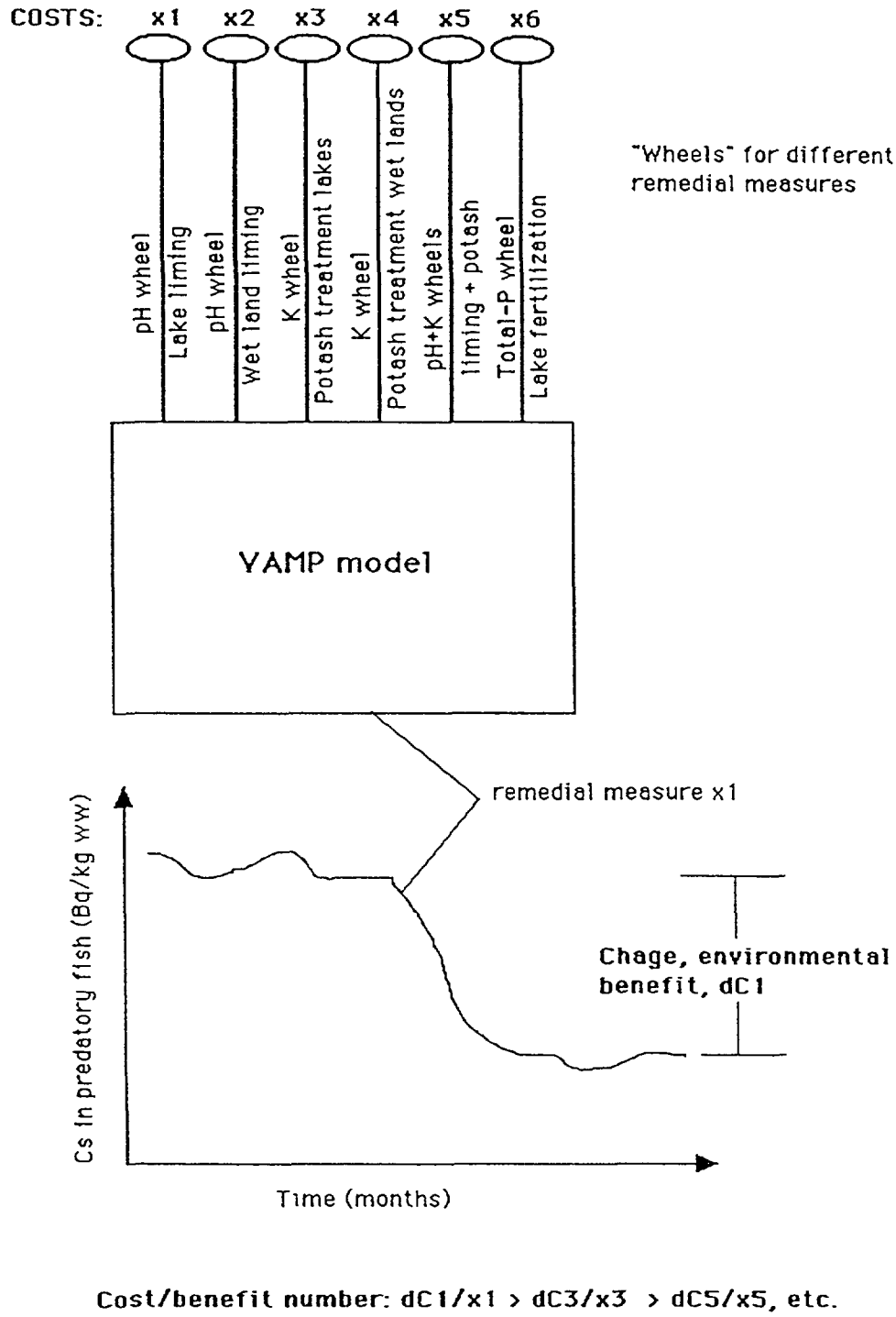

FIG. I-12. Illustration of how to use a model (in this case the VAMP LAKE model) as a practical tool to test various remedial strategies and establish relevant environmental cost/benefit numbers related to the cost for the remedial measures (x1, x2, etc.) and the environmental benefit, as determined by the improvement in target variables (dC1, dC2, etc.).

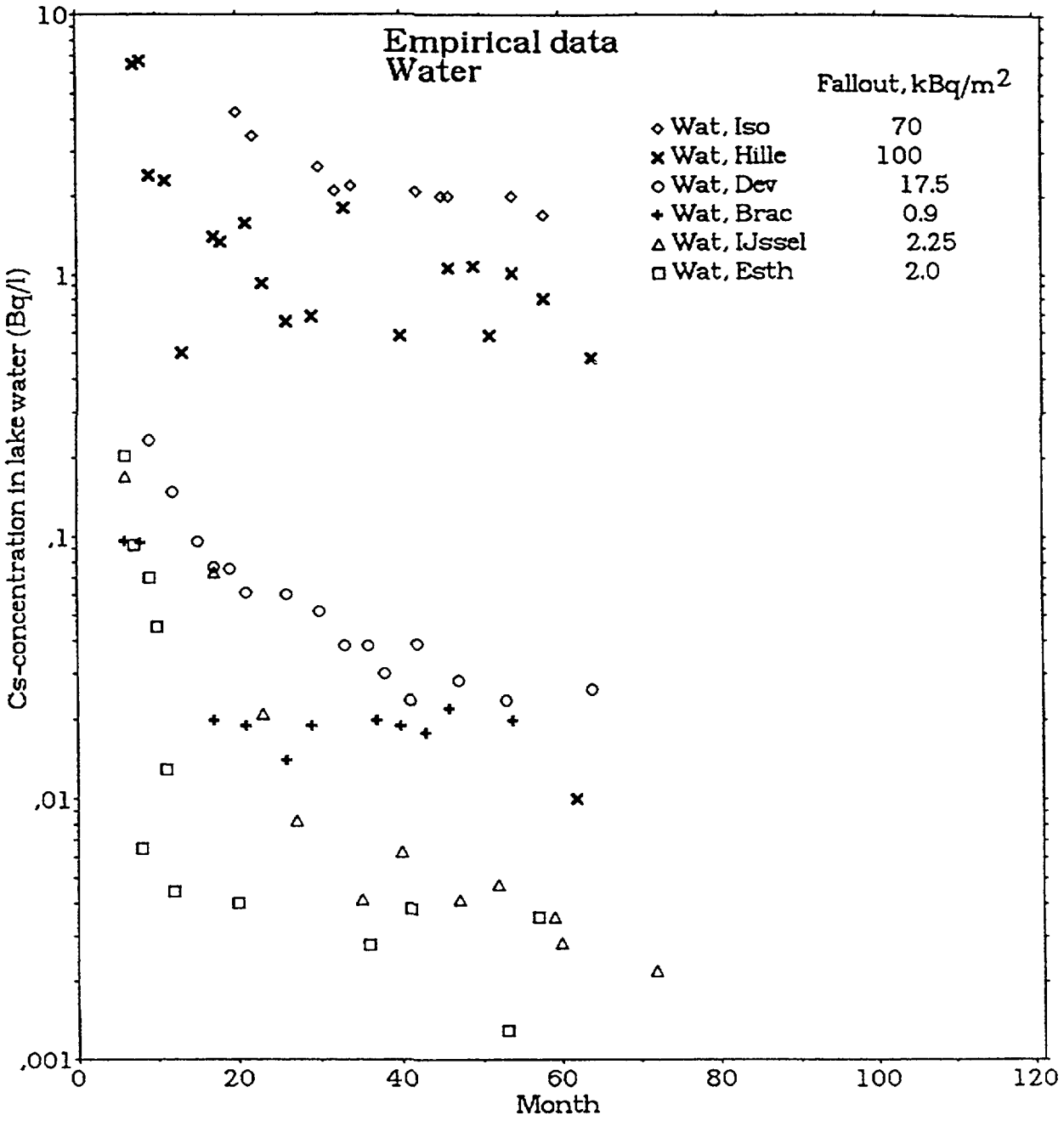

FIG. I-13. Empirical data for Cs-concentrations in lake water on different occasions (month 1 = January 1986) for six of the VAMP lakes.

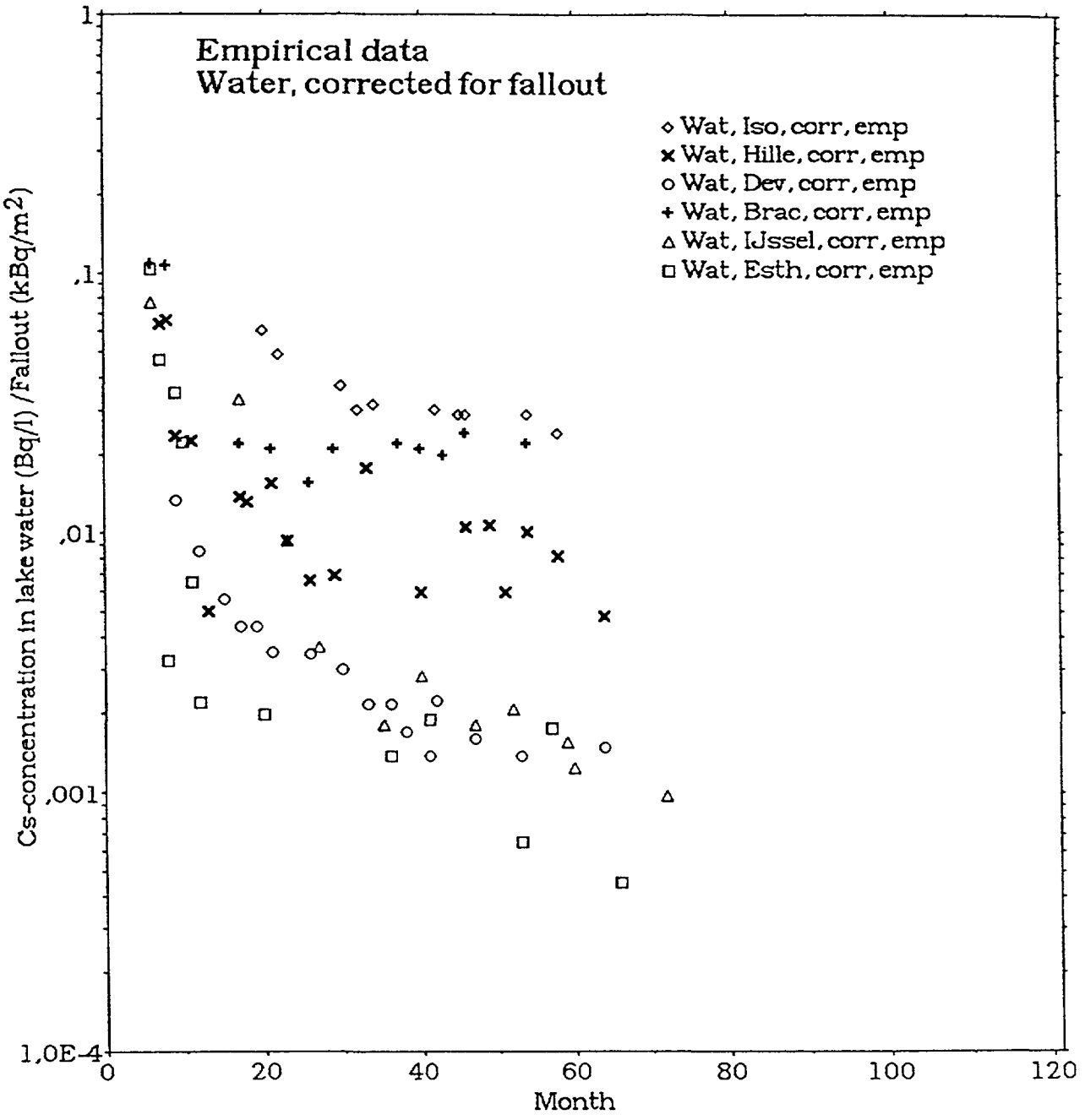

FIG. I-14. Corrected (or normalized) empirical data for Cs-concentrations in lake water on different occasions (month 1 = January 1986) for six of the VAMP lakes.

The VAMP LAKE model includes several such processes, like seasonal (monthly) variability in water discharge and ^{137}Cs input to the lake and retention of ^{137}Cs in the lake, sedimentation, resuspension and uptake of radiocaesium in biota. Figure I-15 gives curves of Cs-concentrations in water (Bq/L), as predicted by the VAMP LAKE model, divided by the fallout for each lake. One can note the marked seasonal variabilities in many small lakes (Esthwaite Water, Heimdalsvatn and Devoke Water), and the low predicted seasonal variations in the deep lake Bracciano and the large IJsselmeer. One can also note that after this simple normalization for fallout, the differences between the lakes in Cs-concentrations remain large (more than one order of magnitude).

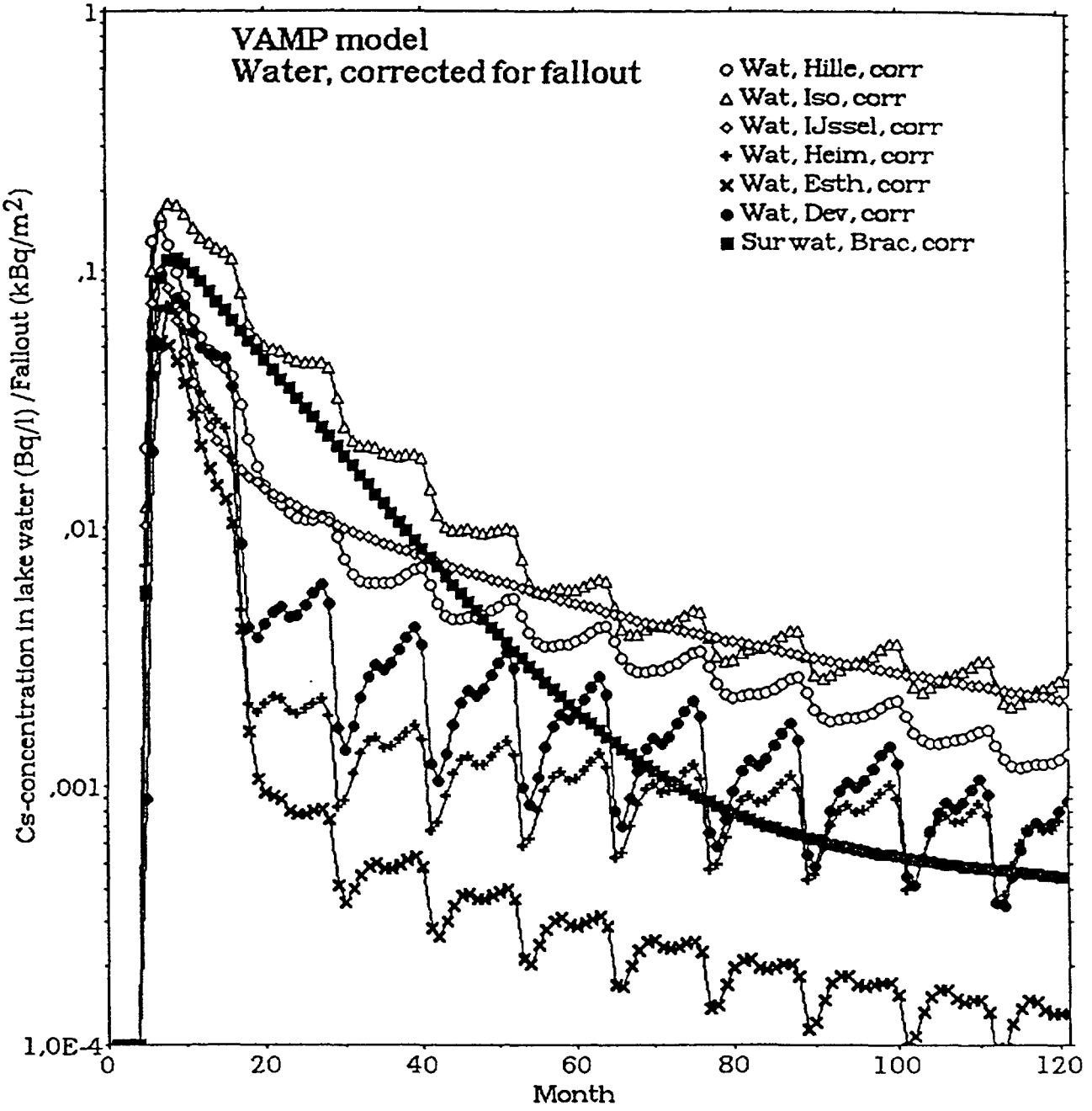

FIG. I-15. Corrected (or normalized) predicted values for Cs-concentrations in lake water on different occasions (month 1 = January 1986) for the VAMP lakes.

These three figures apply to one of the target variables, Cs-concentration in lake water. Figure I-16 gives empirical data in the same manner for Cs-concentrations in predatory fish. One can note that the range without normalization for fallout is greater than 4 orders of magnitude for pike and large perch. When corrected for fallout (Figure I-17), the range is much narrower. The VAMP LAKE model (Figure I-18) predicts similar differences between the normalized values of Cs-concentration in predatory fish.

From the results given in Section 5, one can note that the most important sensitivity factor are ions similar to Cs, like K, Ca, Na and Mg. The more of these ions, the higher the conductivity and the lower the uptake of ^{137}Cs. This is a case of "chemical dilution". Note also that for a "single emission" like after the Chernobyl accident, the biouptake of ^{137}Cs, and the Cs-concentration in fish, is lower in

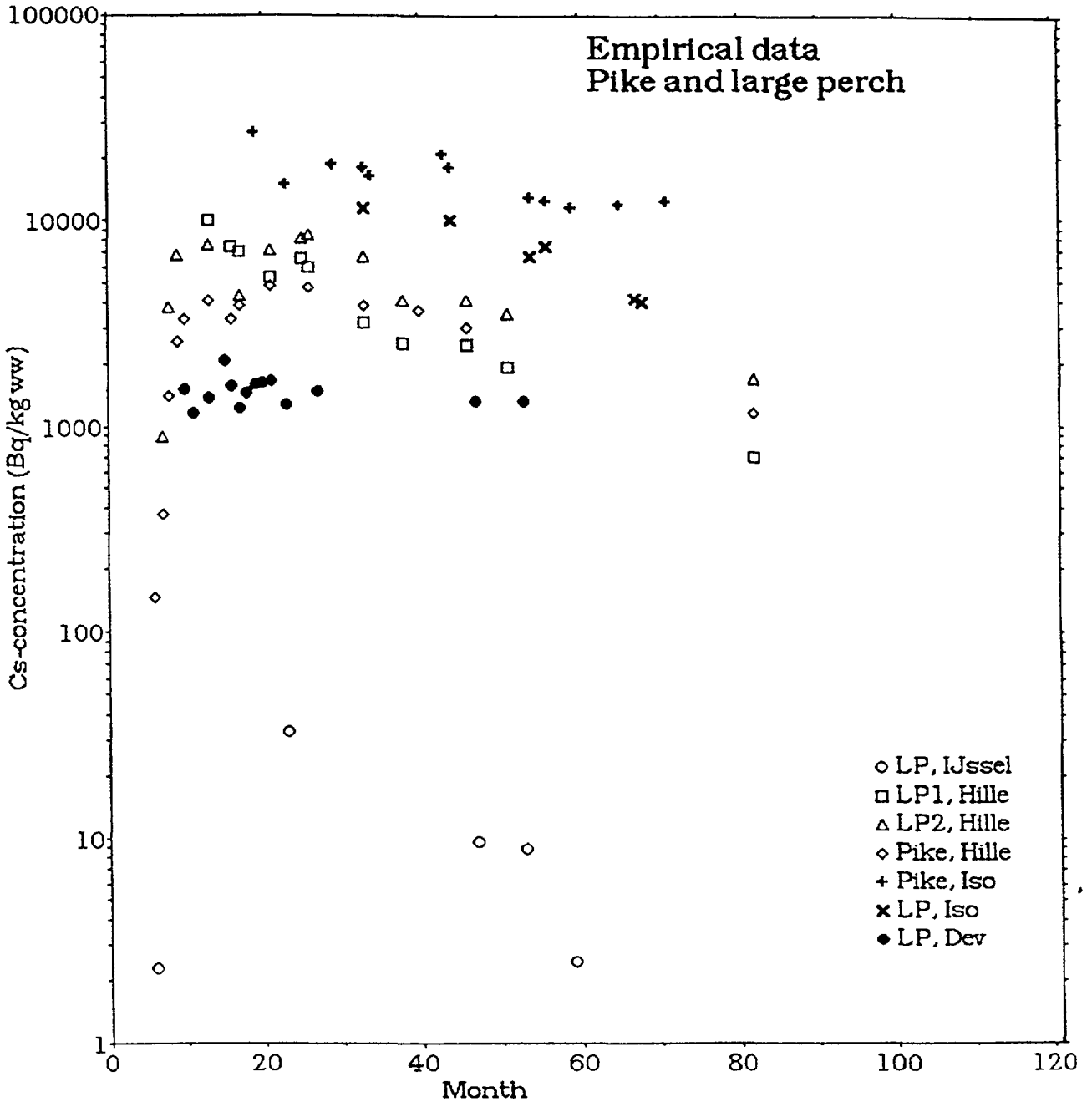

FIG. I-16. Empirical data for Cs-concentrations in pike and large perch on different occasions (month 1 = January 1986) for four of the VAMP lakes.

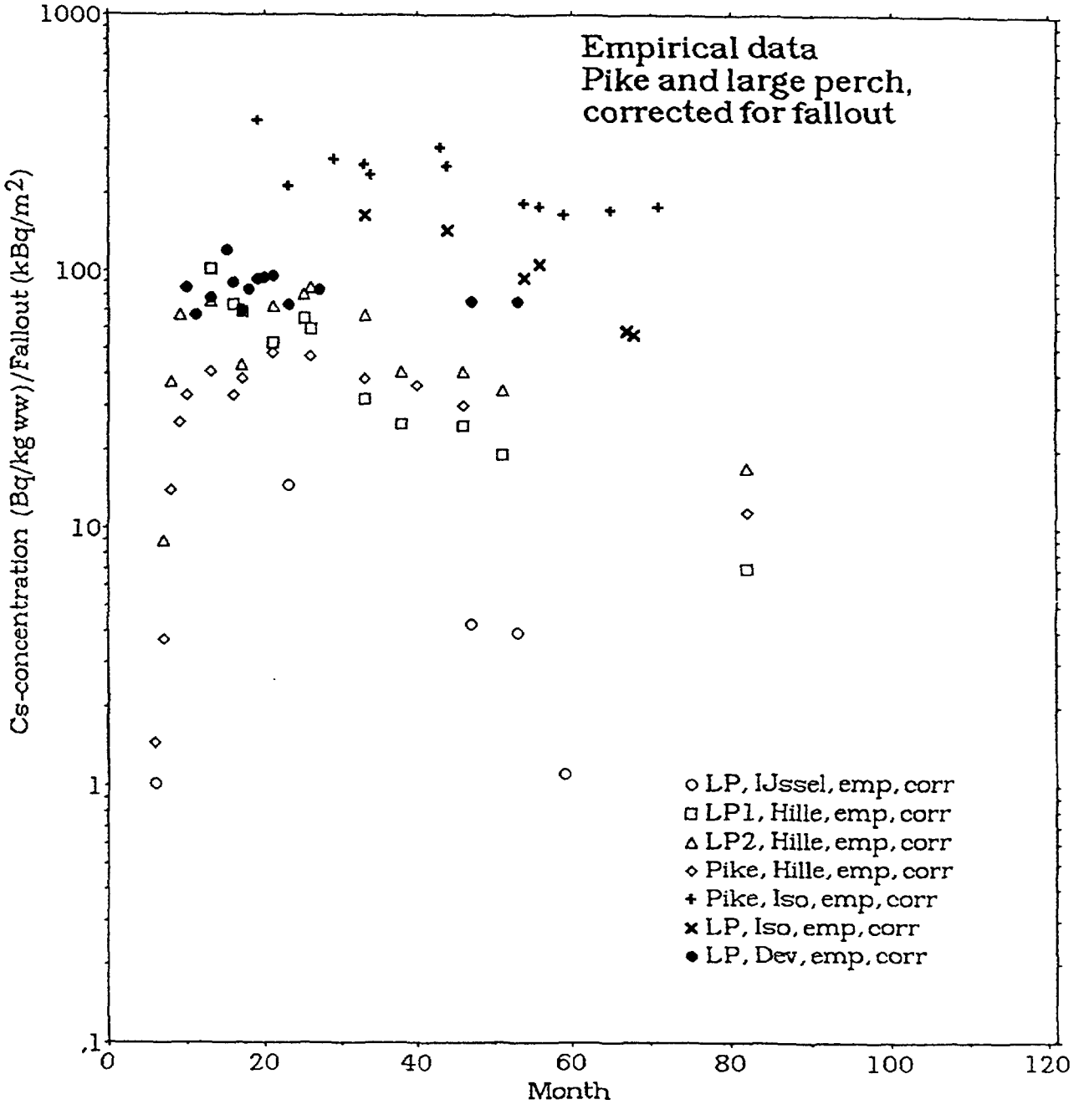

FIG. I-17. Corrected (or normalized) empirical data for Cs-concentrations in pike and large perch on different occasions (month 1 = January 1986) for four of the VAMP lakes.

lakes with fast water turnover than in lakes with slow water turnover – a case of normal "water dilution". The opposite is valid for mercury, which is supplied to the lake "continuously". In that case, the biouptake increase with increased runoff of Hg and water from the catchment [I-30]. Also note that an increase in total-P, i.e. in lake bioproduction, causes a "biological dilution" ^{137}Cs.

From this, one can ask some important questions which will be addressed in the ensuing sections.

- What can be done in practice (in a cost efficient and realistic manner) to reduce (or speed up the recovery of) Cs-concentrations in lake waters and predatory fish?
- Is it possible to reduce the secondary load, i.e. the transport of radiocaesium from land to water, the internal loading, or the bioavailable portion of the lake load?

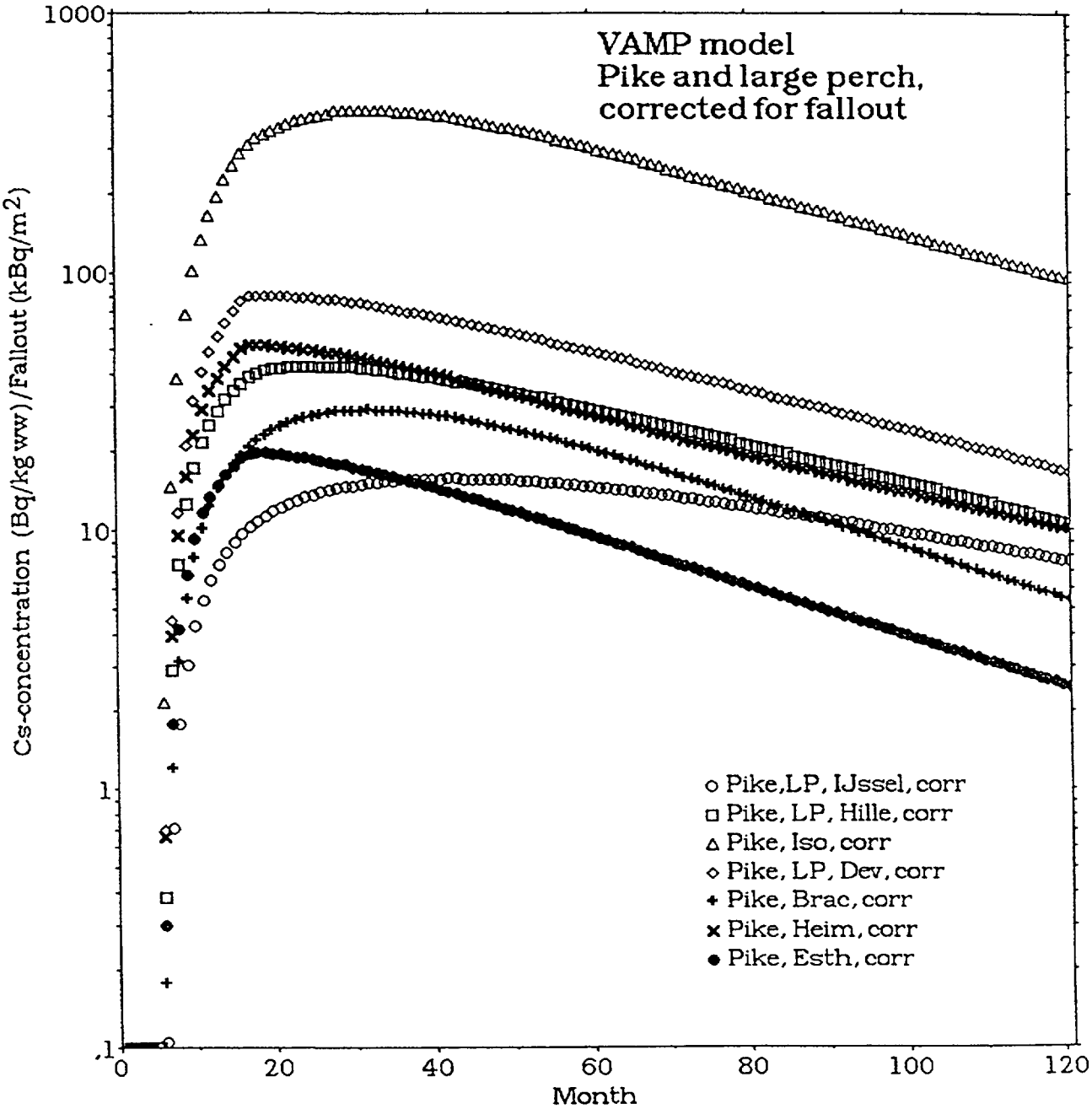

FIG. I-18. Corrected (or normalized) predicted values for Cs-concentrations in pike and large perch on different occasions (month 1 = January 1986) for the VAMP lakes.

- Is it possible to test other remedies linked to the many factors regulating the differences among lakes (illustrated in Figures I-13 to I-18), such as lake liming to change pH, potash treatment to change the K-concentration, or fertilization (adding of phosphorus) to change lake bioproduction?

I-4.3. Effect-dose-sensitivity models

I-4.3.1. Introduction

The terms effect, load and sensitivity are meant to be general terms that may be applied for most contaminants in most environments, including nutrients, metals and organics in lakes, coastal waters and terrestrial ecosystems, and not just for radiocaesium in lakes. The approach discussed here is based on an ecosystem perspective (i.e. it concerns entire lakes).

Ecological effects may be illustrated using results from acidification studies. Figure I-19 shows why the pH of lake water is important in limnology. Many animals accustomed to a circum-neutral pH (pH ≈ 7) cannot reproduce or survive in acidified lakes. Some, like crustaceans, snails and molluscs, are very sensitive to changes in pH, whereas others, like salmon and pike, are less sensitive [I-31]. Since pH is a variable, however, one must also address the problem of "representativity". In other words, what pH-value(s) are most representative and informative for the extinction of crustaceans in lakes, or for the biouptake and concentration of radiocaesium in fish? For crustaceans, the most representative value may be the lowest pH during the spring-flood when they reproduce, and for the content of ^{137}Cs in pike, it may be the mean, long-term lake average pH. This example applies to pH, but the same questions about representativity and compatibility could be raised for any lake variable and any environmental or ecological problem.

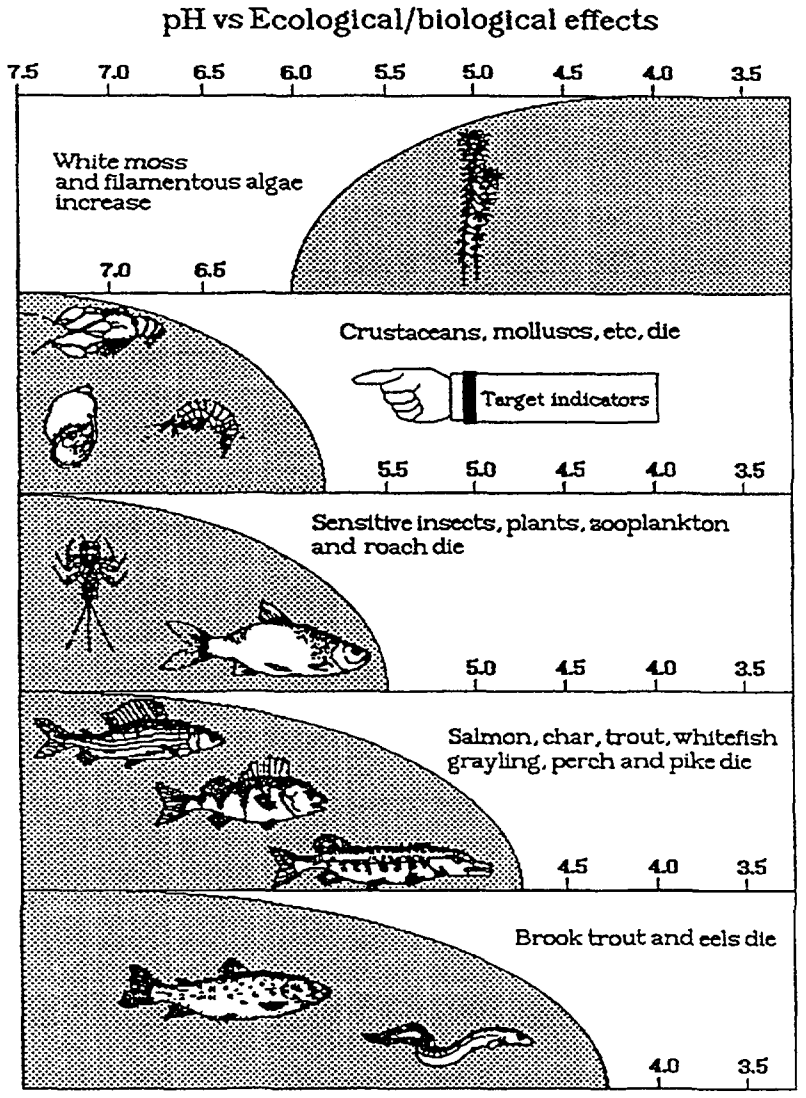

FIG. I-19. Illustration of target organisms using the example of biological and ecological effects of lake acidification.

In predictive liminology, ecology and environmental sciences, a central objective is to find out which organisms are the most sensitive to a given contaminant, whether this is an acidifying substance (like S or N), a nutrient (like P or N) or a toxin (like many metals, organics or radioisotopes). To emphasize their importance, the figure shows examples of key functional groups and target organisms for acidification. Crustaceans react rapidly to changes in pH, whereas certain fish, such as brook trout and eels, do not die until acidification is far advanced. White moss (e.g. *Sphagnum*) and filmentous algae should not be found in these lakes under normal conditions. So, the abundance of such species also indicates ecological effects of acidification [I-31].

For ^{137}Cs in lakes there are no generally accepted ecological/biological effect parameters. The threat does not appear to be directed against life in the lakes but is mainly directed at humans consuming fish. This means that for ^{137}Cs one should focus on fish consumed by man as effect parameters. The fish are caught from several places in each lake. This gives a lake-typical value and not a site-typical value. The Cs-concentration in predatory fish is called an effect parameter in this context.

The term, load = dose, is used in different ways in different connections, e.g. in radioecology, laboratory-based ecotoxicology and ecosystem-directed environmental science. Here, PRIMARY LOAD is considered to be the average fallout (in Bq/m^2) of caesium, whereas SECONDARY LOAD applies to the load of radioactive caesium lakes from catchment to runoff during a given space of time after the fallout event. INTERNAL LOAD applies to the flux of radiocaesium from sediments back to water via different advective and diffusive processes.

The Cs-load can be determined from water samples, but if Cs concentrations in water are low, the analysis is relatively expensive and many samples from different places and at different times must be made. An alternative to water sampling is to use material collected in sediment traps [I-32]. These can be placed out after the spring flood and collected in connection with the fishing of perch in August/September.

Target sensitivity parameters are those that both influence the spread and uptake of caesium in fish and those that can be modified by different practical remedial measures (like lake and wet land liming, lake fertilization, potash treatment and intensive fishing).

The target organisms in Figure I-19 are the most sensitive or important species in the ecosystem, but their roles may only be critical in some freshwater ecosystems, such as oligotrophic lakes. Such lakes are then the target ecosystems for this effect. These species might not be present or might not have the same key function in more productive systems, so such productive systems may withstand higher loads of acidifying substances (or radiocaesium) than oligotrophic systems. This illustrates the term environmental sensitivity – one and the same load may cause different environmental effects in ecosystems with different sensitivity. Consequently, it is important to define both target organisms and target ecosystems relative to a given threat [I-33]. This principle applies to all environmental disturbances, but frequently it is very difficult to apply in practice. When this is the case, it is particularly important to distinguish what one should know from what one knows and what one does not know.

Thus, it is assumed that the ecosystem can be characterized by a number of target organisms at different trophic levels. Five such levels are given in Figure I-19. The functional groups included in these levels (periphyton, plankton, benthos and predatory fish) may be identified as key "ecological groups". It is assumed that an environmental perturbation causes the following reactions among one or more of these key functional groups:

(1) The balance of species biomass and production is initially unaffected, despite an increased load of pollutant;
(2) Eventually, the increasing load causes important changes among the key groups. (Some react extremely rapidly, even to small changes during short episodes). These structural modifications disturb the original balance of the ecosystem until a new successional phase and balance occur in the system;
(3) As the load increases still further, structural modification accelerates to the point that the original ecosystem totally disintegrates.

Figure I-19 illustrates this process with the relationship between acidification and a number of key ecological species. At pH = 7.5, the system is in its original balance. By the time pH drops to 6, some important changes have occurred among the key species of plankton. Changes at this level may be quantified by the influence given by the curve. The influence is less at the other levels. At pH =

4, all key groups are absent. For lakes, complementary indices would also have to be developed along gradients of productivity or phosphorus load and colour, as well as along the pH-gradient.

I-4.3.2. Load models

Vollenweider [I-34] presented his first load model for phosphorus in lakes in the late 1960s. He demonstrated that in many lakes, eutrophication could be reversed by reducing the input of total phosphorus to the lakes so that the mean annual concentration of total-P could be lowered. Since then, many studies have demonstrated where the Vollenweider approach can – and cannot – be used. Different alternative models have been presented, and the most successful of those have one thing in common with the basic Vollenweider model – simplicity!

Today there exist no load models for metals (except for mercury and radiocaesium) or for halogenated toxins (like PCBs and DDTs). This means that there is room for speculations concerning the ecological effects of these contaminants as such, and especially in real situations where many different substances contaminate and antagonistic and synergistic effects can appear. Empirically validated load models provide data so that practically feasible remedial measures can be discussed and the consequences of such measures simulated; thus enabling quantitative environmental cost-benefit calculations to be made [I-35]. Elevated concentrations of contaminants that cause no visible or measurable ecological effects would generally be of less interest for practical water management, and to remedial strategies, in the situation faced today in ecosystems with multiple threats. The aim of load models [I-3] is to provide a tool for quantitative predictions relating operationally defined ecological effects to compatible load and sensitivity parameters. Many factors may have an influence on how an effect parameter varies between aquatic ecosystems. The analysis behind the load models aims at identifying the most important factors in this respect. Frequently, there are no causal explanations of phenomena that can be established statistically. One of the advantages of the empirical/statistical approach is that it provides a possibility to rank factors exerting influence on an effect parameter so that future research can be concentrated on these factors. Naturally, when using models at the ecosystem level (for entire lakes, coastal areas, etc.), it is not possible to describe phenomena at the individual, organ or cellular levels.

I-4.3.3. Mass-balance models and ecometric models

It is possible to confuse the aims and objectives of dynamic, mass-balance load models with empirical load models. Mass-balance models concern fluxes, amounts and concentrations of all types of materials (like radionuclides and nutrients). Empirical models focus on ecological effect variables, defined and determined in relations to given threats. These two model approaches (see Figure I-20) may, as least in theory, both be used to address the same issues with the following constraints:

- At least one operationally defined ecological effect parameter (y) relevant for the load parameter(s) in question should be included in the model. If several ecological/biological effect parameters are used, it may be possible to define a function as the y-parameter to be predicted. Ideally, the y-parameter should express the reproduction, abundance, mass or status of key (target) organisms, which characterize the given ecosystem and which cannot be replaced by similar organisms, which could carry out the same function in the ecosystem. Such ideal effect parameters CANNOT generally be used within dynamic models which are designed to handle fluxes, amounts and concentrations but NOT ecosystems effects. One way to circumvent this problem is to use dynamic models to model concentrations and empirical models to link these concentrations to ecological effect variables. If such ideal ecological effect parameters cannot be operationally defined for practical, economic or scientific reasons, then one should try to seek simpler but relevant alternatives, like mean concentrations of given toxic substances in key functional groups. Environmental goals should be related to ecological effect parameters and not to load parameters, since one and the same load may cause very different ecological effects in ecosystems of different sensitivities. Figure I-21 gives the principle components of a general load

model illustrated as a ELS-diagram. The figure also gives some of the effect, load and sensitivity parameters that may be used for radiocaesium in lakes.

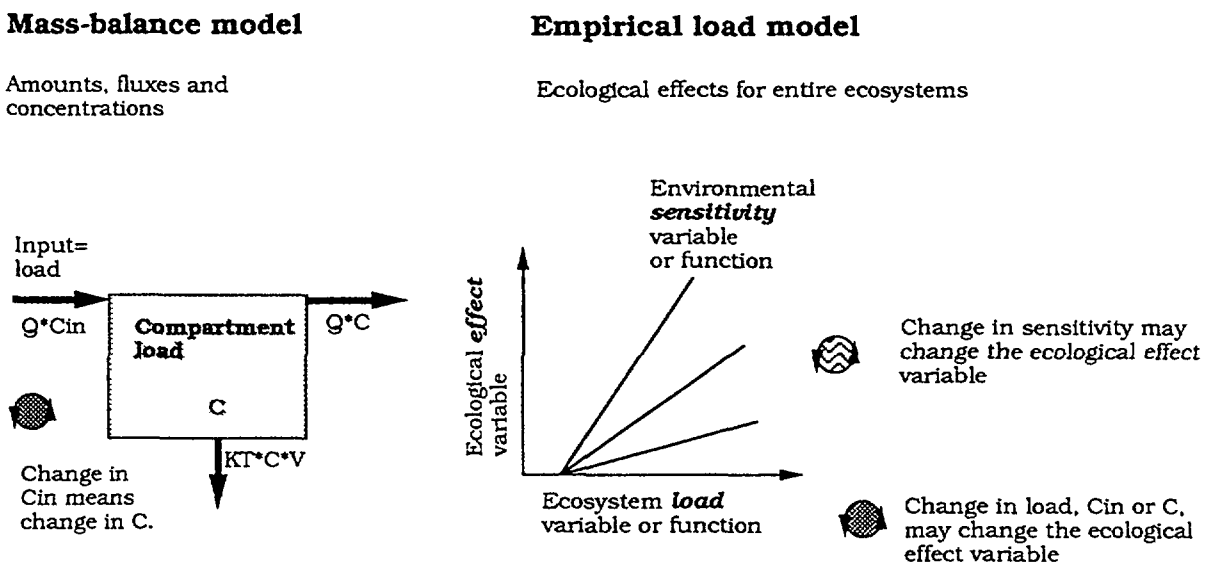

FIG. I-20. Illustration of the fundamental differences between dynamic, mass-balance models and ecometric load models, i.e. ecological effect-load-sensitivity models. The three wheels indicate that by means of remedial measures one may reduce the load variable in dynamic models and the load and the sensitivity variables in ecometric models [I-31].

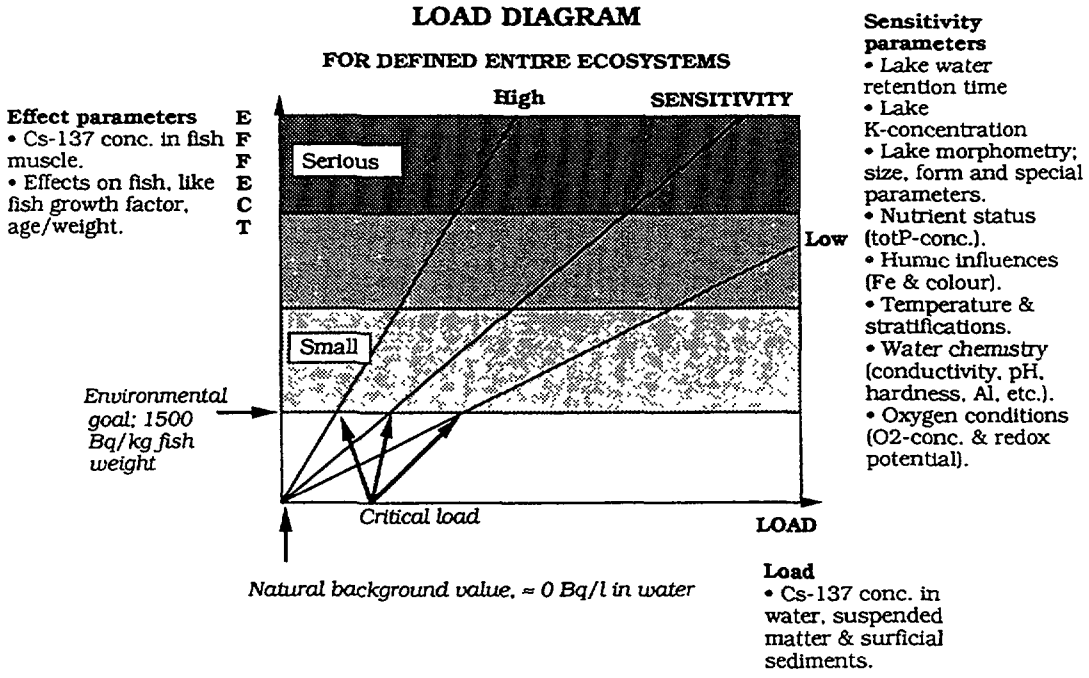

FIG. I-21. The basic set-up of a load diagram from a load model. From this diagram, important concepts like natural background concentration, critical load and environmental goal (linked effect parameters) can be scientifically defined. One and the same load may cause very different ecological effects in ecosystems of different sensitivities. This figure also gives examples of effect, load and sensitivity parameters used for load models for radiocaesium in lakes.

- The primary interest is not on site-specific conditions (the sampling bottle), but at the ecosystem level, which is the perspective that should be of main interest from a management viewpoint. Very large areas (like large lakes) may have to be separated into different ecosystems where different key organisms dominate. Smaller lakes (area <100 km^2) can often be regarded as ecosystems in this context. If a given y-variable (often a mean value for a given area and a given period of time) varies more within a lake than among lakes, it becomes very difficult to develop models that predict the y-variable. In such a case, the definition of the boundaries of the ecosystem may be ecologically inappropriate. An ecosystem in this context is a rather uniform, homogeneous entity with respect to its defining characteristics.

- The predictive accuracy of the model must be stated. The predictive accuracy is generally determined by means of statistical tests (often regressions), where model predictions of y are compared to reliable empirical data of y. Models that provide r^2-values higher than about 0.8 (and p-values lower than 0.05) could generally be used in practice in management for predictions in individual ecosystems. Models providing lower r^2-values (but still p-values <0.05) can be used for regional predictions, when predictive failure in individual ecosystems can be accepted [I-31].

- It is generally not possible to derive load models which apply with equal success for all types of ecosystems. This means that the operational range must be explicitly given to avoid abuse of the model for ecosystems for which it was never intended.

If dynamic mass-balance model meet these requirements, they would generally be preferable to statistical/empirical models because of the better inherent causalities and time dependencies. In this compilation, "mixed" dynamic and statistical models will be presented.

I-4.4. Model simulations of remedial measures using the VAMP LAKE model

The dispersal, retention and biouptake of environmental contaminants vary from substance to substance, but the fundamental principles and processes regulating the distribution and biouptake are more or less the same for all toxic substances. They can be modelled in the same way by means of generic, mass-balance models, but with different rates and model variables for different substances. For radioisotopes dissolved in the water, or absorbed by very small carrier particles, the distribution may be revealed as elevated concentrations in water, suspended materials, sediments and biota over vast areas. However, elevated concentrations in abiotic compartments is one thing – biological uptake and increased ecological effects at the ecosystem level may be quite another [I-30, I-35]. Thus, a fundamental question concerns the ecological effects: how can one detect, describe and predict ecological effects on the ecosystem level for radioisotopes? It should be stressed that it is at least theoretically possible to model concentrations of substances in abiotic compartments like sediments and water in a rather straightforward manner, it is often much more difficult to apply causal models to biological variables and predict biouptake and concentrations in plankton and fish. It is very difficult indeed to develop good predictive models, for the ecological effects on the ecosystem level. In this case, we do not model ecosystem effects, but concentrations in fish and water.

The VAMP LAKE model is used to simulate consequences for Cs-concentrations in predatory fish from (1) liming, (2) potash treatment and (3) fertilization. No simulations are made for measures aiming at speeding up the recovery of Cs-concentrations in lake water, since this is regulated by factors which are very difficult to remediate (e.g. to change precipitation, runoff and internal loading). We will only present realistic simulations, not testing for fertilization for eutrophic lakes and liming for lakes of neutral pH.

I-4.4.1. Liming

Many low-productive lakes with catchments dominated by acidic rocks and mires have naturally low pH. Many processes and properties in the catchment influence lake pH. This means that natural, pre-industrial, values of lake pH vary from lake to lake. It is, clearly, not possible to measure today

what the conditions used to be, but there are methods to predict this [I-36, [I-37]. In Sweden, there exists a rule-of-the-thumb-system applied by the National Environmental Protection Agency and regional authorities, whereby lakes are generally limed to about 6.4–6.5. The "natural" range in mean annual pH would, in small glacial lakes, vary from about 6 to about 7.2. So, 6.4 is only occasionally correct!

The only VAMP lake with a very low pH is the Finnish lake, Iso Valkjärvi (pH = 5.1). Figure I-22 shows the predicted effects of limings on Cs-concentrations in pike when lake pH was increased in steps from 5.1 to 7.5. The higher the lake pH, the lower the Cs-concentrations in pike. In Figure I-22, the liming was simulated to start in different months. The upper curve gives the default conditions (pH = 5.1), the next curve the results when a liming increased pH from 5.1 to 6.5 in month 8 (i.e. August 1986). The following curves give the same results for different starting months (month 10, 12, 15, 18 and 24). The lowest curve gives the conditions when pH is set to 6.5 for the entire period. From this figure one can note that the sooner the liming starts, the better. Similar analyses have been carried out for whitefish (Figure I-23), which has a shorter ecological half-life than pike. From this figure, one can note similar, but quicker changes.

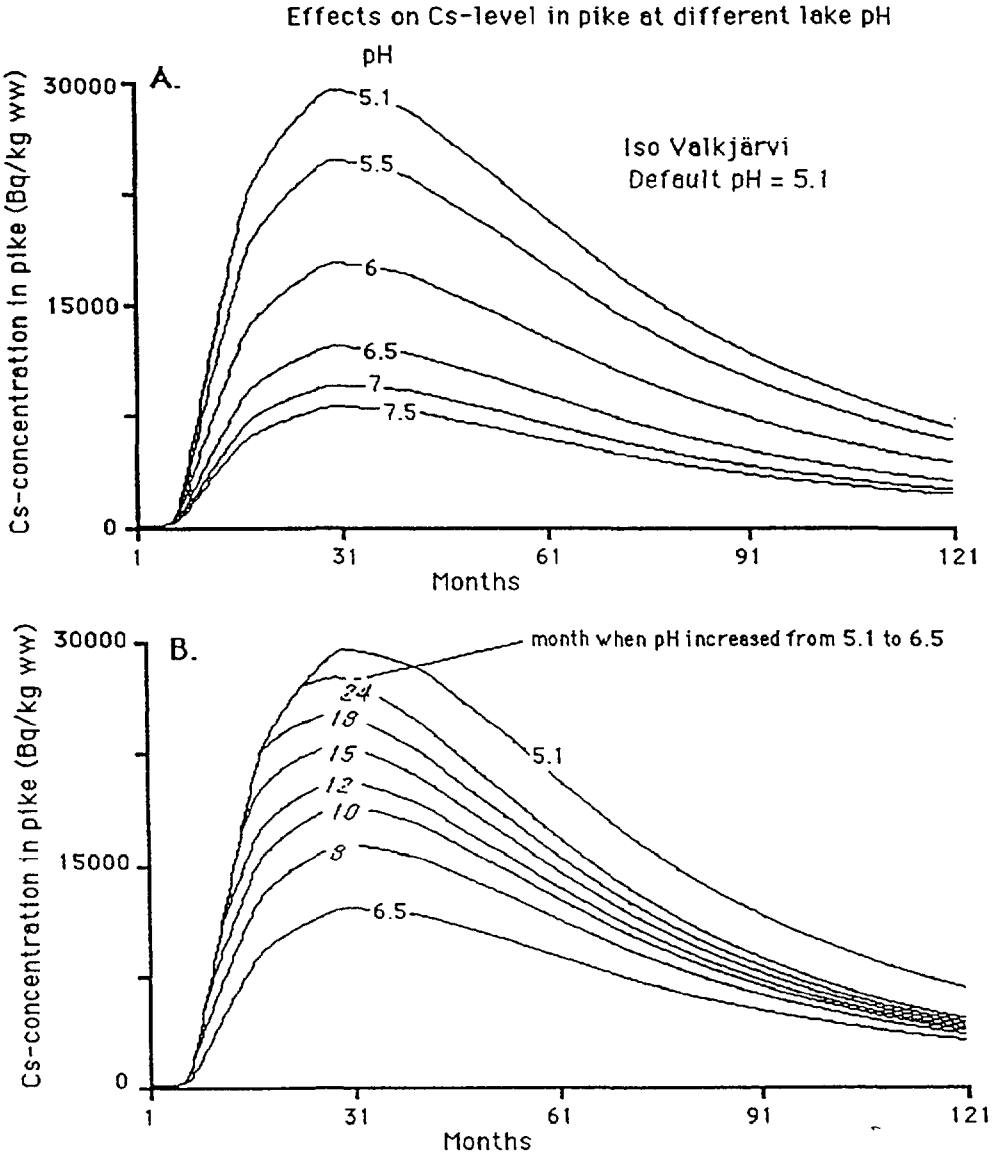

FIG. I-22. Simulations illustrating the effect of liming on Cs-concentration in pike in Iso Valkjärvi using the VAMP LAKE model.

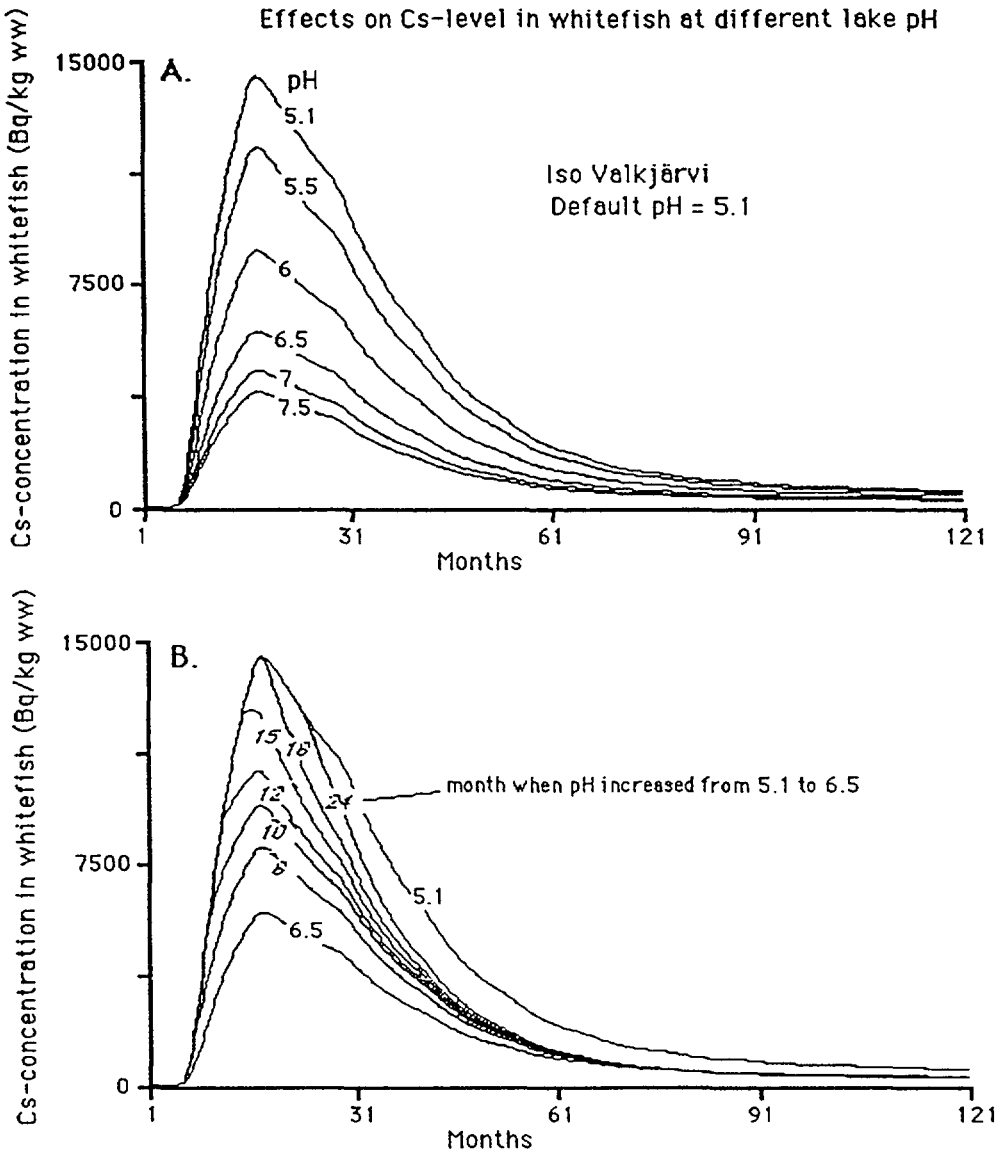

FIG. I-23. Simultaneous illustrating the effect of liming on Cs-concentration in whitefish in Iso Valkjärvi, using the VAMP LAKE model.

It is evident that it is NOT realistic to keep pH, which is a variable, first as a constant of 5.1, then as a constant of 6.5. In Figure I-24, real empirical data on lake pH were used to drive the VAMP LAKE model. Since we do not have access to monthly data lake pH for Iso Valkjärvi, and since the objective was to simulate future development in predatory fish, we have used pH-data from the Swedish lake Ölen for which there is a long record of such data. This lake had a similar low initial pH to Iso Valkjärvi. Ölen was limed with 437 tons of dolomite and with 2815 tons of igneous rock lime (see Figure I-24(b)). The lake pH varies considerably between a low of 4.9 and a high of 7.3. These variations depend on seasonal variations in precipitation, runoff and lake production and on the added lime. This curve will be used as a realistic example for Iso Valkjärvi. Figure I-24(a) gives the results. The upper curve is for a constant pH of 5.1, the lower curve gives predicted Cs-concentrations in pike when the pH-variation is given by the curve in Figure I-24(b). One can note that the model predicts a small but significant reduction of ^{137}Cs in pike after such a liming.

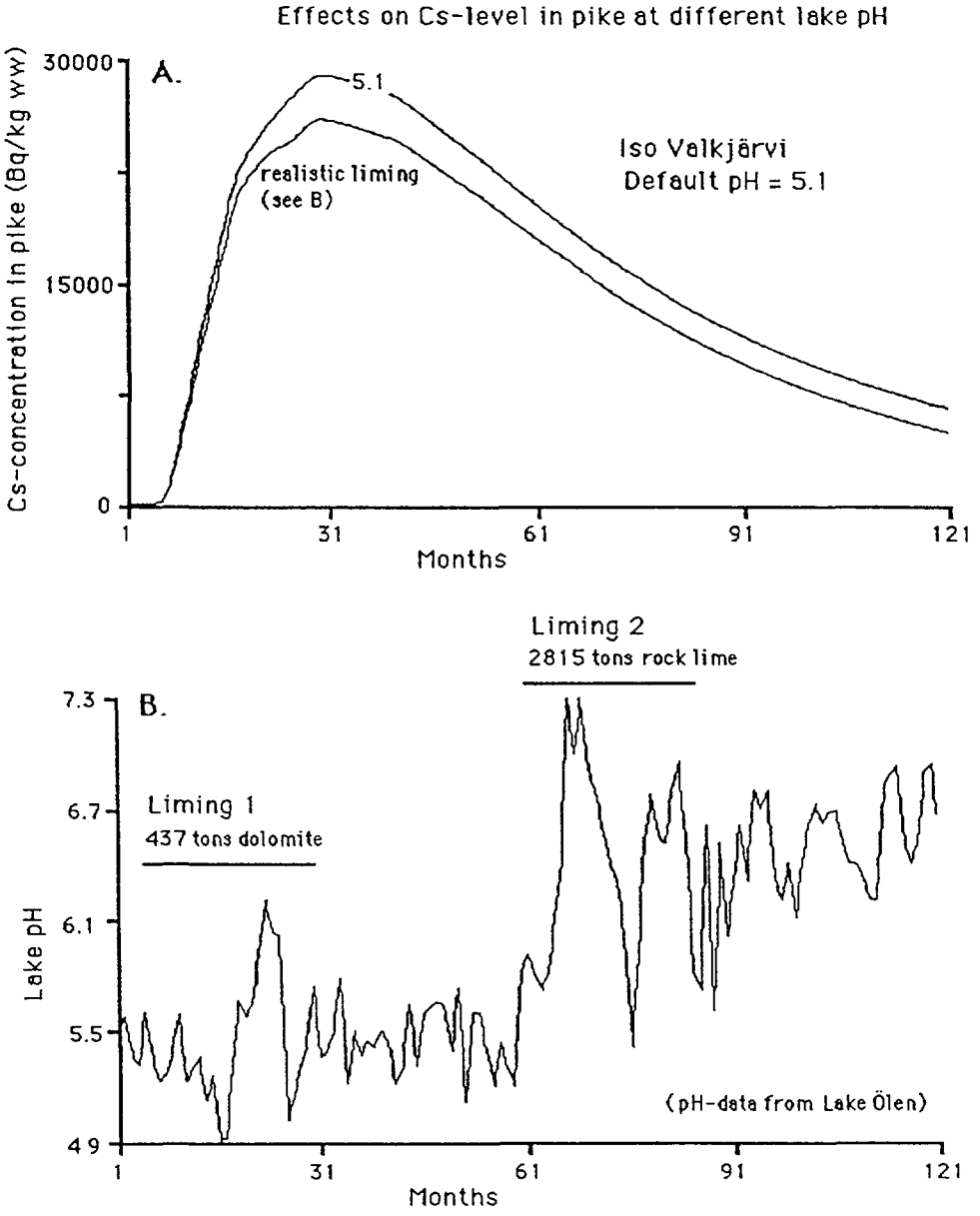

FIG. I-24. Simulations illustrating the effect of liming on Cs-concentration in pike in Iso Valkjärvi using the VAMP LAKE model and more realistic data on lake pH (in this case from Lake Ölen, Sweden).

I-4.4.3. Potash treatment

One can increase pH without changing the concentration of potassium in the lake, such as by adding primary rock lime with no potassium, but it is not possible to increase the K-concentration, and not at the same time also increase lake pH. Figure I-25(a) gives a regression between empirical data on lake pH and K-concentration for the VAMP lakes. One can note a highly significant correlation (r^2 = 0.76, p = 0.01). The regression line is:

$$10^{pH} = 10^7 \times (16.87 \log(K) + 6.492) \quad \text{(I-1)}$$

It should be noted that pH by definition is a logarithmic value. In the following simulations, we have used this equation to simulate increases in lake pH from increasing K-concentrations. The

regression is only valid for lakes with pH greater than 5.1 and lower than 8.5. In these simulations, we have set pH to 5.1 for K-concentration <0.45 (mg/L). For other situations, we have used the regression (but in a simpler form, as shown in Figure I-25(b)).

Figure I-26 shows the predicted effects of potash treatment on Cs-concentrations in pike when lake K-concentration was increased in steps from 0.4 to 38.4. The model predicts significant influences on the Cs-concentrations in pike: the higher the K, the lower the Cs-concentrations in pike. In Figure I-26(B), we have simulated starting the liming in different months: the upper curve gives the default conditions (K = 0.4), the next curve the results when a potash treatment increased K from 0.4 to 4 in month 24 (i.e. December 1987). The following curves give the results for different starting months (18, 15, 12, 10, 8 and 4); and the lowest curve gives the conditions when K is set to 4 for the whole period. One can again note: the sooner the treatment starts, the better. Similar results can be predicted for any species of fish.

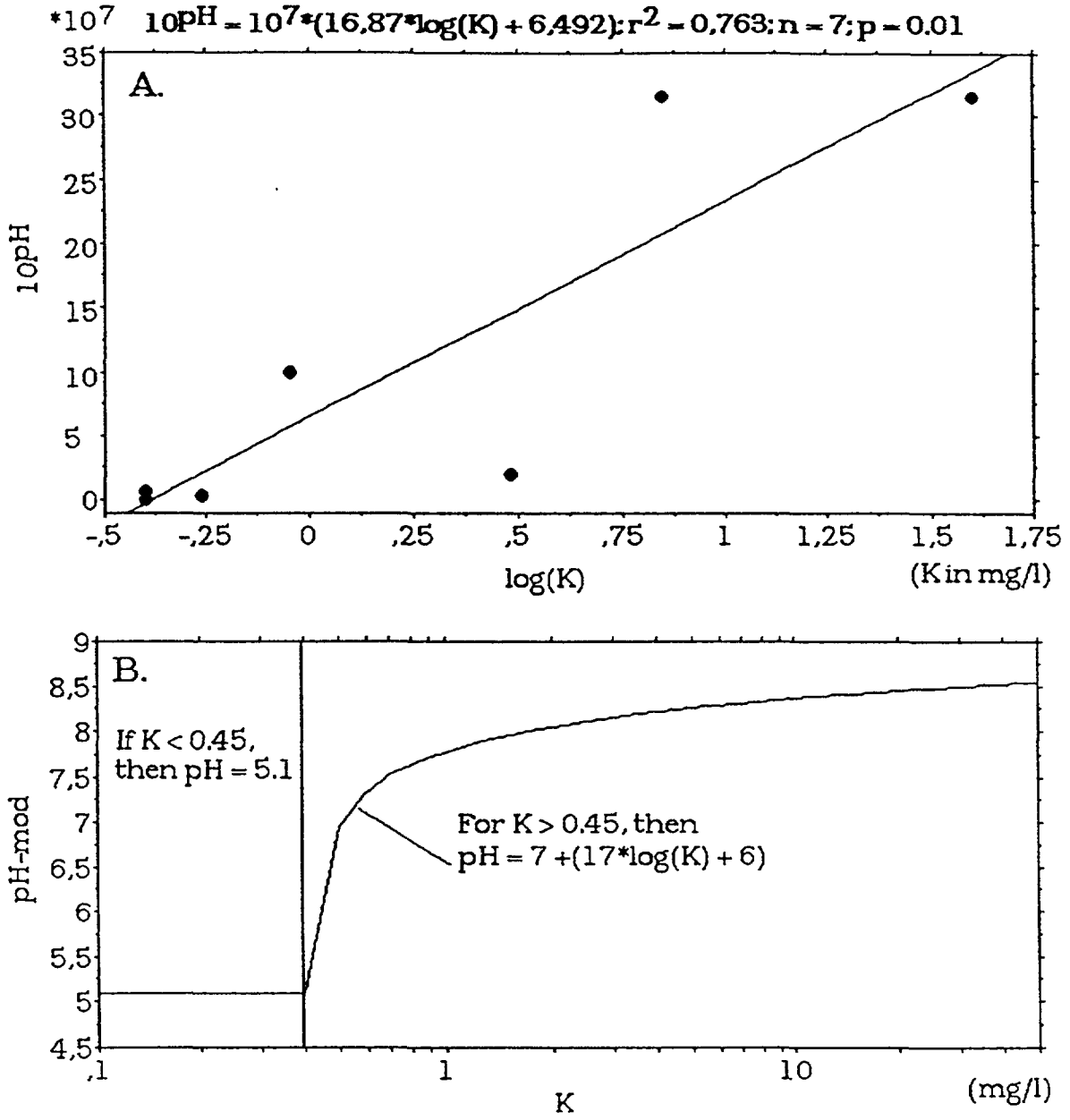

FIG. I-25. (a) The relationship between lake pH and lake K-concentration for the seven VAMP lakes. (b) Illustration of the use of the regression in (a) in simulations.

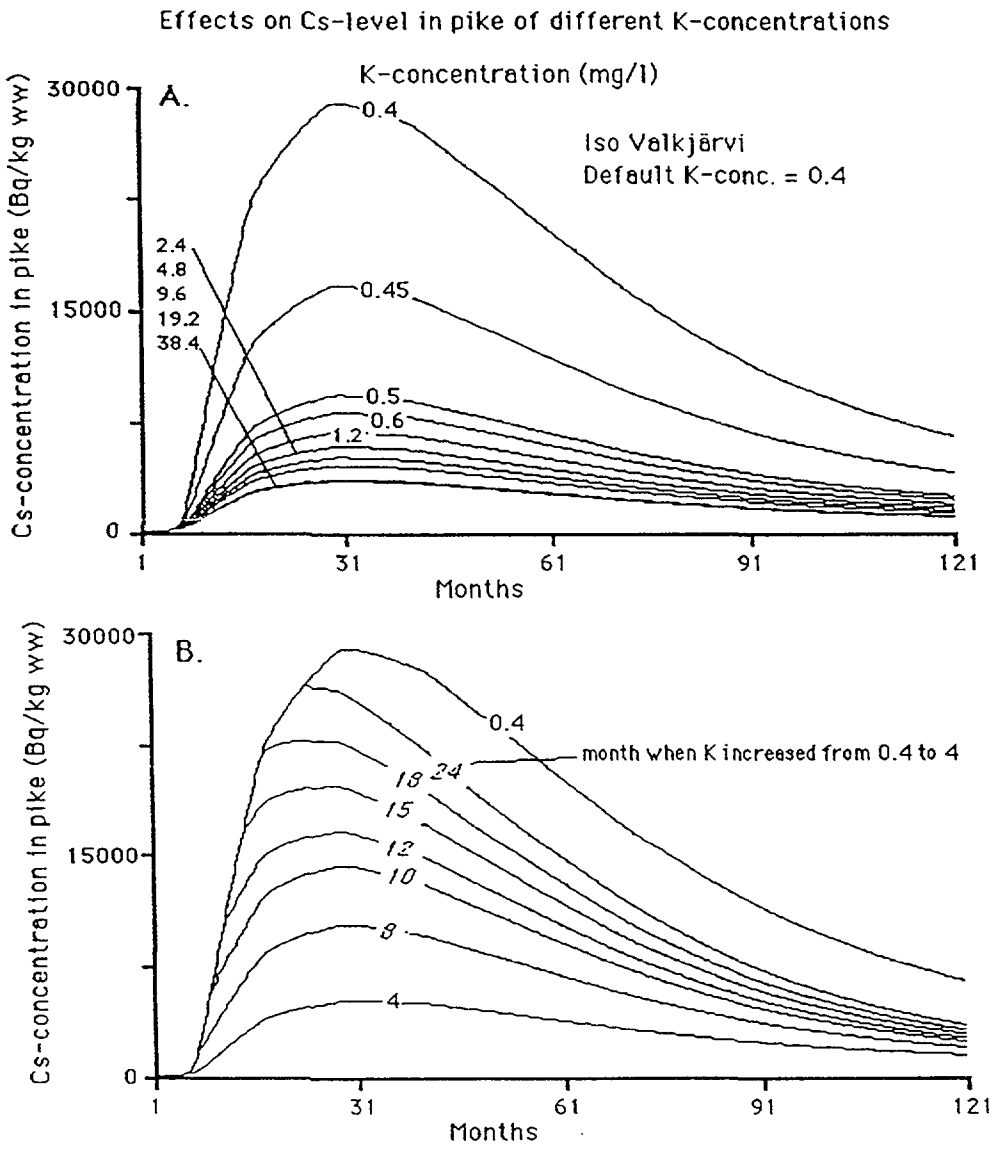

FIG. I-26. Simulations illustrating the effect of potash treatment on Cs-concentration in pike in Iso Valkjärvi using the VAMP LAKE model.

I-4.4.3. Fertilization

The most important nutrients in aquatic ecosystems are phosphorus and nitrogen. Total phosphorus has long been recognized as the nutrient most likely to limit lake primary productivity [I-37]. Several compilations of models, theories and approaches to the role of phosphorus in lake eutrophication exist [I-34, I-38, I-39]. Both experimental and comparative studies have been carried out of whole lake ecosystems to derive loading models for lake management [I-40, I-41]. A key element in this development was Vollenweider's identification of the simple relationship between sedimentation of phosphorus and water turnover in lakes. Water turnover is therefore an important factor regulating the effect of a given load of nutrient on lakes.

It is important to recognize the difference between chemical variables, like lake total-P, and meaningful ecological effect variables describing biological and ecological conditions such as algal biomass. Simple chemical variables may be very useful indicators of ecological effects, but this is only possible when the quantitative relations between those indicators and the biological or ecological effects have been established. Because it describes so much of the lake's status, lake total-P could be considered as a limnological state variable, but it is not an ecological effect variable. Thus, although

the concentration of total phosphorus in a lake (C_{TP}) is not interesting *per se*, total-P is interesting because it can be related to variables of real ecological interest such as hypolimnetic oxygen demand, mean and maximum primary production, Secchi depth, algal volume, fish yield, and various aspects of the communities of the bottom fauna, algae, or fish (see [I-31] and Table I-2).

Figure I-27 shows the predicted effects on the Cs-concentrations in pike in Iso Valkjärvi when fertilization changed the primary production (in g C · m^{-2} · a^{-1}) from 25 in steps to 300: The higher the lake production, the larger the biomass and the lower the Cs-concentrations in pike. In Figure I-27, the fertilization was started in different months. The upper curve gives the default conditions (prim. prod. = 25), the next curve gives the results when fertilization increased primary production from 25 to 100 in month 8; the following curves give the same results for different starting months (10, 12, 15, 18 and 24); and the lowest curve gives the conditions when primary production is set to 100 for the entire period. In the VAMP LAKE model, the Cs-concentration in predatory fish is calculated as the ratio between the amount of Cs in predator and the biomass of the predator. The biomass of the predator is calculated from equations driven by input data on primary production. So, in this case, the VAMP LAKE model simulates a very quick response to a fertilization, as indicated by the curves linking the upper, default curve to the curve for a primary production of 100. It is evident that fertilization should NOT be used as a practical remedy in eutrophic lakes.

From these simulations, one may conclude that potash treatment ought to be the most effective method to speed up the recovery in lakes with initial low K-concentrations.

TABLE I-2. CHARACTERISTIC FEATURES IN LAKES OF DIFFERENT TROPHIC LEVELS [I-31]

Trophic level	Oligotrophic	Mesotrophic	Eutrophic	Hypertrophic
Primary prod. (g C · m^{-2} · a^{-1})	<30	25–60	40–200	130–600
Secchi depth (m)	>5	3–6	1–4	0–2
Chlorophyll-a (mg/m^3)	<2	2–78	6–35	30–400
Algal volume (g/m^3)	<0.8	0.5–1.9	1.2–2.5	2.1–20
Total-P (mg/m^3)	<5	5–20	20–100	>100
Total-N (mg/m^3)	<300	300–500	350–600	>1000
Dominant fish	Trout Whitefish	Whitefish Perch	Perch Roach	Roach Bream

I-4.4.4. Conclusions

One and the same load (fallout) may cause different environmental effects (biouptake and concentration in biota) in ecosystems with different sensitivity. The most important environmental variables regulating the biouptake of radiocaesium and the duration (retention time) of the substance in the a lake are the concentration of potassium in the lake water and the lake water retention time.

There are several ecologically acceptable and practically feasible methods to remediate a lake contaminated by radiocaesium, e.g. liming, potash treatment, and fertilization of low-productive lakes. The results of simulations agree with results obtained from field experiments: the sooner the treatment starts, the better. Potash treatment is also likely to be the most effective remedy.

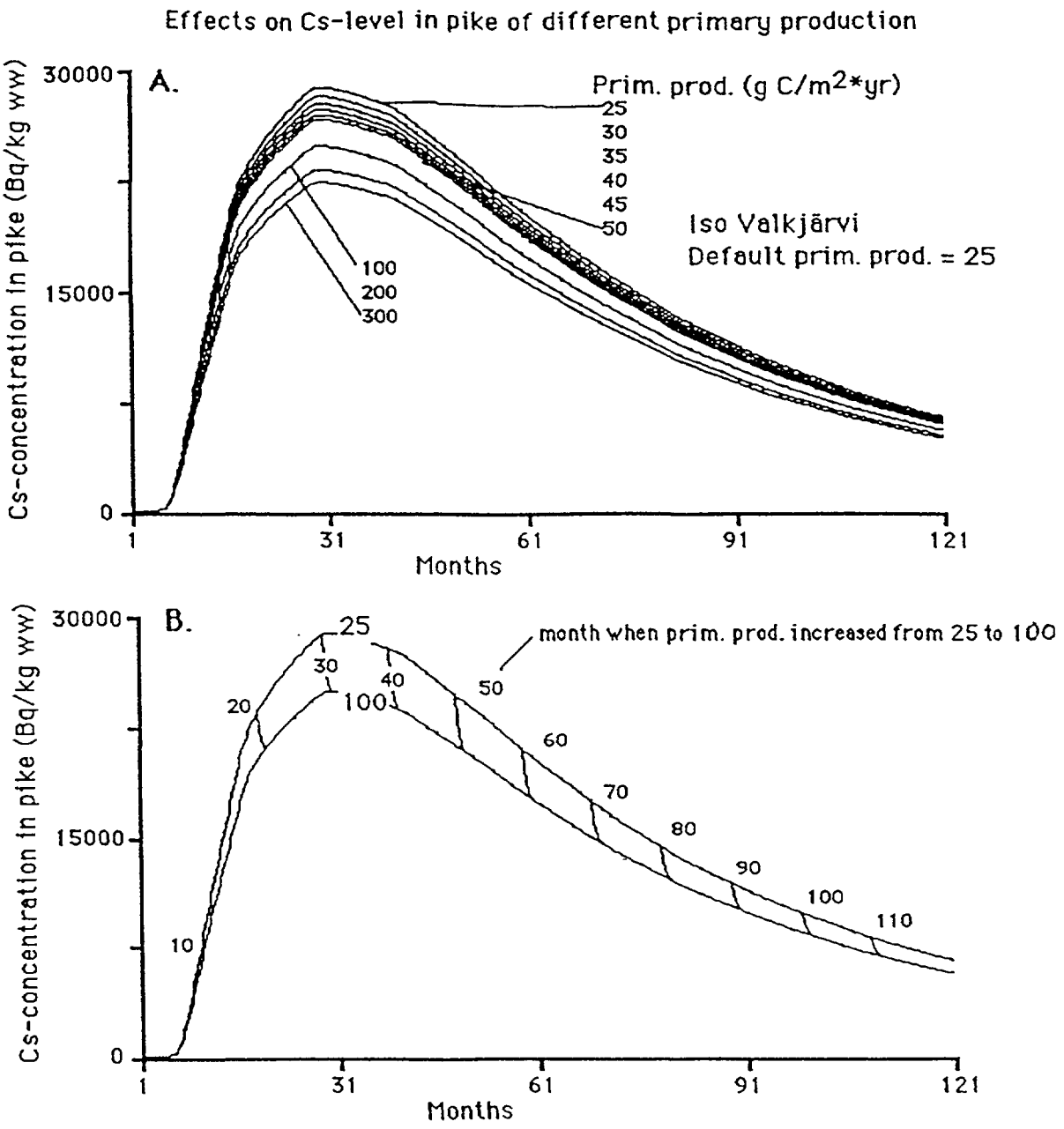

FIG. I-27. Simulations illustrating the effect of fertilization on Cs-concentration in pike in Iso Valkjärvi using the VAMP model.

From the perspective of practical models in radioecology, some very interesting areas of future research open up, i.e. models based on the ecosystem approach should be developed for target variables (like Cs-concentration in water and predatory fish in this work) for many other types of environments, such as forests, agricultural land and urban areas.

There are problems associated with large ecosystem models in predictive contexts, and also problems with statistical models. The VAMP LAKE model may be considered as a "mixed" model in the sense that it is based on approaches used both in traditional dynamic models and in statistical, regression models. In the future, it is possible that such "mixed" models will be developed and used in many practical and scientific contexts.

REFERENCES

[I-1] HÅKANSON, L., et al., Modelling of radiocesium in lakes – lake sensitivity and remedial strategies. J. Environ. Radioactivity **33** (1996) 1–25.

[I-2] ZHELEZNYAK, M.J., et al., "Modelling the Effectiveness of Countermeasures Designed to Reduce the Rate of Transport of Radionuclides in the Pripyat-Dnieper Water System", Intervention Levels and Remedial Measures after Nuclear Accidents, (Proc. Int. Sem. Cadarache, 1991), International Union of Radiologists, Cadarache (1992).

[I-3] HÅKANSON, L., Ecometric and Dynamic Modelling – Exemplified by Caesium in Lakes after Chernobyl, Springer-Verlag, Heidelberg, (1991) 158 p.

[I-4] HÅKANSON, L., Radioactive Caesium in Fish in Swedish Lakes after Chernobyl – Geographical Distributions, Trends, Models and Remedial Measures, (MOBERG, L., Ed.), "The Chernobyl book", Swedish Radiation Protection Institute, Stockholm (1991) 239–281.

[I-5] SANTCHI, P.H., BOLLHALDER, S., ZINGG, S., LUCK, A., FARRENKOTHEN, K., The self-cleaning capacity of surface waters after radioactive fallout, Evidence from European waters after Chernobyl, 1986-1988, Environ. Sci. Technol. **24** (1990) 519–527.

[I-6] VOITSEKHOVITCH, O.V., KANIVETS, V.V., LAPTEV, V. , BILIY, I.Y., "Hydrological Processes and Their Influence on Radionuclide Behaviour and Transport by Surface Water Pathways as Applied to Water Protection after Chernobyl Accident", Hydrological Impact of Nuclear Power Plant, (Proc. Int. Symp. Paris, 1992), UNESCO, Paris (1993).

[I-7] VOITSEKHOVITCH, O.V., "Overview of Water Quality Management in the Areas Affected by the Chernobyl Radioactive Contamination", Radioecology and the Restoration of Radioactive-Contaminated Sites, (LUYKX, F., FRISSEL, M.J., Eds) NATO, Series 2. Environment Vol. 13 (1996).

[I-8] VAKULOVSKY, S.M., et al., "Radioactive Contamination of Water Bodies in the Area Affected by Releases from the Chernobyl Nuclear Power Plant Accident", Environmental Contamination Following a Major Nuclear Accident (Proc. Int. Symp., Vienna 1989), IAEA, Vienna (1990) 231–246.

[I-9] VOITSEKHOVICH, O.V., BORZILOV, V.A., KONOPLEV, A.V., "Hydrological Aspects of Radionuclides Migration in Water Bodies Following the Chernobyl Accident", Comparative Assessment of the Environmental Impact of Radionuclides Released During Three Major Nuclear Accidents: Kyshtym, Windscale, Chernobyl, (Proc. Conf., Luxembourg 1990) Vol. 2, Commission of the European Communities, Radiation Protection – 53, Rep. EUR 13574, CEC, Luxembourg (1991) 528–548.

[I-10] VOITSEKHOVITCH, O.V., "Radioecology of the Water Bodies at the Area Affected as a Result of Chernobyl Accident", Chernobylinterinform, Kiev, Volume 1 (1997).

[I-11] INTERNATIONAL ATOMIC ENERGY AGENCY, Modelling of Radionuclide Transfer into Rivers and Reservoirs, IAEA-TECDOC, Vienna (in preparation).

[I-12] VOITSEKHOVITCH, O.V., KANIVETS, V.V., SHERESHEVSKY, A.I., "The Effectiveness of Bottom Sediment Traps Created with Aim to Catch Contaminated Matter Transported by Suspended Particles", Proc. of Ukr. Hydromet Institute, Kiev, Vol. 228 (1998).

[I-13] VOITSEKHOVITCH, O.V., ZHELEZNYAK, M.I, ONISHI, Y., "Chernobyl Nuclear Accident Hydrologic Analysis and Emergency Evaluation of Radionuclide Distributions in the Dnieper River, Ukraine, during the 1993 Summer Flood", Rep. PNL-9980, Pacific Northwest Laboratory, Richland, WA (1994).

[I-14] BILYI, I.Y., VOITSEKHOVITCH, O.V., ONISHI, Y., GRAVES, R.E., "Modeling of ^{90}Sr Wash-off from the Pripyat Flood Plain by a Four-Year Flood", Isotopes in Water Resources Management (Proc. Symp. Vienna 1995), IAEA, Vienna, (1995).

[I-15] VOITSEKHOVITCH, O.V., On the concept of water protection measures against secondary contamination after Chernobyl accident, Trudy UkrNIGMI, No. 245 (1993) (in Russian).

[I-16] PRISTER, B., LOSCHILOV, N., PEREPELYATNICOVA, L., PEREPELYATNICOV, G., Efficiency of measures aimed at decreasing the contamination of agricultural products in areas contaminated by the Chernobyl NPP accident, Sci. Total Environ. **112** (1992) 79–87.

[I-17] VOITSEKHOVITCH, O.V., NASVIT, O., BERKOVSKY, V., LOST, I., "Present Concept on Water Remedial Activities on the Areas contaminated by the Chernobyl Accident", Freshwater and Estuarine Radioecology, (Proc. Int. Symp., Lisbon, 1994), European Union, Luxembourg (1997).
[I-18] INTERNATIONAL COMMISSION ON RADIOLOGICAL PROTECTION, 1990 Recommendations of the International Commission on Radiological Protection, ICRP Publication 60, Pergamon Press, Oxford and New York (1991).
[I-19] ESPEGREN, M.L., PIERCE, G.A., HALFORD, D.K., Comparison of Risk for Pre-and Post-Remediation of Uranium Mill Tailing from Vicinity Properties in Monticello, Utah Health Physics Society, Salt Lake City, UT, Vol. 70, **4** (1996).
[I-20] ANDERSSON, T., HÅKANSON, L., KVARNÄS, H., NILSSON, A., Measures to Reduce High Levels of Radioactive Caesium in Swedish Lake Fish after Chernobyl (in Swedish with English summary), SSI Report-XX 91–07, Stockholm (Sweden) (1991) 114 p.
[I-21] HÅKANSON, L., et al., Measures to Reduce Mercury in Lake Fish. Final Report from the Liming-mercury-caesium Project. Nat. Environ. Prot. Agency, S-171 25 Solna, Sweden, SNV PM 3818 (1990) 189p.
[I-22] BROBERG, A., ANDERSSON, E., Turnover of Caesium in Limnic Systems, Limnological inst., Uppsala Univ., mimeo (1989) 30 p (in Swedish).
[I-23] SALBU, B., BJØRNSTAD, H.E., BRITTAIN, J.E., Fractionation of Cs-isotopes and Sr-90 in snowmelt, run off and lake waters from contaminated Norwegian mountain catchment, J. Radioanal. Nucl. Chem. **156** (1992) 7–20.
[I-24] HAMMAR, J., NOTTER, M., NEUMANN, G., Caesium in Char Lakes (in Swedish), Report to Swedish Radiation Protection Institute, Stockholm (project P 378.86 and P 378.88) (1989).
[I-25] CARLSSON, S., A model for the turnover of Cs-137 and potassium in pike (*Esox lucius*), Health Phys. **35** (1978) 549–554.
[I-26] JANSSON, M., HAYMAN, U., FORSBERG, C., Acid lakes and "biological buffering", Vatten, **37** (1981) 241–251 (in Swedish).
[I-27] EVANS, S., Biological Half-time of Cs-137 in Fish Exposed to the Chernobyl Fallout. Clearance of Cs-137 in Roach Exposed to Various Potassium Concentrations in the Water, An Experimental Study, Studsvik Report, Np-89/74, Studsvik Energiteknik AB, Nyköping (Sweden) (1989) 17 p.
[I-28] WALLSTRÖM, A., HÅKANSON, L., A Household Method to Reduce Cs-137 in Meat, National Food Administration, Uppsala, Sweden, Report 6, IUP (1991) (in Swedish).
[I-29] HÅKANSON, L., ANDERSSON, T., Remedial measures against radioactive caesium in Swedish lakes fish after Chernobyl, Aquatic Sci. **54** (1992) 141–164.
[I-30] MEILI, M., Mercury in Boreal Forest Lake Ecosystems, Acta Univ. Upsaliensis 336, Thesis, Uppsala Univ. (1991).
[I-31] HÅKANSON, L., PETERS, R.H., Predictive Limnology, Methods for Predictive Modelling, SPB Academic Publishing, Amsterdam (1995).
[I-32] HÅKANSON, L., JANSSON, M., Principles of Lake Sedimentology, Springer-Verlag, Berlin (1983) 316 p.
[I-33] COUNCIL OF GREAT LAKES RESEARCH MANAGERS, A proposal framework for developing indicators of ecosystem health for the Great Lakes Region, (CGLRM), Internat. Joint Comm., Windsor, Ontario (1991).
[I-34] VOLLENWEIDER, R.A., The Scientific Basis of Lake Eutrophication, with Particular Reference to Phosphorus and Nitrogen as Eutrophication Factors, Tech. Rep. DAS/DSI/68.27, OECD, Paris (1968) 159 pp.
[I-35] PETERS, R.H., A Critique for Ecology, Cambridge Univ. Press, Cambridge (1991) 366 p.
[I-36] SVERDRUP, H., WARFVINGE, P., The role of weathering and forestry in determining the acidity of lakes in Sweden, Water, Air and Soil Poll. **52** (1990) 71–78.
[I-37] WETZEL, R.G., Limnology. Saunders College Publ., Philadelphia, PA (1983) 767 p.
[I-38] CHAPRA, S.C., RECKHOW, K., Expressing the phosphorus loading concept in probabalistic terms, J. Fish. Res. Board. Can. **36** (1979) 225–229.

[I-39] VOLLENWEIDER, R.A., "Eutrophication: Conventional and Non-conventional Considerations on Selected Topics", Scientific Perspectives in Theoretical and Applied Limnology (DE BERNARDI, R., GIUSSANI, G. AND BARBANTI, L., Eds), Memorie dell'Istituto Italiano di Idrobiologia Dott. Marco de Marchi, **47**, Pallanza, (1990) 378 p.

[I-40] DILLON, P.J., RIEGLER, F.H., A test of a simple nutrient budget model predicting the phosphorus concentration in lake water, J. Fish. Res. Board Can. **31** (1974) 1771–1778.

[I-41] SCHINDLER, D.W., FEE, E.J., RUSZCZYNSKI, T., Phosphorus input and its consequences for phytoplankton standing crop and production in the experimental lakes area and in similar lakes, J. Fish. Res. Board Can. **35** (1978) 190–196.

Annex II

CIEMAT MODEL RESULTS FOR ESTHWAITE WATER

A. Agüero and A. García-Olivares, CIEMAT-IMA, Spain

II-1. MODEL DESCRIPTION

The main elements of the transfer model, PRYMA-LO, for the transfer of Cs-137 in watershed scenarios, are presented in Figure II-1. The model has been developed by CIEMAT-IMA, Madrid, Spain and the present modelling exercise has been undertaken by A. Agüero and A. García-Olivares. The processes included in the model have been organized as follows:

Firstly, we consider the catchment area and the different processes involved in the transfer of the fallout to the ground. Then, we consider the processes by which isotopes are incorporated into the water flow and eventually leave the system under study. A water inflow-outflow steady state is assumed. Finally, a model for the fate of caesium in the lake is established.

The model for the interception process considers the time dependent deposition, the infiltration of water and the interception of contamination by the vegetation canopy (using fractional interception factors) and the rate of discharge from the canopy. The catchment model attempts to obtain a general picture of the water and sediment flows and the activity coming from the drainage basin to Esthwaite Water. A generic model has been used, which simulates the drainage of water and eroded material in a catchment using a mosaic of cells to represent the basin drainage. The subprocesses considered are the physico-chemical equilibrium (using the K_d approach) between the dissolved and absorbed phases of the radionuclide in the drainage area, erosion of soil by water from the drainage area and infiltration into the surface soil.

Figure II-2 shows the flow chart for the calculation of each single cell in the basin. In this scenario only two rectangular cells have been used to represent the catchment. This rough approach is justified since the direct deposition of contamination on the lake seems to be the dominant fraction in the source term, and since the water and soil inputs into the lake are known from direct observations.

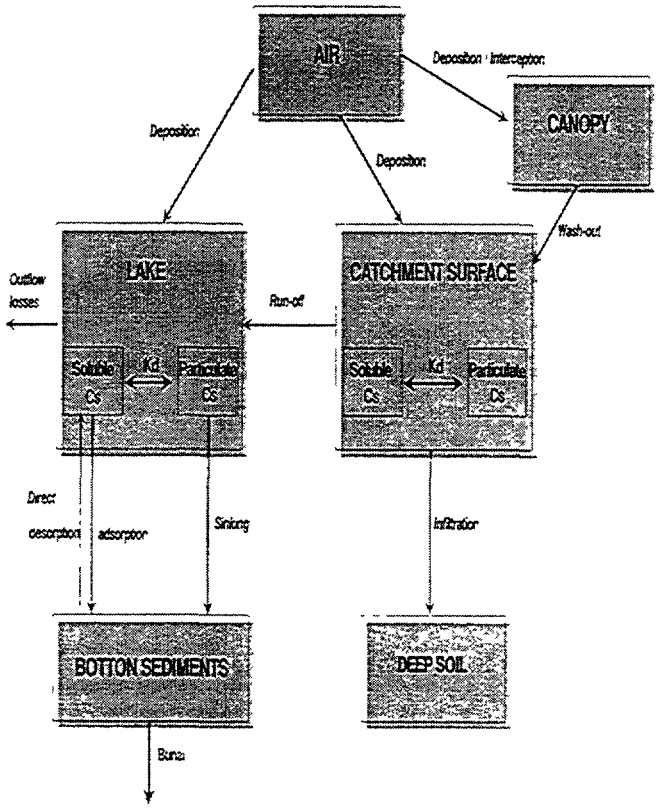

FIG. II-1. Conceptual model of the catchment-lake system.

The concentration in the water and sediments of the lake has been simulated through a dynamic compartmental model based on Codell [II-1, II-2]. This model has been complemented with a set of subsidiary hypotheses to take into account the dynamics during the summer stratification period.

In the following Sections the main assumptions and expressions used in the construction of the different parts of the model are briefly described.

(1) INPUT DATA

$\Downarrow$

(2) Overload flow downslope $f_i = \dot{R}(1 - \frac{I_f}{\dot{R}} S_c(1 - V_i)$ *if* $\dot{R} > I_c$

Number of channels N_c of average diameter Z_0

$\Downarrow$

(3) Estimate the rugosity as a function of median size particle (Strickler):

$$n = 0.0342 \cdot d_m^{1/6}$$

$\Downarrow$

(4) Mean and maximum water depth if the flow is channeled

$$h = \frac{2}{3Z_0}(Z_0 h' - h'^{/2}) \text{ and } h' = (f_i \cdot n/1.527\sqrt{SZ_0} \cdot N_c)^{6/13}$$

$\Downarrow$

(5) Compute water flow velocity (Manning): $v = \frac{1.5}{n} h^{2/3} S^{1/2}$

$\Downarrow$

(6) Reynolds number, $N_r = \frac{vh}{v}$

$\Downarrow$

(7) Overland flow bed material (Peter-Meyer) $g_s = [\frac{\tau - \tau_0}{0.25 \cdot (\frac{1000}{g})^{1/3}}]^{3/2}$

$$\tau_0 = 0.047(\rho_d - 1000\cdot)d_m \text{ and } \tau = \frac{50}{8} \frac{\rho v^2}{N_r}$$

$\Downarrow$

(8) Sediments concentration that are dragged by the bottom (Einstein):

$$SS = \frac{1000 \cdot g_s\sqrt{N_r}}{58 \cdot \rho_b \cdot v \cdot d_m}$$

$\Downarrow$

(9) Deposition velocity of eroded soil (v_s) is defined as the smaller of the two velocities v_1, v_2, obtained from (i) the Stokes formula and (ii) the impact model:

$$v_1 = 2.17777 \cdot (\rho_b - 1000.)\cdot d_m^2/\mu_d \quad v_2 = [\frac{9\mu_d^2 + 3 \cdot 9810 \cdot (\rho_b - 1000)d_m^3]^{1/2} - 3\mu_d}{2.25 \cdot d_m \cdot 1000}$$

$\Downarrow$

FIG. II-2. Flow chart for the calculation of each single cell in the drainage basin. (cont.)

(cont.)

(10) Flow of suspended eroded material $q_s = \frac{q_s}{11/6} \frac{(\frac{a'}{h})^{w-1}}{[1 - (\frac{a'}{h})^w]}[(\frac{v}{\mu_0} + 2.5) \cdot J_1 + 2.5 \cdot J_2]$

$$with\ a' \equiv 2d_m,\ w \equiv \frac{v_g}{0.4 \cdot x_0},\ u_o \equiv 2.5v/\sqrt{N_r}$$

$$J_1 = \int_{a'/h}^{1} (\frac{1 - \xi/h}{\xi/h})^w \cdot d(\frac{\xi}{h}) \quad J_2 = \int_{a'/h}^{1} (\frac{1 - \xi/h}{\xi/h})^w \cdot ln\frac{\xi}{h} d(\frac{\xi}{h})$$

⇓

(11) Flow of water leaving the catchment due to different categories of precipitation
Flow of eroded material leaving the catchment due to different categories or of shower

⇓

(12) Wet surface, total volume of flowing water, for each category of shower

⇓

(13) Compute water-eroded material activity equilibrium for each category of shower

⇓

(14) Water and soil particles concentrations and daily average source term into the next cell

$$C_{water}(t) = \int_0^t \frac{C_{i'}^0(t)}{h(1 + ss \cdot K_d)} \exp([-\frac{I_c' \cdot R}{h_s} - \frac{Q_w}{V_w}(1 + ss \cdot K_d) - \lambda_r]t')dt'$$

$$C_{soil}(t) = K_d \cdot C_{water}(t)$$

⇓

(15) Daily averages weighted to the probability of the shower category

⇓

(16) INPUT into the lake coming from the catchment

FIG. II-2. Flow chart for the calculation of each single cell in the drainage basin.

II-1.1. The catchment

Figure II-2 shows the flowchart of the calculation in the catchment model. Most of these expressions can be found in reference [II-3].

II-1.1.1. Time dependent deposition

Daily deposition for the catchment area and lake surface has been obtained by distributing the deposition over 13 days proportionally to the observed air concentrations in Glasgow, in such a way that the observed total deposition in the basin is obtained [II-4]. The observations in Glasgow are expected to approximately represent the evolution of the Chernobyl cloud in the U.K. The observed deposition ranges between 0 and 2000 Bq/m^2 (Appendix I) in a distribution that we assume to be log-normal with a median value at 666 Bq/m^2 and 99 percentile at 2000 Bq/m^2.

II-1.1.2. Interception

A fraction, V_i= 0.15 of the activity deposition is intercepted by the canopy and gradually released at a rate λ_{wash} = 0.0495 d^{-1} [II-2].

II-1.1.3. Recharge and water catchment

A constant layer of water is assumed to arise from each rain shower with an intensity above the infiltration capacity of the soil I_c. Table II-1 shows the assumed intensity distribution of showers sampled at 30-minute intervals. This is a typical distribution for Northern Spain [II-5]. The precise distribution that should be applied in the Esthwaite area was unknown.

TABLE II-1. INTENSITY DISTRIBUTION OF RAIN SHOWERS SAMPLED AT 30-MINUTE INTERVALS

Intensity ($L \cdot m^{-2} \cdot (30min)^{-1}$)	0–1	1–3	3–5	5–10	10–30	>30
%	39.5	38.5	14.	7.	1.	0.

When a water layer is formed in the drainage area, the water is assumed to flow along the bottom of semi-cylindrical channels, with a mean radius of close to 10 cm., in order to represent the terrain ondulations on the scale between 1 to 50 cm. Consequently the effective surface area of flowing water is not the true basin area but a fraction that is between 5 and 20% depending on the intensity of the shower. In this fraction of the area an equilibrium between dissolved nuclides and nuclides sorbed by resuspendible soil is assumed.

II-1.1.4. Soil erosion by water from the drainage area

The flowchart in Figure II-2 shows the processes modelled. The units in that flowchart are:

$\dot{R}_i$ is the intensity of a shower type-i of 30 minutes ($L \cdot m^{-2} \cdot (30\ min)^{-1}$),
V_i is the fraction of the precipitation intercepted by the canopy (-)
I_c is the infiltration capacity for a shower of 30 minutes ($L \cdot m^{-2} \cdot (30\ min)^{-1}$),
f_i is the flow leaving the cell during the 30 minutes shower i (L/(30 min)),
S_c is the cell area (m^2)
d_m is the median diameter of the particles (m),
h is the mean depth of the channelled approximately equal to the hydraulic radius (m),
h′ is the maximum depth in the channel (m),
v is the velocity of the water leaving the cell (m/s),
g is the gravity constant (9.8 m/s^2),
ρ_b is the bulk density of the soil (kg/m^3),
τ is the critical tractive force (kg/m^2),
τ_0 is the boundary shear stress acting on the particles (kg/m^2),
g_s is the load bed transport rate leaving the cell in mass per unit width ($kg \cdot m^{-1} \cdot s^{-1}$),
ss is the mass of sediments transported per volume unit of water (kg/m^3),
v_1, v_2 are the deposition velocities of the suspended particles (m/s),
q_s is the suspended load leaving the cell in mass per unit width ($kg \cdot m^{-1} \cdot s^{-1}$),
h_s represents the depth of the soil layer that would be resuspended if it were available to the flowing water, according to the Peter-Meyer formula,
C_{water} is the activity concentration in water (Bq/m^3),
C_t^0 is the total surface activity concentration (Bq/m^2),
C_{soil} is the activity concentration bonded to soil particles (Bq/kg),
Q_w is the water outflow which equals the water inflow into the lake (m^3/d),
I_c' is the daily averaged infiltration capacity (m/d).

It is possible to estimulate the flow of eroded soil from catchment into the lake by means of mass balance since the rate of deposition on the bottom and the suspended sediments have been measured in Esthwaite (Appendix I and reference [6]).

Considering an annual steady state between solids entering, leaving and depositing on the bottom, it is easy to obtain the following expression:

$$q_m = ss_l \cdot (S_t \cdot v_{dep} + Q_{out}) \qquad \text{(II-1)}$$

$$v_{dep} = \frac{v_{sed} \cdot \rho_{sed}}{ss_l}$$

where

q_m is the flow of sediments entering the lake (kg/d),
ss_l is the concentration of suspended sediments in the lake (kg/m^3)
S_l is the surface area of the lake (m^2),
v_{dep}, is the deposition velocity of the suspended particles (m/d),
Q_{out} is the outflow (m^3/d),
v_{sed} is the annual averaged sedimentation velocity in daily units (m/d), and
ρ_{sed} is the bulk density of the sediments (kg/m^3).

Since the observed values are: ss_l 1 × 10^3 kg/m^3 (Appendix I), v_{sed} 9 mm/a [II-6] and ρ_{sed} is 100 kg/m^3 [II-6], the basin must contribute about 2 × 10^3 kg/d of soil which is roughly 10^{-4} to 10^{-3} times the quantity that is potentially transportable by the water flowing in the basin. The low factor may be related to the extensive vegetation cover, with 10–15% of forest, 80–90% grassland and less than 5% bare rock.

For these reasons most of the contamination contributed by the basin seems to be washed out from surfaces and not resuspended by the flowing water. Thus, only a minor fraction of the source term seems to be contributed by the eroded soil, at least in the short time scale relevant to this problem (days to months).

The first process has been simulated using a rate of washing by runoff (d^{-1}) of the daily deposited caesium. McDougall, et al., [II-6] used a similar approach in their modelling of Esthwaite Water. To model the second process the resuspended soil is assumed to have an activity concentration roughly in equilibrium with the concentration of the water that carries it:

$$C_w(t) = \frac{C_t^0(t)}{h(1 + ss \cdot K_d)} \qquad \text{(II-2)}$$

and

$$C_s(t) = K_d \cdot C_w(t) \qquad \text{(II-3)}$$

where

$C_{w,s}(t)$ is the concentration of nuclides in water and suspended soil,
$C_t^0(t)$ is the total concentration per unit of surface, obtained from the direct deposition and the canopy washout,
K_d is the soil-water distribution coefficient for C_s,
h(m) is the average height of the channelled water,
ss is the suspended soil concentration (kg/m^3).

II-1.1.5. Infiltration and decay of the available contamination

It has been assumed that the groundwater contribution comes exclusively from the infiltrated flow in the basin.

The infiltration flow drives the surface contamination to deeper soils. We assume that the infiltrated contamination does not became available for dissolution and drainage after it is below a depth h_s.

$$h_s = \frac{h \cdot ss}{\rho_b} \tag{II-4}$$

with ρ_b being the bulk density of the soil (kg/m^3).

This implies a loss rate of contamination due to infiltration K_{out}:

$$K_{out} = \frac{I_c \cdot R}{h_s} \tag{II-5}$$

where

h_s is given by eq. (II-4),
I_c is the infiltration capacity ($m^3 \cdot m^{-2} \cdot d^{-1}$),
G is the soil porosity,
R_c a retardation coefficient:

$$R_c = [1 + \rho_b \cdot K_d \cdot \frac{1 - \varepsilon}{\varepsilon}]^{-1} \tag{II-6}$$

This retardation coefficient expresses the ratio between the radionuclides transport velocity and the groundwater flow velocity. It critically depends on the soil-water distribution coefficient of the nuclide, K_d.

In addition, the deposited contamination is lost at the rate λ_w by which the contaminated water is taking it out into the lake:

$$\lambda_w = \frac{Q_w}{S_w} \cdot \frac{C_w(t)}{C_t^0(t)} \tag{II-7}$$

where

S_w is the wet surface area of the catchment (m^2).

II-1.1.6. Physico-chemical equilibrium

Under the assumptions (II-4) to (II-7), the solution of eqs. (II-2) and (II-3) provides the concentration $C_w(t)$ in the drainage water during a shower able to produce a water height h. This solution is shown in the step (14) of Figure II-2.

In that expression:

$$C_t^0(t) = \int_0^t D(t')dt' \tag{II-8}$$

where

D(t) is the deposition ($Bq \cdot m^{-2} \cdot d^{-1}$),
Qw is the flow of water entering the lake (m^3/d),
λ_r is the radioactive decay (d^{-1}).

The expressions used to obtain h and ss are shown in the steps (6) and (10) of Figure II-2.

II-1.2. The lake

A dynamic lake model developed by Codell [II-1, II-2] and slightly modified by us has been used for the periods of non-stratification. The activity of caesium-137 in the lake is present in two different forms, a fraction of it is dissolved in water and a fraction adsorbed onto suspended particles.

The total source term into the lake, S(t) (Bq/d), is the sum of a direct deposition on the lake surface S_3 which is dominant during the first days after deposition, a contribution from the water inflow S_1, which seems to be dominant after the contaminated cloud has passed over and a contribution from the eroded soils S_2 coming from the catchment which could become dominant in the long term. However, the latter is not an important contribution during the first 100 days and therefore it has a minor influence in the short term dynamics in the lake:

$$S(t) = S_1(t) + S_2(t) + S_3(t) = Q_{out} \cdot C_{water}(t) + Q_m \cdot C_{soil} + S_l \cdot D(t) \qquad \text{(II-9)}$$

where

S_l is the lake surface area (m^2).

The removal of activity from the lake water is due to outflow from the lake and to the transfer of activity to the bottom sediments. The transfer to the sediments includes the direct adsorption/desorption process of the soluble fraction and the sinking of the particulate fraction.

The sedimentation rate is assumed to be constant. The thickness of the sediment layer remains constant because it is assumed that when sedimentation occurs an equivalent portion of the original bed is buried and it is eliminated from the active layer.

The concentrations of activity in water (C), concentration in sediments (C_p), concentration bonded to suspended particles and the contribution initially bonded to particles coming from the catchment are respectively:

where:

$$\frac{dC}{dt} = \frac{S_1(t) + S_3(t)}{V} + C_p\lambda_1 - C\lambda_2 \qquad \text{(II-10)}$$

$$\frac{dC_p}{dt} = C\lambda_3 - C_p\lambda_4 + C_c\lambda_c \qquad \text{(II-11)}$$

$$C_s = ss_l \cdot K_d \cdot C \qquad \text{(II-12)}$$

$$C_c = \frac{S_2(t)}{V \cdot \lambda_{cl}} \qquad \text{(II-13)}$$

where:

$$\lambda_1 = \frac{K_f}{< h > \cdot K} \tag{II-14}$$

$$\lambda_2 = \frac{Q_{out}}{v} + \lambda_r + \frac{v \cdot K}{< h >} + \frac{K_f}{< h >}$$

$$\lambda_3 = \frac{v \cdot K}{d} + \frac{K_f}{d}$$

$$\lambda_4 = \lambda_r + \frac{v}{d} + \frac{K_f}{d \cdot K}$$

$$\lambda_c = v_{dep}/d$$

$$\lambda_{cl} = \lambda_r + v_{dep}/ < h > + Q_{out}/V$$

and

C is the concentration dissolved in water (Bq/m^3),
C_p is the concentration in particles of the bottom sediments (Bq/m^3),
$S_1(t)$, $S_3(t)$ are the source term in dissolved form and the source term from direct deposition (Bq/d),
K_f is the coefficient of direct radionuclide transfer (m/d),
$< h >_l$ is the average lake depth (volume to surface ratio V/S_l), (m),
d is the sediment layer depth (m),
q is the outflow (m^3/d),
V is the lake volume (m^3),
v is the sedimentation rate (m/d),
ρ_{sed} is the bulk density of the sediments kg/m^2,
K is the dimensionless distribution coefficient: $K = K_d\ \rho_{sed}$

The system (II-10) to (II-13) is a linear system of ordinary differential equations with a well known solution for the dissolved concentration:

$$C(t) = \int_0^t \frac{S(t')}{V \cdot (\alpha_1 - \alpha_2)} (\lambda_4 + \alpha_1) e^{\alpha_1 (t - t')} - (\lambda_4 + \alpha_2) e^{\alpha_2 (t - t')} dt' \tag{II-15}$$

with:

$$\alpha_{1,2} \equiv \frac{-(\lambda_2 + \lambda_4) \pm \sqrt{(\lambda_2 + \lambda_4)^2 - 4(\lambda_2 \lambda_4 - \lambda_3 \lambda_1)}}{2} \tag{II-16}$$

The unstratified lake is assumed to be completely mixed. During the stratification period the lake is divided into two layers, the epilimnion and hypolimnion. In the hypolimnion, caesium is lost only by radioactive decay. Outflow is interrupted. On the other hand, physical resuspension of radiocaesium at the sediment water interface is only important in very shallow lakes [II-6]. The turbulence that resuspends particles from the bottom and maintains these particles suspended sufficient time to absorb contamination from the water until the K-equilibrium is reached is assumed to be unimportant during stratification.

It is assumed that the sedimentation continues at the same annually averaged rate but that the suspended particles are not in sufficiently high concentration and simultaneously do not have enough time to absorb a significant quantity of activity from the water. Therefore, the "pump" of contamination $v \cdot K/< h >$ and $v \cdot K/d$ which is the most important terms of transfer between compartments before the stratification is assumed to become negligible during this period.

The dynamics in the hypolimnion are thus described by eqs. (II-10) to (II-13) with the following redefinition of the parameters:

$$\lambda_1 = \frac{K_f \cdot S_h}{V_h \cdot K} \qquad \text{(II-17)}$$

$$\lambda_2 = \lambda_r + \frac{K_f \cdot S_h}{V_h}$$

$$\lambda_3 = \frac{K_f}{d}$$

$$\lambda_4 = \lambda_r + \frac{K_f}{d \cdot K}$$

$$\lambda_c = v_{dep}/d$$

$$\lambda_{cl} = \lambda_r + v_{dep}/ < h > + Q_{out}/V$$

and $S_1(t) = S_3(t) = 0$.

The dynamics of the caesium in the epilimnion are described by the system of equations (II-10) to (II-13). However, the transfer through sedimentation of resuspended particles is neglected; the lake volume V replaced by the epilimnion volume V_e; and the direct absorption transfer term in (II-17) is redefined as the new area of absorption. The transfer rates has been redefined in the following way:

$$\lambda_1 = 0 \qquad \text{(II-18)}$$

$$\lambda_2 = \frac{Q_{out}}{V_c} + \lambda_r + \frac{K_f \cdot V_e}{S_l - S_h}$$

$$\lambda_3 = \frac{K_f}{d}$$

$$\lambda_4 = \lambda_r + \frac{K_f}{d \cdot K}$$

$$\lambda_c = 0$$

$$\lambda_{cl} = \lambda_r + v_{dep}/ < h > + Q_{out}/V$$

The model for the epilimnion and hypolimnion is connected to the day or commencement of stratification ("NESTR1" in Table II-3)) and it is maintained until the day "NESTR2". Between this day and the day of the end of stratification "NESTR3" winter conditions, eqs. (II-10) to (II-13), develop with an increasing mixing of the water layers.

TABLE II-2. A PRIORI PROBABILITY DENSITY FUNCTIONS OF THE PARAMETERS USED IN THE UNCERTAINTY ANALYSIS

Parameter	Distribution	Range	Label
1	TRIANGULAR	WITH PARAMETERS BELOW A= 0.250 B= 0.500 C= 0.750	I_c
2	UNIFORM	5.000E-02 – 0.100	S
3	TRIANGULAR	WITH PARAMETERS BELOW A= 5.00 B= 6.50 C= 8.00	$\dot{R}_i$
4	LOGUNIFORM	5.000E-05 – 1.000E-03	d_m
5	UNIFORM	1.250E+03 – 1.350E+03	ρ_b
6	LOGNORMAL	0.176 – 1.06	$K_{d\text{-}soil}$
7	LOGNORMAL	306. – 991.	D(1)
8	LOGNORMAL	306. – 991.	D(2)
9	NORMAL	0.474 – 0.525	ε
10	UNIFORM	0.100 – 0.500	Z_0
11	TRIANGULAR	WITH PARAMETERS BELOW A= 1.141E-05 B= 2.330E-05 C= 3.650E-05	v_{sed}
12	UNIFORM	90.0 – 120.	ρ_{sed}
13	LOGNORMAL	90.0 – 250.	$K_{d\text{-}sed}$
14	LOGNORMAL	2.730E-04 – 4.380E-03	K_f
15	TRIANGULAR	WITH PARAMETERS BELOW A= 4.000E-04 B= 1.550E-03 C= 2.700E-03	ss_1
16	UNIFORM	1.E-03 – 1.E-01	f_{30}
17	UNIFORM	37.0 – 45.0	NESTR1
18	UNIFORM	115. – 119.	NESTR2
19	UNIFORM	119. – 126.	NESTR3

TABLE II-3. PARAMETERS OF THE MODEL

Parameter	Symbol	Range			Units	Reference
		Median	Min.	Max.		
Interception by vegetation	V_i	0.15			–	[I-1]
Infiltration capacity	I_c	0.5	0.4	0.8	$L \cdot m^{-2} \cdot (30min)^{-1}$	
N° of shower categories	NCAT	7				[I-5]
Frequency of each shower intensity range	$\dot{R}(i)$ f(i)	0.25 0.1975			$L \cdot m^{-2} \cdot (30min)^{-1}$	[I-5]
		0.75 0.1975			$L \cdot m^{-2} \cdot (30min)^{-1}$	[I-5]
		1.75 0.289			$L \cdot m^{-2} \cdot (30min)^{-1}$	[I-5]
		2.75 0.09			$L \cdot m^{-2} \cdot (30min)^{-1}$	[I-5]
		4.00 0.14			$L \cdot m^{-2} \cdot (30min)^{-1}$	[I-5]
		7.50 0.07			$L \cdot m^{-2} \cdot (30min)^{-1}$	[I-5]
		20.0 0.01			$L \cdot m^{-2} \cdot (30min)^{-1}$	[I-5]
Catchment slope	S	0.1	0.05	0.1	–	Appendix I
Total rain	R_t	5.6	5.0	8.0	$L \cdot m^{-2} \cdot d^{-1}$	Appendix I
Density of soil, actual	$\$_d$	2650.0			kg/m^3	[I-7]
Particle size of soil	d_m	0.0002	0.00005	0.001	m	[I-7]
Bulk density of soil	$\$_b$	1250	1250	1350	kg/m^3	[I-1]
Soil distribution coefficient	$K_{d\text{-}soil}$	0.80	0.617	1.06	m^3/kg	[I-8]
Decay	λ_r	6.3E-05			1/d	
Duration of radioactive cloud	NDAY	13.0			days	[I-4]
Daily radioactive deposition	D(I)				$Bq \cdot m^{-2} \cdot d^{-1}$	
First day	I-1	480.8	306.0	991.0	$Bq \cdot m^{-2} \cdot d^{-1}$	[I-4]
Second day	I=2	480.8	306.0	991.0	$Bq \cdot m^{-2} \cdot d^{-1}$	[I-4]
Third to thirteenth days	$3 \leq I \leq 13$	1.7			$Bq \cdot m^{-2} \cdot d^{-1}$	[I-4]
Soil porosity	ε	0.53	0.474	0.53	–	[I-1]
Vegetation washout	λ_{wash}	2.6E-04			1/d	[I-1]
Rugosity height	Z_0	0.1	0.1	0.5	m	
Catchment area	A_c	1.7E+07			m^2	Appendix I
Lake surface area	S_l	1.00E+06			m^2	Appendix I
Lake volume	V_l	6.44E+06			m^3	[I-6]
Deposition velocity	v_{sed}	2.33E-05	1.1E-05	3.6E-05	m/d	Appendix I
Bulk density of sediments	ρ_{sed}	100	90.0	120.0	kg/m^3	[I-6]
Sediment distribution coeff.	$K_{d\text{-}sed}$	170.0	90.0	250.0	m^3/kg	[I-6]
Sediment depth	d	0.02			m	[I-6]
Direct adsorption coefficient	K_f	0.001	0.000273	0.00438	m/d	[I-8]
Initial concentration in sed.	$c_p(0)$	160.0			Bq/kg	[I-6]
Suspended solids in the lake	ss_l	0.001	0.0004	0.0027	kg/m^3	Appendix I
Hypolimnion area	S_h	3.49E+05			m^2	[I-6]
Catchment washout rate	f_{30}	5.E-02	1.E-03	1.E-01	1/d	
Stratification starts at day	NESTR1	41	37	45	days	[I-6]
Stratification breaks at day	NESTR2	119	115	119	days	[I-6]
Stratification ends at day	NESTR3	123	119	126	days	[I-6]
Time period simulated	NEND	480			days	

II-2. APPLICATION OF THE MODEL TO THE ESTHWAITE WATER SCENARIO

To test the model against observational data, measurements obtained in water and sediments of Esthwaite Water, Lake District, UK, have been used. Additionally, this comparison has made it possible to calibrate the parameters of the model to the specific scenario. The uncertainties expected in the predictions of integrated concentrations have also been analysed.

Table II-3 summarizes the parameters and data required by the model with the median value chosen a priori and the range that can be expected from the available information. After the calibration, new median values may be defined for the parameters which are site-specific.

The median value of the interception by the vegetation V_i is calculated by [II-1] and [II-2] as a default value for forage vegetation.

Yearly averaged water inflow into the lake has been measured and range from 7.2×10^7 m^3/d to 2×10^8 m^3/d [II.6] with most values between 7×10^7 m^3/d and 1×10^8 m^3/d (Appendix I). This last range is consistent with the observed mean annual precipitation in the catchment: 1750 mm/a, an infiltration velocity of 0.25 to 0.50 mm/(30min) in showers of 30 minutes, and a mean slope in the catchment from 5 to 10 %. Table II-3 shows the median values and range used for the parameters in the catchment model and in the lake model.

The annual mean precipitation rate $\dot{R}_t$ has an associated natural variability. Two different values have been reported: 5.6 L·m^{-2}·d^{-1} (Appendix I) and 7 L·m^{-2}·d^{-1} [II-6]. The range of the infiltration capacity (I_c) has been chosen in such a way that it may be consistent with R_t and with the observed water balance in the basin, i.e. a lake outflow between 73×10^6 L/d and 200×10^6 L/d [II-6]. However, it is not possible to obtain outflows larger than 100×10^6 L/d without increasing the $\dot{R}_t$ above 7 L·m^{-2} d^{-1}. Since this is not probable except in especially wet years, the value I_c=0.8 L·m^{-2} (30 min)$^{-1}$ corresponding to $= 100 \times 10^6$ L/d has been chosen as the superior bound. In addition, the probability density function (PDF) used in the uncertainty analysis for has been defined as triangular function with extreme points at 5 L·m^{-2}·d^{-1}, 8 L·m^{-2} d^{-1} and mode 5.6 L·m^{-2} d^{-1}.

The effect of the distribution of precipitations f(R) is to control the wet surface and so the decay of the source term bonded to water. The particular distribution f(R) that took place in the basin is not known. According to McDougall [II-6] "the passage of the Chernobyl cloud coincided with isolated, very heavy, advective rainstorms so that the deposition occurred over a very short time period, e.g. 12 h in Cumbria". Therefore, a possible choice is to use the right extreme value in Table II-1. However, the wet surface is not only controlled by this parameter: the soil undulations are expected to widely reduce the total basin surface that is being flushed which is a function of the spatial distribution of rugosities, f(Z_0).

Given the lack of specific information it has been decided not to try and to model this combined uncertainty but to calibrate the "wet surface" parameter. To this effect, the frequency matrix has been fixed to the values of Table II-1 (a rough estimation strictly only applicable to conditions in the North of Spain) and the Z_0 parameter has been calibrated to the best fit. The uncertainty of this parameter adds to the uncertainty of the Z_0 parameter since this has a similar effect on the model; both control the surface of basin that is doused by a shower and thus the decay of the water concentration flowing into the lake. The mean slope of the basin is based on topographical maps (Appendix I).

The particle density ρ_d is a parameter showing relatively little variability for different types of soils [II-7]. The median diameter of the soil particles has been chosen to range between that of very coarse silt and coarse sandy soil [II-7]. The bulk density of the soil ρ_d and the porosity ε have been chosen to range from typical values for very coarse silt to typical values for coarse sandy soil [II-1], p. 5–42. The K_d of the soil ranges typically between 0.6 and 1.1 m^3/kg [II-8]. A median value of 0.8 m^3/kg has been chosen.

The days of presence of the cloud has been reported in several locations of the UK [II-4]. A generic parameter, about 2.6×10^{-4} d^{-1}, has been taken as the washout rate of the contamination intercepted by the vegetation [II-1]. The surfaces of the basin and lake are given in Appendix I.

The thickness of the sediment active zone, the surface area of the hypolimnion and the volume of the lake and hypolimnion have been reported by [II-6], based in experimental observations. The sedimentation velocity has been calculated as the ratio between the annually averaged sedimentation velocity rate (500 to 1200 g $m^{-2} \cdot a^{-1}$ (Appendix I) and the observed bulk density of the sediments (90 to 120 kg/m^3 [II-6].

The distribution coefficient K_d of the sediments has been reported to be between 90 and 250 (m^3/kg) [II-6]). The K_f has been chosen with the generic range reported by [II-8]. The initial caesium concentration in the sediments and the days of start and end of the stratification period are reported in [II-6]. The concentration of suspended sediments in the lake ss_l is from Table 3.1 of this document.

Finally, the washout rate by the running water in the catchment has been calibrated by the best fit.

II-3. UNCERTAINTY AND SENSITIVITY ANALYSES

Many of the parameters defining the scenario and the processes of transfer involved sometimes have: (i) a large natural variability, (ii) associated experimental uncertainties and/or (iii) are not experimentally based but based on theoretical considerations or even ad hoc hypotheses. These parameters have been defined through probability distributions as it shown in Table II-2. Taking the median values of the parameters, the following picture emerges of the water and eroded soil flows in the catchment:

Discounting vegetation interception and evaporation, 99×10^6 L/day are intercepted by the basin from which 14×10^6 L infiltrate and 85×10^6 L drain downslope. For a rugosity size of 10 cm, the height of the drainage channels formed ranges from 3.5 mm to 2.1 cm depending on the shower intensity. The concentration of eroded soil that is potentially transportable has ranges from 99 kg/m^3 to 22 kg/m^3. It means that only a fraction, about 3.5×10^{-3} kg/m^3, of that potentially transportable (or 12% of the eroded soil suspended in the water) flows into the lake. The basin surface that is doused by the drainage ranges between 5% to 20% for different showers. The source term into the lake associate with water and suspended soil is shown in Figures II-9 and II-11.

The direct deposition onto the lake seems to be more important than the contribution from the catchment, generating an input that is close to a pulse of a maximum duration of two days. However, the "tail" after the second day has an influence on the slope of decay in the lake concentration.

In order to quantify the degree of fit between the model predictions p_i at day i (i=1,2,..,N) and the time series with the observed concentrations o_i in epilimnion, hypolimnion and sediments the two following residuals have been used:

$$R = \frac{\sum_{i=1}^{N} (p_i - o_i)}{\sum_{i=1}^{N} o_i} \qquad \text{(II-19)}$$

and:

$$C_{x^2} = \frac{\sum_{i=1}^{N} (p_i - o_i)^2}{\sum_{i=1}^{N} o_i^2} \qquad \text{(II-20)}$$

where N is the number of observations.

The distance R is the integrated residuals of the fit. When R is small, the mean predicted concentration is close to the mean observed concentration. The distance C_{02} is the variance that remains unexplained after the fit. When R and C_{02} are both small then the discrepancies between punctual predictions and the corresponding observation are bounded.

The model can be calibrated a posteriori by selecting the runs providing lowest values for eq. (II-19) [II-9]. Figures II-3 to II-8 show the distribution of these two distances of fit for the three variables simulated.

The integrated residuals for epilimnion, hypolimnion and sediments present forms resembling log-normal distributions, with the following statistical parameters:

Parameter	Epilimnion	Hypolimnion	Sediments
Average	-0.34	-0.22	0.77
Median	-0.34	-0.27	0.71
Variance	0.075	0.11	0.28
Standard deviation	0.27	0.33	0.53
Minimum	-0.8	-0.82	-0.30
Maximum	3.19	3.7	9.77

This implies that the model has a tendency to underpredict in the epilimnion and hypolimnion by roughly 39% and 27%, respectively, and a tendency to overpredict in the sediment mean concentration by 71%, even though in this last case the fit would be inside the experimental bounds. The integrated residual is an index of the error in the predicted integrated concentration relative to the observed integrated concentration.

The statistical parameters of the distribution of C_{02} are:

Parameter	Epilimnion	Hypolimnion	Sediments
Average	0.18	0.35	0.95
Median	0.14	0.27	0.56
Variance	0.089	0.34	4.2
Standard deviation	0.30	0.58	2.06
Minimum	0.02	0.0068	0.0069
Maximum	14.4	22.8	98.7

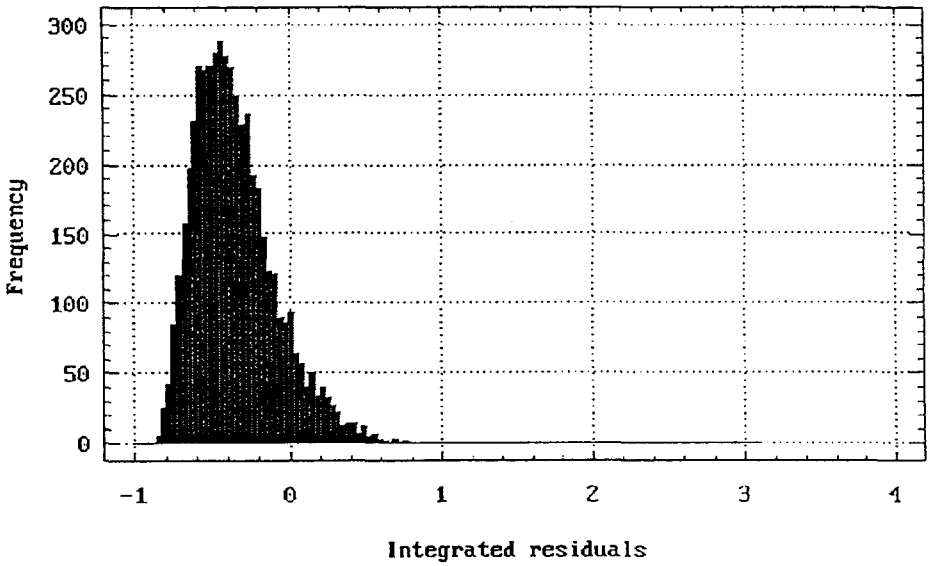

FIG. II-3. Probability distribution function for the integrated residuals in the fit between predicted and observed concentrations in epilimnion.

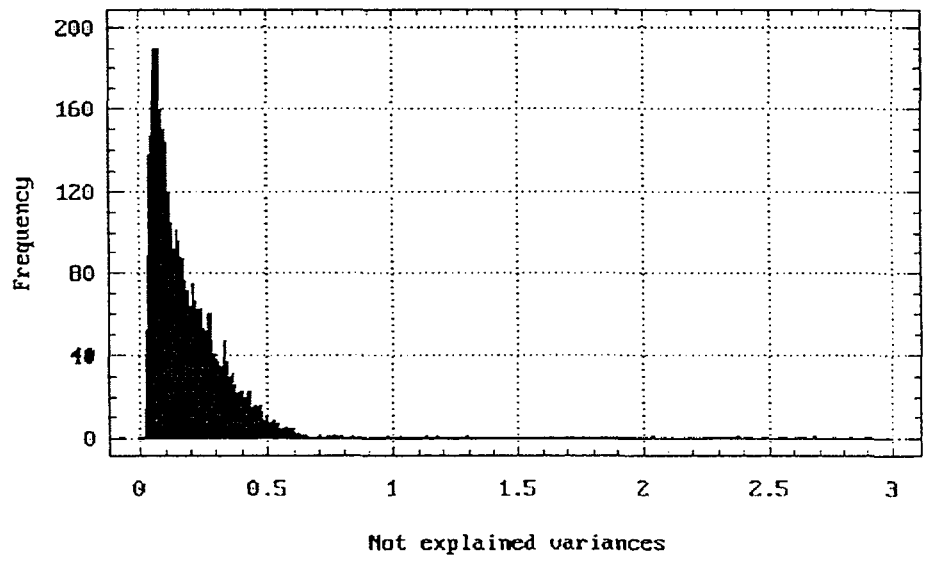

FIG. II-4. Probability distribution function of the unexplained variances in the fit between predicted and observed concentrations in epilimnion.

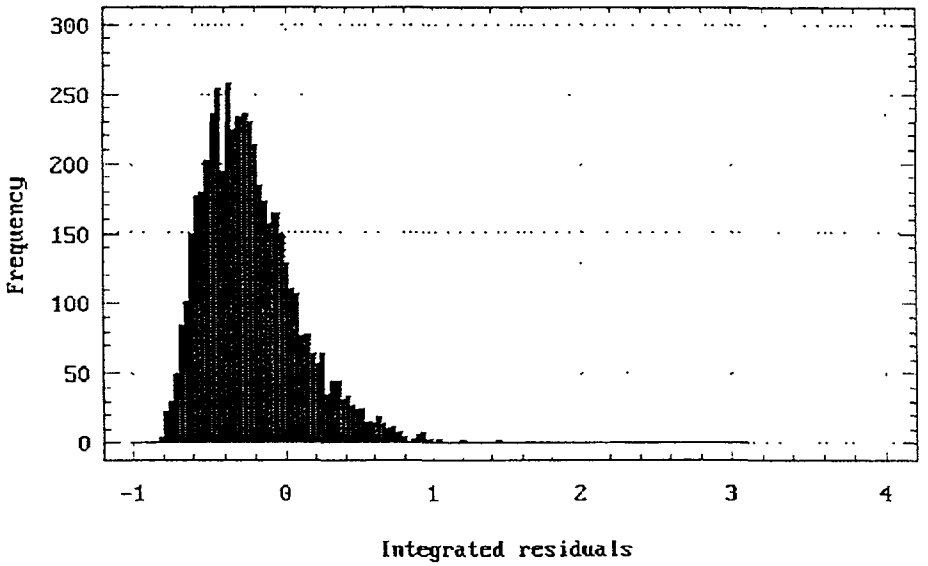

FIG. II-5. Probability distribution function of the integrated residuals in the fit between predicted and observed concentrations in hypolimnion.

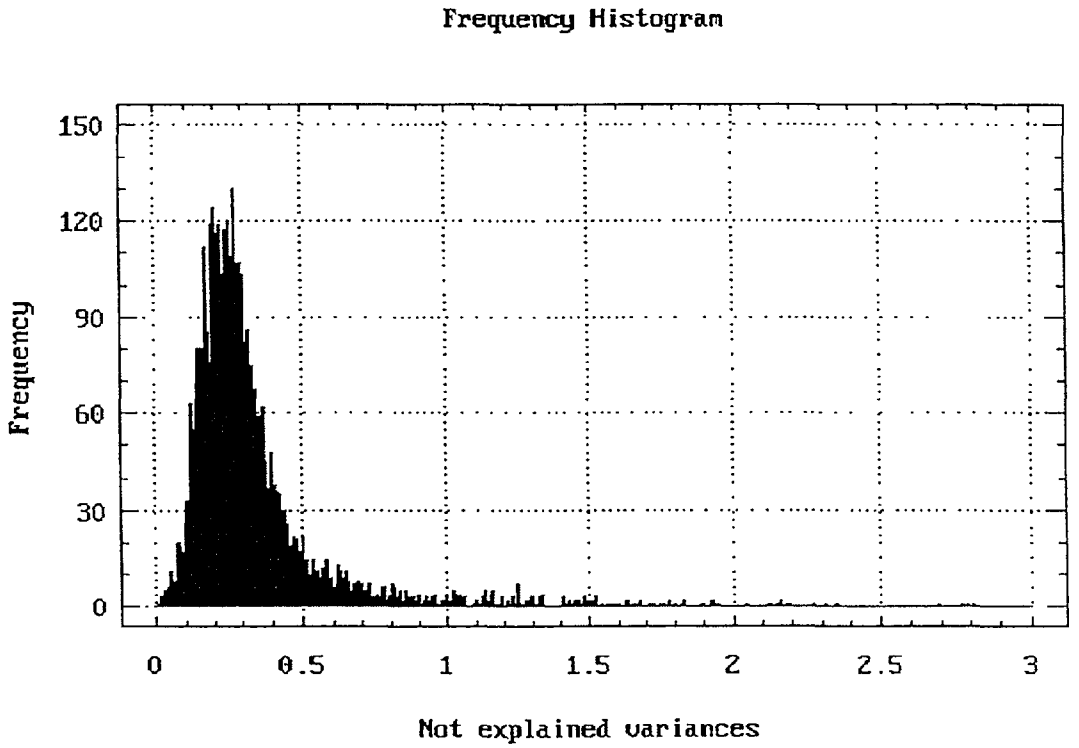

FIG. II-6. Probability distribution function of the unexplained variances in the fit between predicted and observed concentrations in hypolimnion.

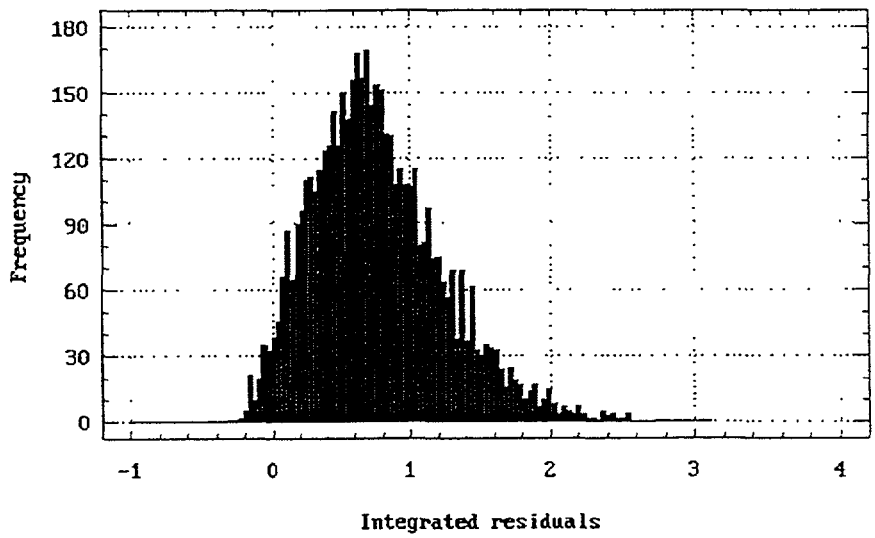

FIG. II-7. Probability distribution function of the integrated residuals in the fit between predicted and observed concentrations in the sediments.

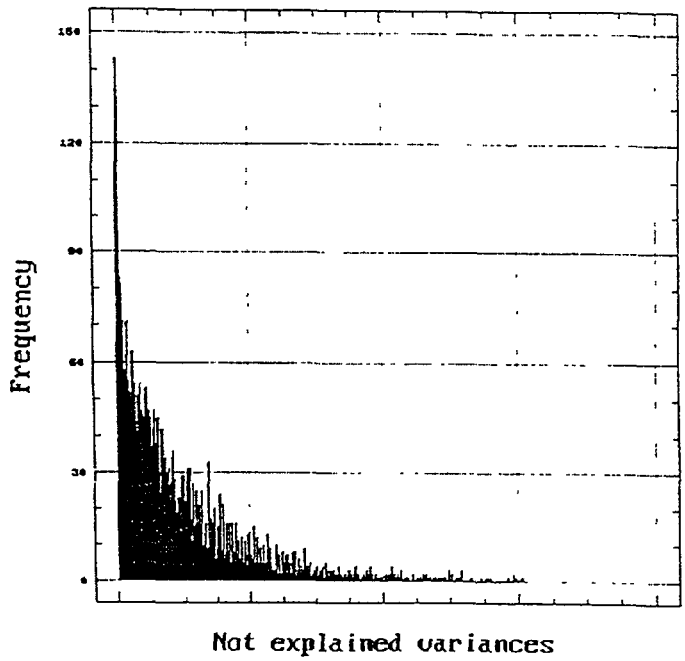

FIG. II-8. Probability distribution function of the unexplained variances in the fit between predicted and observed concentrations in the sediments.

This implies that in a median situation 14% and 27% of the variance in the integrated concentrations for epilimnion and hypolimnion, respectively, would remain unexplained after the fit.

A sensitivity analysis of the parameters used by the model has been implemented. The distance R has been used as the output variable, and the influence of the parameter p_i on this variable is measured through a sensitivity index s_i:

$$s_i = \left| \frac{\partial \ln R}{\partial \ln p_i} \right| \qquad \text{(II-21)}$$

Table II-4 shows the sensitivities of the most uncertain parameters of the model. The most sensitive parameters are the deposition during the first two days and the three parameters controlling the water-sediment exchange in the lake. Next follows the annual precipitation rate controlling the inflow, and subsequently the soil rugosity height and the washout rate of contamination from the catchment, which control the flushed area in the catchment and the rate of flushing, respectively.

To select the best fits obtained, the constraint R<10% and C_{02}<10% has been imposed simultaneously in the epilimnion and hypolimnion. Sediments are always within the range observed. A number of 10 from a total of 5000 runs fulfill this condition. The most sensitive parameters in these 10 runs are shown in Table II-5. Figures II-10 and II-12 compare predictions and observations of the two best fits from this set. The integrated residuals are respectively: R_{epi} = -6% (-6.2%), R_{hypo} = 8% (9%) and R_{sed} = -4.4% (-13%).

The unexplained variances C_{02} (in %) in epilimnion, hypolimnion and sediments are respectively: 3.2% (3.6%), 3% (2.8%) and 1% (2.3%).

The temporal zero corresponds to 2 May 1986.

TABLE II-4. SENSITIVITY OF R_{epi}, R_{sed} TO THE MODEL PARAMETERS

Parameter	Symbol	Sensitivity		
		R_{epi}	R_{hypo}	R_{sed}
Infiltration capacity	I_c	1.3	0.8	0.6
Slope	S	1.2	1.1	0.7
Annual precipitation	I_{tot}	4.1	2.8	2.1
Particle diameter	d_m	0.0	0.0	0.0
Soil density	ρ_b	0.0	0.0	0.0
Soil K_d	$K_{d\text{-}soil}$	0.0	0.0	0.1
1st day deposit	D(1)	7.4	6.4	7.7
2nd day deposit	D(2)	7.6	6.5	7.6
Soil porosity	ε	0.0	0.0	0.0
Soil rugosity	Z_0	2.2	1.9	2.1
Sedimentation velocity	v_{sed}	4.9	4.5	5.1
Sediments density	ρ_{sed}	4.9	4.5	4.3
Sediments K_d	$K_{d\text{-}sed}$	4.9	3.7	6.9
Direct absorption	K_f	0.1	0.1	0.2
Volume ratio epi/lake	f_{eplh}	1.7	0.9	1.6
Suspended sediments	ss_1	0.0	1.0	0.0
Daily washing rate	f_{30}	0.8	0.7	1.5

TABLE II-5. RANGE OF VALUES FOR THE MOST INFLUENTIAL PARAMETERS USED TO OBTAIN THE BEST FITS

Parameter	Symbol	Range		Units
		Min.	Max.	
Total deposition	D(1)+D(2)	660	1430	Bq/m^2
Sedimentation velocity	v_{sed}	1.1×10^{-5}	1.9×10^{-5}	m/d
Bulk density of the sediment	ρ_{sed}	90	118	kg/m^3
Sediment-water distribution coeff.	$K_{d\text{-}sed}$	93	157	m^3/kg
Total rain	$\dot{R}_t$	5.6	6.8	$L \cdot m^{-2} \cdot d^{-1}$
Daily washing rate	f_{30}	1.9×10^{-3}	5.2×10^{-2}	1/d

Some parameters with large associated sensitivity become less important if they have short ranges of uncertainty (Table II-2). This is the case with the parameters I_c, S, I_{tot}, v_{sed}, ρ_{sed} and f_{eplk} all of which are constrained by the experimental evidence (see Section 2).

On the other hand, the parameters D(1) and D(2) have no sensitive effect when one of them is decreased and the other increased in the same proportion. However, some evidence suggests that most of the deposition in the area of Cumbria in UK took place during the first 12 hours of the presence of the cloud [II-6]. For these reasons the integrated parameter $D_{pulse} \equiv (1) + D(2)$ can be used in this scenario instead of the separated parameters D(1) and D(2) with no loss of generality in the conclusions. Therefore, obtaining the best fits is a matter of finding the most favorable combinations of the following parameters: $K_{d\text{-}sed}$, D_{pulse}, f_{30} and Z_0.

When using the pulse D_{pulse} as the only contribution of contamination to the lake ($f_{30} = 0$) the model solution is the "impulse response" of the system (II-10) to (II-13), given by the integral of eq. (II-15) for the period previous to the stratification. It is not possible to fit this "impulse response" to the observed time series of concentration in water without forcing the parameter K_d (or alternatively v_{dep}) below its confidence range. Therefore, it must be concluded that some contribution of contamination coming from the catchment must be acting in this scenario.

Figures II-9 and II-11 show two specific source terms both with contribution from the catchment that have proportional good fits in two different calibrations. The first, with a water outflow at the upper extreme end of the experimental range and the second at the opposite extreme. The contribution from the catchment can be observed as a decay over imposed on a two-day pulse.

Figures II-10 and II-12 show the corresponding concentrations in lake water in both cases. It can be observed from the parameters given in the footnotes in Figures II-10 and II-12 that for a pulse D_{pulse}, of median value 660 Bq/m^2 and all the less-sensitive parameters in their median values, a $K_{d\text{-}sed}$ between 105 and 120 m^3/kg, a f_{30} between 1.5 and 2×10^{-2} d^{-1} and a Z_0 such that the aquatic area in the catchment is between 8.8% and 9.4% make it possible to obtain good fits. It is possible to obtain good fits with high $K_{d\text{-}sed}$ values ($\geq$ 170 m^3/kg) without assuming high values for D_{pulse}. For instance, $D_{pulse} = 900$ Bq/m^2 and $f_{30} \approx 10^{-3}$ or $D_{pulse} = 1400$ Bq/m^2 and $f_{30} \approx 10^{-4}$. However these fits are slightly worse than the previous ones since the high K_d values produce an excessively rapid decay of the "tail" after the stratification period.

The concentration in sediments (Figures 10-B and 12-B) increases quickly until the stratification period, followed by a slower rise after the stratification period and then by a long term decay by burial and radioactive decay. The general trend is quite similar to that observed in the mean experimental values in Figures II-10-B and II-12-B. These means values were obtained by averaging the concentrations in core samples taken from 16 sites in Esthwaite Water [II-6].

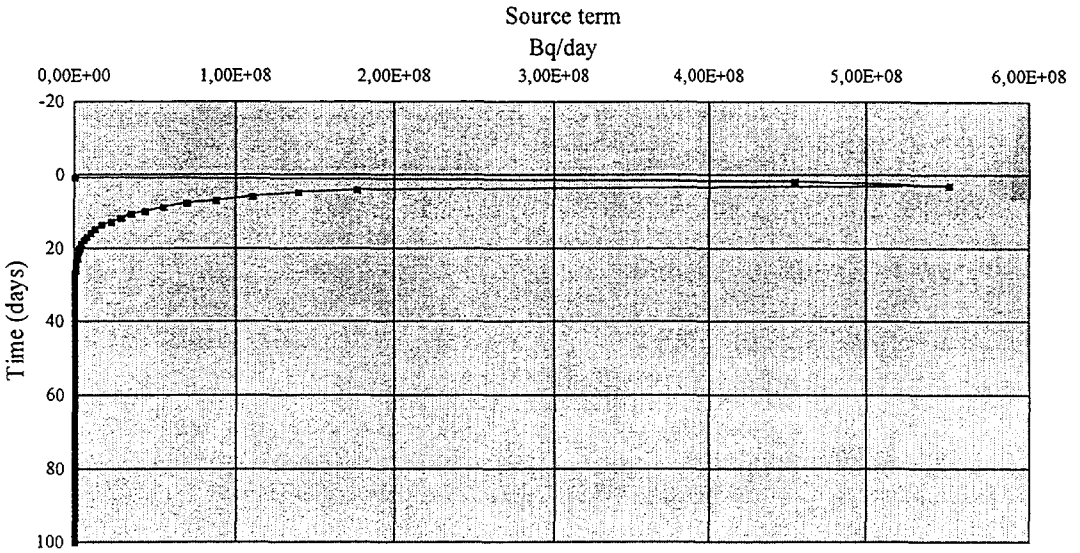

FIG. II-9. Source term of activity into the lake for a low water inflow (this is the input to the lake shown in Figure II-10).

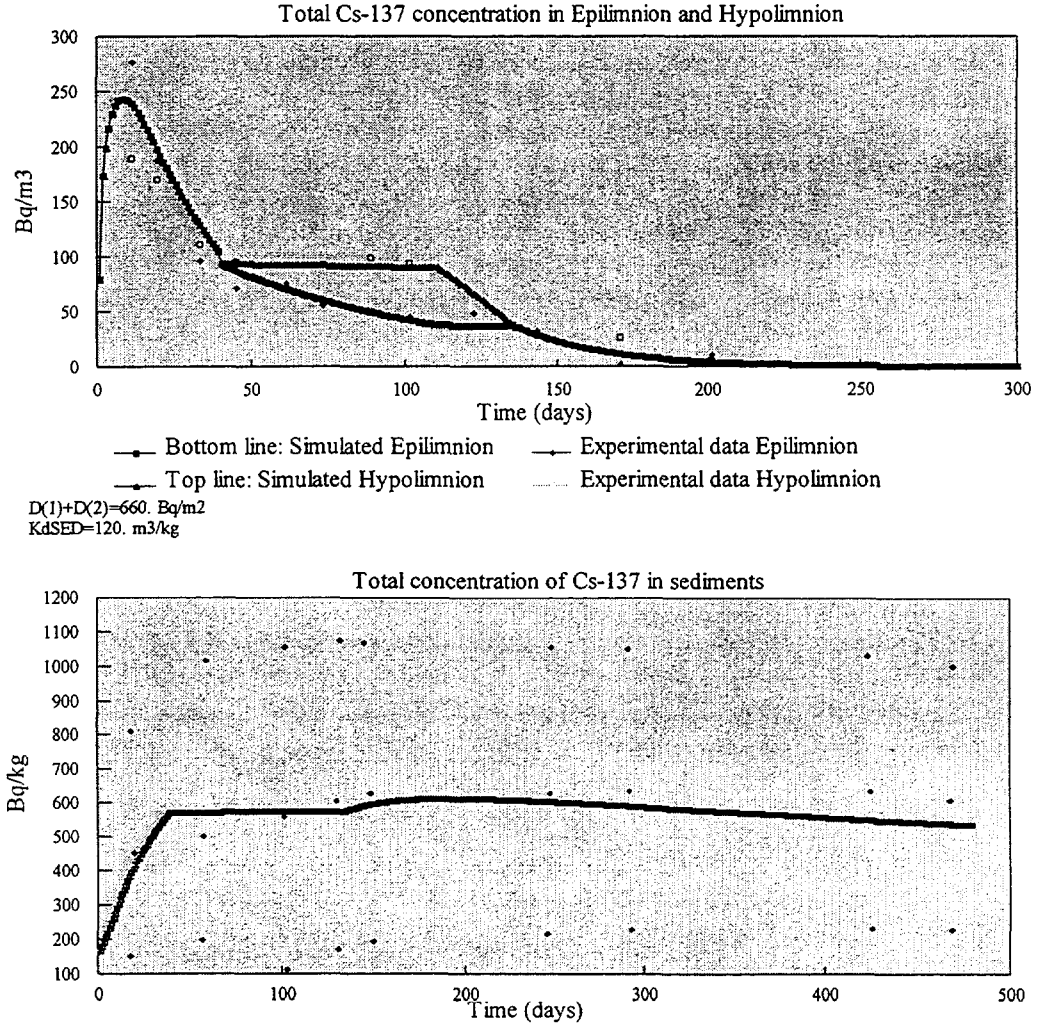

FIG. II-10. Top: Total ^{137}Cs concentration in epilimnion and hypolimnion. Bottom: Total ^{137}Cs concentration in bottom sediments for a low water inflow from the catchment source.

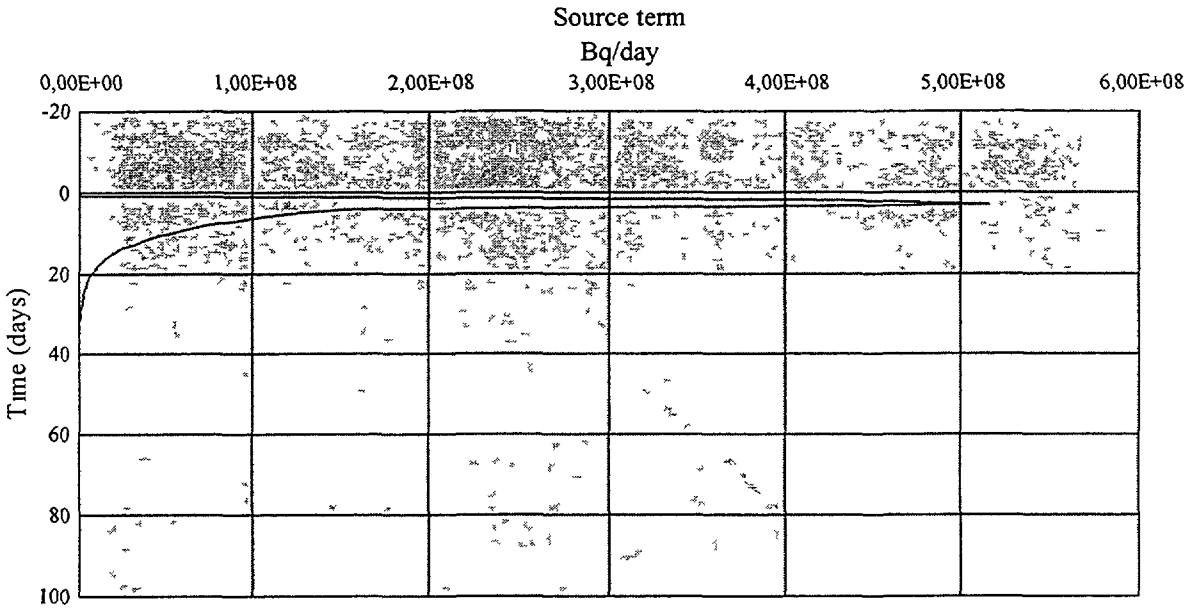

FIG II-11 Source term of activity into the lake for a high water inflow (this is the input to the lake shown in Figure II-12).

II-4. CONCLUSIONS

In this study the Codell model [II-2] has been used as a starting point to simulate the behaviour of caesium-137 in Esthwaite water. With the help of some basic auxiliary models for the input source, the model has made it possible to obtain a good estimation within the range of the integrated concentration expected in water and a qualitatively correct fit for the observed dynamics in water and sediments.

The most sensitive parameters in the model are (i) the direct deposition during the two first days, (ii) the three parameters controlling the interaction water-bottom sediments, i.e. the distribution coefficient (K_d), the sedimentation velocity, and the bulk density of the sediments, followed by (iii) the rate of washout of contamination by water in the basin.

When using a priori probability density functions (PDF) for the parameters in agreement with the existent experimental uncertainties, the predicted median integrated concentrations tend to be biased by -39% (epilimnion), -27% (hypolimnion) and 71% (sediments).

A calibration has been implemented within the expected variability of the parameters to obtain the model solution that best matches the observed dynamics in the epilimnion, hypolimnion and bottom sediments.

Reasonably good fits were obtained when the source term into the lake was assumed to be dominated by the direct atmosphere to lake deposition. This is consistent with a presence of a major atmospheric contamination 2 and 3 May and a minor addition during the following days coming mainly from the activity accumulated in the catchment.

Best fits were obtained when the total deposition during the first two days ranged from 660 to 1430 Bq/m^2, the sedimentation velocity from 1.1×10^{-5} and 1.9×10^{-5} m/d; the distribution coefficient $K_{d\ sed}$ from 93 to 157 m^3/kg and the rate of washout in the basin ranged from 1.9×10^{-3} to 5.2×10^{-2} d^{-1}.

When the PDF's median values of these parameters are redefined to fall inside the previous ranges, a large fraction of the bias disappears. However, a small fraction of the bias derives from the

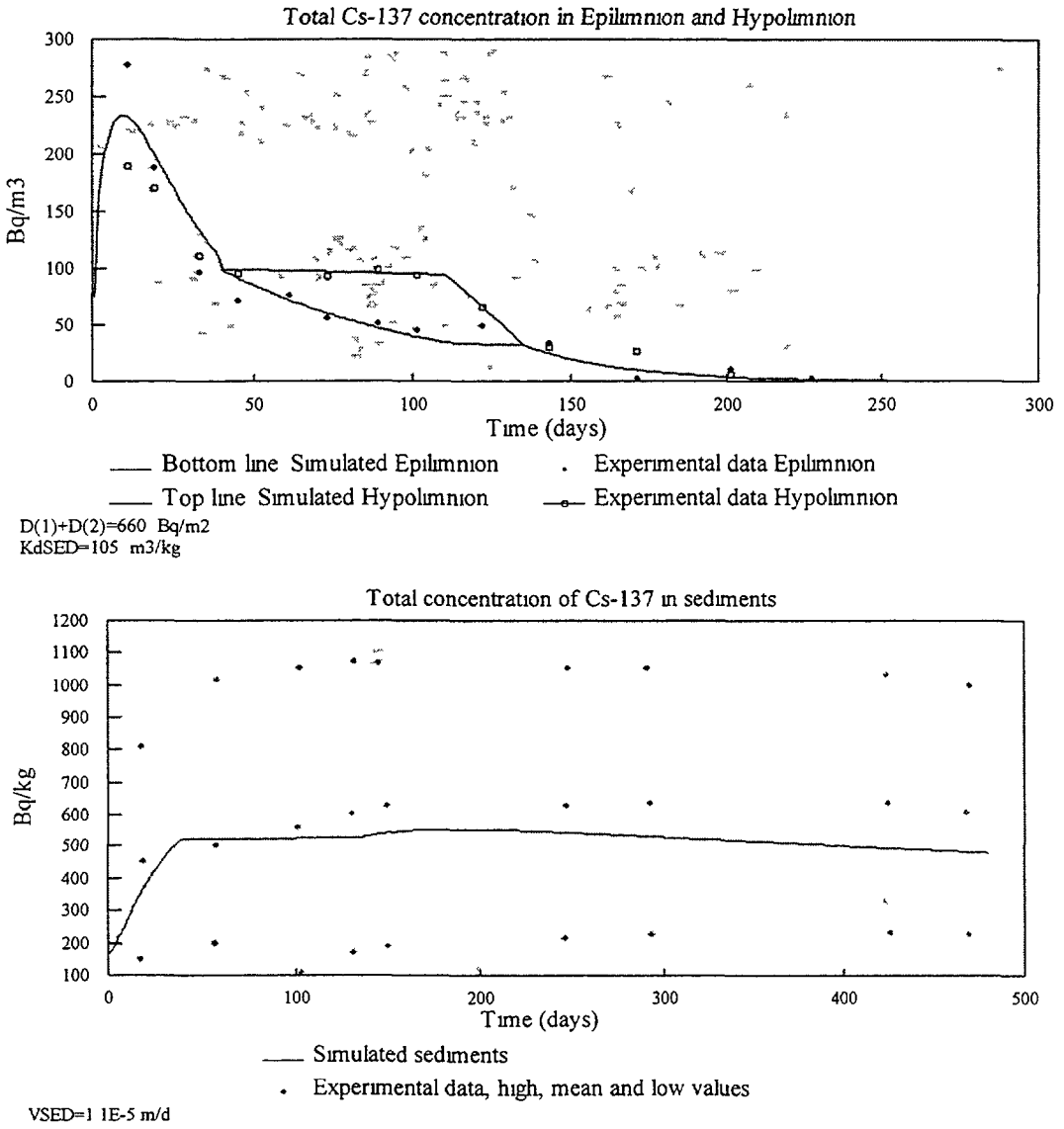

FIG II-12 Top: Total ^{137}Cs concentration in epilimnion and hypolimnion. Bottom Total ^{137}Cs concentration in bottom sediments for a high water inflow from the catchment source.

use of generic parameters which are not easily deducible from site observations and which have been taken from the literature, (e.g. the canopy's interception fraction and washout rate, the distribution coefficient of the catchment's soil, the median soil porosity and the median size of the particles). These parameters have not been quantified locally.

Since 95% of the variance has been taken into account after the calibration, it is possible to conclude that the most of the a priori misperformance of the model derived from the unavailability of accurate information on the parameters controlling the mean transfers between the compartments and their experimental distributions, especially the water/sediments distribution coefficient in the lake. Structural uncertainties may be considered secondary in this scenario. However, the model slightly underpredicted observed concentration in the epilimnion for a few days at the end of the stratification period. In addition, the experimental data show concentrations in the epilimnion greater than in hypolimnion during the period prior to stratification. A possible explanation of these observations is that the activity received by the lake surface during the first two days did not diffuse instantaneously into the hypolimnion. It is clear than compartmental models cannot easily account for diffusive phenomena. Therefore, these misperformances must be considered part of the structural uncertainties of the model.

It may be observed from the Figures II-10 and II-12 that there is no way to simultaneously match the stratification period and the period previous to it without any residuals in the fit with this model. This derives from the decreasing step that the disappearance of a large fraction of contaminated suspended sediments introduces in the initial phase of the stratification period. It can be argued that the model is too definite in its approach to this process.

During stratification, the model considers that contamination of the suspended sediments arises exclusively from the catchment. These sediments have not had time to increase their original contamination by absorption from the lake water and for this reason are not as contaminated as the suspended particles coming from the active layer on the bottom, which are assumed to undergo several cycles of deposition-resuspension before final sedimentation. In fact, suspended sediments are not expected to reach the K_d equilibrium concentrations with the surrounding water if their residence time in suspension is negligible, but it is not realistic to assume that they adsorb no new contamination from the water.

Another detail that remains unexplained is the low epilimnion concentration predicted at the end of the stratification period. This could derive from some unexplained effect of the hypolimnion. The influence of the hypolimnion on the dynamics could be larger than expected from its volume, which can be as small as 9% of the lake volume.

In other kinds of scenarios of contamination after the Chernobyl accident, uncertainties in integrated concentrations larger than an order of magnitude have been frequent, and a bias of one order of magnitude has been observed in many predictive models (see e.g. BIOMOVS studies [II-10]).

For this reason, a bias of 30% and a 2σ confidence level of the prediction with the same order of the mean value may be considered to give a relatively good reliability for dose assessment application.

REFERENCES

[II-1] TILL, J.E., MEYER, H.R. (Eds), "Radiological Assessment, A Textbook on Environmental Dose Analysis", United States Nuclear Regulatory Commission, NUREG CR-3332 Oak Ridge Nat. Lab., Oak Ridge, TN (1983).

[II-2] UNITED STATES NUCLEAR REGULATORY COMMISSION, Liquid Pathway Generic Study. Impacts of Accidental Radioactivity Releases to the Hydrosphere from Floating and Land-Based Nuclear Power Plants, NUREG-0440, Washington, DC (1978).

[II-3] SHEN, H.W. (Ed.), Modelling of Rivers, John Wiley & Sons, New York (1979).

[II-4] EUROPEAN COMMISSION, Environmental radioactivity in the European Community 1984-85-86, Joint Research European Commission Centre, EUR 12254 EN, Brussels-Luxembourg, ISBN 92-825-9928-0 (1989).

[II-5] VIDAL, J.M., POTAU, M., Intensidad de las lluvias en Barcelona, Ministerios del Aire, Servicio Meteorológico Nacional, Madrid (1951).

[II-6] MCDOUGALL, S., HILTON, J., JENKINS, A., A dynamic model of caesium transport in lakes and their catchments, Water Resources **25** 4 (1991) 437–445.

[II-7] FETTER, C.W., Applied Hydrogeology, Mervil Publishing, Columbus, OH (1988).

[II-8] UNITED STATES NUCLEAR REGULATORY COMMISSION, "Simplified Analysis for liquid Pathway Studies", NUREG-1054, Washington, DC (1984).

[II-9] GARCÍA-OLIVARES, A., Calibrating Uncertainties in a Dynamical Environmental Model, Modelling Geo-Biosphere Processes, 1 (1992) 41–81.

[II-10] BIOMOVS, Scenario A4, Multiple Model Testing Using Chernobyl Fallout Data of I-131 in Forage and Milk and Cs-137 in Forage, Milk, Beef and Grain, BIOMOVS Technical Report 13, part 1 and part 2 (1991).

GLOSSARY

adsorption	The process of attachment on to and release from surfaces.
algae	Simple photosynthetic non-vascular plants; mainly aquatic.
alkalinity	The total amount of weak acid salts (largely bicarbonate) per unit volume of water.
allochthonous	From outside (often used to characterize materials transported from the drainage area to a lake).
anoxic sediment	Sediment devoid of free oxygen.
autochthonous	Originating from inside the lake.
benthos	Organisms living in or on the river or lake bed.
bioaccumulation	The increase in the amount of chemical or compound in the tissues of living organisms.
biological half-life	The time required for the amount of a particular radionuclide in a biological system, such as an animal, to be reduced by one half by biological processes, when the contamination has been terminated.
biomass	Mass of living organisms present at any one time within a given area or volume.
biota	The total flora and fauna of a given area.
bioturbation	Mechanical mixing, for example of bottom sediments due to living organisms.
catchment	The drainage basin which channels precipitation into a lake or single outflow.
compartment	Any part of the environment or process which may conveniently be considered as a single entity. Used in developing mathematical models.
compartment model	A model in which a series of **compartments** is used to represent the system of interest. Material can flow between the compartments. Differential or difference equations often are used to represent the rates of flow in the system.
conductivity	Quantity of electricity transferred across unit area per unit of potential gradient and unit of time (in mS/m). It usually gives an indication of total ionic concentration.
confidence interval	An interval which encompasses the true value for a parameter or measurement with a degree of confidence stated in terms of a probability.

default value	A value prescribed for a model parameter in the absence of data directly relevant to the assessment situation.
diffusion	The movement of atoms or molecules from a region of higher concentration of the diffusing species to regions of lower concentration.
dimictic	A lake having two seasonal overturn periods of mixing and two of thermal stratification (see **thermocline**).
dynamic model	A model that simulates the changes that occur through time in a system, especially, in the current context, in containment concentrations in the system.
dystrophic	Lake rich in humic matter mainly in the form of suspended plant colloids and larger plant fragments.
ecological half-life	The time required for the amount of a particular radionuclide in a particular organism living in a natural **ecosystem** to be reduced by one half.
ecosystem	A community of organisms together with the environment they inhabit and with which they interact.
effective half-life	The time required for the amount of a particular radionuclide in a system to be reduced by one half as a consequence of radioactive decay and all other processes.
epilimnion	The upper layer of lake water above the **thermocline** with a comparatively homogeneous temperature profile.
eutrophic	A lake rich in nutrients, usually resulting in high productivity.
evapotranspiration	Loss of water by evaporation from soil and by transpiration from vegetation over a given area with time.
food chain	Sequence of organisms in an **ecosystem** occupying specific hierarchical levels (trophic levels) such that organisms belonging to a superior level survive by eating organisms belonging to inferior levels. The sequence can be represented as **compartments** in a mathematical model or analysis.
food web	The network of interconnected food chains in an **ecosystem**.
generic model	A model that is not built on site-specific information.
hardness (water)	A measure of the amount of calcium and magnesium cations in the water.
hydraulic residence time	The ratio of the volume of a water body to water discharge (corresponding to the theoretical time needed for a complete exchange of water).
hypolimnion	The layer of lake waters below the **thermocline**

load (internal/primary)	Fallout directly onto the lake surface.
load (secondary)	The flux (transport) from the **catchment** to the lake.
macrophytes	Large aquatic plants.
mesohumic	Lake with intermediate levels of humic matter.
monomitic	Lake having a single period of free circulation or overturn per year.
Monte Carlo	A technique involving the use of random numbers in a computer program or simulation model to represent stochastic events.
morphometric	All the geometric characteristics relative to the shape of the basin (volume, surface, depth etc.).
oligohumic	A lake poor in nutrients, usually resulting in low productivity.
oligotrophic	A lake with low primary productivity.
output variables	Variables that are produced as model output. Output variables can be state variables or functions of one or more state variables.
partition coefficient K_d	The ratio between the amount of radionuclide attached to **suspended** matter per unit of mass and the amount of dissolved radionuclide per unit of volume of water.
permeability	Rate of passage of water through a given cylindrical section of a **sediment** core.
pelagic	Pertaining to the water column of the lake; used for organisms inhabiting the open waters of the lake.
periphyton	A community of plants, animals and associated detritus forming a surface coating on stones, plants and other submerged objects.
phytoplankton	Plant members of the **plankton**.
piscivorous	Fish-eating.
plankton	Organisms that float or swim very feebly in the water masses of lakes and rivers.
predator	An animal that kills other animals for food.
primary productivity	The total production by photosynthetic and chemosynthetic activity of organic substances.
resuspension	The remobilization of particles from the sediments of a water body by the action of water movement.
sediment	The matter which has fallen to the bottom of a water body.
sedimentation rate	The amount of matter deposited on the bottom of a water body per unit of surface and time.

sensitivity analysis	The analysis of variation of model output with changes in the values of model parameters.
stratification	Division of lake water masses into horizontal layers with different physical and chemical properties.
suspended matter	Matter suspended in lake and river waters.
thermocline	The boundary layer of lake waters in which temperature changes sharply with depth; situated between the **epilimnion** and **hypolimnion**.
tributary	A smaller river flowing into a larger river or a lake.
trophic level	The hierarchical level which an organism occupies in the food chain. The group of organisms that occupy the same level in the food chain.
uncertainty analysis	An analysis of the way in which the uncertainty in assessment results is affected by uncertainty in the input data used in the model.
validation (model)	The process of comparing model outputs with independent experimental data sets. A model is considered validated when sufficient testing has been performed to ensure an acceptable level of predictive accuracy over the range of conditions over which the model may be applied.
volume development	The ratio between the lake volume and the volume of a cone having the basis equal to the area of lake surface and the height equal to the maximum depth of the lake.
zooplankton	Animal members of the **plankton**.

CONTRIBUTORS TO DRAFTING AND REVIEW

Lake information and data:

Bergström, U.	Studsvik Ecosafe, Sweden
Brittain, J.	University of Oslo, Norway
Hamilton-Taylor, J.	University of Lancaster, United Kingdom
Monte, L.	ENEA, Italy
Saxén, R.	Finnish Radiation and Nuclear Safety Authority, Finland
Van der Steen, J.	KEMA, Netherlands
Woodhead, D.	CEFAS, United Kingdom

Modelling:

Bergström, U.	Studsvik Ecosafe, Sweden
Heling, R.	KEMA, Netherlands
Håkanson, L.	Uppsala University, Sweden
Korhonen, R.	Technical Research Center, Finland
Monte, L.	ENEA, Italy
Suolanen, V.	Technical Research Center, Finland